Agronomy Research

Established in 2003 by the Faculty of Agronomy, Estonian Agricultural University

Aims and Scope:

Agronomy Research is a peer-reviewed international Journal intended for publication of broad-spectrum original articles, reviews and short communications on actual problems of modern biosystems engineering incl. crop and animal science, genetics, economics, farm- and production engineering, environmental aspects, agro-ecology, renewable energy and bioenergy etc. in the temperate regions of the world.

Copyright & Licensing:

Agronomy Research online:

Agronomy Research is available online at: https://agronomy.emu.ee/

Acknowledgement to Referees:

The Editors of *Agronomy Research* would like to thank the many scientists who gave so generously of their time and expertise to referee papers submitted to the Journal.

Abstracted and indexed:

SCOPUS, EBSCO, DOAJ, CABI Full Paper and Clarivate Analytics database: (Zoological Records, Biological Abstracts and Biosis Previews, AGRIS, ISPI, CAB Abstracts, AGRICOLA (NAL; USA), VINITI, INIST-PASCAL.)

Subscription information:

Institute of Technology, EMU
Fr.R. Kreutzwaldi 56,
51006 Tartu,
ESTONIA
e-mail: timo.kikas@emu.ee

Journal Policies:

Estonian University of Life Sciences, Latvia University of Life Sciences and Technologies, Vytautas Magnus University Agriculture Academy, Lithuanian Research Centre for Agriculture and Forestry, and Editors of *Agronomy Research* assume no responsibility for views, statements and opinions expressed by contributors. Any reference to a pesticide, fertiliser, cultivar or other commercial or proprietary product does not constitute a recommendation or an endorsement of its use by the author(s), their institution or any person connected with preparation, publication or distribution of this Journal.

ISSN 1406-894X

CONTENTS

Agronomy Research **22**(1), 5–15, 2024
https://doi.org/10.15159/AR.24.003

Mathematical model for detecting tomato ripeness using chlorophyll fluorescence

M.A. Abdelhamid[1,*], S.A. Rawdhan[2], S.S. Shalaby[1] and M.F. Atia[1]

[1]Ain Shams University, Faculty of Agriculture, Department of Agricultural Engineering, 11241 Egypt
[2]University of Baghdad, Department of Agricultural Machines and Equipment, College of Agricultural Engineering Sciences, 47040 Iraq
[*]Correspondence: mahmoudabdelhamid@agr.asu.edu.eg

Received: October 25th, 2023; Accepted: December 12th, 2023; Published: January 18th, 2024

Abstract. A precise assessment of tomato ripeness is crucial in the harvesting and marketing procedures. Chlorophyll fluorescence is being relied on as a harmless approach for tracking the maturity of tomatoes in postharvest research. In this study, mathematical model is proposed based on measuring the intensity of fast chlorophyll fluorescence of tomatoes depending on their degree of maturity. In the experimental study, four stages of tomato ripening (green, turning, pink, and red) for three varieties ('Alkazar', 'Lezginka', and 'Rosanchik') were used. The Fluorescence Intensity (FI) data over time were represented using a third-degree polynomial function and finding its first derivative curve. The FI parameter was obtained as the fluorescence level at the first inflection point on the fluorescence induction curve (at time t_I on the first derivative curve). According to the obtained mathematical models, the optimal time for monitoring the degree of ripeness of tomatoes was $t_I = 129 \pm 4$ ms. According to the results of experimental studies, there is a general trend, regardless of the variety used, that the FI decreases with tomato maturity. The FI may assist in sorting and grading processes for fresh vegetables and fruits. It can also be used as a system that can be integrated into harvest and post-harvest machinery for agricultural products.

Key words: tomato, model, maturity stage, fast chlorophyll fluorescence.

INTRODUCTION

Tomatoes are sensitive fruits that need to be transported swiftly to the market if they are mature or shipped if they have not reached one of the other maturing phases. As a result, determining the optimal ripeness is critical to maintaining its texture, aroma, and nutrient content. Tomato fruit sorting and postharvest maturing tracking according to fruit maturity levels at harvest are required to ensure the maximum possible quality and ability to sell the fully matured product (Kasampalis et al., 2020). Yet, large-scale measures are inapplicable when using destructive methods. The physical characteristics of tomatoes can be most frequently defined through the quality parameters, including

degree of maturity (Vursavus & Kesilmis, 2016). Human labor is also highly used in fruit crop sorting (Guann., et al., 2022; Wang et al., 2022). In the past few decades, as urbanization has expanded and agricultural labor has become more and more scarce, laborious sorting and classification methods have become progressively costly and fail to meet market needs (Zhou et al., 2018; Bai et al., 2022; Rong et al., 2022; Yang et al., 2023). Recent years have seen attempts to control fruit quality using non-destructive technologies, particularly imaging techniques like thermal, infrared thermography, and microwave imaging; spectral analysis techniques like Raman and hyperspectral image analysis, fluorescent visualizing, and laser light backscatter imaging; nuclear magnetic techniques and other approaches (Avotins et al., 2020).

Tomato ripening includes multiple physiological processes, including the decomposition of chlorophyll and an increase in carotenoids, resulting in higher levels of beta-carotene and lycopene, which are the cause of tomatoes' antioxidant benefits. As tomatoes mature, their chlorophyll content reduces, but their carotenoid content rises until they reach full ripeness (Fraser et al., 2007). Tomatoes are among the world's most desirable fruits due to their wide range of uses in cuisine. Tomatoes are not just tasty, but their high carotene content is commonly recognized. Non-destructive testing procedures are becoming more popular in a variety of industries (Alsiņa et al., 2019). Tomato ripening consists of different changes in fruit color produced by biochemical processes in the fruit's tissues. During the early stages of ripening, the tomato fruit has a significant amount of the green pigment chlorophyll in cells called chloroplasts. During growth, the chloroplast of green tomatoes starts to separate into chromoplasts, which commence the breakdown of chlorophyll to tetrapyrroles, permitting the exposure or release of red pigments called carotenoids, which are also contained in the chloroplast (Wold et al., 2004; Klee & Giovanni, 2011; Saad et al., 2016). Therefore, a fluorescence method was used during different stages of tomato maturity.

The fluorescence of chlorophyll corresponds strongly with the amount of light taken up by cell pigments. The majority of the energy absorbed by light is used for photosynthesis, while one portion disappears as heat, and only a small amount is released as fluorescent light shortly after the charged electron goes to its fundamental state (Maxwell & Johnson, 2000). Among the postharvest techniques accessible, chlorophyll fluorescence has been examined as a useful tool for evaluating the maturation and aging of green cells, used in both green leaves and many pigment-containing fruits (Song et al., 1997). Chlorophyll fluorescence in mature or aged fruit is affected by chlorophyll concentration and chlorophyll's activities. The decrease in fluorescence of chlorophyll throughout the banana and maturation was correlated with chlorophyll concentration and chloroplast ability loss. Maturity is characterized by a rise in cell membrane decomposition (Smillie, 1978), which results in chloroplast aging, a process in which cells degrade their physical integrity, decreasing photosynthetic activity, and, as a result, modifying fluorescence characteristics (Sanxter, 1992; Tucker, 1993).

After illumination, the fluorescence of chlorophyll starts and maintains a characteristic pattern known as the 'Kautsky curve', fluorescence transient, OJIP transient, or OJIP-test. This curve contains four separate phases (O, J, I, and P) and depends on the thylakoid membrane 'energy flow' hypothesis (Strasser et al., 2000). Furthermore, the OJIP method includes variables related to quantum yields, energy changes, and essential values determined and measured. The OJIP test has already been utilized to examine a variety of environmental conditions, including dehydration and

chilling challenges, along with basic temperature impacts, nutritional shortages, and toxic metal loads (Kalaji et al., 2016). Changes in chlorophyll fluorescence can be used to detect changes in photosynthesis. Fig. 1 shows the kinetics of chlorophyll fluorescence in all photosynthetic content which shows an increase in heterogeneity over time and is characterized by four typical steps: the first rise from the origin (O) at 20 s or 50 s, followed by an intermediate state at 2 ms (J step), then a second slower rise involving a second intermediate step at 30 ms (I step), followed by the P step, where maximum fluorescence occurs (Liu et al., 2021).

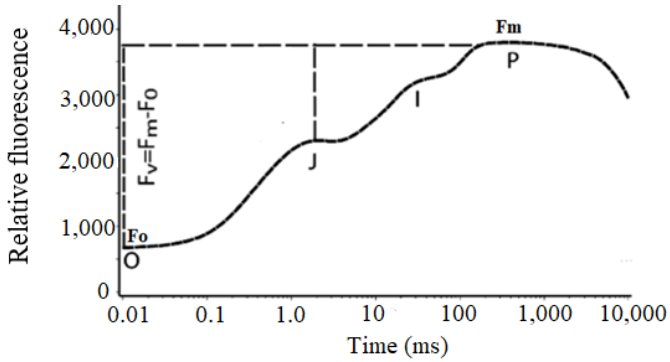

Figure 1. The standard Kautsky curve. Fo represents the initial degree of fluorescence upon illumination. Fm stands for maximum fluorescence, which is the highest level of fluorescence achieved following illumination. Fv stands for variable fluorescence, and it is calculated by subtracting the Fo value from the Fm value (Kargar et al., 2019).

Chlorophyll fluorescence technology is a valuable tool for non-destructive analysis to classify tomato fruit maturity stages (Kasampalis et al., 2020; Abdelhamid et al., 2021). According to the literature, maximum chlorophyll fluorescence (Fm) has been utilized as a non-destructive technique for measuring fruit ripening in postharvest research. In this study aims to propose mathematical model based on chlorophyll fluorescence measurement that can distinguish and classify tomato fruits.

MATERIALS AND METHODS

Tomato samples

For this research, three tomato varieties were chosen: (i) 'Alkazar', (ii) 'Lezginka', and (iii) 'Rosanchik'. Four phases of maturation were used for each variety (green, turning, pink, and red). 100 samples of each variety were chosen at random, 25 for each degree of ripeness. This study was conducted on defect-free tomatoes. Samples of tomatoes were obtained from the greenhouse at the Russian State Agricultural Academy named after K. A. Timiryazev, Russia and they were taken to the laboratory for fluorescence testing after being picked. Within half an hour, all fruits were brought to the laboratory in open boxes of cartons for assessments.

Measurements of chlorophyll fluorescence

The fluorescence emitted for each sample was monitored separately at the four distinct maturity stages of all three varieties under study in order to determine the level of maturity of tomatoes based on chlorophyll fluorescence induction. Fluorescence was recorded at two diametrically opposed locations at the fruit's equator at various ripening phases. A silicon photodiode sensor and a blue light emitting diode (5 W) were used in the fluorimeter to record the fast chlorophyll fluorescence induction curves over a time range of 0.01 ms to 1 s. This allowed for the computational recording of the transitory fluorescence. The blue light (455 nm; 5,000 μmol quanta m^{-2} s^{-1}; 1 s duration) saturating pulse from the light-emitting diode was used to measure the maximum fluorescence (Fm) for the dark-adapted condition. For further information, refer to (Kreslavski et al., 2014). The signal was captured every 10 μs during 1 ms and every 1 ms beginning from 1 ms up to 1 s during data collecting. After the signal was smoothed, it was transferred from the silicon photodiode to the computer for further processing. The fluorescence induction curve illustrates variations in chlorophyll emitted by fluorescence in a photosynthetic item. It can be separated into two phases, each lasting about a second. This fast phase involves photosynthetic light-phase processes. The slow phase, on the other hand, may last for minutes.

Model Fitting

For data analysis, the time was the independent variable, and chlorophyll fluorescence was the dependent variable based on the 'Kautsky curve'. As a result, the suggested generalized model may be written as follows:

$$\mathrm{FI} \sim f\,\mathrm{Time} \quad (1)$$

The data values were fitted with multiple alternative models from several types of fit (polynomial, exponential, linear, power, and logarithmic) to identify the most appropriate relation of FI over time and the degree of confidence of the fit statistics of these models were obtained using 'Mathematica v.12'. The most accurate model within the fitted models was a third-order polynomial correlation between the intensity of fluorescence over time, as shown below:

$$FI = a_3\,t^3 - a_2\,t^2 + a_1\,t + c, \text{ at } 0 \le t < 250 \text{ ms.} \quad (2)$$

where, *FI*: chlorophyll fluorescence intensity, rel. units and *t*: time, ms.

The initial inductive curve was used to derive the first derivative. The *FI* was then approximated as the fluorescence level at the first bend point on the fluorescence induction curve (at time t_I on the first derivative curve). Calculating the second derivatives of the fluorescence induction curve d^2FI/dt^2 yielded the time at the first bending point that defines the fluorescence induction curve (t_I). Then, solve d^2FI/dt^2 = zero to determine the precise period at which the fluorescence induction curve first inverts. At the time, the FI was calculated for each level of maturity of the tomato cultivars under study.

RESULTS AND DISCUSSION

Changes in chlorophyll fluorescence during ripening of tomato fruits

Figs 2–4 show the chlorophyll fluorescence intensity *FI* and their first derivatives (*dFI* / *dt*) dependencies versus time for the 'Alkazar', 'Lezginka', and 'Rosanchik'

cultivars. Figs 2–4 demonstrate that the *FI* increases with time until a specific point (*I*), at which point the curve trend begins to change direction for a reasonably short period and then begins to rise again. The first differential curve of the original chlorophyll fluorescence curve, on the other hand, begins with its maximum value and then begins to drop with time to its lowest value at the point corresponding to point (*I*) on the original fluorescence induction curve. Following that, it begins to rise for a relatively brief amount of time until it reaches its higher values. Then it appeared to fall again.

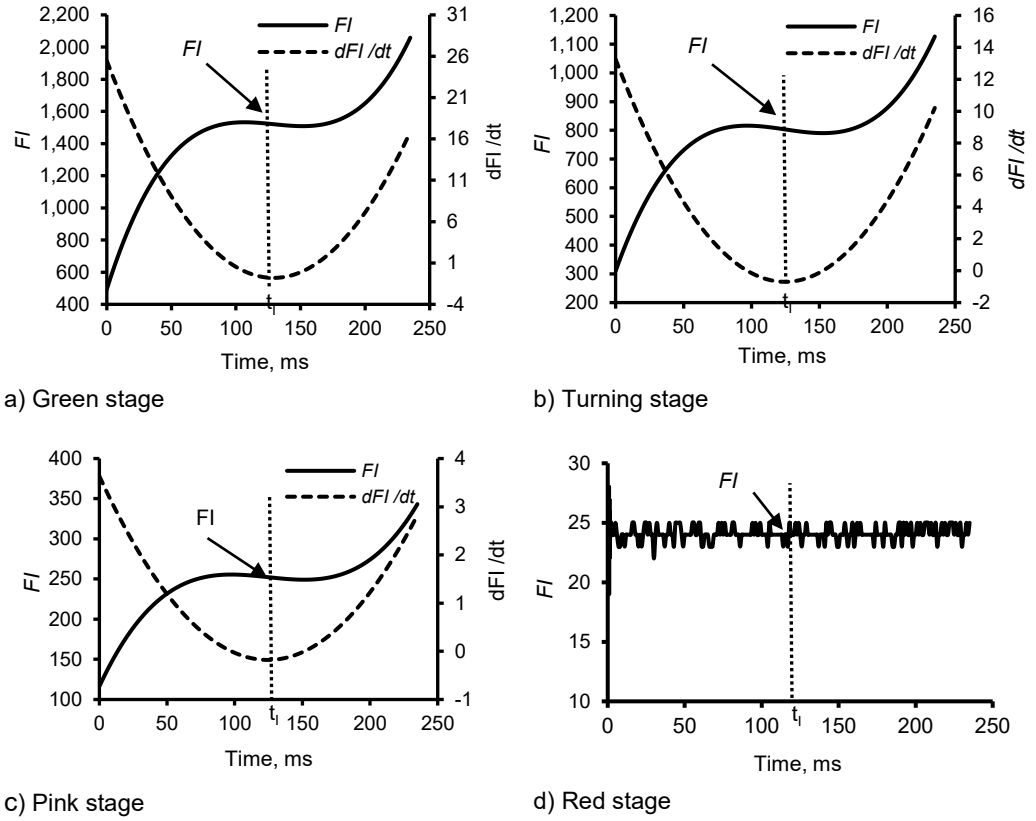

Figure 2. Curves of the fluorescence dependencies of chlorophyll (*FI*) and their first derivatives (*dFI* / *dt*) over time for the 'Alkazar' variety for different degrees of ripeness.

A more recent approach is to find the FI parameter using the first derivative. According to the figures, the *FI* value is equal to the signal level at the short-term deceleration point of the fluorescence induction curve's first inflection point. This is the first minimum of time tI on the first derivative curve of the original fluorescence induction curve. Figures reveal that at various stages of maturation, the first inflection point in the fluorescence induction curve occurs with an average duration of 129 ± 4 ms. The dependence is stationary for red tomatoes (Figs 2, d; 3, d, and 4, d) and varies insignificantly (in magnitude) with time.

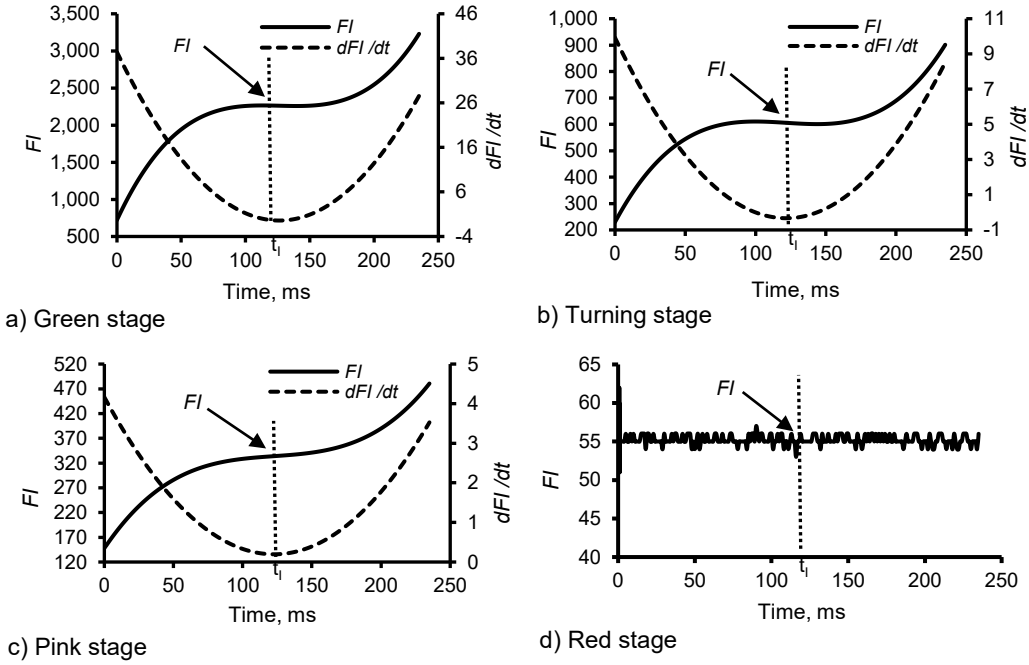

Figure 3. Curves of the fluorescence dependencies of chlorophyll (*FI*) and their first derivatives (*dFI / dt*) over time for the ‘Lezginka’ variety for different degrees of ripeness.

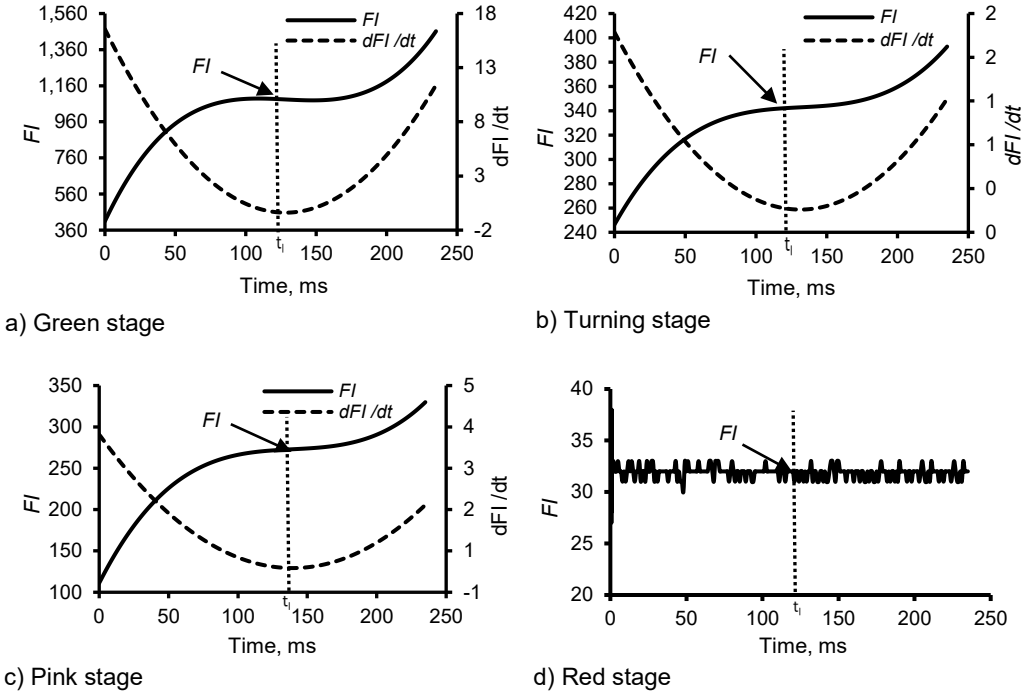

Figure 4. Curves of the fluorescence dependencies of chlorophyll (*FI*) and their first derivatives (*dFI / dt*) over time for the ‘Rosanchik’ variety for different degrees of ripeness.

Development of mathematical models

Table 1 shows the calculated time t_I at the first inflection point of the chlorophyll fluorescence intensity curve (the shortest period for operational control of the degree of ripeness of tomatoes), which was derived by calculating its second derivative (in this case, $d^2FI/dt^2 = 0$), as well as the determined time t_I at the second curvature point of the chlorophyll fluorescence intensity curve (the minimum time for operational control of the degree of ripeness).

Table 1. Mathematical models of chlorophyll fluorescence curves of 'Alkazar', 'Lezginka', and 'Rosanchik' varieties with different degrees of maturity

Tomato variety	Degree of ripeness	Equations of mathematical models
Alkazar	Green	$FI = 0.000525\ t^3 - 0.2033\ t^2 + 25.45\ t + 494$ $dFI/dt = 0.001574\ t^2 - 0.4066\ t + 25.45$ $d^2FI/dt^2 = 0.003149\ t - 0.4066$ (t_I=129 ms)
	Turning	$FI = 0.000299\ t^3 - 0.1119\ t^2 + 13.26\ t + 309$ $dFI/dt = 0.000897\ t^2 - 0.2237\ t + 13.26$ $d^2FI/dt^2 = 0.001793\ t - 0.2237$ (t_I=124 ms)
	Pink	$FI = 0.000082\ t^3 - 0.0306\ t^2 + 3.64\ t + 116$ $dFI/dt = 0.000246\ t^2 - 0.0613\ t + 3.64$ $d^2FI/dt^2 = 0.000492\ t - 0.0613$ (t_I=124 ms)
	Red	$FI = 24 \pm 5$
Lezginka	Green	$FI = 0.000790\ t^3 - 0.2994\ t^2 + 37.40\ t + 721$ $dFI/dt = 0.002370\ t^2 - 0.5989\ t + 37.40$ $d^2FI/dt^2 = 0.004741\ t - 0.5989$ (t_I=126 ms)
	Turning	$FI = 0.000230\ t^3 - 0.0842\ t^2 + 9.92\ t + 229$ $dFI/dt = 0.000691\ t^2 - 0.1684\ t + 9.92$ $d^2FI/dt^2 = 0.001381\ t - 0.1684$ (t_I=122 ms)
	Pink	$FI = 0.000088\ t^3 - 0.032369\ t^2 + 4.16\ t + 147$ $dFI/dt = 0.000264\ t^2 - 0.0647\ t + 4.16$ $d^2FI/dt^2 = 0.000528\ t - 0.0647$ (t_I=122 ms)
	Red	$FI = 55 \pm 5$
Rosanchik	Green	$FI = 0.000344\ t^3 - 0.1322\ t^2 + 16.56\ t + 409$ $dFI/dt = 0.001032\ t^2 - 0.2645\ t + 16.56$ $d^2FI/dt^2 = 0.002063\ t - 0.2645$ (t_I=128 ms)
	Turning	$FI = 0.000039\ t^3 - 0.0154\ t^2 + 2.09\ t + 246$ $dFI/dt = 0.000118\ t^2 - 0.0309\ t + 2.09$ $d^2FI/dt^2 = 0.000235\ t - 0.0309$ (t_I=131 ms)
	Pink	$FI = 0.000055\ t^3 - 0.0232\ t^2 + 3.32\ t + 111$ $dFI/dt = 0.000167\ t^2 - 0.0464\ t + 3.32$ $d^2FI/dt^2 = 0.000333\ t - 0.0464$ (t_I=139 ms)
	Red	$FI = 33 \pm 5$

The mathematical models have been created based on the findings of experimental studies in which tabular data was obtained and related curves were constructed for the time dependences of the chlorophyll fluorescence intensity (*FI*) and its first derivatives (*dFI /dt*) for the tomato variety 'Alkazar', 'Lezginka' and 'Rosanchik' and its four stages of maturity (green, turning, pink, and red).

Effect of chlorophyll on fluorescence induction

Fig. 5 shows that during the green ripening stage, tomatoes have maximum fluorescence intensity values which gradually decrease as the fruits mature. On the contrary, fully ripe tomatoes had the lowest levels of fluorescence intensity. A general trend was observed, during tomato ripening the fluorescence intensity decreases. When fruits ripen, the color of the skin changes due to the decomposition of chlorophyll. This occurs when the color of the fruit turns from green to yellow or red and causes the green spots to disappear (Bramley, 2002). This reduction in fluorescence intensity could be utilized to determine tomato maturity. Many recent investigations showed that excitation-based chlorophyll fluorescence indices applying various wavelengths may estimate grape fruit quality (Agati et al., 2013) apples (Seifert et al., 2014) and tomatoes (Abdelhamid et al., 2020). Chlorophyll fluorescence induction has been used in a number of recent research to classify tomato fruit ripening phases (Hoffmann et al., 2015, Fatchurrahman et al., 2020; Abdelhamid et al., 2021). During the ripening, changes in the fruit's pigment distribution and composition had varying effects on fluorescence. Identifying red or far-red fluorescence by combining several excitation lamps allowed for the observation and definition of distinctive maturation curve patterns. The light absorption spectrum undergoes a major change when the green to red maturation stage is reached (Qin & Lu, 2008). The breakdown of chlorophyll results in a decrease in fluorescence emission. Carotenoids are synthesized in tandem with the breakdown of chlorophyll when chloroplasts transform into chromoplasts, initially in the fruit's core and subsequently in the pericarp (Bramley, 2002). The most reliable indicator of this decline in chlorophyll content is the FI index, which also exhibits high connections with the ripening stage. Thus, fluorescence measurements can be taken as a useful tool for assessing the general state of a fruit and its maturity at various stages. Furthermore, as with apples (Betemps et al., 2012), significant fruit quality attributes might be assessed using this technique. The fluorescence approach could be used to precisely define the optimal harvest time or as a robust tool for fruit categorization in high-speed sorting processes.

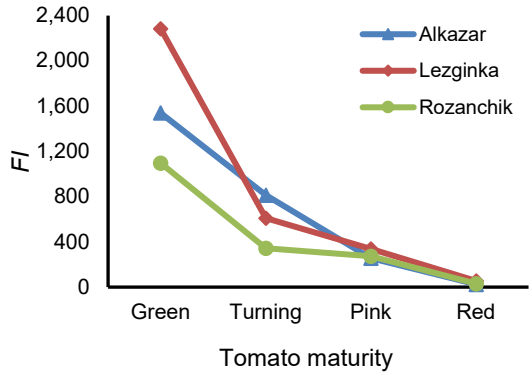

Figure 5. Relationship between *FI* and the degree of maturity for 'Alkazar', 'Lezginka' and 'Rozanchik' varieties.

CONCLUSION

This study investigated the ability to classify the degree of ripeness of tomato fruits using fast fluorescence intensity. The results showed that during the maturity stages, the fluorescence intensity decreases. Mathematical models of chlorophyll fluorescence levels in tomatoes based on ripeness are defined by third-order polynomials. The results indicated that according to the mathematical models obtained, the optimal time to

monitor the degree of tomato maturity was $t_I = 129 \pm 4$ ms. The proposed mathematical models can be used in sorting and grading operations for fresh vegetables and fruits. It can also be used as a system that can be integrated into harvesting and post-harvesting machinery for agricultural products.

REFERENCES

Abdelhamid, M.A., Sudnik, Y.A., Alshinayyin, H.J. & Shaaban, F. 2020. Chlorophyll fluorescence for classification of tomato fruits by their maturity stage. *E3S Web Conf*. **193**, 01065. doi:10.1051/e3sconf/202019301065

Abdelhamid, M.A., Sudnik, Y., Alshinayyin, H.J. & Shaaban, F. 2021. Non-destructive method for monitoring tomato ripening based on chlorophyll fluorescence induction. *Journal of Agriculture Engineering* **52**, 1–7. doi.org/10.4081/jae.2020.1098

Agati, G., D'Onofrio, C., Ducci, E., Cuzzola, A., Remorini, D. & Tuccio, L. 2013. Potential of a multiparametric optical sensor for determining in situ the maturity components of red and white Vitis vinifera wine grapes. *J. Agric. Food Chem.* **61**, 12211–8.

Alsiņa, I., Dubova, L., Dūma, M., Erdberga, I., Avotiņš, A. & Rakutko, S. 2019. Comparison of Lycopene and β-carotene Content in Tomatoes Determined with Chemical and Non- destructive Methods. *Agronomy Research* **17**(2), 343–348. doi:10.15159/AR.19.085

Avotins, A., Kviesis, K., Bicans, J., Alsina, I. & Dubova, L. 2020. Experimental Analysis of IoT Based Camera SI-NDVI Values for Tomato Plant Health Monitoring Application. *Agronomy Research* **18**(S2), 1138–1146. doi.org/10.15159/AR.20.087

Bai, Y., Mao, S., Zhou, J. & Zhang, B. 2022. Clustered tomato detection and picking point location using machine learning-aided image analysis for automatic robotic harvesting. *Precision Agriculture* **24**, p.727–743. doi:10.1007/s11119-022-09972-6

Betemps, D.L., Fachinello, J.C., Galarça, S.P., Portela, N.M., Remorini, D., Massai, R. & Agati, G. 2012. Non-destructive evaluation of ripening and quality traits in apples using a multiparametric fluorescence sensor. *Journal of the Science of Food and Agriculture* **92**(9), 1855–1864.

Bramley, P.M. 2002. Regulation of carotenoid formation during tomato fruit ripening and development. *Journal of Experimental Botany* **53**, 2107–2113. doi.org/10.1093/jxb/erf059

Fatchurrahman, D., Amodio, M.L., Chiara, M.L.V.D., Chaudhry, M.M.A. & Colelli, G. 2020. Early discrimination of mature and immature green tomatoes (Solanum lycopersicum *L.*) using fluorescen imaging method. *Postharvest Biol. Technol*. **169**, 111287.

Fraser, P.D., Enfissi, E.M., Halket, J.M., Truesdale, M.R., Yu, D., Gerrish, C. & Bramley, P.M. 2007. Manipulation of phytoene levels in tomato fruit: effects on isoprenoids plastids and intermediary metabolism. *Plant Cell.* **19**(10), 3194– 211.doi.org/10.1105/tpc.106.049817

Guan, Z., Li, H., Zuo, Z. & Libo, P. 2022. Design a Robot System for Tomato Picking Based on YOLO v5. In Proceedings of the 16th IFAC Symposium on Large Scale Complex Systems Theory and Applications (LSS). Xi'an.China. v.55 p. 166–171. doi.org/10.1016/j.ifacol.2022.05.029

Hoffmann, A.M., Noga, G. & Hunsche, M. 2015. Fluorescence indices for monitoring the ripening of tomatoes in pre- and postharvest phases. *Sci. Hortic*. **191**, 74–81.

Kargar, M., Ghorbani, R., Rashed Mohassel, M.H. & Rastgoo, M. 2019. Chlorophyll fluorescence-A tool for quick identification of accase and als inhibitor herbicides performance. *Planta Daninha* **37**.

Kasampalis, D.S., Tsouvaltzis, P. & Siomos, A.S. 2020. Chlorophyll fluorescence. non- photochemical quenching and light harvesting complex as alternatives to color measurement. in classifying tomato fruit according to their maturity stage at harvest and in monitoring postharvest ripening during storage. *Postharvest Biology and Technology* **161**, 111036. https://doi.org/10.1016/j.postharvbio.2019.111036

Kalaji, H.M., Jajoo, A., Oukarroum, A., Brestic, M., Zivcak, M., Samborska, I.A., Cetner, M.D., Łukasik, I., Goltsev, V. & Ladle, R.J. 2016. Chlorophyll *a* fluorescence as a tool to monitor physiological status of plants under abiotic stress conditions. *Acta Physiol Plant* **38**. 102. doi:10.1007/s11738-016-2113-y

Klee, H.J. & Giovannoni, J.J. 2011. Genetics and control of tomato fruit ripening and quality attributes. *Annual review of genetics* **45**, 41–59. doi.org/10.1146/annurev-genet- 110410-132507

Kreslavski, V.D., Lankin, A.V., Vasilyeva, G.K., Luybimov, V.Y., Semenova, G.N., Schmitt, F.-J., Friedrich, T. & Allakhverdiev, S.I. 2014. Effects of polyaromatic hydrocarbons on photosystem II activity in pea leaves. *Plant Physiology and Biochemistry* **81**, 135–142. doi: 10.1016/j.plaphy.2014.02.020

Liu, X., Lv, Y., Song, G. & Xu, K. 2021. Ofloxacin induces etiolation in Welsh onion leaves. *Chemosphere* **267**, 128918. doi.org/10.1016/j.chemosphere.2020.128918

Maxwell, K. & Johnson, G.N., 2000. Chlorophyll fluorescence - a practical guide. *Journal of experimental botany* **51**, 659–668. doi.org/10.1093/jexbot/51.345.659

Qin, J. & Lu, R. 2008. Measurement of the optical properties of fruits and vegetables using spatially resolved hyperspectral diffuse reflectance imaging technique. *Postharvest Biology and Technology* **49**(3), 355–365.

Rong, J., Wang, P., Wang, T., Hu, L. & Yuan, T. 2022. Fruit pose recognition and directional orderly grasping strategies for tomato harvesting robots. *Computers and Electronics in Agriculture* **202**, 14 pp. doi.org/10.1016/j.compag.2022.107430

Saad, A., Jha, S.N., Jaiswal, P., Srivastava, N. & Helyes, L. 2016. Non-destructive quality monitoring of stored tomatoes using VIS-NIR spectroscopy. *Engineering in agriculture environment and food* **9**, 158–164. doi.org/10.1016/j.eaef.2015.10.004

Sanxter, S.S., Yamamoto, H.Y., Fisher, D.G. & Chan Jr, H.T., 1992. Development and decline of chloroplasts in exocarp of Carica papaya. *Canadian journal of botany* **70**, 364–373. doi:10.1139/b92-049

Seifert, B., Pflanz, M. & Zude, M. 2014. Spectral shift as advanced index for fruit chlorophyll breakdown. *Food Bioproc. Technol.* **7**, 2050-9.

Smillie, R.M. 1987. Application of chlorophyll fluorescence to the postharvest physiology and storage of mango and banana fruit and the chilling tolerance of mango cultivars. *Asian Food J.* **3**, 55–59. https://publications.csiro.au/rpr/pub?list=BRO&pid=procite:f6096c5d-f78a-448e-9c73-3e6b905a0057

Song, J., Deng, W., Beaudry, R.M. & Armstrong, P.R. 1997. Changes in chlorophyll fluorescence of apple fruit during maturation. ripening. and senescence. *HortScience* **32**, 891–896. doi:10.21273/HORTSCI.32.5.891

Strasser, R.J., Srivastava, A. & Tsimilli-Michael, M. 2000. The flouresence transient as atool to characterize and screen photosynthetic samples. In: Yunus M.. Pathre U.. Mohanty P. (ed.): *Probing Photosynthesis: Mechanisms. Regulation and Adaptation*. Taylor and Francis. London, pp. 445–483.

Tucker, G. 1993. *Biochemistry of Fruit Ripening*. Introduction en Seymour GB. Taylor, J.E. and Tucker, G.A. (Eds.). Chapman & Hall. Londres, pp. 1–51. https://link.springer.com/book/10.1007/978-94-011-1584-1

Vursavus, K.K. & Kesilmis, Z. 2016. Modeling of impact parameters for non-destructive evaluation of firmness of greenhouse tomatoes. *Agronomy Research* **14**(S2), 1498–1508. doi: 10.13140/RG.2.1.2857.9448

Wang, Z., Xun, Y., Wang, Y. & Yang, Q. 2022. Review of smart robots for fruit and vegetable picking in agriculture. *International Journal of Agriculture and Biological Engineering* **15**, 33–54.

Wold, A., Rosenfeld, H., Baugerød, H. & Blomhoff, R. 2004. The effect of fertilization on antioxidant activity and chemical composition of tomato cultivars (Lycopersicon esculentum Mill.). *European journal of horticultural science* **69**, 167–174. https://www.pubhort.org/ejhs/2004/file_15106.pdf

Yang, Z., Amin, A., Zhang, Y., Wang, X., Chen, G., Abdelhamid, M.A. 2023. Design of a Tomato Sorting Device Based on the Multisine-FSR Composite Measurement. *Agronomy* **13**, 1778. doi.org/10.3390/agronomy13071778

Zhou, T., Zhang, D., Zhou, M., Xi, H. & Chen, X. 2018. System Design of Tomatoes Harvesting Robot Based on Binocular Vision. In *Proceedings of the Chinese Automation Congress (CAC)*. Xi'an. China, pp. 1114–1118. 2018. doi: 10.1109/CAC.2018.8623150

Agronomy Research **22**(1), 16–32, 2024
https://doi.org/10.15159/AR.24.002

Water deficit stress alleviation by bio-formulated native mycorrhizal species for wheat grown in a saline calcareous soil

Z.A. Abdel-Salam[1,*], M.A. Abouzeid[2], M.M. El-Shazly[1] and D.A.M. Abdou[2]

[1]Department of Soil Fertility and Microbiology, Desert Research Center, Cairo, Egypt
[2]Department of Microbiology, Faculty of Science, Ain Shams University, Cairo, Egypt
[*]Correspondence: zenabahmed5@gmail.com

Received: August 7th, 2023; Accepted: January 12th, 2024; Published: January 18th, 2024

Abstract. Arbuscular mycorrhizal fungi (AMF) are a genus of obligatory root biotrophs that can develop mutualistic symbioses with most terrestrial plants. This study aimed to investigate the impact of three different isolates of AMF (*Acaulospora spinosa* [M1], *Glomus ambisporum* [M2], and *Scutellospora heterogama* [M3]) isolated from native environments and three carriers (biochar, alginate, and polyacrylate) on wheat (*Triticum aestivum* L.) grown in a saline calcareous soil in conditions of water deficit. In a pot experiment, reduced amounts of water were applied at intervals of 4, 8, and 12 days, while in a field experiment, the intervals were 1, 2, and 3 weeks (W1, W2, and W3). By analyzing the chlorophyll index and dry weight data from the pot experiment, it was revealed that two AMF isolates (M1 and M2), along with two carriers (biochar and alginate), showed promising results in stimulating wheat growth. Based on these findings, a field validation experiment was conducted to further evaluate the effects of these isolates and carriers. The wheat plants subjected to water deficit stress exhibited improved vegetation characteristics, grain yield, nutrient uptake, and colonization percentage when treated with the AMF isolate M2 formulated on biochar. For instance, under W2 conditions without any mycorrhiza or carrier, the grain yield was recorded at 6,600 kg ha^{-1}. However, with the inoculation of M2-biochar at the same W2 level, the yield significantly increased to 9110 kg ha^{-1}. The study concluded that AMF formulated on biochar outperformed other carriers, leading to enhanced wheat growth under water stress conditions.

Key words: drought stress, arbuscular mycorrhizal fungi, biocompatible carriers, biochar, alginate, wheat yield.

INTRODUCTION

Wheat (*Triticum aestivum* L.) serves as a staple food worldwide, providing sustenance for approximately one-third of the global population (Acevedo et al., 2018; Grote et al., 2021). However, the occurrence of drought has a significant impact on wheat production, leading to severe consequences for both global food security and economic stability (Daryanto et al., 2016; Leng & Hall, 2019; Pequeno et al., 2021). The growth and development of wheat plants are intricately linked to the availability of water, as it plays a crucial role in various physiological processes such as photosynthesis, nutrient uptake, and protein synthesis (Torrion & Stougaard 2017; Plett et al., 2020). When wheat

plants are exposed to prolonged drought conditions, they experience a range of detrimental effects, including reduced leaf area, impaired stomatal conductance, diminished photosynthetic activity, and altered carbohydrate metabolism (Lonbani & Arzani, 2011; Ahmad et al., 2018; Zhang et al., 2018; Pour-Aboughadareh et al., 2020). Consequently, these stress-induced changes lead to decreased yield and compromised grain quality, posing substantial challenges for farmers and food systems worldwide.

Microbial interactions with plants play a crucial role in our ecosystem. These interactions, as highlighted by Barea et al. (2005) and acknowledged by numerous scientists, can provide valuable support to crop plants during periods of acute stress. One promising approach to enhance plant adaptation strategies involves increasing the presence of arbuscular mycorrhizal fungi (AMF) in soils (Plouznikoff et al., 2016; Diagne et al., 2020). AMF, when established in root cortical cells, actively participate in nutrient exchange, leading to improved plant growth and productivity (Park et al., 2015; Heydarian et al., 2018; Bhantana et al., 2021). Moreover, AMF can mitigate the negative effects of drought by reducing water and nutrient loss, thereby sustaining plant growth and restoring leaf moisture levels (Borriello et al., 2012; Bahadur et al., 2019). The most important mechanisms by which symbiosis can alleviate drought stress in host plants are direct water uptake through the fungal hyphae, changes in soil water holding properties, better osmotic adjustment of plants, enhancement of water-use efficiency, and protection against oxidative damage caused by severe water deficiency (Barea et al., 2011; Ruiz-Lozano et al., 2011; Borde et al., 2017).

Due to environmental limitations and the challenges posed by the short shelf life of inoculum, the adoption of bio-fertilizers by farmers has been relatively low compared to other methods. Consequently, the utilization of specific materials, known as carriers, becomes crucial in facilitating microbial growth and ensuring effective delivery to the rhizosphere (Zafar-ul-Hye et al., 2019). These carriers can be derived from either organic sources such as compost, crushed corn, peat biochar, or inorganic sources like lignite (Zafar-ul-Hye et al., 2019). However, it is imperative that these carrier materials possess certain characteristics. They should be readily available, cost-effective, physically and chemically stable, non-toxic to plant growth-promoting microbes, biodegradable, free from pollutants, and easy to process (Pacheco-Aguirre et al., 2017; Moghadam et al., 2018; Sohaib et al., 2020). To maintain the efficacy of AMF in the field, gel encapsulation techniques have been employed to preserve the isolated vesicles, internal hyphae, or spores of AMF. These techniques have proven effective in enabling AMF to renew hyphae even under adverse conditions (Herrmann & Lesueur, 2013; Pitaktamrong et al., 2018).

Only a limited number of studies have conducted pairwise comparisons between various encapsulation methods. Among these studies, the effects of AMF inoculation in soil, both with and without Na-alginate encapsulated AMF, have been extensively surveyed (Schütz et al., 2018; Basiru et al., 2020). However, there is currently a dearth of information regarding the impact of biochar on soil microbial communities, despite its known role in enhancing soil fertility (Lehmann et al., 2011). The objectives of this study were to investigate the effects of three native AMF isolated from abiotic environments on the growth rate and production of wheat in saline calcareous soils under water deficit conditions. This was accomplished by manipulating irrigation intervals and reducing water amounts. Furthermore, the study aimed to assess the influence of three different carriers (biochar, alginate, and polyacrylate) on the performance of drought-

stressed wheat plants. These carriers were chosen based on their potential to improve water retention and nutrient availability in the soil.

MATERIALS AND METHODS

Isolation and purification of mycorrhizal spores

Soil samples were gathered from the root zones of indigenous plants that thrive in the harshest conditions found across various locations in the West Delta of Egypt. These plants predominantly consisted of wild species that have flourished without any human intervention. These locations, namely El-Khatatba, South El-Tahrir, El-Bostan, North El-Tahrir, and El-Nobaria, are characterized by arid climates, where visible signs of salinization and degradation are evident. At each location, a total of five soil samples were carefully collected from a depth of 15–30 cm. These samples predominantly consisted of calcareous sandy soils with elevated salinity levels. To facilitate further analyses, the collected samples, along with the corresponding plant roots, were promptly transferred to the laboratory.

In the laboratory, sieving in wet condition and decanting technique, as described by Gerdemann & Nicolson (1963), was employed to separate the coarse particles of the soil while retaining mycorrhiza spores and organic particles on sieves of different sizes. Under a dissecting microscope (model SZX9, Olympus, Tokyo, Japan), the spores were carefully selected using a pipette. Morphological identification of the spores was conducted, including measurements of their size and thickness of wall layers, following the methodology outlined by Trappe (1982). To maintain AMF propagules (spores/hyphae/colonized root pieces), the samples taken from cultures that are in the late or stationary phase of growth have been used. These samples were mixed with alginate or biochar, and then dried out before cryopreservation for the utilization in the pot and field experiments.

Treatments and experimental design

A pot experiment consisting of three replicates was conducted in the greenhouse of the Desert Research Center in Cairo during the 2019/2020 season. The experiment followed a completely randomized design. The identified isolates were *Acaulospora spinosa* (M1), *Glomus ambisporum* (M2), and *Scutellospora heterogama* (M3). The three AMF species (M1, M2, M3) in addition to control (M4) were formulated on three different carriers, namely alginate (C1), polyacrylate (C2), biochar (C3), and soil (C4). Treatments also included three levels of irrigation (every 4, 8, and 12 days; W1, W2, and W3, respectively) in low amounts of water to induce further drought stress. For the pot experiment, large plastic polyethylene pots measuring 30 cm in diameter and 35 cm in depth were used. These pots were chosen specifically for their suitability in conducting the research. To ensure consistency, each pot was filled with 10 kg of air-dried soil obtained from the surface layer of the Mariout Research Station in the West Delta region of Egypt. This soil was carefully selected as the field experiment will be implemented in this location in the subsequent season. To sow the seeds, 15 grains of wheat from the Giza 171 variety were distributed into each pot. After a period of three weeks, the plants had grown sufficiently, and it was necessary to thin them out. Eight plants were retained in each pot, ensuring that they had the best chance of thriving and producing accurate results.

The validation field experiment was conducted at the Mariout Research Station in the West Delta region of Egypt during the 2020/2021 season. The experiment location being at altitude of 15 metres above sea level and is located in latitude 31° 0' 12.2" N and longitude 29° 47' 3.0" E. According to the FAO classification, the soil in this area is categorized as Haplic Xerosols (FAO, 1998). The average rainfall in this area during the growing season was around 140 mm $year^{-1}$, mostly in the months of December-February. The average temperature during the growing season ranged between 10 and 20 °C. The main plots were divided into three irrigation intervals: 1, 2, and 3 weeks, with reduced amounts of water. Normally, a hectare requires 5,200 m^3 of water (W1), but for the purpose of this experiment, it was limited to 3,800 m^3 for W2 and 2,800 for W3. The sub-plots were assigned to three different carriers: biochar, alginate, and a control group. The sub-sub-plots were assigned to three AMF as M1, M2, and M3 (control).

Before sowing wheat, the soil was ploughed twice, levelled, before dividing into 3×5 m plots (15 m^2 for sub-sub plots, 45 m^2 for subplots, and 135 m^2 for main plots). Wheat (Giza 171, the most often used variety in the study area) was sown in early November at a seeding rate of 155 kg ha^{-1} (15.5 gm m^{-1}) and harvested in mid-April. A total of 500 gm of beads, consisting of various carriers such as alginates, polyacrylate, and biochar, were utilized for field inoculation. Each plot was enriched with 180 entrapped propagules through the application of these beads during sowing. It is important to note that this particular wheat belongs to the spring type. In accordance with the general recommendations, P fertilizer (60 kg P_2O_5 ha^{-1} as single superphosphate) and K fertilizer (50 kg K_2O ha^{-1} as potassium sulphate) were applied. Standard techniques were applied to control weeds, insects, and diseases.

Optical sensor and chlorophyll meter measurements

The atLEAF chlorophyll meter (FT Green LLC, Wilmington, DE, USA) and the GreenSeeker optical sensor (Trimble, Sunnyvale, CA, USA) were used to measure the spectral properties of wheat leaves at the Feekes 6^{th} growth stage (stem elongation growth stage). This growth stage, which corresponds to 30 on the BBCH scale and occurs approximately 50 days after sowing, was selected based on the research conducted by Ali (2020) and Ali et al. (2021). These studies have identified this particular stage as the optimal time for gathering crucial information and making informed management decisions for wheat crops. Chlorophyll meter readings were obtained from the pot experiment, while both sensors were utilized in the field experiment to gather data. This approach was adopted because the GreenSeeker optical sensor requires canopy volume to collect data, unlike the atLEAF meter which measures readings from a specific spot on the leaf.

The atLEAF chlorophyll meter was used to assess the chlorophyll index, the meter measures light transmittance through the leaf at two different wavelengths of 660 and 940 nm to give a single indicative index. The highest fully expanded leaf was utilized to gather the atLEAF readings by inserting the middle section of the leaf into the meter's slit. Measurements were documented from 10 plants in each plot, and average values were computed. Spectral reflectance of the canopy was measured using the GreenSeeker active optical sensor and expressed as a normalized difference vegetation index (NDVI), the sensor has a red (656 nm) and near infrared (774 nm) self-illumination system. The GreenSeeker measurements were conducted by traversing the plot at an approximate

speed of 0.5 m s^{-1} while maintaining a sensor height of approximately 1 m above the canopy.

Assessment of mycorrhizal characteristics in the field experiment

At harvest, rhizosphere soil samples were collected to determine the characteristics of mycorrhizal spores. Mycorrhizal colonization was assessed using a composite root sample from three plants in the centre of each plot. Mycorrhizal colonization in roots was evaluated by washing and staining of 1-cm root segment cut from the plant. Phillips & Hayman's (1970) staining procedure was used to prepare root samples for microscopic examination.

The gridlines intersect approach developed by Giovannetti & Mosse (1980) was also used to calculate the percentage of mycorrhizal colonization. The formula used for calculating mycorrhizal colonization percentage is:

$$Colonization\ percentage = \frac{Number\ \ of\ positive\ intersect\ points}{Total\ number\ of\ observed\ intersect\ points} \times 100 \quad (1)$$

Soil and plant sampling in the field experiment

Samples from the surface layer of the experimental soil (0–30 cm depth) were collected, mixed, air dried, ground, sieved through a 2 mm sieve, and analysed for several physical and chemical properties prior to sowing, as shown in Table 1. Particle size distribution in soil samples was determined using the pipette technique (Page et al., 1982). Soil pH and electrical conductivity (EC) were measured according to Page et al., 1982. The Walkley & Black (1934) method was used to determine soil organic matter.

Soil cation exchange capacity (CEC) was determined using the ammonium acetate-saturation method (Page et al., 1982). A calcimeter was used to determine the total calcium carbonate content. Soil available N was extracted using a 2 m KCl solution, and then determined using the micro-Kjeldahl method as described by Bremner (1965). Available P and K were extracted by 1 m NH_4HCO_3 in 0.005 m DTPA adjusted to a pH of 7.6. In a spectrophotometer (Pye unican SP1900), P was colorimetrically determined using ascorbic acid and ammonium molybdate, while K was measured using a flame photometer (CL 387).

Table 1. Some physical and chemical properties of the topsoil layer (0–30 cm depth) of the experimental site

Soil characteristics	Values
Sand, %	57.2
Silt, %	26.5
Clay, %	16.3
Texture class	Sandy loam
Saturation percentage, %	35.4
Cation exchange capacity, $cmol_{(+)}$ kg^{-1}	11.5
pH*	8.43
EC**, dS m^{-1}	8.91
$CaCO_3$, %	22.4
Organic matter, %	0.94
Available N, mg kg^{-1}	62.1
Available P, mg kg^{-1}	8.9
Available K, mg kg^{-1}	218

* pH in saturated soil paste. ** Electrical conductivity in saturated soil paste extract.

Aggregate stability was determined as described by Kemper & Rosenau (1986). The soil samples were collected from each plot after harvest and air-dried before determining aggregate stability. The aggregate stability was then determined using the sieving and re-sieving in dry and wet conditions by the following equation:

$$Stable\ aggregate\ (Soil\ >\ 0.25\ mm) = \frac{Weight\ of\ stable\ soil\ aggregates}{Total\ weight\ of\ soil\ samples} \times 100 \quad (2)$$

In mid–April, when the wheat crop reached maturity, it was manually harvested from each plot's net area of 4 m^2. To separate the grains from the straw, a small thresher was used, and the resulting grains were weighed. Additionally, samples were taken for further analysis. To ensure consistency, the collected samples were dried in a hot air oven at 70 °C until they reached a consistent weight. The grain yield was adjusted to 14% moisture content per hectare for reporting. Subsequently, the samples were ground and prepared for analysis. The samples were digested in an H_2SO_4–H_2O_2 mixture, and the total N, P, and K contents were determined according to Kalra (1998). The nutrient uptake was calculated by multiplying the nutrient concentration with dry matter and dividing by 100.

Data processing

Microsoft Excel was utilized for conducting mathematical calculations. According to Gomez & Gomez (1984), the effects of treatments on the collected data were examined using analysis of variance (ANOVA). To assess the disparities between means, the Least Significant Difference (*LSD*) test was employed at a significance level of $P \leq 0.05$. The software utilized for statistical analysis in this study is Statistix 9.0.

RESULTS AND DISCUSSION

Effects of AMF and drought stress on plants in the potted plant experiment

The duration of irrigation intervals had a significant (*P*-value ≤ 0.05) effect on all measurements as shown in Table 2. For example, the chlorophyll index value in the control treatment (M4C4) in W1 (irrigation every 4 days) was 34.1, but dropped to 20.25 in W3 (irrigated every 12 days). A similar pattern was also observed in wheat dry weight. Irrigation intervals of W1, W2, and W3 resulted in dry weights of 12.2, 8.76, and 7.83 g pot^{-1}, respectively.

When different treatments (either alone or in combination) were used, significant effects on wheat parameters were recorded (Table 2). In M1, the highest chlorophyll index was observed in biochar carrier, followed by alginate, polyacrylate, then the control in W1 irrigation regime. In M2, the highest chlorophyll index was observed in alginate, followed by biochar, control and polyacrylate. The difference between biochar, control, and polyacrylate, on the other hand, is not statistically significant. In M3, the highest chlorophyll index was observed in polyacrylate, followed by biochar, alginate, and control. The differences between these carriers are not statistically significant. In M4, the highest chlorophyll index was observed in biochar, followed by control, alginate, and polyacrylate. The differences in these values are not statistically significant, with the exception of biochar and polyacrylate that indicated a significant difference.

Table 2. Effect of different AMF species bio-formulated on different carriers on chlorophyll index and dry weight of wheat in the pot experiment under different water regimes

Mycorrhizae (M)	Carrier (C)	Chlorophyll index			Dry weight (g pot^{-1})		
		Water regime*			Water regime		
		W1	W2	W3	W1	W2	W3
M1 (*Acaulospora* sp.)	Alginate (C1)	60.54	36.08	29.82	26.30	21.92	17.04
	Polyacrylate (C2)	54.52	29.97	33.93	26.97	21.52	16.12
	Biochar (C3)	69.54	33.39	27.73	29.36	25.37	19.71
	Control (C4)	34.39	34.66	29.52	18.23	17.32	14.82
M2 (*Glomus* sp.)	Alginate (C1)	50.38	37.15	31.60	26.39	21.60	14.71
	Polyacrylate (C2)	38.21	34.79	23.88	25.48	23.54	15.65
	Biochar (C3)	43.18	42.18	28.02	27.39	19.35	18.73
	Control (C4)	40.63	39.24	23.86	17.60	18.65	15.70
M3 (*Scutellospora* sp.)	Alginate (C1)	36.60	37.11	31.98	19.44	15.86	11.99
	Polyacrylate (C2)	39.86	37.28	26.11	18.47	14.97	12.16
	Biochar (C3)	38.72	41.60	36.09	21.73	16.01	14.16
	Control (C4)	36.2	41.05	35.1	15.64	13.90	9.65
M4 (No-mycorrhizae)	Alginate (C1)	33.47	33.43	23.03	15.68	13.59	10.77
	Polyacrylate (C2)	30.04	30.92	20.51	16.69	11.41	9.90
	Biochar (C3)	35.81	35.51	21.14	18.36	14.24	10.87
	Control (C4)	34.10	34.83	20.25	12.20	8.76	7.83
LSD W (P-value < 0.05)		1.68			1.04		
LSD m (P-value < 0.05)		1.21			0.65		
LSD C (P-value < 0.05)		1.33			0.62		
LSD W×M (P-value < 0.05)		2.45			1.41		
LSD W×C (P-value < 0.05)		2.5846			1.3759		
LSD M×C (P-value < 0.05)		2.6094			1.2558		
LSD M×W×C (P-value < 0.05)		5.0419			2.3808		

* The water regimes in the pot experiment were irrigation every 4 (W1), 8 (W2), and 12 (W3) days.

Pertaining to wheat dry matter, the highest values were observed in biochar carrier, followed by polyacrylate, alginate, and control in W1 irrigation regime under AMF isolate M1. For AMF isolate M2, the highest dry matter was the one observed in biochar, followed by alginate, polyacrylate and the control.

The increasing in irrigation intervals, or the wheat plants exposed to drought stress, have a significant detrimental influence on wheat growth and productivity. In the pot experiment, the performance of both biochar and alginate (carriers) was better than polyacrylate for wheat dry weight. Findings also suggest that AMF (M1 and M2) isolates were superior than M3 in the tested parameters. Data suggest that AMF isolates (M1 and M2) when using biochar and alginate as carriers gave better data in chlorophyll index values. These are in consistent with those recorded by Nirmala & Selvaraj (2011) and Pitaktamrong et al. (2018), who reported that alginate can be employed as a possible carrier of AMF, and promotes colonization, provides resilience to drought stress. Encapsulation of living cells in polymeric gels, such as alginate, is a well-established technology with a wide and expanding variety of uses (Park & Change, 2000). However, biochar can provide a safe refuge for colonizing fungal and bacterial communities, with a protection from natural soil predators (Warnock et al., 2007) and improvement of both chemical and biological soil properties (Pandian et al., 2016). Biochar with AMF is reported to improve the overall growth and plant yields (Aggangan et al., 2019).

Effect of the bio-formulated AMF on the vegetation growth and grain yield of wheat in the field experiment

Table 3 illustrates the influence of AMF, carrier, and water regime on chlorophyll index, NDVI, and grain yield of wheat in the field experiment. As expected, increase in irrigation intervals (from one week to three weeks) had a significant impact on all measured parameters. The chlorophyll index and NDVI values in the absence of AMF (control) were 34.66 and 0.41 in W1 (every week), significantly decreased to 31.65 and 0.34 in W2 (every two weeks) and 20.92 and 0.16 in W3 (every three weeks), respectively. This resulted in a significant reduction in the grain yield of wheat as well, the grain yield free of AMF was 8243 kg ha^{-1} in W1, decreased to 6,600 kg ha^{-1} in W2 and dropped to 3,390 kg ha^{-1} in W3.

The use of the two isolates of AMF along with the two types of carriers have a significant effect (P-value ≤ 0.05) on vegetation growth and grain yield of wheat (Table 3). In M1W1, the highest chlorophyll index and NDVI was observed using biochar as a carrier, followed by alginate, but they were statistically different. Grain yield took the same trend, as biochar and alginate were the statistically highest values, followed by the control. In W1M2, the chlorophyll index and NDVI were statistically higher in biochar treatment, followed by alginate, and the control.

In W2M1, the chlorophyll index and NDVI were statistically similar in biochar experiment and alginate, but higher than control. Grain yields in biochar and alginate were also statistically similar, but higher than control. In W2M2, the chlorophyll index and NDVI were statistically highest in biochar, followed by alginate, then control.

In W3M1, the chlorophyll index and NDVI in biochar and alginate were statistically similar, but higher than control. However, grain yield in all treatments were statistically similar. In W3M2, biochar gave the statistically highest chlorophyll index and NDVI, followed by alginate, and then control. However, grain yields in all treatments were statistically similar, ranging from 4,906 to 4,500 kg ha^{-1}. In W3M3, biochar and alginate gave statistically similar chlorophyll index and NDVI values, but higher than control. However, grain yields in all treatments were statistically similar, ranging from 3,686 to 3,390 kg ha^{-1}.

In the field experiment, the single effect of AMF/carrier types were examined, the average chlorophyll index and NDVI for AMF M1 were higher than others. The grain yield for M1 and M2 were nearly similar, and higher than the control. For the tested carriers, the overall average of biochar gave the statistical highest values of chlorophyll index and NDVI, followed by alginate, then the control. A similar pattern also observed on grain yield, as biochar gave the highest productivity, followed by alginate. These data emphatically reflect that AMF isolate (M2) and the carrier (biochar) may interact with better results expected.

An accurate analysis of the data revealed that the M2-biochar combination could reduce drought stress caused by irrigation intervals (1–3 weeks) on wheat grain yield. Under W2 the control (free of AMF and carrier), the grain yield was 6,600 kg ha^{-1}. Inoculation with M2-biochar at the same conditions, the value raised to 9,110 kg ha^{-1}. Following the inoculation with M2-biochar increased grain yield of 4,906 kg ha^{-1} compared with 3,390 kg ha^{-1} for the control by inoculation with M2-biochar.

Table 3. Effect of different AMF species bio-formulated on different carriers on chlorophyll index, normalized difference vegetation index (NDVI) and grain yield of wheat in the field experiment under different water regimes

Water regime (W)*	Mycorrhizae (M)	Carrier (C)	Chlorophyll index	NDVI	Grain yield (kg ha^{-1})
W1	M1 (*Acaulospora* sp.)	Alginate (C1)	56.62	0.72	9,303
		Biochar (C2)	57.58	0.79	9,600
		Control (C3)	40.48	0.46	7,623
	M2 (*Glomus* sp.)	Alginate (C1)	51.99	0.75	9,500
		Biochar (C2)	59.98	0.80	9,780
		Control (C3)	45.25	0.47	7,496
	M3 (control)	Alginate (C1)	51.52	0.50	7,956
		Biochar (C2)	52.96	0.51	8,243
		Control (C3)	34.66	0.41	7,050
W2	M1 (*Acaulospora* sp.)	Alginate (C1)	37.66	0.65	9,398
		Biochar (C2)	39.22	0.65	9,120
		Control (C3)	28.72	0.33	6,966
	M2 (*Glomus* sp.)	Alginate (C1)	37.68	0.65	8,950
		Biochar (C2)	42.94	0.70	9,110
		Control (C3)	27.65	0.29	6,776
	M3 (control)	Alginate (C1)	30.63	0.32	6,880
		Biochar (C2)	31.65	0.34	7,586
		Control (C3)	23.05	0.27	6,600
W3	M1 (*Acaulospora* sp.)	Alginate (C1)	24.31	0.23	4,956
		Biochar (C2)	25.65	0.26	4,890
		Control (C3)	21.26	0.21	4,600
	M2 (*Glomus* sp.)	Alginate (C1)	25.71	0.23	4,793
		Biochar (C2)	28.14	0.29	4,906
		Control (C3)	22.48	0.20	4,500
	M3 (control)	Alginate (C1)	22.34	0.19	3,686
		Biochar (C2)	23.98	0.20	3,540
		Control (C3)	19.92	0.16	3390
LSD W (*P*-value < 0.05)			2.61	0.0122	495.4
LSD m (*P*-value < 0.05)			0.71	0.0068	383.2
LSD C (*P*-value < 0.05)			0.47	0.0076	374.6
LSD W×M (*P*-value < 0.05)			2.79	0.0154	729.1
LSD W×C (*P*-value < 0.05)			2.69	0.0161	716.9
LSD M×C (*P*-value < 0.05)			0.98	0.0128	653.5
LSD M×W×C (*P*-value < 0.05)			2.97	0.0226	1,301.2

* The water regimes in the field experiment were irrigation every 1 (W1), 2 (W2), and 3 (W3) weeks in reduced amounts of water.

The soil in this study is a highly saline calcareous soil, which may create unfavourable conditions for AMF growth and development, in addition to the effect of drought stress. Changes in climate, complex soil composition, predation by soil microfauna, and competition amongst better-adapted native microflora, all pose serious challenges to the inoculated microorganisms' survival and viability (Bashan et al., 2014; Tao et al., 2018). Thus, immobilising these cells in an appropriate carrier, such as biochar, may improve tolerance to such challenges and protect cells from indigenous soil microorganisms (Chuaphasuk & Prapagdee, 2019).

Sajedi et al. (2010) previously supported the idea that AMF improves water efficiency in drought-stressed plants, this was later explained by Zou et al. (2015), who owed such improvement to active extraradical AMF mycelium in the soil. The composition of growth-promoting rhizobacteria with biochar found to have beneficial effects on the experimental crops, particularly in agriculturally hard environments such as water scarcity (Nadeem et al., 2017), seasonal differences (Ijaz et al., 2019), and drought (Egamberdieva et al., 2017). Yooyongwech et al. (2019) reported that for maize (*Zea mays* L.) plants, the alginate-AMF type of encapsulation may perform better than the agar-mycorrhiza type, and resulted in superior development under water-limited conditions.

Effect of the bio-formulated AMF on nutrient uptake in the field experiment

Table 4 lists the influence of AMF, carrier, and water regime on N, P, and K uptake by wheat. For the single effect of AMF isolate, the overall N, P, and K uptake in M1 were 215.4, 54.1, and 123.6 kg ha^{-1}, respectively. In M2, these nutrients were 239.2, 56.2, and 151.7 kg ha^{-1}, whereas in M3 (without AMF) were 149.8, 32.7, and 78.8 kg ha^{-1}, respectively.

Regarding the single effect of carrier types, the overall N, P, and K uptake in biochar was the highest even if at par with alginate for N and K uptake. In alginate, these nutrients were 219.1, 50.3, and 129.1 kg ha^{-1}, whereas in control were 165.9, 37.2, and 96.8 kg ha^{-1}, respectively. Biochar is statistically higher in N uptake, but at par with alginate in N and K uptake. The control exhibited statistically lowest values of N, P, and K uptake.

Data revealed that the M2-biochar interaction could reduce drought stress caused by varying irrigation intervals on nutrient uptake. Under W2 in M3-control (without AMF and carrier), N, P, and K uptake were 129.7, 28.4, and 73.6 kg ha^{-1}, respectively. However, with the inoculation with M2-biochar at the same W2 conditions, these values turned to be 177.6, 39.4, and 89.2 kg ha^{-1}, respectively. Under W3 conditions, which can be regarded as severe drought, the M3-control gave N, P, and K values of 57.7, 12.3, 34.4 kg ha^{-1}, respectively. However, the inoculation with M2-biochar at the same W3 conditions increased the N, P, and K uptake values to be 123.5, 17.0, and 63.6 kg ha^{-1}, respectively. This shows the positive impact of the treatments of alleviating the drought negative effects of nutrient uptake.

Ameloot et al. (2015) and Solaiman et al. (2019) showed that biochar application boosted AMF activity. Since the biochar amendment improves nutrient availability and retention in a variety of soils (Yadav et al., 2019), as well as contributing to the enhancement of other physical and biological soil parameters (Igalavithana et al., 2016; Novák et al., 2020; Zhang et al., 2020) and in metal retention (Xing et al., 2020). Positive biochar-AMF interacting effects on beans (*Phaseolus vulgaris* L.) P uptake were found by Vanek & Lehmann (2015) when sparsely soluble Fe-P was paired with biochar. In this regard, Solaiman et al. (2019) linked AMF increases to inadequate soil nutrient availability.

Table 4. Effect of different AMF species bio-formulated on different carriers on N, P, and K uptake by wheat at harvest in the field experiment under different water regimes

Water regime (W)*	Mycorrhizae (M)**	Carrier (C)	N uptake (kg ha^{-1})	P uptake (kg ha^{-1})	K uptake (kg ha^{-1})
W1	M1 (*Acaulospora* sp.)	Alginate (C1)	309.5	85.3	157.6
		Biochar (C2)	300.5	98.9	151.7
		Control (C3)	226.0	66.7	128.3
	M2 (*Glomus* sp.)	Alginate (C1)	326.8	90.0	228.6
		Biochar (C2)	341.7	92.6	207.9
		Control (C3)	213.0	64.1	126.3
	M3 (control)	Alginate (C1)	228.5	48.8	114.4
		Biochar (C2)	244.4	56.2	122.9
		Control (C3)	214.1	42.3	116.2
W2	M1 (*Acaulospora* sp.)	Alginate (C1)	291.1	64.4	205.5
		Biochar (C2)	263.7	64.2	173.6
		Control (C3)	180.8	37.3	116.6
	M2 (*Glomus* sp.)	Alginate (C1)	299.1	63.3	197.4
		Biochar (C2)	329.5	77.5	248.2
		Control (C3)	249.5	51.1	170.9
	M3 (control)	Alginate (C1)	172.4	36.2	96.5
		Biochar (C2)	177.6	39.4	89.2
		Control (C3)	129.7	28.4	73.6
W3	M1 (*Acaulospora* sp.)	Alginate (C1)	131.0	25.4	66.6
		Biochar (C2)	136.8	29.5	71.1
		Control (C3)	99.5	15.2	41.6
	M2 (*Glomus* sp.)	Alginate (C1)	133.5	23.4	59.7
		Biochar (C2)	135.8	27.0	63.2
		Control (C3)	123.5	17.0	63.6
	M3 (control)	Alginate (C1)	65.3	16.3	35.3
		Biochar (C2)	58.8	14.1	26.6
		Control (C3)	57.7	12.3	34.4
LSD W (*P*-value < 0.05)			15.7	10.7	12.3
LSD m (*P*-value < 0.05)			6.3	7.6	5.8
LSD C (*P*-value < 0.05)			5.2	3.8	11.4
LSD W×M (*P*-value < 0.05)			18.0	15.1	13.6
LSD W×C (*P*-value < 0.05)			17.2	11.9	12.4
LSD M×C (*P*-value < 0.05)			9.7	9.3	12.7
LSD M×W×C (*P*-value < 0.05)			21.8	17.1	19.4

* The water regimes in the field experiment were irrigation every 1 (W1), 2 (W2), and 3 (W3) weeks in reduced amounts of water.

Effect of the bio-formulated AMF on the soil aggregation and mycorrhizal colonization in the field experiment

In Table 5, influence of AMF, carrier, and water regime on each of spores count, colonization percentage, and soil aggregates are recorded. For the single effect of AMF isolate: overall spores count, colonization percentage, and soil aggregates in M1 were 52.7 spores 100 g^{-1}, 58.7%, and 24.1%, respectively. For isolate M2, the spores count was higher, but values were at par with M1 in colonization percentage and soil aggregates. For isolate M3 (control) all recorded values were lower.

Table 5. Effect of different AMF species bio-formulated on different carriers on spores count, colonization percentage, and soil aggregates in the wheat field experiment under different water regimes

Water regime (W)*	Mycorrhizae (M)**	Carrier (C)	Spore count (spores 100 g^{-1})	Colonization percentage (%)	Soil aggregates (%)
W1	M1 (*Acaulospora* sp.)	Alginate (C1)	77.1	77.3	35.1
		Biochar (C2)	79.8	79.3	32.4
		Control (C3)	43.4	66.2	23.7
	M2 (*Glomus* sp.)	Alginate (C1)	78.9	80.9	25.5
		Biochar (C2)	100.2	81.5	34.2
		Control (C3)	66.8	72.5	32.1
	M3 (control)	Alginate (C1)	45.9	50.2	23.6
		Biochar (C2)	45.8	36.4	21.3
		Control (C3)	41.7	30.7	21.1
W2	M1 (*Acaulospora* sp.)	Alginate (C1)	55.7	61.7	23.5
		Biochar (C2)	60.3	66.5	23.1
		Control (C3)	38.4	48.9	19.7
	M2 (*Glomus* sp.)	Alginate (C1)	60.5	64.2	23.0
		Biochar (C2)	66.4	65.5	22.4
		Control (C3)	39.0	51.7	19.8
	M3 (control)	Alginate (C1)	61.7	32.1	20.1
		Biochar (C2)	65.2	33.8	20.4
		Control (C3)	39.9	22.0	19.9
W3	M1 (*Acaulospora* sp.)	Alginate (C1)	41.8	45.8	21.4
		Biochar (C2)	46.0	46.1	19.4
		Control (C3)	32.1	36.2	18.5
	M2 (*Glomus* sp.)	Alginate (C1)	45.0	40.0	15.4
		Biochar (C2)	43.9	43.4	14.9
		Control (C3)	35.9	35.0	14.1
	M3 (control)	Alginate (C1)	30.0	25.2	14.2
		Biochar (C2)	29.6	23.1	12.3
		Control (C3)	25.7	19.1	12.9
LSD W (*P*-value < 0.05)			16.2	18.4	2.8
LSD m (*P*-value < 0.05)			10.3	11.7	2.8
LSD C (*P*-value < 0.05)			10.7	15.0	3.4
LSD W×M (*P*-value < 0.05)			21.7	22.4	4.9
LSD W×C (*P*-value < 0.05)			21.9	15.6	5.6
LSD M×C (*P*-value < 0.05)			18.3	21.2	5.6
LSD M×W×C (*P*-value < 0.05)			35.9	39.4	9.5

* The water regimes in the field experiment were irrigation every 1 (W1), 2 (W2), and 3 (W3) weeks in reduced amounts of water.

The AMF isolate M2-biochar changed the most spores, counting 100.2 spores 100 g^{-1} under W1 conditions. The highest colonization percentage was that recorded also for AMF isolate M2-biochar which statistically little higher than the one recorded under W1 conditions for AMF isolate M2-alginate. The highest soil aggregates were in AMF isolate M1-alginate, which statistically at par with those recorded under W1 conditions in treatments: AMF isolate M2-biochar and AMF isolate M2-control. The AMF isolate

M2-biochar interaction, generally, resulted in overall improved values for drought stress relief.

Regarding the root colonization, the findings seem to be in line with those recorded by Videgain-Marco et al. (2021) who found that biochar addition boosted AMF root colonization, number of spores, and the infective potential of indigenous AMF. Also, biochar addition is very recalcitrant and capable of improving soil characteristics through affecting both biochemical and biological processes (Arif et al., 2017; Song et al., 2019). However, few studies, on the other hand, have documented successful rhizospheric colonization of immobilized growth-promoting rhizobacteria strains when biochar was utilised as the inoculant carrier, which also encouraged root colonization by native AMF (Saxena et al., 2013).

CONCLUSIONS

In the pot experiment, the three tested isolates of AMF and the three proposed carriers had diverse effects on wheat performance under water deficit stress. The treatment effects were refined using the chlorophyll index and dry weight of wheat for two AMF isolates (*Acaulospora spinosa*, and *Glomus ambisporum*) and two carriers (biochar and alginate), both of which performed better. When applied in the field experiment, wheat plants exposed to water deficit stress performed better (grain yield, nutrient uptake, and colonization percentage) for AMF isolate *Glomus ambisporum* formulated on biochar and alginate, with better performance of biochar over alginate. For example, *Glomus*-biochar treatment could save 2,510 kg ha^{-1} grain yield lost when irrigation was shifted from W1 (irrigation every week) to W2 (irrigation every two weeks). This indicates that *Glomus*-biochar was effective in relieving water deficit stress in wheat. The results of this study hold significant implications for enhancing wheat growth under drought conditions.

REFERENCES

Acevedo, M., Zurn, J.D., Molero, G., Singh, P., He, X., Aoun, M., Juliana, P., Bockleman, H., Bonman, M., El-Sohl, M., Amri, A., Coffman, R. & McCandless, L. 2018. The role of wheat in global food security. In: Nagothu U.S., Bloem E., Borrell A. (eds) *Agricultural Development and Sustainable Intensification*. Routledge, London. https://doi.org/10.4324/9780203733301

Aggangan, N.S., Cortes, A.D. & Reaño, C.E. 2019. Growth response of cacao (Theobroma cacao L.) plant as affected by bamboo biochar and arbuscular mycorrhizal fungi in sterilized and unsterilized soil. *Biocatalysis and Agricultural Biotechnology* **22**, 101347.

Ahmad, Z., Waraich, E.A., Akhtar, S., Anjum, S., Ahmad, T., Mahboob, W., Hafeez, O.B.A., Tapera, T., Labuschagne, M. & Rizwan, M. 2018. Physiological responses of wheat to drought stress and its mitigation approaches. *Acta Physiologiae Plantarum* **40**, 1–13.

Ali, A.M. 2020. Development of an algorithm for optimizing nitrogen fertilization in wheat using GreenSeeker proximal optical sensor. *Experimental Agriculture* **56**(5), 688–698.

Ali, A.M., Ibrahim, S.M., Hassany, W.M., El-Sadek, A.N. & Bijay-Singh. 2021. Fixed-time corrective dose fertilizer nitrogen management in wheat using atLeaf meter and leaf colour chart. *Experimental Agriculture* **57**(4), 232–243.

Ameloot, N., Sleutel, S., Das, K.C., Kanagaratnam, J. & De Neve, S. 2015. Biochar amendment to soils with contrasting organic matter level: effects on N mineralization and biological soil properties. *Gcb Bioenergy* **7**(1), 135–144.

Arif, M., Ilyas, M., Riaz, M., Ali, K., Shah, K., Haq, I.U. & Fahad, S. 2017. Biochar improves phosphorus use efficiency of organic-inorganic fertilizers, maize-wheat productivity and soil quality in a low fertility alkaline soil. *Field Crops Research* **214**, 25–37.

Bahadur, A., Batool, A., Nasir, F., Jiang, S., Mingsen, Q., Zhang, Q., Pan, J., Liu, Y. & Feng, H. 2019. Mechanistic insights into arbuscular mycorrhizal fungi-mediated drought stress tolerance in plants. *International Journal of Molecular Sciences* **20**(17), 4199.

Barea, J.M., Palenzuela, J., Cornejo, P., Sánchez-Castro, I., Navarro-Fernández, C., Lopéz-García, A., Estrada, B., Azcón, R., Ferrol, N. & Azcón-Aguilar, C. 2011. Ecological and functional roles of mycorrhizas in semi-arid ecosystems of Southeast Spain. *Journal of Arid Environments* **75**(12), 1292–1301.

Barea, J.M., Pozo, M.J., Azcon, R. & Azcon-Aguilar, C. 2005. Microbial co-operation in the rhizosphere. *Journal of Experimental Botany* **56**(417), 1761–1778.

Bashan, Y., de-Bashan, L.E., Prabhu, S.R. & Hernandez, J.P. 2014. Advances in plant growth-promoting bacterial inoculant technology: formulations and practical perspectives (1998–2013). *Plant and Soil* **378**(1), 1–33.

Basiru, S., Mwanza, H.P. & Hijri, M. 2020. Analysis of arbuscular mycorrhizal fungal inoculant benchmarks. *Microorganisms* **9**(1), 81.

Bhantana, P., Rana, M.S., Sun, X.C., Moussa, M.G., Saleem, M.H., Syaifudin, M., Shah, A., Poudel, A., Pun, A.B., Bhat, M.A. & Mandal, D.L. 2021. Arbuscular mycorrhizal fungi and its major role in plant growth, zinc nutrition, phosphorous regulation and phytoremediation. *Symbiosis* **84**, 19–37.

Borde, M., Dudhane, M. & Kulkarni, M. 2017. Role of arbuscular mycorrhizal fungi (AMF) in salinity tolerance and growth response in plants under salt stress conditions. *Mycorrhiza-eco-physiology, secondary metabolites, nanomaterials*, 71–86.

Borriello, R., Lumini, E., Girlanda, M., Bonfante, P. & Bianciotto, V. 2012. Effects of different management practices on arbuscular mycorrhizal fungal diversity in maize fields by a molecular approach. *Biology and Fertility of Soils* **48**(8), 911–922.

Bremner, J.T. 1965. Inorganic forms of nitrogen. Methods of Soil Analysis: Part 2 Chemical and Microbiological Properties, Agronomy Monographs 9. *American Society of Agronomy,* Madison (**WI**, 1179–1237).

Chuaphasuk, C. & Prapagdee, B. 2019. Effects of biochar-immobilized bacteria on phytoremediation of cadmium-polluted soil. *Environmental Science and Pollution Research* **26**(23), 23679–23688.

Daryanto, S., Wang, L. & Jacinthe, P.A. 2016. Global synthesis of drought effects on maize and wheat production. *PloS One* **11**(5), e0156362.

Diagne, N., Ngom, M., Djighaly, P.I., Fall, D., Hocher, V. & Svistoonoff, S. 2020. Roles of arbuscular mycorrhizal fungi on plant growth and performance: Importance in biotic and abiotic stressed regulation. *Diversity* **12**(10), 370.

Egamberdieva, D., Reckling, M. & Wirth, S. 2017. Biochar-based Bradyrhizobium inoculum improves growth of lupin (*Lupinus angustifolius* L.) under drought stress. *European Journal of Soil Biology* **78**, 38–42.

FAO. 1998. World Reference Base for Soil Resources. Rep.84. Rome.

Gerdemann, J.W. & Nicolson, T.H. 1963. Spores of mycorrhizal Endogone species extracted from soil by wet sieving and decanting. *Transactions of the British Mycological Society* **46**(2), 235–244.

Giovannetti, M. & Mosse, B. 1980. An evaluation of techniques for measuring vesicular arbuscular mycorrhizal infection in roots. *New Phytologist*, 489–500.

Gomez, K.A. & Gomez, A.A. 1984. *Statistical Procedures for Agricultural Research*. Hoboken, NJ: John Wiley & Sons, New York, 680 pp.

Grote, U., Fasse, A., Nguyen, T.T. & Erenstein, O. 2021. Food security and the dynamics of wheat and maize value chains in Africa and Asia. *Frontiers in Sustainable Food Systems* **4**, 617009.

Herrmann, L. & Lesueur, D. 2013. Challenges of formulation and quality of biofertilizers for successful inoculation. *Applied Microbiology and Biotechnology* **97**(20), 8859–8873.

Heydarian, A., Moghadam, H.T., Donath, T.W. & Sohrabi, M. 2018. Study of effect of arbuscular mycorrhiza (*Glomus intraradices*) fungus on wheat under nickel stress. *Agronomy Research* **16**(4), 1660–1667.

Igalavithana, A.D., Ok, Y.S., Usman, A.R., Al-Wabel, M.I., Oleszczuk, P. & Lee, S.S. 2016. The effects of biochar amendment on soil fertility. In book: Agricultural and Environmental Applications of Biochar: Advances and BarriersEdition: SSSA Special Publication 63Publisher: *Soil Science Society of America, Inc.* pp. 123–144. doi:10.2136/sssaspecpub63.2014.0040

Ijaz, M., Tahir, M., Shahid, M., Ul-Allah, S., Sattar, A., Sher, A., Mahmood, K. & Hussain, M. 2019. Combined application of biochar and PGPR consortia for sustainable production of wheat under semiarid conditions with a reduced dose of synthetic fertilizer. *Brazilian Journal of Microbiology* **50**(2), 449–458.

Kalra, Y. 1998. *Handbook of Reference Methods for Plant Analysis*. CRC press, 287 pp.

Kemper, W.D. & Rosenau, R.C. 1986. Aggregate stability and size distribution. Methods of soil analysis: Part 1 *Physical and mineralogical methods* **5**, 425–442.

Lehmann, J., Rillig, M.C., Thies, J., Masiello, C.A., Hockaday, W.C. & Crowley, D. 2011. Biochar effects on soil biota–a review. *Soil Biology and Biochemistry* **43**(9), 1812–1836.

Leng, G. & Hall, J. 2019. Crop yield sensitivity of global major agricultural countries to droughts and the projected changes in the future. *Science of the Total Environment* **654**, 811–821.

Lonbani, M. & Arzani, A. 2011. Morpho-physiological traits associated with terminal drought stress tolerance in triticale and wheat. *Agronomy Research* **9**(1–2), 315–329.

Moghadam, H.T., Donath, T.W., Ghooshchi, F. & Sohrabi, M. 2018. Investigating the probable consequences of super absorbent polymer and mycorrhizal fungi to reduce detrimental effects of lead on wheat (*Triticum aestivum* L.). *Agronomy Research* **16**(1), 286–296.

Nadeem, S.M., Imran, M., Naveed, M., Khan, M.Y., Ahmad, M., Zahir, Z.A. & Crowley, D.E. 2017. Synergistic use of biochar, compost and plant growth-promoting rhizobacteria for enhancing cucumber growth under water deficit conditions. *Journal of the Science of Food and Agriculture* **97**(15), 5139–5145.

Nirmala, P. & Selvaraj, T. 2011. Mass Production of sodium alginate entrapped arbuscular mycorrhizal inoculum and their influence on growth and nutrition of Sorghum vulgare Pers. *Indian Journal of Applied Microbiology* **13**(1), 63–68.

Novák, V., Křížová, K. & Šařec, P. 2020. Biochar dosage impact on physical soil properties and crop status. *Agronomy Research* **18**(4), 2501–2511.

Pacheco-Aguirre, J.A., Ruíz-Sánchez, E., Ballina-Gómez, H.S. & Alvarado-López, C.J. 2017. Does polymer-based encapsulation enhance performance of plant growth promoting microorganisms? A meta-analysis view. *Agrociencia* **51**(2), 173–187.

Page, A.L., Miller, R.H. & Keeney, D.R. 1982. Methods of soil analysis. Part 2. Chemical and Microbiological properties. 2nd ed. American Soc. of Agronomy. *In Soil Science Society of America*, Vol. **1159**.

Pandian, K., Subramaniayan, P., Gnasekaran, P. & Chitraputhirapillai, S. 2016. Effect of biochar amendment on soil physical, chemical and biological properties and groundnut yield in rainfed Alfisol of semi-arid tropics. *Archives of Agronomy and Soil Science* **62**(9), 1293–1310.

Park, H.J., Floss, D.S., Levesque-Tremblay, V., Bravo, A. & Harrison, M.J. 2015. Hyphal branching during arbuscule development requires Reduced Arbuscular Mycorrhiza1. *Plant Physiology* **169**(4), 2774–2788.

Park, J.K. & Chang, H.N. 2000. Microencapsulation of microbial cells. *Biotechnology Advances* **18**(4), 303–319.

Pequeno, D.N., Hernandez-Ochoa, I.M., Reynolds, M., Sonder, K., MoleroMilan, A., Robertson, R.D., Lopes, M.S., Xiong, W., Kropff, M. & Asseng, S. 2021. Climate impact and adaptation to heat and drought stress of regional and global wheat production. *Environmental Research Letters* **16**(5), 054070.

Phillips, J.M. & Hayman, D. 1970. Improved procedures for clearing roots and staining parasitic and vesicular–arbuscular mycorrhizal fungi for rapid assessment of infection. *Transactions of the British Mycological Society* **55**, 158–161.

Pitaktamrong, P., Kingkaew, J., Yooyongwech, S., Cha-um, S. & Phisalaphong, M. 2018. Development of arbuscular mycorrhizal fungi-organic fertilizer pellets encapsulated with alginate film. *Engineering Journal* **22**(6), 65–79.

Plett, D.C., Ranathunge, K., Melino, V.J., Kuya, N., Uga, Y. & Kronzucker, H.J. 2020. The intersection of nitrogen nutrition and water use in plants: new paths toward improved crop productivity. *Journal of Experimental Botany* **71**(15), 4452–4468.

Plouznikoff, K., Declerck, S. & Calonne-Salmon, M. 2016. Mitigating abiotic stresses in crop plants by arbuscular mycorrhizal fungi. *Belowground defence strategies in plants*, 341–400.

Pour-Aboughadareh, A., Mohammadi, R., Etminan, A., Shooshtari, L., Maleki-Tabrizi, N. & Poczai, P. 2020. Effects of drought stress on some agronomic and morpho-physiological traits in durum wheat genotypes. *Sustainability* **12**(14), 5610.

Ruíz-Lozano, J.M., del Carmen Perálvarez, M., Aroca, R. & Azcón, R. 2011. The application of a treated sugar beet waste residue to soil modifies the responses of mycorrhizal and non mycorrhizal lettuce plants to drought stress. *Plant and Soil* **346**(1), 153–166.

Sajedi, N.A., Ardakani, M.R., Rejali, F., Mohabbati, F. & Miransari, M. 2010. Yield and yield components of hybrid corn (*Zea mays* L.) as affected by mycorrhizal symbiosis and zinc sulfate under drought stress. *Physiology and Molecular Biology of Plants* **16**(4), 343–351.

Saxena, J., Rana, G. & Pandey, M. 2013. Impact of addition of biochar along with Bacillus sp. on growth and yield of French beans. *Scientia Horticulturae* **162**, 351–356.

Schütz, L., Gattinger, A., Meier, M., Müller, A., Boller, T., Mäder, P. & Mathimaran, N. 2018. Improving crop yield and nutrient use efficiency via biofertilization–A global meta-analysis. *Frontiers in Plant Science* **8**, 2204.

Sohaib, M., Zahir, Z.A., Khan, M.Y., Ans, M., Asghar, H.N., Yasin, S. & Al-Barakah, F.N. 2020. Comparative evaluation of different carrier-based multi-strain bacterial formulations to mitigate the salt stress in wheat. *Saudi Journal of Biological Sciences* **27**(3), 777–787.

Solaiman, Z.M., Abbott, L.K. & Murphy, D.V. 2019. Biochar phosphorus concentration dictates mycorrhizal colonisation, plant growth and soil phosphorus cycling. *Scientific Reports* **9**(1), 1–11.

Song, D., Xi, X., Zheng, Q., Liang, G., Zhou, W. & Wang, X. 2019. Soil nutrient and microbial activity responses to two years after maize straw biochar application in a calcareous soil. *Ecotoxicology and Environmental Safety* **180**, 348–356.

Tao, S., Wu, Z., He, X., Ye, B.C. & Li, C. 2018. Characterization of biochar prepared from cotton stalks as efficient inoculum carriers for Bacillus subtilis SL-13. *Bioresources* **13**(1), 1773–1786.

Torrion, J.A. & Stougaard, R.N. 2017. Impacts and limits of irrigation water management on wheat yield and quality. *Crop Science* **57**(6), 3239–3251.

Trappe, J.M. 1982. Synoptic keys to the genera and species of zygomycetous mycorrhizal fungi. *Phytopathology* **72**(8), 1102–1108.

Vanek, S.J. & Lehmann, J. 2015. Phosphorus availability to beans via interactions between mycorrhizas and biochar. *Plant and Soil* **395**(1), 105–123.

Videgain-Marco, M., Marco-Montori, P., Martí-Dalmau, C., Jaizme-Vega, M.D.C., Manyà-Cervelló, J.J. & García-Ramos, F.J. 2021. The Effects of Biochar on Indigenous Arbuscular Mycorrhizae Fungi from Agroenvironments. *Plants* **10**(5), 950.

Walkley, A. & Black, I.A. 1934. An examination of the Degtjareff method for determining soil organic matter, and a proposed modification of the chromic acid titration method. *Soil Science* **37**(1), 29–38.

Warnock, D.D., Lehmann, J., Kuyper, T.W. & Rillig, M.C. 2007. Mycorrhizal responses to biochar in soil–concepts and mechanisms. *Plant and Soil* **300**(1), 9–20.

Xing, D., Magdouli, S., Zhang, J. & Koubaa, A. 2020. Microbial remediation for the removal of inorganic contaminants from treated wood: Recent trends and challenges. *Chemosphere* **258**, 127429.

Yadav, V., Jain, S., Mishra, P., Khare, P., Shukla, A.K., Karak, T. & Singh, A.K. 2019. Amelioration in nutrient mineralization and microbial activities of sandy loam soil by short term field aged biochar. *Applied Soil Ecology* **138**, 144–155.

Yooyongwech, S., Suriyan, C.U., Tisarum, R., Therawitaya, C., Samphumphung, T., Aumtong, S., Kingkaew, J. & Phisalaphong, M. 2019. Influence of different encapsulation types of arbuscular mycorrhizal fungi on physiological adaptation and growth promotion of maize (*Zea mays* L.) subjected to water deficit. *Notulae Botanicae Horti Agrobotanici Cluj-Napoca* **47**(1), 213–220.

Zafar-ul-Hye, M., Bhutta, T.S., Shaaban, M., Hussain, S., Qayyum, M.F., Aslam, U. & Zahir, Z.A. 2019. Influence of plant growth promoting rhizobacterial inoculation on wheat productivity under soil salinity stress. *Phyton* **88**(2), 119–129.

Zhang, J., Zhang, S., Cheng, M., Jiang, H., Zhang, X., Peng, C., Lu, X., Zhang, M. & Jin, J. 2018. Effect of drought on agronomic traits of rice and wheat: A meta-analysis. *International Journal of Environmental Research and Public Health* **15**(5), 839.

Zhang, Q., Song, Y., Wu, Z., Yan, X., Gunina, A., Kuzyakov, Y. & Xiong, Z. 2020. Effects of six-year biochar amendment on soil aggregation, crop growth, and nitrogen and phosphorus use efficiencies in a rice-wheat rotation. *Journal of Cleaner Production* **242**, 118435.

Zou, Y.N., Srivastava, A.K., Ni, Q.D. & Wu, Q.S. 2015. Disruption of mycorrhizal extraradical mycelium and changes in leaf water status and soil aggregate stability in rootbox-grown trifoliate orange. *Frontiers in Microbiology* **6**, 203.

Agronomy Research **22**(1), 33–51, 2024
https://doi.org/10.15159/AR.24.005

In vivo evaluation of antioxydant potential and antihyperglycemic effect of *Stevia rebaudiana* Bertoni

O. Aissaoui[1,2,*], L. Terki[1,3], S. Ait Ameur[2] and A. Bitam[2]

[1]University of Saad Dahlab, Faculty of natural and life sciences, Institute of Science and Applied Technology, Department of Food Science, DZ09000 Blida, Algeria
[2]National Higher School of Agronomy, Food Technology and Human Nutrition Laboratory, Food Technology Department, DZ16000, El Harrach, Algiers, Algeria
[3]University of Bejaia, Research Laboratory of Biomathematics, Biochemistry, Biophysics and Scientometrics, DZ06000, Bejaia, Algeria
[*]Correspondence: aissaoui_ourida@univ-blida.dz

Received: October 1st, 2023; Accepted: December 23rd, 2023; Published: January 22nd, 2024

Abstract. *Stevia rebaudiana* Bertoni (SR) has a high concentration of phytochemicals that promote health and well-being in conditions such as diabetes. This study aims to assess the antihyperglycemic, antioxidant, and antihyperlipidemic effects of SR on diabetes in male rats caused by Alloxan. Forty adult male rats were divided into five groups. For 28 days, SR was administered by gavage. Spinreact and ELISA kits were used to detect serum levels of blood glucose, insulin, liver function, lipid profiles, antioxidant enzymes, and lipid peroxidation. Histopathology was also investigated. Stevia's free radical scavenging capabilities have an IC_{50} value of between 34.49 and 39.66 mg L^{-1}. Stevia therapy reduced biochemical markers in diabetic rats (DR). After 28 days, SR raised fasting blood glucose, insulin, and lipid peroxidation serum levels by 52%, 40%, and 27%, respectively. Also, in DR treated with SR, there was a substantial increase in high-density lipoprotein cholesterol (35.8%), superoxide dismutase (30%), total antioxidant status (20%), glutathione peroxidase and reductase. SR improves DR's pancreas and liver function by enhancing the endogenous antioxidant system. These findings revealed that SR counteracted Alloxan's necrotic effects by reducing insulin resistance in DR, hence revitalizing pancreatic β–cells.

Key words: HOMA-IR, glycemia, liver, oxidative stress, pancreas, Stevia.

INTRODUCTION

Mellitus diabetes, a major public health problem due to its high incidence and morbidity, is divided into Type 1 and Type 2. It is a prevalent chronic condition characterized by cellular metabolic disruptions such as hyperglycemia and insulinemia, which cause abnormalities in many organs and systems by producing reactive oxygen species (ROS) (Jiménez et al., 2020). Free radicals' induction of oxidative stress may have numerous health consequences, including pathogenic and degenerative processes such as diabetes (Ameer et al., 2020). In Type 2 diabetes patients, oral non-insulin medications are the first-line therapy, along with lifestyle adjustments. Eight

pharmacological categories, anti-diabetic medications (with their action mechanism, benefits and drawbacks), are presently accessible to manage this condition (Abdel-Daim & Halawa, 2014; Hernández et al., 2020). Metformin was the first oral anti-diabetic drug (OAD) approved for treating type 2 diabetes. The research problem is the limited and side-effects of chemical OAD mentioned above, in addition to their high cost. Therefore, the search for an alternative way to treat diabetes is necessary. That's why the cognitive goal of this study is to find a natural remedy for diabetes and has a number of health-promoting properties.

Plants and algae such as *Stevia rebaudiana* (SR) and *Spirulina platensis* are important natural bioactive and antioxidant compounds sources, gradually replacing synthetic antioxidants (Aissaoui et al., 2017; Ameer et al., 2017). The utilitarian goal of the undertaken research study is to demonstrate the effect of SR on Alloxan-induced metabolic and histological problems associated with diabetes in rats.

SR is a perennial shrub of the Compositae family that is cultivated for its leaves in South America. It is grown around the world from March to September. SR propagated by seed or by cuttings or clump division (Peteliuk et al., 2021). Its bioactive components are responsible for several activities and sweetness. Unfortunately, stevia cultivation faces 2–25% yield penalty due abiotic and biotic constraints which further adds to its cultivation cost (Taak et al., 2020; Patel & Navale, 2023).

Agriculture requires mastery of certain parameters (climatic conditions, fertilization, irrigation, optimal harvest periods and geographical dispersion) to assure high stevia yields (Hirich et al., 2022).

Stevia is one of the plants with a nutritional and therapeutic value that has been reported in many traditional pharmacopeias around the world. SR has a history of ethnobotanical applications in various countries, food, and therapeutic medicine. Furthermore, extensive Stevia use has not been shown to have a negative impact on the human body. It is considered safe (Carakostas et al., 2008; Kasti et al., 2022). Stevia bioactive components or extract have been used to reduce oxidative stress and anticipate the aggression of various diseases, including obesity, diabetes, and gut bacteria (Savita et al., 2017; Ameer et al., 2020 & Kasti et al., 2022).

Stevia's bioactive components (stevioside and polyphenols) make it a plant with nutritional, pharmaceutical, and therapeutic value, and it is used to treat metabolic syndrome. Stevia can thus be used to create cosmetic, pharmaceutical, and functional food products (Thomas & Glade, 2010; Ameer et al., 2020). SR has significant curative properties as a natural treatment for metabolic imbalance. The European Food Safety Authority has declared Stevia and the US Food and Drug Administration a natural sweetener and an additive food (4 mg kg^{-1} body weight as acceptable daily intake) (Yu et al., 2017; Thomas & Glade, 2010). To this end, this paper investigates SR's influence on glucose metabolism, cellular and metabolic aggression of Alloxan diabetes in animals.

MATERIALS AND METHODS

Phytochemical profile of SR

In 2020, fresh green leaves were collected from Ouled Fayet, southwest of Algiers. After waste removal, stevia leaves were dried at 25 °C. The mixture was blended in a blender (Miyako BL152, 25,000 rpm, China) and kept at a +4 °C temperature.

Determination of total polyphenols and flavonoids

Pure ethanol was used to extract phenolics from Stevia powder, according to Makkar et al. (1993). The SR powder was broken down (0.2 mg in 10 mL of solvent for 20 min). The solution was centrifuged at 3,000 rpm for 10 min before filtering through Whatman No.1 filter paper.

The ethanol was volatilized at low pressure at approximately 78 °C using a rotary evaporator (SE) to obtain the Stevia extract. Total polyphenols and flavonoids in SE were measured using the Folin-Ciocalteu and $AlCl_3$ methods. Gallic acid and quercetin were used as standards, respectively (Singleton et al., 1999; Chang et al., 2002).

In vivo *antioxydant* profile resolution

The Şahin et al. (2004) technique was used to evaluate the free radical scavenging abilities of Stevia extract against the 2,2–diphenyl–1–picrylhydrazyl (DPPH). However, 100 g mL^{-1} of butylated hydroxyl toluene (BHT) was used as an experimental control. We calculated the anti-free radical activity of the samples using Eq. (1).

was used as a positive control. The antiradical activity of the tested samples was calculated using Eq. (1):

$$\mathrm{DPPH}(\%) = \frac{1 - A_{.SR}}{A_{.DPPH}} 100 \qquad (1)$$

where $A_{.SR}$ and $A_{.DPPH}$ represent the absorbances of Stevia and DPPH separately.

The peroxidase reaction of SR and ABTS (2,2–azino-bis (ethylbensothiazoline–6–sulfonic acid ABTS), in comparison to that of positive control BHT (EQ.2) (Sacan & Yanardag, 2010):

$$\mathrm{ABTS}(\%) = \left(A_C \frac{A_t}{A_C}\right) 100 \qquad (2)$$

where the absorbance of the tested samples are A_t and A_C with $ABTS^{+}$.

The extract concentration that results in 50% inhibition (IC_{50}) of the DPPH, ABTS and BHT parameters was calculated using the graph correlating the inhibition percentages with the extract concentration of the antioxidant parameters. They were purchased from Sigma Aldrich GMBH in Sternheim, Germany.

Animals and diabetes induction

Forty adult Wistar rats (10–13 weeks; 180 ± 70 g) were obtained from the Pasteur Institute of Algeria for this study. On a standard pellet diet, the rats were kept in polypropylene cells in an animal space (12 h light: 12 h darkness, 24 ± 2 °C and 60% relative humidity) (National Office for Food Livestock, Algiers, Algeria) with free access to water. The Algerian Institutional Animal Care Committee approved the National Administration of Algerian Higher Education and Scientific Research's experimental procedures (Algiers). Before the Alloxan injection, the animals fasted overnight. Alloxan monohydrate was given as a subcutaneous injection at a [150 mg kg^{1} body weight (b.w)] dose (Kameswara Rao et al., 1999). We added a 5% glucose solution to daily water consumption to avoid endocrine and metabolic imbalances and a hypoglycemic crisis. After 72 hours, the animals' fasting blood sugar (FBS) was measured. Diabetic animals had hyperglycemia levels greater than 2 g L^{-1}. Following that, we began data analysis.

Experimental procedure

The Pasteur National Institute (Algeria) provided all the animals under study. Over 28 days, the therapeutic effect of SR was studied. The Stevia plant aqueous extract was collected from an upper part vegetable substance (leaves, 1:100 w v^{-1}) by steeping in distilled water for 30 min and incubating at 40 °C/24 h with low movement on an orbital shaker. The hydrosoluble fraction was centrifuged (6,000 g for 10 min), and the insoluble precipitate was discarded. Whatman No.1 paper was used to filter the supernatant. The rotary evaporator's two pressure/temperature settings (40 °C) concentrated the SR filtrate. Then the water was removed to obtain the SR extract.

Animals in group 1 (normal control rats; G1: NC) and group 2 (diabetic control group; G2: DC) received distilled water. In Group 3 (stevia control), the rats were treated with 400 mg kg^{-1} of Stevia, gavaged daily (G3: SC). Diabetic rats in Groups 4 and 5 were given 200 mg kg^{-1} body weight of metformin (G4: DTM) and 400 mg kg^{-1} body weight of Stevia (G5: DTS), respectively. Over 28 days, the SR and metformin (Met) powders were administered to animals by mouth at the equivalent of 1 mL per day. All animals were fed normally while taking Stevia, metformin, or distilled water.

Biochemical analysis

After fasting the rats for the whole night, blood is collected from the retro-orbital plexus every weekend for 28 days. The blood samples were centrifuged for 900 sec at 25 °C and 6,000 rpm. Then, the plasma was stocked at –20 °C in clean tubes for biochemical interpretations. Serum glucose, triglycerides (TGs), total cholesterol (TC), HDL-c (High-density lipoprotein cholesterol), urea, creatinine, and liver function tests [GPT and GOT] were performed by the automated Random Access Clinical Analyzer PICTUS 200–DIATRON using SPINREACT diagnostic kits (UAA Ctra, Santa Coloma 7 E 17176 Sant Esteve de BAS (GI), Spain). On the 28th day, serum insulin levels were determined using an ELISA kit (Boehringer Manheim Diagnostic, Mannheim, Germany). Insulin resistance was assessed using HOMA–IR (the Homeostasis-Model-Assessment estimate of Insulin-Resistance), and pancreatic β–cells function was evaluated using HOMA–B (the Homeostasis-Model-Assessment insulin β–cells) (Song et al., 2007):

$$\mathrm{HOMA-IR} = \frac{\text{fasting insulin level } \left(\frac{\mu U}{mL}\right) \text{ x fasting blood glucose } \left(\frac{mmol}{mL}\right)}{22.5} \quad (3)$$

$$\mathrm{HOMA-B} = \frac{20 \times \text{Insulin } \left(\frac{\mu U}{mL}\right)}{\text{fasting blood glucose } \left(\frac{mmol}{mL}\right)} \quad (4)$$

Using laboratory kits, the serum oxidative stress enzyme parameters (superoxide dismutase; SOD, glutathione peroxidase; GPx, glutathione reductase; GRx, and total antioxidant status; TAS) were measured (Randox Laboratories Antrim, UK). The serum TBARS levels were determined as described by (Quintanilha et al., 1982).

Body weight gain (BWG)

Every 7 days, the rats' weight was measured. At the end of the experiment (28 days), the rats were sacrificed.

$$\mathrm{BWG\ (g)} = \text{Final BW} - \text{Initial BW} \quad (5)$$

Histology

On the 28th day of the study, pancreatic and liver biopsies were taken to estimate the tissue and organ (pancreas and liver) transformations of Alloxan-induced-diabetic of Forty-rats. In 10% formaldehyde, the samples were fixed and dehydrated. Afterward, paraffin, hematoxylin, and eosin (H & E) were used to embed and stain the samples (Gomori, 1950). These sections were examined in the Anapathology Department, University Hospital Centres, Parnet, Algiers, Algeria, using a Leica microscope that works with light and is equipped with a camera.

Statistical analysis

The results were presented as the mean ± standard error (SE). The ANOVA test was used for the statistical analysis of variance. The statistical significance of the means was determined using the STATESTICA 8.0 software and a Student Test of ANOVA (*t–test*) from the *Newman-Keuls test*. A value of $p < 0.05$ was considered significant, $p < 0.01$ was considered highly significant, and ($p < 0.001$) was considered extremely significant.

RESULTS

Stevia phytochemical and antioxidant characterization

Stevia extract contains 54.57 ± 0.35 mg EAG g^{-1} total polyphenols and 20.35 ± 0.09 mg EQ g^{-1} total flavonoids. Stevia leaves have a higher total phenol content (91 mg g^{-1}). The same results were observed by Serio et al. (2010), Gaweł-Bęben et al. (2015) (60.15 mg EAG g^{-1} of total polyphenols; 20.96 mg EQ g^{-1} of total flavonoids). They have numerous health advantages (Ozola & Dūma, 2020). The most important are antioxidant and anti-diabetic properties (Turkoglu et al., 2007; Molina-Calle et al., 2017). By scavenging free radicals, antioxidants inhibit lipid peroxidation in a relatively short period. DPPH and ABTS tests revealed that Stevia has higher antioxidant activity (79.58 and 70.03%, respectively) than BHT (99.56 and 85.39%, respectively) (Table 1). The percent inhibition of ethanolic Stevia extracts by DPPH-radical inhibition activity was 67.07% and 49.27% (Ahmad et al., 2010, Mohammad AL-Mamun et al., 2018). Stevia's claim to be a natural source of antioxidant compounds with significant antioxidant potential has been confirmed. Stevia extract had a higher tannin content, indicating its antioxidant potential. The lower the IC_{50} value, the greater the DPPH-radical inhibition activity (Shukla et al., 2012; Barba et al., 2015; Savita et al., 2017; Joseph et al., 2019).

Table 1. Antioxidant activities of ethanolic extract of Stevia

Antioxidant activity (%) in 100 (g mL^{-1})				IC_{50} (mg L^{-1})			
DPPH	BHT	ABTS	BHT	DPPH	BHT	ABTS	BHT
79.58 ± 0.43	85.39 ± 0.44	70.03 ± 0.30	99.56 ± 0.05	34.49 ± 0.7	13.33 ± 0.41	39.66 ± 0.33	5.3 ± 0.07

DPPH: 2–2–Diphenyl–1–picrylhydrazyl; BHT: Butyl hydroxytoluene; ABTS: 2.2 Azino–bis (3–ethylbenzthiazoline–6–sulphonic acid) ; IC_{50}: extracts concentration providing 50% inhibition.

Biochemical parameters

In our animal study, Alloxan caused an improvement in the fasting blood glucose level (BGL) and plasma insulin level of diabetic rats, indicating that SR had an antihyperglycemic effect (Figs 1, 2, respectively). The diabetic rats had a 70% increase in BGL compared to the normal rats ($P < 0.001$). When compared to diabetic animals (G2), groups treated with Met or Stevia had a significant decrease in blood glucose ($P < 0.001$). G5: DTS reduced BGL by 52% compared to the untreated diabetic control (G2) ($P < 0.001$), ranging from 3.12 to 1.50 g L^{-1} over 28 days. G4 BGL decreased by 62%, ranging from 3.20 to 1.2 g L^{-1}. Stevia-ed rats (G3) had no decrease in BGL (Fig. 1). Naveen et al. (2012) and Assaei et al. (2016) found similar results.

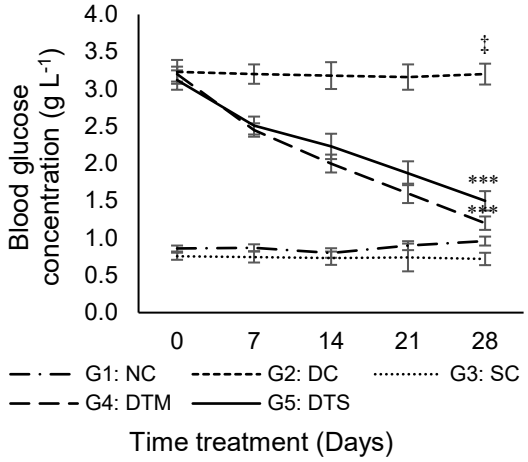

Figure 1. Effect of stevia administration on blood glucose level.

NC: Normal Control; DC: Diabetic Control ; SR: Stevia Control; DTM: Diabetic rats treated with Metformin; DTS: Diabetic rats treated with Stevia. Each value represents mean ± SE ($n=8$). ‡$p < 0.001$, compared with group 1 values ; *** $p < 0.001$ compared with group 2 values at the end of experiment.

The diabetic group had a lower serum insulin level (9.8 U mL^{-1}) than the normal Group (20.01 U mL^{-1}) ($P < 0.001$). During the 28 day study, the serum insulin level in the powder Stevia leaves and metformin-fed groups was higher [11% (G4) versus 40% (G5)] than in the alloxan Group ($P < 0.05$; $P < 0.001$). Normal rats were fed Stevia, and no significant changes were observed (Fig. 2). Except in metformin-treated animals, there was a significant ($p < 0.001$) decrease in HOMA-IR-DC and HOMA-IR-G5 (Fig. 2). As a result, SR has antihyperglycemic activity. Furthermore, in diabetic rats, this plant increased insulin levels. On the other hand, HOMA-B levels in rats treated with Stevia aqueous or metformin increased significantly ($p < 0.001$) compared to diabetic control rats (Fig. 2). Several studies have shown the same result (Naveen et al., 2012; Akbarzadeh et al., 2015; Ahmad & Ahmad, 2018; Han et al., 2022).

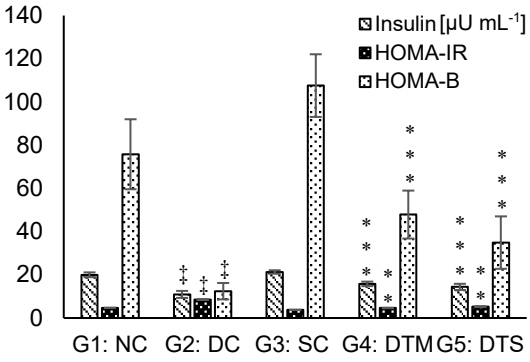

Figure 2. Effect of stevia administration on blood insulin level, HOMA-IR and HOMA-B.

NC: Normal Control; DC: Diabetic Control ; SR: Stevia Control; DTM: Diabetic rats treated with Metformin; DTS: Diabetic rats treated with Stevia. Each value represents mean ± SE ($n = 8$). ‡$p < 0.001$, compared with group 1 values; *** $p < 0.001$ compared with group 2 values at the end of experiment.s

Fig. 3 depicts the effect of SR on the levels of liver enzymes. Serum levels of GOT and GPT were measured (G2) to assess the extent of liver damage caused by Alloxan. Fig. 3 shows that GOT and GPT levels were reduced ($p < 0.001$) in Stevia aqueous extract-fed rats (G5) compared to the diabetic control group (25 and 50%, respectively). After 28 days of OAD treatment, G4 showed a slight decrease in GOT and GPT levels (6 and 17%, respectively) compared to G2 (Fig. 3). Peteliuk et al. (2021) noted the same observations.

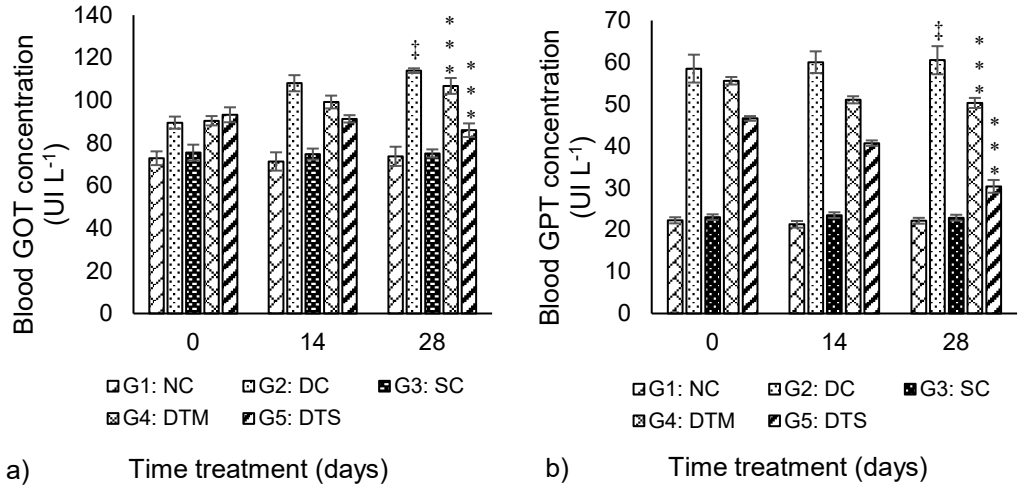

Figure 3. Effect of stevia on serum liver function levels.

GOT (a) : glutamate oxaloacetate transaminase ; GPT (b) : glutamate pyruvate transaminase; NC: Normal Control; DC: Diabetic Control ; SR: Stevia Control; DTM: Diabetic rats treated with Metformin; DTS: Diabetic rats treated with Stevia. Each value represents mean ± SE ($n=8$). ‡$p < 0.001$, compared with group 1 values ; *** $p < 0.001$compared with group 2 values at the end of experiment.

As shown in Table 2, i.p., alloxan injection significantly increased ($P < 0.001$) the levels of TGs (by 66%) and TC (by 49%) when compared to the NC Group. Met and SR treatment, on the other hand, significantly reversed ($p < 0.01$; $p < 0.001$) the increase in plasma TGs and TC by (44% and 35% for SR) and (29.6 and 8% for Met), respectively. G2 had a 51% decrease in HDL-c ($P < 0.001$). On the other hand, SR increased HDL-c levels by 35.8% in G5 and 18% in G4 gavaged with OAD ($p < 0.05$; $p < 0.001$). Similar conclusion were observed by Park & Cha, (2010); Sudha et al. (2017); Ibrahim Ahmed et al. (2019); Peteliuk et al. (2021).

Diabetic animals in G2 had a 64 and 47.5% increase ($P < 0.001$) in urea and creatinine after Alloxan injection, respectively. Met and SR, on the other hand, reduced these effects ($p < 0.01$; $p < 0.001$) by (27.5 and 45% for Met) and (12 and 26% for SR), respectively. No significant differences in TC, TGs, HDL-c, urea, and creatinine levels were found between the SR (G3) and NC (G1) groups (Table 2). The results also show that Alloxan significantly reduced the oxidative stress parameters ($p < 0.001$) compared to the controls. However, after 28 days of Stevia consumption, Group 5 had a significant increase ($p < 0.01$; $p < 0.001$) in TAS (20%), SOD (30%), GPx (27%), and GRx (18%) compared to G2. TAS, SOD, GPx, and GRx levels in G4 were slightly lower than in G2 (4%, 9%, 14%, and 8.6%, respectively) (Table 2).

Table 2. Chemical, oxidative stress parameters and body weight gain at the end of the study

	G1 : NC	G2 : DC	G3 : SC	G4 : DTM	G5 : DTS
Lipid profile					
TG (mg dL^{-1})	57.20 ± 8.56	168.47 ± 14.04‡	58.00 ± 9.23	118.63 ± 12.03***	94.47 ± 8.20 ***
TC (mg dL^{-1})	66.57 ± 11.02	130.51 ± 10.4‡	69.2 ± 11.06	120.06 ± 11.12 **	84.45 ± 8.60 ***
HDL-c (mg dL^{-1})	41.05 ± 4.98	20.14 ± 6.72‡	43.72 ± 5.17	24.6 ± 8.31 *	31.37 ± 7.33 **
Urinary profile					
Urea (mg dL^{-1})	30.89 ± 4.70	85.80 ± 7.61‡	32.95 ± 4.12	62.14 ± 4.05 ***	75.42 ± 2.87 **
Creatinine (mg dL^{-1})	0.64 ± 0.15	1.22 ± 0.23 ‡	0.66 ± 0.29	0.67 ± 0.18 ***	0.90 ± 0.16 ***
Oxidative stress parameters					
TAS [mmol L^{-1}]	1.21 ± 0.11	0.65 ± 0.08‡	1.30 ± 0.04	0.68 ± 0.27	0.81 ± 0.21 **
SOD [U mL^{-1}]	61.78 ± 7.20	40.13 ± 5.71‡	65.31 ± 6.06	44.23 ± 5.52 *	56.75 ± 7.25 ***
GPx [U mL^{-1}]	8.43 ± 0.58	5.13 ± 1.62‡	9.13 ± 0.83	5.96 ± 1.34 *	7.02 ± 1.21 ***
GRx [U g^{-1} protein]	24.32 ± 2.41	17.05 ± 3.42‡	25.11 ± 2.12	18.67 ± 3.73	20.82 ± 3.48 **
TBARS [mmol g^{-1} protein]	24.04 ± 3.12	48.27 ± 6.8‡	23.91 ± 2.17	44.60 ± 4.32 *	35.13 ± 3.75 ***
Body weight gain and loss (g)	28.44 ± 2.50	-13.78 ± 3.13‡	30.18 ± 2.23***	18.30 ± 3.50***	-8.07 ± 3.40***

NC: Normal Control; DC: Diabetic Control; SR: Stevia Control; DTM: Diabetic rats treated with Metformin; DTS: Diabetic rats treated with Stevia. Each value represents mean ± SE (n = 8). ‡$p < 0.001$, compared with group 1 values, (* $p < 0.05$, **$p < 0.01$, *** $p < 0.001$ compared with group 2 values at the end of experiment. TG : triglyceride; TC : total cholesterol, HDL-c : High–density lipoprotein cholesterol. Superoxide dismutase (SOD), glutathione peroxidase (GPx), and glutathione reductase (GRx) and total antioxidant status (TAS), TBARS : Thiobarbituric acid reactive substances.

In contrast, Alloxan significantly increased serum TBARS levels in G2 ($p < 0.001$ by 50%) compared to G1. In G5, SR treatment reduced TBARS levels by 27% (Table 2). Body weight gain was significantly reduced ($p < 0.001$) in diabetic rats groups G2, G4, and G5 (–13.78 g, +18.30 g, and –8.07 g, by 7.13%, 8.84%, and 4%, respectively) when compared to the control group (+28.44 g), as shown in Table 2, whereas no significant changes were observed in G3, BWG (30.18 g) for the rats treated with SR. The same results were obtained for animals treated with Streptozotocin, a known diabetogen (Naveen et al., 2012; Assaei et al., 2016).

Histology

In diabetic rats, damage to the liver and pancreatic tissues causes insulin resistance, affecting glucose metabolism. Histological examinations of the pancreas and liver in diabetic animals were performed to determine whether SR could protect these tissues (Fig. 4). Normal (G1) and SR-fed (G3) rats' pancreatic and hepatic histopathology slides revealed no structural changes. The NC rats' pancreas structure had a regular size and shape with full and entire Langerhans islet organization and many pancreatic β–cells (Fig. 4). Diabetic rats in G2 have lower pancreatic β–cell islet mass, cell necrobiosis, and atrophied Langerhans islet.

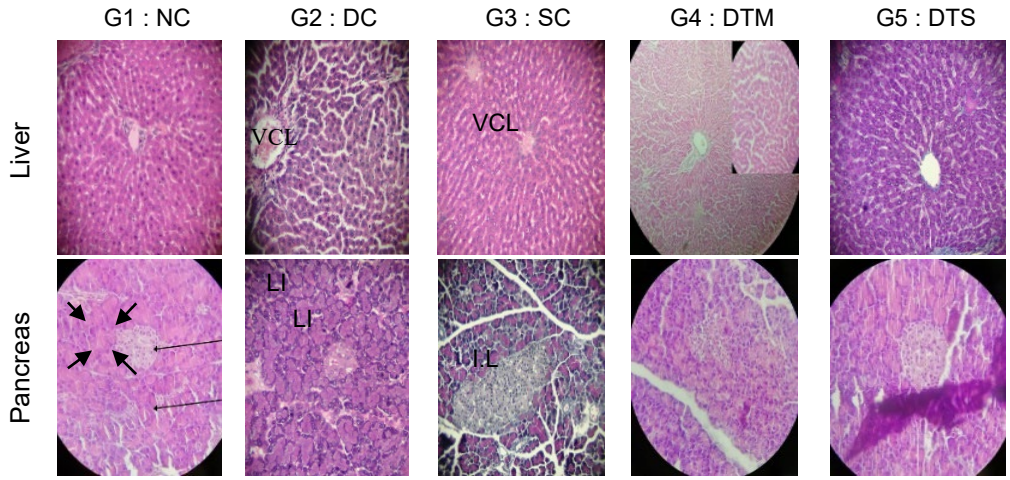

Figure 4. Effect of stevia on the pancreas and liver of normal and diabetic rats H&E, 40x and 10x. Group 1 [NC: the non-diabetic control], group 2 [DC: the diabetic control], group 3 [SC: Stevia control], group 4 [DTM: Diabetic rats treated with metformin], group 5 [DTS: Diabetic rats treated with Stevia], LI: Langerhans islet, AC: Acinus cells.

Treatment with either SR or Met alleviated these pathological changes (Fig. 4). Stevia aqueous extract stimulates active nuclei and regeneration and increases the number of β–cells in pancreatic islet-treated groups (G5). We also saw structural changes, decreased islet size and number, cell necrobiosis, condensed nuclei, and partial damage restoration in G4 pancreases. However, SR or Met treatment alleviated pathological changes (atrophied Langerhans islets, cell rupture, cytolysis, and apoptosis). It was discovered that islets regenerate, particularly in G5 (Fig. 4). As shown in Fig. 4, Stevia extract demonstrates nucleoprotein synthesis as evidenced by big cells

with several cytoplasmic granules, net vesicular nuclei and a high concentration of blood cells called eosinophils that play a role in the immune system stimulation. Studies conducted by Vaiserman et al. (2019a, 2019b); Jeppesen et al. (2000) have detailed the effect of diabetes on the pancreas, liver, glucose and insulin levels.

H&E staining revealed normal liver parenchyma with hepatocytes and central veins in G1 and G3, as shown in Fig. 4. On the other hand, most hepatocytes were damaged and inflamed, with rigid hepatic lobules, empty storage vesicles, and cell injury with central vein congestion, resulting in the premature death of liver cells by autolysis.

Similarly, in diabetic rats treated with Alloxan, the nucleus of hepatocytes showed significant pathological damage (G2). SR treatment, on the other hand, effectively alleviated non–hepatosteatosis and hepatocyte restoration (G5) (Fig. 4). Connective tissue with abnormal hepatocyte structure accompanied by damage and irritants cells in animals of G4.

DISCUSSION

Mesoxalylurea-Alloxan is an organic compound that inactivates islet β–cells and causes chemical diabetes in animals. Diabetes mellitus is a disorder of the metabolic mechanism that slowly sets in with IR, hyperglycemia, and hyperlipidemia. Then, the insulin allows cells to use and convert glucose into energy (Pankaj & Varma, 2013). Substances with no toxic an adverse effect that manages diabetes problems by improving IR and abnormally elevated levels of any or all lipids are needed. *Stevia rebaudiana* Bertoni (family: Asteraceae) commonly known as honey leaf-candy leaf or sweet herb is a perennial shrub of South America. There are 154 species of genus Stevia, and among them *S. rebaudiana* is the only species which synthesize steviol glycosides like stevioside, dulcoside A and rebaudioside (rebaudioside A, B, C, D and E) in its leaves (Taak et al., 2020). SR natural, non-caloric sugar substitute, is a rich source of pharmacologically important glycoside stevioside and has been employed in the world as a treatment for diabetic problems (Akbarzadeh et al., 2015; Ahmad & Ahmad, 2018; Abdel-Aal et al., 2021). The conventional strategies used for stevia cultivation are not reliable because of poor viability of seeds and germination percentage 8. Hence, to overcome such limitations, in vitro propagation is the only remedy that can facilitate large-scale production of genetically identical stevia plants (Jagatheeswari & Ranganathan, 2012; Taak et al., 2020).

In diabetic rats, SR treatment improved the biochemical, histological, and oxidative stress parameters studied. This improvement was also more pronounced in the SR than in the OAD group. Furthermore, most diabetic patients now prefer Stevia, a second option to artificial substances used instead of sugar to sweeten foods and drinks. Steviol glycosides are the most important component of SR because of the intensity of sweetness of a sweetener (300 times sweeter than saccharose) with zero caloric content (Park & Cha, 2010; Khiraoui et al., 2017).

This study aims to demonstrate the effect of Stevia on Alloxan-induced diabetes in rats based on this information. The role of Stevia in lowering glucose levels was investigated using FBG, insulin levels in plasma, and insulin resistance parameters.

When the Stevia treatment rats were compared to the control diabetic group, the results showed reduced blood glucose, insulin resistance (HOMA-IR), and increased insulin level and HOMA-B, as indicated by improved β–cell functions. These findings

support previous research on diabetic rats treated with 4% and 400 mg kg^{-1} b.w. after Streptozotocin injections at 60 and 40 mg kg^{-1} for 5 and 4 weeks, respectively (Naveen et al., 2012; Assaei et al., 2016). More than five mechanisms are leads to reduce BGL by SE through its chemical constituent, namely (Toskulkao et al., 1995; Chang et al., 2005; Naveen et al., 2012; Bender, 2016; Abdel-Aal et al., 2021):

1. Decreasing in the rate of glucose absorption by the intestines
2. Increasing the use of glucose in the muscles by eliminating glucose
3. Changing glucose transport
4. Regulation of gluconeogenesis,
5. Improving insulin sensitivity and/or secretion.

A higher HOMA–IR indicates Insulin-Resistance, whereas a lower HOMA-IR indicates Insulin-Sensitivity. We believe that decreased insulin secretion caused by Alloxan pancreatic damage increased insulin sensitivity. As a result, even at very low serum insulin levels, SR may still sensitize pancreatic system tissues to insulin force, assisting in the reduction of hyperglycemia. According to the DPPH and ABTS tests, stevia leaves have a high antioxidant potential due to polyphenols, flavonoids, and tannins (Krumina-Zemture et al., 2018; Peteliuk et al., 2021). These bioactive molecules with strong antioxidant properties promote the passage of the hormone secreted by the pancreatic ß–cells into the blood or the opposite of the blood glucose to other tissues (Gaweł-Bęben et al., 2015; Molina-Calle et al., 2017; Joseph et al., 2019).

The combination and control of arbuscular mycorrhizal fungi with the addition of P during the growth of stevia allows the modulation of the accumulation of bioactive compounds, improves the nutraceutical value and the exploitation of the raw material as a functional ingredient for foods, dietary supplements and cosmetics (Tavarini et al., 2020).

Previous research has also highlighted the importance of Stevia leaves' hypoglycemic components, which are high in diterpene glycosides and counteract free radicals, Rebaudioside A, stevioside, isosteviol, steviol, and polyphenolic compounds. These ingredients have been shown to help prevent diabetes and its complications (Wheeler et al., 2008; Thomas & Glade, 2010; Ameer et al., 2017; Ameer et al., 2020). Compared to the control, Alloxan elevated BGL contrary to insulin. The addition of MET to diabetic rats reversed these changes, as Met increases glucose utilization by muscles and decreases glucose absorption mechanisms from the intestinal tract (Goodman et al., 2011; Jin et al., 2017; Ibrahim Ahmed et al., 2019).

Some researchers have proposed that, in addition to sweetness and stevioside, the extract obtained from SR-leaves, as well as related compounds such as rebaudioside A, steviol, and isosteviol, may have curative and/or preventive health benefits, including hyperglycemia and blood pressure, oxidation, tumors, diarrhea, stomach, kidney and immune disorders and others (Chatsudthipong & Muanprasat, 2009; Lemus-Mondaca et al., 2012; Periche et al., 2014; Ramos-Tovar et al., 2019). Because the increases in mean GOT and GPT enzymes, urea, and creatinine were relatively higher after Alloxan induction, the findings suggest that the increases in liver and urinary serum parameters were due to physiological rather than toxicological effects. Our findings show that the Stevia supplement improved hepatic and urinary parameters in diabetic rats by significantly lowering GOT, GPT, urea, and creatinine serum levels over 28 days.

Other studies have suggested that Stevia can improve human and animal liver health by lowering serum hepatic biomarkers with daily administration of Stevia (400 mg kg^{-1} b.w.) for four weeks. This could be due to the antioxidant activity of SR combined with free radical–scavenging activity provided by the DPPH and ABTS tests (Assaei et al., 2016; Muriel et al., 2017). According to Carakostas et al. (2008), male rats treated with rebaudioside A have higher plasma urea and creatinine concentrations than female rats. Another study found no significant changes in the blood parameters listed below after long-term stevioside sweetener feeding in male rats (Awney et al., 2010). Anomalies in the lipid and lipoprotein profiles are metabolic factors that contribute to insulin resistance. However, increased total cholesterol, triglyceride serum, and decreased good cholesterol levels in DC rats could be a sign of increased pyruvate dehydrogenase activity (Ford et al., 2008; Latha & Daisy, 2011; Zhang et al., 2013; Castro et al., 2015).

The findings also highlight that taking Stevia aqueous extract daily significantly changes the lipid profile. This spot is reliable with Sharma et al. (2009) research which found that TC and TGs were significantly reduced after one month of daily Stevia extract consumption in women with high cholesterol, while HDL–c was increased in experimental animals (Sudha et al., 2017; Ahmad et al., 2018; Abdel-Aal et al., 2021). The effect of Stevia on lipid characteristics in G2 demonstrates that SR has good hypolipidemic properties. A wealth of information is available regarding using SR to prevent cardiovascular complications in diabetic patients (Khiraoui et al., 2017). As a result, it is possible that consuming SR may help to reduce the prevalence of diabetes and hyperlipidemia and good management of glycemic metabolism. Metformin has also been shown in diabetic animals to have mild hypolipidemic effects. The effect was seen in all parameters studied, including TGs, TC, and HDL-c.

Compared to control male rats, treatment with a high dose of stevioside (1,500 mg kg^{-1} b.w/day), Rebaudioside A and SH significantly increased total cholesterol and HDL-c levels. This is explained by changes in bile acid homeostasis (Nikiforov & Eapen, 2008; Awney et al., 2010). By producing reactive oxygen species, environmental factors and stress levels in animals, Alloxan causes oxidative damage (Sapsuha et al., 2022). As a result, Stevia's hepatoprotective properties and antioxidant effects on pancreatic activity can be used to manage diabetes-related oxidative stress (Kangralkar et al., 2010; Assaei et al., 2016). Stevia aqueous extract significantly increased stress oxidant parameters (TAS, GPx, GRx, and SOD), which are enzymes that degrade free radicals. ABTS levels were significantly reduced. Our conclusions are consistent with those of Naveen et al. (2012), who discovered that feeding diabetic rats with Stevia leaves in their various states reverses the effect of ROS molecules and reactive oxygen species accompanied by lowering MDA levels. Many studies have shown that SR contains numerous biomolecules (*steviosides, polyphenols, flavonoids, alkaloids, water–soluble chlorophylls and xanthophylls, hydroxycinnamic acids, austroinullin, β–carotene, dulcoside, nilacin, rebaudi oxides, riboflavin, steviol and thiamine)* that have antioxidant activity, prevent oxidative DNA damage, inhibit lipid peroxidation in diabetic rats, and significantly increase GSH levels (Gezer et al., 2006; Turkoglu et al., 2007; Jayaraman et al., 2008; Khiraoui et al., 2017; Rotimi et al., 2018).

Serum insulin levels were found to be higher in the Stevia-treated groups in this study. This means some biomolecules in Stevia may stimulate beta cells to release insulin, thereby improving carbohydrate metabolizing enzymes and restoring normal BGL. Moreover, this finding demonstrates that Stevia can improve glucose tolerance and cellular insulin sensitivity (Naveen et al., 2012; Assaei et al., 2016). Rats in the diabetic model Group induced by Alloxan lost weight gradually. Alloxan is toxic, causing pancreatic, hepatic, and renal damage. This type of diabetes causes weight loss, muscle wasting, and the degradation of the muscle protein complex over time (Naveen et al., 2012; Han et al., 2022). In contrast, oral administration of SR, a non-caloric natural sweetener, to G2:DC rats at the last of the experiment highlighted a critical augmentation in BWG, pointing out that Stevia considerably enhanced their health status and she has launched a series of metabolic processes by good blood sugar management and reversed gluconeogenesis (Abdel-Daim & Halawa, 2014; Ameer et al., 2020).

This study also examined how islet endocrine cell populations reorganized during the development of alloxan diabetes in rats. Alloxan is thought to cause Type 1 diabetes by damaging islets of Langerhans β–cells (Aissaoui et al., 2017; Ibrahim Ahmed et al., 2019). In insulin-dependent diabetes, islet α and δ cells are unused autoimmune destruction directed at beta-cells. This result encourages increasing non-beta endocrine cells in the islet core (Plesner et al., 2014). Alloxan is a crystalline compound $C_4H_2N_2O_4$, a toxic glucose analog, which selectively destroys insulin-producing cells in the pancreas when administered to animal species, damaging cell membrane structure, and generating harmful molecules ROS, reactive oxygen species, which are indirectly responsible for causing pancreatic tissue failure, particularly β–cells, and activating protein kinases, hexosamines, and others (Jorns et al., 1997; Ha & Kim, 1999; Brownlee, 2005; Simmons, 2012; Han et al., 2022).

SE may scavenge free radicals and aid in the reconstruction of pancreatic units, allowing them to release more insulin, resulting in an anti–diabetic effect. By revitalizing pancreatic β-cells and antagonizing Alloxan's β-necrotic action, SR synthesized and aggregated insulin in diabetic rats' pancreas tissue (Misra et al., 2011; Assaei et al., 2016). Furthermore, no evidence of pancreas or liver tissue disorder was observed in histo-pathology slides after SE gavage in Group 1. MET did not significantly affect pancreatic islet cell size in the diabetic Group (Jin et al., 2017). After SR treatment, diabetic rats had moderately sized islets of Langerhans with active nuclei cells (G5). Stevia leaves may protect rats from acute and hepatic toxicity, disturbance in the balance between the production of reactive oxygen species (free radicals) and antioxidant defenses, cellular damage and death and a decrease in biliary secretion known by cholestasis by improving the endogenous antioxidant system and exerting anti-inflammatory activity (Shakoori et al., 1994). Stevia leaf primarily benefits from its bioactive, biochemical, and nutritional composition, which are mostly related to the harvest time and P supply. They are original organic phenolic compounds (total phenols and flavonoids as well as antioxidant activities, carbohydrates, protein, and crude fiber), promoting wellness and decreasing metabolic attacks (Najafian & Moradi, 2017; Tavarini et al., 2020).

CONCLUSION

This study investigated the ant-diabetic activity and potential antioxidant mechanism of SR in diabetic rats caused by Alloxan. The findings show that an aqueous extract of Stevia has anti-diabetic effects by lowering abnormal biochemical and histological parameters and oxidative stress markers in rats with Alloxan-induced diabetes. Natural Stevia's antioxidant potential and relevant bioactive properties appeal to consumers.

Further research in the field covering metabolic and health disorders presented in this article are necessary, citing the most important research perspectives, the biological activity of SR and its relationship to human health; the use of other parts of the shrub such as flowers, stems or seeds, and find solutions to stevia cultivation problems to increase yields and reduce costs. The industrial application of SR to prevent diseases that set in over time from food additives and chemical sweeteners. Finally, the use of stevia as a treatment for other diseases. Human applications are desirable too.

ACKNOWLEDGMENTS. The authors would like to express their gratitude to the National Institute Pasteur (Medical Center in Algeria) and the National Higher School of Agronomy in Algiers, Algeria, for providing technical assistance in evaluating the biological effects of *Stevia rebaudiana*.

REFERENCES

Abdel-Aal, R.A., Abdel-Rahman, M.S., Al Bayoumi, S. & Ali, L.A. 2021. Effect of Stevia aqueous extract on the antidiabetic activity of saxagliptin in diabetic rats. *J Ethnopharmacol* **265**, 113188. doi: 10.1016/j.jep.2020.113188

Abdel-Daim, M. & Halawa, S. 2014. Synergistic hepatocardio protective and antioxidant effects of myrrh and ascorbic acid against diazinon–induced toxicity in rabbits. *Int. Research Journal Humanit Eng. Pharmaceutical Sciences* **1**, 1–7. Available at https://api.semanticscholar.org/CorpusID:88227618?utm_source=wikipedia

Ahmad, N., Fazal, H., Abbasi, B.H. & Farooq, S. 2010. Efficient free radical scavenging activity of Ginkgo biloba, *Stevia rebaudiana* and *Parthenium hysterophorous* leaves through DPPH (2, 2–diphenyl–1–picrylhydrazyl). *Int. J. Phytomed* **2**(2), 231–239. doi: 10.5138/ijpm.2010.0975.0185.02034

Ahmad, U., Ahmad, R.S., Arshad, M.S., Musthaq, Z., Hussain, S.M. & Hameed, A. 2018. Antihyperlipidemic efficacy of aqueous extract of *Stevia rebaudiana* Bertoni in albino rats. *Lipids Health Dis* **17**(1), 1–8. doi: 10.1186/s12944-018-0810-9

Ahmad, U. & Ahmad, R.S. 2018. Anti diabetic property of aqueous extract of *Stevia rebaudiana* Bertoni leaves in streptozotocin-induced diabetes in albino rats. *BMC Complementary and Alternative Medicine* **18**(1), 179. doi: 10.1186/s12906-018-2245-2

Aissaoui, O., Amiali, M., Bouzid, N., Belkacemi, K. & Arezki, B. 2017. Effect of *Spirulina platensis* ingestion on the abnormal biochemical and oxidative stress parameters in the pancreas and liver of alloxan-induced diabetic rats. *Pharm Biol.* **55**(1), 1304–1312. doi: 10.1080/13880209.2017.1300820

Akbarzadeh, S., Eskandari, F., Tangestani, H., Bagherinejad, S.T., Bargahi, A., Bazzi, P., Daneshi, A., Sahrapoor, A., O'Connor, W.J. & Rahbar, A.R. 2015. The Effect of *Stevia Rebaudiana* on Serum Omentin and Visfatin Level in STZ–Induced Diabetic Rats. *Journal of Dietary Supplements* **12**(1), 11–12. doi: 10.3109/19390211.2014.901999

Ameer, K., Bae, S.W., Jo, Y., Lee, H.G., Ameer, A. & Kwon, J.H. 2017. Optimization of microwave-assisted extraction of total extract, stevioside and rebaudioside–A from *Stevia rebaudiana* (Bertoni) leaves, using response surface methodology (RSM) and artificial neural network (ANN) modelling. *Food Chem* **229**, 198–207. doi: 10.1016/j.foodchem.2017.01.121

Ameer, K., Jiang, J.H., Amir, R.M. & Eun, J.B. 2020. Chapter 33–Antioxidant potential of *Stevia rebaudiana* (Bertoni). *Pathology, Oxidative Stress and Dietary Antioxidants* pp. 345–356. doi: 10.1016/B978-0-12-815972-9.00033-0

Assaei, R., Mokarram, P., Dastghaib, S., Darbandi, S., Darbandi, M., Zal, F., Akmali, M. & Ranjbar Omrani, G.H. 2016. Hypoglycemic effect of aquatic extract of Stevia in pancreas of diabetic rats: PPARγ-dependent regulation or antioxidant potential. *Avicenna J. Med. Biotech.* **8**(2), 65–74. PMCID: PMC4842244, PMID: 27141265

Awney, H.A., Massoud, M.I. & El-Maghrabi, S. 2010. Long–term feeding effects of stevioside sweetener on some toxicological parameters of growing male rats. *J. Appl. Toxicol.* **31**(5), 431–438. doi: 10.1002/jat.1604

Barba, F.J., Grimi, N. & Vorobiev, E. 2015. Evaluating the potential of cell disruption technologies for green selective extraction of antioxidant compounds from *Stevia rebaudiana* Bertoni leaves. *J. Food Eng.* **149**, 222–228. doi: 10.1016/j.jfoodeng.2014.10.028

Bender, C. 2016. *Stevia rebaudiana*'s antioxidant properties. In: Merillon, J.M., Ramawat, K., editors. Sweeteners. Reference series in phytochemistry. San Diego, Cham: *Springer International Publishing* pp. 1–27.

Brownlee, M. 2005. The pathobiology of diabetic complications: a unifying mechanism. *Diabetes* **54**(6), 1615–1625. doi: 10.2337/diabetes.54.6.1615

Carakostas, M.C., Curry, L.L., Boileau, A.C. & Brusick, D.J. 2008. Overview: the history, technical function and safety of rebaudioside A, a naturally occurring steviol glycoside, for use in food and beverages. *Food Chem Toxicol* **46**(7), S1–S10. doi: 10.1016/j.fct.2008.05.003

Castro, G.S.D., Deminice, R., Simões-Ambrosio, L.M.C., Calder, P.C., Jordão A.A. & Vannucchi, H. 2015. Dietary docosahexaenoic acid and eicosapentaenoic acid influence liver triacylglycerol and insulin resistance in rats fed a high-fructose diet. *Mar Drugs* **13**(4), 1864–1881. doi: 10.3390/md13041864

Chang, C., Yang, M. & Wen Handhern, J. 2002. Estimation of total flavonoid content in propolis by two complementary colorimetric methods. *Food Drug Anal* **10**(3), 178–182. doi: 10.38212/2224-6614.2748

Chang, J.C., WU, M., Liu, I.M. & Cheng, J.T. 2005. Increase of insulin sensitivity by stevioside in fructose-rich chow–fed rats. *Hormone and Metabolic Research* **37**(10), 610–616. doi: 10.1055/s-2005-870528

Chatsudthipong, V. & Muanprasat, C. 2009. Stevioside and related compounds: Therapeutic benefits beyond sweetness. *Pharmacology et Therapeutics* **121**(1), 41–54. doi: 10.1016/j.pharmthera.2008.09.007

Ford, E.S., Li, C. & Sattar, N. 2008. Metabolic syndrome and incident diabetes: current state of the evidence. *Diabetes care* **31**(9), 1898–1904. DOI: 10.2337/dc08-0423

Gaweł-Bęben, K., Bujak, T., Nizioł-Łukaszewska, Z., Antosiewicz, B., Jakubczyk, A., Karas, M. & Rybczyńska, K. 2015. *Stevia rebaudiana* Bert. leaf extracts as a multifunctional source of natural antioxidants. *Molecules* **20**(4), 5468–5486. doi: 10.3390/molecules20045468

Gezer, K., Duru, E., Kivrak Turkaglu, A., Mercan, N., Turkoglu, H. & Gukan, S. 2006. Free radical scavenging capacity and antimicrobial activity of wild edible mushroom from Turkey. *Afr. J. Biotechnol.* **5**(20), 1924–1928. doi: 10.5897/AJB2006.000-5073

Gomori, G. 1950. Aldehyde–fuchsin, a new staining for elastic tissue. *Am. J. Clin. Pathol* **17**, 665–666.

Goodman, L.S., Brunton, L.L., Chabner, B. & Knollmann, B.C. 2011. Goodman and Gilman's The pharmacological basis of therapeutics. 10th edition, New York: McGraw-Hill. doi: 10.1021/jm020026w

Ha, H. & Kim, K.H. 1999. Pathogenesis of diabetic nephropathy: the role of oxidative stress and protein kinase C. *Diabetes Res Clin Pract* **45**(2-3), 147–151. doi: 10.1016/s0168-8227(99)00044-3

Han, Q., Sun, J., Xie, W., Bai, Y., Wang, S., Huang, J., Zhou, S., Li, Q., Zhang, H. & Tang, Z. 2022. Repeated Low–Dose Streptozotocin and Alloxan Induced Long-Term and Stable Type 1 Diabetes Model in Beagle Dogs. *BioMed Research International* Article ID 5422287, 6 pages. doi: 10.1155/2022/5422287

Hernández, E.L., Jiménez, P.G. & Sevilla, J.J.M. 2020. Therapeutic strategy in diabetic patient (II). Oral lipid-lowering drugs. Advices to the patient. *Medicine* **13**(17), 949–956. doi: 10.1038/s41440-021-00773-4

Hirich, E.H., Bouizgarne, B., Zouahri, A. & Azim, K. 2022. Agronomic Practices and Performances of Stevia rebaudiana bertoni under Field Conditions: A Systematic Review. *Environ. Sci. Proc* **16**(44). doi.org/10.3390/ environsciproc2022016044

Ibrahim Ahmed, M.A., Fudal Idris, O., Asad, A., Abdelsalam Ahmed, K., Ali Mohammed, A.M. & AI Alyahya, A.R. 2019. Effect of olive oil on insulin release, insulin resistance and lipid profile and its interaction with metformin in alloxan induced diabetic rats. *Int. J. Biol. Biotech.* **16**(4), 895–900. Available at (17) EFFECT OF OLIVE OIL ON INSULIN RELEASE, INSULIN RESISTANCE AND LIPID PROFILE AND ITS INTERACTION WITH METFORMIN IN ALLOXAN INDUCED DIABETIC RATS. | Request PDF (researchgate.net)

Jagatheeswari, D. & Ranganathan, P. 2012. Studies on Micropropagation of *Stevia rebaudiana* Bert. *Int. J. Pharm. Biol. Archit*. **3**, 315–320.

Jayaraman, S., Manoharan, M. & Illanchezian, S. 2008. In–vitro antimicrobial and antitumor activities of *Stevia rebaudiana* (Asteraceae) leaf extracts. *Trop J Pharm Res* **7**(4), 1143–1149.

Jeppesen, P.B., Gregersen, S., Poulsen, C.R. & Hermansen, K. 2000. Stevioside acts directly on pancreatic β cells to secrete insulin: Actions independent of cyclic adenosine monophosphate and adenosine triphosphate-sensitivie K+-channel activity. *Metabolism* **49**(2), 208–14. doi.org/10.1016/S0026-0495(00)91325-8

Jiménez, P.G., Martín-Carmona, J. & Hernández, E.L. 2020. Diabetes mellitus. *Medicine-Programa de Formación Médica Continuada Acreditado* **13**(16), 883–890. doi: 10.1016/j.med.2020.09.010

Jin, J., Lim, S.W., Jin, L., Yu, J.H., Kim, H.S., Chung, B.H. & Yang, C.W. 2017. Effects of metformin on hyperglycemia in an experimental model of tacrolimus- and sirolimusinduced diabetic rats. *Korean J. Intern. Med.* **32**(2), 314–322. doi: 10.3904/kjim.2015.394

Jorns, A., Munday, R., Tiedge, M. & Lenzen, S. 1997. Comparative toxicity of alloxan, N–alkyl-alloxans and ninhydrin to isolated pancreatic islets in-vitro. *J Endocrinol* **155**(2), 283–93. doi: 10.1677/joe.0.1550283

Joseph, D., George, J., Mathews, M.M., Mathew, F., Varghese, B. & Sunny, B. 2019. A comprehensive exploration on therapeutic options of *Stevia rebaudiana* with emphasize on anti–diabetic attribute. *Res. J. Pharm Technol.* **12**(10), 4981–4988. doi: 10.5958/0974-360X.2019.00863.1

Kameswara Rao, B., Kesavulu, M.M., Giri, R. & Appa Rao, C. 1999. Antidiabetic and hypolipidemic effects of *Momordica cymbalaria* Hook. Fruit powder in alloxan–diabetic rats. *J. Ethnopharmacol* **67**(1), 103–109. doi: 10.1016/s0378-8741(99)00004-5

Kangralkar, V., Shivraj, A., Patil, D. & Bandivadekar, R.M. 2010. Oxidative stress and diabetes: A review. *International Journal of Pharmaceutical Applications* **1**(1), 38–45. Available at https://api.semanticscholar.org/CorpusID:27294896?utm_source=wikipedia

Kasti, A.N., Nikolaki, M.D., Synodinou, K.D., Katsas, K.N., Petsis, K., Lambrinou, S, Pyrousis I.A. & Triantafyllou, K. 2022. The Effects of Stevia Consumption on Gut Bacteria: Friend or Foe? *Microorganisms* **10**, 744. doi: 10.3390/microorganisms10040744

Khiraoui, A., Hasib, A., Al Faiz, C., Amchra, F., Bakha, M. & Boulli, A. 2017. *Stevia Rebaudiana* Bertoni (Honey Leaf): A magnificent natural bio-sweetener, biochemical Ccomposition, nutritional and therapeutic values. *J Nat Sci Res* **7**(14), 75–85. Available at (17) (PDF) *Stevia rebaudiana* Bertoni (Honey Leaf): A Magnificent Natural Bio-sweetener, Biochemical Composition, Nutritional and Therapeutic Values (researchgate.net)

Krumina-Zemture, G., Beitane, I. & Cinkmanis, I. 2018. Flavonoids and total phenolic content in extruded buckwheat products with sweet and salty taste. *Agronomy Research* **16**(S2), 1425–1434. doi: 10.15159/AR.18.042

Latha, R.C.R. & Daisy, P. 2011. Insulin–secretagogue, antihyperlipidemic and other protective effects of gallic acid isolated from *Terminalia bellerica* Roxb in streptozotocin-induced diabetic rats. *Chem-Biol Interact* **189**(1–2), 112–118. doi: 10.1016/j.cbi.2010.11.005

Lemus-Mondaca, R., Vega-Gálvez, A., Zura-Bravo, L. & Ah-Hen, K. 2012. *Stevia rebaudiana* Bertoni, source of a high-potency natural sweetener: a comprehensive review on the biochemical, nutritional and functional aspects. *Food Chem* **132**(3), 1121–1132. doi: 10.1016/j.foodchem.2011.11.140

Makkar, H.P.S., Blummel, M., Borowy, N.K. & Becker, K. 1993. Gravimetric determination of tannins and their correlations with chemical and protein precipitation methods. *J. Sci. Food Agric.* **61**(2), 161–165. doi: 10.1002/jsfa.2740610205

Misra, H., Soni, M., Silawat, N., Mehta, D., Mehta, B.K. & Jain, D.C. 2011. Antidiabetic activity of medium-polar extract from the leaves of *Stevia rebaudiana* Bert. (Bertoni) on Alloxan-induced diabetic rats. *J Pharm Bioall Sci* **3**(2), 242–8. doi: 10.4103/0975-7406.80779

Mohammad, AL-Mamun, Shuvo, M.M.A. & Absar, N. 2018. In Vitro Determination of Total Phenolics, Flavonoids and Free Radical Scavenging Activities of *Stevia rebaudiana* Dry Leaves Powder in Different Solvents Extract. *EC Nutrition* **13**(3), 71–78.

Molina-Calle, M., Priego-Capote, F. & Luque, de Castro, M.D. 2017. Characterization of stevia leaves by LCQTOF MS/MS analysis of polar and non–polar extracts. *Food Chem* **219**, 329–338. doi: 10.1016/j.foodchem.2016.09.148

Muriel, P., Ramos-Tovar, E., Montes-Páez, G. & Buendía-Montaño, L.D. 2017. Experimental models of liver damage mediated by oxidative stress. In: Muriel P, editor. *Liver pathophysiology* 529–546.

Najafian, S. & Moradi, M. 2017. Polyphenolic compounds (HPLC analysis) and antioxidant activity of *Stevia rebaudiana* (Asteraceae) by FRAP and DPPH assay in greenhouse and free space condition. *Int. J. Farm & Alli. Sci.* **6**(2), 49–55. Available at http://ijfas.com/wp-content/uploads/2017/04/49-55.pdf

Naveen, S., Mahadev, N., Farhath, K. & Vijay, K.K. 2012. Antioxidant, anti-diabetic and renal protective properties of *Stevia rebaudiana*. *J Diabetes Complications* **27**(2), 103–113. doi: 10.1016/j.jdiacomp.2012.10.001

Nikiforov, A.I. & Eapen, A.K. 2008. A 90-day oral (dietary) toxicity study of rebaudioside A in Sprague–Dawley rats. *Int. J. Toxicol.* **27**(1), 65–80. doi: 10.1080/10915810701876

Ozola, B. & Dūma, M. 2020. Antioxidant content of dark colored berries. *Agronomy Research* **18**(S3), 1844–1852. doi : 10.15159/AR.20.123.

Pankaj, P.P. & Varma, M.C. 2013. Potential role of *Spirulina platensis* in maintaining blood parameters in alloxan-induced diabetic mice. *Int. J. Pharm Sci.* **5**, 450–456. Available at (17) Potential role of spirulina platensis in maintaining blood parameters in alloxan induced diabetic mice | Request PDF (researchgate.net)

Park, J.E. & Cha, Y.S. 2010. *Stevia rebaudiana* Bertoni extract supplementation improves lipid and carnitine profiles in C57BL/6J mice fed a high-fat diet. *J. Sci. Food Agric.* **90**(7), 1099–1105. doi: 10.1002/jsfa.3906

Patel, S. & Navale, A. 2023. The Natural Sweetener Stevia: An Updated Review on its Phytochemistry, Health Benefits, and Anti-diabetic study. *Curr Diabetes Rev* **20**(2), e010523216398. doi: 10.2174/1573399819666230501210803

Periche, A., Koutsidis, G. & Escriche, I. 2014. Composition of antioxidants and amino acids in Stevia leaf infusions. *Plant Foods Hum Nutr* **69**(1), 1–7. doi: 10.1007/s11130-013-0398-1

Peteliuk, V., Rybchuk, L., Bayliak, M., Storey, K.B. & Lushchak, O. 2021. Natural sweetener *Stevia rebaudiana*: Functionalities, health benefits and potential risks. *EXCLI J.* **22**(20), 1412–1430. doi: 10.17179/excli2021-4211

Plesner, A., ten Holder, J.T. & Verchere, C.B. 2014. Islet Remodeling in Female Mice with Spontaneous Autoimmune and Streptozotocin-Induced Diabetes. *PLoS ONE* **9**(8), e102843. doi: 10.1371/journal.pone.0102843

Quintanilha, A.T., Packer, L., Davies, J.M., Racanelli, T.L. & Davies, K.J. 1982. Membrane effects of vitamin E deficiency: bioenergetic and surface charge density studies of skeletal muscle and liver mitochondria. *Ann N. Y. Acad Sci.* **393**(1), 32–47. doi: 10.1111/j.1749-6632.1982.tb31230.x

Ramos-Tovar, E., Flores-Beltrána, R.E., Galindo-Gómez, S., Camachoc, J., Tsutsumi, V. & Muriel, P. 2019. An aqueous extract of *Stevia rebaudiana* variety Morita II prevents liver damage in a rat model of cirrhosis that mimics the human disease. *Annals of Hepatology* **18**(3), 472–479. doi: 10.1016/j.aohep.2018.10.002

Rotimi, S.O., Rotimi, O.A., Adelani, I.B., Onuzulu, C., Obi, P. & Okungbaye, R. 2018. Stevioside modulates oxidative damage in the liver and kidney of high fat/low streptozocin diabetic rats. *Heliyon* **4**(5), e00640. doi: 10.1016/j.heliyon.2018.e00640

Sacan, O. & Yanardag, R. 2010. Antioxidant and antiacetylcholineesterase activities of chard (*Beta vulgaris* L. var. cicla). *Food Chem Toxicol* **48**(5), 1275–1280. doi: 10.1016/j.fct.2010.02.022

Şahin, F., Güllüce, M., Daferera, D., Sökmen, A., Sökmen, M., Polissiou, M., Agar, G. & Özer, H. 2004. Biological activities of the essential oils and methanol extract of *Origanum vulgare ssp*. vulgare in the Eastern Anatolia region of Turkey. *Food Control* **15**(7), 549–557. doi: 10.1016/j.foodcont.2003.08.009

Sapsuha, Y., Suprijatna, E., Kismiati, S. & Sugiharto, S. 2022. Possibility of using nutmeg flesh (Myristica fragrans houtt) extract in broiler diet to improve intestinal morphology, bacterial population, blood profile and antioxidant status of broilers under high-density condition. *Agronomy Research* **20**(S1), 1134–1150. doi : 10.15159/AR.22.077

Savita, S.M., Sheela, K., Sunanda, S., Shankar, A.G. & Ramakrishna, P. 2017. *Stevia rebaudiana*–A functional component for food industry. *J. Hum. Ecol.* **15**, 261–264. doi: 10.1080/09709274.2004.11905703

Serio, L. 2010. La *Stevia rebaudiana*, une alternative au sucre. *Phytothérapie* **8**(1), 26–32. doi.org/10.1007/s10298-010-0526-4

Shakoori, A.R., van Wijnen, A.J., Bortell, R., Owen, T.A., Stein, J.L., Lian, J.B. & Stein, G.S. 1994. Variations in vitamin D receptor transcription factor complexes associated with the osteocalcin gene vitamin D responsive element in osteoblasts and osteosarcoma cells. *J. Cell. Biochem.* **55**(2), 218–229. doi: 10.1002/jcb.240550209

Sharma, N., Mogra, R. & Upadhyay, B. 2009. Effect of Stevia extract intervention on lipid profile. *Studies on ethno–medicine* **3**(2), 137–140. http://www.krepublishers.com/02-Journ...

Shukla, S., Mehta, A., Mehta, P. & Bajpai, V.K. 2012. Antioxidant ability and total phenolic content of aqueous leaf extract of *Stevia rebaudiana* Bert. *Exp. Toxicol. Pathol.* **64**(7–8), 807–811. doi:10.1016/j.etp.2011.02.002

Simmons, R.A. 2012. Developmental origins of diabetes: The role of oxidative stress. *Best Pract. Res. Clin Endocrinol Metab.* **26**(5), 701–708. doi:10.1016/j.beem.2012.03.012

Singleton, V.L., Orthofer, R. & Lamuela–Raventos, R.M. 1999. Analysis of total phenols and other oxidation substrates and antioxidants by means of Folin–Ciocalteu reagent. *Methods Enzymol* **299**, 152–178. doi:10.1016/s0076-6879(99)99017-1

Song, Y., Manson, J.E., Tinker, L., Howard, B.V., Kuller, L.H., Nathan, L., Rifal, N. & Liu, S. 2007. Insulin sensitivity and insulin secretion determined by homeostasis model assessment and risk of diabetes in a multiethnic cohort of women. The women's health initiative observational study. *Diabetes care* **30**(7), 1747–1752. doi: 10.2337/dc07-1288

Sudha, T., Devi, D.A. & Kaviarasan, L. 2017. Antihyperlipidemic effect of *Stevia rebaudiana* on alloxan induced diabetic rats. *Asian J. pharm technol.* **7**(4), 202–208.

Taak, P., Tiwari, S. & Koul, B. 2020. Optimization of regeneration and *Agrobacterium*-mediated transformation of Stevia (*Stevia rebaudiana* Bertoni): a commercially important natural sweetener plant. *Sci. Rep.* **10**, 16224. doi.org/10.1038/s41598-020-72751-8

Tavarini, S., Clemente, C., Bender, C. & Angelini, L.G. 2020. Health-Promoting Compounds in Stevia: The Effect of Mycorrhizal Symbiosis, Phosphorus Supply and Harvest Time. *Molecules* **25**(22), 5399. doi: 10.3390/molecules25225399

Thomas, J.E. & Glade, M.J. 2010. Stevia: it's not just about calories. *Open Obes. J.* **2**(1), 101–109. doi: 10.2174/1876823701103010085

Toskulkao, C., Sutheerawatananon, M., Wanichanon, C., Saitongdee, P. & Suttajit, M. 1995. Effects of stevioside and steviol on intestinal glucose absorption in hamsters. *J. Nutr. Sci. Vitaminol* **41**(1), 105–113. doi: 10.1016/0378-4274(95)03391-w

Turkoglu, A., Duru, M.E., Mercan, N., Kivrak, I. & Gezer, K. 2007. Antioxidant and antimicrobial activities of *Laetiporus sulphureus* (Bull.) Murill. *Food Chem* **101**(1), 267–273. doi:10.1016/j.foodchem.2006.01.025

Vaiserman, A., Koliada, A. & Lushchak, O. 2020a. Neuroinflammation in pathogenesis of Alzheimer's disease: Phyto-chemicals as potential therapeutics. *Mech Ageing Dev* **189**, 111259. doi: 10.1016/j.mad.2020.111259

Vaiserman, A., Koliada, A., Zayachkivska, A. & Lushchak, O. 2020b. Curcumin: A therapeutic potential in ageing-related disorders. *PharmaNutrition* **14**, 100226. doi.org/10.1016/j.phanu.2020.100226

Wheeler, A., Boileau, A.C., Winkler, P.C., Compton, J.C., Prakash, I., Jiang, X. & Mandarino, D.A. 2008. Pharmacokinetics of rebaudioside A and stevioside after single oral doses in healthy men. *Food Chem. Toxicol* **46**(7), S54–S60. doi: 10.1016/j.fct.2008.04.041

Yu, H., Yang, G., Sato, M., Yamaguchi, T., Nakano, T. & Xi, Y. 2017. Antioxidant activities of aqueous extract from *Stevia rebaudiana* stem waste to inhibit fish oil oxidation and identification of its phenolic compounds. *Food Chem* **232**, 379–386. doi: 10.1016/j.foodchem.2017.04.004

Zhang, Y.H., An, T., Zhang, R.C., Zhou, Q., Huang, Y. & Zhang, J. 2013. Very high fructose intake increases serum LDL–cholesterol and total cholesterol: A meta-analysis of controlled feeding trials. *J. Nutr.* **143**(9), 1391–1398. doi: 10.3945/jn.113.175323

Agronomy Research **22**(1), 52–71, 2024
https://doi.org/10.15159/AR.24.031

Fusarium head blight in winter wheat: development peculiarities and protective strategies

G.V. Avagyan[1,*] and H.S. Martirosyan[2]

[1]Armenian National Agrarian University, Chair of Horticulture and Plant Protection, 74 Teryan Str., AM0009 Yerevan, Republic of Armenia (RA)
[2]'Agrobiotechnology Scientific Center' Branch of Armenian National Agrarian University (ANAU), 1 Isi–Le–Mulino Str., AM1101 Ejmiatsin, Republic of Armenia (RA)
[*]Correspondence: gayaneavagyan@yahoo.com

Received: February 24th, 2024; Accepted: April 25th, 2024; Published: May 2nd, 2024

Abstract. *Fusarium* head blight (FHB, caused by the fungal plant pathogen *Fusarium graminearum* Schwabe) is a widespread fungal disease in the Republic of Armenia, affecting various cereal crops, including wheat, leading to a decrease in productivity and grain quality. However, comprehensive research aimed at selecting proper fungicides and determining the optimal application timing has not been conducted before.
FHB can undergo epidemic development during years characterized by favorable weather conditions. Conversely, during periods of adverse weather conditions, the severity and incidence of FHB tend to decrease notably. Abundant rainfall and mild temperatures render plants more susceptible, facilitating the spread of infection not only during the flowering of winter wheat but also at the waxy ripening stage, thereby increasing the risk of an FHB epidemic.
The experiments were carried out during the 2022 and 2023 growing seasons under rain-fed conditions, with the primary focus on treating winter wheat with triazole group fungicides.
During years with adverse weather conditions for FHB development, a single application of Falcon (0.5 L ha^{-1}) or Prosaro (1.0 L ha^{-1}) at Feekes 10.5.1 proved to be an effective strategy for managing FHB, particularly when integrated with cultural practices. These treatments provided a biological efficacy of 80.6% to 83.3% at Feeks 11.2, and from 76.6% to 79.4% at harvest, respectively, increasing wheat yield by 37.62% to 42.9%.
In the case of epidemic development of FHB during years with more favorable weather conditions, a double fungicide treatment (Falcon or at Feekes 10.3 and Prosaro at Feekes 10.5.1) was the most effective option, showing high biological efficacy (97.4% at Feeks 11.2 and 90.3% at harvest) against FHB of winter wheat, increasing wheat yield by 40.1%.

Key words: *Fusarium* head blight, winter wheat, triazole fungicides, biological efficacy.

INTRODUCTION

Cereal crops play indispensable roles in global food systems, serving as critical components in nutrition, economics, and food security worldwide. They are cultivated in larger quantities and contribute more food energy worldwide than any other crop type, making them essential staple food crops (Sarwar et al., 2013).

The production of grain is of strategic importance for ensuring the food and national security of the Republic of Armenia. Out of 227.2 hectares of cultivated land in the RA territory, 124,96 hectares, or 55%, are occupied by grain and leguminous crops. In 2021, the average yield of wheat (both autumn and spring varieties) was 1.68 metric tons per hectare (t ha^{-1}), and it was lower than the yield recorded in 2017 (which was 2.18 t ha^{-1}) by 0.5 tons or 22.9% (Statistical Yearbook of Armenia, 2022).

Climate change, violations of cultivation technology (such as improper selection of seeds, monoculture of cereal crops, and inadequate control of harmful organisms), among other factors, significantly contribute to low yield levels. Herbicides are the main pesticides that are used during the cultivation of grain crops in RA, and in the conditions of monoculture, an intensive development of diseases and pests is observed, their harmfulness continues to increase over time. Climate change, along with violations of cultivation technology such as improper seed selection, monoculture of cereal crops, and insufficient control of harmful organisms, are significant contributors to low yield levels. In the Republic of Armenia, herbicides serve as the primary pesticides used during the cultivation of grain crops. Under monoculture conditions, there is a noticeable intensification of diseases and pests, with their harmful impact progressively worsening over time.

Considering the nutritional value and economic importance of cereal crops for food security, as well as the impact of global climate change on grain yield quality and quantity, especially in arid and semiarid regions, research in recent years by numerous authors from different countries has aimed at increasing the productivity of cereal crops and grain quality using various technologies and agricultural practices. Research areas encompass various aspects, including:

– Implementation of soil tillage practices and weed management strategies (Bani Khalaf et al., 2021); exploration of short-term tillage and no-tillage methods in conjunction with chemical treatments (Guedioura et al., 2023); evaluation of different cultivation technologies (Zargar et al., 2018);

– Optimization of plant nutrition systems (Radchenko et al., 2021), particularly focusing on nitrogen fertilizer rates in winter wheat (Litke et al., 2019); investigation into the impact of bio-humus on soil fertility and spring wheat productivity (Muhamedyarova et al., 2020); study of the effects of environmentally friendly fertilizer (acceptable in green agriculture) on cereal crops (Martirosyan et al., 2023);

– Development of farming practices aimed at enhancing the productivity of winter wheat through the utilization of pesticides from different groups (Kuznetsov et al., 2020); adoption of new technologies for fungicide treatment schemes (both chemical and biological); protection of cereal crops from root rot development using Bacillus subtilis (Kolesnikov et al., 2021); combatting leaf rust and blotches (Švarta et al., 2022), *Fusarium* head blight (González-Domínguez et al., 2021), etc.

The importance of *Fusarium* head blight on wheat cannot be overstated (Shude et al., 2020). It is a severe fungal disease that profoundly impacts cereal crops worldwide, representing a substantial threat to both agricultural productivity and food safety. FHB not only reduces crop yield and quality but also poses health risks due to the production of mycotoxins. These mycotoxins can contaminate grain, posing harm to humans and animals upon ingestion (Mudge et al., 2006; Malekinejad et al., 2007; Duffeck et al., 2020; Mesterhazy, 2020; Wu et al., 2023; Miedaner et al., 2024).

Fusarium head blight (FHB) epidemics have become an increasing problem over the last decades (Alisaac et al., 2019; Ma et al., 2022), likely due to the increased adoption of conservation tillage practices, the use of susceptible wheat varieties, and climate variability (Haile et al., 2019; Spanic et al., 2019; Dong et al., 2020). Moreover, yield losses due to the disease can reach up to 80% of the crop (Alisaac & Mahlein, 2023).

Fungicides have historically served as the primary method for managing FHB (Siranidou & Buchenauer, 2001; Haidukowski et al., 2005; Lehoczki-Krsjak et al., 2010; Shude et al., 2020). However, their effectiveness is often hampered by the development of fungicide resistance (Anderson et al., 2020; Chen et al., 2021; Zhao et al., 2022) and environmental concerns.

Crop rotation and tillage practices have also been implemented as strategies to mitigate FHB by reducing the levels of inoculum in the soil (Schaafsma et al., 2005; McMullen et al., 2012; Wegulo et al., 2015; Fernando et al., 2021). Concurrently, breeding efforts aimed at developing FHB-resistant crop varieties (Mesterházy et al., 1999; Buerstmayr et al., 2019; Fernando et al., 2021) represent a long-term approach to disease management.

Biological control methods, such as the use of antagonistic microbes, beneficial fungi (Khan et al., 2001; Chen et al., 2018; Drakopoulos et al., 2019; Drakopoulos et al., 2020), and essential oils derived from plant sources, have been explored (Kumar et al., 2016; Ferreira et al., 2018) as potential alternatives to chemical fungicides for suppressing *Fusarium* spp. However, the practical implementation of these methods has faced challenges due to practical constraints. The efficacy of biocontrol agents is contingent upon various factors, including weather conditions, crop stage, formulation, and the specific type of agent (Elnahal et al., 2022).

Recent literature underscores the importance of integrating diverse management practices, including cultural, chemical, and biological approaches, to effectively combat FHB (Shah et al., 2018; Chen et al., 2022; Alisaac & Mahlein, 2023).

Fusarium head blight is a common fungal disease in the Republic of Armenia (RA); however, there has been no comprehensive research conducted previously to select appropriate fungicides and determine the optimal timing for their application. This study aims to investigate the development peculiarities of FHB and develop strategies to reduce disease development while enhancing the productivity of winter wheat under rain-fed agricultural conditions. This research represents a novel approach, focusing on the assessment of triazole-group fungicides and identifying the optimal application timing in combating FHB.

MATERIAL AND METHODS

Experimental site and meteorological data recorded

The research was conducted during the 2022 and 2023 growing seasons in rain-fed cultivation conditions in the Spitak community of Lori marz in the Republic of Armenia, situated at coordinates 40°49'55.96"N, 44°16'2.32"E. The climate in Spitak is characterized by winters with a permanent snow cover and warm, relatively humid summers. The average air temperature ranges from -8 °C in winter to +18 °C in summer, with a mean temperature of +5 °C. August marks the hottest, while January is the coldest month. May typically receives the highest amount of precipitation, averaging 89.4 mm, with annual precipitation totaling 398.1 mm per year.

The multi-annual monthly agroclimatic data for the Spitak region were sourced from Arazyan & Shekoyan, 2006. Meteorological data for both the 2022 and 2023 vegetation periods were provided by the 'Hydrometeorology and Monitoring Center' SNCO of the Ministry of Environment of RA.

Experimental design

The experiments were conducted during the 2022 and 2023 growing seasons in rain–fed cultivation conditions, with the primary focus on applying fungicides to winter wheat. Both single and double preventive applications of fungicides were considered as the main factors in the study.

The winter wheat cultivar Bezostaya 1, widely cultivated in Armenia, was planted on September 20, 2021, and September 15, 2022. Comprehensive agricultural practices were implemented throughout the entire experimental field, including tillage, residue, and weed management, to mitigate inoculum levels. Additionally, early sowing dates were chosen to avoid the peak of *Fusarium* spore production, while careful attention was paid to avoiding excessive nitrogen fertilization to enhance crop health and reduce susceptibility to disease.

The experimental field for testing fungicides was divided into plots, each measuring 10 m², with three replicates for each treatment option. Additionally, 40 cm -wide wheat stripe areas with no treatments were left between plots to minimize potential interference or contamination between treatments.

Fusarium graminearum, the causative species of *Fusarium* head blight (FHB), was isolated from sampled infected kernels using PDA media.

Assessment of disease development

Severity and incidence of FHB in winter wheat, disease development degree (DDD, which is a metric similar to the Disease Severity Index (DSI)), and biological efficacy of applied pesticides were determined using methods accepted in plant pathology (Dementyeva, 1985; Avagyan, 2006; Shin et al., 2014; Arcibal et al., 2016).

One hundred spikes from various locations within the plot were assessed to measure *Fusarium* head blight (FHB) severity (in scores) and disease incidence (%).

FHB severity was evaluated as the percentage of spikelets on the spikes displaying visually detectable disease symptoms at the wheat late milk growth stage Feekes 11.2 (Large, 1954), as well as at harvest (Feekes 11.4). This assessment was conducted using a 5-point severity scale:

- 0-point score severity: absence of FHB infection, indicating a healthy spike.
- 1-point severity score: up to 10% of spikelets of the spike (head) are infected, showing discoloration or covered with perithecia.
- 2-point severity score: 10.1–25% of spikelets of the spike (head) are infected, displaying discoloration or covered with perithecia.
- 3-point severity score: 25.1–50% of spikelets of the spike (head) are infected.
- 4-point severity score: more than 50% of spikelets of the spike (head) are infected.

FHB incidence was calculated using the following formula:

Incidence = (Number of infected spikes/Total number of calculated spikes) × 100%.

The Disease Development Degree (DDD) was calculated using the following formula:

DDD = [∑(disease severity score×number of infected spikes with corresponding severity score)]/[(total number of calculated spikes)×(maximal score (4) in the disease severity score scale)]×100%.

The Biological Efficacy of fungicides was calculated using the following formula:

Be = [(disease development degree in untreated check (control) option-disease development degree in the option with fungicide application)] / [disease development degree in untreated check option]×100% (Dementyeva, 1985).

Additionally, yield was calculated using the metric method, with data collected from three repetitions of each variant (Kuznetsov, 1980).

Statistical assessment of the results

Statistical assessment was conducted using the single-factor or one-way ANOVA test (analysis of variance). The MS Excel package was utilized to compare the average data across the experimental options and to display standard deviation and error bars. The indicator of the least significant difference (*LSD* 0.5) was applied with the lower limit of the permissible level of significance set at $p < 0.05$.

RESULTS AND DISCUSSION

The host plants for *Fusarium* head blight are wheat (*Triticum aestivum* L.), durum wheat (*Triticum durum* L.), barley (*Hordeum vulgare* L.), oats (*Avena sativa* L.), rye (*Secale cereale* L.), corn (*Zea mays* L.), etc. Wheat and barley are among the most frequently infected crops by *Fusarium* head blight.

The causal agents of *Fusarium* head blight are encompassing various species within the *Fusarium* Link genus (Zemánková & Lebeda, 2001). *Fusarium graminearum* Schwabe, with its sexual stage known as *Gibberella zeae* (Schwein.) Petch, stands out as one of the most prevalent and significant species linked to FHB. However, other *Fusarium* species such as *F. culmorum* (W.G.Sm.) Sacc., *F. avenaceum* (Corda ex Fries) Sacc., *F. sporotrichioides* Sherb., and several others can also cause FHB in cereal crops. The negative effect of *Fusarium* spp. is manifested in the yield decrease, as well as in the accumulation of the mycotoxin deoxynivalenol (DON) in the infected grain (Parry et al., 1995; Stack, 2000; Bekele, 2018; Shah et al., 2018).

Fusarium head blight was first identified in England in 1884 (Shah et al., 2018). FHB is now widespread throughout the world (McMullen et al., 2017). The symptoms of the disease can be both visible and hidden-latent. If symptoms are noticeable, grains are deformed and orange spore masses appear on the margin of the glumes of infected spikelets. In the case of latent symptoms, no diagnostic signs of FHB are observed, as noted by Parry et al. (1995), which leads to the synthesis of the DON in the grains (Clement et al., 1998).

The severity of FHB symptoms can vary depending on factors such as environmental conditions, host susceptibility, etc. During our observations in 2022–2023, the most common symptom of FHB was premature bleaching of the

entire spike or individual spikelets (Fig. 1, a). Premature bleaching progresses over time on most or all spikelets, eventually causing the entire head to bleach (Avagyan, 2006).

Figure 1. Symptoms of *Fusarium* head blight: bleached spikes during milky ripening stage (a), infected heads during waxy ripening stage (b), perithecia on the spikes (c).

Bleached spikelets are sterile or contain shriveled and lightweight kernels compared to healthy ones. In case of severe infection, the spike becomes completely deformed and wrinkled (Fig. 1, b). During waxy ripening stage, the pathogen forms perithecia on the surface of wheat spikelets (Fig. 1, c). Under favorable wet conditions, perithecia may also appear on the leaves and stem of wheat (Fig. 2). Infected heads ripen prematurely, leading to reduced yield.

Additionally, the pathogen can cause symptoms of crown and root rot, characterized by the rotting and decay of the crown tissue at the soil surface (Fig. 3).

Our observations during the 2022 and 2023 growing seasons in different regions of RA have revealed outbreaks of massive FHB development, particularly in regions such as Spitak and Aparan, situated at elevations ranging from 1,650 to 1,880 meters above sea level. These regions were characterized by high levels of precipitation, especially during the heading and flowering stages of winter wheat. This pattern persisted during years with substantial

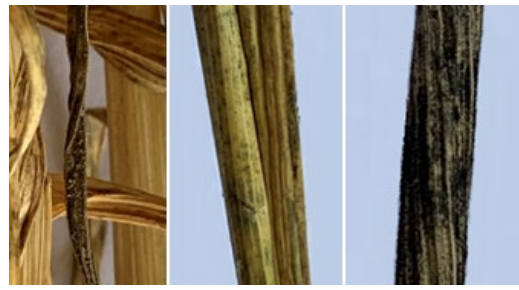

Figure 2. Perithecia of *F. graminearum (G. zeae)* on wheat leaves and stem.

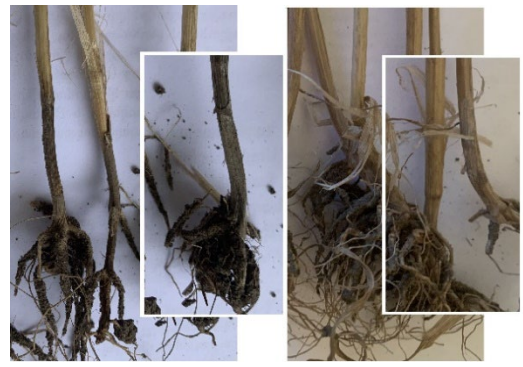

Figure 3. Symptoms of *Fusarium* crown rot: infected (left) and healthy (right) plants.

precipitation, such as 2023, observed in regions like Ararat, Armavir, and Kotayk, which are situated at elevations ranging from 825 to 1,450 meters above sea level.

F. graminearum overwinters either as perithecia (*G. zeae*) or mycelia in the soil or within host crop residues, which serving as a source of primary infection during the subsequent spring. In spring, under favorable weather conditions (warm and humid), ascospores and/or conidia are released from crop residues. These spores are then disseminated by wind or splashing water, and upon landing on wheat heads, they germinate and infect glumes, flowers, and other parts of the heads (Vaughan et al., 2016; Shah et al., 2018; Teli et al., 2020; Windels, 2000).

An effective strategy to manage *Fusarium* head blight in wheat is the use of fungicides. Some research studies have indicated that the application of strobilurin fungicides can lead to increased DON levels in the harvested grains (Bonfada, et al., 2019; Gaurilèikienë et al., 2005).

Therefore, for the experiments, fungicides from the chemical group of triazoles were selected, including Tilt® (applied at a rate of 0.5 L ha^{-1}), Alto super (0.5 L ha^{-1}), Falcon (0.8 L ha^{-1}), Folicur® (0.5 L ha^{-1}), Prosaro® (1.0 L ha^{-1}).

It is widely recognized that the development of *Fusarium* head blight is strongly influenced by climatic conditions. Wheat becomes susceptible to FHB from the heading stage to the beginning of the waxy ripening stage, with the critical window for head infection occurring during anthesis (Bai et al., 1996; Hooker et al., 2002; Yoshida et al., 2007; Sioua et al., 2014; Brauer et al., 2020). Thus, during the 2022 growing season, pesticides were applied preventively at the wheat growing stage Feekes 10.5.1 (early anthesis). During the 2023 growing season, pesticides were applied preventively mostly at the wheat growing stage Feekes 10.5.1, similar to 2022. However, double sprayings were carried out in two options: the first at Feekes 10.3, when half of the heading process had been completed, and the second at Feekes 10.5.1.

The basis for carrying out double spraying was the data obtained during 2022, which demonstrated that from the milky ripening stage to the waxy ripening stage and harvest of winter wheat, the disease can progress, intensively forming perithecia on the ears, stems and leaves. We have also considered the data on weather conditions of 2022 and 2023 (Table 1), as the severity of FHB in rain–fed agriculture mainly depends on weather conditions.

The average monthly air temperature during April–July months of 2022 was generally higher (10.5–19.7 °C), whereas the total amount of precipitation during some months was lower (10.5–34.8 mm during July and April) or higher (90.3–111.2 mm during June and May), compared to the multi–annual monthly averages (Table 1). The average monthly air temperature during 2023 was generally lower (9.3–18.8 °C) compared to 2022, but it was higher compared to the multi–annual data. Meanwhile, the total amount of precipitation was higher (65.6–107.9 mm) compared to 2022, as well as the multi–annual monthly averages. Under such conditions of high precipitation and moderate temperature, it is necessary to spray not only during the phase of massive maturation and release of the pathogen's ascospores – when plants are at the flowering stage (Feekes 10.5.1), potentially facing massive infection - but also earlier, when half of the heading process is completed (Feekes 10.3). The first application of fungicides at Feekes 10.3 will coincide with the initial stage of maturation and release of the pathogen's ascospores from perithecia, whereas the second one (at Feekes 10.5.1) will

align with the phase of massive maturation and release of the ascospores. This approach reduces the amount of inoculum and the likelihood of subsequent infection of the spikes.

Table 1. Total amount of precipitation, average air temperature and relative humidity data for Spitak region, RA

Indicators of climate conditions	Year	Months				
		April	May	June	July	August
Average air temperature, °C	2022	10.5	11.4	17.7	19.7	20.3
	2023	9.3	12.5	16.4	18.8	21.2
Multi-annual temperature, °C	-	6.4	11.6	14.8	18.0	18.0
Total amount of precipitation, mm	2022	34.8	111.2	90.3	10.5	22.6
	2023	65.6	93.01	107.9	84.1	19.5
Multi-annual precipitation, mm	–	56	78	78	50	36
Average relative humidity, %	2022	70	81	85	63	60
	2023	63	66	70	69	66
Multi-annual relative humidity, %	-	66	69	70	68	65

According to the data presented in Table 2, the incidence of FHB in the untreated check (control) option was 22.3% and 26.8% at Feekes 11.2 and Feekes 11.4, respectively, in 2022. The average disease severity scores were 1.3 and 1.6, and the degree of disease development being 7.2% and 10.7%, respectively. The high amount of precipitation (90.3 mm) in June 2022 contributed to the development of FHB.

Table 2. Impact of fungicide treatment on development of *Fusarium* head blight of winter wheat (Spitak, 2022)

Fungicides/options, consumption norm, application time		During stage Feekes 11.2			During stage Feekes 11.4		
		FHB incidence, %	severity score (avg)	FHB DDD, %	FHB incidence, %	severity score (avg)	FHB DDD, %
Tilt, 0.5 L ha^{-1}	at Feekes 10.5.1	9.3	1	2.3	14.7	1	3.7
Alto super, 0.5 L ha^{-1}		8.5	1	2.1	13.9	1	3.5
Folicur, 0.5 L ha^{-1}		6.9	1	1.7	11.1	1	2.8
Falcon, 0.8 L ha^{-1}		5.8	1	1.4	9.9	1	2.5
Prosaro, 1.0 L ha^{-1}		4.9	1	1.2	8.9	1	2.2
Untreated check	-	22.3	1.3	7.2	26.8	1.6	10.7

With a single application of fungicides from the triazole group at Feekes 10.5.1, the incidence of FHB decreased compared to the untreated check option, ranging from 4.9% to 9.3% (at Feekes 11.2) and 8.9% to 14.7% (at Feekes 11.4). The degree of disease development ranged from 1.2% to 2.3% and 2.2% to 3.7%, respectively. The highest percentage reduction of FHB was recorded in the options, where plants were sprayed with the fungicides Falcon at 0.8 L ha^{-1} or Prosaro at 1.0 L ha^{-1}.

High incidence and severity of FHB were recorded, especially during the 2023 growing season (see Table 3). The incidence of FHB in the untreated check option was 34.6% during the late milk stage (Feekes 11.2) and increased to 65.3% at harvest (Feekes 11.4). The average severity of the disease ranged from 1.8 (Feekes 11.2) to 2.1 scores (Feekes 11.4), with the degree of disease development ranging from 15.6% to 35.9%, respectively. These findings indicate a very high rate of infection and massive

development of FHB. It was also observed that abundant rainfall (84.1 mm) and moderate temperatures (18.8 °C) in July 2023 contributed to the spread of the infection during the waxy ripening stage.

Table 3. Impact of fungicide treatment on development of *Fusarium* head blight of winter wheat (Spitak, 2023)

Fungicides/options, consumption norm, application time			During stage Feekes 11.2			During stage Feekes 11.4		
			FHB incidence, %	severity score (avg)	FHB DDD, %	FHB incidence, *%	severity score (avg)	FHB DDD, %
Tilt		at Feekes 10.5.1	17.1	1.3	5.6	35.7	1.6	14.3
Alto super			16.4	1.3	5.3	33.5	1.6	13.4
Folicur			14.4	1.2	4.3	33.4	1.4	11.7
Falcon			12.1	1.1	3.6	31.7	1.2	9.5
Prosaro			10.4	1.1	3.1	29.7	1.2	8.9
Folicur and Prosaro	at Feekes 10.3	at Feekes 10.5.1	3.7	1	0.9	17.1	1.1	4.7
Falcon and Prosaro			1.7	1	0.4	12.7	1.1	3.5
untreated check	-	-	34.6	1.8	15.6	65.3	2.1	35.9

Our research findings revealed variations in *Fusarium* head blight (FHB) disease severity, incidence, and harmfulness between the 2022 and 2023 growing seasons in Spitak, attributable to differences in weather conditions. The significant development of FHB was correlated with lower average air temperatures from heading to the waxy ripening stage during the June–July months (16.4 and 18.8 °C in 2023) and a notably higher amount of precipitation (107.9 and 84.1 mm), along with high relative humidity (refer to Table 1). Moderate temperatures and abundant rainfall extended the flowering stage, prolonging the plants' susceptibility period (flowering stage), thereby heightening the risk of epidemics.

Our research results align with findings from several studies. According to Parry et al. (1995), a prolonged flowering stage increases the risk of an epidemic. Additionally, the severity of FHB primarily depends on air temperature (Mentewab et al., 2000; Brennan et al., 2005; Nita et al., 2005; Okereke et al., 2016) and humidity levels (Lacey et al., 1999; Cowger et al., 2005; Stenglein, 2009).

The results of our research showed that in 2023, with a single application of triazole fungicides at Feekes 10.5.1, the incidence of *Fusarium* head blight decreased, ranging from 10.4% to 17.1% (at Feekes 11.2) and 29.7% to 35.7% (at Feekes 11.4). Meanwhile, the degree of disease development varied between 3.1% to 5.6% and 8.9% to 14.3%, respectively. However, during years of epidemic FHB development, the degree of disease development with a single application of fungicides reduced below the harmful level (10%) only when plants were sprayed with the fungicides Prosaro or Falcon. In contrast, a single application of fungicides Tilt, Alto Super, and Folicur couldn't significantly suppress the development of FHB.

Spraying winter wheat twice (at Feekes 10.3 and Feekes 10.5.1) during 2023 significantly reduced the development of FHB. The disease incidence and the degree of disease development ranged from 1.7% to 3.7% and 0.4% to 0.9%, respectively, at the Feekes 11.2 late milk stage, while ranging from 12.7% to 17.1% and 3.5% to 4.7%,

respectively, at the Feekes 11.4 harvest stage. These figures represent a rather low index in the case of epidemic development of FHB.

Evaluating the biological efficacy of the used fungicides, we can conclude that when weather conditions during the growing season are not favorable for the development of FHB, Prosaro (applied at a rate of 1.0 L ha^{-1}), Falcon (applied at a rate of 0.8 L ha^{-1}), as well as Folicur (applied at a rate of 0.5 L ha^{-1} demonstrate higher efficacy (ranging from 76.4 to 83.3% at Feekes 11.2 and from 73.8 to 79.4% at harvest, respectively) against FHB with a single application at the beginning of the flowering stage (Feekes 10.5.1, early anthesis). However, the fungicides Tilt (0.5 L ha^{-1}) and Alto super (0.5 L ha^{-1}) exhibited the lowest biological efficacy, ranging from 68.1% to 70.8% at Feeks 11.2, and from 65.4% to 67.6% at harvest, respectively (see Fig. 4). Conversely, Falcon and Prosaro demonstrated the highest biological efficacy, ranging from 80.6 to 83.3% at Feeks 11.2 and from 76.6 to 79.4% at harvest, respectively.

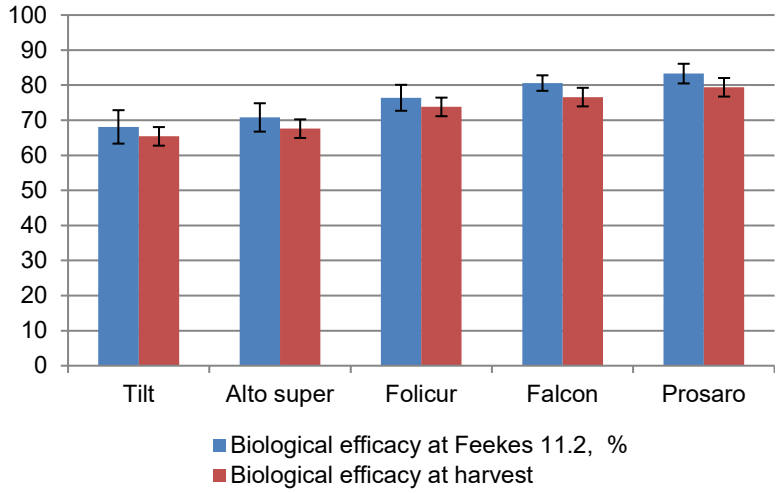

Figure 4. Biological efficacy of fungicides against FHB of winter wheat, 2022: error bars are equivalent to standard deviations.

However, during years of epidemic FHB development, spraying only at the beginning of the flowering stage (Feekes 10.5.1, early anthesis) did not provide high biological efficacy (refer to Fig. 5). These results are consistent with those of Caldwell et al. (2017), indicating that a single fungicide application may not be sufficient to achieve high yields with good seed quality. Two preventive applications during the growing season, the first at Feekes 10.3 (half of heading process completed) with Folicur, 0.5 L ha^{-1} or Falcon, 0.8 L ha^{-1}, and the second at Feekes 10.5.1 (early anthesis) with Prosaro, 1.0 L ha^{-1}, demonstrated high biological efficacy (ranging from 94.2% to 97.4% and 86.9% to 90.3%, respectively) against FHB. However, the Falcon + Prosaro option yielded the highest results.

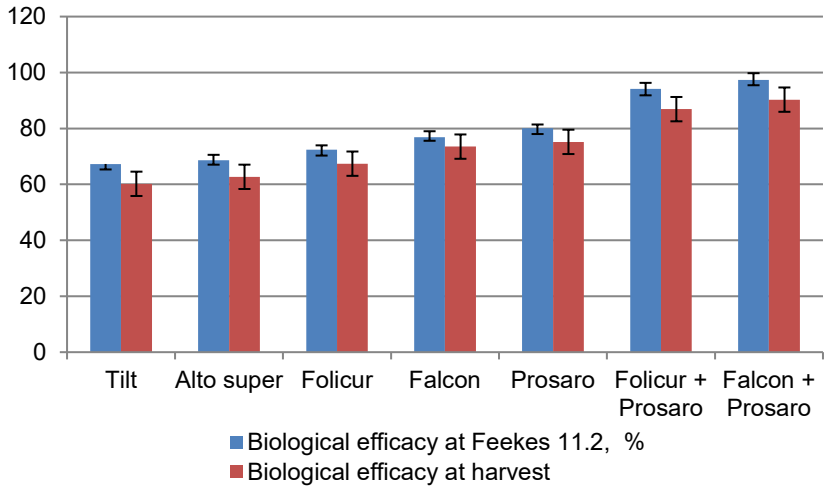

Figure 5. Biological efficacy of fungicides against FHB of winter wheat, 2023: error bars are equivalent to standard deviations.

Analyzing previous research on the efficacy of fungicides against *Fusarium* head blight (FHB) from different chemical groups, it is notable that Bolanos-Carriel et al. (2020) identified triazole and strobilurin fungicides commonly used for controlling FHB and other wheat diseases. The most effective fungicide treatment in reducing FHB severity, damaged kernels, deoxynivalenol (DON) contamination, and yield loss was found to be prothioconazole-containing fungicides (Proline® or Prosaro®) applied during early anthesis, consistently reducing FHB disease severity compared to the untreated/inoculated control (Haidukowski et al., 2012; Bolanos-Carriel et al., 2020). According to other research studies, triazoles such as tebuconazole, metconazole, and prothioconazole (Paul et al., 2008) and benzimidazole fungicides, including carbendazim, control FHB (Zhou et al., 2016; Machado et al., 2017). They inhibit hyphal growth (Hollomon et al., 1998) and regulate DON levels in wheat (Paul et al., 2018). In contrast, strobilurin fungicides are generally ineffective in controlling FHB; moreover, their application increases DON concentration in grain compared to untreated controls (Shah et al., 2018). However, it's worth noting that the control efficacy of carbendazim and other benzimidazole fungicides against *F. graminearum* has declined due to the development of resistance in *F. graminearum* against carbendazim (Liu et al., 2019).

The results of our research in agreement with Maryland Agronomy News, which suggests that tebuconazole-containing Folicur® is less effective compared to prothioconazole-based treatments and should not be used if the risk of FHB is high. Tilt (propiconazole) has become less effective for managing FHB and currently provides poor control.

The effect of the used fungicides on the productivity of winter wheat is presented in Table 4. The yield of winter wheat was 2.12 t ha^{-1} in 2022 and 2.39 t ha^{-1} in 2023 in the untreated check option of the experiment. However, the yield increased to 2.71–3.03 t ha^{-1} in 2022 (an increase of 27.95–42.9%) and to 2.79-3.12 t ha^{-1} in 2023 (an increase of 16.7–30.5%) in the options with a single treatment of fungicides.

Table 4. Effect of preventive fungicides on productivity of winter wheat

Fungicide, consumption norm	2022			2023		
	yield, t ha^{-1}	increase in yield, %	weight of 1,000 kernels, g	yield, t ha^{-1}	increase in yield, %	weight of 1,000 kernels, g
Tilt, 0.5 L ha^{-1}	2.71	27.95	36.5	2.79	16.7	36.2
Alto super, 0.5 L ha^{-1}	2.74	29.44	37.1	2.82	17.8	36.3
Folicur, 0.5 L ha^{-1}	2.86	35.13	38.4	2.87	20.2	36.5
Falcon, 0.8 L ha^{-1}	2.92	37.62	39.3	3.02	26.3	36.8
Prosaro, 1.0 L ha^{-1}	3.03	42.9	40.0	3.12	30.4	37.4
Folicur, 0.5 L ha^{-1} and Prosaro, 1.0 L ha^{-1}	-	-	-	3.33	38.3	39.7
Falcon, 0.8 L ha^{-1} and Prosaro, 1.0 L ha^{-1}	-	-	-	3.51	40,1	40.2
Untreated check	2.12	-	33.5	2.39	-	32.9
LSD_{05}	0.09	-	0.6	0.16	-	1.25

In the options with double preventive spraying of fungicides at Feekes 10.3 and Feekes 10.5.1, the yield of winter wheat ranged from 3.33 to 3.51 t ha^{-1} in 2023, exceeding the results of the untreated check option by 0.94–1.12 t ha^{-1} (an increase of 38.3-40.1%). The highest yield of winter wheat was achieved in the option where Falcon (at a rate of 0.8 L ha^{-1}) was applied first, followed by Prosaro (at a rate of 1.0 L ha^{-1}) for the second spraying.

Similar data were recorded when analyzing the weight of 1,000 kernels. In the case of a single preventive application of fungicides during Feekes 10.5.1 in both 2022 and 2023, the highest weight of 1,000 kernels was recorded when winter wheat was treated with Falcon (39.3 and 36.8 g, in 2022 and 2023, respectively) or Prosaro (40.0 and 37.4 g in 2022 and 2023, respectively), surpassing the results of the untreated check option by 5.8–6.5 and 3.9–4.5 g, respectively. In the case of double preventive spraying with triazole group fungicides during Feekes 10.3 and 10.5.1 in 2023, the highest weight of 1,000 kernels (40.2 g) was observed when plants were treated with Falcon (at a rate of 0.5 L ha^{-1}), and Prosaro (at a rate of 1.0 L ha^{-1}), exceeding the results of the untreated check option by 7.3 g.

Upon comparing the yield data from 2022, it is noteworthy that all experimental variants utilizing fungicide applications exhibited a least significant difference higher than 0.09 t ha^{-1}, ranging from 0.59 to 0.91 t ha^{-1} difference compared to the control option. Additionally, the 1,000 grain weight of all experimental variants demonstrated a least significant difference exceeding 0.6 g, ranging from 3 to 6.5g difference compared to the control option, indicating significant disparity. Particularly promising results in 2022 were observed with a single application of Falcon or Prosaro.

Comparing the yield data from 2023, the least significant difference for all experimental variants with fungicide applications surpassed 0.16 t ha^{-1}, ranging from 0.4 to 0.74 t ha^{-1} (for single applications) and from 0.94 to 1.12 t ha^{-1} (for double applications) difference compared to the control option. Similarly, the 1,000 grain weight of all experimental variants exhibited a least significant difference exceeding 1.25 g, ranging from 3.3 to 4.5 g (for single applications) and from 6.8 to 7.3 g (for double applications) difference compared to the control option, indicating significant differences. Notably, the most promising results in 2022 were achieved with a single

application of Falcon or Prosaro, while in 2023, double applications with Folicur + Prosaro or Falcon + Prosaro fungicides proved to be the most effective.

So, we can conclude that based on cultural practices, the application of fungicides has been shown to decrease *Fusarium* head blight incidence, severity, and development, while simultaneously boosting wheat yield. The results corroborate the findings of Kuznetsov et al. (2020), Kolesnikov et al. (2021), and Švarta et al. (2022), demonstrating that the use of pesticides led to an increase in the grain yield of winter wheat.

Based on our research findings, we recommend farmers to apply fungicides to winter wheat at the onset of the flowering stage (Feekes 10.5.1, early anthesis) to effectively control *Fusarium* head blight in rain-fed agriculture. Specifically, we suggest using Falcon at a rate of 0.5 L ha^{-1} or Prosaro at a rate of 1.0 L ha^{-1}. This recommendation is particularly pertinent during years with less favorable weather conditions for disease development. Additionally, during years with the most favorable weather conditions for *Fusarium* head blight development (moderate temperature and abundant rain during heading and flowering stages), it is advisable to implement a double preventive treatment with fungicides against FHB in winter wheat in rain-fed agriculture. The initial application should occur when half of the heading process is completed (Feekes 10.3). We suggest using Folicur at a rate of 0.5 L ha^{-1} or Falcon at a rate of 0.8 L ha^{-1} for this first application. The second application should be conducted during early anthesis (Feekes 10.5.1) using Prosaro at a rate of 1.0 L ha^{-1}. This two-step protocol provides comprehensive protection against *Fusarium* head blight and is especially effective when implemented during the specified growth stages.

It's essential to acknowledge the contentious nature of the data concerning the impact of strobilurins and triazole fungicides on post-harvest grain infection with *Fusarium* spp. and mycotoxin contamination. Butkutė et al. (2008) noted that while the concentration of zearalenone (ZEN) was lower in strobilurin and triazole fungicide-treated plots compared to untreated ones, the concentration of deoxynivalenol (DON) was significantly higher. Despite negligible contamination with T-2 toxin, there was a tendency for it to decrease in grain from fungicide-treated plots. Moreover, the correlation between the percentage of grain kernels infected with *Fusarium* spp. and mycotoxin levels was found to be weak (Butkutė et al., 2008).

In contrast, another study by Bolanos-Carriel et al. (2019) suggested that the reduction in deoxynivalenol (DON) observed in the field from applying a triazole fungicide (Prosaro) at anthesis could be sustained throughout the grain storage period. However, the application of a strobilurin fungicide (Headline) at anthesis was ineffective in reducing DON and even led to an increase during storage. Conversely, DON levels were lower at the beginning of storage and remained stable over time with the use of the triazole fungicide Prosaro, indicating its efficacy in controlling mycotoxins in stored grain (Bolanos-Carriel et al., 2019).

Furthermore, it's noteworthy that fungicides containing strobilurins should not be used beyond flag leaf emergence on wheat because they can potentially increase DON vomitoxin accumulation in the grain (Bonfada et al., 2019; Gaurilèikienë et al., 2005). These findings underscore the complexity of managing *Fusarium* head blight and mycotoxin contamination, emphasizing the importance of careful consideration and monitoring when employing fungicide treatments.

CONCLUSION

Concluding the results of the research, it can be stated that winter wheat is particularly sensitive to *Fusarium* head blight, especially during the flowering stage. Prolonged rains during flowering contribute to the delay of the flowering stage, prolonging the susceptibility of plants thereby increasing the risk of FHB epidemics.

A massive development (epidemic) of *Fusarium* head blight was recorded in Spitak in 2023 due to favorable weather conditions for the development of the pathogen. Abundant rainfall and moderate temperatures contributed to the spread of the infection during the waxy ripening stage as well.

Based on agricultural practices, it is recomended to apply fungicides to winter wheat at the onset of the flowering stage (Feekes 10.5.1, early anthesis), utilizing Falcon at a rate of 0.5 L ha^{-1} or Prosaro® at a rate of 1.0 L ha^{-1} to manage *Fusarium* head blight in rain-fed agriculture. This strategy is particularly crucial during years with less favorable weather conditions for disease development. Implementing these fungicides can potentially increase yields by 37.62% to 42.9% and the weight of 1,000 kernels by 5.8 to 6.5 g, respectively, compared to the untreated check option in the experiment.

The use of a double fungicide treatment is recommended for managing *Fusarium* head blight of winter wheat in rain–fed agriculture, particularly during years with more favorable weather conditions conducive to disease development (moderate temperatures and abundant rain during heading and flowering). This strategy is especially beneficial when integrated with cultural practices, such as those aimed at reducing inoculum levels and optimizing crop health. The first application should be done at Feekes 10.3 (when half of the heading process is completed), using Falcon at a rate of 0.5 L ha^{-1}, followed by a second application at Feekes 10.5.1 (early anthesis) using Prosaro® at a rate of 1.0 L ha^{-1}. Implementing this strategy can potentially increase yields by 40.1% and the weight of 1,000 kernels by 7.3 g compared to the untreated check option in the experiment.

The data acquired will serve as a foundation for ongoing research aimed at enhancing protective strategies against *Fusarium* head blight across various regions of the Republic of Armenia, encompassing both rain-fed and irrigated agricultural systems. Furthermore, this information will play a crucial role in controlling the presence of deoxynivalenol mycotoxin in harvested grains. Additionally, it will serve as essential training material for farmers, equipping them with the knowledge and skills needed to effectively address *Fusarium* head blight in their crops.

ACKNOWLEDGEMENTS. This work was supported by the Higher Education and Science Committee of the RA MoESCS (The Ministry of Education, Science, Culture and Sports of the Republic of Armenia), within the framework of the research project No. 21T–4C050.

The authors extend their heartfelt appreciation to the reviewers for their valuable insights, thoughtful comments, and constructive feedback, all of which significantly enhanced the quality of this manuscript.

REFERENCES

Alisaac, E. & Mahlein, A.-K. 2023. *Fusarium* head blight on wheat: biology, modern detection and diagnosis and integrated disease management. *Toxins* **15**(3), 192. https://doi.org/10.3390/toxins15030192

Alisaac, E., Behmann, J., Rathgeb, A., Karlovsky, P., Dehne, H.W. & Mahlein, A.K. 2019. Assessment of *Fusarium* infection and mycotoxin contamination of wheat kernels and flour using hyperspectral imaging. *Toxins*. **11**(10), 556. https://doi.org/10.3390/toxins11100556

Anderson, N.R., Freije, A.N., Bergstrom, G.C., Bradley, C.A., Cowger, C., Faske, T., Hollier, C., Kleczewski, N., Padgett, G.B., Paul, P., Price, T. & Wise, K.A. 2020. Sensitivity of *Fusarium* graminearum to metconazole and tebuconazole fungicides before and after widespread use in wheat in the United States. *Plant Heal. Prog*. **21**, 85–90. https://doi.org/10.1094/PHP-11-19-0083-RS

Arazyan, K. Yev. & Shekoyan, Z.S. 2006. *Methodical instructions on the use of meteorological and agroclimatic data in course and diploma works*. ANAU, Yerevan, 19 pp. (in Armenian).

Arcibal, S.S., Jackson, C.A., Shelman, T.L., Jones, L.L. & Marshall, J.M. 2016. Integrated FHB management of spring wheat in Idaho. *FHB management. National Fusarium Head Blight Forum. December 2016,* pp. 3–6 https://scabusa.org/pdfs/nfhbf16_proc_mgmt.pdf

Avagyan, G.V. 2006. *Practical guide to agricultural phytopathology*. Armenian Agricultural Academy, Yerevan. 142 pp. https://library.anau.am/images/stories/grqer/Gyughatntesutyun/gyux.pdf (in Armenian).

Bani Khalaf, Y., Aldahadha, A., Samarah, N., Migdadi, O. & Musallam, I. 2021. Effect of zero tillage and different weeding methods on grain yield of durum wheat in semi-arid regions. *Agronomy Research* **19**(1), 13–27. https://doi.org/10.15159/AR.20.236

Bai, G.H. & Shaner, G.H. 1996. Variation in *Fusarium graminearum* and Cultivar Resistance to Wheat Scab. *Plant Disease* **80**, 975–979. https://doi.org/10.1094/PD–80–0975

Bekele, B. 2018. Review on the status and management strategies of *Fusarium* head blight (*Fusarium graminearum*) of wheat. *Academic Research Journal of Agricultural Science and Research* **4(**6), 2348–3997. https://doi.org/10.14662/ARJASRD2017.069

Bolanos-Carriel, C., Wegulo, S.N., Hallen-Adams, H., Baenziger, P.S., Eskridge, K.M., Funnell-Harris, D., McMaster, N. & Schmale, D.G. 2019. Effects of field-applied fungicides, grain moisture, and time on deoxynivalenol during postharvest storage of winter wheat grain. *Canadian Journal of Plant Science* **100**(3). https://doi.org/10.1139/cjps-2019-0075

Bolanos-Carriel, C., Wegulo, S.N., Baenziger, P.S., Funnell-Harris, D., Hallen-Adams, H.E. & Eskridge, K.M. 2020. Effects of fungicide chemical class, fungicide application timing, and environment on *Fusarium* head blight in winter wheat. *Eur. J. Plant Pathol*. **158**, 667–679. https://doi.org/10.1007/s10658-020-02109-3

Bonfada, E.B., Honnef, D., Friedrich, M.T., Boller, W. & Deuner, C.C. 2019. Performance of fungicides on the control of *Fusarium* head blight (*Triticum aestivum* L.) and deoxynivalenol contamination in wheat grains. *Summa Phytopathologica* **45**(4), 374–380. https://doi.org/10.1590/0100-5405/191941

Brauer, E.K., Balcerzak, M., Rocheleau, H., Leung, W., Schernthaner, J., Subramaniam, R. & Ouellet, T. 2020. Genome editing of a deoxynivalenol–induced transcription factor confers resistance to *Fusarium graminearum* in wheat. *Molecular Plant–Microbe Interactions* **33**, 553–560. https://doi.org/10.1094/MPMI-11-19-0332-R

Brennan, J.M., Egan, D., Cooke, B.M. & Doohan, F.M. 2005. Effect of temperature on head blight of wheat caused by *Fusarium culmorum* and *F. graminearum. Plant Pathology* **54**, 156–160. https://doi.org/10.1111/j.1365-3059.2005.01157.x

Buerstmayr, M., Steiner, B. & Buerstmayr, H. 2019. Breeding for *Fusarium* head blight resistance in wheat-Progress and challenges. *Plant Breed*. **139**, 429–454. https://doi.org/10.1111/pbr.12797

Butkutė, B., Mankevičienė, A. & Gaurilčikienė, I. 2008. A comparative study of strobilurin and triazole treatments in relation to the incidence of *Fusarium* head blight in winter wheat, grain quality and safety. *Cereal Research Communications* **36**, 671–675. https://doi.org/10.1556/crc.36.2008.suppl.b.

Caldwell, C.D., MacDonald, D., Jiang, Y., Cheema, M.A. & Li, J. 2017. Effect of fungicide combinations for *Fusarium* head blight control on disease incidence, grain yield, and quality of winter wheat, spring wheat, and barley. *Canadian Journal of Plant Science* **97**. https://doi.org/10.1139/cjps-2017-0001

Chen, A-H., Islam, T. & Ma, Z.-h. 2022. An integrated pest management program for managing *Fusarium* head blight disease in cereals. *Journal of Integrative Agriculture* **21**(12), 3434–3444. https://doi.org/10.1016/j.jia.2022.08.053

Chen, C., Long, L., Zhang, F., Chen, Q., Chen, C., Yu, X., Liu, Q., Bao, J. & Long, Z. 2018. Antifungal activity, main active components and mechanism of *Curcuma longa* extract against *Fusarium graminearum. PLoS One*. https://doi.org/10.1371/journal.pone.0194284

Chen, J., Wei, J., Fu, L., Wang, S., Liu, J., Guo, Q., Jiang, J., Tian, Y., Che, Z., Chen, G. & Liu, S. 2021. Tebuconazole resistance of *Fusarium graminearum* field populations from wheat in Henan province. *Phytopathol.* **169**, 525–532. https://doi.org/10.1111/jph.13021

Clement, J.A. & Parry, D.W. 1998. Stem–base disease and fungal colonisation of winter wheat grown in compost inoculated with *Fusarium culmorum, F. graminearum* and *Microdochium nivale*. *European Journal of Plant Pathology* **104**, 323–330. https://doi.org/10.1023/A:1008681618351

Cowger, C. & Sutton, A.L. 2005. The southeastern U.S. *Fusarium* head blight epidemic of 2003. *Plant Health Progress* **6**. https://doi.org/10.1094/PHP-2005-1026-01-RS

Dementyeva, M.I. 1985. *Phytopathology.* Agropromizdat, Moscow, 397 pp. (in Russian).

Dong, F., Xu, J., Zhang, X., Wang, S., Xing, Y., Mokoena, M.P., Olaniran, A.O. & Shi, J. 2020. Gramineous weeds near paddy fields are alternative hosts for the *Fusarium graminearum* species complex that causes *Fusarium* head blight in rice. *Plant Pathology* **69**, 433–441. https://doi.org/10.1111/ppa.13143

Drakopoulos, D., Luz, C., Torrijos, R., Meca, G., Weber, P., Bänziger, I., Voegele, R.T., Six, J. & Vogelgsang, S. 2019. Use of botanicals to suppress different stages of the life cycle of *Fusarium graminearum. Phytopathology* **109**, 2116–2123. https://doi.org/10.1094/PHYTO-06-19-0205-R

Drakopoulos, D., Meca, G., Torrijos, R., Marty, A., Kägi, A., Jenny, E., Forrer, H.R., Six, J. & Vogelgsang, S. 2020. Control of *Fusarium graminearum* in wheat with mustard-based botanicals: from in vitro to in planta. *Front. Microbiol.* **11**, 1595. https://doi.org/10.3389/fmicb.2020.01595

Duffeck, M.R., Alves, K.d-S., Machado, F.J., Esker, P.D. & Del Ponte, E.M. 2020. Modeling Yield Losses and Fungicide Profitability for Managing *Fusarium* Head Blight in Brazilian Spring Wheat. *Phytopathology* **110**, 370–378. https://doi.org/10.1094/PHYTO-04-19-0122-R

Elnahal, A.S.M., El-Saadony, M.T., Saad, A.M., Desoky, E.S.M., El-Tahan, A.M., Rady, M.M., AbuQamar, S.F. & El-Tarabily, K.A. 2022. The use of microbial inoculants for biological control, plant growth promotion, and sustainable agriculture: A review. *Eur. J. Plant Pathol.* **162**, 759–792. https://doi.org/10.1007/s10658-021-02393-7

Fernando, W.G.D., Oghenekaro, A.O., Tucker, J.R. & Badea, A. 2021. Building on a foundation: Advances in epidemiology, resistance breeding, and forecasting research for reducing the impact of *Fusarium* head blight in wheat and barley. *Can. J. Plant Pathol.* **43**, 495–526. https://doi.org/10.1080/07060661.2020.1861102

Ferreira, F.M.D., Hirooka, E.Y., Ferreira, F.D., Silva, M.V., Mossini, S.A.G. & Machinski, M. 2018. Effect of *Zingiber officinale* roscoe essential oil in fungus control and deoxynivalenol production of *Fusarium graminearum* schwabe in vitro. *Food Addit Contam.* - Part A Chem. **35**, 2168–2174. https://doi.org/10.1080/19440049.2018.1520397

Gaurilèikienë, I., Mankevičienė, A. & Dabkevičius, Z. 2005. Impact of triazole and strobilurin fungicides on the incidence of toxic fungi and mycotoxins on winter wheat grain. *Botanica Lithuanica* **8**, https://www.researchgate.net/publication/228489433

González-Domínguez, E., Meriggi, P., Ruggeri, M. & Rossi, V. 2021. Efficacy of fungicides against *Fusarium* head blight depends on the timing relative to infection rather than on wheat growth stage. *Agronomy* **11**, 1549. https://doi.org/10.3390/agronomy11081549

Guedioura, I., Rahmoune, B., Khezzaren, A., Dahoumane, A. & Laouar, N. 2023. Combined effect of soil practices and chemical treatments on weeds growth, soil features, and yield performance in field wheat crop under Mediterranean climate. *Agronomy Research* **21**(1), 62–77. https://doi.org/10.15159/AR.22.079

Haidukowski, M., Pascale, M., Perrone, G., Pancaldi, D., Campagna, C. & Visconti, A. 2005. Effect of fungicides on the development of *Fusarium* head blight, yield and deoxynivalenol accumulation in wheat inoculated under field conditions with *Fusarium graminearum* and *Fusarium culmorum*. *Sci. Food Agric.* **85**, 191–198, https://doi.org/10.1002/jsfa.1965

Haidukowski, M., Visconti, A., Perrone, G., Vanadia, S., Pancaldi, D., Covarelli, L., Balestrazzi, R. & Pascale, M. 2012. Effect of prothioconazole-based fungicides on *Fusarium* head blight, grain yield and deoxynivalenol accumulation in wheat under field conditions. *Phytopathologia Mediterranea* **51**(1), 236–246. http://hdl.handle.net/20.500.11937/67934

Haile, J.K., N'Diaye, A., Walkowiak, S., Nilsen, K.T., Clarke, J.M., Kutcher, H.R., Steiner, B., Buerstmayr, H. & Pozniak, C.J. 2019. *Fusarium* Head Blight in Durum Wheat: Recent Status, Breeding Directions, and Future Research Prospects. *Phytopathology: Review*. https://doi.org/10.1094/PHYTO-03-19-0095-RVW

Hollomon, D.W., Butters, J.A., Barker, H. & Hall, L. 1998. Fungal beta-tubulin, expressed as a fusion protein, binds benzimidazole and phenylcarbamate fungicides. *Antimicrob. Agents Ch.* **42**(9), 2171–2173. https://doi.org/10.1128/aac.42.9.2171

Hooker, D.C., Schaafsma, A.W. & Tamburic–Ilincic, L. 2002. Using Weather Variables Pre– and Post–heading to Predict Deoxynivalenol Content in Winter Wheat. *Plant Disease* **86**(6), 611–619. https://doi.org/10.1094/PDIS.2002.86.6.611

Khan, N.I., Schisler, D.A., Boehm, M.J., Slininger, P.J. & Bothast, R.J. 2001. Selection and evaluation of microorganisms for biocontrol of *Fusarium* head blight of wheat incited by *Giberella zeae. Plant Dis*. **85**, 1253–1258. https://doi.org/10.1094/PDIS.2001.85.12.1253

Kolesnikov, L.E., Belimov, A.A., Kudryavtseva, E.Y., Hassan, B.A. & Kolesnikova, Yu.R. 2021. Identification of the effectiveness of associative rhizobacteria in spring wheat cultivation. *Agronomy Research* **19**(3), 1530–1544. https://doi.org/10.15159/AR.21.145

Kumar, K.N., Venkataramana, M., Allen, J.A., Chandranayaka, S., Murali, H.S. & Batra, H.V. 2016. Role of *Curcuma longa* L. essential oil in controlling the growth and zearalenone production of *Fusarium graminearum. LWT - Food Sci. Technol*. **69**, 522–528. https://doi.org/10.1016/j.lwt.2016.02.005

Kuznetsov, I.Yu., Alimgafarov, R.R., Akhiyarov, B.G., Safin, F.F. & Nafikova, A.R. 2020. Effect of different pesticides combined with Melafen on grain yield and quality of winter wheat. *Agronomy Research* **18**(1), 163–176. https://doi.org/10.15159/AR.20.006

Kuznetsov, B.S. 1980. *Practical guide on plant breeding*, 235 pp. (in Russian).

Lacey, J., Bateman, G.L. & Mirocha, C.J. 1999. Effects of infection time and moisture on development of ear blight and deoxynivalenol production by *Fusarium* spp. in wheat. *Annals of Applied Biology – AAB* **134**(3), 277–283. https://doi.org/10.1111/j.1744-7348.1999.tb05265.x

Large, E.C. 1954. Growth Stages in Cereals. Illustration of The Feekes Scale. *Plant Pathology* **3**, 128–129. https://doi.org/10.1111/j.1365-3059.1954.tb00716.x

Lehoczki-Krsjak, S., Szabó-Hevér, Á., Tóth, B., Kótai, C., Bortók, K., Varga, M., Farády, L. & Mesterházy, Á. 2010. Prevention of *Fusarium* mycotoxin contamination by breeding and fungicide application to wheat. *Food Addit. Contam.* **27**, 616–628, https://doi.org/10.1080/19440041003606144

Litke, L., Gaile, Z. & Ruža, A. 2019. Effect of nitrogen rate and forecrop on nitrogen use efficiency in winter wheat (Triticum aestivum). *Agronomy Research* **17**(2), 582–592. https://doi.org/10.15159/ar.19.040

Liu, S., Fu, L., Wang, S., Chen, J., Jiang, J., Che, Z., Tian, Y. & Chen, G. 2019. Carbendazim Resistance of *Fusarium graminearum* From Henan Wheat. *Plant disease* **103**, https://doi.org/10.1094/PDIS-02-19-0391-RE

Ma, H., Yongjiang, Liu Y., Zhao, X., Zhang, S. & Ma, H. 2022. Exploring and applying genes to enhance the resistance to *Fusarium* head blight in wheat. *Front Plant Sci.* **13**. https://doi.org/10.3389/fpls.2022.1026611

Malekinejad, H., Schoevers, E.J., Daemen, I.J.J.M, Zijlstra, C., Colenbrander, B., Fink-Gremmels, J. & Roelen, B.A.J. 2007. Exposure of oocytes to the *Fusarium* toxins zearalenone and deoxynivalenol causes aneuploidy and abnormal embryo development in pigs. *Biol. Reprod.* **77**, 840–847. https://doi.org/10.1095/biolreprod.107.062711

Machado, F.J., Santana, F.M., Lau, D. & Del Ponte, E.M. 2017. Quantitative Review of the Effects of Triazole and Benzimidazole Fungicides on *Fusarium* Head Blight and Wheat Yield in Brazil. *Plant Dis.* **101**(9), 1633–1641. https://doi.org/10.1094/PDIS-03-17-0340-RE

Maryland Agronomy News. *Fusarium* Head Blight Fungicide Recommendations. By Andrew Kness. https://blog.umd.edu/agronomynews/2018/05/03/fusarium-head-blight-fungicide-recommendations/ (accessed on 14 April, 2024)

Martirosyan, H.S., Mikaelyan, A.R., Asatryan, N.L. & Babayan, B.G. 2023. Assessment of 'Complex–co' preparation efficiency for some cereal crops growth stimulation. *Agronomy Research* **21**(3), 1213–1220. https://doi.org/10.15159/AR.23.105

McMullen, M., Bergstrom, G., De Wolf, E., Dill–Macky, R., Hershman, D., Shaner, G. & Van Sanford, D. 2012. A Unified Effort to Fight an Enemy of Wheat and Barley: *Fusarium* Head Blight. *Plant Disease* **96**(12), 1712–1728. https://doi.org/10.1094/PDIS-03-12-0291-FE

Mentewab, A., Rezanoor, H.N, Gosman, N., Worland, A.J. & Nicholson, P. 2000. Chromosomal location of *Fusarium* head blight resistance genes and analysis of the relationship between head blight and brown foot rot. *Plant Breeding* **119**, 15–20. https://doi.org/10.1046/j.1439-0523.2000.00439.x

Mesterhazy, A. 2020. Updating the Breeding Philosophy of Wheat to *Fusarium* Head Blight (FHB), Resistance Components, QTL Identification, and Phenotyping-A Review. *Plants.* **9**(12), 1702. https://doi.org/10.3390/plants9121702

Mesterházy, Á., Bartók, T., Mirocha, C.G. & Komoróczy, R. 1999. Nature of wheat resistance to *Fusarium* head blight and the role of deoxynivalenol for breeding. *Plant Breed* **118**, 97–110. https://doi.org/10.1046/j.1439-0523.1999.118002097.x

Miedaner, T., Flamm, C. & Oberforster, M. 2024. The importance of *Fusarium* head blight resistance in the cereal breeding industry: Case studies from Germany and Austria. *Plant Breeding* **143**, 1–15. https://doi.org/10.1111/pbr.13098

Mudge, A.M., Dill-Macky, R., Dong, Y., Gardiner, D.M., White, R.G. & Manners, J.M. 2006. A role for the mycotoxin deoxynivalenol in stem colonisation during crown rot disease of wheat caused by *Fusarium graminearum* and *Fusarium pseudograminearum. Physiol. Mol. Plant Pathol.* **69**, 73–85. https://doi.org/10.1016/j.pmpp.2007.01.003

Muhamedyarova, L.G., Derkho, M.A., Meshcheriakova, G.V., Gumenyuk, O.A. & Shakirova, S.S. 2020. Influence of bio-humus on soil fertility, productivity and environmental safety of spring wheat grain. *Agronomy Research* **18**(2), 483–493. https://doi.org/10.15159/AR.20.152

Nita, M., Tilley, K., De Wolf, E. & Kuldau, G. 2005. Effects of moisture during and after anthesis on the development of *Fusarium* head blight of wheat and mycotoxin production. Canty, S.M., Boring, T., Wardwell, J., Siler L. & & Ward, R.W. (eds), *Proceedings of the 2005 National Fusarium Head Blight Forum. Session 3: Etiology, Epidemiology, and Disease Forecasting,* pp. 125–128. https://scabusa.org/pdfs/forum05_proc_complete.pdf

Okereke, V., Jones, H. & Gooding, M. 2016. Time of *Fusarium* inoculation and post–anthesis temperature stress affect FHB severity and DON concentration in winter wheat. *Journal of Advances in Agricultur* **6**(2), 953–962. DOI: https://doi.org/10.24297/jaa.v6i2.5378

Parry, D.W., Jenkinson, P. & McLeod, L. 1995. *Fusarium* ear blight (scab) in small grain cereals –a review. *Plant Pathology* **44**, 207–238. https://doi.org/10.1111/j.1365-3059.1995.tb02773.x

Paul, P.A., Lipps, P.E., Hershman, D.E., McMullen, M.P., Draper, M.A. & Madden, L.V. 2008. Efficacy of triazole-based fungicides for *Fusarium* head blight and deoxynivalenol control in wheat: a multivariate meta-analysis. *Phytopathology* **98**(9), 999–1011. https://doi.org/10.1094/PHYTO-98-9-0999

Paul, P.A., Bradley, C.A., Madden, L.V., Lana, F.D., Bergstrom, G.C., Dill-Macky, R., Wise, K.A., Esker, P.D., McMullen, M., Grybauskas, A., Kirk, W.W., Milus, E. & Ruden, K. 2018. Effects of Pre- and Postanthesis Applications of Demethylation Inhibitor Fungicides on *Fusarium* Head Blight and Deoxynivalenol in Spring and Winter Wheat. Plant Dis. **102**(12), 2500–2510. doi: https://doi.org/10.1094/PDIS-03-18-0466-RE

Radchenko, M.V., Trotsenko, V.I., Hlupak, Z.I., Zakharchenko, E.A., Osmachko, O.M., Moisiienko, V.V., Panchyshyn, V.Z. & Stotska, S.V. 2021. Influence of mineral fertilizers on yielding capacity and quality of soft spring wheat grain. *Agronomy Research* **19**(4), 1901–1913. https://doi.org/10.15159/AR.21.104

Sarwar, M.H., Sarwar, M.F., Sarwar, M., Qadri, N.Q. & Moghal, S. 2013. The importance of cereals (Poaceae: Gramineae) nutrition in human health: A review. *Journal of Cereals and Oilseeds* **4**, 32–35. https://doi.org/10.5897/JCO12.023

Schaafsma, A.W., Tamburic-Ilincic, L. & Hooker, D.C. 2005. Effect of previous crop, tillage, field size, adjacent crop, and sampling direction on airborne propagules of *Gibberella zeae/Fusarium graminearum, Fusarium* head blight severity, and deoxynivalenol accumulation in winter wheat. *Can. J. Plant Pathol.* **27**, 217–224. https://doi.org/10.1080/07060660509507219

Stenglein, S. 2009. *Fusarium poae*: A pathogen that needs more attention. *Journal of Plant Pathology* **91**(1), 25–36. doi:10.4454/jpp.v91i1.621

Shah, L., Ali, A., Yahya, M., Zhu, Y., Wang, S., Si, H., Rahman, H. & Ma, C. 2018. Integrated control of *Fusarium* head blight and deoxynivalenol mycotoxin in wheat. *Plant Pathology*. **67**, 532–548. https://doi.org/10.1111/ppa.12785

Shude, S.P.N., Yobo, K.S. & Mbili, N.C. 2020 Progress in the management of *Fusarium* head blight of wheat: An overview. *S. Afr. J. Sci*. **116**(11/12). https://doi.org/10.17159/sajs.2020/7854

Sioua, D., Gelissea, S., Lavala, V., Repincayb, C., Canalesc, R., Suffertaand, F., Lannoua, C. 2014. Effect of wheat spike infection timing on *Fusarium* head blight development and mycotoxin accumulation. *Plant Pathology* **63**, 390–399. https://doi.org/10.1111/ppa.12106

Siranidou, E. & Buchenauer, H., 2001. Chemical control of *Fusarium* head blight on wheat *Journal of Plant Diseases and Protection* **108**(3), 231–243. http://www.jstor.org/stable/45154854

Spanic, V., Zdunic, Z., Drezner, G. & Sarkanj, B. 2019. The Pressure of *Fusarium* Disease and Its Relation with Mycotoxins in the Wheat Grain and Malt. *Toxins.* **11**(4), 198. https://doi.org/10.3390/toxins11040198

Stack, R.W. 2000. Return of an old problem: *Fusarium* head blight of small grains. *Plant Health Progress* **1**. doi: https://doi.org/10.1094/PHP-2000-0622-01-RV

Statistical Yearbook of Armenia, 2022. https://armstat.am/file/doc/99533308.pdf

Švarta, A., Bimšteine, G., Gaile, Z., Kaneps, J. & Pluduma-Paunina, I. 2022. Winter wheat leaf blotches development depending on fungicide treatment and nitrogen level in two contrasting years. *Agronomy Research* **20**(2), 414–423. https://doi.org/10.15159/AR.21.160

Teli, B., Purohit, J., Rashid, Md.M., Jailani, A.K. & Chattopadhyay, A. 2020. Omics Insight on *Fusarium* Head Blight of Wheat for Translational Research Perspective. *Current Genomics* **21**, 411–428. https://doi.org/10.2174/1389202921999200620222631

Yoshida, M., Kawada, N. & Nakajima, T. 2007. Effect of infection timing on *Fusarium* Head Blight and mycotoxin accumulation in open– and closed–flowering barley. *Phytopathology* **97**, 1054–1062. https://doi.org/10.1094/PHYTO-97-9-1054

Vaughan, M.M., Backhouse, D. & Del Ponte, E.M. 2016. Climate change impacts on the ecology of *Fusarium graminearum* species complex and susceptibility of wheat to Fusarium head blight: A review. *World Mycotoxin Journal* 9, 1–16. doi: https://doi.org/10.3920/WMJ2016.2053

Wegulo, S.N., Baenziger, P.S., Nopsa, J.H., Bockus, W.W. & Hallen-Adams, H. 2015. Management of *Fusarium* head blight of wheat and barley. *Crop Prot.* **73**, 100–107. https://doi.org/10.1016/j.cropro.2015.02.025

Windels, C.E. 2000. Economic and social impacts of *Fusarium* head blight: changing farms and rural communities in the northern great plains. *Phytopathology* **90**, 17–21. https://doi.org/10.1094/PHYTO.2000.90.1.17

Wu, J., Ackerman, A., Gaire, R., Chowdhary, G. & Rutkoski, J. 2023. A neural network for phenotyping *Fusarium*-damaged kernels (FDKs) in wheat and its impact on genomic selection accuracy. *Plant Phenome* **6**(1). https://doi.org/10.1002/ppj2.20065

Zargar, M., Polityko, P., Pakina, E., Bayat, M., Vandyshev, V., Kavhiza, N. & Kiselev, E. 2018. Productivity, quality and economics of four spring wheat (Triticum aestivum L.) cultivars as affected by three cultivation technologies. *Agronomy Research* **16**(5), 2254–2264. https://doi.org/10.15159/AR.18.204

Zemánková, M. & Lebeda, A. 2001. *Fusarium* species, their taxonomy, variability and significance in plant pathology – a review. *Plant Protection Science* **37**, 25–42. https://doi.org/10.17221/8364–PPS

Zhao, H., Tao, X., Song, W., Xu, H., Li, M., Cai, Y., Wang, J., Duan, Y. & Zhou M. 2022. Mechanism of *Fusarium graminearum* resistance to ergosterol biosynthesis inhibitors: G443S substitution of the drug target FgCYP51A. *Agric. Food Chem.* **70**, 1788–1798. https://doi.org/10.1021/acs.jafc.1c07543

Zhou, Y., Xu, J., Zhu, Y., Duan, Y. & Zhou, M. 2016. Mechanism of Action of the Benzimidazole Fungicide on *Fusarium graminearum*: Interfering with Polymerization of Monomeric Tubulin But Not Polymerized Microtubule. *Phytopathology* **106**(8), 806–813 https://doi.org/10.1094/PHYTO-08-15-0186-R

Agronomy Research **22**(1), 72–84, 2024
https://doi.org/10.15159/AR.24.009

Testing outcomes of IoT based continuous crop weight and PAR sensors at industrial greenhouse

A. Avotins[1,*], A. Potapovs[1], J. Gruduls[2] and R. Ceirs[2]

[1]Riga Technical University, Institute of Industrial Electronics and Electrical Engineering, Azenes 12, LV-1048 Riga, Latvia
[2]SIA 'Latgales darzenu logistika' greenhouse, Kloneshniki, Mezvidi parish, Ludza region, Latvia
[*]Correspondence: ansis.avotins@rtu.lv

Received: January 31st, 2023; Accepted: December 12th, 2023; Published: February 6th, 2024

Abstract. Industrial greenhouses have automated control systems for climate, lighting, irrigation, ventilation, and heating regulation using different types of feedback sensors. Nowadays it is a trend to increase the data precision and measurement data amount, thus various additional IoT sensors are installed, and the regulation becomes more precise, due to available data, which enables new analytical features to create new control rules or strategies. The general aim is to raise the level of process automation, quality, energy efficiency, and other important parameters. Still, further, we go into data resolution and amount, and the problem of data reliability and interpretation starts to become a challenging problem. In this article, authors focus on earlier developed PAR sensor modules and continuous tomato crop weight sensor modules (TWS) testing and received data analysis from an industrial greenhouse. Both sensors were tested in detail at the tomato greenhouse of 'Latgales Darzenu Logistika' in Mezvidi parish, with a total growing area of 5,062.4 m^2 from 1.05.2022 to 30.06.2022., and gathered data is analysed for this period. Received sensor data can be used as the main feedback signal to create a lighting control strategy, same time increasing energy efficiency and reducing also costs. As artificial lighting energy consumption costs make 20–40% of total greenhouse costs, it is worth having a more precise lighting control system algorithm, integrating the crop growth increase and accumulated light energy during the day from the sun, and then adding only the missing amount (also period) of light provided by artificial lighting. Experimental studies of both sensor data, show that plants reaction can be monitored, as by decreasing the lighting period and temperature setpoint by 6% each, the plants daily weight gain decreases by 14%, and it can be measured already in first day after the new settings were set in place.

Key words: greenhouse control systems, IoT, sensors, weight measurement.

INTRODUCTION

Nowadays industrial management systems are changing, using various Internet of Things (IoT) based sensor technologies, to create cloud-based databases. Industrial greenhouse control systems are no exception in this regard, as they have recently become

more popular with the use of various sensors and cloud-based databases for the automation of vegetable and other crop cultivation processes (Singh et al., 2020; Blahins et al., 2021).

Each of these management systems has a control signal from a feedback loop, typically gained from some physical sensor, to control the vegetable growing process.

IoT technologies and sensors (Afzali et al., 2021; Potapovs & Avotins, 2022) are widely used in various fields of agronomy, for example for fermentation process of rice wine (Vošahlik & Hart, 2021; Vošahlik, 2023). Authors remark, that during the rice wine fermentation process, variety of measurable attributes are created which affect the quality of the resulting. With IoT they can be monitored with the help of automation elements (pH, temperature, humidity etc.) and the result is that, if the right environment is chosen, the quality of the fermented wine will improve. IoT sensor system can be used also for lighting system optimisation, where study (Afzali et al., 2021) shows, that electricity costs can be reduced by 4.16% reduction (winter) and 33.85% (spring).

The relevance of the importance of using and correct calibration of physical sensors is confirmed by studies of other authors, for example in the article (Shchuklina et al., 2021; Shchuklina et al., 2022) authors using optical sensors for efficient diagnostics of nitrogen nutrition. Results of their research show the efficiency of using optic sensors (N-testers) for efficient diagnostics of nitrogen nutrition of plants. Authors make conclusion, that such a modern optical device as N-tester, whose action is based on measuring the concentration of leafy chlorophyll, can replace chemical methods and increase the efficiency of nitrogen fertilization, which means increasing the productivity of plants and reducing the negative impact of unreasonable use of nitrogen fertilizers.

Also, popular sensor type is computer vision (CV). For example (Kurras et al., 2023) uses CV for automatic monitoring of dairy cows' lying behavior in open barns.

Authors in paper (Pažuls et al., 2018) describing system where using application of ultrasonic sensors in evaluation of distribution and depth of ruts in forest thinning, but (Bazhenov et al., 2021) using radar sensors for method for determining the moisture content of the upper layers of agricultural lands on the basis of mathematical modeling of a radar signal reflected from the soil.

Authors (Tkach et al., 2021) provide milk-meter based on electric capacitive sensors, where use of certain correction factors for sensor signal ensures sufficient measurement accuracy both for installations with stall milk pipelines and for milking parlors, including during milking of high-performance cows. Authors mark, that challenges include reliable approaches for object detection and tracking as well as pose estimation for images in the barn environment that are characterized by visual obstructions due to overlapping cows and barn infrastructure - occlusion. The authors also conducted studies about long-term testing and measurement data analysis of tomato crop weight sensor module (Potapovs & Avotins, 2022).

Also one of the parameters which is needed to monitor in exactly tomato greenhouses is photosynthetically active radiation (PAR) or photosynthetic photon flux density (PPFD) (Van Straten, 2011; Witkowski & Korzeniewska, 2019; Potapovs & Avotins, 2022).

PPFD monitoring allows recording the cumulative number of micromoles per day the plant has received, which in turn allows monitoring and analysing the impact of this parameter on other physical and technical parameters of the vegetable industrial

greenhouse and, as a result, more effectively control the artificial lighting system and the parameters of the greenhouse.

Other type of important sensors is different types of weight sensors (WS), thus to control irrigation process of tomatoes, it is needed to monitor weight of tomato plants and its soil pod (Witkowski & Korzeniewska, 2019). Weight measurements show tendency of water (fertilizer) consumption and gives precise timing when irrigation must be started and stopped (change in moisture level between start and the end of watering is about 7 to 13%).

Also, weight sensors can be used for tomato weight measuring and it helps to show tendency of crops biomass increase (Moon et al., 2022), plants overall health, balance between parts of the plant according to programmed greenhouse climate values (Van Straten, 2011; Afzali, 2021).

Control system with such type of sensors can enable new features (Afzali, 2021):

- decrease of electrical energy consumption;
- decrease lamp burning hours per year;
- decrease CO_2 emissions;
- new lighting strategies avoiding or minimizing lighting in peak hours of electricity market.

Photosynthesis is almost instantly dependant on light increase/decrease on plant leaves, also according to 'shading' impact on crop yield decrease (Reed et al., 1988) we can define research hypothesis that a plant reaction on light decrease will result also on yield gain loss, but this effect is shifted by several days and it is not instant. The goal is to create an IoT sensor-based measurement setup, obtain measurement data and analyse them to see the tomato plant reaction time.

After the conducted research and the experimental use of sensors in real working conditions, the authors put forward the following main tasks:

- Compare the data provided by PAR sensor modules in different types of greenhouses and compare them with the irradiance data of industrial weathering, evaluate the operation of PAR sensor modules from the point of view of their operational stability, as well as evaluate their interaction with the data storage server;
- Compare tomato weight sensor module (TWS) data with official harvest data, evaluate sensor performance from the point of view of their operational stability, as well as evaluate their interaction with the data storage server;
- To perform mutual data analysis of PAR and TWS sensor modules, to determine the possible correlation between these two parameters, and use the obtained information for further adaptive control of the artificial lighting system.

MATERIALS AND METHODS

Description of PAR sensor and analysis of accumulated server data

Testing environment, greenhouse and PAR sensor module development and testing process in detail was described in the authors© previous work (Potapovs & Avotins, 2022). In developed IoT sensor modules, to measure the PAR parameter in industrial greenhouse conditions, the Apogee ePAR sensor SQ-615-SS with an analogue signal output (Apogee Instruments, 2022) was chosen, which operates in the range of 383 to 757 nm (+/-5nm), and allows to classify it to ePAR for sensors.

As the selected ePAR sensor model SQ-615-SS is an analogue sensor, so for measuring, its output signal needs to be connected to the microcontroller or the external ADC module. In this particular case, the authors chose the connection to the analogue input of the microcontroller according to the following schematic given in Fig. 1.

Two types of PAR sensor modules were developed (see Fig. 2). First type of PAR sensor is for static measurements, but second type is for portable measurements, for example passing through the whole row of plants.

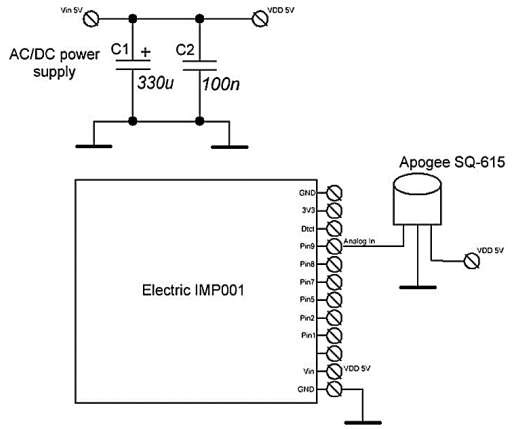

Figure 1. Electric scheme of PAR sensor prototype.

a) Static sensor

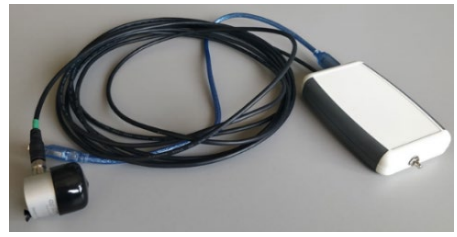

b) Portable sensor

Figure 2. Developed PAR sensor modules.

In IoT server side was developed data base, where was displayed following data (Fig. 3):

- current value PARmom,
- graph of PARmom historical data for the last 72 h,
- cumulative current day value PARsumm,
- graph of PARsumm of the daily cumulative values of the last month.

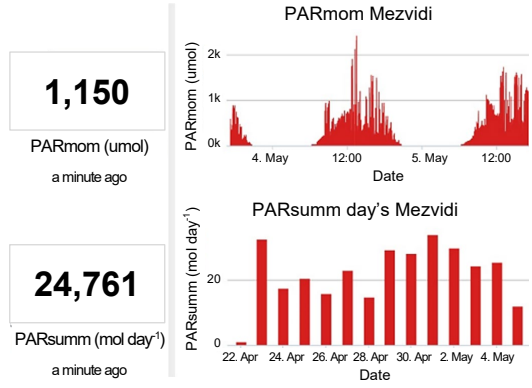

Figure 3. PAR sensor data example from the data server.

Growing conditions are not studied in this research, as they are maintained unchanged during the tests, and overall production/growing process is according to industrial greenhouse control system (PRIVA) and growing procedures. In June/July average temperature in greenhouse is maintained in 23–25 °C range (16–17 °C during night and 25 °C+/-3oC during the day), CO_2 injection was not used, relative humidity level is maintained 75% (night: 85%, day: 55–60%), only 'vegetation' heating pipe is used during night time only (45 °C), artificial lighting is not used, irrigation system/ cycles follows sun, where first is started 2–3 h

after sunrise and last 3 h before sundown. Main focus lies on ePAR and TWS sensor reading and data analysis. More details on the sensor are given in author previous research (Potapovs et al., 2021 and Potapovs & Avotins, 2022).

The obtained two PAR sensor PARsumm data (cumulative PAR by days) from 1.05.2022 to 30.6.2022 (Fig. 4):

- One of them was installed in tomato greenhouse Mezvidi, which has venlo-type glass cover;
- Second in nearby located greenhouse of Aberry, which has double-film cover material and is growing strawberries).

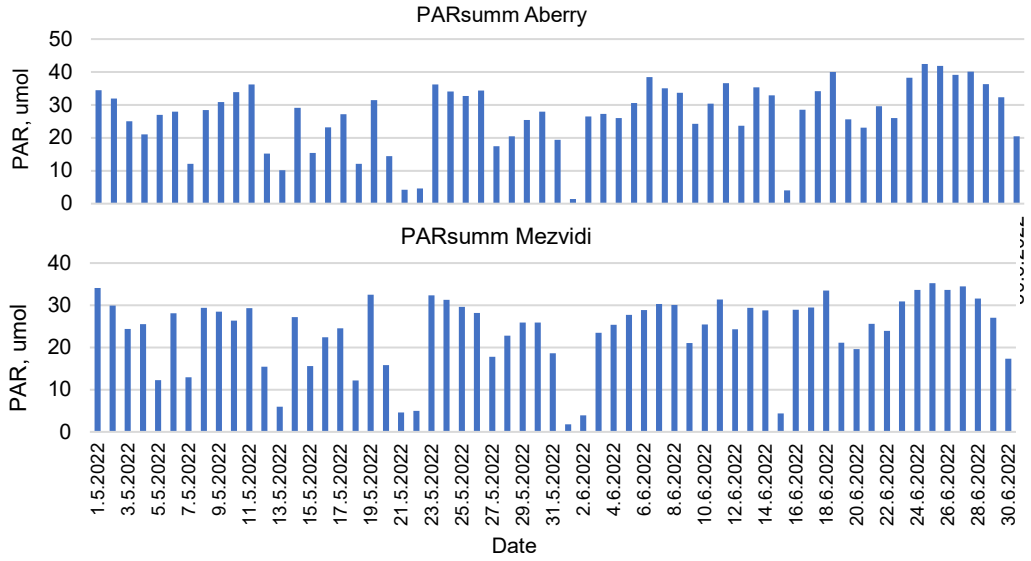

Figure 4. PAR sensor module PARsumm data of two type greenhouse from 1.05.2022 to 30.06.2022.

This data was compared with irradiation sensor data (Fig. 5) from weather station of the *Priva* industrial control system (see graphs below). The obtained data show that by installing PAR sensors inside the greenhouse, it is possible to measure the actual PAR value received by plants with much higher accuracy.

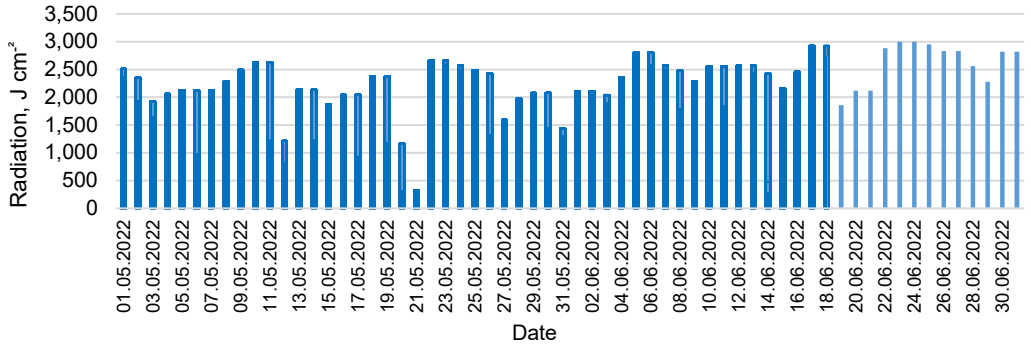

Figure 5. Industrial weather station data of irradiation.

Tomato weight sensors (TWSs)

Two types of weight sensor modules were developed and tested in industrial greenhouse conditions (Fig. 6):

- load sensor module (LSM),
- tomato weight sensor (TWS).

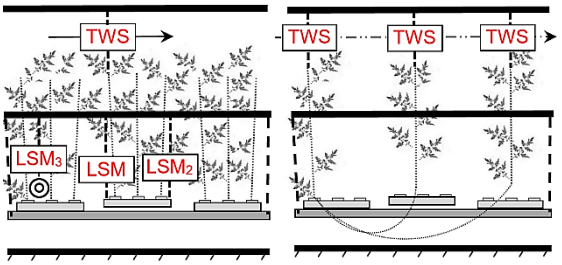

Figure 6. LSM and TWS testing schematic for real greenhouse environment: 1 – LSM sensors; 2 – TWS sensors.

Development and testing of both sensors in details is described in previous research of Potapovs et al. (2021). LSM sensors are designed for weighing the base of the tomato plant substrate, for evaluating the efficiency of the automatic watering system. Also, one of these modules (LSM3) is used for testing the stability of the WS readings of the selected weight sensors over a long time period.

On the other hand, TWS sensor, was developed to be used for measuring the weight of the specific/individual tomato plant, with the possibility to follow its overall (leaves, fruit, stem) mass gain in all its growth stages. The goal is to determine its yield or yield gain during daily period, especially in cases when conducting experiments with different types of lighting levels or periods, or, for example, the nutrient volume supplied and/or mix combination.

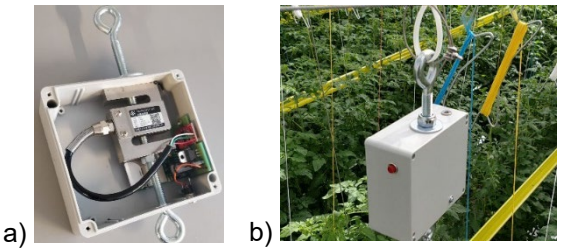

Figure 7. Developed and installed TWS sensor examples: a) TWS internal design; b) installed TWS in greenhouse.

Developed and installed TWS sensor examples are shown in Fig. 7.

To store sensor data, a data base was developed at the IoT server side, where also following data can be displayed (Fig. 8):

- Graph of plant weight of the last 3 days, g (Fig. 8, a);
- Graph of plant weight growth of the daily cumulative values of the last 5 days, g d^{-1} (Fig. 8, b).

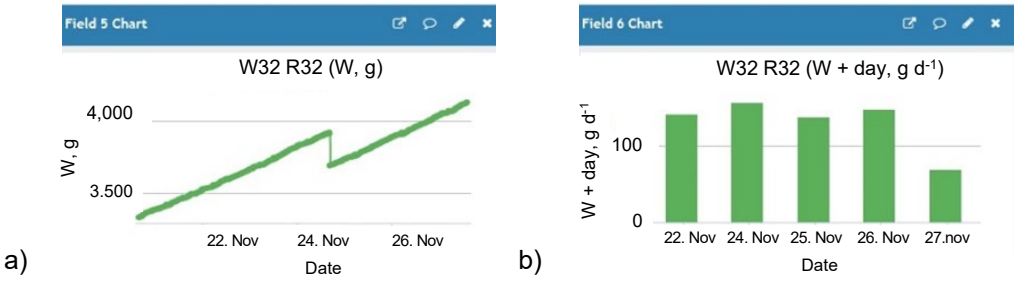

Figure 8. TWS sensor data example from the data server.

RESULTS AND DISCUSSION

For further analysis of stored data, we will use the readings of the first weight sensor W1 and calculated parameter W_{summ}, which is the daily (cumulative) weight gain in plant mass (Fig. 9). This sensor was installed in the row R16 of the Mezvidi greenhouse growing area with 40 growing rows in total.

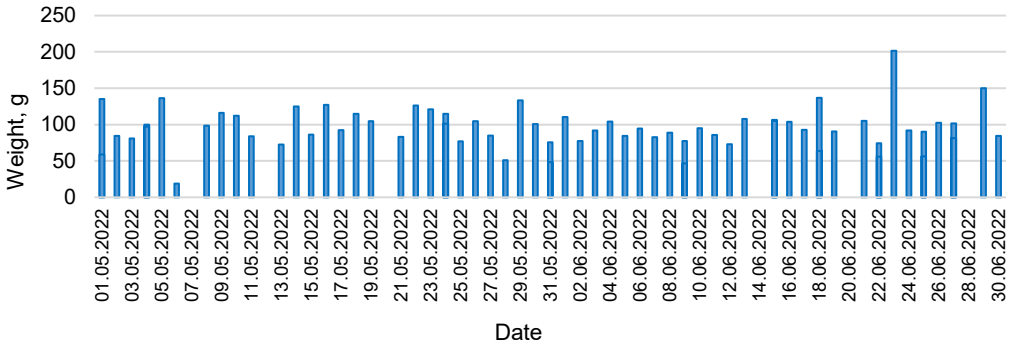

Figure 9. TWS sensor module W16 (R16) Wsumm data 01.05.2022–30.06.2022.

Fig. 10 shows harvested (manually measured) crop yield of a larger zone in the greenhouse, where the W1 sensor was installed. We can observe, that single sensor daily increase readings also show same tendency in reference zone weight increase or decrease. Normally 100 g per day gain is the targeted weight gain and could be accounted as good result for given situation (available solar light amount), thus everything above or below this threshold can give some predictive values. If we look at Fig. 9, at date 25.06.2022 we got twice the amount of daily weight increase, namely 200 g per day, and this is reflected also in Fig. 10 weekly harvest data of 29.06.2022. The 50 g and 0 g per day values in Fig. 9, can be explained by fruit cuts/drops in the morning or by leaf cuts during the day, as the weight can drop by 250 g or even more, so the cumulative daily plant mass gain value can get even negative (zero in our case, as logic rule is applied).

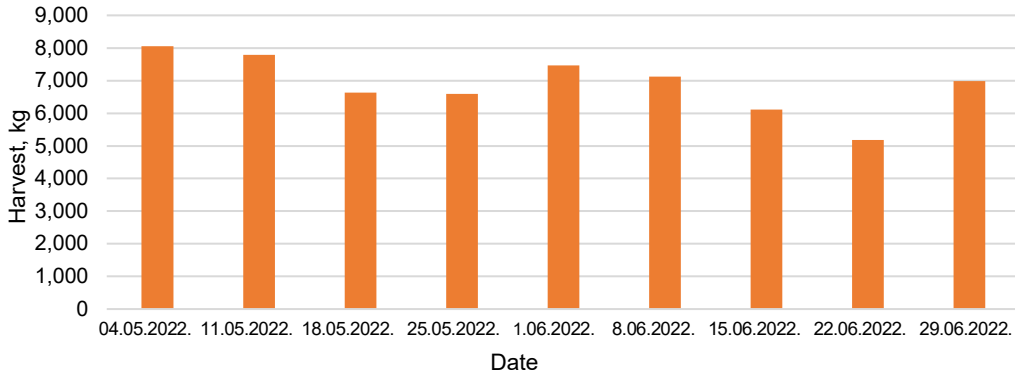

Figure 10. Reference harvest data from greenhouse 01.05.2022–30.06.2022.

Fig. 11. shows the effect of lighting period decrease by 1 hour per day (from 17.45 to 16.45 h) and temperature decrease by 1 °C (from 20.2 °C to 19.7 °C) starting from 01.01.2023. As we can see, the plants reaction happens much earlier - within few days, where before it was anticipated to have reaction in weeks.

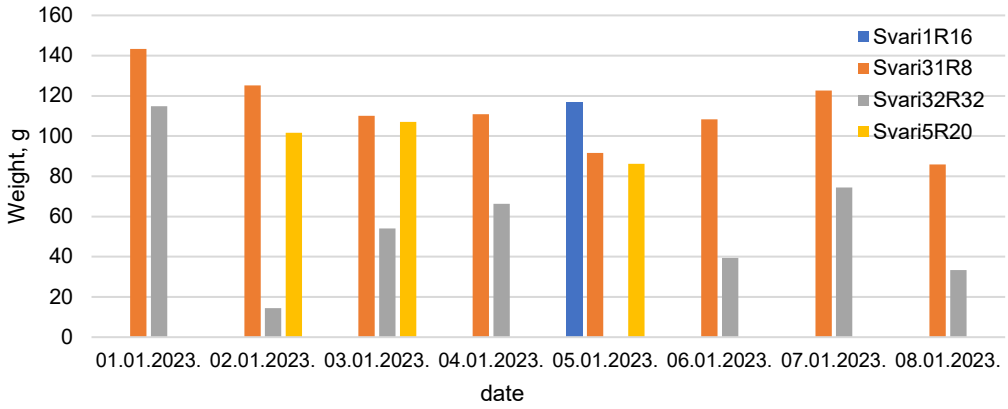

Figure 11. TWS sensor module readings in row 8 (Svari31R8), row 20 (Svari5R20), row 32 (Svari32R32) and row 16 (Svari1R16).

Analysing the data obtained from both installed PAR sensors, it can be concluded that their data differ significantly from each other and the characteristic curve differs even more from the data of the radiation characteristic curve of the external weather station (see Fig. 12), because the readings of the installed PAR sensors inside the greenhouse are influenced by such factors such as:

a) artificial lighting;
b) cleanliness of greenhouse windows;
c) the shadow cast by shading curtains;
d) greenhouse constructive materials;
e) greenhouse screens (motorised curtains for shading).

However, the installation of several such sensors inside the greenhouse above the top of the plants, might allow more accurate recording of the PPFD received by the tomato plants, than using the data of an external weather station, which does not observe all parameters in its readings.

In Fig. 12, we can see that Aberry greenhouse (growing strawberries) has double-film cover material, and Mezvidi tomato greenhouse has venlo-type glass cover, and for Aberry we observe 23–34% less instant PAR values, depending on sun's position during the day. These data were confirmed throughout the experiment lasting 2 months.

However, we can observe (Fig. 12) that the PAR sensor readings are also affected by the shadows cast by the greenhouse structures (they are more pronounced in the Mezvidi glass and metal frame greenhouse, but less in the Aberry greenhouse with less constructive elements), which introduces local drops in the sensor readings. Irradiation sensor, of the weather station, doesn't has such problem, as it is located outside the greenhouse, but it is unable to record the accumulated energy of the plants according to the 4 points described above.

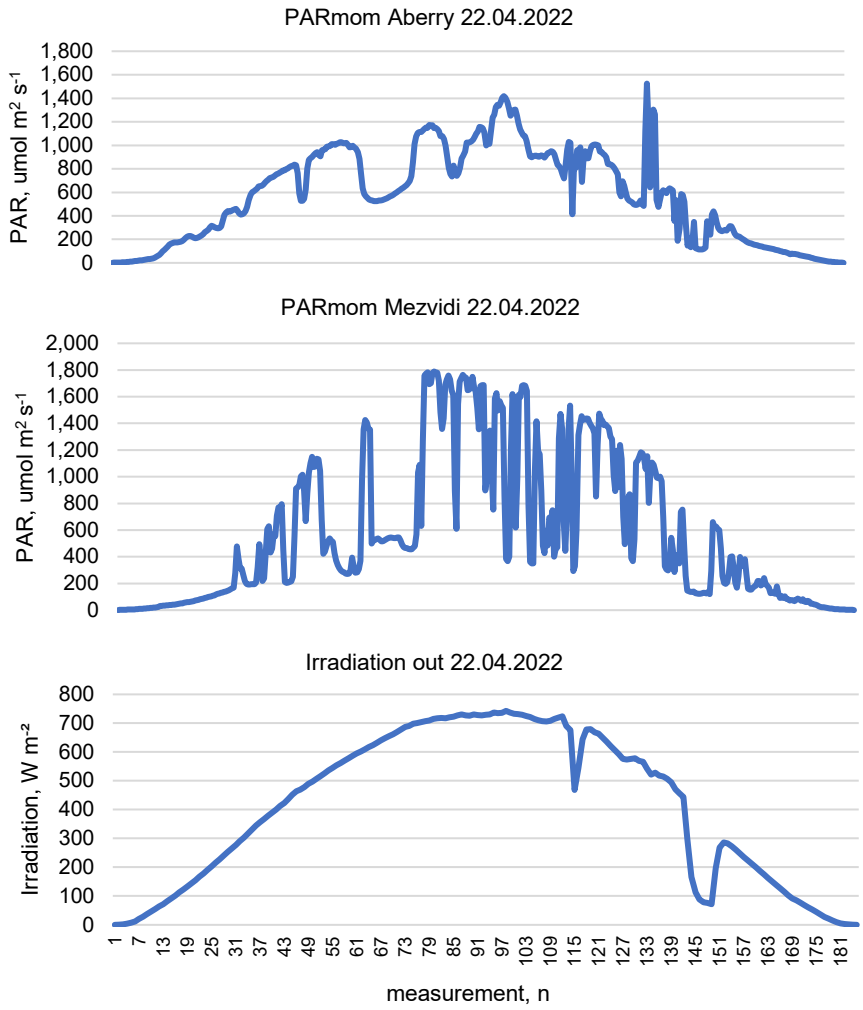

Figure 12. PAR and irradiation sensors data detailed comparison for 1 day.

During the processing of the data accumulated on the server after the 2-month experiment, the problem of the PAR sensor module, which was not resolved in time when developing the algorithm of recording and saving the daily cumulative reading, manifested itself in such a way that the value of the PARsumm previously accumulated in the current day becomes zero if the power voltage disappears. This can be addressed in two ways:

• Periodically saving this value in the energy-independent memory, thereby minimizing the lost volume of the cumulative value;

• Summation of several PARsumm inventory amounts (if its zeroing has been detected) in one day on the data storage server before saving the final value of PARsumm in the database.

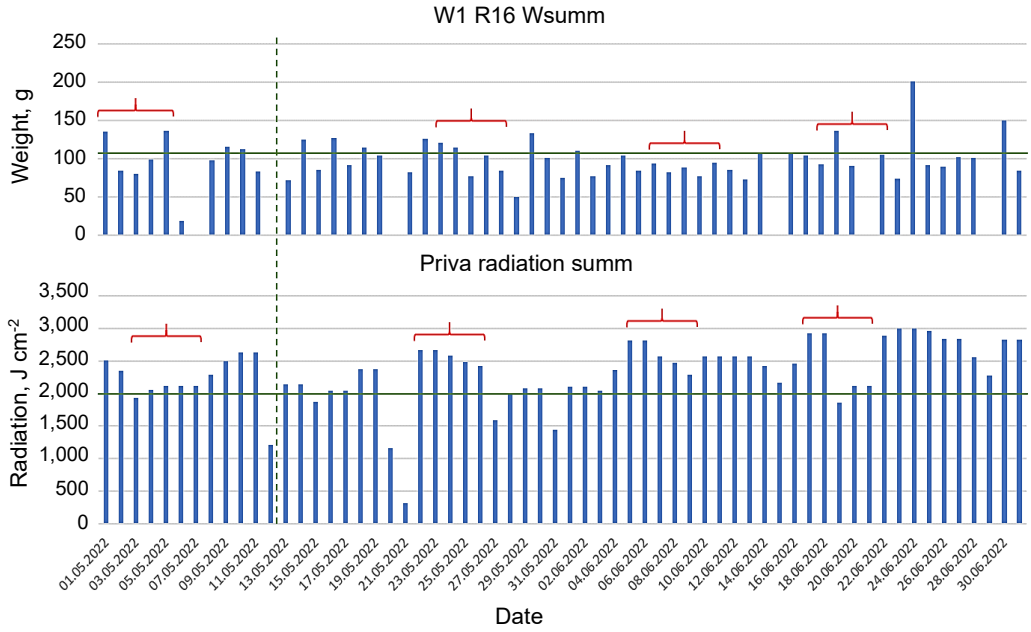

Figure 13. Obtained solar radiation values from greenhouse PRIVA control system and weight sensor data.

Fig. 13. shows solar radiation data from weather-station (located on greenhouse roof) stored by PRIVA system used for greenhouse control and developed weight sensor obtained daily weight increase data. It doesn't show clearly visible and repeatable relationship between light loss and daily weight decrease, but surely, we can observe some correlation here. According to greenhouse and growing technology manuals, this effect is considered to be one week, but we can see it happens between 1–4 days, which is much faster than prescribed. Also, we can observe, that some weight data are missing (around 16%), due to communication problems between hardware and database, thus raising the question about data reliability, which must be improved further in order to obtain more precise data for further evaluation and analytic method development. Sensor readings time to time were affected by the human factor, i.e. the workers who perform the operations around the plants (harvest, care for the plant, hang it, etc.), sometimes didn't hang the plant back in the scale after the last-mentioned operations, so further data from them were lost or faulty. The further use of this type of sensors within creates additional demands on the greenhouse service personnel. With TWS and PAR sensor application and data monitoring, plants reaction can be monitored, as we found out that in one row, the light period and maintained greenhouse temperature decrease by 6% each, resulted in decreased plants daily weight gain by 14% already in first day after the new settings were set in place. This effect dynamics must be studied further, also placing a focus on predictive algorithm studies and testing.

As stated in Perin et al. (2018), the accumulated incoming light radiation has larger impact on plant growth variables than temperature. The shading experiments by other researchers also confirm that tomato is sensitive to light decrease, where measured plant dry matter decreased by 19%–31% and yield loss was observed (Kläring & Krumbein, 2013).

For tomato greenhouse manager, the yield predication is an important parameter, as it directly affects the income or contract demands fulfilling for supermarkets. One of the IoT sensor benefits is the data that can be obtained in hourly, daily or weekly basis, enabling automatic data recoding and feeding into prediction algorithms (Higashide, 2009) or enabling new control algorithms for supplemental LED lighting, as it can compensate the yield decrease if reacted in advance (Tewolde et al., 2018). In case of neural network variant application, the research by Rajashree et al. (2022) indicates, that Vanilla GRU method gives higher precision prediction results, but as it is used in different field, it should be confirmed also for tomato crop prediction application.

CONCLUSIONS

When analysing the collected data from the TWS sensors, it became clear that the not all data were recorded, and after deeper analysis we can conclude, that possible issues for this problem are related with availability of AC mains voltage, WiFi router connectivity or data packet collisions, microcontroller code (program or sequence), instability of reference voltage value or human factor (tomato harvesters). As the data are obtained distantly, it would be advisable to integrate internal system self-check routines and parameters that are also sent to the database - to have more details about failure type for further improvements.

The second factor affecting full data collection from several TWS was the operating algorithm of the data server version used at the time, which was unable to record the sent data packets from several sensors at the same time (under certain conditions of synchronization of the working modes of the sensors, the data of the first sensor was recorded, the rest were ignored). This factor strongly influenced the fixation of the daily cumulative value, which was sent only once a day.

Experimental studies of PAR and TWS sensor data, show that plants reaction can be monitored this way, as by decreasing the lighting period and temperature setpoint by 6% each, results in decreased plants daily weight gain by 14%, already in first day after the new settings were set in place. The dynamics of this effect must be studied further, also placing a focus on predictive algorithm studies and testing.

ACKNOWLEDGEMENTS. Publication is created with support of the Latvian Rural Development Program Project N.18-00-A01620-000006 project ‘Development of greenhouse complex lighting system evaluation method’.

REFERENCES

Afzali, S., Mosharafian, S., Van Iersel, M.W. & Velni, J.M. 2021. Optimal Lighting Control in Greenhouses Equipped with High-intensity Discharge Lamps Using Reinforcement Learning. *2021 American Control Conference (ACC)*, pp. 1414–1419. doi: http://dx.doi.org/10.23919/ACC50511.2021.9482964

Afzali, S., Mosharafian, S., van Iersel, M.W. & Mohammadpour Velni, J. 2021. Development and implementation of an IoT-enabled optimal and predictive lighting control strategy in greenhouses. *Plants* **10**(12), 2652. doi: http://dx.doi.org/10.3390/plants10122652

Apogee Instruments, SQ-610 Datasheet, internet website: *https://www.apogeeinstruments.com/content/SQ-610-spec-sheet.pdf* (last accessed 28.11.2022.)

Bazhenov, A., Sagdeev, K., Goncharov, D. & Grivennaya, N. 2021. Bistatic system for radar sensing of soil moisture. *ERDV*, 919–925. doi: http://dx.doi.org/10.22616/ERDev.2021.20.TF207

Blahins, J., Kalnins, G., Kalnins, K. & Zabasta, A. 2021. IoT smart add-on for small-farms milking machine. *ERDV*, 1494–1500. doi: http://dx.doi.org/10.22616/ERDev.2021.20.TF320

Higashide, T. 2009. Prediction of Tomato Yield on the Basis of Solar Radiation Before Anthesis under Warm Greenhouse Conditions. *HortScience horts* **44**(7), 1874–1878. doi: https://doi.org/10.21273/HORTSCI.44.7.1874

Moon, T., Kim, D., Kwon, S., Ahn, T.I. & Son, J.E. 2022. Non-Destructive Monitoring of Crop Fresh Weight and Leaf Area with a Simple Formula and a Convolutional Neural Network. *Sensors* **22**, 7728. doi: http://dx.doi.org/10.3390/s22207728

Kläring, H.-P & Krumbein, A. 2013. The Effect of Constraining the Intensity of Solar Radiation on the Photosynthesis, Growth, Yield and Product Quality of Tomato. *Journal of Agronomy and Crop Science* **199**(5). doi: http://dx.doi.org/10.1111/jac.12018

Kurras, F., Gravemeier, L.S., Dittmer, A., Kümper, D. & Jakob, M. 2023. Automatic Monitoring of dairy cows lying behaviour using a computer vision system in open barns. *Agronomy Research* **21**(S2), 482–493. doi: https://doi.org/10.15159/AR.23.029

Perin, L., Marins, R.P.N., Trentin, R., Streck, E.A., Schulz Bergmann da Rosa, D., Hohn, D. & Silveira Schaun, W. 2018. Solar radiation threshold and growth of mini tomato plants in mild autumn/winter condition. *Scientia Horticulturae* **239**, 156–162, ISSN 0304-4238, https://doi.org/10.1016/j.scienta.2018.05.037

Potapovs, A. & Avotins, A. 2022. ePAR Sensor Testing for Industrial Greenhouse Lighting Control System Application, *2018 IEEE 59th International Scientific Conference on Power and Electrical Engineering of Riga Technical University (RTUCON)*, pp. 1–6. doi: http://dx.doi.org/10.1109/RTUCON56726.2022.9978897.

Potapovs, A., Avotins, A., Gruduls, J, Čeirs, R. 2021. Long-term testing and measurement data analysis of tomato crop weight sensor module *ERDV*, 1590–1597. doi: http://dx.doi.org/10.22616/ERDev.2021.20.TF339

Rajashree, K., Prema, K.V., Rajath, G. & Angad, S. 2022. 'Prediction of fruit rot disease incidence in Arecanut based on weather parameters'. *Agronomy Research* **20**(S1), 1117–1133. doi: https://doi.org/10.15159/AR.22.076

Reed, A., Singletary, G., Schussler, J., Williamson, D. & Christy, A. 1988. Shading effects on dry matter and nitrogen partitioning, kernel number, and yield of maize. *Crop Science* **28**(5), 819–825. doi: http://dx.doi.org/10.2135/cropsci1988.0011183X002800050020x

Shchuklina, O., Afanasiev, R., Voronchikhina, I., Klimenkova, I. & Komkova, A. 2021. Differentiated application of nitrogen fertilizers based on optical sensor readings. *Agronomy Research* **19**(2), pp. 595–600. doi: https://doi.org/10.15159/AR.21.093

Shchuklina, O., Afanasiev, R., Gulevich, A., Baranova, E., Kvitko, V. & Kvitko, O. 2022. Using data of optic sensors and pigment content in leaves for efficient diagnostics of nitrogen nutrition. *Agronomy Research* **20**(4), 805–813. doi: https://doi.org/10.15159/ar.22.048

Singh, R.K., Berkvens, R. & Weyn, M. 2020. Energy Efficient Wireless Communication for IoT Enabled Greenhouses. 2020 International Conference on COMmunication Systems & NETworkS (COMSNETS*)*, pp. 885–887. doi: 10.1109/COMSNETS48256.2020.9027392

Tewolde, F.T., Shiina, K., Maruo, T., Takagaki, M., Kozai, T. & Yamori, W. 2018. Supplemental LED inter-lighting compensates for a shortage of light for plant growth and yield under the lack of sunshine. *PLoS One* **13**(11). doi: http://dx.doi.org/10.1371/journal.pone.0206592

Tkach, V., Achkevych, V., Bratishko, V. & Achkevych, O. 2021. Milkmeter based on electric capacitive flow sensor. *ERDV*, 528–533. doi: http://dx.doi.org/10.22616/ERDev.2021.20.TF108

Van Straten, G., Van Willigenburg, G., Van Helten, E. & Van Ooteghem, R. 2011. *Optimal Control of Greenhouse Cultivation*. Book (318 pp.). Taylor & Francis Group, pp. 26. doi: http://dx.doi.org/10.1201/b10321

Vošahlík, J. & Hart, J. 2021. Measurability of quality in fermentation process of rice wine by IoT in the field of industry 4.0. *Agronomy Research* **19**(S3), 1318–1324. doi: https://doi.org/10.15159/AR.21.063

Vošahlík, J. 2023. IoT and measurement of fermentation process of rice wine. *Agronomy Research* **21**(3), 1419–1426. doi: https://doi.org/10.15159/ar.23.081

Witkowski, P. & Korzeniewska, E. 2019. Comparative analysis of HPS and LED luminaries in terms of effectiveness of greenhouse plant lighting and light emission. *2019 Applications of Electromagnetics in Modern Engineering and Medicine (PTZE)*, pp. 254–257. doi: http://dx.doi.org/10.23919/PTZE.2019.8781713

Pažuls, K., Štāls, T., Zimelis, A. & Lazdiņš, A. 2018. Preliminary conclusions on application of ultrasonic sensors in evaluation of distribution and depth of ruts in forest thinning. *Agronomy Research* **16**(S1), 1209–1217. doi: http://dx.doi.org/10.15159/ar.18.051

Agronomy Research **22**(1), 85–95, 2024
https://doi.org/10.15159/AR.24.004

Tomato nutrition with the application of *Trichoderma* spp. on different soils

E.D. Conte[1], D. Fiorini[1,2], N.M.B. Vargas[3], L.F.B. Bertoni[2], L.N.T. Santos[2], T.D. Magro[2], W.P. Silvestre[3,*], C. Cocco[4] and J. Schwambach[1,4,5]

[1]University of Caxias do Sul, Institute of Biotechnology, Laboratory of Biological Control of Plant Disease and Laboratory of Plant Biotechnology, Street Francisco Getúlio Vargas, 1130, Petrópolis, ZIP Code 95070-560, Caxias do Sul, Brazil
[2]University of Caxias do Sul, Vacaria Campus, Course of Agronomy, Street Dom Frei Cândido Maria Bampi, 2800, Barcellos, ZIP Code 95206-364, Vacaria, Brazil
[3]University of Caxias do Sul, Postgraduate Program in Process Engineering and Technologies and Course of Agronomy, Street Francisco Getúlio Vargas, 1130, Petrópolis, ZIP Code 95070-560, Caxias do Sul, Brazil
[4]University of Caxias do Sul, Course of Agronomy, Street Francisco Getúlio Vargas, 1130, Petrópolis, ZIP Code 95070-560, Caxias do Sul, Brazil
[5]University of Caxias do Sul, Postgraduate Program in Biotechnology, Street Francisco Getúlio Vargas, 1130, Petrópolis, ZIP Code 95070-560, Caxias do Sul, Brazil
[*]Correspondence: wpsilvestre@ucs.br

Received: August 24th, 2023; Accepted: December 18th, 2023; Published: January 22nd, 2024

Abstract. The present work aimed to evaluate the effect of *Trichoderma* spp. on the nutrition and development of tomato plants in three soil types under protected environments. One experiment was conducted with ferralsol and acrisol soil (conducted in pots in a greenhouse), and another used cambisol soil (conducted in beds in a commercial greenhouse). The experiments were carried out in a randomized block design with twelve replications. The treatments consisted of a control (no application of *Trichoderma* spp.), an application of *Trichoderma* spp. before seedling transplantation, and monthly *Trichoderma* spp. applications in tomato plants cv. Itaipava®. The evaluations included plant nutrition at full flowering, development (height and fresh and dry mass of shoots), crop yield components of number, weight, and diameter of fruits, and average yield per plant. A second nutritional evaluation was repeated in the cambisol. The application of *Trichoderma* spp. in the soil did not modify the nutrition parameters of plants until flowering. However, at the end of the cycle in cambisol, the treatment increased the available contents of N, P, Cu, and Mn. The application of *Trichoderma* spp. did not affect the development and yield of tomato plants in the conditions tested.

Key words: acrisol, bioinputs, cambisol, ferralsol, *Solanum lycopersicum*.

INTRODUCTION

The cultivation of vegetables in Brazil, in general, is carried out with intense soil disturbance and with high use and dependence on inputs (Lima et al., 2014). Vegetables

are productive and have high nutrient demand, so they extract and export more nutrients from the soil than grain crops, requiring more extensive fertilization. As a result, mineral fertilization has been applied in horticulture at higher levels than in other crops (Filgueira, 2008).

The tomato crop (*Solanum lycopersicum*) is among the vegetables with the highest fertilizer demand, especially in protected cultivation, where yield tends to be higher than in unprotected cultivation (Rusu et al., 2023). Although the application of chemical fertilizers drives agricultural production in Brazil (Oliveira et al., 2019), the excessive use of these compounds can cause soil pollution, especially in protected cultivations, contributing to the increase in salinity levels, eutrophication, and surface and groundwater contamination (Silva et al., 2013). In addition, the large consumption of fertilizers associated with exhaustible reserves has increased the search for alternatives to supply nutrients to plants and increase fertilization efficiency.

Natural systems, such as forests and native grasslands, are self-sustaining, without the addition of synthetic fertilizers, and with low nutrient availability (Gamage et al., 2023). Plant nutrition occurs in a complex system of plant, substrate/soil, and many microorganisms, encompassing bacteria and fungi. The relationship between crops and soil microorganisms, including plant growth-promoting fungi such as *Trichoderma* spp., makes them natural biostimulants (López-Bucio et al., 2015). *Trichoderma* is a fungal genus with a cosmopolitan distribution and high biotechnological value. Several species are used as biological control agents (Hermosa et al., 2013). These microorganisms help plants withstand environmental stresses, such as salinity and water imbalances and can help plant defense against pathogenic bacteria and fungi (López-Bucio et al., 2015; Smolińska et al., 2016; Kowalska et al., 2017; Di Vaio et al., 2021).

The control of phytopathogens by fungal inhibition and induction of resistance in tomato induced by *Trichoderma* spp. is well reported (Jayaraj et al., 2006; Lee et al., 2006; Lisboa et al., 2007; You et al., 2016; Patel & Saraf, 2017; Kuzmanovska et al., 2018; Li et al., 2020). However, plant nutrition can interfere with biological disease control (Abro et al., 2014). Furthermore, there is evidence that using *Trichoderma* spp. can increase the bioavailability of nutrients and their absorption by plants (Yedidia et al., 2001). Divergent results are found in the literature, where *Trichoderma* spp. may compete with plants for nutrient absorption (Santiago et al., 2011) and negatively affects the development of tomato and other crops (Souza et al., 2018). Li et al. (2015) observed that tomato seedlings inoculated with *Trichoderma* spp. and grown under copper (Cu) deficient hydroponic conditions exhibited an increase in the dry biomass of plants and Cu uptake compared to control plants. However, the same authors demonstrated that *Trichoderma* spp. competed for phosphorous (P) and zinc (Zn) with tomato seedlings, suppressing root development and releasing phytase and/or chelating minerals. The authors suggested that growth induction directly affects root development, combined with indirect mechanisms such as mineral solubilization (including solubilization via acidification, redox, chelation, and hydrolysis mechanisms). Thus, these effects can be influenced by the soil or substrate, growing conditions, among other factors.

In southern Brazil, particularly the Serra Gaúcha, Campos de Cima da Serra, and Vale do Caí regions, the predominant soils are of the cambisol, ferralsol, and acrisol types (Streck et al., 2008), which are often used in the production of vegetables. Cambisol is a soil in a transformation process with insufficient characteristics to be included in other soil classes. On the other hand, ferralsol is clayey, deep, homogeneous along with the

profile, and suffers from high weathering. In addition, it has high acidity, low nutrient reserve, and aluminum (Al) toxicity for plants. Finally, acrisol has a sandy surface horizon and a more clayey subsurface horizon (Santos et al., 2018). These soils can vary in depth, texture, drainage, and organic matter content but typically have high acidity, aluminum saturation, and low natural fertility (Streck et al., 2008). According to Rodrigues (2010), the response of *Trichoderma* spp. relative to soil characteristics is little known, which may cause oscillation in its performance. Therefore, research is needed so that the beneficial biostimulant potential of *Trichoderma* spp. can be translated to crops grown in different soil types. Based on the influence of soil characteristics and interaction with microbial communities, this work aimed to evaluate the effect of the application of *Trichoderma* spp. in the nutrition and development of tomato plants in three soil types grown under a protected environment.

MATERIALS AND METHODS

Site and soil description

The experiments were conducted in two locations from October 8, 2018 to February 11, 2019. Experiment 1 was carried out in a greenhouse used for research located at UCS Campus Vacaria (geographical coordinates of 28°31'02" S; 50°54'27" W, and an altitude of 960 m above sea level) with Ferralsol and Acrisol (IUSS, 2015), stored in pots with a capacity of 8 L. Experiment 2 was performed in a greenhouse used for commercial production located in the municipality of Caxias do Sul (geographical coordinates of 28°52'58" S; 51°02'38" W, and an altitude of 690 m above sea level) in Cambisol (IUSS, 2015). The temperature during the experiment varied between the minimum of 11.2 °C registered in October 2018 and the maximum of 29.0 °C registered in January 2019 (Embrapa Uva e Vinho, 2023).

The soils used in experiment 1 were collected at a 0–20 cm depth in Campos de Cima da Serra, and Vale do Caí regions, corresponding to a ferralsol and an acrisol, respectively. Experiment 2 was carried out on the ground in Cambisol in an area with a three-year history of tomato cultivation. The three soils were sampled (0–20 cm deep) and had their fertility parameters evaluated according to the methods described by Tedesco et al. (1995). Clay was determined by the densimeter method. Organic matter was determined using sulfochromic solution followed by colorimetry. Ca, Mg, Mn, and Al were extracted with KCl 1 mol·L^{-1}. Al and H + Al contents were assesed by titration; and Ca, Mg, and Mn were determined by atomic absorption spectroscopy (AAS). S was extracted with 500 mg L^{-1} $Ca(H_2PO4)_2$, and assessed by turbidimetry with $BaCl_2$. B was extracted with hot water and determined by colorimetry with azomethine-H. K, P, Cu, and Zn were extracted with Mehlich-1 solution; K was determined by flame photometry; Cu and Zn by AAS; and P by the molybdenum blue method. Cation exchange capacity (CEC) was calculated by the summation of cations (K, Ca, and Mg), and base saturation was calculated based on the percentage of CEC composed of the cations other than Al (Susin et al., 2023).

The fertility parameters of the three soils tested in the experiment are compiled in Table 1.

Before the experiments, the soils were corrected for fertility and acidity (pH 6.0) following the recommendations of the Manual of Fertilization and Liming for the Soils of Rio Grande do Sul and Santa Catarina for tomato crops (CQFS, 2016).

Experimental design and treatments

The experiments were carried out in randomized blocks with four blocks containing three plants per treatment, totaling 12 plants per treatment. In experiment 1, all plants in the pots were evaluated. In experiment 2, the plots were composed of 5 plants, and each plot's two lateral plants/borders were discarded.

Table 1. Fertility parameters of the three soils used in the experiments

Parameter	Unit	Ferralsol	Acrisol	Cambisol
pH	-	6.1	5.0	5.1
pH-SMP	-	5.9	5.6	5.7
Organic matter	% w/v	5.6	1.0	1.1
Ca	$cmol_c \cdot dm^{-3}$	9.4	0.5	6.9
Mg	$cmol_c \cdot dm^{-3}$	6.5	0.5	2.0
Al	$cmol_c \cdot dm^{-3}$	0.6	38.9	0.4
H+Al	$cmol_c \cdot dm^{-3}$	4.9	6.9	6.7
P	$mg \cdot dm^{-3}$	5.0	2.9	242.0
K	$mg \cdot dm^{-3}$	287.0	27.0	252.0
S	$mg \cdot dm^{-3}$	8.7	3.1	101.0
Zn	$mg \cdot dm^{-3}$	4.0	4.0	7.9
Cu	$mg \cdot dm^{-3}$	13.2	0.7	9.6
Mn	$mg \cdot dm^{-3}$	15.7	9.7	12.5
B	$mg \cdot dm^{-3}$	0.5	0.1	1.6
Na	$mg \cdot dm^{-3}$	6.0	4.0	19.6
Effective CTC	$cmol_c \cdot dm^{-3}$	16.7	1.8	9.9
CTC at ph 7	$cmol_c \cdot dm^{-3}$	21.5	8.0	16.2
Saturation of Bases	%	77.7	13.4	59.9

CTC: cation exchange capacity.

The treatments consisted of a control (without application of the fungus *Trichoderma* spp.), an application of *Trichoderma* spp. before seedling transplantation and monthly applications (one application per month) of *Trichoderma* spp. in tomato crops. The commercial product used in this experiment was a liquid produced with propagules of *Trichoderma harzianum*, *T. asperellum*, and *T. koningiopsis* at 1×10^{11} $CFU \cdot mL^{-1}$, with the concentration checked before application.According to the manufacturer's recommendation, the product was applied at 300 $mL \cdot ha^{-1}$ on the surface of the soil/pots. Transplantation of tomato seedlings cv. 'Itaipava'® were carried out using seedlings grafted onto the TD1 rootstock, produced by the Hidroceres nursery (São Paulo, Brazil).

In experiment 1, manual watering was performed daily to reach each soil's field capacity. The fertilization regime followed the recommendations of the Manual of Fertilization and Liming for the Soils of Rio Grande do Sul and Santa Catarina for tomato crops (CQFS, 2016), applied by fertigation. In experiment 2, fertigation was carried out according to the management adopted by the producer and using two drip strips with a 20 cm spacing between drippers placed on each side of the plant row.

Sampling procedures and evaluations

Plant nutrition (plant tissue nutrient content), development (height, fresh and dry mass of shoots), and tomato yield components of plant yield, number of fruits, and average fruit mass and diameter were evaluated. The test was carried out for 120 days after transplanting in experiment 1 and 180 days in experiment 2. In experiment 1, the cycle was reduced because of the higher temperatures (> 35 °C) inside the greenhouse, considering that it did not allow the opening of the side walls.

The nutritional evaluation of the plants was carried out at full flowering, collecting the fourth leaf from the tip of three plants per repetition and five repetitions per treatment. A second nutritional evaluation was repeated after 180 days, with the collection criterion being the removal of the leaf opposite the last bunch with full flowering. This evaluation

was carried out only in experiment 2 because, in experiment 1, the plants did not reach this cultivation stage. Nutrient content in plant tissue was determined following the methods described by Malavolta (2006).

Relative to biometric parameters, plant height was measured from the insertion of the soil to its apex. Fresh plant mass was determined by cutting at the plant insertion in soil and weighting on a digital scale. To determine the dry mass, the plants were dried in an oven for 15 days at 50 °C, and the mass was weighed on a digital scale.

For yield components, during the entire production phase, the fruits were collected harvest point and weighed with a digital scale. Fruit diameter was measured using a digital calliper, and the number of fruits per plant was determined by counting.

Statistical analysis

Data were analysed for normality using the Shapiro-Wilk test. In the case of normality, the comparison of means was performed using the t-test ($p \leq 0.05$) and analysis of variance (ANOVA), and Tukey's test ($p \leq 0.05$) according to the number of treatments compared. In the case of non-normality, the variables were analysed using the U-Mann-Whitney test ($p < 0.05$) and the Kruskal-Wallis test ($p \leq 0.05$). All statistical analyses were performed using SPSS version 21.0 (IBM, USA).

RESULTS AND DISCUSSION

Results

The application of *Trichoderma* spp. application did not significantly impact the plant tissue contents of macro and micronutrients in tomato plants, regardless of the soil class. The plant tissue analysis results are compiled in Table 2.

Table 2. Contents of macro and micronutrients in the plant tissue of 'Itaipava'® tomato plants at full flowering stage, with different application regimes of Trichoderma spp. under protected environment, in Ferralsol, Acrisol, and Cambisol soils. Caxias do Sul, University of Caxias do Sul, 2021

Trichoderma spp.	N	Ca	Mg	P	K	S	Zn	Cu	B	Mn	Fe
application	g·kg^{-1}						mg·kg^{-1}				
Ferralsol (pot)											
Without	20.9 ^{ns}	22.9 ^{ns}	8.0 ^{ns}	4.0 ^{ns}	40.0 ^{ns}	5.2 ^{ns}	31 ^{ns}	16 ^{ns}	32 ^{ns}	71 ^{ns}	207 ^{ns}
With	19.7	21.8	7.2	4.2	32.6	5.6	28	17	37	68	209
CV (%)	27.4	29.3	20.8	12.2	21.0	17.3	1.0	18.5	16.4	55.4	9.5
Acrisol (pot)											
Without	29.0 ^{ns}	32.3 ^{ns}	5.3 ^{ns}	4.7 ^{ns}	50.6 ^{ns}	7.2 ^{ns}	33 ^{ns}	13 ^{ns}	42 ^{ns}	165 ^{ns}	228 ^{ns}
With	33.3	29.4	6.0	4.7	43.9	6.0	34	13	37	225	212
CV (%)	18.7	29.3	16.8	10.2	15.1	17.1	11.9	16.3	15.3	25.8	9.6
Cambisol (soil)											
Without	42.1^{ns}	52.7 ^{ns}	9.0 ^{ns}	5.4 ^{ns}	42.0 ^{ns}	6.1 ^{ns}	87 ^{ns}	110 ^{ns}	88 ^{ns}	154 ^{ns}	152 ^{ns}
With	43.9	54.0	9.6	5.9	42.5	5.9	80	129	90	141	161
CV (%)	7.8	14.3	8.1	8.3	18.6	7.2	15.6	15.2	5.2	13.7	13.5

Macronutrients (N, P, K, Ca, Mg, and S) are shown in g·kg^{-1}, while micronutrientes (Cu, Zn, Mn, Fe, and B) are shown in mg·kg^{-1}. ^{ns}: not significant by the statistical analysis at a 5% error probability. CV: Coefficient of variation.

In the evaluation of leaf nutrient contents at the end of the tomato crop cycle (180 days after transplanting) conducted in cambisol, it was observed that a single application of *Trichoderma* spp. increased the contents of N, P, and Cu. The monthly application increased the plant tissue contents of N, Cu, and Mn, as shown in Table 3.

Table 3. Contents of macro and micronutrients in the plant tissue of 'Itaipava'® tomato plants 180 days after transplanting with different application regimes of *Trichoderma* spp. under a protected environment, grown in a cambisol. Caxias do Sul, University of Caxias do Sul, 2021

Trichoderma	N	Ca	Mg	P	K	S	Zn	Cu	B	Mn	Fe
spp. application	g·kg^{-1}						mg·kg^{-1}				
Without	36.4 b	26.7 ^{ns}	5.0 ^{ns}	2.8 b	35.8 ^{ns}	7.0 ^{ns}	317 ^{ns}	17 b	47 ^{ns}	157 b	256 ^{ns}
Single	45.3 a	30.1	5.9	3.8 a	40.8	7.6	455	24 a	46	212 ab	243
Monthly	43.9 a	35.0	5.9	3.4 ab	34.0	7.6	414	26 a	56	228 a	334
CV (%)	14.1	23.1	13.1	15.9	15.8	8.3	27.3	19.4	17.5	24.4	58.4

Macronutrients (N, P, K, Ca, Mg, and S) are shown in g·kg^{-1}, while micronutrientes (Cu, Zn, Mn, Fe, and B) are shown in mg·kg^{-1}. Means in columns followed by the same lowercase letter do not differ statistically by Tukey's test at a 5% error probability ($p \leq 0.05$). ^{ns}: not significant by the statistical analysis at a 5% error probability. CV: coefficient of variation.

Among the macronutrients, N had the highest concentration in the tissues of the aerial part, and P had the lowest concentration. At the same time, among the micronutrients, the decreasing order of accumulation was Zn>Fe>Mn>B> Cu, regardless of the treatments.

According to Table 4, plant height and fresh and dry matter production at the end of the tomato cycle were not influenced by the application of *Trichoderma* spp. in the evaluated soils and conditions.

The parameters related to tomato production were also not influenced by the application of *Trichoderma* spp. in the soil, regardless of the soil and form of cultivation used, as compiled in Table 5.

Table 4. Plant height and fresh and dry matter of aerial part of tomato cv. 'Itaipava'® plants at the end of the cycle (120 days for ferralsol and acrisol and 180 days for cambisol) with different *Trichoderma* spp. application regimes on the soil surface in a protected environment grown in ferralsol, acrisol, and cambisol soil types. Caxias do Sul, University of Caxias do Sul, 2021

Trichoderma spp. application	Plant height (m)	Fresh plant mass (g)	Dry plant mass (g)
Ferralsol (pot)			
Without	1.10 ^{ns}	178.84 ^{ns}	34.89 ^{ns}
Single	1.13	151.94	31.01
Monthly	1.13	170.34	34.89
CV (%)	12.80	21.74	19.05
Acrisol (pot)			
Without	0.91^{ns}	165.76 ^{ns}	30.59 ^{ns}
Single	0.90	146.91	29.60
Monthly	0.88	123.01	24.01
CV (%)	13.97	34.44	28.29
Cambisol (soil)			
Without	3.68 ^{ns}	2,283.33 ^{ns}	366.00 ^{ns}
Single	3.88	2,340.00	409.33
Monthly	3.95	2,210.67	406.00
CV (%)	7.91	19.15	18.3

^{ns}: not significant by the statistical analysis at a 5% error probability. CV: coefficient of variation.

It is important to note that the differences in the crop yield components observed in Table 5 regarding the cambisol and the other two soil types occurred because cambisol was tested in a field experiment. In contrast, acrisol and ferralsol were conducted in pots.

Table 5. Crop yield components of tomato cv. 'Itaipava'® grown in ferralsol, acrisol, and cambisol with different *Trichoderma* spp. application regimes on the soil surface in a protected environment. Caxias do Sul, University of Caxias do Sul, 2021

Trichoderma spp. application	Number of fruits per plant	Fruit diameter (cm)	Average fruit mass (g)	Fruit yield ($g \cdot plant^{-1}$)
Ferralsol (pot)				
Without	13.00 ^{ns}	4.92 ^{ns}	62.11 ^{ns}	803 ^{ns}
Single	14.58	4.98	62.88	909
Monthly	13.75	5.08	66.42	873
CV (%)	19.17	6.69	18.25	18.94
Acrisol (pot)				
Without	14.67 ^{ns}	5.06 ^{ns}	65.95 ^{ns}	940 ^{ns}
Single	14.45	5.07	66.00	945
Monthly	14.17	4.89	61.86	876
CV (%)	25.57	5.90	14.38	22.41
Cambisol (soil)				
Without	63.93 ^{ns}	7.34 ^{ns}	181.28 ^{ns}	6,392 ^{ns}
Single	69.33	7.32	179.62	7,176
Monthly	65.47	7.42	180.20	6,803
CV (%)	13.04	7.8	22.44	18.71

^{ns}: not significant by the statistical analysis at a 5% error probability. CV: coefficient of variation.

Discussion

The nutritional content of macronutrients in plant tissue found in the full flowering stage in each soil was considered adequate according to Malavolta (2006), except for N and K in Ferralsol, which were below sufficient levels (30 g kg^{-1} and 40 $g \cdot kg^{-1}$, respectively). According to Mello Prado et al. (2011), the elements whose nutritional requirements are highest for tomato plants are K, N, and Ca.

Regarding the micronutrients, B and Zn presented mean values below the adequate range for ferralsol and acrisol. Fe and Mn contents were considered insufficient in all soils, and Cu had excess values in Cambisol and Ferralsol. The observed results indicated that the nutrients provided via mineral fertilization were sufficient for most plant requirements until this stage of development. However, even in those below adequate values, the application of *Trichoderma* spp. did not affect the absorption of nutrients in any soil and growing conditions assessed.

Li et al. (2015) observed that the inoculation of *Trichoderma harzianum* (strain SQR-T037) significantly improved tomato seedlings' biomass and nutrient uptake. However, in this respective study, the seedlings were grown in nutrient-limited soil with a high pH (8.1) and packed in pots. In the present study, the soils were corrected to pH 6.0, and the nutrient contents were provided according to the official recommendation in force for each evaluated soil (CQFS, 2016). It should be noted that soil turning over and packaging in pots accelerates the decomposition of organic matter, and some nutrients may be temporarily immobilized by microbial biomass (Brandani & Santos, 2016). That can explain the lower contents of nutrients in plant tissue, especially in the ferralsol, whose organic matter content is higher than the other soil types (Table 1).

The increase observed in the concentration of foliar nutrients at the end of the tomato cycle with *Trichoderma* spp. in cambisol indicates that the fungus was efficient in helping plant absorption of nutrients through biochemical mechanisms or by root development, facilitating nutrient absorption. According to Samolski et al. (2012), qid74-induced modifications in root architecture increased the total absorptive surface, facilitating nutrient uptake and translocation of nutrients in the shoots and efficient use of NPK and micronutrients by the plants.

The increase in the absorption of N, P, Cu, and Mn observed in the cambisol using *Trichoderma* spp. was not reflected in the development of tomato plants. According to Sani et al. (2020), *Trichoderma* increased the plant growth and yield of tomatoes with half of the recommended NPK dose for the crop, unlike the present experiment in which the entire NPK fertilizer recommendation was provided. According to Li et al. (2015), the mechanisms by which *Trichoderma* regulates plant growth and mineral solubilization partially depend on the absence of a specific nutrient. This situation probably did not occur significantly in the present experiment because of the fertilizer dose.

Furthermore, according to Szczech et al. (2017) and Conte et al. (2022), the complexity of the relationships between the soil's chemical, physical, and biological components influence the efficiency of biological products and vice-versa. In this respective study, the resulting balance between the effects on chemical and biological soil parameters affected by the application of *Trichoderma* spp. provided an absence of effect in the development and productivity of the soybean crop.

Information about the adaptation and efficiency of applying *Trichoderma* spp. in field conditions and its interaction with the soil's chemical, physical, and biological quality and the resulting balance among them are scarce. Therefore, it is imperative to better understand the interaction dynamics of *Trichoderma* spp. with the soil and plant to allow for greater applicability and more confidence in the field dynamics of interaction (Smolińska et al., 2014; Mahfudz et al., 2019). Thus, further studies are needed to reduce the application of fertilizers and/or establish novel and corroborate already observed applications of *Trichoderma* spp. at longer intervals before planting. This is necessary to clarify further its potential for use and applicability in tomatoes and other horticultural crops in different soil types.

CONCLUSIONS

The application of *Trichoderma* spp. did not interfere with the production and development of tomato plants using mineral fertilizers following current recommendations and the absence of phytopathogens, regardless of the soil type, indicating its potential use without prejudice to tomato development and productive capacity in different soil types.

ACKNOWLEDGEMENTS. The authors would like to thank the Coordination for the Improvement of Higher Education Personnel (*Coordenação de Aperfeiçoamento de Pessoal de Nível Superior* – CAPES) for providing the scholarships that allowed for the development of this study.

REFERENCES

Abro, M.A., Lecompte, F., Bardin, M. & Nicot, P.C. 2014. Nitrogen fertilization impacts biocontrol of tomato gray mold. *Agronomy for Sustainable Development* **34**(3), 641–648. doi: 10.1007/s13593-013-0168-3

Brandani, C.B. & Santos, D.G. 2016. Carbon transformations in soil]. In: E.J.B. Cardoso & F.D. Andreote (eds), *Soil Microbiology*. Esalq, Piracicaba, 81–98 (in Portuguese).

Comissão de Química e Fertilidade do Solo (CQFS). 2016. *Liming and fertilizing manual for the Rio Grande do Sul and Santa Catarina States*. Sociedade Brasileira de Ciência do Solo – Núcleo Regional Sul, Porto Alegre, 404 pp. (in Portuguese).

Conte, E.D., Dal Magro, T., Dal Bem, L.C., Dalmina, J.C., Matté, J.A., Schenkel, V.O. & Schwambach, J. 2022. Use of *Trichoderma* spp. in no-tillage system: effect on soil and soybean crop. *Biological Control* **171**, 104941. doi: 10.1016/j.biocontrol.2022.104941

Di Vaio, C., Testa, A., Cirillo, A. & Conti, S. 2021. Slow-release fertilization and *Trichoderma harzianum*-based biostimulant for the nursery production of young olive trees (*Olea europaea* L.). *Agronomy Research* **19**(3), 1396–1405.

Embrapa Uva e Vinho. 2023. Meteorological data (in Portuguese). Available from: https://www.embrapa.br/uva-e-vinho/dados-meteorologicos/vacaria

Filgueira, F.A.R. 2008. *New horticulture manual*. UFV, Viçosa, 421 pp. (in Portuguese).

Gamage, A., Gangahagedara, R., Gamage, J., Jayasinghe, N., Kodikara, N., Suraweera, P., Merah, O. 2023. Role of organic farming for achieving sustainability in agriculture. *Farming System* **1**(1), 100005. doi: 10.1016/j.farsys.2023.100005

Hermosa, R., Rubio, M.B., Cardoza, R.E., Nicolás, C., Monte, E. & Gutiérrez, S. 2013. The contribution of *Trichoderma* to balancing the costs of plant growth and defense. *International Microbiology* **16**(2), 69–80. doi:10.2436/20.1501.01.181

IUSS Working Group WRB. 2015. *World Reference Base for Soil Resources* (WRB). FAO, Rome.

Jayaraj, J., Radhakrishnan, N.V. & Velazhahan, R. 2006. Development of formulations of *Trichoderma harzianum* strain M1 for control of damping-off of tomato caused by *Pythium aphanidermatum*. *Archives of Phytopathology and Plant Protection* **39**(1), 1–8. doi: 10.1080/03235400500094720

Kowalska, B., Smolińska, U., Szczech, M. & Winciorek, J. 2017. Application of organic waste material overgrown with *Trichoderma atroviride* as a control strategy for *Sclerotinia sclerotiorum* and *Chalara thielavioides* in soil. *Journal of Plant Protection Research* **57**(3), 205–211. doi: 10.1515/jppr-2017-0027

Kuzmanovska, B., Rusevski, R., Jankulovska, M. & Oreshkovikj, K.B. 2018. Antagonistic activity of *Trichoderma asperellum* and *Trichoderma harzianum* against genetically diverse *Botrytis cinerea* isolates. *Chilean Journal of Agricultural Research* **78**(3), 391–399. doi: 10.4067/S0718-58392018000300391

Lee, S.K., Sohn, H.B., Kim, G.G. & Chung, Y.R. 2006. Enhancement of biological control of *Botrytis cinerea* on cucumber by foliar sprays and bed potting mixes of *Trichoderma harzianum* YC459 and its application on tomato in the greenhouse. *The Plant Pathology Journal* **22**(3), 283–288.

Li, R.X., Cai, F., Pang, G., Shen, Q.R., Li, R. & Chen, W. 2015. Solubilisation of Phosphate and Micronutrients by *Trichoderma harzianum* and its relationship with the Promotion of Tomato Plant Growth. *Plos One* **10**(6), e0130081. doi: 10.1371/journal.pone.0130081

Li, T.T., Zhang, J.D., Tang, J.Q., Liu, Z.C., Li, Y.Q., Chen, J. & Zou, L.W. 2020. Combined use of *Trichoderma atroviride* CCTCCSBW0199 and brassinolide to control *Botrytis cinerea* infection in tomato. *Plant disease* **104**(5), 1298–1304. doi: 10.1094/PDIS-07-19-1568-RE

Lima, C.E.P., Castro, J.S., Madeira, N.R. & Fontenelle, M.R. 2014. *Assessment of environmental impacts with Ambitec-Agro: case study of no-till planting of horticultural crops*. Boletim Pesquisa e Desenvolvimento. Embrapa Hortaliças, Brasília, 24 pp. (in Portuguese).

Lisboa, B.B., Bochese, C.C., Vargas, L.K., Silveira, J.R.P., Radin, B. & Oliveira, A.M.R. 2007. Efficiency of *Trichoderma harzianum* and *Gliocladium viride* to reduce *Botrytis cinerea* incidence in tomatoes grown in protected environement. *Ciência Rural* **37**(5), 1255–1260 (in Portuguese). doi: 10.1590/S0103-84782007000500006

López-Bucio, J., Pelagio-Flores, R. & Herrera-Estrella, A. 2015. *Trichoderma* as biostimulant: exploiting the multilevel properties of a plant beneficial fungus. *Scientia Horticulturae* **196**, 109–123. doi: 10.1016/j.scienta.2015.08.043

Mahfudz, M., Saleh, S., Antara, M., Anshary, A., Bachri, S., Made, U., Hasanah, U. & Rauf, R.A. 2019. Adoption and advantages of eco-friendly technology application at the Shallot farming system in Indonesia. *Agronomy Research* **17**(4), 1679–1687.

Malavolta, E. 2006. *Manual of mineral nutrition of plants*. Agronômica Ceres, São Paulo, 638 pp. (in Portuguese).

Mello Prado, R., Santos, V.H.G., Gondim, A.R.O., Alves, A.U., Cecílio Filho, A.B. & Correia, M.A.R. 2011. Growth and nutrient intake in Raisa tomatoes grown in hydroponics. *Semina: Ciências Agrárias* **32**(1), 19–30 (in Portuguse).

Oliveira, M.P., Malagolli, G.A. & Cella, D. 2019. Fertilizer market: Brazilian dependence from imports. *Revista Interface Tecnológica* **16**(1), 489–498 (in Portuguese).

Patel, S. & Saraf, M. 2017. Biocontrol efficacy of *Trichoderma asperellum* MSST against tomato wilting by *Fusarium oxysporum f. sp. lycopersici*. *Archives of Phytopathology and Plant Protection* **50**(5–6), 228–238. doi: 10.1080/03235408.2017.1287236

Rodrigues, J. 2010. *Trichoderma spp. asociated toNPK fertilizing levels in the Sclerotinia sclerotiorum-bean plant pathosystem*. Master's thesis, Universidade Federal de Santa Maria, Santa Maria, Brazil, 85 pp. (in Portuguese).

Rusu, O.R., Mangalagiu, I., Amăriucăi-Mantu, D., Teliban, G. C., Cojocaru, A., Burducea, M., Mihalache, G., Roșca, M., Caruso, G., Sekara, A. & Stoleru, V. 2023. Interaction Effects of Cultivars and Nutrition on Quality and Yield of Tomato. *Horticulturae* **9**(5), 541. doi: 10.3390/horticulturae9050541

Samolski, I., Rincon, A.M., Pinzón, L.M., Viterbo, A. & Monte, E. 2012. The qid74 gene from *Trichoderma harzianum* has a role in root architecture and plant biofertilization. *Microbiology* **158**(1), 129–138.

Sani, M.N.H., Hasan, M., Uddain, J. & Subramaniam, S. 2020. Impact of application of *Trichoderma* and biochar on growth, productivity and nutritional quality of tomato under reduced NPK fertilization. *Annals of Agricultural Sciences* **65**(1), 107–115. doi: 10.1016/j.aoas.2020.06.003

Santiago, A., Quintero, J.M., Avilés, M. & Delgado, A. 2011. Effect of *Trichoderma asperellum* strain T34 on iron, copper, manganese, and zinc uptake by wheat grown on a calcareous medium. *Plant and Soil* **342**, 97–104. doi: 10.1007/s11104-010-0670-1

Santos, H.G., Jacomine, P.T., Anjos, L.H.C., Oliveira, V.A., Lumbreras, J.F., Coelho, M.R., Almeida, J.A., Araujo Filho, J.C., Oliveira. J.B. & Cunha, T.J.F. 2018. *Brazilian System of Soil Classification*. Embrapa Solos, Brasília (in Portuguese).

Silva, P.F., Lima, C.J.G.S., Barros, A.C., Silva, E.M. & Duarte, S.N. 2013. Fertilizing salts and fertigation management in tomato production in protected environment. *Revista Brasileira de Engenharia Agrícola e Ambiental* **17**(11), 1173–1180 (in Portuguese). doi: 10.1590/S1415-43662013001100007

Smolińska, U., Kowalska, B., Kowalczyk, W., Szczech, M. & Murgrabia, A. 2016. Eradication of *Sclerotinia sclerotiorum* sclerotia from soil using organic waste materials as *Trichoderma* fungi carriers. *Journal of Horticultural Research* **24**(1), 101–110. doi: 10.1515/johr-2016-0012

Smolińska, U., Kowalska, B., Kowalczyk, W. & Szczech, M. 2014. The use of agro-industrial wastes as carriers of *Trichoderma* fungi in the parsley cultivation. *Scientia Horticulturae* **179**, 1–8. doi: 10.1016/j.scienta.2014.08.023

Souza, E., Amaral, H., Santos Neto, J. & Nunes, M. 2018. High *Trichoderma harzianum* doses in tomato negatively influences seedling production and yield. *Revista Terra & Cultura* **34**, 20–36 (in Portuguese).

Streck, E.V., Kampf, N., Dalmolin, R.S.D., Klamt, E., Nascimento, P.C. & Schneider, P. 2008. *Soils of Rio Grande do Sul*. UFRGS, Porto Alegre, 252 pp. (in Portuguese).

Susin, F.M.C., Silvestre, W.P., Cocco, C., Dal Magro, T., Pauletti, G.F., Conte, E.D. 2023. Soil Chemical Parameters with the Use of Agricultural Gypsum and Effects on the Apple Tree Crop. *International Journal of Plant Biology* **14**(4), 986–997. doi: 10.3390/ijpb14040072

Szczech, M., Nawrocka, J., Felczyński, K., Małolepsza, U., Sobolewski, J., Kowalska, B., Maciorowski, R., Jas, K. & Kancelista, A. 2017. *Trichoderma atroviride* TRS25 isolate reduces downy mildew and induces systemic defense responses in cucumber in field conditions. Scientia Horticulturae **224**, 17–26. doi: 10.1016/j.scienta.2017.05.035.

Tedesco, M.J., Gianello, C., Bissani, C.A., Bohnen, H. & Volkweiss, S.J. 1995. *Analysis of soil, plant tissue, and other materials*. Departamento de solos da UFRGS, Porto Alegre, 174 pp. (in Portuguese).

Yedidia, I., Srivastva, A.K., Kapulnik, Y. & Chet, I. 2001. Effect of *Trichoderma harzianum* on microelement concentrations and increased growth of cucumber plants. *Plant and Soil* **235**(2), 235–242.

You, J., Zhang, J., Wu, M., Yang, L., Chen, W. & Li, G. 2016. Multiple criteria-based screening of *Trichoderma* isolates for biological control of *Botrytis cinerea* on tomato. *Biological Control* **101**, 31–38. doi: 10.1016/j.biocontrol.2016.06.0

Agronomy Research **22**(1), 96–109, 2024
https://doi.org/10.15159/AR.24.013

Breeding and genetic screening of F_1 hybrids of soft winter wheat (*Triticum aestivum* L.) by manifestation of resistance to *Fusarium graminearum* Schwabe

O.A. Demydov[1], V.V. Kyrylenko[1], L.A. Murashko[1], O.V Humenyuk[1], Yu.M. Suddenko[1], T.I. Mukha[1], H.B. Volohdina[1], N.P. Zamlila[1], N.V. Novytska[2] and B.O Mazurenko[2,*]

[1]The V.M. Remeslo Myronivka Institute of Wheat, NAAS of Ukraine, Tsentralna Str., 68, UA-08853 v. Tsentralne, Kyiv region, Ukraine
[2]National University of Life and Environmental Sciences of Ukraine, Department of Plant Science, Heroiv Oborony Str., 15, Kyiv 03041, Ukraine
[*]Correspondence: mazurenko.bohdan@nubip.edu.ua

Received: august 12th, 2023; Accepted: February 24th, 2024; Published: March 19th, 2024

Abstract Diseases of field crops significantly reduce yield and the quality of agricultural products. Developing resistant varieties is one of the tasks for enhancing agroecosystem resilience. The creation of infectious material for the background pathogen and heterosis analysis of F_1 hybrids of soft winter wheat for resistance against *Fusarium graminearum* Schwabe (*F. graminearum*) and elements of spike productivity was the goal of the conducted research. The analysis of F_1 genotypes of wheat for resistance against *F. graminearum* was carried out in field infections and natural nurseries of the wheat breeding laboratory of The V.M. Remeslo Myronivka Institute of Wheat of the NAAS of Ukraine (located in the northern part of the Right-Bank Forest-Steppe of Ukraine) during 2021 and 2022. The most aggressive isolates of the *F. graminearum* fungus were identified for developing inoculum and creating an artificial infection background in field conditions. In terms of the inheritance of resistance and spike productivity traits, 29.4% of hybrid populations of the first generation were selected. Positive dominance for the complex of investigated traits was found in hybrid combinations where sources of resistance against *Fusarium graminearum* (MV 20-88 × Smuhlianka, (Mikon × ALMA) × Lehenda Myronivska and local winter wheat varieties MIP Knyazhna, MIP Vyshyvanka were involved in the crossbreeding. It was established that cytoplasmic genes enhance the dominance of genes for complex resistance in one crossbreeding group. The best combinations with positive dominance in resistance to fusarium can be utilized in the development of highly resistant varieties.

Key words: soft winter wheat (*Triticum aestivum* L.), variety, hybrid, spike, heterosis, fusarium.

INTRODUCTION

Soft winter wheat plays a major role in food security. In modern conditions, with a rapid change in climatic scenarios (Liu et al., 2021) and an increase in the phytopathogenic pressure of the variety, a special role is assigned to the biological factor of wheat and agricultural intensification (Lozinskiy et al., 2021). Cereals are damaged

by a wide range of pathogens during the growing season, among which fungi of the genus *Fusarium* Link occupy a significant niche (Ward et al., 2008, Gao et al., 2023).

The causative agents of numerous diseases and pests annually affect significant losses of the wheat harvest and decrease in grain quality. The antidote to this effect is an integrated system of plant protection, which includes various measures that affect the final result - obtaining a high yield in terms of quantity and quality. The key direction of this system is the creation and introduction into the production of varieties resistant and tolerant to common pathogens (Pagán & García-Arenal 2018; Mazurenko et al., 2020; Mikaberidze & McDonald, 2020). The variety is a reliable and economically beneficial factor in increasing crop yield under any growing technology. Wheat varieties created by breeders have productivity potential that has not yet been realized in production, the limit of which is not only not reached, but has not even been established and is growing as varieties are selectively improved and growing conditions are optimized (Kovalyshyna et al., 2020; Moisienko et al., 2020).

Creation of primary material in Ukraine for breeding winter wheat with group resistance against *Erysiphe graminis* DC. f. sp. *tritici* Em. Marchal, *Puccinia recondita* Rob. et Desm., *Septoria tritici* Rob. et Desm., *F. graminearum* Shwabe, *Tilletia caries* Tul., *Cercosporella herpotrichoides* Fron are successfully researched at the Institute of Plant Protection of the National Academy of Agrarian Sciences of Ukraine, The V.M. Remeslo Myronivka Institute of Wheat of the National Academy of Agrarian Sciences of Ukraine (MIP), The Plant Breeding and Genetics Institute - National Center of Seed and Cultivar Investigation of the National Academy of Agricultural Sciences of Ukraine (SGI) and others (Kovalyshyna et al., 2018).

It is known that grain crops can be affected by more than 300–350 species of various organisms, but the main threat to crop loss, especially in the initial phases of development, in the autumn and winter period, are pathogens of fungal infections, among which one of the leading places is occupied by micromycetes of the genus *Fusarium* Link (Ryabovol et al., 2019; Diakite et al., 2022). They cause damage at all stages of the organogenesis of winter wheat plants. Infection of wheat grain with pathogenic fungal species of this genus reduces the energy of its germination and germination, deteriorates gluten density and baking properties of flour (Hysing & Wiik, 2014; El Chami at el., 2023). Mycotoxins (fusariotoxins) accumulate in grain, among which fumonisin B1 (FB1), deoxynivalenol (DON) and zearalenone (ZEA) are the largest (Klyszejko et al., 2005; Tančić, 2013; Obradović et al., 2022). The greatest harmfulness of micromycetes of the genus *Fusarium* Link is detected when infecting the spike of plants, including one of the most dangerous diseases of cereals - Fusarium head blight. The danger of the latter lies not only in the reduction of grain yield, but also in the contamination of grain with fusariotoxins, this disease is of a hidden nature, and therefore the cause of the weakening of plants during their development, it can be detected by mycological analysis (Muthomi et al., 2008; Kovalyshyna et al., 2016).

The problem of grain fusarium infection has now reached international significance. The widespread distribution of fusarium fungi, their variability, as well as indisputable evidence of the danger posed by mycotoxins to human and animal health, determine the interest that the scientific community shows in *Fusarium* (Muthomi et al., 2008; Foroud et al., 2014; Ostrovskyi et al., 2017; Shikur Gebremariam et al., 2018). A complex of fungi of this genus takes part in the intensity of damage to plants, which differ in biology and adaptation to the conditions of the biocenosis in different zones of

grain cultivation (Champeil et al., 2004; Panwar et al., 2016). Significant efforts of scientists are aimed at researching the morphological features, biology, biochemistry, physiology and genetics of fungi of the genus Fusarium Link, as well as finding ways to limit their number in agrobiocenoses and reduce their number (Mostovyiak et al., 2020). The solution to this important scientific problem determines the relevance of the topic of our research, which consisted of identifying sources of resistance among winter wheat varieties that were studied for a certain time on an artificial infectious background of fusarium head blight and involving them in breeding studies.

The purpose of the research is to create infectious material for the background of the pathogen and heterosis analysis of F_1 hybrids of soft winter wheat for resistance to the pathogen *Fusarium graminearum* Schwabe (*F. graminearum*) and spike productivity elements.

MATERIALS AND METHODS

The research was conducted in the field of infectious and natural nurseries (Tribel et al., 2010) of the winter wheat breeding laboratory of The V.M. Remeslo Myronivka Institute of Wheat of the National Academy of Agrarian Sciences of Ukraine (MIP), during 2021 and 2022.

The relief of the territory is a broad plateau, the microrelief is shallow depressions of 0.2–1 ha. Groundwater lies at a depth of 50–60 m. The soil is low-humus, slightly leached, medium loamy chernozem. The thickness of the humus horizon is 38–40 cm. The carbonate layer lies at a depth of 45–65 cm. Soil structure according to the scale of S.P. Dolgov is good, aggregates 0.25–10 mm in the range of 60–80% of the total mass are air-dry, and 55–70% are waterproof. The content of humus in the 0–20 cm layer of the soil is 3.7–4.0%, easily hydrolyzed nitrogen – 12 (11.6–13.0) mg per 100 g of soil, mobile phosphorus is 23 (21–25) mg per 100 g of soil and exchangeable potassium is 11 (10–16) mg per 100 g of soil. Hydrolytic acidity is 1.7–2.2 mg. equiv. per 100 g of soil, pH_{KCl} - 5.4–6.0.

Climate conditions

The meteorological conditions of the 2020/2021 growing season were favorable for the development of the pathogen *Fusarium graminearum* Schwabe. In the spring-summer period of wheat vegetation, average monthly temperatures were observed to be higher than long-term ones: in March and June by 1.0 °C and 1.5 °C, respectively, and in April and May, a decrease in air temperature was noted in comparison with long-term data (–1.4 °C and –0.8 °C respectively). The hydrothermal coefficient (HTC) for May, June, and July 2021 corresponded to 3.1; 2.7; and 2.6, overmoistening contributed to the manifestation and intensity of development of the causative agent of fusarium head blight.

The meteorological conditions of the 2021/2022 vegetation year were very unfavorable for the development of the pathogen *F. graminearum*. The average air temperature in July 2021 and August 2022 recorded 9.3 °C, which is 0.4 °C more than the long-term average (Table 1). In the spring-summer wheat growing season, average monthly temperatures were determined to be lower than the long-term norms by 0.1–1.5 °C, only in June they were noted to increase by 1.4 °C. From August 2021 to July 2022, 663 mm of precipitation fell (108% of the long-term average). Precipitation

in August (109 mm, 198% of the annual amount) contributed to obtaining uniform wheat shoots.

Table 1. Hydrothermal conditions at 2020/2021 and 2021/2022 vegetative period[1]

Year	Month	Air temperature			Precipitation, mm			
		Fact	Multi-annual	±**	Fact	Multi-annual	±, mm**	±, %**
2020/2021	August	21.1/20.5*	20.4	1.6/0.1	11.4/109	55	-46.6/54	19.7/198
	September	18.5/13.2	14.9	4.0/-1.7	33.8/27	58	-24.2/-31	58.3/46
	October	13.2/7.6	8.7	5.0/-1.1	67/26	43	27.0/-17	167.5/60
	November	3.8/4.8	2.4	1.6/2.4	39.8/41	40	-1.2/1	97.1/101
	December	-0.3/-1.1	-1.8	1.9/0.7	49.6/94	42	7,6/52	118.1/223
2021/2022*	January	-2.3/-1.2	-3.7	2.3/2.5	83.7/33	39	48,7/-6	239.1/86
	February	-4.7/1.7	-2.5	-1.2/4.2	73.9/10	33	42.9/-23	238.4/32
	March	2.3/2.3	2.4	1.0/-0.1	39.3/13	39	2.3/-26	106.2/32
	April	7.7/8.3	9.8	-1.4/-1.5	58.6/143	41	16.6/102	139.5/349
	May	14.5/14.7	15.7	-0.8/-1.0	117.9/42	61	58.9/-19	199.8/70
	June	20.1/20.7	19.3	1.5/1.4	157.9/58	87	70.9/-30	181.5/66
	Jule	23.3/20.4	21.1	3.0/-0.7	172.1/68	75	98.1/-7	232.6/91
Per Year		**9.8/9.3**	**8.9**	**1.6/0.4**	**905/663**	**615**	**302/48**	**150.1/108**

[1] Data according to meteostation Myronivka, #33466; *First number - 2020–2021 vegetative period, second - 2021–2022 vegetative period; ** ± according to multi-annual means.

In the spring-summer period of winter wheat vegetation, a sufficient amount of moisture was observed, at least the amount of precipitation was lower than the multi-annual amount by 7–30 mm, and only in April 349% of the average multi-annual amount of precipitation fall. The duration of the period from germination to the end of autumn vegetation in 2021 was on par with long-term data (59 days), the period of rest was shorter by 8 days. According to the indicator of moisture supply, this year was characterized by a weak drought (HTC = 0.9), and in the spring-summer period of winter wheat vegetation, insufficient moisture (HTC = 0.8).

Sampling and methods

The research material included 34 F_1 hybrids resulted from direct (×) and backcrossing (↔) in 2020 with the involvement of soft winter wheat sources of resistance to *F. graminearum* (MV 20-88 × Smuhlianka, BILINMEVEN-49 × Natalka, Donskoy prostor × Slavna, Myronivska rannostyhla × CATALON, and (Mikon × ALMA) × Lehenda Myronivska) and new soft winter varieties (MIP Kniazna, MIP Fortuna, MIP Vyshyvanka, Avrora Myronivska, Podolianka).

In the study, plant protection chemicals and fertilizers were not used. The seeds were sown untreated in standard sowing periods (2nd decade of September). The sowing rate was 133 plants per 1 m².

The seeds of the hybrids were sown by hand, according to the scheme: mother form, hybrid, father form (pollinator). Threshing of spikes was carried out manually. For the maximum implementation of the program, a sparse sowing method was used: the distance between plants in a row is up to 5 cm, and between rows is 15–30 cm. During the growing season, phenological observations were made, and upon the onset of full

maturity, a structural analysis of the elements of the spike productivity of parental components and crossing combinations (F_1 – 25 plants) was carried out (Perepelytsia et al., 2022).

The intensity of damage against *Fusarium graminearum* of wheat was carried out according to the methods of scientists (Babayants et al., 1988; Shelepov et al., 2005; Babayants & Babayants, 2014; Kyrylenko et al., 2017). The intensity was determined by the ratio of affected plants to the total sample.

The degree of phenotypic dominance in hybrid combinations for this quantitative trait was calculated according to the formula of B. Griffing (1950):

$$hp = (F_1 - MP) / (BP - MP),$$

where hp – degree of dominance; F_1 – the average arithmetic value of the indicator in the hybrid; MP – the average arithmetic value of the indicator of both parent forms; BP – the average arithmetic value of the parental component with a stronger development of the symptom (the lowest proportion (%) of the intensity of the infection).

The range in which the degree of dominance (hp) lies covers any values from $-\infty$ to $+\infty$ (Zhupina et al., 2022). Data were grouped according to the methodise of Beil & Atkins (Table 2).

Phytopathological analysis of grain samples in laboratory conditions was used to isolate pathogens of *Fusarium* fungi in pure culture. The studied grain of the hybrid populations was surface sterilized, by passing it over the flame of an alcohol still and soaking it in the Domestos solution. Sterile grain was laid out in Petri dishes on a nutrient medium of potato-glucose agar (PGA), ten seeds in ten cups (100 seeds). Isolates were examined for 5–7 days, recording the presence or absence of microconidia. The final identification of pathogens was carried out by microscopic examination, taking into account the morphological features of macroconidia characteristic of F. graminearum (spindle-sickle, ellipsoidal curved, with a gradually and evenly narrowed conical, elongated upper cell, with a distinct stalk at the base, usually with five septa, whitish-pink, golden-yellow, carmine-purple in mass), the presence or absence of chlamydospores. As a result of the research, the most aggressive isolates of the causative agent of the fungus *F. graminearum* were selected for inoculum development and the creation of an artificial infectious background in field conditions (Mukha & Murashko, 2019).

Table 2. Classification of dominance (Beil & Atkins, 1965)

Type of dominance	hp range
Positive overdominance (heterosis) (POD)	$hp > +1$
Positive dominance (PD)	$+0.5 < hp \leq +1$
Intermediate inheritance (II)	$-0.5 \leq hp \leq +0.5$
Negative dominance (ND)	$-1 \leq hp < -0.5$
Negative overdominance (depression) (D)	$hp < -1$

RESULTS AND DISCUSSION

The impact of climate change on the contamination of agricultural crops by *Aspergillus* and toxigenic *Fusarium* species may lead to a sharp increase in morbidity worldwide with higher food safety risks for humans and animals due to high levels of mycotoxin contamination in the final product (Sarrocco & Vannacci, 2018; Moretti et al., 2019; Thanushree et al., 2019). Recent decades have been characterized by

extraordinary changes in weather conditions, which negatively affect not only cultivated plants but also their development by pathogens (Juroszek & von Tiedemann, 2015; Vozhegova, 2020; Miedaner & Juroszek, 2021).

In the conducted studies, the development of winter wheat diseases and appearance in crops was primarily influenced by the weather conditions of the year, namely the sum of the effective air temperatures and the amount of precipitation. Cereal crops can significantly alter the expression of certain phenotypic dominance depending on the yearly conditions (Spriazhka et al., 2022).

In 2021, overdominance (heterosis) in terms of resistance to the causative agent of Fusarium head blight was established in four (11.76%) hybrid combinations (Fig. 1, A), namely, MIP Kniazna × (Donskoy prostor × Slavna); [(Mykon × ALMA) × Lehenda Myronivska] × Podolianka; MIP Vyshyvanka × (MV 20-88 × Smuhlianka); MIP Vyshyvanka × (BILINMEVEN-49 × Natalka). In 2022, overdominance (heterosis) was found in nine (26.47%) hybrid combinations, namely, (BILINMEVEN-49 × Natalka) × MIP Kniazhna, (Myronivska rannostyhla × CATALON) × MIP Kniazhna, Podolianka × (Donskoy prostor × Slavna), Podolianka × [(Mikon × ALMA) × Lehenda Myronivska], MIP Fortuna × (BILINMEVEN-49 × Natalka), (BILINMEVEN-49 × Natalka) × MIP Fortuna, MIP Fortuna × (Donskoy prostor × Slavna), (Donskoy prostor × Slavna) × MIP Fortuna (Fig. 1, B).

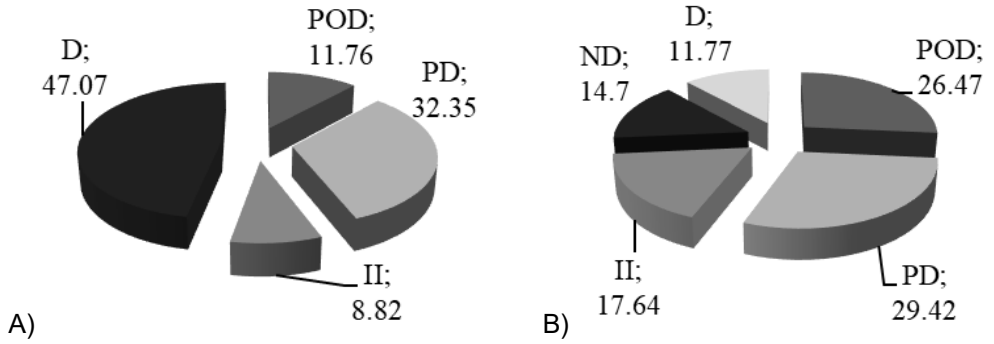

Figure 1. Distribution of phenotypic dominance indicators by the intensity of infection with F. graminearum in F_1 of soft winter wheat. (POD – heterosis; PD – positive dominance; II – intermediate inheritance; ND – negative dominance; D – depression (A – 2021, B – 2022)).

The transmission of resistance to the pathogen *Fusarium graminearum* was observed in the varieties MIP Knyazna, MIP Vyshivanka, MIP Podolyanka, MIP Fortuna, which were involved in crossing as the mother form and the pollinator variety of the source of resistance. Agostinelli et al. (2012) indicate that breeders often use phenotypic selection to develop fusarium-resistant soft winter wheat cultivars.

In the studies of Jin et al. (2013) resistance to Fusarium wilt in wheat is determined either by gene products that contribute to plant defense (active resistance factors) or by plant properties that indirectly affect susceptibility reduction, such as morphological characters and developmental features (passive resistance factors). In F_1, resistance to fusarium wilt was mostly at the level of one of the parental forms, partially positive inheritance was present in 11 (32.35%) hybrids, in 2022 was 10 hybrids (29.42%). Three hybrids (8.8%) and six (17.64%) hybrids had intermediate inheritance, respectively. In

the 2022 studies, five (14.7%) hybrid combinations had partial negative inheritance. Depression was identified in 16 hybrids of the first generation, which is (47.07%) and four (11.77%), respectively. It is worth noting that this provision complements the general principle of the formative process (Miedaner, 1997; Motsnyy et al. 2017; Khalikulov et al., 2022) as a result of which such a proportion of the probability of selection of new resistant genotypes for a given pathogen is formed.

Grain yield is a complex feature and the result of multiplicative interaction of components (Slafer et al., 1996). Previous studies of wheat have identified some quantitative trait loci affecting grain yield that are co-located with those associated with its components, suggesting partially shared genetic control of these traits (Kuchel et al., 2007; Cuthbert et al., 2008; Sukumaran et al., 2015; Schulthess et al., 2017). Wheat yield components are multifaceted Slafer et al. (2014) and cover two main parameters: grain yield per area and grain yield per spike. The output of grain from the area includes grains in the spike, mass of grain and spikes from the area; while grain yield per spike consists of the number of spikes per ear, the number of grains and the size of grains per spikes and/or spike. There are numerous interactions and compensation mechanisms between different yield components, depending on genotype x environment x agronomy interactions (Gegas et al., 2010).

Therefore, studies of the nature of the variability of this trait in the parent-offspring system were conducted based on biometric analysis, and the degree of dominance of this trait in the first-generation hybrids was determined. Motsnyy et al. (2017) note that the interaction is characterized by partial or complete dominance or even overdominance of the trait and low or medium heritability. Khalikulov et al. (2022) add that alleles that have a weaker direct negative effect or do not have such an effect prevail over alleles that contribute to a more pronounced decrease. During the research period of 2021, 2022, heterosis for the trait 'grain number per the main spike' was noted in the group of crosses 29 (85.29%) hybrids F_1 (Fig. 2, A) and 19 (55.88%) (Fig. 2, B), respectively; partial positive dominance was noted in four (11.77%) and 12 (35.29%) hybrids F_1, respectively. In 2021, intermediate inheritance was noted only in the hybrid combination (BILINMEVEVN-49 × Natalka) × Podolianka.

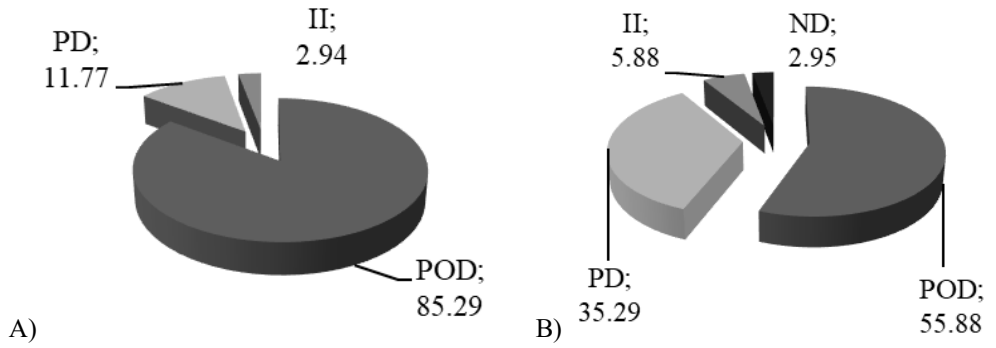

Figure 2. Distribution of phenotypic dominance indicators by the grain number per spike in F_1 of soft winter wheat. (POD – heterosis; PD – positive dominance; II – intermediate inheritance; ND – negative dominance (A – 2021, B – 2022)).

In 2022, intermediate inheritance for this trait was observed in hybrid combinations ntermediate inheritance for this trait was observed in two hybrid combinations (BILINMEVEN-49 × Natalka) × MIP Fortuna, (Donskoy prostor × Slavna) × MIP Fortuna, and negative dominance (ND was found in the combination Svitanok Myronivskyi × (Myronivska rannostyhla × CATALON).

Grain weight from the main spike is one of the important elements of productivity (Zhou et al., 2007; Zheng et al., 2011; Xiao et al., 2012; Feng et al., 2018). The results of research by Zhang et al. (2022) showed that a significant increase in grain yield over the past 60 years was mainly due to an increase in the number of grains in spike and grain weight, while the number of spikes per m^2 did not change significantly. According to the grain weight per the main spike, heterosis (superdominance) was revealed in 82.35% (2021) (Fig. 3, A) and 61.77% of new genotypes (2022) (Fig. 3, B). Positive dominance was found in three (8.82%) and ten (29.41%) hybrid combinations, respectively.

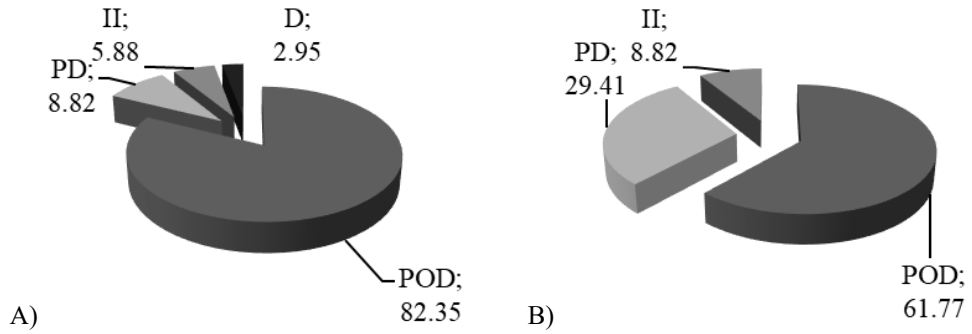

Figure 3. Distribution of phenotypic dominance indicators by the grain weight per main spike in F1 of soft winter wheat. (POD – heterosis; PD – positive dominance; II – intermediate inheritance; ND – negative dominance (A – 2021, B – 2022)).

In 2021, in two (5.88%) hybrid combinations (BILINMEVEN-49 × Natalka) × Podolianka, [(Mikon × ALMA) × Lehenda Myronivska] × MIP Fortuna; and in 2022, in three (8.82%) MIP Kniazna × (MV 20-88 × Smuhlianka), MIP Fortuna × (BILINMEVEN-49 × Natalka), (Donskoy prostor × Slavna) × MIP Fortuna intermediate inheritance of grain weight per main spike was noted. An expression of depression was recorded in one hybrid combination (in 2021) MIP Fortuna × (Donskoy prostor × Slavna).

Ten (29.41%) hybrid populations of the first generation were identified according to the nature of inheritance of resistance and yield components of the main spike (Table 3). In 2021, the following direct hybrid combinations [(Mikon × ALMA) × Lehenda Myronivska] × Podolianka, MIP Vyshyvanka × (MV 20-88 × Smuhlianka) were singled out for resistance to Fusarium head blight with heterosis (overdominance), and in 2022, they were Podolianka × [(Mikon × ALMA) × Lehenda Myronivska] and the reverse hybrid combination MIP Fortuna ↔ (BILINMEVEN-49 × Natalka).

According to the yield components of the main spike in eight F_1, the most expression of heterosis was observed in the conditions of 2021, positive dominance was found in two reverse hybrids Podolianka ↔ [(Mikon × ALMA) × Lehenda Myronivska]. In the conditions of 2022, heterosis is established in direct hybrid combinations:

MIP Kniazna × (MV 20-88 × Smuhlianka), (MV 20-88 × Smuhlianka) × MIP Kniazna, (BILINMEVEN-49 × Natalka) × MIP Fortuna and the reverse combination Podolianka ↔ [(Mikon × ALMA) × Lehenda Myronivska].

Table 3. Degree of phenotypic dominance for resistance against *F. graminearum* and main spike productivity traits in F_1 winter wheat, 2021–2022.

Hybrid combination	Degree of phenotypic dominance*					
	2021			2022		
	Resistance to *F. graminearum*	Grain number per spike	Grain weight per spike	Resistance to *F. graminearum*	Grain number per spike	Grain weight per spike
MIP Kniazhna × (MV 20-88	PD	POD	POD	PD	POD	II
× Smuhlianka)	0.51	3.76	17.61	0.80	7.40	0.45
(MV 20-88 × Smuhlianka)	PD	POD	POD	PD	POD	POD
× MIP Knyazhna	0.52	5.34	24.65	0.80	13.70	17.61
Podolianka × [(Mykon × ALMA)	II	PD	POD	POD	POD	POD
× Lehenda Myronivska]	0.43	0.92	1.12	1.40	3.90	1.12
[(Mykon × ALMA) × Lehenda	POD	PD	PD	II	POD	POD
Myronivska] × Podolianka	2.41	0.53	0.64	0.40	2.30	1.64
MIP Vyshyvanka × (MV 20-88	POD	POD	POD	PD	PD	PD
× Smuhlianka)	3.17	2.43	24.63	0.94	0.87	0.94
(MV 20-88 × Smuhlianka)	PD	POD	POD	PD	PD	PD
× MIP Vyshyvanka	0.76	8.50	23.37	0.71	0.52	0.71
MIP Vyshyvanka × [(Mykon × ALMA)	PD	POD	POD	PD	PD	PD
× Lehenda Myronivska]	0.87	1.61	1.98	0.83	0.96	0.50
[(Mykon × ALMA) × Lehenda	PD	POD	POD	PD	PD	PD
Myronivska] × MIP Vyshyvanka	0.51	2.29	2.57	0.50	0.51	0.73
MIP Fortuna × (BILINMEVEN-49	II	POD	POD	POD	PD	II
× Natalka)	0.45	1.81	2.23	1.30	0.73	0.27
(BILINMEVEN-49 × Natalka)	PD	POD	POD	POD	II	POD
× MIP Fortuna	0.52	2.86	8.0	1.60	0.35	3.04

*Degree of phenotypic dominance: POD – heterosis; PD – positive dominance; II – intermediate inheritance.

Positive dominance of the set of investigated traits was found in hybrid combinations in which sources of resistance to the pathogen *Fusarium graminearum* (MV 20-88 × Smuhlianka, (Mikon × ALMA) × Lehenda Myronivska) and local varieties of winter wheat (MIP Kniazhna, MIP Vyshyvanka) were involved in crossing.

The obtained results give grounds for asserting that cytoplasmic genes strengthened the dominance of complex resistance genes in the crossbreeding group: (MV 20-88 × Smuhlianka) × MIP Kniazna; [(Mikon × ALMA) × Lehenda Myronivska] × Podolianka; (MV 20-88 × Smuhlianka) × MIP Vyshyvanka; [(Mikon × ALMA) × Lehenda Myronivska] × MIP Vyshyvanka; (BILINMEVEN-49 × Natalka) × MIP Fortuna. The dependence of the level of resistance to *Fusarium graminearum* of the progeny of winter wheat on the level of resistance of the parental forms is visible in hybrids: MIP Kniazna

× (MV 20-88 × Smuhlianka); Podolianka × [(Mikon × ALMA) × Lehenda Myronivska]; MIP Vyshyvanka × (MV 20-88 × Smuhlyanka); MIP Vyshyvanka × [(Mikon × ALMA) × Lehenda Myronivska]; MIP Fortuna × (BILINMEVEN-49 × Natalka).

It should be noted that in order to increase the percentage of selectively valuable new forms, it is necessary to have as few negative signs and properties as possible or to detect them as early as possible at the initial stages of selection. The selection of transgressive forms for resistance to pathogens in combination with elements of productivity in the second, third and fourth generation of hybrids can be effective. Selection for ecologically stable resistance must be carried out in multiple environments with a maximal range of different infection levels (Miedaner, 1997; Agostinelli et al., 2012).

CONCLUSIONS

To improve the efficiency of winter wheat breeding for immunity, it is promising to create a qualitatively new source material that is maximally adapted to zonal conditions. When developing new varieties, selection plays a central role, regardless of the method used to create the source material. At the same time, it is important for the breeder to determine the characteristics of the nature of inheritance of traits. 10 combinations of F_1 crosses out of 34 studied combine in one genotype resistance to *Fusarium graminearum* and main spike yield components that exceed the parental components for these traits. These genotypes are recommended for further breeding work to develop high-yielding winter bread wheat varieties resistant to *Fusarium graminearum*, as these hybrid combinations are potentially highly transgressive.

In 2021, overdominance (heterosis) in terms of resistance to the causative agent of Fusarium head was found in four (11.76%) hybrid combinations (MIP Kniazhna × (Donskoy prostor × Slavna); [(Mikon × ALMA) × Lehenda Myronivska] × Podolianka; MIP Vyshyvanka × (MV 20-88 × Smuhlianka); MIP Vyshyvanka × (BILINMEVEN-49 × Natalka)); in 2022, overdominance (heterosis) was found in nine (26.47%) hybrid combinations (BILINMEVEN-49 × Natalka) × MIP Kniazhna, (Myronivska rannostyhla × CATALON) × MIP Kniazhna, Podolianka × (Donskoy prostor × Slavna), Podolianka × [(Mikon × ALMA) × Lehenda Myronivska], MIP Fortuna × (BILINMEVEN-49 × Natalka), (BILINMEVEN-49 × Natalka) × MIP Fortuna, MIP Fortuna × (Donskoy prostor × Slavna), (Donskoy prostor × Slavna) × MIP Fortuna).

29.4% of hybrid populations of the first generation were distinguished by the nature of inheritance of resistance and productivity elements of the main ear. Positive dominance of the set of investigated traits was found in hybrid combinations in which sources of resistance against the pathogen *Fusarium graminearum* (MV 20-88 × Smuhlianka, (Mikon × ALMA) × Lehenda Myronivska) and local varieties of winter wheat MIP Knyazhna, MIP Vyshivanka were involved in crossing.

The obtained results give reason to assert that cytoplasmic genes strengthened the dominance of genes of complex resistance in one crossing group, and the dependence of the level of resistance against *Fusarium graminearum* of winter wheat offspring on the level of resistance of parental forms in other hybrids was observed.

REFERENCES

Agostinelli, A.M., Clark, A.J., Brown-Guedira, G. & Van Sanford, D.A. 2012. Optimizing phenotypic and genotypic selection for Fusarium head blight resistance in wheat. *Euphytica* **186**, 115–126.

Babayants, L.T., Mesterhazy, A., Wachter, V., Neklesa, N., Dubinina, L., Omelchenko, L., Klechkovskaya, H., Syusarenko, A. & Bartosh, P. 1988. *Methods of selection and evaluation of wheat and barley resistance in member countries of the CMEA*. Prague, 321 pp. (in Russian).

Babayants, O.V. & Babayants, L.T. 2014. Fundamentals of wheat breeding and methodology for assessing resistance to pathogens. Odessa: VMV (in Ukrainian).

Beil, G.M. & Atkins, R.E. Inheritance of quantitative characters in grain sorghum. 1965. *Iowa State Journal* **39**. P. 3

El Chami, J., El Chami, E., Tarnawa, Á., Kassai, K.M., Kende, Z. & Jolánkai, M. 2023. Effect of Fusarium infection on wheat quality parameters. *Cereal Research Communications* **51**(1), 179–187.

Champeil, A., Doré, T. & Fourbet, J.F. 2004. Fusarium head blight: epidemiological origin of the effects of cultural practices on head blight attacks and the production of mycotoxins by Fusarium in wheat grains. *Plant Science* **166**(6), 1389–1415.

Cuthbert, J.L., Somers, D.J., Brule-Babel, A.L., Brown, P.D. & Crow, G.H. 2008. Molecular mapping of quantitative trait loci for yield and yield components in spring wheat (*Triticum aestivum* L.). *Theoretical and Applied Genetics* **117**(4), 595–608.

Diakite, S., Pakina, E., Zargar, M., Aldaibe, A.A.A., Denis, P., Gregory, L. & Behzad, A. 2022. Yield losses of cereal crops by *Fusarium* Link: A review on the perspective of biological control practices. *Research on Crops* **23**(2), 418–436.

Feng, F., Han, Y., Wang, S., Yin, S., Peng, Z., Zhou, M., Gao, W., Wen, X., Qin, X. & Siddique, K.H. 2018. The effect of grain position on genetic improvement of grain number and thousand grain weight in winter wheat in North China. *Frontiers in Plant Science* **9**, 129.

Foroud, N.A., Chatterton, S., Reid, L.M., Turkington, T.K., Tittlemier, S.A. & Gräfenhan, T. 2014. Fusarium diseases of Canadian grain crops: impact and disease management strategies. *Future Challenges in Crop Protection Against Fungal Pathogens*, 267–316.

Gao, X.L., Fan, L.I., Sun, Y.K., Jiang, J.Q., Tian, X.L., Li, Q.W., Duan, K.L, Lin, J., Liu, H.Q. & Wang, Q.H. 2023. Basal defense is enhanced in a wheat cultivar resistant to Fusarium head blight. *Journal of Integrative Agriculture*. (in press).

Gegas, V.C., Nazari, A., Griffiths, S., Simmonds, J., Fish, L., Orford, S., Fish, L., Sayers, L., Doonan, J.H. & Snape, J.W. 2010. A genetic framework for grain size and shape variation in wheat. *Plant Cell* **22**(4), 1046–1056.

Griffing, B. 1950. Analysis of quantitative gene-action by constant parent regression and related techniques. *Genetics* **35**, 303–321.

Hysing, S.C. & Wiik, L. 2014. Fusarium seedling blight of wheat and oats: effects of infection level and fungicide seed treatments on agronomic characters. *Acta Agriculturae Scandinavica, Section B—Soil & Plant Science* **64**(6), 537–546.

Jin, F., Zhang, D., Bockus, W., Baenziger, P.S., Carver, B. & Bai, G. 2013. Fusarium Head Blight Resistance in U.S. Winter Wheat Cultivars and Elite Breeding Lines. *Crop Science* **5**, 2006–2013. https://doi.org/10.2135/cropsci2012.09.0531

Juroszek, P. & von Tiedemann, A. 2013. Climate change and potential future risks through wheat diseases: a review. *European Journal of Plant Pathology* **136**, 21–33.

Juroszek, P. & von Tiedemann, A. 2015. Linking plant disease models to climate change scenarios to project future risks of crop diseases: a review. *Journal of Plant Diseases and Protection* **122**, 3–15.

Khalikulov, D.K., Gulboev, O.Y. & Gulbaev, Y.I. 2022. Inheritance of the quantity of grains in first generation durum wheat hybrids. *Universum* **10**(100)), 15–17.

Klyszejko, A., Kubus, Z. & Zakowska, Z. 2005. Mycological analysis of cereal samples and screening of Fusarium strains' ability to form deoxynivalenole (DON) and zearalenone (ZEA) mycotoxins-a pilot study. *Polish journal of microbiology* **54**, 21–25.

Kovalyshyna, H.M., Demidov, O.A., Mukha, T.I., Murashko, L.A. & Zaima, O.A. 2016. Mironivka winter wheat varieties with group resistance to diseases for the Forest-Steppe of Ukraine. *Scientific Reports of the National University of Life and Environmental Sciences of Ukraine*. Issue 5.

Kovalyshyna, H.M., Dmytrenko, Yu.M., Demidov, O.A., Mukha, T.I. & Murashko, L.A. 2018. Results of winter wheat selection for resistance to major pathogens at the Mironivka Wheat Institute. *Scientific Bulletin of the National University of Life and Environmental Sciences of Ukraine. Series: Agronomy* **294**, 96–103 (in Ukrainian).

Kovalyshyna, H., Dmytrenko, Y., Tonkha, O., Makarchuk, O., Demydov, O., Humeniuk, O., Kozub, N., Karelov, A., Sozinov, I. & Mushtruk, M. 2020. Diversity of winter common wheat varieties for resistance to leaf rust created in the V.M. Remeslo Myronivka Institute of wheat. *Potravinarstvo Slovak Journal of Food Sciences* **14**, 1001–1007.

Kuchel, H., Williams, K.J., Langridge, P., Eagles, H.A. & Jefferies, S.P. 2007. Genetic dissection of grain yield in bread wheat. I. QTL analysis. *Theoretical and Applied Genetics* **115**(8), 1029–1041.

Kyrylenko, V.V., Demidov, O.A., Humeniuk, O.V., Dubovik, N.S., Bliznyuk, B.V., Lisova, H.M. 2018. *Utility Model Patent* No. 128676 Ukraine. Method of selection for complex resistance against major pathogens of soft winter wheat diseases. IPC (2018.01), A01N 1/00, A01N 3/00, Application No. 2017 11026; filed on November 13, 2017; published on October 10, 2018, Bulletin No. 19.

Liu, Y., Chen, Q., Chen, J., Pan, T. & Ge, Q. 2021. Plausible changes in wheat-growing periods and grain yield in China triggered by future climate change under multiple scenarios and periods. *Quarterly Journal of the Royal Meteorological Society* **147**(741), 4371–4387. https://doi.org/10.1002/qj.4184

Lozinskiy, M., Burdenyuk-Tarasevych, L., Grabovskyi, M., Lozinska, T., Sabadyn, V., Sidorova, I., Panchenko, T., Fedoruk, Y. & Kumanska, Y. 2021. Evaluation of selected soft winter wheat lines for main ear grain weight. *Agronomy Research* **19**(2), 540–551. doi: https://doi.org/10.15159/ar.21.071

Mazurenko, B., Novytska, N., & Honchar, L. 2020. Response of spring and facultative triticale on microbial preparation (*Azospirillum brasilense* and *Bacillus polymyxa*) by different nitrogen nutrition. *Journal of Central European Agriculture* **21**(4), 763–774.

Miedaner, T. 1997. Breeding wheat and rye for resistance to Fusarium diseases. *Plant Breeding* **116**, 201–220. https://doi.org/10.1111/j.1439-0523.1997.tb00985.x

Miedaner, T. & Juroszek, P. 2021. Climate change will influence disease resistance breeding in wheat in Northwestern Europe. *Theoretical and Applied Genetics* **134**(6), 1771–1785.

Mikaberidze, A. & McDonald, B.A. 2020. A tradeoff between tolerance and resistance to a major fungal pathogen in elite wheat cultivars. *New Phytologist* **226**(3), 879–890.

Moretti, A., Pascale, M. & Logrieco, A.F. 2019. Mycotoxin risks under a climate change scenario in Europe. *Trends in Food Science & Technology* **84**, 38–40.

Mostovyiak, I.I., Demianyuk, O.S. & Borodai, V.V. 2020. Formation of phytopathogenic fond in agrocenoses of cereals of the right-bank Forest-steppe of Ukraine. *Agroecological Journal* **1**, 28–38 (in Ukrainian).

Motsnyy, I.I., Goncharova, A.I., Chebotar, G.O. & Chebotar, S.V. 2017. Degree of phenotypic dominance and heritability of the plant height in wheat hybrids with different alleles of Rht genes. *Cytology and Genetics* **51**(1), 18–25.

Moisiienko, V.V., Nazarchyk, O.P. & Ishchenko, M.V. 2020. Increasing the Yield and Quality of Winter Wheat through Autumn Herbicide Treatment. *Scientific Horizons* **08**(93), 98–103 (in Ukrainian).

Mukha, T.I. & Murashko, L.A. 2019. Resistance of variety samples from collection nursery of winter bread wheat against Fusarium head blight and group of diseases. *Myronivka bulletin* **9**, 53–58.

Muthomi, J.W., Ndung'u, J.K., Gathumbi, J.K., Mutitu, E.W. & Wagacha, J.M. 2008. The occurrence of *Fusarium* species and mycotoxins in Kenyan wheat. *Crop Protection* **27**(8), 1215–1219.

Obradović, A., Stanković, S., Krnjaja, V., Nikolić, M., Savić, I., Stevanović, M. & Stanković, G. 2022. Fusariotoxins on wheat grain. Collection of summaries of Works. In: *XVII Conference on Plant Protection*, Zlatibor, 28. Novembar-1. Decembar 2022. godine, 48–48 (in Serbian).

Ostrovskyi, D.M., Korniienko, L.Ye. & Andriichuk, A.V. 2017. Toxigenic Properties of Microfungi *Fusarium* and *Aspergillus*. *Scientific Bulletin of Veterinary Medicine* **1**, 157–162 (in Ukrainian).

Pagán, I. & García-Arenal, F. 2018. Tolerance to plant pathogens: theory and experimental evidence. *International Journal of Molecular Sciences* **19**(3), 810.

Panwar, V., Aggarwal, A., Paul, S., Singh, V., Singh, P.K., Sharma, D. & Shaharan, M.S. 2016. Effect of temperature and pH on the growth of Fusarium spp. causing Fusarium head blight (FHB) in wheat. *South Asian Journal of Experimental Biology* **6**(5), 186–193.

Perepelytsia, L.O., Patsiuk, M.K. & Korevo, N.I. 2022. *Educational Practice in Plant Physiology and Genetics. Guidelines for Laboratories*. Zhytomyr: Zhytomyr Ivan Franko State University Publishing, 36 pp. (in Ukrainian).

Ryabovol, Ya.S., Ryabovol, L.O. & Diordiieva, I.P. 2019. Resistance to Diseases of Soft Winter Wheat Samples Created by HybridiFzation of Geographically Distant Forms. *Submontane and Mountain Farming and Animal Husbandry* **65**, 124–133.

Sarrocco, S. & Vannacci, G. 2018. Preharvest application of beneficial fungi as a strategy to prevent postharvest mycotoxin contamination: A review. *Crop Protection* **110**, 160–170. https://doi.org/10.1016/j.cropro.2017.11.013

Schulthess, A.W., Reif, J.C., Ling, J., Plieske, J., Kollers, S., Ebmeyer, E., Korzun, V., Argillier, O., Stiewe, G., Röder, M. & Jiang, Y. 2017. The roles of pleiotropy and close linkage as revealed by association mapping of yield and correlated traits of wheat (*Triticum aestivum* L.). *Journal of Experimental Botany* **68**(15), 4089–4101.

Shelepov, V.V., Dubovyi, V.I., Kyrylenko, V.V., Sabadin, V.Ya., Dubyna, L.V., Lisovyi, M.P., Fedorenko, V.P., Parfeniuk, A.I., Dovhal, Z.M., Sokolovska, M.P., Vusatyi, R.O. & Yarynchyin, A.M. 2005. *Creation of Resistant Winter Wheat Varieties Using Complex Infectious Pathogen Backgrounds in Breeding Process*. (Methodological Guidelines) / edited by M.P. Lisovyi, V.V. Shelepov. Kyiv: Kolobih, 20 pp. (in Ukrainian).

Shikur Gebremariam, E., Sharma-Poudyal, D., Paulitz, T.C., Erginbas-Orakci, G., Karakaya, A. & Dababat, A.A. 2018. Identity and pathogenicity of Fusarium species associated with crown rot on wheat (*Triticum* spp.) in Turkey. *European Journal Of Plant Pathology* **150**, 387–399.

Slafer, G.A., Savin, R. & Sadras, V.O. 2014. Coarse and fine regulation of wheat yield components in response to genotype and environment. *Field Crops Research* **157**, 71–83.

Slafer, G.A., Calderini, D.F. & Miralles, D.J. 1996. Yield components and compensation in wheat: opportunities for further increasing yield potential. *Increasing yield potential in wheat: Breaking the Barriers*, 101–133.

Spriazhka, R.O., Zhemoida, V.L., Makarchuk, O.S., Dmytrenko, Y.M. & Bahatchenko, V.V. 2022. Selection value of initial material according to the main biochemical parameters of grain in new maize hybrids creation. *Agronomy Research* **20**(S1), 1151–1162.

Sukumaran, S., Dreisigacker, S., Lopes, M., Chavez, P. & Reynolds, M.P. 2015. Genome-wide association study for grain yield and related traits in an elite spring wheat population grown in temperate irrigated environments. *Theoretical and Applied Genetics* **128**(2), 353–363.

Tančić, S. 2013. Fusariotoxins in cereals – occurrence, risk and prevention. *Zbornik referata*, **17** (in Serbian).

Thanushree, M.P., Sailendri, D., Yoha, K.S., Moses, J.A. & Anandharamakrishnan, C. 2019. Mycotoxin contamination in food: An exposition on spices. *Trends in Food Science & Technology* **93**, 69–80. https://doi.org/10.1016/j.tifs.2019.08.010

Tribel, S.O., Hetman, M.V., Stryhun, O.O., Kovalyshyna, H.M. & Andriushchenko, A.V. 2010. *Methodology for Assessing the Resistance of Wheat Varieties to Pests and Pathogens*; edited by S.O. Tribel. Kyiv: Kolobih 392 pp. (in Ukrainian).

Vozhegova, R.A. 2020. Scientific and practical aspects of creating climate-adapted varieties and hybrids of agricultural crops and technologies for their cultivation under irrigation in the southern regions of Ukraine. Publishing House 'Baltija Publishing'. 67–84. (in Ukrainian)

Ward, T.J., Clear, R.M., Rooney, A.P., O'Donnell, K., Gaba, D., Patrick, S., Starkey, D.E., Gilbert, J., Geiser, D.M. & Nowicki, T.W. 2008. An adaptive evolutionary shift in Fusarium head blight pathogen populations is driving the rapid spread of more toxigenic *Fusarium graminearum* in North America. *Fungal Genetics and Biology* **45**(4), 473–484.

Xiao, Y.G., Qian, Z.G., Wu, K., Liu, J.J., Xia, X.C., Ji, W.Q. & He, Z.H. 2012. Genetic gains in grain yield and physiological traits of winter wheat in Shandong Province, China, from 1969 to 2006. *Crop Science* **52**(1), 44–56.

Zhang, C., Zheng, B. & He, Y. 2022. Improving grain yield via promotion of kernel weight in high yielding winter wheat genotypes. *Biology* **11**(1), 42.

Zheng, T.C., Zhang, X.K., Yin, G.H., Wang, L.N., Han, Y.L., Chen, L., Huang, F., Tang, J.W., Xia, X.C. & He, Z.H. 2011. Genetic gains in grain yield, net photosynthesis and stomatal conductance achieved in Henan Province of China between 1981 and 2008. *Field Crops Research* **122**(3), 225–233.

Zhou, Y., He, Z.H., Sui, X.X., Xia, X.C., Zhang, X.K. & Zhang, G.S. 2007. Genetic improvement of graiFn yield and associated traits in the northern China winter wheat region from 1960 to 2000. *Crop Science* **47**(1), 245–253.

Zhupina, A.Yu., Bazaliy, G.G., Usyk, L.O., Marchenko, T.Yu., Suchkova, V.M., Mishchenko, S.V. & Lavrinenko, Yu.O. 2022. Inheritance of ear grain mass by winter wheat hybrids of different ecological and genetic origin under irrigation conditions. *Agrarian Innovations* **14**, 152–160 (in Ukrainian).

Agronomy Research **22**(1), 110–126, 2024
https://doi.org/10.15159/AR.24.030

Spatial variability of methane and carbon dioxide gases in a Compost-Bedded Pack Barn system

J.C. Ferreira[1], P.F.P Ferraz[1,*], G.A.S. Ferraz[1], F.M. Oliveira[1], V.G. Cadavid[2], G. Rossi[3] and V. Becciolini[3]

[1]Federal University of Lavras, Department of Agricultural Engineering, University Campus, PO Box 3037 - CEP 37200-000 Lavras, Minas Gerais, Brazil
[2]Universidad Nacional de Colombia, sede Medellín, Facultad de Ciencias Agrarias, Grupo de Investigación en Biodiversidad y Genética Molecular (BIOGEM). Carrera 65 #59A-110, postal code 050034 Medellín, Colombia
[3]University of Firenze, Department of Agriculture, Food, Environment and Forestry, 13 Via San Bonaventura, IT 50145 Firenze, Italy
[*]Correspondence: patricia.ponciano@ufla.br

Received: February 2nd, 2024; Accepted: April 10th, 2024; Published: May 2nd, 2024

Abstract. The dairy sector significantly contributes to global food production, however, it is closely associated with environmental concerns, specifically the emission of greenhouse gases such as methane (CH_4) and carbon dioxide (CO_2). The research problem focuses on the environmental impact of livestock farming, particularly in relation to the emission of greenhouse gases (GHG) such as methane (CH_4) and carbon dioxide (CO_2). Therefore, the objective of this paper was to assess the spatial variability of CH_4 and CO_2, as well as the thermal environment through the Temperature and Humidity Index (THI) and of air velocity (V, m s^{-1}) in a Compost Bedded Pack (CBP). The experiment was carried out in October 2023, in a commercial dairy cattle facility measuring 54×22×4.5 m (length×width×height) that housed 80 lactating cows. Measurements were collected at 75 points, 0.25 m above the bedding, for one minute in each point. To characterize the distribution of gases and the thermal environment, the data were underwent geostatistical techniques and kriging maps. THI values ranged from 72.4 to 78.4, categorizing the animals into two environments within the facility, comfort and alert to thermal conditions. The maximum recorded for CO_2 was 713.60 ppm in the region with a low ventilation incidence. CH_4 reached a ranging from 103.38 to 196.73 ppm in areas with low ventilation and higher temperatures. The use of geostatistics enabled the characterization of spatial variability of greenhouse gases CH_4 and CO_2, as well as THI and V. Analyzing these variables is crucial for implementing mitigation actions and developing an increasingly sustainable production system.

Key words: animal welfare, dairy cattle, gas monitoring, geostatistics, greenhouse gases.

INTRODUCTION

In the 21st century, we face crucial challenges in attempting to reduce emissions and control the accumulation of greenhouse gases (GHG) in the atmosphere (Su et al., 2020). In this scenario, livestock farming significantly contributes to climate change.

Studies indicate that livestock farming is responsible for 14.5% of anthropogenic greenhouse gas emissions in the atmosphere, with dairy cattle contributing to 20% of total gas emissions produced in livestock farming (Gerber et al., 2013; Singaravadivelan et al., 2023).

Methane (CH_4) and carbon dioxide (CO_2) represent some of the main GHGs emitted by ruminants primarily generated through enteric fermentation, feed production, manure production, and management (Naranjo et al., 2020).

In contemporary dairy farming, intensive housing systems are commonly adopted as strategies to mitigate heat stress, improve milk quality, ensure herd health, and increase animal productivity (Frigeri et al., 2023b).

In Brazil, an intensive system that has aroused the interest of dairy producers is the Compost Barn system (Black et al., 2013). This system seeks to meet the demand for animal welfare, featuring a large common area covered with bedding made of soft and comfortable material (sawdust or wood shavings), where the animals remain free to lie down and move, expressing their natural behaviours (Damasceno, 2020). However, high humidity and inadequate composting can lead to dirty cows, risk of bovine mastitis, reduced comfort and gas emissions due to the continuous accumulation of decomposing organic material (Blanco-Penedo et al., 2020; Leso et al., 2020; Emanuelson et al., 2022; Fuertes et al., 2023).

In intensive housing systems for dairy cows, gas emissions can be influenced by regional climate conditions and the housing system employed, particularly those without mechanical ventilation. In such systems, the decomposition of waste and gas emissions depend on the gradient formed by external variables, including air temperature (t, °C), relative humitidy (RH, %), and air velocity (V, m s^{-1}) (Ngwabie et al., 2009; Ding et al., 2016).

Although in the literature there is no specific reference addressing harmful CH_4 concentrations, it is essential to consider the potential adverse effects of CH_4 exposure on animal health. Excessive production of CH_4 in the enteric fermentation process in ruminants may indicate a lower efficiency in converting feed into usable energy by animals (Haque, 2018; Honan et al., 2022). This can negatively impact animals' productivity, as this energy could be used for growth, milk production, or weight gain (Lôbo et al., 2017; Pragna et al., 2018). In terms of climate effects, CH_4 emissions could become a global problem, due to its contribution to climate change, highlighting its importance even at low concentrations. (Niero et al., 2020). Despite CH_4 being more impactful for global warming, it does not persist in the atmosphere as long as CO_2 (Sejian et al., 2015), which is a natural component of the air and part of the animal respiration process (Zou et al., 2020).

High concentrations of CO_2 can cause irritation in the respiratory tract of animals, compromising the well-being and sustainability of the dairy industry (Stokstad et al., 2020). Moreover, in confined environments with inadequate ventilation, CO_2 accumulation can contribute to thermal stress, leading to reduced food and water intake and thereby adversely impacting the general performance of the animals (Pereira et al., 2013).

For dairy cattle, the concentration of CO_2 that is harmful to their health is not specified; however, when inhaled in large quantities, CO_2 can cause irritation in the airways, vomiting, nausea and death from asphyxiation (Damasceno, 2020). Ostovic et al. (2017) mention that CO_2 is present in the atmosphere at a concentration of

300–400 ppm. For agriculture, the concentration of CO_2 in the atmosphere affects carbon storage in the soil and microbial populations (Yu & Chen, 2019; Baveye et al., 2020).

In addition to direct impacts on animal health, CH_4 and CO_2 emissions contribute to the carbon footprint of animal production and have environmental implications, especially regarding climate change (Gerber et al., 2013). Elevated levels of CH_4 and CO_2 promote heat retention in the Earth's atmosphere and elevate global temperatures. This phenomenon has far-reaching consequences, including altered weather patterns, rising sea levels, ocean acidification, and impacts on animal health (IPCC, 2014; Beauchemin et al., 2020).

In this context, precision livestock farming, through detailed monitoring of animals and the environment, aims to discover non-invasive methods for evaluating animal production systems, such as using livestock indices and analyzing gas emissions (Cruz et al., 2023; Siegford et al., 2023), with the goal of enhancing decision-making and welfare control for confined animals.

Among the techniques employed by several researchers is the application of geostatistics, which investigates the spatial variability of variables, such as the distribution of GHGs, by extracting and organizing available data based on the similarity between neighboring georeferenced points (Ferraz et al., 2020; Andrade et al., 2022; Oliveira et al., 2023). This approach facilitates comprehension of the collected data and their influence on the animals' development environment.

Taking into account these factors and with the aim of providing valuable information about the distribution of these gases and their relationship with thermal conditions within the installation, the primary objective was to assess the spatial variability of the greenhouse gases CH_4 and CO_2 in a Compost Barn. Additionally, it aimed to characterize the thermal environment through the Index of Temperature and Humidity (THI) and air speed (V, m s^{-1}).

MATERIALS AND METHODS

The experiment was conducted in October 2023, in a Compost Barn-type facility for dairy cattle, located in the municipality of Lavras/MG, Brazil, at an altitude of 920.62 m and geographic coordinates 21°15' South latitude and 45°09' West longitude.

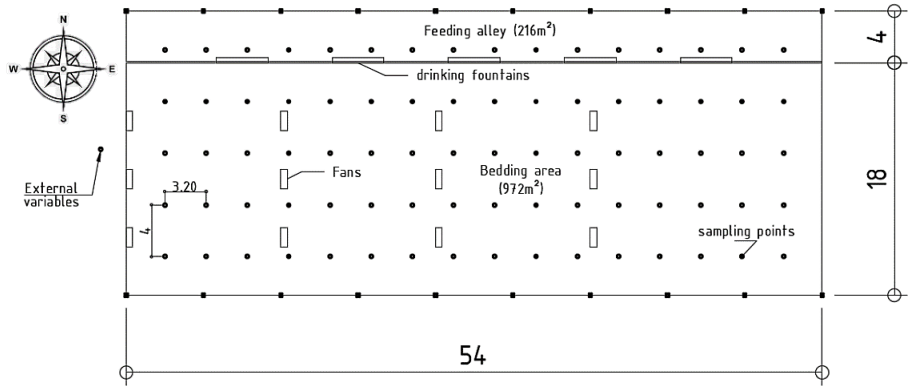

Figure 1. Schematic diagram com as dimensions (meter) and arrangements of points collected in the Compost Barn.

The facility is oriented from East to West and measures 54×22×4.50 m (length×width×ceiling height), including the integrated four-meter feeding alley, located on the North side (Fig. 1). The facility is open, without sidewalls, and there is a roof constructed of galvalume tiles with a 30% slope. Additionally, there are eaves extending three meters on the North and South sides, and one meter long on the East and West sides.

The Compost Barn system is an open, freely accessible facility for animals to rest and feed, a bedding area of 7.9 m^2 to 9.3 m^2 per animal, variable according to breed (Bewley et al., 2012). The studied facility holds 80 lactating cows, at a density of 1 cow/12.15 m^2, which remained throughout the data collection period.

The compost bed consists of sawdust, measuring 65 cm deep. The bedding material is turned over twice daily during this time of year (spring). The bed volume is restored according to the level reduction and removal after one year of use (Fig. 2).

Figure 2. West side view of the Compost Barn.

Mechanical ventilation occurs from the West to the East, aided by 12 fans positioned 2.5 meters above the bed and arranged in four lines. The Ziehl-Abegg® axial fans operate at high speed and low volume (LVHS), with a diameter of 1.10 m, three propellers, rotation 950 rpm, power consumption of 0.86 kW, and an airflow of 23.000 $m^3\ h^{-1}$. The data was collected without any interference in farm management; therefore, the fans remained on throughout the process.

Data collection was asynchronous, starting at 7:00 AM and ending at 10:30 AM. For each point, data were collected for one minute, with intervals of ten seconds for each recording. The data collection height was 0.25 meters above the sawdust bed (Fig. 3).

The sampling grid points comprises 75 points, spaced 3.40 meters apart longitudinally and 4.00 meters apart laterally within the facility (Fig. 1).

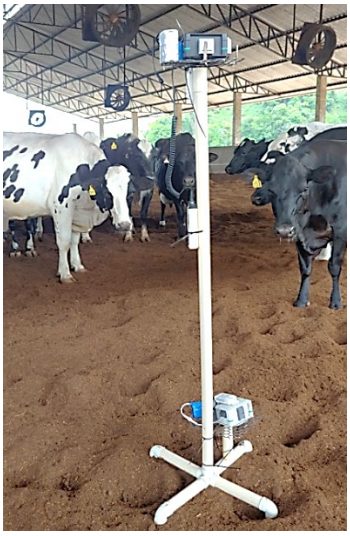

Figure 3. Support fabricated for fixing the sensor at a height of 0.25 m.

The dry bulb temperature (t_{db}, °C), dew point temperature (t_{dp}, °C) and relative air humidity (RH, %) were logged by the datalogger Hobo® MX2301A, with precisions of 0.2 °C and 2.5%, respectively. Air velocity (V, m s^{-1}) was measured using a propeller anemometer, KR-835, with a measuring range of 0.4 to 30 m s^{-1} and a resolution of 0.1.

To record methane (CH_4, ppm) and carbon dioxide (CO_2, ppm) gases, a multi-sensor platform with a modular design and flexible architecture was employed. This platform is equipped with low-cost sensors that have been tested and calibrated in the laboratory (Fig. 4).

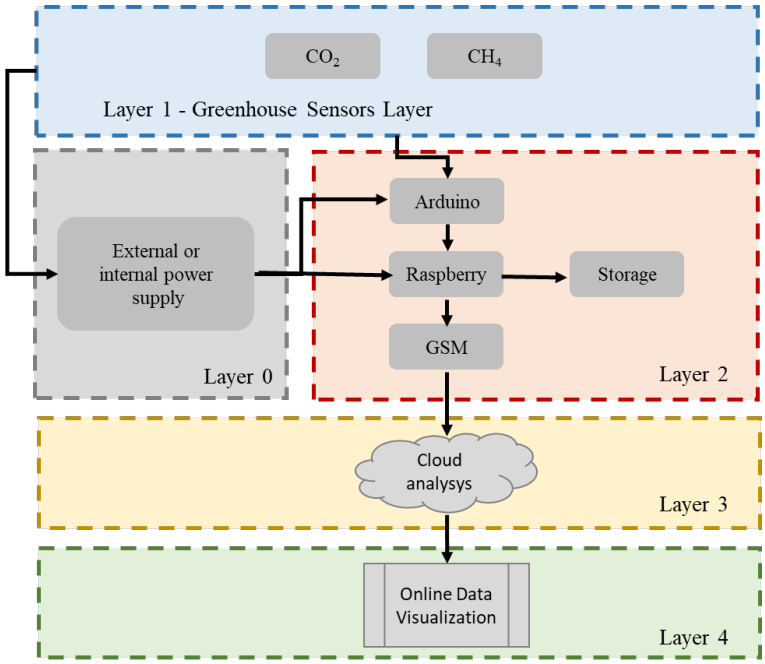

Figure 4. Layer organization of the system architecture (adapted from Becciolini et al., 2022a).

The entire multi-sensor platform design comprises four modules: gas measurement units, processor, server and dashboard. The processing unit includes an ARM Cortex M0+ core, ATM2560 microcontroller for data processing and transmission, and a Raspberry Pi Compute module. Low-cost commercial sensors, selected to meet the monitoring objective, have technical characteristics summarized in Table 1.

Table 1. Technical characteristics of the tested sensors

Target measurement	Sensor name	Type of sensor	Measurement range	Accuracy
CH_4 (ppm)	IRC-AT	Eletrochemical	200–10,000	± 100 ppm
CO_2 (ppm)	SCD30	NDIR	400–10,000	± 30 ppm

The thermal variables (t_{db}, t_{dp}, and RH) were also recorded externally from the Compost Barn using a Hobo® MX2301A datalogger. It was positioned one meter from the West face and at a height of one meter from the ground. Air velocity (V, m s^{-1}) was

measured using a propeller anemometer, KR-835, which has a measuring range of 0.4–30 m s^{-1} and a resolution of 0.1. The assessment of the thermal environment was determined using the temperature and humidity index (THI) equation, developed by Thom (1959):

$$\text{THI: } t_{db} + 0.36\,(t_{dp}) + 41.5 \quad (1)$$

where THI is temperature and humidity index (dimensionless); t_{db} is the dry bulb temperature (°C); t_{dp} is the dew point temperature (°C).

To obtain the spatial variability of CH_4 and CO_2 gases, and the environmental variables of the THI and V inside the Compost Barn, geostatistical analysis was applied, using the software R DEVELOPMENT CORE TEAM (2022). The semivariance was estimated by equation 2, described by Bachmaier & Backes (2008):

$$\hat{\gamma}\,(h) = \frac{1}{2N(h)} \sum_{i=1}^{N(h)} [Z(Xi) - Z(Xi + h)]^2 \quad (2)$$

where $N(h)$ is the number of experimental pairs of observations $Z(Xi)$); and $Z(Xi + h)$ are positions separated by a distance h.

Semivariance adjustments and interpolation by ordinary kriging were applied to verify the dependence and visualize the spatial distribution. The method adopted was restricted maximum likelihood (REML), which results in less biased estimates (Ferraz et al., 2019).

The mathematical model used to adjust the semivariance was Gaussian. The parameters nugget effect (C_0), contribution ($C_0 + C_1$) and range (a) were obtained from the semivariance equation adjusted according to the behaviour of the graphs.

The quality of the fit was assessed by the degree of spatial dependence (DSD) according to the classification that considers values greater than 75%, a weak spatial dependence; values between 25% and 75%, a moderate spatial dependence; and values below 25%, a strong spatial dependence (Cambardella et al., 1994).

The choice of method applied can be reinforced by cross-validation, to compare the predicted values with the observed value, thus obtaining the mean error (ME), standard deviation of the mean error (SDm), reduced error (RE) and the standard deviation reduced error (SDR) (Ferraz et al., 2020).

The spatial distribution patterns of variables in the facilities were generated by maps plotted using Surfer® 13 software. These maps predict, through interpolation and spatial dependence, the value of a variable at a non-sampled point, based on a set of information obtained at other points.

RESULTS AND DISCUSSION

Understanding the variability of thermal variables enables the identification and management of the thermal stress occurrences within the facilities. Therefore, Fig. 5 presents these results, comparing the internal variables (t_{db}, RH, and V) to the external variables during the experimental period.

According to Fig. 5, the three thermal variables studied (t_{db}, RH, and V) exhibited discrepant values when comparing the internal and external environment of the facility.

The t_{db} measured inside the Compost Barn registered an average of 26.9 °C while the external t_{db} registered one average of 29 °C (Fig. 5, a). The average temperature indoors draws attention to the need for additional strategies to control environmental

variables, such as relative humidity and mechanical ventilation. The environmental temperature limit at which cows can regulate their temperature through metabolic processes is 27 °C; temperatures above this threshold are considered critical, compromising both well-being and productivity (Broucek et al., 2009).

The uncontrolled increase in the facility's temperature exposes the animals to thermal stress conditions, leading to behavioural changes (Becker & Stone, 2020). The primary behavioural changes observed in cattle include reduced time spent resting on the bed, decreased feed consumption, and increased time spent standing, walking, or at the water fountains (Frigeri et al., 2023a).

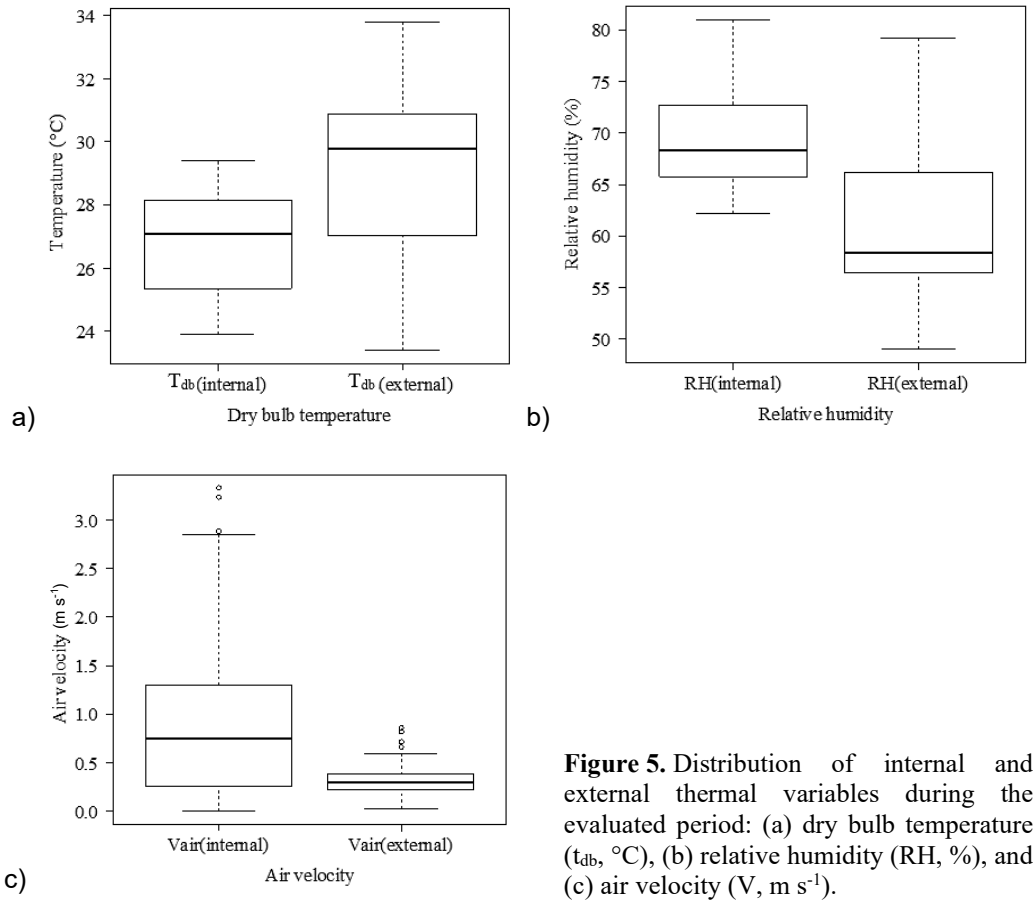

Figure 5. Distribution of internal and external thermal variables during the evaluated period: (a) dry bulb temperature (t_{db}, °C), (b) relative humidity (RH, %), and (c) air velocity (V, m s^{-1}).

In Fig. 5, b, it is observed that the internal RH registered an average of 69.7%, while the average of the external RH was 61.9%. In the internal environment, the predominance above 69.7% reinforces the need for a good ventilation system within the Compost Barn, since the maximum limit considered for animals is 70% (Ferreira, 2016). For situations where relative humidity is greater than 70%, only the use of ventilation allows good dissipation of the heat released by the animals through convection (Baêta & Souza, 2010).

In the Compost Barn production system, RH also directly affects the bedding where the animals lie. In this case, turnover strategies for the bedding material are adopted to reduce its humidity, which should ideally range between 40 and 65% (Shane et al., 2010). These strategies involve incorporating animal waste, which promotes microbial activity in the aerobic composting process (Leso et al., 2020).

Regarding the variable V, based on Fig. 5, c, it is observed that the greatest variability occurred inside the installation, where the average recorded was 0.99 m s^{-1}, while externally the average recorded was 0.32 m s^{-1}. High speed within the facility is desired and results from mechanical fans that provide high rotational speed and low entrained air volume (LVHS). However, most of the time the V was between 0.26 and 1.3 m s^{-1}. For Compost Barn type production systems, V must be maintained close to 1.80 m s^{-1} throughout the installation area, encouraging thermal exchanges, allowed drying of the bed and gas removal (Black et al., 2013).

It is plausible that the climatic variables, t_{db}, RH and V, influence both the physiology of the animals and the indices, and dispersion of gases within the installation. To access the dispersion of these variables and gases within the CBP, geostatistical analysis was applied, allowing the magnitude and spatial dependence of the microclimatic variables to be quantified, as shown in Table 2.

Table 2. Parameters estimated by the REML method and Gaussian model of the experimental semivariograms for the variables: Methane (CH_4), Carbon Dioxide (CO_2), Temperature and Humidity Index (THI) and Air velocity (V, m s^{-1})

Variable	C_0	C_1	$C_0 + C_1$	a	a'	DSD	ME	SDm	RE	SDR
CH_4	256.45	1,736.09	1,992.54	6.78	11.74	12.87	0.259	0.005	25.945	1.076
CO_2	1,170.60	8,296.02	9,466.62	24.99	43.25	12.37	-0.200	-0.003	37.611	1.020
THI	0.10	2.64	2.74	18.85	32.63	3.59	0.001	0.001	0.359	1.015
I	0.44	0.49	0.93	16.47	28.50	47.21	-0.003	-0.002	0.699	1.001

C_0 – Nugget effect; C_1 – Contribution; $C_0 + C_1$ – sill variance; a – range; a' – practical range; DSD – Degree of spatial dependence; ME – Mean error; SDm – Standard deviation of the mean error; RE – Reduced error; SDR – Standard deviation of reduced error.

The parameters of the experimental semivariograms adjusted to the Gaussian model using the REML method (restricted maximum likelihood) presented satisfactory results. Where the ME and RE should presenting values close to zero (Ferraz et al., 2020). Furthermore, the adjustments were satisfactory for all variables, the SDm value should result in the lowest possible value, and the SDR should present the closest value to 1.0. Although CH_4 and CO_2 exhibited RE values that were not proximate to zero, they demonstrated satisfactory values for the other three error evaluation metrics studied, thus characterizing them as well-fitted adjustments.

The nugget effect (C_0) is an important parameter that indicates the discontinuity of the semivariogram for distances smaller than the shortest distance between samples (Ferraz et al., 2017). The variables surveyed presented different C_0 values, which may be due to the fluid characteristics of each. The nugget effect occurs due to small-scale variability not captured by sampling, measurement errors, local variations, among others, without the possibility of individual quantification of the magnitude of these components (Oliveira et al., 2021).

According to Cambardella et al. (1994), the gases CH_4 and CO_2 as well as the THI presented a strong DSD, and the air speed variable presented a moderate DSD, that is, the variables present spatial dependence.

Practical range values obtained from semivariograms represent the distance within which samples are spatially correlated (Ferraz et al. 2017). All variables presented a practical range greater than the shortest distance sampled (3.4 m), with CO_2 having the greatest range (43.25 m) and CH_4 having the smallest recorded range (11.74 m). With this, it is possible to establish that distances greater than that used in this sampling can be considered (Oliveira et al., 2021).

To construct spatial distribution maps (isocolors), the values of the variables were estimated using ordinary kriging. In this way, the maps made it possible to visualize the spatial variability of the THI index, the variable V and the gases CH_4 and CO_2 (Fig. 6).

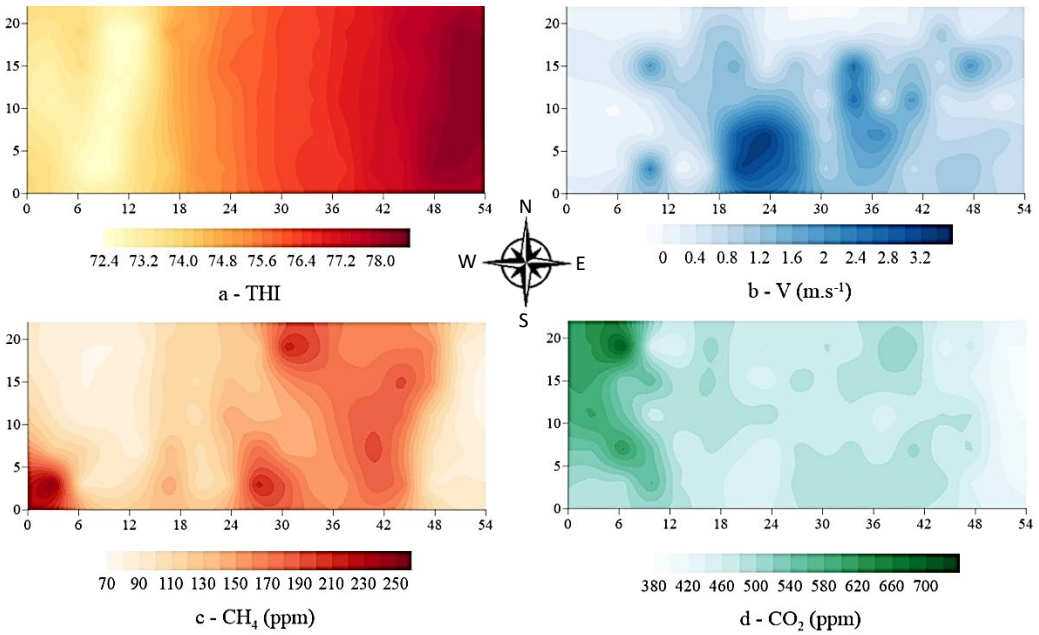

Figure 6. Spatial distribution of variables, where the X-axis represents the length (54 meters) and Y-axis represents the width (22 meters): (a) Temperature and Humidity Index (THI – dimensionless); (b) air speed (V, m s^{-1}), greenhouse gases concentration; (c) CH_4 (ppm) and (d) CO_2 (ppm).

The THI brings together in its formula the effect of two climatic properties, being widely applied to verify the thermal comfort conditions in which animals are subjected (Frigeri et al., 2023a).

In this study, THI values ranged from 72.4 to 78.4 throughout the entire experimental period. Reference ranges for cattle classify values below 74 as ideal conditions for thermal comfort; between 74 and 79 as a warning for producers; between 79 and 84 as dangerous conditions requiring safety measures to prevent losses in the herd; and greater than 84 as an emergency situation (Mader et al., 2006).

In Fig. 6, a, the yellow regions, primarily located on the west side of the facility, denote the lowest THI values, suggesting that the animals were within a comfortable range (below 74). There is an observed trend of increasing THI values along the length of the barn towards the East. As the shades darken in Fig. 6, a, it is evident that THI values also rise, with areas depicted in darker red indicating THI values surpassing the recommended threshold.

When dairy cattle are subjected in environments with high THI values, they can decrease dry matter consumption, rumination, and food bolus (Soriani et al., 2013). Consequently, these alterations directly affect milk production (Tao et al., 2018). When assessing conditions inducing heat stress in animals, it is crucial to analyze the duration and accumulation of heat load over successive days (Heinicke et al., 2018; Frigeri et al., 2023a).

To identify critical THI thresholds is valuable for decision-making regarding productivity and animal welfare, it should not be the sole determinant but rather complemented with behavioural, physiological, and regional considerations (Foroushani & Amon, 2022). The rise in temperature can also stem from metabolic processes, such as the generation of metabolic heat during rumination and food digestion in cows (Liu, 2019). Therefore, integrating THI with other factors becomes essential, given the variations among dairy cow breeds, age, milk production, geographic location of the barn, and housing types (Hoffmann et al., 2020).

Lack of mechanical ventilation may result in higher THI values, causing discomfort for animals (Mota et al., 2019). However, with the LVHS ventilation system, THI values ranging from 73 to 76 can be achieved under conditions similar to those in this study (Oliveira et al., 2019).

In Compost Barn type facilities, natural ventilation does not ensure comfortable conditions for the animals or adequate aeration for the bedding (Caldato et al., 2019). Therefore, it is necessary to utilize mechanical ventilation and regularly assess its effectiveness at two levels (animal and bedding), as it is not uniformly distributed (Oliveira et al., 2023).

For this survey, the values of V at a height of 0.25m from the bed (Fig. 6, b) showed large variations along the length of the installation, with a minimum of 0 m s^{-1} and a maximum of 3.3 m s^{-1}. The V values lower than 1 m s^{-1} were recorded mainly in the feeding area, which is a region with no direct mechanical ventilation, and low animal permanence. For Compost Barn type installations, it is common for air velocity to present high dispersion, due to sudden changes in magnitude and direction (Faria et al., 2008; Oliveira et al., 2023).

Insufficient ventilation results in increased RH and the accumulation of gases within facilities (Ding et al., 2016). Indeed, V will influence the intensity of gas dispersion and the time they remain inside the installations. This dispersion for CH_4 and CO_2 gases can be observed in Fig. 6c and Fig. 6, d, respectively.

The distribution of CH_4 (Fig. 6, c), at a height of 0.25m, shows a range of 24 meters (between coordinates 24 and 48 on the X axis) in which concentrations vary between 130 and 210 ppm. A single point recorded the maximum value of 253 ppm for CH_4 on the West side of the installation (indicated by dark red color). These values are above the limits for CH_4 concentration in milk production, which vary between 60 and 117 ppm (Jungbluth et al., 2001).

High values of CH_4 can cause discomfort to the animal, mainly reducing feed efficiency (Honan et al., 2022), if the scenario persists, the producer may consider adopting other strategies, such as reformulating the animal's diet (Schären et al., 2017; Wesemael et al., 2019; Ku-Vera et al., 2020; Bharathidhasan, 2022).

The heat retained inside the installation is responsible for altering the behaviour of the gases. In the case of CH_4 (lower density), it disperses quickly and is retained in the highest part of the installation (Damasceno, 2020). These concentrations must always be validated for each region due to factors that affect the production and emission of GHGs, including the type of facility for the animals, breed, consumption and composition of feed, local climate, among others (Huang & Guo, 2018).

According to Becciolini et al. (2022b), the methane electrochemical sensor used in this research yielded plausible yet lower values compared to other methane measurements using sampled air. Nevertheless, it is still possible to utilize this sensor to assess the variability of gas within the Compost Barn and the differences in regions with higher or lower concentrations of the methane.

Among the sources and strategies for reducing GHG emissions are: (1) storage of liquid and unprocessed waste, which is a more polluting source than dry waste, with processing capable of reducing these emissions (Aguirre-Villegas & Larson, 2017); (2) the animal's metabolism, in which case emissions are controlled by adding or replacing feed components (Hammond et al., 2016; Holtshausen et al., 2021; Baceninait et al., 2022). Research involving CH_4 emissions from livestock mainly considers emissions from eructation (Sorg, 2022), however, it is necessary to develop cost-effective technologies and methods for monitoring and systematizing emissions present in facilities, in order to establish other ways to mitigate GHG (Becciolini et al., 2022a; Becciolini et al., 2022b).

The CO_2 distribution (Fig. 6, d) indicates that concentrations in the largest areas vary from 380 to 500 ppm. This range falls below the limits found by Jungbluth et al. (2001) for dairy farming, which may vary between 970 and 1,480 ppm. Notably, a peak concentration of 713.6 ppm was recorded on the west side, within the feeder lane. According to Bewley et al. (2017), the concreted corridor retains approximately 25% to 30% of all manure and urine produced, which in some cases can result in elevated gas concentrations. The presence of CO_2 in the corridor may also be attributed to the animals' feeding behaviors, as they are metabolically active and tend to cluster together (Zou et al., 2020).

As it is a dense gas, CO_2 tends to concentrate in the lowest parts of the installation (Damasceno, 2020), which can be accentuated in the Compost Barn due to the decomposition of the material used for bedding. According to Ding et al. (2016), CO_2 emissions from waste increase considerably with increasing t_{db} and become more dispersed with increasing V on the surface.

In general, the production of polluting gases within the facility is affected by V, t_{db}, and RH, which strongly depend on constantly changing weather conditions (Hempel et al., 2016).

The use of geostatistics enabled the assessment of the spatial distribution of greenhouse gases within a Compost Barn during the evaluated period. The concentration of these gases can impact air quality and consequently the comfort and well-being of the animals, while also contributing to the emission of these gases into the atmosphere, which may contribute to global warming. Moreover, geostatistical analysis allows

producers to identify areas with higher or lower concentrations of these gases, aiding in decision-making and the identification of management issues.

CONCLUSION

The semivariograms allowed us to characterize the instantaneous spatial variability of the greenhouse gases CH_4 and CO_2, as well as environmental variables such as THI and V at the height of the bed, inside the Compost Barn. For gases and the thermal index, the predominance of spatial dependence was strong, while for V the dependence was moderate.

Spatial maps were created to identify spatial variability based on kriging interpolation. The concentration of CH_4 at 0.25 m of bed height was more evident on the east side, except for a small region to the west of the installation. For CO_2, the highest values were on the west side of the installation. The analysis of greenhouse gas concentrations is crucial for mitigation actions and the development of an increasingly sustainable production system.

The V at 0.25 m bed height resulted in a very heterogeneous distribution, with a small region presenting values above 3.2 m s^{-1}. The non-uniform behavior of V indicates the possibility of promoting greater intensification of ventilation for unreached regions. The THI gradient showed elevations from west to east, following the direction of air circulation caused by the fans. The THI allows decisions to be made regarding the animal's thermal comfort and can be used in conjunction with observations of the animal's physical state.

Due to the various climatic variations in Brazil, this survey can be considered in other regions to better characterize the dispersion of gases in the Compost Barn system.

ACKNOWLEDGEMENTS. The authors would like to thank the Federal University of Lavras and Florence University for their support. We also extend our appreciation to CNPq, CAPES, and FAPEMIG for the scholarships provided. Special thanks to CNPq (404420/2021-4), Fapemig (APQ-01082-21), and Fapemig (BPD-00034-22) for the financial support provided.

REFERENCES

Aguirre-Villegas, H. & Larson, R.A. 2017. Evaluating greenhouse gas emissions from dairy manure management practices using survey data and lifecycle tools. *Journal of Cleaner Production* **143**, 169–179. doi: 10.1016/j.jclepro.2016.12.133

Andrade, R.R., Tinôco, I.F.F., Damasceno, F.A., Ferraz, G.A.S., Freitas, L.C.S.R., Ferreira, C.F.S., Barbari, M. & Teles Junior, C.G.S. 2022. Spatial analysis of microclimatic variables in compost-bedded pack barn with evaporative tunnel cooling. *An Acad Bras Cienc*. **94**(3), 1–23. doi: 10.1590/0001-3765202220210226

Baceninait, D., Dzermeikaite, K. & Antanaitis, R. 2022. Global Warming and Dairy Cattle: How to Control and Reduce Methane Emission. *Animals* **12**(19), 1–22. doi: 10.3390/ani12192687

Bachmaier, M. & Backes, M. 2008. Variogram or semivariogram? understanding the variances in a variogram. *Precision Agriculture* **9**(1), 173–175. doi: 10.1007/s11119-008-9056-2

Baêta, F.C. & Souza, C.F. 2010. *Ambience in rural buildings: environmental comfort*. 2ª ed., Viçosa: UFV, 246 pp. (in Portuguese).

Baveye, P.C., Schnee, L.S., Boivin, P., Laba, M. & Radulovich, R. 2020. Soil organic matter research and climate change: merely re-storing carbon versus restoring soil functions. *Front. Environ. Sci.* **10**(8), 1–20. doi: 10.3389/fenvs.2020.579904

Beauchemin, K.A., Ungerfeld, E.M., Eckard, R.J. & Wang, M. 2020. Review: Fifty years of research on rumen methanogenesis: lessons learned and future challenges for mitigation. *Animal* **14**(S1), 2–16. doi: 10.1017/S1751731119003100

Becciolini, V., Conti, L., Rossi, G., Marin, D.B., Merlini, M., Coletti, G. & Barbari, M. 2022a. Real-time measurements of gaseous and particulate emissions from livestock buildings and manure stores with novel UAV-based system. In: *Conference of the Italian Society of Agricultural Engineering.* Springer International Publishing, pp. 1049–1056.

Becciolini, V., Conti, L., Rossi, G., Merlini, M., Gabriele, C., Ugo, R. & Barbari, M. 2022b. A UAV-based system for greenhouse gases and particulate measurement in livestock farms. In: *European Conference on Precision Livestock Farming*. Precision livestock farming 22, pp. 450–456.

Becker, C.A. & Stone, A.E. 2020. Graduate Student Literature Review: Heat abatement strategies used to reduce negative effects of heat stress in dairy cows. *J. Dairy Sci*. **103**(10), 9667–9675. doi: 10.3168/jds.2020-18536

Bewley, J.M., Robertson, L.M. & Eckelkamp, E.A. 2017. A 100-Year Review: Lactating dairy cattle housing management. *Journal of dairy science* **100**(12), 10418–10431. doi: 10.3168/jds.2017-13251

Bewley, J.M., Taraba, J.L., Day, G.B., Black, R.A. & Damasceno, F.A. 2012. Compost bedded pack barn design features and management considerations. *Cooperative Extension Service*, **206**, pp.1–32.

Bharathidhasan, A. 2022. Effect of supplemental malic acid on methane mitigation in paddy straw based complete diet for sustainable animal production in indigenous dairy cattle. *The Indian Journal of Animal Sciences* **92**(11), 1314–1319. doi: 10.56093/ijans.v92i11.100033

Black, R.A., Taraba, J.L., Day, G.B., Damasceno, F.A. & Bewley, J.M. 2013. Compost bedded pack dairy barn management, performance, and producer satisfaction. *J. Dairy Sci.* **96**(12), 8060–8074. doi: 10.3168/jds.2013-6778

Blanco-Penedo, I., Ouweltjes, W., Ofner-Schröck, E., Brügemann, K.& Emanuelson, U. 2020. Symposium review: Animal welfare in free-walk systems in Europe. *J. Dairy Sci.* **103**, 5773–5782. Doi: 10.3168/jds.2019-17315

Broucek, J., Novák, P., Vokrálová, J., Soch, M., Kisac, P. & Uhrincat, M. 2009. Effect of high temperature on milk production of cows from freestall housing with natural ventilation. *Slovak J. Anim. Sci.* **42**(4), 167–173.

Caldato, E.M.R., Caldato, A., Marcondes, M.I. & Rotta, P.P. 2019. *Technical manual for construction and management of Compost Barn for dairy cows*. 1ª ed. Viçosa: UFV. 35 pp. (in Portuguese).

Cambardella, C.A., Moorman, T.B., Novak, J.M., Parkin, T.B., Karlen, D.L., Turco, R.F. & Konopka, A.E. 1994. Field scale variability of soil properties in Central Iowa soils. *Soil Science Society of America Journal* **58**(5), 1501–1511. doi: 10.2136/sssaj1994.03615995005800050033x

Cruz, E.F.L., Hernández, R.O., Damasceno, F.A., Tinôco, I.F.F, Andrade, R.R., Nascimento, J.A.C., Rossi, G., Becciolini, V. & Barbari M. 2023. Energetic analysis in compost dairy barn: a case study in southeastern Brazil. *Agronomy Research* **21**(3), 1064–1082. doi: 10.15159/AR.23.073

Damasceno, F.A. 2020. *Compost barn as an alternative to dairy farming*. 1ª ed. Divinópolis: Adelante. 396 pp. (in Portuguese).

Ding, L., Cao, W., Shi, Z., Li, B., Wang, C., Zhang, G. & Kristensen, S. 2016 Carbon dioxide and methane emissions from the scale model of open dairy lots. *Journal of the Air & Waste Management Association* **66**(7), 715–725. doi: 10.1080/10962247.2016.1173605

Emanuelson, U., Brügemann, K., Klopcic, M., Leso, L., Ouweltjes, W., Zentner, A. & Blanco-Penedo, I. 2022. Animal Health in Compost- Bedded Pack and Cubicle Dairy Barns in Six European Countries. *Animals* **12**(3), 396. doi: 10.3390/ani12030396

Faria, F.F, Moura, D.J., Souza, Z.S. & Maratazzo, S.V. 2008. Climatic spatial variability of a dairy freestall barn. *Rural Science* **38**(9), 2498–2505. doi: 10.1590/S0103-84782008000900013 (in Portuguese).

Ferraz, G.A.S., Silva, F.M., Oliveira, M S., Custódio, A.A.P. & Ferraz, P.F.P. 2017. Spatial variability of plant attributes in a coffee plantation. *Revista Ciência Agronômica* **48**(1), 81–91. doi: 10.5935/1806-6690.20170009

Ferraz, P.F.P., Ferraz, G.A.S., Schiassi, L., Nogueira, V.H.B., Barbari, M. & Damasceno, F.A. 2019. Spatial variability of litter temperature, relative air humidity and skin temperature of chicks in a commercial broiler house. *Agronomy Research* **17**(2), 408–417. doi: 10.15159/AR.19.112

Ferraz, P.F.P., Gonzalez, V.C., Ferraz, G.A.S., Damasceno, F.A., Osorio, J.A.S. & Conti, L. 2020. Assessment of spatial variability of environmental variables of a typical house of laying hens in Colombia: Antioquia state Case. *Agronomy Research* **18**(S2), 1244–1254. doi: 10.15159/AR.20.099

Ferreira, R.A. 2016. *Greater production with better environment: for poultry, pigs and cattle*. 3ª ed. Viçosa: Learn Easy Editor. 528 pp. (in Portuguese).

Foroushani, S. & Amon, T. 2022. Thermodynamic assessment of heat stress in dairy cattle: lessons from human biometeorology. *Int. J. Biometeorol.* **66**, 1811–1827 doi: 10.1007/s00484-022-02321-2

Frigeri, K.D.M., Deniz, M., Damasceno, F.A., Barbari, M., Herbut, P. & Vieira, F.M.C. 2023a. Effect of Heat Stress on the Behavior of Lactating Cows Housed in Compost Barns: A Systematic Review. *Appl. Sci*. **13**(2044), 1–15. doi: 10.3390/app13042044

Frigeri, K.D.M, Kachinski, K.D., Ghisi, N.C., Deniz, M., Damasceno, F.A., Barbari, M., Herbut, P. & Vieira, F.M.C. 2023b. Effects of Heat Stress in Dairy Cows Raised in the Confined System: A Scientometric Review. *Animals* **13**(350), 1–22. doi: 10.3390/ani13030350

Fuertes, E., Balcells, J., Maynegre, J., Fuente, G., Sarri, L. & Seradj, A.R. 2023. Measurement of methane and ammonia emissions from compost-bedded pack systems in dairy barns: tilling effect and seasonal variations. *Animals* **13**(1871), 1–13. doi: 10.3390/ani13111871

Gerber, P.J., Steinfeld, H., Henderson, B., Mottet, A., Opio, C., Dijkman, J., Falcucci, A. & Tempio, G. 2013. *Tackling climate change through livestock – A global assessment of emissions and mitigation opportunities*. Food and Agriculture Organization of the United Nations (FAO), Rome, p. 136.

Hammond, K.J., Crompton, L.A., Bannink, A., Dijkstra, J. & Yáñez-Ruiz, D.R. 2016. Review of current in vivo measurement techniques for quantifying enteric methane emission from ruminants. *Anim. Feed Sci*. Technol. **219**. 13–30. doi: 10.1016/j.anifeedsci.2016.05.018

Haque, M.N. 2018. Dietary manipulation: a sustainable way to mitigate methane emissions from ruminants. *J. Anim. Sci. Technol*. **60**(15). doi: 10.1186/s40781-018-0175-7

Heinicke, J., Hoffmann, G., Ammon, C., Amon, B. & Amon, T. 2018. Effects of the daily heat load duration exceeding determined heat load thresholds on activity traits of lactating dairy cows. *J. Therm. Biol*. **77**. 67–74. doi: 10.1016/j.jtherbio.2018.08.012

Hempel, S., Saha, C.K., Fiedler, M., Berg, W., Hansen, C., Amon, B. & Amon,T. 2016. Non-linear temperature dependency of ammonia and methane emissions from a naturally ventilated dairy barn. *Biosystems Engineering* **145**. 10–21. doi: 10.1016/j.biosystemseng.2016.02.006

Hoffmann, G., Herbut, P., Pinto, S., Heinicke, J., Kuhla, B. & Amon, T. 2020. Animal-related, non-invasive indicators for determining heat stress in dairy cows. *Biosystems Engineering* **199** (Special Issue), 83–96. doi: 10.1016/j.biosystemseng.2019.10.017

Holtshausen, L., Benchaar, C., Kröbel, R. & Beauchemin, K.A. 2021. Canola Meal versus Soybean Meal as Protein Supplements in the Diets of Lactating Dairy Cows Affects the Greenhouse Gas Intensity of Milk. *Animals* **11**(6), 1–22. doi: 10.3390/ani11061636

Honan, M., Feng, X., Tricarico, J.M & Kebreab, E. 2022. Feed additives as a strategic approach to reduce enteric methane production in cattle: modes of action, effectiveness and safety. *Review Animal Production Science* **62**, 1303–1317. doi: 10.1071/AN20295

Huang, D. & Guo, H. 2018. Diurnal and seasonal variations of greenhouse gas emissions from a naturally ventilated dairy barn in a cold region, *Atmospheric Environment* **172**, 74–82. doi: 10.1016/j.atmosenv.2017.10.051

Intergovernmental Panel on Climate Change (IPCC). 2014. Climate Change 2014: Impacts, Adaptation, and Vulnerability. Part A: Global and Sectoral Aspects. Contribution of Working Group II to the Fifth Assessment Report of the Intergovernmental Panel on Climate Change.

Jungbluth, T., Hartung, E. & Brose, G. 2001. Greenhouse gas emissions from animal houses and manure stores. *Nutrient Cycling in Agroecosystems* **60**, 133–145 doi: 10.1023/A:1012621627268

Ku-Vera, J.C., Castelán-Ortega, O.A., Galindo-Maldonado, F.A., Arango, J., Chirinda, N., Jiménez-Ocampo, R., Valencia-Salazar, S.S., Flores-Santiago, E.J., Montoya-Flores, M.D., Molina-Botero, I.C., Pin˜ eiro-Vázquez, A.T., Arceo-Castillo, J.I., Aguilar-Pérez, C.F., Ramírez-Avilés, L. & Solorio-Sánchez, F.J. 2020. Review: Strategies for enteric methane mitigation in cattle fed tropical forages. *Animal* **14**(S3), 453–463. doi: 10.1017/S1751731120001780

Leso, L., Barbari, M., Lopes, M.A., Damasceno, F.A., Galama, P., Taraba, J.L. & Kuipers, A. 2020. Invited review: Compostbedded pack barns for dairy cows. *J. Dairy Sci.* **103**(2), 1072–1099. doi: 10.3168/jds.2019-16864

Liu, J., Li, L., Chen, X., Lu, Y. & Wang, D. 2019. Effects of heat stress on body temperature, milk production, and reproduction in dairy cows: A novel idea for monitoring and evaluation of heat stress—A review. *Asian-Australas. J. Anim. Sci.* **32**(9), 1332–1339. doi: 10.5713/ajas.18.0743

Lôbo, A.M.B.O., Lôbo, R.N.B., Facó, O., Souza, V., Alves, A.A.C., Costa, A.C. & Albuquerque, M.A.M. 2017. Characterization of milk production and composition of four exotic goat breeds in Brazil. *Small Ruminant Research* **153**. 9–16. doi: 10.1016/j.smallrumres.2017.05.005

Mader, T.L., Davis, M S. & Brown-Brandl, T. 2006. Environmental factors influencing heat stress in feedlot cattle*. J. An. Sci.* **84**(3), 712–719. doi: 10.2527/2006.843712x

Mota, V.C., Andrade, E.T. & Leite, D.F. 2019. Characterization of the spatial variability of animal comfort indices in Compost Barn confinement systems. *Pubvet* **13**(2), 1–14. doi: 10.31533/pubvet.v13n3a276.1-14

Naranjo, A., Johnson, A., Rossow, H. & Kebreab, E. 2020. Greenhouse gas, water, and land footprint per unit of production of the California dairy industry over 50 years. *Journal of Dairy Science* **103**(4), 3760–3773. doi: 10.3168/jds.2019-16576

Ngwabie, N.M., Jeppsson, K.H., Nimmermark, S., Swensson, C. & Gustafsson, G. 2009. Multi-location measurements of greenhouse gases and emission rates of methane and ammonia from a naturally-ventilated barn for dairy cows. *Biosystems Engineering* **103**(1), 68–77. doi: 10.1016/j.biosystemseng.2009.02.004

Niero, G., Cendron, F., Penasa, M., Marchi, M., Cozzi, G. & Cassandro, M. 2020. Repeatability and Reproducibility of Measures of Bovine Methane Emissions Recorded using a Laser Detector. *Animals* **10**(606). doi: doi.org/10.3390/ani10040606

Oliveira, C.E.A., Damasceno, F.A., Ferraz, P.F.P., Nascimento, J.A.C., Ferraz, G.A.S. Barbari, M. 2019. Geostatistics applied to evaluation of thermal conditions and noise in compost dairy barns with different ventilation systems. *Agronomy Research* **17**(3), 783–796. doi: 10.15159/AR.19.116

Oliveira, C.E.A., Damasceno, F.A., Ferraz, G.A.S., Nascimento, J.A.C., Vega, F.A.O., Tinôco, I.F.F. & Andrade, R.R. 2021. Assessment of spatial variability of bedding variables in compost bedded pack barns with climate control system. *An Acad Bras Cienc* **93**(3), 1–14. doi: 10.1590/0001-3765202120200384

Oliveira, C.E.A., Tinôco, I.F.F., Damasceno, F.A., Oliveira, V.C., Rodrigues, P.H.M., Ferraz G.A.S., Sousa, F.C., Andrade, R.R., Nascimento, J.A.C. & Silva, L.F. 2023. Air velocity spatial variability in open Compost-Bedded Pack Barn system with positive pressure ventilation. *An Acad Bras Cienc* **95**(Suppl. 1). doi: 10.1590/0001-3765202320220415

Ostovic, M., Mencik, S., Ravic, I, Zuzul, S., Pavicic, Z., Matkovic, K., Antunovic, B., Tomic, D.H. & Kabalin, A.E. 2017. Relation between microclimate and air quality in the extensively reared turkey house. *Mac Vet Rev* **40**(1). doi: 10.1515/macvetrev-2017-0015

Pereira, M.H.C., Rodrigues, A.D.P., Martins, T., Oliveira, W.V.C., Silveira, P.S.A., Wiltbank, M.C. & Vasconcelos, J.L.M. 2013. Timed artificial insemination programs during the summer in lactating dairy cows: Comparison of the 5-d Cosynch protocol with an estrogen/ progesterone-based protocol. *Journal of Dairy Science* **96**(11), 6904–6914. doi: 10.3168/jds.2012-6260

Pragna, P., Chauhan, S.S., Sejian, V., Leury, B.J. & Dunshea, F.R. 2018. Climate Change and Goat Production: Enteric Methane Emission and Its Mitigation. *Animals* **8**(12), 1–17. doi: 10.3390/ani8120235

R Core Team. 2022. R: A language and environment for statistical computing. R Foundation for Statistical Computing, Vienna, Austria. URL https://www.R-project.org/

Schären, M., Drong, C., Kiri, K., Riede, S., Gardener, M., Meyer, U., Hummel, J., Urich, T., Breves, G. & Dänicke, S. 2017. Differential effects of monensin and a blend of essential oils on rumen microbiota composition of transition dairy cows. *Journal of Dairy Science* **100**(4), 2765–2783. doi: 10.3168/jds.2016-11994

Sejian, V., Bhatta, R., Soren, N.M., Malik, P.K., Ravindra, J.P., Prasad, C.S. & Lal, R. 2015. Introduction to concepts of climate change impact on livestock and its adaptation and mitigation. In V. Sejian, J. Gaughan, L. Baumgard & C. Prasad (Eds.), Climate change Impact on livestock: adaptation and mitigation (pp. 1–23), New Delhi: Springer. doi: 10.1007/978-81-322-2265-1_1

Shane, E.M., Endres, M.I. & Janni, K.A. 2010. Alternative bedding materials for compost bedded pack barns in minnesota: a descriptive study. *Applied Engineering in Agriculture* **26**(3), 465–473. doi: 10.13031/2013.29952

Siegford, J.M., Steibel, J.P., Han, J., Benjamin, M., Brown-Brandl, T., Dórea, J.R.R., Morris, D., Norton, T., Psota, E. & Rosa, G.J. 2023. The quest to develop automated systems for monitoring animal behaviour. *Applied Animal Behaviour Science* **265**(106000), 1–12 doi: 10.1016/j.applanim.2023.106000

Singaravadivelan, A., Sachin, P.B., Harikumar, S., Vijayakumar, P., Vindhya, M.V., Beegum Farhana, F.M., Rameesa, K.K. & Mathew, J. 2023. Life cycle assessment of greenhouse gas emission from the dairy production system – review. *Tropical Animal Health and Production* **55**(320). doi: 10.1007/s11250-023-03748-4

Sorg, D. 2022. Measuring Livestock CH_4 Emissions with the laser methane detector: a review. *Methane* **1**. 38–57. doi: 10.3390/methane1010004

Soriani, N., Panella, G. & Calamari, L. 2013. Rumination time during the summer season and its relationships with metabolic conditions and milk production. *J. Dairy Sci*. **96**(8), 5082–5094. doi: 10.3168/jds.2013-6620

Stokstad, M., Klem, T.B., Myrmel, M., Oma, V.S., Toftaker, I., Østerås, O. & Nødtvedt, A. 2020. Using Biosecurity Measures to Combat Respiratory Disease in Cattle: The Norwegian Control Program for Bovine Respiratory Syncytial Virus and Bovine Coronavirus. *Front. Vet. Sci*. **7**(167). doi: 10.3389/fvets.2020.00167

Su, Y., Yu, Y. & Zhang, N. 2020. Carbon emissions and environmental management based on Big Data and Streaming Data: A bibliometric analysis. *Science of The Total Environment* **733**(138984), 1–11. doi: 10.1016/j.scitotenv

Tao, S., Orellana, R.M., Weng, X., Marins, T.N., Dahl, G.E. & Bernard, J.K. 2018. Symposium review: The influences of heat stress on bovine mammary gland function. *J. Dairy Sci*. **101**(6), 5642–5654. doi: 10.3168/jds.2017-13727

Thom, E.C. 1959. The discomfort index. *Weatherwise* **12**, 57–59.

Wesemael, D.V., Vandaele, L., Ampe, B., Cattrysse, H., Duval, S., Kindermann, M., Fievez, V., Campeneere, S. & Peiren, N. 2019. Reducing enteric methane emissions from dairy cattle: Two ways to supplement 3-nitrooxypropanol. *Journal of Dairy Science* **102**(2), 1780–1787. doi: 10.3168/jds.2018-14534

Yu, T. & Chen, Y. 2019. Effects of elevated carbon dioxide on environmental microbes and its mechanisms: A review. *Sci Total Environ* **10**(655), 865–879. doi: 10.1016/j.scitotenv

Zou, B., Shi, Z.X. & Du, S.H. 2020. Gases emissions estimation and analysis by using carbon dioxide balance method in natural-ventilated dairy cow barns. *Int. J. Agric. & Biol. Eng.* **13**(2), 41–47. doi: 0.25165/j.ijabe.20201302.4802

Agronomy Research **22**(1), 127–145, 2024
https://doi.org/10.15159/AR.24.014

Adaptability of apricot varieties in the Right-Bank Subzone of the Western Forest-Steppe of Ukraine

O. Ignatenko[1], N. Moiseichenko[1], D. Makarova[1], H. Trokhymchuk[1], V. Vasylenko[1], O. Havryliuk[2,*], O. Kishchak[1], Y. Honcharuk[1] and V. Hrusha[1]

[1]Institute of Horticulture of the National Academy of Agrarian Sciences of Ukraine, 23 Sadova Str., UA03027 Novosilky, Kyiv Region, Ukraine
[2]National University of Life and Environmental Sciences of Ukraine, Heroiv Oborony Str., 13, UA03041 Kyiv, Ukraine
[*]Correspondence: o.havryliuk@nubip.edu.ua

Received: October 25th, 2023; Accepted: February 24th, 2024; Published: March 19th, 2024

Abstract. The research reveals the main reasons that prevent the extension of commercial apricot plantations in Ukraine and worldwide. This brief description includes eight cultivars from Ukrainian and foreign breeding programmes. The trials conducted in the Right-Bank subzone of the Western Forest Steppe of Ukraine. The plants from Ukrainian breeding programme 'Melitopolskyi Rannii', 'Botsadivskyi', 'Siaivo', 'Kumir', 'Osoblyvyi Denysiuka', as well as the foreign one – 'Robada', 'Harogem', 'HJA-19', were distinguished by high adaptability to the complex of adverse overwintering factors in the above-mentioned region. These samples did not lose the acquired level of frost resistance under the influence of provoking thaws. A comprehensive assessment of drought resistance, based on water-holding capacity, turgor recovery degree, water deficiency, and leaves' hydration of the presented varieties, established that all variants of the experiment were not inferior to the best popular cultivars. According to the the biological feature of buds' formation at an early age, the cultivars 'Robada' and 'HJA-19' were characterized as early-fruiting. The yield and quality indicators for the 2021–2022 years of research were evaluated. Average fruit weight was noted in all samples, with the cultivar 'Siaivo' exceeding the average. To improve the assortment and enrich the apricot gene pool collections with the best samples suitable for cultivation in the Forest-Steppe Zone of Ukraine, according to the results of the study, the following researched cultivars were included in the collection of valuable samples of the common apricot gene pool of the Institute of Horticulture of the National Academy of Sciences of Ukraine: 'Melitopolskyi Rannii,' 'Botsadivskyi,' 'Siaivo,' and 'Osoblyvyi Denysiuka'. These cultivars are sources of productivity and adaptability to abiotic factors of cultivation (winter and frost resistance, drought resistance). They are certified by the National Center of Plant Genetic Resources of Ukraine.

Key words: *Prunus armeniaca,* winter hardiness, abiotic factors, water deficiency, hydration, fruit quality.

INTRODUCTION

Apricot (*Prunus armeniaca* or *Armeniaca vulgaris*) is a valuable stone fruit not only within the territory of Ukraine but also well beyond its borders. The trees are

characterized by high yields, short-term fertility, and regenerative ability. This plant has been valued for its taste, nutritious, high-vitamin fruit with a rich mineral composition and excellent medicinal properties (Zhou et al., 2020; Groppi et al., 2021).

According to FAOSTAT (Food and Agriculture Organization of the United Nations. Link), in 2021 the world production of Apricot fruits was 4.2 million tons, mainly from European and Asian countries. The largest plantation areas are situated in China, Turkey, and Iran.

Ukraine is among the countries that have their own industrial areas of apricot plantations but do not significantly impact the international market. In 2021, Ukraine produced 8 thousand tons of fruit. The largest cultivated areas in Ukraine are in Crimea, Odesa, and Mykolaiv regions (Voitovyk et al., 2023).

Tong Zhao et al. (2022) notes that the significant restraint in the extension of industrial apricot plantations area in the world is due to the periodicity of fruiting of this crop. The latter phenomenon is primarily associated with the death of generative buds during sharp temperature variations in the winter-spring period and under adverse weather conditions during flowering (Havryliuk & Kondratenko, 2019; Havryliuk et al., 2022a; 2022b). Such problems in the industrial cultivation of apricots in Ukraine also exist. The main productive orchards of this crop in Ukraine are concentrated in the Steppe zone (Spriazhka et al., 2022). At the same time, the later periods of phenophases in the Forest-Steppe, compared to the Steppe, make it possible to avoid frost damage to flower buds in the early spring period. Therefore, promoting industrial apricot plantations in the forest-steppe zone of Ukraine can significantly increase the productivity of such orchards due to the alignment of morphophysiological development phases with the natural and climatic conditions of the environment (Vasylenko et al., 2021; Ivanova et al., 2022).

Improving the assortment and enriching apricot gene pool collections with the best samples from foreign and Ukrainian breeding programmes, suitable for cultivation in the Forest-Steppe zone of Ukraine, is an extremely urgent task of horticultural science. This will make it possible to establish an industrial apricot fruiting conveyor in the aforementioned growing area. It will also significantly increase the effectiveness of selection by utilizing sources with genetically determined high productivity, excellent commercial and consumer qualities of fruits, resistance to diseases, and significant adaptability to specific pedoclimatic climatic condition. Frost and drought stresses strongly affect the altitudinal and latitudinal fruit plants distribution (Gansert, 2004; Charrier et al., 2013; Litvinova et al., 2023a; 2023b). Among various weather hazards, frost causes the greatest economic losses in agriculture (Snyder & Melo-Abreu, 2005; Vasylenko et al., 2021; Pavlichenko et al., 2023). A frost can cause losses of hundreds of thousands of hryvnias in fruit and plant production. Most fruit crops currently grown in temperate zones originate from warm regions, especially Asia, such as walnut, apple, pear, and plum trees (Fornari et al., 2001). High yield and strong resistance to pathogens, rather than frost or drought tolerance, were the main goals of the breeding process (Fady et al., 2003). Although frost severely limits life forms and causes enormous economic losses, it has not been studied as thoroughly as other biotic or abiotic stresses, such as drought tolerance. The main reason for this may be that damage occurs when trees appear not to be active, but they become visible only in the next growing season (Havryliuk et al., 2022b).

Phenological stages control the effects of frost on susceptible organs (e.g., bud break, flower, and leaf budding (Lang et al., 1987). Hence, dormancy induction and release occur concurrently with frost acclimation and deacclimation (Charrier et al., 2011). After cessation of growth, frost acclimation and release from endodormancy are regulated by cold temperatures, whereas deacclimation and exit from ecological dormancy are subsequently controlled by warmer, milder temperatures (Bonhomme et al., 2013). For some fruit crop species, photoperiod can also influence dormancy and the timing of bud break. Photoperiod has its greatest effect when chilling requirements have not been met (Basler & Koerner, 2012; Laube et al., 2014). The 'safety margin' (calculated as the difference between damage-inducing and minimum temperatures) is usually wide enough at the end of the ecological dormancy period to avoid bud damage (Lenz et al., 2013). However, frosts may still occur (Cittadini et al., 2006).

The effects of frost on above ground vegetative parts have been less thoroughly investigated than on economically important parts such as flowers and fruits (Winkel et al., 2009; Havryliuk et al., 2022a). However, the architecture of the above-ground part of the tree affects the temperature distribution (microclimate) and, therefore, the potential damage (Karbivska et al., 2022). In all plant parts, the shoot apical meristem plays a key role, as its temperature damage affects survival, ecological distribution, and fruit formation (Nobel, 1980; Rodrigo, 2000). When apical buds are damaged, the loss of apical dominance results in altered growth patterns, especially in columnar apple trees. Thus, subsequent changes in tree architecture will alter local environmental conditions (e.g., light, temperature, and humidity).

The study of frost resistance is detailed in the research of many authors (Honcharuk, 2012; Trokhymchuk, 2012). The investigation of this phenomenon is based on the analysis of various physiological and biochemical indicators or the use of the direct laboratory freezing method. This method allows for the determination of plants' frost resistance based on objective signs of damage when they are exposed to low temperatures using freezers.

One of the significant factors for apricot productivity, especially in dense plantations, is its drought resistance. Apricot is drought-resistant and can withstand a lack of moisture in the air and soil for an extended period without significant dimensional changes. However, unstable temperature and water conditions, especially droughts, significantly affect the quantitative (size, total volume per tree) and qualitative (external attractiveness, taste) characteristics of the crop. Therefore, the field determination of drought resistance provided by the 'Methodology of state cultivar testing...' for apricot plantations of various degrees of intensification is not sufficiently informative. Comprehensive information on drought resistance can be provided by a laboratory assessment (based on a set of methods) with mandatory consideration of weather conditions at the time of the experiment. In the future, such a study will allow for the creation of sufficiently productive apricot plantations in conditions of unstable water supply through the use of more adaptive cultivars, without additional capital investments (Havryliuk et al., 2022a).

The main negative biotic factor for apricot in the conditions of the Western Forest Steppe of Ukraine is brown rot caused by the pathogen *Monilia Cinerea Bonord*. The susceptibility of apricot cultivars to moniliosis varies significantly. Although absolute resistance to the disease does not exist, by selection of appropriate cultivars, it is possible

to create apricot plantations with high resistance to Monilia Cinerea Bonord., capable of forming economic productivity and high-quality fruits even in epiphytotic years.

The collection of the common apricot gene pool at the Institute of Horticulture of the National Academy of Agrarian Sciences of Ukraine (IS NAAS) includes 157 specimens at the Melitopol Research Station of Horticulture named after M.F. Sydorenko and 73 cultivars at the Research Station of Pomology L.P. Symyrenko. However, at the beginning of 2023, scientists at the IH of the National Academy of Sciences began to passport and register samples of the working collection of common apricot at the National Center of Plant Genetic Resources of Ukraine (NCPGRU). Based on the results of the initial varietal study presented in this article, valuable samples of common apricot are being registered to obtain the 'Certificate of Registration of Samples of the Gene Pool of Plants in Ukraine'.

MATERIALS AND METHODS

The research was conducted during 2021–2022 in the laboratory of Breeding and Cultivation System of fruit crops and Technologies for growing fruit crops of the Institute of Horticulture of the National Academy of Agrarian Sciences of Ukraine (Kyiv region), as well as at the technological base and with the assistance of specialists from the laboratory of Plant Physiology and Microbiology of the same institution. The quality indicators of the fruits were studied using equipment from the laboratory of post-harvest quality processing of fruit and berry products. According to our research, the certification of samples was carried out based on the National Center of Plant Genetic Resources of Ukraine.

Apricot plantations of the 2018 planting year were established in the spring period according to the scheme of 5.0×2.5 m, with one-year seedlings grafted on cherry-plums. The objects of research were 8 new, promising apricot cultivars from Ukrainian and foreign Breeding programmes, based on preliminary varietal studies: 'Melitopolskyi Rannii', 'Kumir', 'Robada', 'HJA-19', 'Harogem', 'Botsadivskyi', 'Osoblyvyi Denysiuka', 'Siaivo'.

Soil profile of the researched area

The soil is dark gray, podzolized, light loam on carbonate loess, typical for the northern part of the Forest Steppe. The humus content in one soil layer is 3.8%, mobile phosphates (according to Kirsanov) - 180.9 mg kg^{-1} (optimal), exchangeable potassium (according to Kirsanov) - 202.8 mg kg^{-1} (high), easily hydrolyzed nitrogen (according to Kornfield) - 98.0 mg kg^{-1} soil (average). At the depth of the main mass of roots (60–80 cm), the content of these substances decreases to 48.1, 68.9, and 35 mg kg^{-1}, respectively. At a meter depth, it is 37.0, 66.0, and 28.7 mg kg^{-1}. The reaction of the soil solution (pH) ranges from slightly acidic (6.1) to slightly alkaline (7.2). Groundwater is at a depth of 2.0–2.5 m.

The practical value of the study is the development of recommendations for new cultivars for their use in production and breeding programs. This will make it possible to enhance the assortment of apricots in the Right-Bank subzone of the Western Forest Steppe of Ukraine with samples more adapted to the climatic conditions of the region.

In the process of conducting research, field, laboratory, and comparative methods were used. The main studies on strain investigation conducted according to the Methodology of state testing of plant cultivars for suitability for is in Ukraine (Methodology..., 2005), namely: phenological observations, winter and frost resistance, drought resistance, features of flowering, pollination, and fertilization, time of initiation of fruiting, and fruit quality.

The winter and frost resistance of apricot were studied directly in the trial plots according to the 'Methodology of State Cultivar Testing...' (Methodology..., 2005). However, for evaluating the frost resistance of garden crops, including apricot, the laboratory method is considered the main one (Bublyk et al., 2013). Direct freezing was performed under two different temperature regimes with a maximum temperature drop to -25 and -30 °C, and the results were compared with samples taken from the experimental plots without artificial freezing. One-year shoots were selected three times during the period of forced dormancy (second half of winter). One-year shoots were selected three times during the period of forced dormancy (second half of winter). Before freezing, the samples were pre-hardened for 3–5 days in a refrigerating chamber with an adjusted temperature (0–(-5) °C)), simulating real conditions in the plantation. Direct freezing was performed in a specialized CRO/400/40 freezer with a gradual decrease to the required minimum negative temperature. The latter was held for 4 hours. Thawing of test samples was also gradual, with the use of an additional freezer (Palahecha et al., 2005). This measure is necessary to prevent an artificial increase in the degree of damage to tissue growths, which is not characterise the natural conditions but is observed during laboratory freezing followed by ultra-fast thawing of experimental samples. In this case, gaps in growth tissues increase, and the degree of their damage does not correspond to the reality and real frost resistance of the cultivar (Hrokholskyi, 2003). growths (in triple repetition with triple replication), fixed in glycerin, and an ocular assessment of the condition of the main plant tissues (bark, cambium, wood, pith) was conducted, as well as the degree of frost damage to buds (taking into account the condition of bud tissues and the parenchymal mass beneath it) under a microscope MBI-6 at 90x magnification. The maximum score for frost damage for a particular type of tissue or cut through the bud according to the laboratory freezing method is 5 points. The total score for tissue damage in a cross-sectional anatomical cut of one-year growth is 25 points (four types of tissues and a bud cut). The total score for damage to one-year growth as a whole is 65 points (four types of tissues from the abaxial and adaxial parts of one-year growth, 20 points each; a cut through the internode, 20 points for complete destruction; and a cut through the bud, 5 points for complete destruction).

Drought resistance was studied directly in experimental plantations (Methodology..., 2005), as well as by a complex of laboratory methods (Trokhymchuk & Makarova, 2022). Namely, according to hydration, water deficit, water-holding capacity, and turgor of leaves. The selection of leaves (in 15-fold repetition for each of the drought resistance above parameters) of all cultivars in the orchard was carried out at 10–11 in the morning, at a relative humidity of 30–35%. The method of collecting experimental data was standard for this kind of research (Trokhymchuk & Makarova, 2022).

Developmental stages of bud mutagenesis according to Vytkovskyi (1984) method. Anatomical sections of generative buds of apricot cultivars were made using an OmE freezing microtome, with a fixed thickness of 50–75 μm. Sections were fixed in

glycerol and viewed under an MBI-6 microscope at a magnification of 90–180 times (Havryliuk et al., 2022a; 2022b).

The climate is moderately continental and mild, with sufficient humidity. According to the average long-term data (for the last 20 years), the average temperature in January is minus 6.0 °C, in July plus 19.5 °C, and the duration of the growing season is 198–204 days. The sum of active temperatures of 10.0 °C and above gradually increases from north to south and ranges from 3,200 to 3,600 °C.

Statistical analysis

Quantitative indicators of the yield and quality of valuable apricot varieties were assessed using a variance analysis. The assessment of frost resistance and flowering intensity was done on a scale, and these calculations currently do not require statistical processing. Factors influence by the correlation re categorized as weak $0 \leq 0.29$, moderate: 0.30–0.49, noticeable: 0.50–0.69, high: 0.70–0.89, very high: 0.9–0.99 (*LSD*: Least significantly difference at $P < 0.05$). Statistical processing was performed in Microsoft Excel 2016 in combination with XLSTAT.

RESULTS AND DISCUSSION

Field and laboratory winter hardiness of promising apricot cultivars

According to frost damage resistance during the winter of 2021/2022, the variants were distributed as follows (in the direction of improvement according to the percentage of tissue and organ damage): 'Osoblyvyi Denysiuka' (39.50) < 'Kumir' (38.25) < 'NJA-19' (33.03) < 'Harogem' (31.07) < 'Robada' (28.85) < 'Melitopolskyi Rannii' (21.45) < 'Siaivo' (20.13) < 'Botsadivskyi' (16.83). It is worth noting that the apricot of the 'Botsadivskyi' cultivar was characterized by consistently high frost resistance in the plantations, regardless of the wintering conditions during the entire period of research.

As a result of laboratory freezing in 2021–2022 at temperatures of -25 °C and -30 °C (the latter is critical for culture), the cultivars 'Botsadivskyi' and 'Melitopolskyi Rannii' turned out to be more resistant. The damage to generative formations in these cultivars ranged from 2.8 to 3.5 points (without indexing the importance of the tissue for the vital activity of the plant; the maximum tissue damage score is 5.0). 'Osoblyvyi Denysiuka', 'Robada', and 'Kumir' were marked as more vulnerable to the stress factors of the cold period of the Forest-Steppe zone of Ukraine, especially to critical temperatures, whose generative formations were damaged from 3.9 to 5.0 points, respectively (on a 20-point scale). The data of direct laboratory freezing confirmed the high frost resistance of tissues of most of the studied cultivars. Even the most susceptible cultivars demonstrated sufficient frost resistance potential for plant preservation and high-yield formation (Table 1).

Negative biotic and abiotic factors of the environment worsen the productive potential and functional state of the apricot, even to the point of complete death. One of the most important goals of modern varietal research is the climatic adaptation of new cultivars. Namely, the selection of cultivars that will have a longer period of generative buds' development. No less important is the selection of intensive-type cultivars: quick-fruiting, self-pollination, high-yielding (Hel, 2015).

Table 1. Damage to one-year growths of apricot in the winter periods of 2021–2022, Institute of Horticulture of the National Academy of Agrarian Sciences of Ukraine*

Cultivar	Control (with no freezing)		-25		-30	
	2020–2021	2021–2022	2020–2021	2021–2022	2020–2021	2021–2022
Melitopolskyi Rannii	3.2	14.0	8.5	32.9	52.0	52.0
Siaivo	10.8	13.1	15.3	28.1	28.9	48.6
Botsadivskyi	6.4	10.9	20.7	21.7	43.6	56.1
Kumir	5.1	24.9	16.3	29.6	44.7	52.7
Harogem	7.0	20.2	28.6	43.6	48.2	53.7
NJA-19	5.2	21.5	17.3	41.2	37.2	52.7
Robada	16.5	18.8	16.6	41.0	43.0	50.2
Osoblyvyi Denysiuka	7.7	25.7	16.6	27.2	44.7	51.5

Note to the Table 1 – * A maximum score of organ damage (complete tissue death of growths and generative buds) is 65 points.

Winter hardiness of apricot plants, the main deterrent factor for the spread of this culture, depends on external and internal factors - temperature changes in the cold season, and the degree of generative sphere development during wintering. Which collectively determine one or another level of spring frost resistance. Generative buds during the rest period from October to January, which coincides with the formation of sporogenous tissue in anthers, are the most resistant to low temperatures (Yablonsky & Elmanova, 1986). Winter-hardy cultivars are characterized by slowed physiological rhythms in the autumn-winter period, as well as at the beginning of spring. To get out of the rest state, they require longer exposure to positive temperatures - from 0 to 7 °C. Their spring development takes place at a greater sum of effective temperatures (from 5 °C and higher) than in non-winter-hardy apricot cultivars (Yablonsky & Elmanova, 1983).

A decrease in temperature in cold-resistant apricot plants does not cause visible damage, let alone the death of cells. At the same time, it stimulates the launch of intracellular processes to prevent ice formation and reduce the harmfulness of this phenomenon at the cellular and subcellular levels. The low-temperature resistance of apricot trees during spring frosts depends on the ability of photosynthesis to function and the suppression of other metabolic processes. At low temperatures, changes in the chemical composition of cell membranes occur, where the lipid layer acquires the ability to retain liquid properties, which causes the cell to retain a complex of membrane-bound functions (Klimov, 1997).

Szalay et al. (2021) note that apricot plants have a short period of rest, bloom early, and are quite often damaged by spring frosts. Therefore, it is very important to study the flowering characteristics and to select genotypes with later flowering. Generative buds in apricots are formed in the years preceding flowering, and their differentiation begins after the active spring-summer growth and development of the plants. Differentiation of generative buds begins after active spring and summer growth and plant development. The bud formation depends to a greater extent on the biological characteristics of the cultivar and on the natural growth conditions (Bulatović & Bulatović, 1981; Kaya & Kose, 2019). In the future, apricot cultivars adapted to local conditions at the stage of buds morphophysiological development in the phyllosperm stage practically do not lose their resistance to frost after thawing. They react to environmental temperature fluctuations to a lesser extent and less actively irrigate tissues during thaws. In their

experiments, Salazar-Gutierrez & Chaves-Cordoba (2020) observed the maximum saturation of apricot tissues with water during the thaw period at (+15) – (+20 °C). The same authors and others emphasized that the degree of apricot plants' resistance depended on the speed and direction of related processes: accumulation of dry mass and water in buds, changes in the overall hydration of functionally related generative and vegetative organs at various stages of morphogenesis (Salazar-Gutierrez & Chaves-Cordoba, 2020).The gradual decrease in temperature before wintering in 2020–2021 contributed to the acquisition of winter and frost resistance by experimental apricot trees and the smooth entry into deep rest. No sharp temperature fluctuations were observed during the specified winter period (from 30.11.20 to 24.02.21). During the three winter months of 2020–2021, precipitation was sufficient (123.2 mm of precipitation was recorded, while the average long-term data is 103 mm). The minimum air temperature in mid-January (January 17, 2021) reached -20 °C. Thaws lasting 5–7 days (2.0–7.1 °C) did not provoke a significant loss of the frost resistance acquired level by the experimental trees, which was confirmed by field studies. We noted minor damage to one-year growths - up to 12.9% (minor damage to bark and cambium from 0.1 to 0.5 points, heartwood from 0.3 to 1.8 points, generative formations from 0.3 to 1.0 points; with a maximum tissue damage score of 5.0 points). In promising apricot cultivars that are more sensitive to cold, there was a freezing of the growths tops ('Kumir', 'Harogem' up to 3.3 points), bark and cambium damage was from 0.3 to 1.2 points, generative formations from 0.3 to 2.5 points (5.0 points - the maximum damage score). The total percentage of damage to one-year growths ranged from 4.0 ('Siaivo') to 43.4% ('Harogem'). In general, according to the resistance to frost damage during the winter of 2020–2021, the studied variants were distributed as follows (in the direction of improvement of the characteristic, according to the percentage of tissues and organs damage): 'Robada' (25.35) < 'Siaivo' (16.60) < 'Osoblyvyi Denysiuka' (11.85) < 'Harogem' (10.75) < 'Botsadivskyi' (9.90) < 'NJA-19' (7.95) < 'Kumir' (7.85) < 'Melitopolskyi Rannii' (4.90).

The winter period 2021/2022 was mild, with little snow, and short-lived. The maximum decrease in air temperature was observed on December 23 -13.5 °C, January 13 at -15.4, and February 5 at -10.1 °C. The greatest temperature drop to minus 16.8 °C (13.01.22) led to minor damage to one-year growth in apricot cultivars ranging from 16.83% to 39.50%. A prolonged thaw was recorded in mid-February, with positive air temperatures during the day (up to 10.3 °C on February 22) and slight frosts at night ((-0.5)–(-4.1 °C)). During the winter months, 89.8 mm of precipitation fell, with the majority (68.7 mm) occurring in December, and 12.4 mm and 8.7 mm in January and February, respectively.

In general, the weather conditions during the 2021–2022 research years for apricot wintering were satisfactory. Before the onset of cold weather, the generative buds of most apricot cultivars were in the phase of phyllosperm formation. In this state, cultivars of this crop have a high risk of damage from low temperatures. Field studies indicated sufficient winter hardiness of the most promising cultivars (except for the more vulnerable 'Kumir' and 'Harogem'). They were well adapted to wintering conditions in the right-bank subzone of the Western Forest-Steppe of Ukraine, without a tendency to lose the level of frost resistance during forced dormancy under the influence of provoking thaws.

The influence of abiotic factors of the vegetative period on the growth and development of promising apricot cultivars.

Apricot is a drought-resistant crop with low transpiration intensity and low osmotic pressure. The effect of dehydration on the change in the chemical composition of leaves is less pronounced than in grain crops. At the same time, during fruit ripening, moisture is of great importance for the normal formation of the apricot crop. The laboratory method, and not the field method, of determining drought resistance is methodologically correct for an accurate assessment of orchard crops' drought tolerance, including apricot, especially in denser plantings.

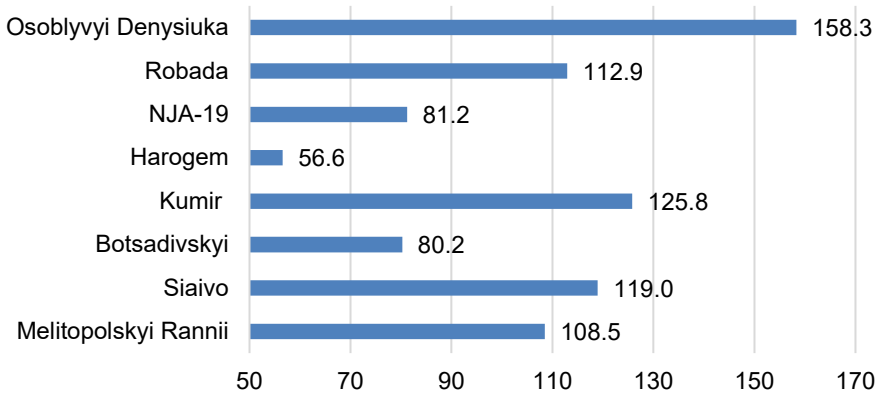

Figure 1. The ability of apricot cultivars to retain water in tree leaves after 24 hours of exposure, % (average for 2021–2022).

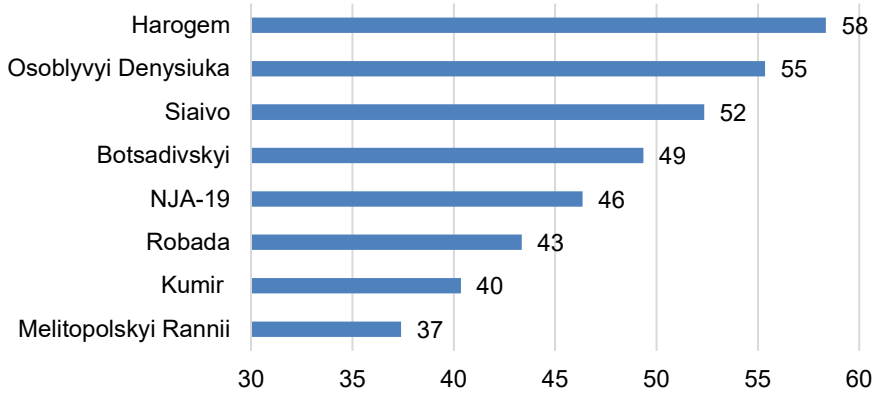

Figure 2. The ability of apricot cultivars to restore water in leaf tissues, % (average for 2021–2022).

In 2021–2022, a comprehensive study was carried out to determine the drought resistance of valuable apricot cultivars of Ukrainian and foreign selection, namely: water-holding capacity (Fig. 1) and turgorescence (Fig. 2), water deficit, and hydration of leaf tissues. The first two of these studies confirmed the sufficient and high drought resistance of all test cultivars under the weather conditions of the research period. Plants of the cultivars ‘Botsadivskyi’, ‘NJA-19’, and, especially, ‘Harogem’, retained water better during wilting followed the restoration of turgor in laboratory conditions.

The laboratory study results of the experimental apricot plants' reaction to water stress in terms of **hydration** and water deficit were indicative.

The hydration of apricot tissues of all studied variants in 2021 and 2022 was within the normal range. Plants, in the second half of the growing season during significant dry periods, maintained their water balance at an appropriate level of 60–70%. Univariate variance analysis showed that in 2021 and 2022, all variants of the experiment did not differ from the control in terms of tissue hydration.

Apricot **water deficiency** in 2021 and 2022 was within the norm and did not exceed 30% even 24 hours after the start of the experiment in all variants. This proves the absence of significant stress due to the lack or excess of moisture and the good functioning of experimental apricot trees during the experiment (the second half of the growing season).

Individual variants significantly outperformed control trees in terms of adaptability and water stress, as indicated by lower values of water deficit. Plants of the early-ripening cultivar 'Robada' (17.00) showed better drought resistance throughout the experiment. The water deficit of these apricot leaves did not exceed 19.00% even 24 hours after the start of the experiment. The plants of other cultivars from the group of mid- and late-ripening groups were better than the control in terms of drought resistance to water deficit and were distributed as follows (in the direction of the trait improvement): 'Siaivo' (28.65%) < 'Osoblyvyi Denysiuka' (18.62%) < 'Harogem' (17.29) < 'NJA-19' (17.16%) < 'Botsadivskyi' (13.97%).

In general, the weather conditions of 2021–2022 were favorable for the water regime, but periods of drought were also noted, allowing the assessment of the resistance of experimental apricot trees to water stress. In laboratory conditions, experimental trees were not inferior to control cultivars in terms of drought resistance. According to turgorescence, water-holding capacity, water deficit, and hydration of leaf tissues, apricot trees from the group of early-ripening cultivars - 'Robada' showed a tendency towards higher drought resistance; from the group of medium and late-ripening - 'Harogem', 'Botsadivskyi', 'NJA-19'.

Compliance with growing conditions in terms of drought resistance in 2021–2022 was high in almost all cultivars. The most adapted foreign cultivars, such as 'Harogem,' 'Robada,' and 'NJA-19,' which can be used in breeding programs to strengthen the above-mentioned economic trait, have been identified.

Resistance of promising apricot cultivars to moniliosis

One of the most important tasks in the initial varietal study of apricots is to determine their resistance to diseases, especially in the Forest-Steppe zone, such as brown rot. In the research plantation of the Institute of Horticulture (IH) of the National Academy of Sciences during 2021–2022, susceptibility to the pathogen *Monilia Cinerea* Bonord varied significantly depending on the cultivar. In 2021, during apricot blossoming (April 21–May 7), wet and moderately warm weather (the average monthly temperature reached 4.6–11.2 °C, and atmospheric humidity was 70–86%) contributed to the spread of the causative agent of the disease and damage to inflorescences. The outbreak of the disease in the orchard planting was estimated at 0.5–5.0 points, depending on the cultivar (Table 2). More susceptible to moniliosis in 2021 were 'Botsadivskyi', 'Kumir', 'NJA-19' (4.0–5.0 points each, average level of damage). Trees of the 'Siaivo' cultivar were distinguished by their high field resistance this year.

In 2022, we recorded slight precipitation only at the beginning of the apricot flowering (April 18). In general, the weather was cool and rainless, with air frosts at the beginning of flowering ((-0.9)–(-1.6 °C), April 19–20)). Such conditions extended the flowering period by 13 days, but the lack of moisture significantly reduced the damage risk to trees. Susceptibility to moniliosis in 2022, despite a fairly long period of potential plant damage, ranged from very low (0.1 points) to medium (4.5 points). Apricot 'Robada' and 'Siaivo' in the experimental plantation differed in very low susceptibility to the disease causative agent (0.8 and 0.1 points, respectively), as well as 'Osoblyvyi Denysiuka' (1.4 points). 'Botsadivskyi' was characterized by average susceptibility (4.5 points), NJA-19, the second most susceptible to moniliosis in 2022, was affected by 3.4 points.

Table 2. The degree of damage to apricot cultivars for 2021 and 2022

Cultivar	Affection by moniliosis, score *	
	2021	2022
Melitopolskyi Rannii	3.1	2.2
Harogem	2.5	2.2
Kumir	4.0	3.1
Robada	2.3	0.8
NJA-19	4.0	3.4
Botsadivskyi	5.0	4.5
Siaivo	0.5	0.1
Osoblyvyi Denysiuka	2.9	1.4

Note: *9.0 – maximum damage score.

Phenological phases of development of valuable apricot cultivars in 2021–2022

The spring period of 2021 was cool and rainy. Apricot flowering in 2021 began at the end of April, with the early ripening cultivars 'Melitopolskyi Ranniii' and 'Kumir' (April 23). Cultivars 'Robada', 'Bodsadivsky' bloomed on April 24. The duration of flowering in these cultivars was 9 calendar days and ended at the beginning of May (May 12). Such cultivars as 'Bodsadivskyi' and 'Robada' began to bloom on April 24 and ended at the same time (May 3), and the duration of flowering was 9 days. The mid-late maturing cultivars, namely 'NJA-19', 'Harogem', 'Osoblyvyi Denysiuka', and 'Siaivo', flowered on April 25–29, within 8–10 days. The degree of flowering varied significantly depending on the cultivar (1.0 to 7.5 points). During apricot flowering in 2021, air frosts of up to -0.4 °C were recorded (from 04/08/2021 to 04/09/2021). This worsened the process of pollination and fertilization and led to the falling of flowers and fruits. At the same time, during the fruit-setting phase (May), significant precipitation (71.4 mm) was recorded, which caused oxidative stress in plants and provoked further falling of flowers and fruits. The temperature and water regime during the spring period of 2021 led to a dropping of 75% in the initial number of flowers and fruits. The trees of the 'NJA-19', 'Robada' cultivars kept the maximum number of useful ovaries (pollinated flowers). It is worth noting that in 2021, the experimental apricot plantation began to bear fruit even under the influence of a complex of adverse weather factors in the spring period. The above-mentioned two cultivars formed a certain crop already in the first year of fruiting (at the age of four). The spring period of 2022 was marked by rainy weather at the beginning of flowering and air frosts on April 19–20 (-0.9–1.6 °C). Due to the weather conditions, apricot blossoming was extended for 18 days (from April 18). The first to bloom were 'Melitopolskyi Ranniii' and 'Kumir', within 8 days. 'NJA-19', 'Harogem' (April 22), 'Osoblyvyi Denysiuka' (April 23), and, especially, 'Siaivo' (April 25) had the latest onset of the flowering phase in 2022. Flowering within

the cultivar lasted 8–10 days, the intensity of which was very high (8.0–9.0 points, on a nine-point scale). The degree of flowering of the 'Robada' and 'Kumir'.

The study of phenological features makes it possible to determine the adaptability of apricot cultivars to specific soil and climatic conditions. The duration of the growing season, the pace of growth and development, and adaptability to certain conditions are determined by the peculiarities of the ontogenesis of cultivars (Havryliuk et al., 2022a; 2022b).

Growth, differentiation, and formation of flower organs in apricot occur after passing the annual temperature maximum. When the average daily air temperature drops below +10–15 °C, sporogenous tissue begins to form in the anthers. Between the duration of the sporogenous tissue formation period and the sums of average daily temperatures in the range of 0–10 °C, there is a direct correlation from $r = 0.70 \pm 0.21$ to $r = 0.80 \pm 0.15$, depending on the considered cultivar. Knowing the dependence of the rest period and the duration of the phases of generative buds' development on the characteristics of the temperature regimes of apricot orchard cultivation regions allows for their more rational placement on the territory.

Yield and quality of apricot fruits

In 2021, at the age of four, the first crop of cultivars was formed: 'Melitopolskyi Rannii', 'Osoblyvyi Denysiuka', 'Harogem', 'Botsadivskyi', 'Siaivo', 'Robada' and 'NJA-19'. Trees of the last two cultivars entered the fruiting season earlier, their productivity immediately reached 5.0 kg/tree (Table 3).

Table 3. Apricot yield and fruit quality, 2021–2022

Cultivar	Yield and quality indicators						Overall tasting score, points, average for 2021–2022
	kg per tree		t ha^{-1}		Fruit weigh, g		
	2021	2022	2021	2022	2021	2022	
Melitopolskyi Rannii	0.5	7.3	0.3	4.9	35.7	64.6	8.9
Harogem	single fruits	4.0	-	2.6	40.2	38.8	8.4
Botsadivskyi	single fruits	4.5	-	3.0	55.4	56.2	8.8
Robada	5.0	2.2	3.4	1.5	42.1	44.9	8.4
Kumir	-	3.0	-	2.0	-	36.6	8.5
NJA-19	5.0	4.1	3.3	2.7	59.6	42.3	8.6
Osoblyvyi Denysiuka	0.5	4.5	0.3	3.0	43.2	37.0	8.8
Siaivo	single fruits	4.5	-	3.0	61.8	68.5	8.8
LSD_{05}	0.1	1.6	0.19	0.86	2.60	3.09	

In 2021, the trees formed fruits of medium size, ranging from 42.1 to 59.6 g. In the next year, 2022, all studied cultivars started fruiting. Apricot trees are considered precocious if they form a yield of 2.0 kg/tree or more at the age of three to four years. 'Robada' and 'NJA-19' were distinguished as precocious (in the 4th year). Some reduction in the yield of 'NJA-19' in 2022 is attributed to the trees being overloaded in the previous period combined with their significant stunting (Havryliuk et al., 2022b). The 'Robada' cultivar in 2022 bloomed with average intensity (5.5 points), and the beginning of the phase coincided with spring frosts. The combination of adverse weather conditions with a phase of morphophysiological development vulnerable to them led to a significant decrease in the yield of the above-mentioned variant in

comparison with last year's data. All experimental samples, except for the cultivar ‘Siaivo’, formed fruits of medium size (35.7–56.2 g), with the latter cultivar having above-average fruit size (68.5 g).

A varietal study of promising apricot cultivars in the right-bank subzone of the Western Forest Steppe of Ukraine showed that all studied cultivars exhibited a tendency to rapidly increase productivity. In the second year after the beginning of fruiting, the productivity ranged from 1.5 to 4.9 t ha^{-1}. The ‘NJA-19’ cultivar stood out as precocious (bearing fruit at the age of 4 years) and productive (yielding 2.7 t ha^{-1} and above) for the mentioned growing region.

According to the results of the apricot varietal study conducted by the Institute of Horticulture of the National Academy of Sciences, some valuable samples were certified by the National Center of Plant Genetic Resources of Ukraine. Specifically:

– ‘Melitopolskyi Rannii’ (national catalog number UN0500557) - utilized in breeding as a source of early ripening fruits with high taste, marketability, and transportability.

– ‘Botsadivskyi’ (national catalog no. UN0500723) - a source of early fertility, winter hardiness, and high productivity.

– ‘Siaivo’ (national catalog number UN0500905) - a source of transportability, productivity, and winter hardiness.

– ‘Osoblyvyi Denysiuka’ (national catalog number UN0501199) - a source of prematurity and a long ripening period.

Description of cultivars

‘Melitopolskyi Rannii’ is an early ripening cultivar bred in the Melitopol Horticulture Experimental Station named after M.F. Sydorenko in Melitopol. It was obtained as a result of crossing the ‘Chervonoshchokyi’ × ‘Ahrori’ cultivars. The tree is medium-sized and forms an inverted pyramidal crown of medium density. Fruiting typically commences in the 5th to 6th year after planting, and the yield is annual. This cultivar is self-fertile.

Winter hardiness is high. It is also resistant to bacterial gummosis and shows moderate resistance to moniliosis.

Fruits are medium to above-medium size, weighing 35–55 g, with a wide oval shape, beveled along the dorsal seam, and slightly compressed on the sides. The skin is thin, delicate, yellowish-orange, with a slight crimson-red blush on the sunny side of the fruit. Pubescence is weak and velvety. The flesh is orange, juicy, of medium density, fiberless, offering a pleasant wine-sweet taste with a well-defined apricot aroma, and a dessert-like flavor (8.0–8.5 points). The pit is medium-sized and oval, not always separating freely from the pulp. The seeds taste sweet.

The fruits contain dry matter - 12.14%, sugars - 7.8–8.18%, organic acids - 0.94–1.11%, and vitamin C - 6.98–9.53 mg per 100 g of raw mass. It is a dessert cultivar with fruiting concentrated on one-year growth and shortened shoots. The fruits ripen from June 20 to July 10, and the transportability is good, making it different destination variety. Since 1980, the cultivar has been included in the Register of Plant Cultivars of Ukraine. Trees of this cultivar do not require special care; timely pruning to thin out the crown is essential.

‘Botsadivskyi’ is a medium-ripening cultivar developed by Ukrainian breeder of the National Botanical Garden named after M.M. Hryshko (Kyiv). It is a result of crossing of form of ‘Kashchenko 84’ with ‘Lytovchenko’. The tree is medium-sized, with a spherical, spreading, and medium-thickened crown. The cultivar is quick fruiting, entering the fruiting season in the 3rd to 4th year after planting, and the yield is annual. ‘Botsadivskyi’ exhibits very high winter hardiness and its resistant to fungal diseases.

The fruits of ‘Botsadivskyi’ are large, weighing 40–50 g, with a maximum weight of 80–120 g. They have a spherical-oval shape and are flattened on the sides. The skin is medium hairy, delicate, thin, smooth, and yellow, with a blurred blush covering 40–50% of the fruit's surface. The flesh is yellowish-orange, tender, juicy, and sweet, with a dessert taste (8.5–9.0 points). The stone is medium size and well separated from the pulp. Fruits ripen on July 15. ‘Botsadivskyi’ is a cultivar of different destination and is recommended for cultivation in the Steppe and Forest Steppe regions of Ukraine.

‘Siaivo’ is a late-ripening apricot cultivar developed by the Institute of Horticulture of the National Academy of Agrarian Sciences of Ukraine (Kyiv). The tree is vigorous and forms a spherical, thin, slightly thickened crown with thick red-brown shoots. It exhibits very high winter hardiness, although occasional damage by moniliosis (brown rot) is observed in some years, necessitating chemical treatment against fungal diseases. It is a self-pollinate cultivar and enters the fruiting season in the 4–5th year after planting.

The fruits of ‘Siaivo’ are large, weighing 55–73 g, with a maximum weight of 150 g, and have a wide-oval shape. The skin is intensely yellow, covered with a thick blurred red blush on the sunny side of the fruit. The pulp is very dense, intensely yellow, sweet, and sour, with excellent taste (8.5 points). The stone is of medium size and easily separated from the pulp. The fruits have different destination suitable for fresh consumption, making high-quality jams, candied fruits, juices with pulp, compotes, and are excellent for obtaining dried apricots.

‘Siaivo’ ripens from July 20 to August 10, and the fruits do not crack during ripening. They exhibit excellent transportability and good marketability. This cultivar is promising for cultivation in industrial and amateur horticulture in the Forest-Steppe and Southern Polissia regions of Ukraine.

‘Osoblyvyi Denysiuka’ is a medium-late ripening apricot cultivar developed by the Ukrainian Institute of Horticulture of the National Academy of Agrarian Sciences (Kyiv). The tree is medium-sized, fast-growing, and forms a spherical, slightly spreading, powerful, slightly thickened crown. It exhibits very high winter hardiness and is highly resistant to fungal diseases. Early fruiting begins in the 3–4th year after planting, and the yield is very high. However, it is prone to crop overload, leading to a decrease in fruit size. Strong, regulatory pruning for fruit rationing is recommended.

The fruits of ‘Osoblyvyi Denysiuka’ are large, weighing 50–60 g, and have an oval shape. The peel is yellow, covered with a thick, bright carmine blush on most of the fruit surface. The flesh is yellow, medium-density, fleshy, juicy, aromatic, and sweet, with excellent taste (8.9–9.0 points). The stone is of medium size but poorly separated from the pulp. The fruits have Different destination, suitable for fresh consumption, as well as for technical processing.

‘Osoblyvyi Denysiuka’ ripens from July 15 to 30. The fruits do not crumble, do not rot, and hang on the crown for a long time. Overripe fruits on the tree shrivel and acquire a honey taste. Maturation is non-simultaneous and extended over 1–1.5 months, allowing consumption until the end of September. They are typically harvested 2–3 times. This cultivar is intended for private gardening.

‘Kumir’ is an early cultivar, a progeny seedling of Melitopolskyi 4/150 x Melitopolskyi Rannii. The tree is medium-sized, with a spreading, flat-rounded crown of medium density. Fruiting begins in the 4th-5th year of planting. ‘Kumir’ is resistant to moniliosis, winter- and frost-resistant, and productive.

The fruits of ‘Kumir’ are large, weighing 57–67 g, with an elongated-rounded shape, and a light golden color with a blush in the form of dots on the sunny side. The flesh is yellow, tender, very juicy, not fibrous, and has a sour-sweet taste (8.5–8.8 points). It separates well from the stone.

The chemical composition of the pulp, %: dry soluble substances - 11.80–15.20, sugars - 7.70–8.30, acids - 0.41–0.65, as well as 5.70–8.00 mg of vitamin C and 190–203 mg of phenolic compounds per 100 g of raw mass.

‘Kumir’ ripens at the end of the second decade of June.

The presented brief description of the varieties is based on the results of collection cultivar studies, which precede the initial evaluation, according to the ‘Methodology of the state testing of plant varieties for suitability for distribution in Ukraine’ (Methodology..., 2005). Collective varietal research was conducted through the network of scientific institutions and farms of the Institute of Horticulture of the National Academy of Agrarian Sciences of Ukraine (the main scientific institution of fruit growing in Ukraine) in various growing zones. The study of the collection revealed sufficient economic and biological potential for the promotion of the described varieties in the northern growing regions.

CONCLUSIONS

A comprehensive study of apricot cultivars from Ukrainian and foreign breeding programmes according to the influence of abiotic factors of the environment confirmed their compliance with the pedo-climatic conditions of the right-bank subzone of the Western Forest Steppe of Ukraine. The morphophysiological phases of the domestic breeding programme cultivars ‘Melitopolskyi Rannii’, ‘Botsadivskyi’, ‘Siaivo’, ‘Osoblyvyi Denysiuka’, as well as the foreign - ‘HJA-19’, coincided with the meteorological conditions of the above-mentioned growing region for all years of the study. These cultivars did not lose the level of acquired frost resistance under the influence of provoking thaws. In terms of drought resistance, the investigated cultivars were not inferior to the control trees, which are confirmed by a comprehensive assessment of water-holding capacity, the degree of turgor recovery, water deficiency, and leaf hydration.

Due to the biological feature of buds' formation at an early age, ‘Robada’ and ‘HJA-19’ cultivars were characterized as precocious. In 2021–2022, there was a propensity of domestic bred cultivars ‘Melitopolskyi Rannii’, ‘Botsadivskyi’, ‘Osoblyvyi Denysiuka’ and ‘Siaivo’ to gradually increase the yield and form fruits with high taste qualities. The ‘HJA-19’ cultivar was selected for both yield and fruit quality.

Most cultivars in the experiment formed fruits of medium size, while 'Siaivo' produced above-average size fruits.

According to the preliminary data of the primary cultivar study, the 'HJA-19' cultivar from foreign breeding programme is promising for commercial cultivation in the right-bank subzone of the Western Forest-Steppe of Ukraine in terms of early fruiting and yield in the first years of fruiting.

A comprehensive assessment of domestically bred apricots confirmed their high adaptability to adverse abiotic factors of the environment, a tendency to quickly increase productivity in the first years of fruiting, and a dessert fruit taste for the cultivars 'Botsadivskyi' and 'Osoblyvyi Denysiuka'. The latter, along with the 'Siaivo' cultivar, exhibited high and very high resistance to moniliosis (the main apricot disease in Ukraine) throughout the entire study period in the experimental plot at the Institute of Horticulture of the National Academy of Agrarian Sciences of Ukraine.

According to our research results, several cultivars can be involved in to thebreeding programs as sources of valuable breeding traits, namely: 'Melitopolskyi Rannii', 'Botsadivskyi', 'Siaivo', and 'Osoblyvyi Denysiuka'. Presently, they have been certified by the National Center of Plant Genetic Resources of Ukraine and deposited in the collection of valuable samples of the apricot gene pool at the Institute of Horticulture of the National Academy of Agrarian Sciences. These cultivars serve as sources of early fruiting, productivity, and adaptability to abiotic cultivation factors.

REFERENCES

Basler, D. & Koerner, C. 2012. Photoperiod sensitivity of bud burst in 14 temperate forest tree species. *Agricultural and Forest Meteorology* **165**, 73–81. https://doi.org/10.1016/j.agrformet.2012.06.001

Bonhomme, M., Lacointe, A. & Rageau, R. 2013. Evidence for non-occurrence of node-to-node or stem-to-bud transfer of chilling temperature signal for dormancy release. *Advances in Horticultural Science* **1–2**(27), 33–43.

Bublyk, M.O., Patyka, T.I. & Kytaiev, O.I. 2013. Laboratory and field methods for determining the frost resistance of fruit breeds and crops: methodical recommendations. Kyiv: Publishing House of the National Academy of Agrarian Sciences of Ukraine, Institute of Horticulture, 26 pp. (in Ukrainian).

Bulatović, S. & Bulatović, M. 1981. The effect of air temperature on the stability of rest period and longevity of apricot trees. *Acta Horticulturae* **85**, 107–118. https://doi.org/10.17660/ActaHortic.1981.85.33

Charrier, G., Bonhomme, M., Lacointe, A. & Améglio, T. 2011. Are budburst dates, dormancy and cold acclimation in walnut trees (*Juglans regia* L.) under mainly genotypic or environmental control?. *International Journal of Biometeorology* **55**, 763–774. https://doi.org/10.1007/s00484-011-0470-1

Charrier, G., Cochard, H. & Améglio, T. 2013. Evaluation of the impact of frost resistances on potential altitudinal limit of trees. *Tree Physiology* **33**(9), 891–902. https://doi.org/10.1093/treephys/tpt062

Cittadini, E.D., de Ridder, N., Peri, P.L. & Keulen, H. 2006. A method for assessing frost damage risk in sweet cherry orchards of South Patagonia. *Agricultural and Forest Meteorology* **141**(2–4), 235–243. https://doi.org/10.1016/j.agrformet.2006.10.011

Fady, B., Ducci, F., Aleta, N., Becquey, J., Vazquez, R.D., Lopez, F., Jay-Allemand, C., Lefèvre, F., Ninot, A., Panetsos, K., Paris, P., Pisanelli, A. & Rumpf, H. 2003. Walnut demonstrates strong genetic variability for adaptive and wood quality traits in a network of juvenile field tests across Europe. *New Forests* **25**, 211–225. https://doi.org/10.1023/A:1022939609548

Food and Agriculture Organization of the United Nations. Available at https://www.fao.org/home/en

Fornari, B., Malvolti, M.E., Taurchini, D., Fineschi, S., Beritognolo, I., Maccaglia, E. & Cannata, F. 2001. Isozyme and organellar DNA analysis of genetic diversity in natural/naturalised European and Asiatic walnut (*Juglans regia* L.) populations. *Acta Horticulturae* **544**, 167–178. https://doi.org/10.17660/ActaHortic.2001.544.23

Gansert, D. 2004. Treelines of the Japanese Alps—altitudinal distribution and species composition under contrasting winter climates. *Flora - Morphology, Distribution, Functional Ecology of Plants* **199**(2), 143–156. https://doi.org/10.1078/0367-2530-00143

Groppi, A., Liu, S., Cornille, A., Decroocq, S., Bui, Q.T., Tricon, D., ... & Decroocq, V. 2021. Population genomics of apricots unravels domestication history and adaptive events. *Nature Communications* **12**(1), 3956. https://doi.org/10.1038/s41467-021-24283-6

Havryliuk, O. & Kondratenko, T. 2019. Specific of the Assimilation Surface of Columnar Apple-Tree. *Agrobiodiversity for Improving Nutrition, Health and Life Quality* (**3**), 57–65. http://dx.doi.org/10.15414/agrobiodiversity.2019.2585-8246.057-065

Havryliuk, O., Kondratenko, T., Mazur, B., Kutovenko, V., Mazurenko, B., Voitsekhivska, O. & Dmytrenko, Y. 2022a. Morphophysiological peculiarities of productivity formation in columnar apple cultivars. *Agronomy research* **20**(1), 148–160. https://doi.org/10.15159/AR.22.007

Havryliuk, O., Kondratenko, T., Mazur, B., Tonkha, O., Andrusyk, Y., Kutovenko, V., Yakovlev, R., Kryvoshapka, V., Trokhymchuk, A. & Dmytrenko, Y. 2022b. Efficiency of productivity potential realization of different-age sites of a trunk of grades of columnar type apple-trees. *Agronomy research* **20**(2), 241–260. https://doi.org/10.15159/AR.22.031

Hel, I.M. 2015. *Workshop on applied breeding of fruit and vegetable crops*, part II. Fruit, berry and nut crops. Lviv. 327 pp. (in Ukrainian).

Honcharuk, Yu.D. 2012. Winter hardiness of scab-immune cultivars of apple (Malus domestica Borkh.). *Scientific Bulletin of the NULES of Ukraine* (**180**), 192–199 (in Ukrainian).

Hrokholskyi, V.V. 2003. Methods of determining damage to fruit crops due to wintering, spring and autumn frosts. Monitoring of fruit crops, 127–135 (in Ukrainian).

Ivanova, I., Serdyuk, M., Malkina, V., Tonkha, O., Tsyz, O., Mazur, B., Shkinder-Barmina, A., Gerasko, T. & Havryliuk, O. 2022. Cultivar features of polyphenolic compounds and ascorbic acid accumulation in the cherry fruits (*Prunus cerasus* L.) in the Southern Steppe of Ukraine. *Agronomy research* **20**(3), 588–602. https://doi.org/10.15159/AR.22.065

Karbivska, U., Butenko, Y., Nechyporenko, V., Shumkova, O., Shumkova, V., Tymchuk, D.S., Litvinov, D., Hotvianska, A. & Toryanik, V. 2022. Ecological and economic efficiency of growing on dark gray soils of bean-cereal grasses. *Journal of Agricultural Science* **2**(32), 404–409. https://dx.doi.org/10.15159/jas.22.25

Kaya, O. & Kose, C. 2019. Cell death point in flower organs of some apricot (*Prunus armeniaca* L.) cultivars at subzero temperatures. *Scientia horticulturae* **249**, 299–305. https://doi.org/10.1016/j.scienta.2019.01.018

Klimov, S.V. 1997. Bioenergy concept of plant resistance to low temperatures. *Advances in modern biology* **11**(2), 133–154.

Lang, G.A., Early, J.D., Martin, G.C. & Darnell, R.L. 1987. Endo-, para- and ecodormancy: physiological terminology and classification for dormancy research. *HortScience* **22**(3), 371–377.

Laube, J., Sparks, T.H., Estrella, N., Hofler, J., Ankerst, D.P. & Menzel, A. 2014. Chilling outweighs photoperiod in preventing precocious spring development. *Global Change Biology* **20**(1), 170–182. https://doi.org/10.1111/gcb.12360

Lenz, A., Hoch, G., Vitasse, Y. & Koerner, C. 2013. European deciduous trees exhibit similar safety margins against damage by spring freeze events along elevational gradients. *New Phytologist* **200**(4), 1166–1175. https://doi.org/10.1111/nph.12452

Litvinova, O., Dehodiuk, S., Litvinov, D., Havryliuk, O., Kyrychenko, A., Borys, N. & Dmytrenko, O. 2023a. Efficiency of technology elements for growing winter wheat on typical chernozem. *Agronomy research* **21**(3), 1199–1212. https://doi.org/10.15159/AR.23.079

Litvinova, O., Tonkha, O., Havryliuk, O., Litvinov, D., Symochko, L., Dehodiuk, S., Zhyla, R. 2023b. Fertilizers and pesticides impact on surface-active substances accumulation in the dark gray podzolic soils. *Journal of Ecological Engineering* **24**(7), 119–127. https://doi.org/10.12911/22998993/163480

Methodology of state cultivar testing of agricultural crops for suitability for distribution in Ukraine (fruit, berry, nut, subtropical, grape and mulberry). 2005. Protection of rights to plant cultivars. Kyiv. *Ministry of Agricultural Policy* **2**(2), 161–221. (in Ukrainian)

Nobel, P.S. 1980. Morphology, nurse plants, and minimum apical temperatures for young Carnegiea gigantea. *Botanical Gazette* **141**(2), 188–191. https://doi.org/10.1086/337142

Palahecha, R.M., Hrokholskyi, V.V., Kytaiev, O.I. & Fomichova, S.V. 2005. Frost resistance of deciduous magnolia shoot tissues. Introduction and conservation of plant diversity. *Bulletin of the Kyiv National University named after Taras Shevchenko* (**8**), 52–55 (in Ukrainian).

Pavlichenko, A., Dmytrenko, O., Litvinova, O., Kovalova, S., Litvinov, D. & Havryliuk, O. 2023. Changes in gray forest soil organic matter pools under anthropogenic load in agrocenoses. *Agronomy research* **21**(3), 1266–1277. https://doi.org/10.15159/AR.23.095

Rodrigo, J. 2000. Spring frosts in deciduous fruit trees-morphological damage and flower hardiness. *Scientia Horticulturae* **85**(3), 155–173. https://doi.org/10.1016/S0304-4238(99)00150-8

Salazar-Gutierrez, M.R. & Chaves-Cordoba, B. 2020. Modeling approach for cold hardiness estimation on cherries. *Agricultural and Forest Meteorology* **287**, 107946. https://doi.org/10.1016/j.agrformet.2020.107946

Snyder, R.L. & Melo-Abreu, J.P. 2005. *Frost Protection: Fundamentals, Practice and Economics*. Environment and Natural Resources Series. Rome: Food and Agriculture Organization of the United Nations, 223 pp. Available at https://www.fao.org/3/y7231e/y7231e.pdf

Spriazhka, R.O., Zhemoida, V.L., Makarchuk, O.S., Dmytrenko, Y.M. & Bahatchenko, V.V. 2022. Selection value of initial material according to the main biochemical parameters of grain in new maize hybrids creation. *Agronomy Research* **20**(S1), 1151–1162. https://doi.org/10.15159/AR.22.037

Szalay, L., Bakos, J., Tósaki, Á., Keleta, B.T., Froemel-Hajnal, V. & Karsai, I. 2021. A 15-year long assessment of cold hardiness of apricot flower buds and flowers during the blooming period. *Scientia Horticulturae* **290**, 110520. https://doi.org/10.1016/j.scienta.2021.110520

Trokhymchuk, A.I. & Makarova, D.H. 2022. Scientific and methodological recommendations for the study and storage of genetic resources of fruit, berry, nut and rare crops [Naukovo-metodychni rekomendatsii z vyvchennia i zberihannia henetychnykh resursiv plodovykh, yahidnykh, horikhoplidnykh ta maloposhyrenykh kultur], 24 pp. (in Ukrainian).

Trokhymchuk, A.I., Makarova, D.H. & Kytaiev, O.I. 2012. Frost resistance potential of introduced cultivars of apple (Malus domestica Borkh.) in the conditions of the Western forest-steppe of Ukraine. *Scientific reports of NULES of Ukraine* (**180**), 187–192 (in Ukrainian).

Vasylenko, O., Kondratenko, T., Havryliuk, O., Andrusyk, Y., Kutovenko, V., Dmytrenko, Y., Grevtseva, N. & Marchyshyna, Y. 2021. The study of the productivity potential of grape cultivars according to the indicators of functional activity of leaves. *Potravinarstvo Slovak Journal of Food Sciences* **15**, 639–647. https://doi.org/10.5219/1638

Voitovyk, M., Butenko, A., Prymak, I., Mishchenko, Yu., Tkachenko, M., Tsiuk, O., Panchenko, O., Slieptsov, Yu., Kopylova, T. & Havryliuk, O. 2023. Influence of fertilizing and tillage systems on humus content of typical chernozem. *Agraarteadus* **34**(1), 44–50. https://dx.doi.org/10.15159/jas.23.03

Vytkovskyi, V.L. 1984. *Morphogenesis of fruit plants*. Kolos, 207 pp. (in Ukrainian).

Winkel, T., Lhomme, J.P., Nina Laura, J.P., Alcon, C.M., del Castillo, C. & Rocheteau, A. 2009. Assessing the protective effect of vertically heterogeneous canopies against radiative frost: the case of quinoa on the Andean Altiplano. *Agricultural and Forest Meteorology* **149**(10), 1759–1768. https://doi.org/10.1016/j.agrformet.2009.06.005

Yablonsky, E.A. & Elmanova, T.S. 1983. Morphogenesis of generative buds of peach and apricot and the influence of extreme temperatures on it. *Bull. State Nikit. nerd. garden* **52**, 87–89.

Yablonsky, E.A. & Elmanova, T.S. 1986. Physiology of apricot resistance to unfavorable winter conditions. Increasing the productivity of apricot plantations: collection. scientific works of State Nikit. nerd. *Garden* **100**, 81–91.

Zhao, T., Cheng, L., Chen, C.L., Wu, Y.X., Wang, H., Zhang, J.Q., Zhu, Y. & Wang, Y.X. 2022. Microstructural observation on pistil abortion of 'Li Guang'apricot and transcriptome reveal the mechanism of endogenous hormones involved in pistil abortion. *Scientia Horticulturae* **293**, 110749. https://doi.org/10.1016/j.scienta.2021.110749

Zhou, W., Niu, Y., Ding, X., Zhao, S., Li, Y., Fan, G., Zhang, S. & Liao, K. 2020. Analysis of carotenoid content and diversity in apricots (*Prunus armeniaca* L.) grown in China. *Food chemistry* **330**, 127223. https://doi.org/10.1016/j.foodchem.2020.127223

Agronomy Research **22**(1), 146–156, 2024
https://doi.org/10.15159/AR.24.040

Processing of Latvian peat and waste coffee as a biocomposite material for the oil spill collection

K. Irtiseva[1,*], M. Zhylina[1,2], R. Baumanis[1], J. Kuzmina[3], J. Ozolins[1] and V. Lapkovskis[4]

[1]Riga Technical University, Faculty of Materials Science and Applied Chemistry, Institute of General Chemical Engineering, Rudolfs Cimdins Riga Biomaterials Innovations and Development Centre, Pulka street 3, LV-1007 Riga, Latvia
[2]Institute of Agricultural Resources and Economics, Stende Research Centre, LV-3258, Dizstende, Latvia
[3]Riga Technical University, Faculty of Mechanical Engineering, Scientific Laboratory of Powder Materials and Institute of Aeronautics, Kipsalas street 6B, LV-1048 Riga, Latvia
[4]Riga Technical University, Institute of General Chemical Engineering, Riga Technical University, 3/7 Paula Valdena street, LV-1048 Riga, Latvia
[*]Correspondence: kristine.irtiseva@rtu.lv

Received: January 31st, 2023; Accepted: November 17th, 2023; Published: May 13th, 2024

Abstract. There is a growing interest in adsorbents of natural origin that are renewable, effective, and able to treat water contaminated by oil products. The current paper investigates a novel bio-based 'peat - spent coffee grounds' SCG-HP bio-based composite pellets as a perspective adsorbent for spilt oil products. The preparation and characterisation of SCG-HP bio-based composite material in pellet form is described. This research used homogenised peat (HP) as an efficient, natural binder. The SCG in different proportions (from 12 wt% to 50 wt%) with HP were used for the different types of SCG-HP granulated sorbents. The granule size obtained ranged from 2 to 6 mm with a total porosity of 56–61%. The sorption of the test oil (fresh engine oil Pilot 10W-40 SJ/CF) was investigated. Sorption studies showed maximum adsorption (capacity) from 90 to 125 wt% for SCG-HP granules.

Key words: spent coffee grounds, adsorption, peat bio-based composite, oil spill, sustainable production, waste recycling.

INTRODUCTION

There is a significant focus within the scientific community on using by-products to develop novel materials. One of specific but prospective organic waste is coffee waste from coffee making. Recent data show increased consumption of used coffee grounds (SCG), which are the waste from the coffee brewing process. Around 6 million tonnes of SCG were generated in 2020–2021 (Hu et al., 2022). Coffee residues are the largest waste product because they are a highly sought-after commodity on the international

market, resulting in large quantities of coffee waste in the form of SCG (Kim & Kim 2020).

Despite the specific properties of SCGs, there are many potential applications for SCGs and SCG-based products. Table 1 summarises some of the promising application fields of SCGs in environmental areas and for developing new materials.

Table 1. Concise overview of recent research on applications of Spent Coffee Grounds

	SCG application area	References
1.	SCG as an additive for food (bakery) products	(Benincá et al., 2023; Cavanagh et al., 2023)
2.	SCG for obtaining electrospun composite nanofiber	(Rubio-Valle et al., 2023)
3.	SCG for graphene oxide production	(Challa et al., 2023)
4.	SCG application in fluorescent chemosensors	(Jeong et al., 2023)
5.	Development of nanostructured and KOH-activated carbon for energy storage application.	(Padilla-Martínez et al., 2023; Sangprasert et al., 2022)
6.	Microporous carbons from SCG for selective extraction (explosives removal) from water samples	(Charmas et al., 2022)
7.	Biochar obtained by carbonisation of SCG for an energy storage device	(Andrade et al., 2020)
8.	Ceramic materials with clay and SCG	(Kłosek-Wawrzyn et al., 2023)
9.	Films from lignocellulosic fibers of SCG	(Bhattarai & Janaswamy, 2023)
10.	SCG for bio-based phase change materials for thermal energy storage	(Jin Ong et al., 2023)
11.	Enhancement of building materials (concrete)	(Roychand et al., 2023; Saeli et al., 2023)
12.	SCG valorisation in biorefinery applications	(Lauberts et al., 2023; Sharma et al., 2021)
13.	Hydrogen production from SCG	(Bekirogullari, 2020; Rodrigues et al., 2022)
14.	SCG as a fuel for small boilers	(Kang et al., 2017)
15.	Microalgae growth on SCG substrate for biodiesel production	(Rosmahadi et al., 2022)

Using SCG as an adsorbent for petroleum products is considered an innovative application, as evidenced by existing research in this field (Lee et al., 2022; Shi et al., 2023).

Peat as a binder is also novel in the context of use with SCG. Peat is a complex system with a wide variety of properties. Intense mechanical action can be used to alter the physicochemical properties of peat and the properties of the macromolecular compounds it contains (Mazlan et al., 2023). Mechanical activation of peat by dispersion increases specific surface area and the opening of closed pores. The deformation of the peat components causes changes in the interatomic and intermolecular bonds, leading to their weakening and, in some cases, their destruction, resulting in the formation of free radicals.

The mechanical activation of the peat is carried out in a disperser. The treatment can be carried out without reagents or with their addition for different purposes. For example, adding solid NaOH/KOH promotes the release of humic substances. It increases the release of soluble peat fractions such as polyphenols and polysaccharides and its binding capacity (Klavins & Purmalis 2013).

MATERIALS AND METHODS

The SCGs used in this study were obtained from local coffee shops in Riga, Latvia. The collected SCGs were dried at 105 °C until constant weight; otherwise, the samples tended to mould and then sieved through a 0.250 mm sieve. The sieved SCGs were stored in polyethene bags until use and did not undergo any physical or chemical pretreatment before use. SCG was characterised as having a broad particle size range from 20 μm to 30 mm, being composed of fibre (> 50%) and lignin with high molecular composition and having a high surface area (7.5 m^2g^{-1}).

The binder used in this study is ZTK low-type peat (Lielvārde, Latvia). The material was subjected to metal analysis to rule out the presence of heavy metals. ZTK was mixed with distilled water in proportions 1:2, taking into account the moisture content of the peat. Performing ZTK pretreatment with the hydrodynamic cavitation method, obtaining a homogeneous peat suspension (HP) (Irtiseva et al., 2021, 2022).

The complete technological process of granulation is shown in Fig. 1. The process consists of 3 stages: preparation of raw materials and preparation of a homogeneous mixture, granulation process and drying of granules. Each stage significantly affects the mass proportions of raw materials, moisture content, granule quality, and physical-chemical properties.

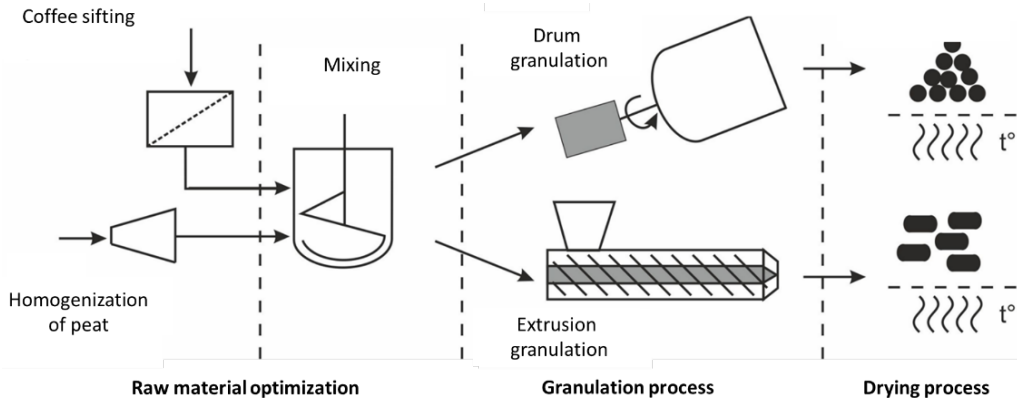

Figure 1. Technological scheme for pellet processing (Vincevica-Gaile et al., 2019).

Fig. 1 shows that 2 granulation methods were used: drum granulation and extrusion. The aim is to identify which granules are mechanically robust and can adsorb more.

Rotary pelletising uses the principle that as the drum containing the mixture rotates, the mixture begins to roll by friction between the mixture and the drum walls, forming agglomerates of particles that further agglomerate to form spherical pellets (Fig. 2). With this technology for producing pellets, the mixture must be precisely prepared so that, as it mixes, the granulation process is initiated. In this process, it was also observed that there was a large excess mass of the mixture, which did not form pellets, which is a significant disadvantage of this technology for producing pellets.

During the experiments, it was observed that the mixture started to granulate badly after a specific time, the reason being the high moisture content of the mixture, which inevitably decreases as it evaporates, so such a mixture needs to be both moistened and

powdered with the dry mixture in order to prevent the granules from dissolving but continuing to roll in the drum. Powdering technology makes it possible to form layered spherical pellets with different compositions.

Since in extrusion pelletisation, the mixture must be drier to form solid pellets (due to the pressure when the mixture is extruded), a smaller amount of binder is used initially than in rotary pelletisation experiments. Similarly to rotational granulation experiments, extrusion granulation experiments vary the composition of the mixture to see the effect of the composition on the resulting granules and their properties.

The pelletising part of the extrusion pelletising machine consists of 2 parts: rollers and a disc with holes. The mixture to be pelletised is introduced into the compartment above these parts. The mixture is discharged under pressure through the slots in the matrix, where a cut-off further adjusts its length. The extrusion pelletising machine used is shown in Fig. 2.

Figure 2. Two machines were used for pelletising: extrusion pelletising: a – working wheel with matrix, b – overall operating diagram of the granulating system. Drum granulation: c – Working rotating cylinder with adjustable angle.

After pelletisation, it is pyrolysed at the following temperatures: 550 °C, 600 °C, and 650 °C. The pyrolysis process converts the carbon to CO_2, thus forming a channel and pores in the pellet. The size of the molecule of the decomposed substance significantly influences the size of the pores.

The source peat is a low-type peat with a 40–50% decomposition rate. SCGs (K), taken from Circle K Latvia, were used after drying to a coffee fraction > 3 mm. Dried peat was used as additional filler.

Moisture analyser KERN MRS 120-3 (UK) is used to determine the moisture content for samples (Table 2). Since the materials used in the work are porous,drying is performed at a temperature of 120 °C, and the mass of the sample is greater than 1 g.

Table 2. Moisture content of components, raw materials

Sample	Moisture, %	Sample	Moisture, %
Raw peat (ZTK)	70.0 ± 2.5	Dry peat (P)	12.0 ± 0.5
Raw SCGs (RK)	67.6 ± 0.6	Peat binder (HP)	94.0 ± 0.5
Dry SCGs (K)	4.0 ± 0.1		

The proportions of raw materials were based on previous experiments (Irtiseva et al., 2022). Initially, experiments were carried out by visual observation of the mixture and its granulation process, from which successful experiments, a specific formulation was further derived, which is further investigated. In the composition tables and for the

raw materials below, the following abbreviations are used: SCGs – K; dried peat – P; peat binder – HP.

The Archimedes method is used to determine the open porosity of bio-based adsorbents: the sample to be studied is completely saturated with a defined liquid, e.g., distilled water (ISO 2738). The resulting biosorbents are subjected to oil sorption testing. The resulting biosorbent is tested in Pilot 10W – 40 SJ/CF semi-synthetic engine oil. The samples were kept together for 15 minutes, with the mass of the oil-impregnated sample being determined every 3, 6, 10 and 15 minutes to observe the adsorption kinetics.

The compressive strength of the specimens was determined using a Moeller (Germany) mechanical strength testing machine.

RESULTS AND DISCUSSION

In order to be able to make a further evaluation of the composition of the final bio-based adsorbent product, the composition of the raw materials needs to be clarified.

Since pyrolysis carbonises organic compounds to form a carbon structure, it is necessary to analyse the mineral composition, as these minerals will be retained in the bio-based adsorbent. The metal content of the raw material used, peat, was determined Summarising the metal concentrations gives the following results: calcium (3384$\mu g \cdot g^{-1}$), aluminium (1,674 $\mu g \cdot g^{-1}$), sulphur (1,538 $\mu g \cdot g^{-1}$), iron (806 $\mu g \cdot g^{-1}$), magnesium (747 $\mu g \cdot g^{-1}$), silicon (436 $\mu g \cdot g^{-1}$), phosphorus (313 $\mu g \cdot g^{-1}$), potassium (747 $\mu g \cdot g^{-1}$), lead (55 $\mu g \cdot g^{-1}$), titan (48 $\mu g \cdot g^{-1}$), manganese (40 $\mu g \cdot g^{-1}$), barium (26 $\mu g \cdot g^{-1}$), sodium (25 $\mu g \cdot g^{-1}$), boron, lithium, strontium, copper, antimony, selenium, arsenic, thallium, vanadium, chromium, cadmium, nickel, cobalt, molybdenum, beryllium have ion concentrations < 10 $\mu g \cdot g^{-1}$.

Table 3 illustrates the recipes suitable for the drum granulation method and extrusion. It should be noted that the granulation methods vary according to the type of technological process, and the recipes also show how the amount of binder mass varies concerning the fillers.

Table 3. Composition of pellets by weight (wt%) and method of pelleting

Composition mass proportion, wt%			
Sample	K	P	HP
Drum Granulation			
1. K-HP	35 ± 1	0	65 ± 1
2. K-HP	45 ± 1	0	55 ± 1
3. K-HP	50 ± 1	0	50 ± 1
4. K-P-HP	12 ± 1	7 ± 1	81 ± 1
5. K-P-HP	14 ± 1	14 ± 1	72 ± 1
Extrusion			
E1	67 ± 1	20 ± 1	13 ± 1
E2	69 ± 1	21 ± 1	10 ± 1
E3	65 ± 1	19 ± 1	16 ± 1
E4	84 ± 1	0	16 ± 1

The mass proportions were based on the principle of a homogeneous mass. Initially, no binder was mixed, to which fillers were added. Each pellet has its mass proportions because of the different methods of pelleting.

Spherical pellets are obtained with a higher binder content, while the extrusion method uses more filler. Table 3 shows that the highest binder content (HP) for spherical pellets is for sample 4. K – P – HP means this sample should have better physical properties and be more durable. The extruded granules show how the highest filler content (K) is for the E4 sample, thus giving good physical properties.

The pyrolysis process retains from the samples pellets that are extruded: E1, E2; E3, E4 and spherical 4. K – P – HP.

The results of the open porosity analysis showed the following: the best result for extruded granules is E2 – 48 ± 4% at 600 °C, and the worst is E4 – 41 ± 3% at 600 °C. However, for spherical granules at 550 °C, 61 ± 4%.

The open porosity data show that the pyrolysis temperatures used have no significant influence on the open porosity of the resulting product. It can be seen that the open porosity of the pellets obtained by rotary pelletisation is higher than that obtained by extrusion pelletisation. The rounded pellets have a significantly lower density than the extruded pellets. These pellets may also have closed pores, which can be converted to open pores by changing the pyrolysis temperature.

The apparent density data show that the rounded pellets are not as compacted in the raw form as the extruded pellets, indicating a higher porosity after pyrolysis treatment. The high errors in the apparent densities of the rounded pellets indicate differences in the composition of the pellets (Fig. 3). It can be concluded that the apparent density may differ from the bulk density by a factor of 1.5 to 2.1. It is important to note that there will be a volume change when the pellets are transported, as the self-weight of the pellets will compact the pellets between them, reducing voids in the buried material and resulting in a denser arrangement.

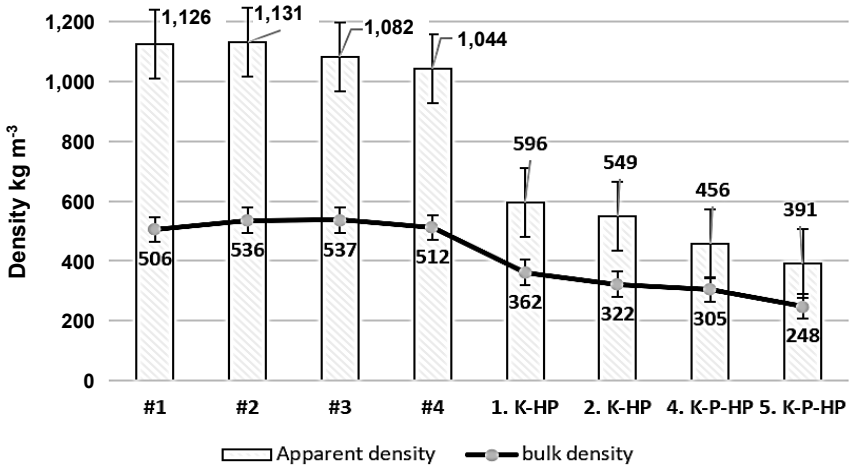

Figure 3. Bulk and apparent densities of the produced pellets before pyrolysis.

The apparent density strength of extruded granules ranges from 900 to 1,100 kg·m^{-3} (Fig. 3). The bulk density is 2 times lower, around 500–540 kg·m^{-3}. Spherical pellets have an apparent friability of 350–650 kg m^{-3}, where the burial density is 1.6 less between 200–400 kg·m^{-3}. The best mechanical properties are found for samples E2-600, E4-550 and E3- 650, which are between 180 and 230 kPa. The mechanical properties of the pyrolysed samples increase by a factor of 1.8 compared to the root sample dried at 105 °C to constant weight (Fig. 4).

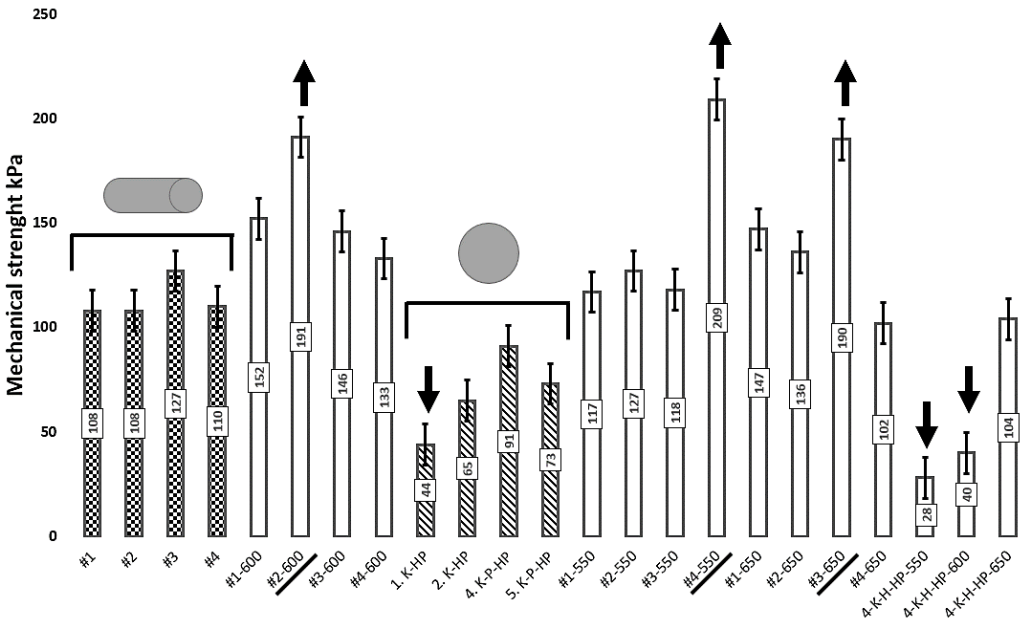

Figure 4. Mechanical properties before and after pyrolysis for extruded and spherical pellets.

The results of the tests on the sorption of the resulting bio-based adsorbents in oil (Pilot 10W – 40 SJ/CF semi-synthetic engine oil) can be seen in the following graphs. In Fig. 5 and Fig. 6, the adsorption capacity is highest at minute 3 for the granules of the E4 – 600 and E4 – 550 compounds, which account for 55–66% of the initial mass.

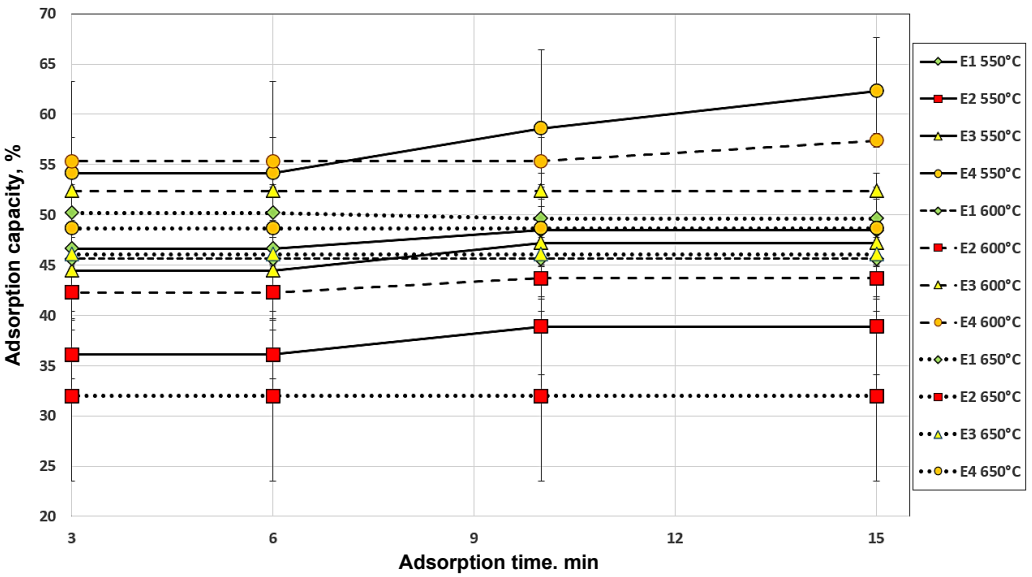

Figure 5. Adsorption kinetics of extruded pellets in Pilot 10W-40 SJ/CF oil.

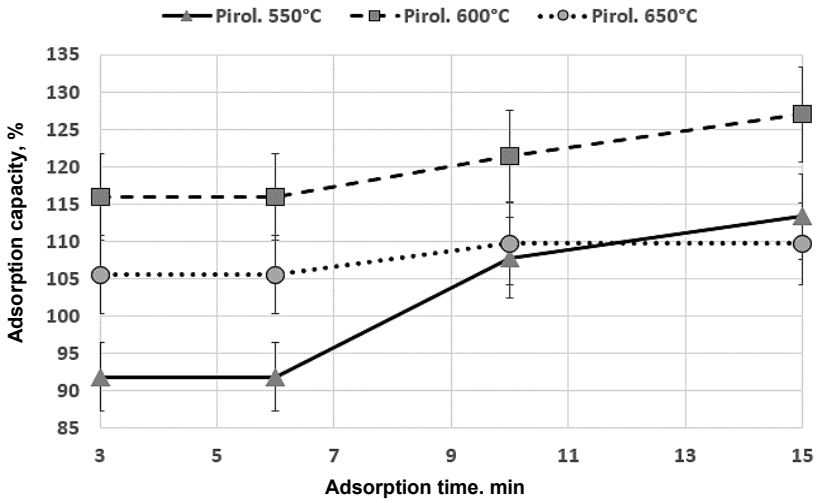

Figure 6. Adsorption kinetics of spheric pellets 4. K – P – HP of Pilot 10W-40 SJ/CF oil.

It can be seen that the bio-based adsorbent produced by rotary granulation adsorbs a greater amount of oil relative to the mass of the sorbent itself. Considering the physical parameters described above, it can be concluded that the resulting rotary granulation bio-based adsorbent has a highly porous structure. The data obtained demonstrate the effectiveness of the bio-based adsorbent in the sorption of petroleum products. When the samples were placed in the oil, air bubbles were observed to be released from the biosorbent within the first few seconds, indicating that sorption was taking place. The same picture can be seen where the same observation is seen in the water. The first observations suggested a reaction of the biosorbent with the water, but no environmental changes were observed when the pH of the water was checked.

Given that the moisture content of the samples is 60–70%, the shelf life of the samples was analysed. For the uncured samples, moulding was observed and the drying process was then carried out (Fig. 7).

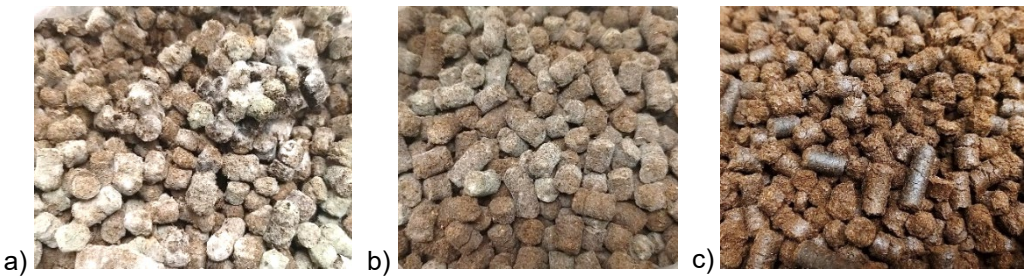

Figure 7. Side effects for samples with and without drying: observation of mould formation in undried, untreated (a), undried with disinfectant treatment (b) and dried untreated (c) pellets after 7 days (a), 14 days (b) 56 days (c).

CONCLUSIONS

This study used SCGs from local Circle K Latvia shops in Riga, Latvia, which were dried at 105 °C until constant weight and sieved. The binder used was ZTK low-type peat, which was subjected to metal analysis and pre-treated with hydrodynamic cavitation to obtain a homogeneous peat suspension. The mass proportions were based on the principle of a homogeneous mass, with spherical pellets having higher binder content and extrusion methods using more filler. The results showed that the best results for extruded granules were E2 – 48 ± 4% at 600 °C, while the worst were E4 – 41 ± 3% at 600 °C. The mechanical properties of pyrolysed samples increased by 1.8 compared to raw samples dried at 105 °C to constant weight. The sorption of the resulting bio-based adsorbents in oil showed the highest adsorption capacity at 3rd minute of the test. E-2 pellets have potential for use in the treatment of soil and water from petroleum products.

ACKNOWLEDGEMENTS. This research/publication was supported by Riga Technical University's Doctoral Grant programme.

REFERENCES

Andrade, T.S., Vakros, J., Mantzavinos, D. & Lianos, P. 2020. Biochar Obtained by Carbonization of Spent Coffee Grounds and Its Application in the Construction of an Energy Storage Device. *Chemical Engineering Journal Advances* **4**, 100061. doi: 10.1016/j.ceja.2020.100061

Bekirogullari, M. 2020. Hydrogen Production from Sodium Borohydride by ZnCl2 Treated Defatted Spent Coffee Ground Catalyst. *International Journal of Hydrogen Energy* **45**(16), 9733–43. doi: 10.1016/j.ijhydene.2020.01.244

Benincá, D.B., do Carmo, L.B., Grancieri, M., Aguiar, L.L., Lima Filho, T., Costa, A.G.V., Oliveira, D. da S., Saraiva, S.H. & Silva, P.I. 2023. Incorporation of Spent Coffee Grounds in Muffins: A Promising Industrial Application. *Food Chemistry Advances* **3**, 100329. doi: 10.1016/j.focha.2023.100329

Bhattarai, S. & Janaswamy, S. 2023. Biodegradable, UV-Blocking, and Antioxidant Films from Lignocellulosic Fibers of Spent Coffee Grounds. *International Journal of Biological Macromolecules* **253**, 126798. doi: 10.1016/j.ijbiomac.2023.126798

Cavanagh, Q., Brooks, M.S.-L. & Rupasinghe, H.P.V. Vasantha Rupasinghe. 2023. Innovative Technologies Used to Convert Spent Coffee Grounds into New Food Ingredients: Opportunities, Challenges, and Prospects. *Future Foods* **8**, 100255. doi: 10.1016/j.fufo.2023.100255

Challa, A.A., Saha, N., Szewczyk, P.K., Karbowniczek, J.E., Stachewicz, U., Ngwabebhoh, F.A. & Saha, P. 2023. Graphene Oxide Produced from Spent Coffee Grounds in Electrospun Cellulose Acetate Scaffolds for Tissue Engineering Applications. *Materials Today Communications* **35**, 105974. doi: 10.1016/j.mtcomm.2023.105974

Charmas, B., Zięzio, M., Tomaszewski, W. & Kucio, K. 2022. Smart Preparation of Microporous Carbons from Spent Coffee Grounds. Comprehensive Characterization and Application in Explosives Removal from Water Samples. *Colloids and Surfaces A: Physicochemical and Engineering Aspects* **645**, 128889. doi: 10.1016/j.colsurfa.2022.128889

Hu, Y., Gallant, R., Salaudeen, S., Farooque, A.A. & He, S. 2022. Hydrothermal Carbonization of Spent Coffee Grounds for Producing Solid Fuel. *Sustainability* **14**(14), 8818. doi: 10.3390/su14148818

Irtiseva, K., Lapkovskis, V., Mironovs, V., Ozolins, J., Thakur, V.K., Goel, G., Baronins, J. & Shishkin, A. 2021. Towards Next-Generation Sustainable Composites Made of Recycled Rubber, Cenospheres, and Biobinder. *Polymers* **13**(4), 1–14. doi: 10.3390/polym13040574

Irtiseva, K., Mosina, M., Tumilovica, A., Lapkovskis, V., Mironovs, V., Ozolins, J., Stepanova, V. & Shishkin, A. 2022. Application of Granular Biocomposites Based on Homogenised Peat for Absorption of Oil Products. *Materials* **15**(4), 1306. doi: 10.3390/ma15041306

Jeong, G., Park, C.H., Yi, D. & Yang, H. 2023. Green Synthesis of Carbon Dots from Spent Coffee Grounds via Ball-Milling: Application in Fluorescent Chemosensors. *Journal of Cleaner Production* **392**, 136250. doi: 10.1016/j.jclepro.2023.136250

Jin Ong, P., Leow, Y., Yun Debbie Soo, X., Hui Chua, M., Ni, X., Suwardi, A., Kiang Ivan Tan, C., Zheng, R., Wei, F., Xu, J., Jun Loh, X., Kai, D. & Zhu, Q. 2023. Valorization of Spent Coffee Grounds: A Sustainable Resource for Bio-Based Phase Change Materials for Thermal Energy Storage. *Waste Management* **157**, 339–47. doi: 10.1016/j.wasman.2022.12.039

Kang, S.B., Oh, H.Y., Kim, J.J. & Choi, K.S.2017. Characteristics of Spent Coffee Ground as a Fuel and Combustion Test in a Small Boiler (6.5 kW). *Renewable Energy* **113**, 1208–14. doi: 10.1016/j.renene.2017.06.092

Kim, M.-S. & Kim, J.-G. 2020. Adsorption Characteristics of Spent Coffee Grounds as an Alternative Adsorbent for Cadmium in Solution. *Environments* **7**(4), 24. doi: 10.3390/environments7040024

Klavins, M. & Purmalis, O. 2013. Properties and Structure of Raised Bog Peat Humic Acids. *Journal of Molecular Structure* **1050**, 103–13. doi: 10.1016/j.molstruc.2013.07.021

Kłosek-Wawrzyn, E., Frąc, M. & Pichór, W. 2023. Influence of Pregranulation and Low-Pressure Compaction on the Properties of Ceramic Materials Incorporating Clay and Spent Coffee Grounds. *Applied Clay Science* **245**, 107154. doi: 10.1016/j.clay.2023.107154

Lauberts, M., Mierina, I., Pals, M., Latheef, M.A.A. & Shishkin, A. 2023. Spent Coffee Grounds Valorization in Biorefinery Context to Obtain Valuable Products Using Different Extraction Approaches and Solvents. *Plants* **12**(1), 30. doi: 10.3390/plants12010030

Lee, K.-T., Cheng C.-L., Lee, D.-S., Chen, W.-H., Vo, D.-V.N., Ding, L. & Lam, S.S. 2022. Spent Coffee Grounds Biochar from Torrefaction as a Potential Adsorbent for Spilled Diesel Oil Recovery and as an Alternative Fuel. *Energy* **239**, 122467. doi: 10.1016/j.energy.2021.122467

Mazlan, S.A., Abang Hasbollah, D.Z., Legiman, M.K.A., Mohd Taib, A., Ibrahim, A., Ramli, A.B., Jusoh, S.N., Abdul Rahman, N., Md Dan, M.F. & Zukri, A. 2023. Effectiveness of Coffee Husk Ash and Coconut Fiber in Improving Peat Properties. *Physics and Chemistry of the Earth* **130**, 103361. doi: 10.1016/j.pce.2023.103361

Padilla-Martínez, E.D., Pérez-Buendía, S.K., López-Sandoval, R. & Sánchez-Rodríguez, C.E. 2023. Electrochemical Energy Storage from Spent Coffee Grounds-Derived Carbon by KOH Activation. *Journal of Energy Storage* **71**, 108115. doi: 10.1016/j.est.2023.108115

Rodrigues, J.P., Ghesti, G.F., Silveira, E.A., Lamas, G.C., Ferreira, R. & Costa, M. 2022. Waste-to-Hydrogen via CO2/Steam-Enhanced Gasification of Spent Coffee Ground. *Cleaner Chemical Engineering* **4**, 100082. doi: 10.1016/j.clce.2022.100082

Rosmahadi, N.A., Rawindran, H., Lim, J.W., Kiatkittipong, W., Assabumrungrat, S., Najdanovic-Visak, V., Wang, J., Chidi, B.S., Ho, C.-D., Abdelfattah, E.A., Lam, S.M. & Sin, J.C. 2022. Enhancing Growth Environment for Attached Microalgae to Populate onto Spent Coffee Grounds in Producing Biodiesel. *Renewable and Sustainable Energy Reviews* **169**, 112940. doi: 10.1016/j.rser.2022.112940

Roychand, R., Kilmartin-Lynch, S., Saberian, M., Li, J., Zhang, G. & Li, C.Q. 2023. Transforming Spent Coffee Grounds into a Valuable Resource for the Enhancement of Concrete Strength. *Journal of Cleaner Production* **419**, 138205. doi: 10.1016/j.jclepro.2023.138205

Rubio-Valle, J.F., Valencia, C., Sánchez, M.C., Martín-Alfonso, J.E. & Franco, J.M. 2023. Upcycling Spent Coffee Grounds and Waste PET Bottles into Electrospun Composite Nanofiber Mats for Oil Structuring Applications. *Resources, Conservation and Recycling* **199**, 107261. doi: 10.1016/j.resconrec.2023.107261

Saeli, M., Capela, M.N., Piccirillo, C., Tobaldi, D.M., Seabra, M.P., Scalera, F., Striani, R., Corcione, C.E. & Campisi, T.2023. Development of Energy-Saving Innovative Hydraulic Mortars Reusing Spent Coffee Ground for Applications in Construction. *Journal of Cleaner Production* **399**, 136664. doi: 10.1016/j.jclepro.2023.136664

Sangprasert, T., Sattayarut, V., Rajrujithong, C., Khanchaitit, P., Khemthong, P., Chanthad, C. & Grisdanurak, N. 2022. Making Use of the Inherent Nitrogen Content of Spent Coffee Grounds to Create Nanostructured Activated Carbon for Supercapacitor and Lithium-Ion Battery Applications. *Diamond and Related Materials* **127**, 109164. doi: 10.1016/j.diamond.2022.109164

Sharma, A., Ray, A. & Singhal, R.S. 2021. A Biorefinery Approach towards Valorization of Spent Coffee Ground: Extraction of the Oil by Supercritical Carbon Dioxide and Utilizing the Defatted Spent in Formulating Functional Cookies. *Future Foods* **4**, 100090. doi: 10.1016/j.fufo.2021.100090

Shi, C., Wang, T., Roy, S., Chopra, S.S., Chen, G., Shang, J., Tian, J. & Ok, Y.S. 2023. From Waste to Resource: Surface-Engineered Spent Coffee Grounds as a Sustainable Adsorbent for Oil–Water Separation. *ACS ES&T Engineering* **3**(9), 1297–1307. doi: 10.1021/acsestengg.3c00096

Vincevica-Gaile, Zane, Stankevica, K., Irtiseva, K., Shishkin, A., Obuka, V., Celma, S., Ozolins, J. & Klavins, M. 2019. Granulation of Fly Ash and Biochar with Organic Lake Sediments – A Way to Sustainable Utilization of Waste from Bioenergy Production. *Biomass and Bioenergy* **125**, 23–33. doi: 10/gf45v3

Agronomy Research **22**(1), 157–167, 2024
https://doi.org/10.15159/AR.24.049

Effectiveness of reducing ammonia emissions from solid manure by using bio-covers

I. Knoknerienė*, I. Strelkauskaitė-Buivydienė and R. Bleizgys

[1]Vytautas Magnus University, Agriculture Academy, Faculty of Engineering, Department of Mechanical, Energy, and Biotechnology Engineering, Studentu 15a, LT-53362 Akademija, Kauno r., Lithuania
*Correspondence: ieva.knokneriene@vdu.lt

Received: January 31st, 2024; Accepted: May 7th, 2024; Published: May 23rd, 2024

Abstract. According to the European Environment Agency, in 2021, 93 percent of ammonia was released into the environment due to agricultural activities. Almost half of the pollutants were released from cowsheds. The next significant source of pollution is liquid and/or solid manure storage facilities. Many dairy farms use liquid manure systems, but inevitably there is some solid manure produced in every cattle farm. Ammonia emissions increase when air penetrates the top layer of the manure pile. This is the reason why it is recommended to reduce the surface area of the manure piles that contact with open air. Straw, peat, sawdust, or other materials can be used as bio-covers. The purpose of this study is to determine the efficiency of bio-covers while covering solid manure. Experimental studies were carried out in field conditions, covering solid cattle manure with a > 10 cm thick layer of chopped straw. As the results show, chopped straw reduced ammonia emissions by up to 44.49 percent, but the emission declination rate is 1.85 times higher during the period when NH_3 volatilization is the most intensive.

Key words: air pollution, ammonia, bio-covers, cattle manure, emissions.

INTRODUCTION

Researches conducted by many scientists have provided a perception of how ammonia (NH_3) emissions alter natural structures and function of ecosystems. Ammonia can easily form new compounds with water vapor in the atmosphere, develop into acid rain, and acidify oceans, forests, freshwaters, and other ecological communities (Pereira et al., 2010; Kitidis et al., 2011; Driscoll & Wang, 2019). According to the European Environmental Agency (2023), in 2021, 93 percent of ammonia gas was released due to agricultural activities. Medėkšaitė & Čingienė (2014) established that 49 percent of these harmful gases volatilize from cattle sheds. Another significant source of ammonia gas is manure heaps, slurry pits, composting systems, and heaps of manure in the field (Hassouna et al., 2016; Kavanagh et al., 2019).

The type of manure is determined by the amount of dry matter (DM) found in the substance. The content of DM in solid cattle manure reaches 20 percent or more (Skurdenienė et al., 2007; Bagdonienė et al., 2011). In Lithuania, if there are not more

than 50 livestock units kept on the farm, solid manure can be stored in manure stacks near barns or in fields that will be fertilized with manure. In all cases, it is desirable to use measures that reduce emitting odors and gas emissions into the environment. Manure should be covered with flexible, waterproof artificial coatings or a layer of bio-coatings (peat, soil, chopped or unchopped straw, sawdust) no thinner than 10 cm (Inventory of Environmental Requirements…, 2005).

NH_3 volatilization into the environment is a complex process influenced by various biological, chemical, and physical factors. Besides air humidity and temperature, air velocity, protein content in manure, and pH of the manure, DM content, concentration of ammonia at the surface of the manure, and the area of manure exposed to the air are the most common contributors affecting the intensity of ammonia emission (Freney et al., 1981; Philippe et al., 2011; van der Weerden et al., 2023). The phenomenon of NH_3 volatilization occurs when the ammonium-N present in the manure or slurry is converted to dissolved ammonia gas in the manure (Meisinger & Jokela, 2000). The higher the pH and ambient temperature of the manure, and the higher the NH_4-N concentration, the more active this process is (Holly et al., 2017). This results in a high amount of dissolved ammonia gas in the manure. Then liquid ammonia turns into gaseous form and evaporates from the manure due to convective mass exchange (Meisinger & Jokela, 2000; Grzyb et al., 2021).

In solid manure, the emission of ammonia is induced by the air that penetrates the outer layer of the manure stack. Therefore, the area exposed to the air needs to be reduced as much as possible (Karlsson & Tersmeden, 2001; Ye et al., 2011; McCollough et al., 2022). This can be done by forming higher manure heaps or covering the surface of manure with various materials (Guarino et al., 2006; Zhu et al., 2014). Most of the research is focused on liquid manure (Zhu et al., 2014). However many small and medium-sized farms still use livestock housing systems where solid manure is produced.

For small and medium-sized farms in many cases, it is uneconomical to install manure pits. Furthermore, even commercial farms have facilities in which solid manure is formed, such as calf barns, calving pens, etc. The Environmental Requirements For Manure And Slurry Management in Lithuania allow the storage of thick manure in heaps near barns or in crop fields. But recently, discussions were going on that manure heaps should be prohibited. This research was conducted to scientifically prove the advantage of using recommendations mentioned in The Environmental Requirements For Manure And Slurry Management under realistic field conditions, found in farms in Lithuania. Therefore, the experiment shows the scientifically investigated efficiency of bio-based manure covers and also demonstrates that it is possible to store manure in piles, posing a lower threat to environmental pollution by ammonia gas.

MATERIALS AND METHODS

Cattle housing system and diets

Fresh solid cattle manure used for the research was collected from the Vytautas Magnus University Agriculture Academy (VMU-AA) Training farm. Approximately 160 Holstein cows are kept on this farm. Cows are divided into two groups: dry cows and lactating cows. The group of dry cows consists of ~40 cows all year round. The rest of the cows form a lactating cow group which includes various lactation-stage cows: early, mid, and late.

All cows were fed with a feed mixture that included wheat, barley, or other kinds of crop straw, corn silage, grass silage, hay, water, essential mineral compounds, additional nutrients, and trace elements. The feed mixture for lactating cows is enriched with rapeseed oilcake, soy groats, minced wheat, barley, and oat blend to meet their feed intake needs.

To ensure animal welfare, the cowshed was designed relying on loose housing system parameters. However, beds for cows were built by combining two major types of loose systems: cubicle system and straw yard system. Cubicles and straw yard are cleaned every day by using farm machinery and bedded with fresh good quality chopped straw. In summer time, 5–6 bales of straw, weighing approx. 200 kg each, are used for bedding. During cold season, the number of bales used for bedding increases up to 8 each day.

Manure samples

Experimental studies in field conditions were carried out in the VMU-AA Training farm crop field. Manure pile (MP) (Fig. 1. a) and manure stack (MS) (Fig. 1, b) were formed in crop field which later was fertilized with manure used for the experimental study.

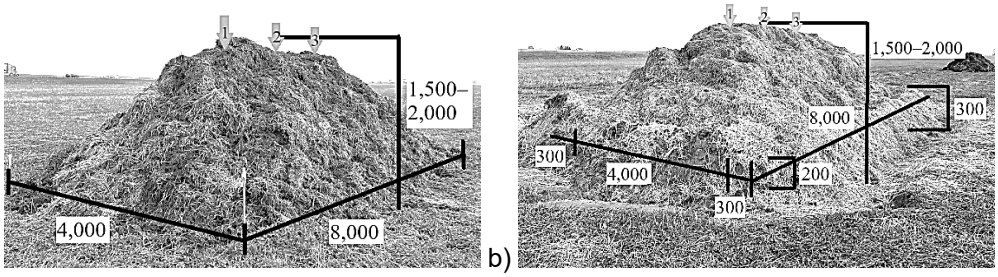

Figure 1. Measurements of manure pile and manure stack used for the experiment.

Both, the manure stack, and manure pile were 8 m long, 4 m wide, and 1.5–2 m high. Each pile consisted of 35 t (or 48 m^3) of fresh solid cattle manure. The difference between the MP and MS is:

– Manure Pile (MP) was formed simply by piling layers of manure straight on the surface of the ground. It also didn't have any kind of bio-based cover and the surface of the manure was in contact with open air;

– Manure Stack (MS) was formed according to Environmental Requirements for Manure and Slurry Management in Lithuania. MS was formed on top of an 8.6 m long, 4.6 wide (clarification: underlayer has to be 0.3 m wider than the manure stack on all sides), and 0.2 m thick underlayer made of compressed chopped straw. Additionally, the manure stack was covered in a >10 cm thick layer of chopper straw. Furthermore, a 0.3 m high embankment encircled the same manure stack.

The amount of dry matter in manure samples varied from 21.01% to 28.76%. The total amount of nitrogen content at the beginning of the experiment was 0.52–0.67%. Elemental composition studies were carried out in the Lithuanian Research Centre for Agriculture and Forestry, Institute of Agriculture, Chemical Research Laboratory.

Instrumentation

A portable air monitor 'Aeroqual Series 500' (range: 0–1,000 ppm; accuracy: < ± 0.5 ppm + 10%) was used for measuring ammonia (NH_3) concentration (ppm) during experimental studies in field conditions. At least 3 measurements were taken at the top of the manure stack and manure pile. Measuring sites are marked with arrows and numbered as '1', '2', and '3' (Fig. 1, a & b).

Methods

Direct measurement of the NH_3 emission fluxes at the manure-air interface was measured using the method of Static Chamber. During sampling, the cylindrical plastic chamber (H = 37 cm; Ø = 32 cm; V = 30 L) was deployed above the surface of the manure. Ammonia concentration readings were recorded at the 3-minute mark from when the air monitor was covered with the chamber (Fig. 2). At least 3 measurements were taken at different areas of the same stack. All measurements were done at the top of the heap.

The waiting duration (3 minutes) was chosen experimentally. The intensity of ammonia volatilization is bound to a concentration gradient. When a static chamber is used, NH_3 gasses accumulate under the hood, the diffusion coefficient declines until equilibrium is reached and the evaporation process to the air hardly occurs. Numerous attempts showed that a duration of 3 minutes is enough to reach an equilibrium of gas concentrations between the surface of the manure and the air inside the chamber.

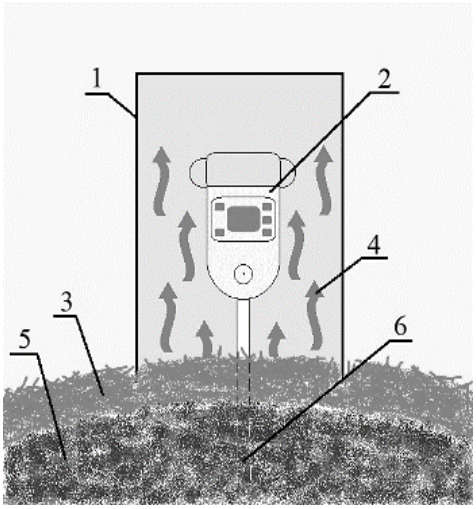

Figure 2. Schematic image of measuring ammonia gas concentration at the manure-air interface using static chamber: 1 – static chamber with a volume of 30 L; 2 – NH3 gas concentration monitor; 3 – manure cover (straw); 4 – NH_3 evaporation flux; 5 – manure; 6 – monitor mounting rod.

Ammonia concentration measurements in ppm then are used to determine the intensity of gas emission into the environment in mg $m^{-2}h^{-1}$. The calculations are done using the equation written below:

$$E = \frac{\Delta C}{\Delta \tau} \cdot \frac{V_k}{F_k} \quad (1)$$

where ΔC – the difference of ammonia concentration at the beginning and end of measurement, mg $m^{-2}h^{-1}$; $\Delta \tau$ – time difference ($\tau_{beginning} - \tau_{end}$), h; V_k – the capacity of the static chamber, m^3; F_k – floor area of the static chamber, m^2.

The research data were statistically evaluated by calculating the arithmetic averages of the indicators and their confidence intervals. Statistical reliability was assessed according to the methodology of Student's *t-test* and Tukey *HSD test*. The level of

statistical significance is $p < 0.05$. Thus, the results were presented using descriptive statistics.

The results of this research are valid only for the case under consideration. This case study represents the actual approach to forming manure piles in crop fields and does not provide ideal conditions such as homogenization of the manure before storing. Therefore, the study results can be related to fundamental knowledge of what processes occur while storing manure in piles and how they progress but do not represent situations in other farms than VMU-AA Training farm.

RESULTS AND DISCUSSION

Experimental field research was conducted from November to March. This period coincides with the period in which it is prohibited to fertilize the fields with manure. Therefore, the study conditions correspond to real conditions when farmers store manure in stacks in crop fields until they are allowed to use manure as a fertilizer again.

To ensure the reliability of results, ammonia concentration rates were measured after 2 weeks since manure heaps were formed. The 2 weeks were designated to ensure that biological and thermodynamical processes in manure had stabilized. The results of experimental studies in field conditions are shown in Table 1.

Table 1. Statistical evaluation of calculated ammonia emission rates in mg m^{-2} h^{-1}, according to the data results of experimental studies in field conditions (MS – manure stack, covered with straw; MP – manure pile, uncovered)

Date (day of the experiment)		Emission, mg m^{-2} h^{-1}					
		$\bar{y}$[1]	S[2]	n[3]	s[4]	$t_{n-1,\,P}$[5]	$\pm\Delta y_{n-1,\,P}$[6]
11–11 (22)	MS	**713.20**	28.89	3	16.68	4.30	71.77
	MP	**611.03**	13.72	3	7.92	4.30	34.08
11–28 (28)	MS	**168.94**	18.85	4	9.42	3.18	29.99
	MP	**359.00**	60.63	4	30.32	3.18	96.48
12–02 (43)	MS	**36.28**	3.88	3	2.24	4.30	9.63
	MP	**71.99**	6.54	3	3.77	4.30	16.24
01–16 (88)	MS	**11.90**	0.50	3	0.29	4.30	1.25
	MP	**15.38**	0.50	3	0.29	4.30	1.25
02–03 (106)	MS	**9.58**	0.00	3	0.00	4.30	0.00
	MP	**7.26**	1.33	3	0.77	4.30	3.30
03–02 (133)	MS	**9.58**	0.87	3	0.50	4.30	2.16
	MP	**7.84**	1.74	3	1.01	4.30	4.33
03–24 (155)	MS	**12.48**	0.5	3	0.29	4.30	1.25
	MP	**10.74**	1.33	3	0.77	4.30	3.30

[1] Average; [2] Standard deviation; [3] Number of samples; [4] Standard error of the mean; [5] t value; [6] Confidence interval.

During the experiment, average air temperature was 1.15 ± 0.79 °C in the range from lowest at -10.30 °C in December and the highest at 12.90 °C in March. The meteorological data was gathered from Kaunas' meteorological station which the Lithuanian Hydrometeorological Service operates under the Ministry of the Environment.

According to the data in Table 1, ammonia volatilization into the atmosphere during the first 30 days is the most intense. The same tendencies are described by Zhuang et al. (2020) in their study. Based on other authors' research, this occurrence corresponds to the temperature of manure. When solid cattle manure is stored in heaps, the process of composting develops due to bacterial activity (Flynn & Wood, 1996; Petric & Selimbašić, 2008; Chen et al., 2011). During the first 30 days, the temperature of the manure reached 74–76 °C in both heaps, 0.1 m – 1.2 m deep. After day 30 of the experiment, the temperature started to subside until it reached the maturation stage temperature of 18.48 ± 0.52 °C on average. The only exception was a 0.1 m deep manure layer in an uncovered manure pile (MP) with an average temperature of 8.17 ± 0.47 °C which was close to the air temperature at the same period (88–155 days of the experiment).

The highest emission rate from MS was 713.20 ± 71.77 mg m^{-2} h^{-1} on the 22nd day of the experiment. The highest NH_3 emission rate from MS was also established on the 22nd day of the research (611.03 ± 34.08 mg m^{-2} h^{-1}). Although at the beginning of the research, it is acknowledged that the ammonia flux rate from the covered manure stack is more intense, on the 28th day of the research a radical change can be noted (Fig. 3).

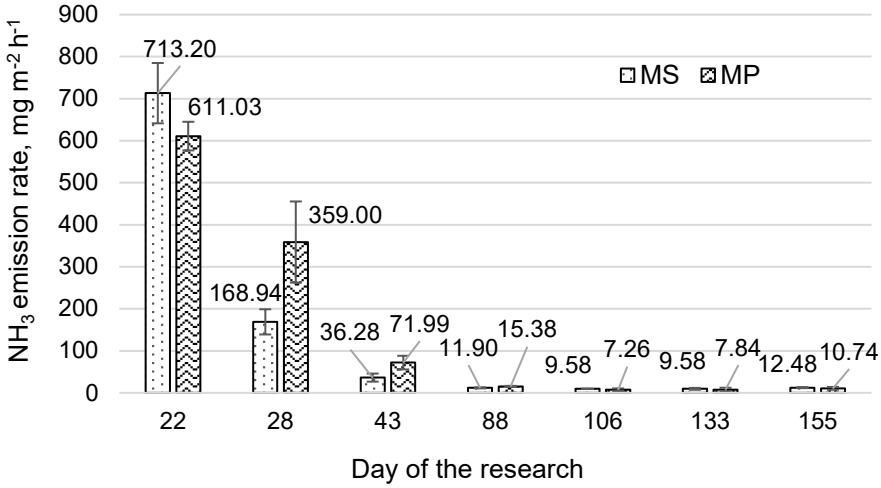

Figure 3. Tendencies in the change of ammonia volatilization from solid manure during field experiment (MS – manure stack, covered with straw; MP – manure pile, uncovered).

On the 22nd day of the research, the NH_3 volatilization flux rate from the manure stack covered in straw was 14.32 percent higher than from the uncovered manure pile. However, according to Student's *t-test* and Tukey *HSD test* the difference is not significant. A completely different situation was acknowledged on the 28th day of research. A significant difference of 52.94 percent between MS and MP was recorded. During the rest of the research, no significant differences were observed.

As results show, when manure is not covered with a layer of straw or another substance, the highest rate of ammonia emission declination can be seen until day 88 of the research (Fig. 4). Due to natural causes, between day 22 and 28, NH_3 volatilization decreased by 41.25 percent. The data implies that the lesion of ammonia emission is 6.88 percent a day on average. However, NH_3 emission rate abatement drops to 3.13 percent

a day on average, between days 28 and 43. The declination rate lessens to 0.21 percent a day on average during the 43rd–88th day period. A decrease in ammonia emission lux rate can be observed until day 106 of the research. On this day, the lowest emission rate (7.26 ± 3.30 mg m^{-2} h^{-1}) was observed. But from this point of the research, NH_3 volatilization started to increase until the end of the experiment.

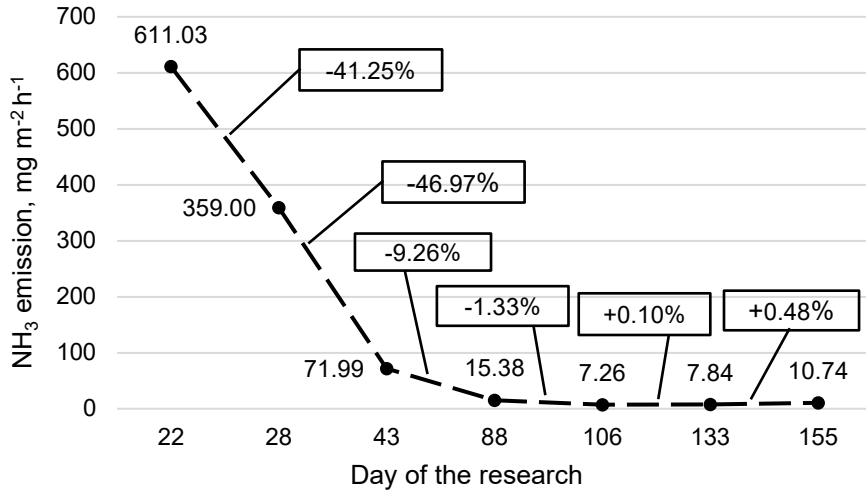

Figure 4. NH_3 emission flux rate declination from manure pile (MP) without cover.

According to data gathered during the research in field conditions, when manure is covered with chopped straw, the NH_3 volatilization flux rate declines much faster (Fig. 5).

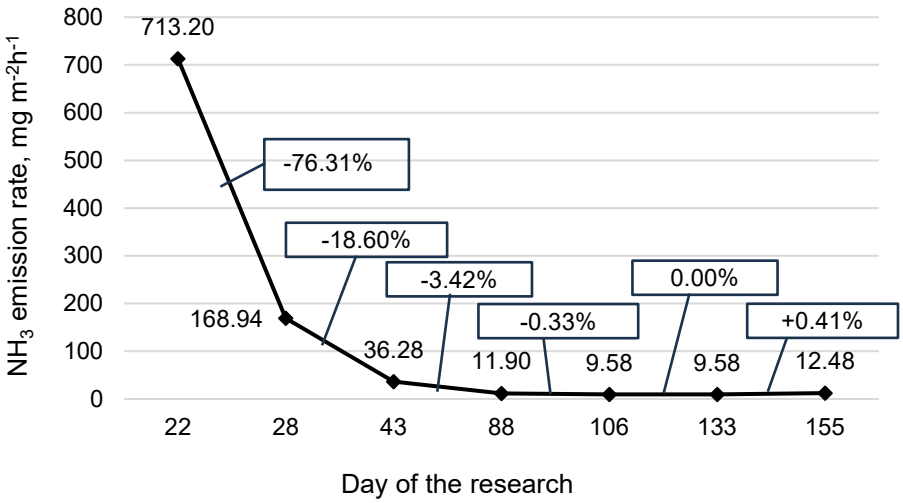

Figure 5. NH_3 emission flux rate declination from manure stack (MS) covered in chopped straw.

Between days 22 and 28 of the study NH_3 emission rate decreased by 76.31 percent. Results suggest that ammonia emission from manure stacks covered in straw diminishes by 12.72 percent a day on average. The decline rate between days 28 and 43 lowers to 1.24 percent a day on average. The ammonia volatilization rate continued decreasing until day 133 of the research and declined to the lowest rate of 9.58 ± 2.16 mg m^{-2} h^{-1}. At the very end of the research, between days 133 and 155, a slight increase in ammonia emission was observed. Compared to previous results, the emission rate increased by 0.41 percent and reached 12.48 ± 1.25 mg m^{-2} h^{-1} but this change was not statistically significant.

The biggest amount of NH_3 volatilizes into the atmosphere in the first 30 days from the formation of manure stack or pile. The most intense ammonia vaporization occurs at 10–14 days of manure storage. Some researchers found that evaporation of NH_3 from an uncovered manure pile is the most intense in the first 7 days (VanderZaag et al., 2015). Whereas, the formation of the natural crust begins after 10 to 20 days and stabilizes after 40 to 60 days (Nielsen et al., 2010; Aguerre et al., 2012). This tendency implies that measures and tools to reduce air pollution with ammonia gas are the most necessary in the first month after stacking manure. >10 cm thick layer of straw helps reduce NH_3 emissions 1.85 times faster.

This occurrence can be explained by processes happening in the manure during the storage period. The composting process naturally occurs in manure due to bacterial activity. In the first and second composting stages (active phase), bacterial activity is very high, therefore the temperature of manure increases (Chen et al., 2011; Nozhevnikova et al., 2019). Temperature is one of the factors that amplifies NH_3 emissions from manure. Hence, ammonia volatilization depends on bacterial activity. Bacteria found in solid manure are aerobic, which means they require oxygen to digest compounds found in manure. When manure has an open surface, air with oxygen keeps penetrating manure, and bacteria are continuously provided with the vital gas. While covered manure does not have an open surface and air access to the manure surface is restricted. Bacteria experience a lack of oxygen much sooner and cannot continue aerobic digestion, thus ammonia emission is reduced.

According to previously conducted laboratory research, chopped straw lowers the NH_3 emission flux rate up to 73.42 percent. However, experimental studies in field conditions indicate that a > 10 cm thick layer of chopped straw lessens the vaporization of ammonia gas only by 44.49 percent. This is thought to be due to the porosity of the straw layer.

CONCLUSIONS

1. The highest NH_3 emission rates were acknowledged on day 22 of the trial and were as high as 713.20 ± 71.77 mg m^{-2} h^{-1} from manure stack (MS) and 611.03 ± 34.08 mg m^{-2} h^{-1} from manure pile (MP).

2. During experimental studies in field conditions, it was found that ammonia evaporates into the environment most intensively in the first 30 days after the manure is piled up. During this period, ammonia emission reduction measures are needed the most.

3. Due to natural causes, ammonia emission lowers on itself, but it takes ~1.85 times longer. When chopped straw is used as a bio-cover, the NH_3 emission reduction rate can reach up to 12.72 percent a day between days 22 and 28 of research. Meanwhile, ammonia emissions declined only by 6.88 percent a day at the same time from the uncovered manure pile.

4. The effectiveness of > 10 cm thick chopped straw layer on field conditions can reach up to 44.49 percent. The porosity of the substance could be the cause of such results. To confirm or deny this hypothesis, it is suggested to complement research results with material porosity studies.

5. In both, the manure stack and manure pile, high ammonia emission rates were noticed at the beginning of the trial. It is believed that the activity of aerobic bacteria caused this. Therefore, on day 28 a significant decline in NH_3 volatilization was observed which supposedly could be caused by a lack of oxygen in the covered manure stack. To confirm or deny this hypothesis, it is suggested to complement the results of the research with oxygen level data during the composting process.

6. The experimental research scientifically proves the positive effect of methods mentioned in the Inventory of Environmental Requirements for Manure and Slurry Management reducing air pollution with ammonia gasses from thick cattle manure stored in heaps in the case under consideration.

7. Reduced ammonia emissions are related to lessened loss of nitrogen from the manure. Therefore, manure remains more beneficial as a fertilizer. Hence, using such manure as fertilizer, fewer inorganic fertilizers are needed which is economically beneficial.

REFERENCES

Aguerre, M.J., Wattiaux, M.A. & Powell, J.M. 2012. Emissions of ammonia, nitrous oxide, methane, and carbon dioxide during storage of dairy cow manure as affected by dietary forage-to-concentrate ratio and crust formation. *Journal of Dairy Science* **95**(12), 7409–7416. doi: 10.3168/jds.2012-534

Bagdonienė, I., Bleizgys, R. & Naujokienė, V. 2011. Technological factors of cowshed influence for gas emission intensity from manure. In *Žemės ūkio inžinerija, mokslo darbai* **43**(2), 40–49 (in Lithuanian, English absrt.)

Chen, L., de Haro Marti, M., Moore, A. & Falen, C. 2011. The composting process. *Dairy Manure Compost Production and Use in Idaho* **2**, 513–532.

Driscoll, C.T. & Wang, Z. 2019. Ecosystem effects of acidic deposition. *Encyclopedia of Water: Science. Technology. and Society*, 1–12. doi: 10.1002/9781119300762.wsts0043

EEA. 2023. Air pollution in Europe: 2023 reporting status under the National Emission reduction Commitments Directive. https://www.eea.europa.eu/publications/national-emission-reduction-commitments-directive-2023 pp.13

Flynn, R.P. & Wood, C.W. 1996. Temperature and chemical changes during composting of broiler litter. *Compost Science & Utilization* **4**(3), 62–70. doi: 10.1080/1065657X.1996.10701841

Freney, J.R., Simpson, J.R. & Denmead, O.T. 1981. Ammonia volatilization. *Ecological Bulletins*. No. **33**, 291–302.

Grzyb, A., Wolna-Maruwka, A. & Niewiadomska, A. 2021. The significance of microbial transformation of nitrogen compounds in the light of integrated crop management. *Agronomy* **11**(7), 1415, 1–27. doi: 10.3390/agronomy11071415

Guarino, M., Fabbri, C., Brambilla, M., Valli, L. & Navarotto, P. 2006. Evaluation of simplified covering systems to reduce gaseous emissions from livestock manure storage. *Transactions of the ASABE* **49**(3), 737–747. doi: 10.13031/2013.20481

Hassouna, M., Eglin, T., Cellier, P., Colomb, V., Cohan, J.P., Decuq, C., Delabuis, M., Edouard, N., Espagnol, S., Eugene, M., Fauvel, Y., Fernandes, E., Fischer, N., Flechard, C., Genermont, S., Godbout, S., Guingand, N., Guyader, J., Lagadec, S., Laville, P., Lorinquer, E., Loubet, B., Loyon, L., Martin, C., Meda, B., Morvan, T., Oster, D., Oudart, D., Personne, E., Planchais, J., Ponchant, P., Renand, G., Robin, P. & Rochette, Y. 2016. *Measuring emissions from livestock farming: greenhouse gases, ammonia and nitrogen oxides*, INRA-ADEME, 220 pp.

Holly, M.A., Larson, R.A., Powell, J.M., Ruark, M.D. & Aguirre-Villegas, H. 2017. Greenhouse gas and ammonia emissions from digested and separated dairy manure during storage and after land application. *Agriculture. Ecosystems & Environment* **239**, 410–419. doi: 10.1016/j.agee.2017.02.007

Inventory of Environmental Requirements for Manure and Slurry Management. 2005. Ministry of Environment of the Republic of Lithuania. Vilnius, Lithuania.

Karlsson, S. & Tersmeden, M. 2001. Ammonia emissions from storing and spreading of manure–reference measurements. *LIFE–Ammonia* **31**, 1–11.

Kavanagh, I., Burchill, W., Healy, M.G., Fenton, O., Krol, D.J. & Lanigan, G.J. 2019. Mitigation of ammonia and greenhouse gas emissions from stored cattle slurry using acidifiers and chemical amendments. *Journal of Cleaner Production* **237**, 117822, 1–9. doi: 10.1016/j.jclepro.2019.117822

Kitidis, V., Laverock, B., McNeill, L.C., Beesley, A., Cummings, D., Tait, K., Osborn, M.A. & Widdicombe, S. 2011. Impact of ocean acidification on benthic and water column ammonia oxidation. *Geophysical Research Letters* **38**(21), 1–5. doi: 10.1029/2011GL049095

McCollough, M.R., Pedersen, J., Nyord, T., Sørensen, P. & Melander, B. 2022. Ammonia Emissions. Exposed Surface Area. and Crop and Weed Responses Resulting from Three Post-Emergence Slurry Application Strategies in Cereals. *Agronomy* **12**(10), 2441, 1–19. doi: 10.3390/agronomy12102441

Medėkšaitė, J. & Čingienė, R. 2014. Investigation of the factors influencing pollution from livestock production sites. In *Human and nature safety 2014: proceedings of the 20th international scientific-practice conference*. Aleksandras Stulginskis University, Akademija, Lietuva, pp. 90–93. (in Lithuanian, English abstr.)

Meisinger, J.J. & Jokela, W.E. 2000. Ammonia volatilization from dairy and poultry manure. *Managing nutrients and pathogens from animal agriculture (NRAES-130).* Natural Resource, Agriculture, and Engineering Service, Ithaca, NY, 334–354.

Nielsen, D.A., Nielsen, L.P., Schramm, A. & Revsbech, N.P. 2010. Oxygen distribution and potential ammonia oxidation in floating, liquid manure crusts. *Journal of Environmental Quality* **39**(5), 1813–1820. doi: 10.2134/jeq2009.0382

Nozhevnikova, A.N., Mironov, V.V., Botchkova, E.A., Litti, Y.V. & Russkova, Y.I. 2019. Composition of a microbial community at different stages of composting and the prospects for compost production from municipal organic waste. *Applied Biochemistry and Microbiology* **55**, 199–208. doi: 10.1134/S0003683819030104

Pereira, J., Misselbrook, T.H., Chadwick, D.R., Coutinho, J. & Trindade, H. 2010. Ammonia emissions from naturally ventilated dairy cattle buildings and outdoor concrete yards in Portugal. *Atmospheric Environment* **44**(28), 3413–3421. doi: 10.1016/j.atmosenv.2010.06.008

Petric, I. & Selimbašić, V. 2008. Development and validation of mathematical model for aerobic composting process. *Chemical Engineering Journal* **139**(2), 304–317. doi: 10.1016/j.cej.2007.08.017

Philippe, F.X., Cabaraux, J.F. & Nicks, B. 2011. Ammonia emissions from pig houses: Influencing factors and mitigation techniques. *Agriculture. ecosystems & environment* **141**(3-4), 245–260. doi: 10.1016/j.agee.2011.03.012

Skurdenienė, I., Ribikauskas, V. & Bakutis, B. 2007. *Advantages of organic farming in animal husbandry*. Institute of Animal Husbandry of the Lithuanian Veterinary Academy, Baisiogala, 143 pp. (Available in Lithuanian).

van der Weerden, T.J., Noble, A.N., Beltran, I., Hutchings, N.J., Thorman, R.E., de Klein, C.A.M. & Amon, B. 2023. Influence of key factors on ammonia and nitrous oxide emission factors for excreta deposited by livestock and land-applied manure. *Science of The Total Environment* **889**, 164066, 1–12. doi: 10.1016/j.scitotenv.2023.164066

VanderZaag, A., Amon, B., Bittman, S. & Kuczyński, T. 2015. Ammonia abatement with manure storage and processing techniques. *Costs of ammonia abatement and the climate co-benefits*, 75–112. doi: 10.1007/978-94-017-9722-1_5

Ye, Z., Zhu, S., Kai, P., Li, B., Blanes-Vidal, V., Pan, J., Wang, C. & Zhang, G. 2011. Key factors driving ammonia emissions from a pig house slurry pit. *Biosystems engineering* **108**(3), 195–203. doi: 10.1016/j.biosystemseng.2010.12.001

Zhu, H., Dong, H., Zuo, F., Yuan, F. & Rao, J. 2014. Effect of covering on greenhouse gas emissions from beef cattle solid manure stored at different stack heights. *Transactions of the Chinese Society of Agricultural Engineering* **30**(24), 225–231.

Zhuang, M., Shan, N., Wang, Y., Caro, D., Fleming, R.M. & Wang, L. 2020. Different characteristics of greenhouse gases and ammonia emissions from conventional stored dairy cattle and swine manure in China. *Science of the Total Environment* **722**, 137693. doi: 10.1016/j.scitotenv.2020.137693

Agronomy Research **22**(1), 168–179, 2024
https://doi.org/10.15159/AR.24.012

Importance of mosaic augmentation for agricultural image dataset

S. Kodors[1,*], M. Sondors[1], I. Apeinans[1], I. Zarembo[1], G. Lacis[2], E. Rubauskis[2] and K. Karklina[2]

[1]Rezekne Academy of Technologies, Faculty of Engineering, Institute of Engineering, Atbrivosanas Str. 115, LV-4601 Rezekne, Latvia
[2]Institute of Horticulture (LatHort), Graudu Str. 1, LV-3701 Cerini, Krimunu pagasts, Dobeles novads, Latvia
[*]Correspondence: sergejs.kodors@rta.lv

Received: August 24th, 2023; Accepted: February 6th, 2024; Published: February 23rd, 2024

Abstract. The yield estimation using artificial intelligence is based on object detection algorithms. Firstly, the object detection algorithms identify the number of fruits on images, then tree fruit load is predicted using regression algorithms. YOLO is a popular convolution neural network architecture for object detection tasks. It is sufficiently well studied for fruit yield estimation. However, the experiments are traditionally restricted to only one specific fruit category and growing season. This is a big shortcoming for the smart solutions like agro-drones, which must automatically complete yield monitoring of the most popular fruit species in commercial orchards. Therefore, the modern studies related to yield estimation increasingly raise attention to multi-stage, multi-state and multi-specie detection tasks. The multi-stage datasets can be described as a collection of multiple sub-datasets, e.g. flowers, fruitlets and fruits. The multi-state dataset can contain classes like mature, immature or damaged fruits. Meanwhile, the multi-specie dataset contains images with representatives of multiple cultures. However, if classic object-detection tasks like urban or indoor object detection have multiple classes presented in one image, then yield estimation datasets usually have images with only one class presented on them. Therefore, an image shuffle or mosaic augmentation are the intuitive training strategies of YOLO for object detection working with a collection of multiple single class datasets. We applied the YOLOv5m model to test both strategies, which were verified on three datasets: apple fruits (MinneApple), pear fruits (Pear640) and pear fruitlets (PFruitlet640). Our experiment showed that mosaic augmentation improves mAP@0.5:0.95 better than simple image shuffle. The mean difference between both strategies is equal to 0.0438.

Key words: augmentation, deep learning, yield estimation, object detection, precision horticulture.

INTRODUCTION

Fruit growing is an important branch of agriculture, an important sector of the economy, and provides a significant part of a healthy diet. It currently faces a number of challenges: climate change, new diseases and pests, public demand for less pesticide use, and competitive production. These contradictory tasks require effective decision-making

and prognosis tools based on knowledge-intensive smart fruit-growing solutions and diverse orchard management information. One of the prerequisites for successful decision-making is the availability of up-to-date and accurate orchard monitoring data (Kodors et al., 2021). Regular collection of such data requires involvement of appropriately skilled human resources, which is not always possible in terms of time and costs, especially in small farms. Therefore, the automation of these processes is relevant, including drone-based imaging, recognition and tracking of different stages of fruit development for yield prediction modelling (Moravec et al., 2017).

The automatic fruit yield forecasting consists of three stages: 1) yield estimation; 2) tree fruit load prediction; 3) and yield prediction. The yield estimation is object detection task, which estimates the number of fruits visible on images. However, the actual number of fruits is different than visible on images, because some fruits can be occluded by leaves or counted multiple times on different photos. Therefore, the actual tree load must be predicted by regression algorithms. For example, Vijayakumar et al. (2023) presented combination of YOLO and regression algorithms for citrus load prediction (Vijayakumar et al., 2023), meanwhile, the similar combination of methods was applied by for blueberry load prediction (MacEachern et al., 2023). The yield prediction is based on the application of regression algorithms too, only the fruit load is forecasted by the number of fruits calculated in the previous season or development stage. For example, Cheng et al. (2017) applied simple back propagation neural networks to complete early fruit yield prediction within one season and for next year (Cheng et al., 2017).

Traditionally the experiments are restricted to only one specific fruit category and growing season. This is a big shortcoming for the smart solutions like agro-drones, which must automatically complete yield monitoring of the most popular fruit species in commercial orchards. Therefore, the modern studies related to yield estimation increasingly raise attention to multi-stage, multi-state and multi-specie detection tasks. The multi-stage datasets can be described as a collection of multiple sub-datasets, e.g. flowers, fruitlets and fruits. The multi-state dataset can contain classes like mature, immature or damaged fruits. Meanwhile, the multi-specie dataset contains images with representatives of multiple cultures.

The object of our study is the automation of yield estimation using unmanned aerial vehicles (UAV) and artificial intelligence (AI) in the commercial orchards. In this article we focus on training a neural network to recognize different fruits and their different development stages and states.

The automatic yield estimation using computer vision is sufficiently well studied. For example, Wang et al. (2022) applied modified YOLOv5 architecture for litchi fruit detection and obtained accuracy 92.4% mAP. Meanwhile, Lyu et al. (2022) experimented with yield estimation of green citrus achieving 98.23% mAP@0.5 by using YOLOv5-CS architecture. Many different types of fruits and berries can be mentioned as the object of yield estimation study: tomatoes (Liu et al., 2020), strawberries (Chen et al., 2019), pears (Parico & Ahamed, 2021), etc. However traditionally these studies are scoped by only one specie.

If we are speaking about practical application of unmanned ground vehicles (UGV) or UAV for automatic yield estimation, prediction or harvesting, single-specie and single-stage restrictions are strongly unattractive product features, therefore CNN must be trained to detect many classes.

The intuitive solutions to train convolution neural network (CNN) on a collection of multiple single class datasets are two strategies: image shuffle or mosaic augmentation. The goal of the study is to identify the most suitable strategy for CNN training on collections with multiple single class datasets: image shuffle or mosaic augmentation.

The following objectives are defined to achieve the study goal:

1. Prepare datasets for CNN training.
2. Train CNN using two strategies: image shuffle and mosaic augmentation.
3. Compare obtained accuracies.

A short summary of findings, which presents the novelty of our study:

• PFruitlet640 dataset was collected and annotated for the experiment. PFruitlet640 contains images of pear fruitlets. This dataset was required to evaluate the multi-stage object detection with visually similar objects like a pair of pear fruits (Pear640) and pear fruitlets (PFruitlet640). PFruitlet640 is published in Kaggle repository under CC-BY licence (Web, a).

• Our experiment showed that mosaic training strategy is more suitable for the agricultural image datasets. It showed 4.38% better mAP@50:95 results than image shuffle strategy.

The experiment was completed using the YOLOv5m model, which was selected in our previous experiment (Kodors et al., 2023).

BACKGROUND

Two strategies of CNN training on multiple single class datasets are discussed in this article: image shuffle and mosaic augmentation (see Fig. 1). Image shuffle strategy considers new dataset creation when images of A and B datasets are mixed one after another. Mosaic augmentation: when images of A and B datasets are split in parts and combined as new images.

The transfer-learning and augmentation disciplines are the most suitable for the theoretical analysis of both solutions because the transfer-learning is related to training on multiple datasets, but the augmentation - image generation by modifying existing images.

For example, Ngiam et al. (2018) found that transfer-learning using fine-grained classified datasets provides better performance. It can be concluded that both strategies, image shuffle and mosaic augmentation, must improve object detection results. Additionally, Ngiam et al. (2018) mention that multiple different categories in datasets provide better results. Therefore, the combination of visually different objects like red apples and green pears must provide better results than visually similar objects like pears and pear fruitlets. Interesting study was completed by Rotshtein et al. (2004), they completed an experiment morphing the photos of Marilyn Monroe and Margaret

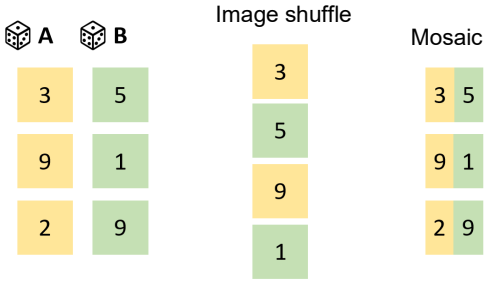

Figure 1. Two training strategies: image shuffle and mosaic augmentation.

Thatcher. They experimentally showed that it is harder for people to recognize morphed photos and the mistakes depend on the amount of the added foreign person visual features. Considering that, Chu et al. (2020) mention: 'when there is simply no sufficient data for the tail classes to recover their underlying distribution, the problem of finding an optimal decision boundary becomes ill-defined. In this scenario, it becomes extremely difficult to guess the location of the decision boundary without recovering the distribution first'. So, the increase of visually similar content can stabilise the object recognition finding more correct hyperplanes. Meanwhile, Barman et al. (2019) mention that transfer-learning requires less data than training from scratch. But Sun et al. (2017) has shown that the performance of deep learning models is logarithmically related to the number of training samples (Sun et al., 2017). It means if the number of categories is increased the number of images per class can be decreased. The similar conclusion is mentioned by Li et al. (2023), that collection and production of training samples require a high cost, but augmentation provides low-cost data (Li et al., 2023). Therefore, it is more economically interesting to collect multiple single class datasets than to solve simply one-class problem.

It must be told that the authors of YOLOv4 (Bochkovskiy et al., 2020) mention mosaic augmentation as important element of improvement combination to achieve better performance (Bochkovskiy et al., 2020). Meanwhile, Li et al. (2023) presented Dynamic Mosaic algorithm and Multi-Type Data Augmentation (MDTA) strategy, which were tested and compared with simple mosaic using YOLOv5s and Pascal VOC dataset (Li et al., 2023). The experiment of Li et al. (2023) showed that simple mosaic improved mAP by 7.81%, Dynamic Mosaic - by 8.54%, but MDTA provided additional 3.68% for Dynamic Mosaic. Summers & Dinneen (2019) experimented with different mosaic types, they identified importance of another transformation, which must be applied to the mosaic parts; that was considered by Li et al. (2023) as MDTA strategy.

Considering multiple stage recognition, the most popular subject is plant disease detection. For example, Cruz et al. (2022) trained YOLOv5 models for strawberry disease detection (gray mold, leaf spots, powdery mildew, anthracnose fruit rot, blossom blight), which were integrated to edge computing solution (Cruz et al., 2022). Liu et al. (2023) trained YOLOv5s model to detect disease 'brown rot' on tomatoes. The authors achieved accuracy 89.8% mAP@0.5 (Liu et al., 2023). Tian et al. (2019) applied YOLOv3-dense for the detection of infected apples (Tian et al., 2019).

Speaking about existing studies with mosaic augmentation in agriculture, Dulal et al. (2022) compared the YOLOv5 training strategies with and without mosaic augmentation. By developing a cattle identification solution, they showed that mosaic strategy improves object detection accuracy. Considering similar studies, Ge et al. (2022) developed UGV solution for tomato yield estimation in a greenhouse. Their solution was able to detect tomato-fruit development in the multi-stages. They applied the YOLO-Deepsort network and highlighted the importance of mosaic augmentation. Phan et al. (2023) applied YOLOv5m for tomato multi-state recognition: immature tomato, ripe tomato and damaged tomato. The augmentation description mentions only geometric transformations. However, they obtained 0.97% accuracy, which can be associated with image shuffle.

MATERIALS AND METHODS

Object detection model YOLOv5m

The object detection solution YOLO was firstly presented by Redmon et al. (2016) in the publication 'You Only Look Once: Unified, Real-Time Object Detection' (Redmon et al., 2016). The main idea of YOLO was to replace slow post-processing classification of bounding-boxes in older solutions like R-CNN. From limitations of YOLOv1 Redmon et al. (2016) mention struggles with small objects that appear in groups, such as flocks of birds. In YOLOv2 (YOLO9000), Redmon & Farhadi (2017) introduced anchor box architecture, which allowed to detect many objects inside the same grid cell. The anchor boxes of YOLOv2 were calculated with a k-means clustering algorithm. Meanwhile, the 5th generation of YOLO architecture (YOLOv5) provides auto-learning of anchor boxes from training datasets.

The YOLOv5m is a medium-sized version of the YOLOv5 architecture. YOLOv5 framework is available in GitHub repository (Web, b). YOLOv5 was not published in any scientific publication, all related documentation is available in GitHub Wiki of Ultralytics project.

The YOLOv5m model was applied, because it is the most efficient and compatible according to our previous experiments (Kodors et al., 2023). The YOLOv5m model is less GPU intensive than for example the YOLOv5l model, while YOLOv5m provides worse results than YOLOv5l considering Ultralytics experiments (Web, b). However, our experiments showed that YOLOv5l does not provide sufficient increase of accuracy for yield estimation tasks (Kodors et al., 2023). Phan et al. (2023) completed the similar experiments with the yield estimation, and they selected YOLOv5m as the most optimal model too. We have not tuned (changed) YOLOv5m architecture and applied the default model available in yolov5m.yaml, that was marked v6.0.

Experiment datasets

Three datasets were used for the experiment: MinneApple, Pear640 and PFruitlet640 (see Fig. 2). MinneApple and Pear640 are existing image datasets, which are specially prepared for yield estimation studies, which were firstly presented in the articles of Häni et al. (2020) and Kodors et al. (2023). Both datasets are developed under research projects, have good annotation quality and are sufficiently large. Meanwhile, PFruitlet640 is a novel dataset collected and annotated by our team, which is firstly presented in this publication.

Apples and pears belong to the multi-specie problem, but pear fruitlets and pears - to the multi-stage problem. Additionally, we use knowledge results from our previous study (Kodors et al., 2023), which provides baselines for YOLOv5m accuracy in the case of each dataset independently.

MinneApple is a dataset of apple tree photographs (Fig. 2, a), which was collected and annotated by Häni et al. (2020). The dataset details can be found in the paper of Häni et al. (2020), who completed similar experiments and achieved mAP@0.5 77.5% by applying method Faster RCNN. We cropped the images to size of 640×640 px, which are suitable with a YOLOv5m input layer. This was done to save the original image resolution, because the images contained some examples of apples with size 25×25 px, which could disappear after image resizing.

Pear640 is a dataset of pear fruits (Fig. 2, b) specially prepared for YOLO training with input size 640×640 px. The collection of fruit images was obtained at the end of August (105 days after full bloom) prior to the harvest. The dataset is freely available in Kaggle repository under CC BY 4.0 license. The dataset details can be found in the paper of Kodors et al. (2023).

PFruitlet640 is a dataset of pear fruitlet instances (Fig. 2, c), which was collected for this experiment due to the shortage of the similar dataset. The digital images of pear fruitlets were collected in the experimental site of the Institute of Horticulture (LatHort) with cultivars 'Suvenirs', 'Vasarine Sviestine' and 'Mramornaya' on seedling rootstocks 'Kazraushu' with planting distances 4×5 m (500 trees per 1 ha). (Krimūnu parish, Dobeles district, Latvia: 56.610169, 23.305956). The collection of fruitlet images of 'Suvenirs', 'Vasarine Sviestine' and 'Mramornaya' was done at the beginning of August (79 days after full bloom).

Figure 2. Image examples of datasets: a) MinneApple; b) Pear640; c) PFruitlet640.

The collection of digital images was carried out using a photo camera of mobile device Huawei P 40: 50 MP Ultra Vision Camera (Wide Angle, f/1.9 aperture) + 16 MP Ultra-Wide Angle Camera (f/2.2 aperture) + 8 MP Telephoto Camera (f/2.4 aperture, OIS), the image size: 3,000×4000 px; 5.0 MP.

The collection of images was carried out in field conditions in 2022, in the orchard at the distance from the tree planting point 2.5 m (middle of alleyway). The whole canopy of trees was photographed as separate objects. The images were taken in the front of a tree (a tree trunk, a planting point), perpendicularly the tree row from the west side of rows (the rows of pear trees oriented from north to south) before noon (10:00–12:00) at natural light conditions.

The dataset is available in Kaggle repository under CC BY 4.0 license (Web, a).

Experiment design

The experiment was completed in three stages (see Fig. 3): 1st and 2nd stages prepare datasets for CNN training, but 3rd stage trains CNN using two strategies: image shuffle and mosaic augmentation.

1st stage: each dataset (MinneApple, Pear640 and PFruitlet640) were split into training, validation and testing subdatasets. 20% of each dataset was taken out to create the testing baseline to compare the results of trained YOLOv5m models.

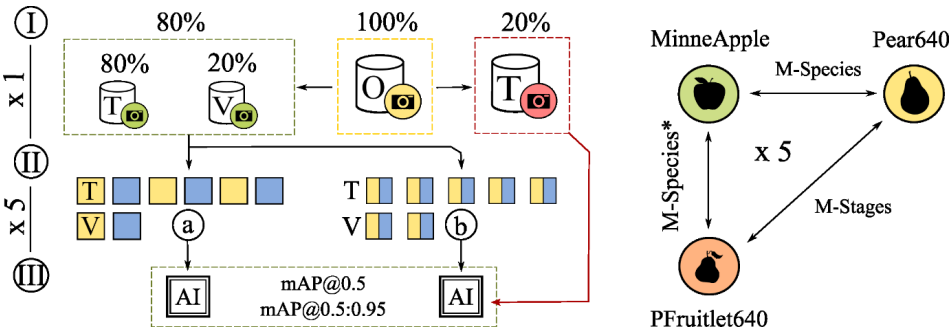

Figure 3. Experiment design: I – each dataset is split on training, validation and testing subdatasets; II – two datasets are joint using strategies: (a) image shuffle and (b) mosaic augmentation; III – YOLOv5m model is trained using each strategy and verified on testing dataset.

2nd stage: the training and validation datasets were preprocessed using two strategies: image shuffle and mosaic augmentation. Our mosaic augmentation is different from YOLOv5 framework - it joins two parts of images, which belong to different classes, taking the left and right vertical sides of images (see Fig. 4). The Python script was written to create balanced datasets with equal proportion of each category, that was achieved by image repeating of smaller datasets.

Figure 4. Example of mosaic augmentation applied in experiment (two images joint together).

3rd stage: the YOLOv5m model was trained using the datasets preprocessed in the 2nd stage. The length of training time was 300 epochs. The default augmentation of YOLOv5 framework was modified by setting mosaic and mix-up augmentation to 0. The 2nd and 3rd stages were repeated 5 times to collect statistics for box-plot diagrams and visual comparison of obtained results.The experiment was conducted on an NVIDIA RTX 2070 GPU, which provided sufficient memory and performance for this experiment.

Accuracy comparison

Two accuracy parameters of YOLOv5 framework were applied for the quality comparison: mAP@0.5 and mAP@0.5:0.95.

$$AP_k = \int_0^1 p(r)dr, \tag{1}$$

where p – a precision; r – a recall; AP_k – an average precision of the k-th class.

$$mAP = \sum_{k=1}^{Q} \frac{AP_k}{Q}, \tag{2}$$

where mAP – a mean average precision for Q classes.

More math details can be found, for example, in the work of Wang et al. (2022).

Considering our experiment, we measured the trained YOLOv5m models on the testing datasets with only one class, therefore mAP (Eq. 2) is equal to AP (Eq. 1). In our study, the more important parameter is the difference between @0.5 and @0.5:095. The mAP@0.5 is a mean average precision for objects with Intersection over Union (IoU) greater than 0.5. Meanwhile, mAP@0.5:0.95 is means of mAP over different IoU thresholds, from 0.5 to 0.95 with step 0.05. In our case, mAP@0.5 shows the accuracy improvement, but mAP@0.5:0.95 depicts the stable object detection and classification.

RESULTS AND DISCUSSIONS

The experiment results of YOLOv5m training are depicted in Fig. 5. Looking at the results of trained YOLOv5m models, it is required to say that the results should be analysed independently for each combination of datasets, then all separate results must be summarised as the final conclusion that helps to evaluate the best training strategy to improve the accuracy of YOLOv5m.

Analysing the results of Multi-Species (see Fig. 5), where two different species of fruits were used for CNN training, it can be seen that mAP@0.5 results do not differ among image shuffle, mosaic augmentation and even the baseline results obtained in the previous study (Kodors et al., 2023). But there is a significant difference of 5.6% at mAP@0.5:0.95 for the Pear640 dataset, where the results of mosaic augmentation are significantly greater than image shuffle and the baseline results. Even the MinneApple dataset had better results with mosaic augmentation showing accuracy improvement of 2.6%. Additionally, the box-plots of mosaic augmentation results are very narrow, showing stable accuracy results regardless of the case of training.

Moving to the next case, Multi-Stage presents the results (see Fig. 5) where the same fruit in the different growth stages was looked at. The experiment shows the similar results to the previous case (Multi-Species): the lack of difference in the case of mAP@0.5 and the mAP@0.5:0.95 improvement of 6.2% in the case of mosaic augmentation for the Pear640 dataset. And the improvement of 3.9% can be seen with the PearFruitlets dataset using mosaic augmentation as well.

Analysing the last case, Multi-Species* (see Fig. 5) was the dataset where mature apples and pear fruitlets were used for the experiment. The mAP@0.5 results had insignificant differences between image shuffle and mosaic augmentation, similarly to the previous cases. However, looking at mAP@0.5:0.95 results, similarly to the previous cases, mosaic augmentation provides significant improvement of mAP@0.5:0.95 accuracy: PearFruitlets – +3.8% and MinneApple – +4.2%; compared to image shuffle strategy.

To summarise the accuracy difference among three dataset combinations, the accuracy difference was calculated using Eq. 3, the results are depicted in Table 1:

$$\Delta x = (x_1 - x_2), \tag{3}$$

where x_1 is the result accuracy of mosaic augmentation strategy; x_2 – of image shuffle.

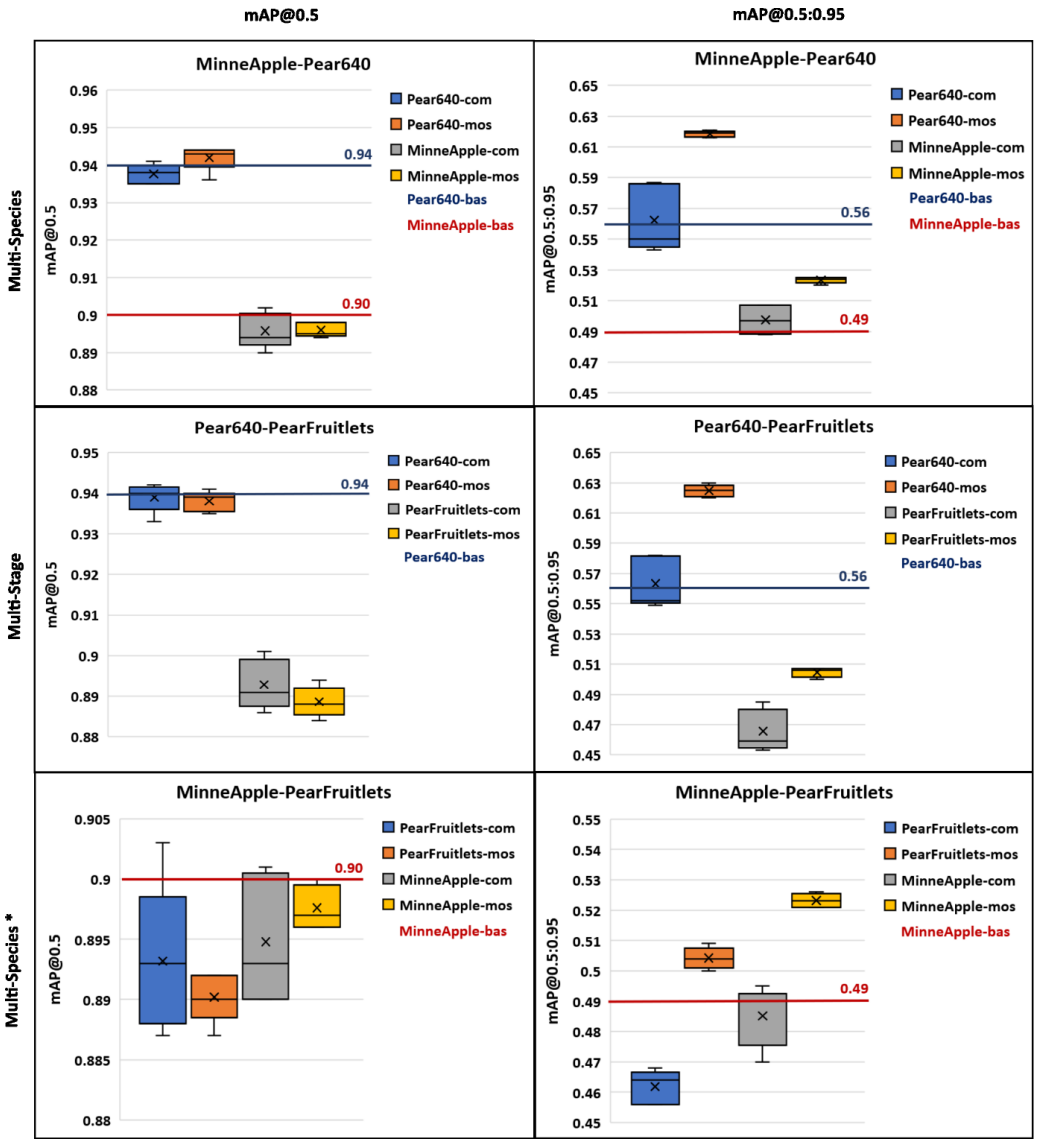

Figure 5. Experiment results of YOLOv5m training: *com* – image shuffle strategy; *mos* – mosaic augmentation strategy; *bas* – baselines obtained in previous study (Kodors et al., 2023).

In summary of all three cases, it can be seen that the mosaic augmentation made significant mAP@0.5:0.95 improvement of 4.38% (see Table 1) compared with image shuffle. Meanwhile, the mean value of mAP@0.5 difference is close to zero.

Table 1. Difference Δx calculation between mosaic augmentation (x_1) and image shuffle (x_2)

Combination	M-Species		M-Stage		M-Species*		Mean
Category	Apple	Pear	Pear	PFruitlet	Apple	PFruitlet	
mAP@0.5	0.004	0.000	-0.001	-0.004	-0.003	0.003	-0.0001
mAP@0.5:0.95	0.056	0.026	0.062	0.039	0.042	0.038	0.0438

Considering to Li et al. (2023) experiment results, the simple mosaic increased mAP@0.5 of YOLOv5s by 7.81%, that is higher than in our case. However, Sun et al. (2017) mentioned about logarithmical relation to the number of training samples. Li et al. (2023) worked in the range 70%–80% of mAP@0.5, meanwhile, our YOLOv5m worked in the range 88%-95%. Therefore, considering to logarithmic relation, our study should show smaller accuracy increase than in the case of Li et al. (2023). Ngiam et al. (2018) and Li et al. (2023) mentioned that multiple different categories improve accuracy. Comparing with Li et al. (2023), we only mixed two classes in each combination. Therefore, it would be required to continue experiment to investigate dependence on the number of combined datasets for the yield estimation. Additionally, Barman et al. (2019) mentioned that transfer-learning requires less data than training from scratch. It is useful to verify the accuracy dependence from the number of images per each dataset, which are combined for the yield estimation. That must have stronger impact in the case of small datasets, considering to logarithmical relation detected by Sun et al. (2017).

CONCLUSIONS

The goal of study was to evaluate image shuffle and mosaic augmentation strategies to select the most appropriate solution for CNN training on an agricultural image collection, which contain multiple single class datasets. The obtained results show that in all cases mAP@0.5 results are negligible as difference between image shuffle and mosaic augmentation strategies and it was close to 0 with mean difference value of -0.0001. Meanwhile, mAP@0.5:0.95 showed all results in favour of mosaic augmentation with mean difference value of 0.0438. Based on experiment results it can be concluded that the most appropriate strategy for the agricultural datasets with multiple single class sub-datasets is the usage of mosaic augmentation. Considering the baselines, which showed better results for one-class problem in the case of mAP@0.5, it can be concluded that mosaic augmentation is strongly required for YOLO CNN training to improve accuracy for the yield estimation. Additionally mosaic augmentation provides more stable accuracy results, which are training case independent.

ACKNOWLEDGEMENTS. This research is funded by the Latvian Council of Science, project 'Development of autonomous unmanned aerial vehicles based decision-making system for smart fruit growing', project No. lzp2021/1-0134.

REFERENCES

Barman, R., Deshpande, S., Agarwal, S. & Inamdar, U. 2019. Transfer Learning for Small Dataset. *In proceedings of National Conference on Machine Learning*. Amity University Mumbai, Mumbai, India, pp. 132–137.

Bochkovskiy, A., Wang, C.Y. & Liao, H.Y.M. 2020. Yolov4: Optimal speed and accuracy of object detection. arXiv preprint arXiv:2004.10934.

Chen, Y., Lee, W. S., Gan, H., Peres, N., Fraisse, C., Zhang, Y. & He, Y. 2019. Strawberry Yield Prediction Based on a Deep Neural Network Using High-Resolution Aerial Orthoimages. *Remote Sens* **11**(13), 1584. doi: 10.3390/rs11131584

Cheng, H., Damerow, L., Sun, Y. & Blanke, M. 2017. Early Yield Prediction Using Image Analysis of Apple Fruit and Tree Canopy Features with Neural Networks. *J. Imaging* **3**(6). doi: 10.3390/jimaging3010006

Chu, P., Bian, X., Liu, S. & Ling, H. 2020. Feature Space Augmentation for Long-Tailed Data. In: *Vedaldi, A., Bischof, H., Brox, T., Frahm, JM. (eds) Computer Vision - ECCV 2020. ECCV 2020. Lecture Notes in Computer Science,* vol. **12374**. Springer, Cham. doi: 10.1007/978-3-030-58526-6_41

Cruz, M., Mafra, S., Teixeira, E. & Figueiredo, F. 2022. Smart Strawberry Farming Using Edge Computing and IoT. *Sensors* **2022**(22), 5866. doi: 10.3390/s22155866

Dulal, R., Zheng, L., Kabir, M.A., McGrath, S., Medway, J., Swain, D. & Swain, W. 2022. Automatic Cattle Identification using YOLOv5 and Mosaic Augmentation: A Comparative Analysis. *2022 International Conference on Digital Image Computing: Techniques and Applications (DICTA),* 1–8. doi: 10.1109/DICTA56598.2022.10034585

Ge, Y., Lin, S., Zhang, Y., Li, Z., Cheng, H., Dong, J., Shao, S., Zhang, J., Qi, X. & Wu, Z. 2022. Tracking and Counting of Tomato at Different Growth Period Using an Improving YOLO-Deepsort Network for Inspection Robot. *Machines 2022* **10**, 489. doi: 10.3390/machines10060489

Häni, N., Roy, P. & Isler, V. 2020. MinneApple: A Benchmark Dataset for Apple Detection and Segmentation. *IEEE Robotics and Automation Letters* **5**(2), 852–858. doi: 10.1109/LRA.2020.2965061

Kodors, S., Lacis, G., Sokolova, O., Zhukovs, V., Apeinans, I. & Bartulsons, T. 2021. Apple scab detection using CNN and Transfer Learning. *Agronomy Research* **19**(2), 507–519. doi: 10.15159/AR.21.045

Kodors, S., Sondors, M., Lācis, G., Rubauskis, E., Apeināns, I. & Zarembo, I. 2023. RAPID PROTOTYPING OF PEAR DETECTION NEURAL NETWORK WITH YOLO ARCHITECTURE IN PHOTOGRAPHS. ENVIRONMENT. TECHNOLOGIES. RESOURCES, *Proceedings of the International Scientific and Practical Conference* **1**, 81–85. doi: 10.17770/etr2023vol1.7293

Li, Y., Cheng, R., Zhang, Ch., Chen, M., Liang, H. & Wang, Z. 2023. Dynamic Mosaic algorithm for data augmentation. *Mathematical Biosciences and Engineering* **20**(4), 7193–7216. doi: 10.3934/mbe.2023311

Liu, G., Nouaze, J.C., Touko Mbouembe, P.L. & Kim, J.H. 2020. YOLO-Tomato: A Robust Algorithm for Tomato Detection Based on YOLOv3. *Sensors* **20**(7), 2145. doi: 10.3390/s20072145

Liu, J., Wang, X., Zhu, Q. & Miao, W. 2023. Tomato brown rot disease detection using improved YOLOv5 with attention mechanism. *Frontiers in Plant Science* **14**. doi: 10.3389/fpls.2023

Lyu, S., Li, R., Zhao, Y., Li, Z., Fan, R. & Liu, S. 2022. Green Citrus Detection and Counting in Orchards Based on YOLOv5-CS and AI Edge System, *Sensors* **22**(2), 576. MDPI AG. doi: 10.3390/s22020576

MacEachern, C.B., Esau, T.J., Schumann, A.W., Hennessy, P.J. & Zaman, Q.U. 2023. Detection of fruit maturity stage and yield estimation in wild blueberry using deep learning convolutional neural networks, *Smart Agricultural Technology* **3**. doi: 10.1016/j.atech.2022.100099

Moravec, D., Komárek, J., Kumhálová, J., Kroulík, M., Prošek, J. & Klápště, P., 2017. Digital elevation models as predictors of yield: Comparison of an UAV and other elevation data sources. *Agronomy Research* **15**(1), 249–255. Available at https://agronomy.emu.ee/wp-content/uploads/2017/03/Vol15Nr1_Moravec.pdf

Ngiam, J., Peng, D., Vasudevan, V., Kornblith, S., Le, Q. & Pang, R. 2018. Domain Adaptive Transfer Learning with Specialist Models. Available at https://arxiv.org/pdf/1811.07056.pdf

Parico, A.I.B. & Ahamed, T. 2021. Real Time Pear Fruit Detection and Counting Using YOLOv4 Models and Deep SORT. *Sensors* **21**, 4803. doi: 10.3390/s21144803

Phan, Q.-H., Nguyen, V.-T., Lien, C.-H., Duong, T.-P., Hou, M.T.-K. & Le, N.-B. 2023. Classification of Tomato Fruit Using Yolov5 and Convolutional Neural Network Models. *Plants* **12**(4), 790. MDPI AG. doi: 10.3390/plants12040790

Redmon, J., Divvala, S., Girshick, R. & Farhadi, A. 2016. You only look once: Unified, real-time object detection. In: *Proceedings of the IEEE conference on computer vision and pattern recognition*, pp. 779–788. Available at https://arxiv.org/abs/1506.02640

Redmon, J. & Farhadi, A. 2017. YOLO9000: better, faster, stronger. In: *Proceedings of the IEEE conference on computer vision and pattern recognition*, pp. 7263–7271. Available at https://arxiv.org/abs/1612.08242

Rotshtein, P., Henson, R., Treves, A., Driver, J. & Dolan, R. 2004. Morphing Marilyn into Maggie dissociates physical and identity face representations in the brain. *Nat Neurosci* **8**, 107–113. doi: 10.1038/nn1370

Summers, C. & Dinneen, M.J. 2019. Improved mixed-example data augmentation. In: *2019 IEEE winter conference on applications of computer vision (WACV)*, pp. 1262–1270. Available at https://arxiv.org/abs/1805.11272

Sun, C., Shrivastava, A., Singh, S. & Gupta, A. 2017. Revisiting Unreasonable Effectiveness of Data in Deep Learning Era, In: *2017 IEEE International Conference on Computer Vision (ICCV)*, Venice, Italy, pp. 843–852. doi: 10.1109/ICCV.2017.97

Tian, Y., Yang, G., Wang, Zh., Li, E. & Liang, Z. 2019. Detection of Apple Lesions in Orchards Based on Deep Learning Methods of CycleGAN and YOLOV3-Dense. *Journal of Sensors* **2019**. doi: 10.1155/2019/7630926

Vijayakumar, V., Ampatzidis, Y. & Costa, L. 2023. Tree-level citrus yield prediction utilizing ground and aerial machine vision and machine learning. *Smart Agricultural Technology* **3**. doi: 10.1016/j.atech.2022.100077

Wang, L., Zhao, Y., Xiong, Z., Wang, S., Li, Y. & Lan, Y. 2022. Fast and precise detection of litchi fruits for yield estimation based on the improved YOLOv5 model. *Frontiers in Plant Science* **13**, doi: 10.3389/fpls.2022.965425

Web (a) PFruitlet640 dataset.
Available at https://www.kaggle.com/datasets/projectlzp201910094/pfruitlet640

Web (b) Ultralytics, YOLOv5-7.0 GitHub repository. Available at https://github.com/ultralytics/yolov5

Agronomy Research **22**(1), 180–189, 2024
https://doi.org/10.15159/AR.24.006

Agro-biological evaluation of different groundnut (*Arachis hypogaea* L.) varieties on the background of phosphorous-potash fertilizers in conditions of semi-desert soil zone

L.G. Matevosyan*, A.A. Barbaryan, R.H. Ghazaran, A.G. Ghukasyan, M.H. Galstyan and S.S. Harutyunyan

Scientific Centre of Agriculture, Isi-le-Mulino 1, AM1101 Ejmiatsin, Armavir region, Armenia
*Correspondence: lusnyak.matevosyan81@mail.ru

Received: October 25th, 2023; Accepted: January 12th, 2024; Published: January 26th, 2024

Abstract. In conditions of semi-desert soil zones of Armenia (1,130 m high above the sea level) the agro-biological properties of groundnut varieties Lia, Virginia, Mocket, TMV 3, Sevahatik (Black Seed) and Chinese have been studied with the aim of selecting their best options for further regionalization in the piedmont zones. The field experiments were conducted in 2020–2022. The calculations and laboratory analyses have indicated that the field germination capacity of the mentioned varieties is rather high fluctuating within the range of 77.5–81.0%, whereas the weight of 1,000 grains equaled to 515–545 g, the average yield - 2.77–3.33 t ha^{-1}, the total nitrogen in the grains were 4.39–4.61%, crude proteinhnıմ (per 5.70 factor of nitrogen) - 25.02–26.28%, total sugar contents - 14.11–16.63%, and fat content - 44.8–48.0%. The Mocket and Chinese varieties were distinguished by their yield capacity and qualitative indices of the yield and thus, the latter have been recommended for the cultivation in the farm households of the mentioned zone.

Key words: grondnut, variety, yield, quality.

INTRODUCTION

In the intensive and organic agricultural systems the permanent application of crop rotation technique is pivotal to ensure soil fertility recovery and to overcome soil fatigue. In this respect the perennial and annual *Fabaceae* plants have exceptional role. Lucerne, sainfoin, trifolium, lupine, ornithopus /common bird's-foot/, chickpea, lentil, pea, bean, soy, groundnut, etc. not only enrich the soil with biological nitrogen, but they are also directly connected with the production of plant and animal protein so important for humanity.

In the croplands of lucerne and trifolium 150–200 kg ha^{-1} N is accumulated annually, whereas in those of annual *Fabaceae* plants - 50–100 kg ha^{-1}, since their root system is unable to get so much strength, as that of the perennial plants (Orlova & Litvak, 1983). Nitrogen accumulated by different genotypic forms of pea (*Pisum sativum* L.) in meadow-black soil conditions of Western Siberia ensured high wheat yield and high

protein content in grain for about 3 years (Nazaryuk et al., 2016). In the Ukrainian soils with low humus content the chickpea plants have fixed 109–288, soybeans - 264–312, while the *Lucerne/alfalfa* - 486 kg ha^{-1} N. In the options without the mentioned *Fabaceae* plants, the nitrogen fixation made about 9%, against the afore stated indices (Tanchyk, et al., 2021).

According to the European Food Program, it is necessary to increase the production of food rich in plant protein, the demand for which is increasing parallel to the growth of the world population, whereas the proteins in the cereal and leguminous plants are evidently indispensable for mankind (Nigam et al., 2004).

In Armenia the leguminous crops are cultivated in limited areas, and the groundnut cultivation started in the last 23 years, whereas for crop rotation, as well as from the point of view of food and ecological security of the country they are critically significant, as it concerns the full supply of the population with plant food products (Matevosyan, 2014, Galstyan & Matevosyan, 2015). To meet the optimal demand of the organism for proteins, fats and carbohydrates, their ratio in the human diet should be 1:1.2:4. Moreover, the proteins in the energy portion of the diet should make 12%, fats - 30–35%, and the rest part is complemented with carbohydrates. According to medicinal justifications the daily intake of total proteins is 100–120 g, the annual optimal intake - 35 kg, out of which 21 kg should be animal proteins. Upon the breakdown of 1 g protein 4 kkal energy is released, from 1 g fat - 9 kkal energy and from 1 g carbohydrate - 4 kkal energy is released (Harutyunyan & Sargsyan, 2018).

Among the leguminous crops, the groundnut is a leading oilseed crop, the seeds of which contains 40–60% fat, 30–37% protein, 26–28% crude protein, while the groundnut cake/pomace produced from the seed contains 8% fat. Groundnut also stands out for its rather high digestibility, as well as for the full amino acid content. The percentage of essential amino acids (tryptophan, phenylalanine, methionine, lysine, valine, leucine, threonine, isoleucine) in the proteins is also rather high (Hammons, 1980, Kishlyan et al., 2020). Groundnut is cultivated in the tropical and subtropical regions. The world production of groundnut in 2015 was 37,535,000 tons. China is the largest producer of groundnut - 16,500,000 tonnes (43% of world production), followed by India (11.9%), Nigeria (8%), the United States (7.5%) and Sudan (4.9%) (Stalker, 2017).

Intensification in the symbiotic function of groundnut occurs at the flowering stage, during which plants actively absorb nitrogen from the atmosphere. All tuber bacteria that enter into a symbiotic relationship with leguminous crops belong to the genus *Rhizobium* (Arrendelle et al., 1988, Basu, 2011). Being fed with nitrogen, groundnut badly needs phosphorus and potassium. If the phosphorus content is low in the soil, the tuber bacteria migrate into the plant roots but don't form tubercles. Air nitrogen fixation occurs with the participation of ATP, the main energy supplier of which is phosphorus. In conditions of phosphorus deficiency, small amount of ATP is formed and air nitrogen is poorly fixed. Nitrogen-fixing activity is also due to the high potassium content, which accounts for the high demand of groundnut for this nutrient, as it ensures the constant movement of carbohydrates from the leaf to the tuber (Jana et al., 1990). A higher yield of early-ripening soybean cultivars in typical black soils of the forest-steppe zone of Ukraine is obtained by the application of $N_{60}P_{60}K_{60}$ pattern when the seeds are treated with rhizobium. Further increase of nitrogen doses (N_{90}, N_{120}, N_{150}, N_{180}) on the plants roots inhibits the development of tuber bacteria (Kalenska et al., 2022).

Groundnut is a non-traditional crop for Armenia, but the climatic conditions of several agricultural zones are favorable for the cultivation of this valuable crop. The lack of high-yielding, early-maturing varieties has been an obstacle to the expansion of groundnut croplands. The only variety cultivated in the republic (Meghri local) has a long vegetation period and is cultivated in the Meghri region with favorable climatic conditions for that variety (630–700 m above sea level), so there is a need for the individual selection of new high-yielding varieties from the global collection of peanuts, which is a relatively quick and available method (Matevosyan et al., 2020). Scientific research activities on the groundnut cultivation have been mainly carried out in conditions of the Ararat valley in the territory of production-experimental farm (853 m high above sea level) at the Scientific Center of Agriculture, since 2000. As a result of the research, varieties with best biological and economic characteristics were selected, which showed high adaptability in the given zone, and some of them were tested in different zones after receiving the status of variety, meanwhile the early-mature variety 'Lia' was also registered in the RA State Register of Selection Achievements in 2015 (registration N 28-L).

Purpose of the research and problems

The aim of the research is to study 5 varieties, identified by the individual selective method from 80 groundnut variety samples of the International Crops Research Institute for the Semi-Arid Tropics (*ICRISAT*) and tested in conditions of Ararat valley, and to test them also in conditions of piedmont zones, to identify their yield capacity against the Lia variety, disclose their qualitative properties and to recommend the selected varieties to the production, which would promote the expansion of groundnut croplands also in conditions of piedmont subzones of semi-desert soil zone, which will be partially involved in the crop rotation alternations of cereal crops. Within the frame of the above stated goal the similar sowing rates and density has been observed, against this background calculation of yield structural elements and analysis of qualitative indicators has been conducted in view of maturation times of the varieties.

Materials and methods

The field expriments were carried out within the period of 2020–2022 years, in the semi-desert soil zone (800–1,250 m high above sea level) on the Virginia, Mocket, TMV 3, Sevahatik, Chinese variety samples, the yield and qualitative indices of which were compared with Lia variety the latter coming forth as a control variant. The experimental pattern of the varieties is introduced in the Table 2–6. The studies were conducted in the land areas near Ashtarak city in the Aragatsotn region/marz, 1,130 m high above sea level on the soils belonging to the light brown subtype. The experiment was set up in 3 replications (70 m^2 each replication) with 70×25 cm feeding area, i.e., 6 plants per 1 m^2. The yielding capacity of the groundnut depending on the plants' density is a very important issue, which has been studied by multiple researchers. In regular conditions the density of plants varies within the range of 4–10 plants per m^2, in case of which the highest ield capacity is ensured. Higher densities than the afore stated range do not increase the yield capacity of pods, whereas in case of the density lower than 4 plants per m^2, yield capacity decline is observed (Morla et al., 2018).

In the experimental years the sowing was implemented in the second decade of April, at the depth of 6–8 cm. During the autumn ploughing the experimental plot was fertilized with the phosphorus-potassium fertilizers with $P_{80}K_{120}$ kg ha^{-1} dosage, as a general background. Before sowing the seeds were subjected to pre-sowing treatment in the 0.5% water solution of carbon + growth stimulant keeping them for 24 hours. Carbon plus stimulator is an organic fertilizer derived from active carbon compounds that contains many components. It contributes to the active development of the root system, promotes the emergence of hair roots, which results in the increase of roots feeding area, absorption of greater amounts of nutrients and moisture from the soil and their active movement from the root to the stem. As a result of all these the yield capacity of the crops and resistance towards high and low temperatures increase (http://agroservice.am/hy/product/504).

The overall area of the experimental plot made 0.2 ha, where the experimental/tested varieties per their replications took up 1,260 m^2, whereas in the other 740 m^2 land area nurseries for the breeding of Lia and Mocket varieties were established. The fall and spring soil cultivation, sowing and weed control during the vegetation period were implemented through the agro-technological methods developed for groundnut cultivation. To struggle against weeds, Gesagard herbicide with 3.5 L ha^{-1} dosage (solution volume- 600 L ha^{-1}) was sprayed across the experimental plot after the first watering. The investigations have indicated that weeds become serious threats in the period of groundnut crops formation. The weed biomass slows down the penetration of groundnut genophores into the soil, interferes with the process of pods maturation, which increases the yield loss amounts (Grichar et al., 2015).

The irrigation water source is the Arzni-Shamiram canal, which starts from Lake Sevan. During the vegetation period the plants were irrigated 6 times (600 m^3 ha^{-1} watering rate), irrigation rate - 3,600 m^3 ha^{-1}. Harvest was carried out in the second decade of October (70 m^2 total yield and qualitative indicators of all replications were estimated).

The climate in this region is rather dry with cold winters and warm summers. The sum of active temperatures (higher than 10 °C) amounts to 3,300–3,800 °C, average annual air temperature is 10.9 °C, maximum temperature - 41 °C, minimum - 29 °C. The annual precipitation amount makes 300–400 mm, annual evaporation deficit is 680 mm, Shashko's humidity coefficient - 0.07–0.15. The crops can't grow in this zone without artificial irrigation (Agroclimatic resources of Armenia, edited by R.S. Mkrtchyan et al., 2011).

During the vegetation, hilling and loosening activities for the plants were conducted thrice, which is not only aimed at the mechanical weed control but it also promotes the penetration of more genophores into the soil developing higher number of pods, which is the main guarantee for getting high groundnut yield. At the shrubbing stage, prior to watering, the plants were treated with foliar feeding through the fulvomix bio-liquid fertilizer with 9 L ha^{-1} dosage (600 L ha^{-1}). Fulvomix fertilizer contains fulvic acids, macro-micro nutrients, as well as amino acids. It strengthens the root system of plants, restores soil microflora (https://brand.am/products/?l =e&barcode=5852886000118).

During the vegetation period phenological observations and biometric measurements were conducted. After harvesting, the yield structural elements in the laboratory conditions were determined. The yield capacity of the varieties was calculated

by weighing the total yield of the experimental bed. The laboratory analysis of the soil and plant was conducted with the general methods (Arinushkina, 1970, Yagodin, 1987). The soil mechanical composition was determined through the classic pipette method and estimated according to the Kachinskiy's grading scale. The hygroscopic humidity was determined through weighing method, pH in the water extract - with potentiometer, humus content - per the method of I.V. Turin, total nitrogen - pe the Kjeldahl's method, mobile nirogen forms - per the methods of I.V. Turin and M.M. Kononova and the phosphorus content - according to the Machigin's method.

The results of yield amount were subjected to mathematical processing according to the method of dispersion analysis by the calculation of the least significant difference (*LSD*) and the relative error of the experiment- Sx, % (Dospekhov, 1985). The crude protein content in legumes according to the total nitrogen determination (Peterburgsky, 1968). Fats were determined by the extraction method with the Soxhlet apparatus (Yagodin, 1987).

In the samples of the average grain the contents of dry matters, crude protein, total sugar and fats were determined in the laboratory of Organic Agriculture at the Armenian National Agrarian University (ANAU).

RESULTS AND DISCUSSION

The land area is a homogeneous plane, and soil sampling was done in the central part of the experimental field from the A and B horizons, taking into account the depth of the groundnut root (*rhizosphere*) distribution (Table 1).

Table 1. Physico-mechanical and agrochemical characteristics of test/experimental site soils

Genetic horizon and depth, cm	< 0.01 mm - sum of particles (phys. clay), %	Hygroscopic humidity, %	Humus, %	The pH of the water draft	Total N, %	Mobile forms mg per 100 g in the soil		
						N	P_2O_5	K_2O
A 0–19	34.2	4.2	2.1	7.7	0.09	4.0	3.0	26.0
B 19–35	39.0	4.7	1.9	8.2	0.07	3.9	2.8	22.5

The table data show that the mechanical composition of the experimental plot is mid clay and sandy, where the physical clay makes 34.2–39.0%, (Soil science edited by J.S. Kaurichev, 1982), hygroscopic humidity is 4.2–4.7% (which is typical to the light brown soils), pH of water extract is basic/alkaline (7.7–8.2), humus content in the accumulative layers fluctuates within 1.9–2.1%, total nitrogen - 0.07–0.09%, the content of available nutrients per the respective scales is characterized by the average indicators (Yagodin, 1987).

Groundnut is a light-demanding plant. Seeds start sprouting in 10–12 °C heat conditions. The sprouts withstand up to - 0.5–1 °C. For the regular growth of the plants 25–28 °C temperature is required. Plants need maximum temperature in the flowering and fruit formation period. Plants are hardy towards the autumn heat up to 0.5 °C, while in conditions of 3 °C they dry out. The seeds harvested under these conditions, which don't get dry in natural way, are characterized with low germination capacity and are unfit as seeds. And the seeds harvested under the conditions of 4 °C become unfit for processing (Taille, 1997). Groundnut can grow under insufficient moisture conditions from the germination to the blossoming period, anyhow, in the period of fruit formation

its soil moisture demand is extremely high. The critical stage of moisture demand starts 25–30 days after germination and lasts about 2–3 months. Throughout this period the 20 cm soil layer should be provided with moisture. By the end of vegetation this demand declines and starting from September the water excess can retard the fruit maturation (Roy et al., 1988).

The duration of groundnut vegetation period depends on the varietal characteristcs, cultivation place and climatic conditions. In favorable climatic conditions the sprouts emerge 8–10 days after sowing. After 25–30 days of sprouting, plants enter the flowering stage, which lasts up to the harvesting period. First, the flowers of lower part of stem are developed. Parallel to flowering, the groundnut vegetative part and pods grow up. Such a combination of growing stages is related to the plants demand for moisture and nutrients, particularly at the mass flowering and fruit formation stages. The period from flowering to fruit maturation lasts 1.5–2 months (Colvin et al., 1988).

The vegetation duration of the varieties (Table 2) indicates, that the sprouting stage of the Mocket and Chinese varieties was observed simultaneously with the control variety of Lia and lasted 13 days, while TMV-3 and Sevahatik (black seed) varieties stay behind the Lia variety by 2 days and Virginia variety - by 3 days.

Table 2. Vegetation duration of experimented groundnut varieties, day

Varieties	From seeding to sprouting	From sprouting to			
		bush formation	flowering	pod formation	pod maturation
Lia (control)	13	15	34	90	179
Virginia	16	17	32	94	189
Mocket	13	13	24	83	172
TMV - 3	15	15	25	86	174
Sevahatik	15	15	25	85	176
Chinese	13	13	24	83	172

The bush formation stage in the Mocket and Chinese varieties started 2 days earlier as compared to Lia variety; in Sevahatik and TMV-3 varieties the bush formation period took place simultaneously with that of the control variety, whereas in Virginia variety it was 5 days later. The pod formation phase in the tested varieties fluctuated within 83–86 days compared to Lia variety, except from the Virginia variety, in case of which the mentioned phase started 4 days later than that of the control variant. At this stage again Mocket and Chinese varieties stand apart, since the pod formation stage in these varieties also started earlier.

As a result, in the tested Mocket and Chinese varieties (except from Virginia variety) the pod formation stage was reduced by 7 days and in case of TMV-3 variety - by 5 days, whereas in case of Sevahatik variety - by 3 days. Virginia variety ripens 10 days later than the control variant, whereas 8–12 days later than the other varieties.

Thus, it can be clearly stated, that the experimented Mocket and Chinese varieties, which can avoid early autumn frostbite in climatic conditions of piedmont zones, are distinguished by early maturation and provide high yield.

The studies have indicated that the tested varieties compared to the Lia variety are endowed with higher laboratory and field sprouting/germination ability (Table 3).

The data of Table 3 show that the laboratory germination of the varieties fluctuates within 85.0–88.0% (in the control variant - 84.0%), while the field germination - within 78.5–81.0% (in the control variant - 77.5%). Hence, as compared to Lia variety the laboratory and field germination ability of the studied varieties is slightly higher.

Table 3. Biological indicators of groundnut varieties in conditions of piedmont zones

Varieties	Laboratory germination		Field germination	
	n	%	n	%
Lia (control)	100	84.0	310	77.5
Virginia	100	85.0	314	78.5
Mocket	100	88.0	324	81.0
TMV - 3	100	86.0	320	80.0
Sevahatik	100	85.0	319	79.7
Chinese	100	87.0	322	80.5

In terms of groundnut yield efficiency increase, bush-type varieties are considered more valuable, which differ from the standing varieties by their biological, morphological and economic features. In the bush-type varieties the genophores resulted after flowering, are usually close to the soil and just by slightly bending are able to easily enter in the soil and develop pods (Patil et al., 1988).

The research results have also indicated that Lia groundnut variey is a rather self-righting variety, it is distinguished by the height of the plants (46.3 cm), which complicates the process of genophores migration into the soil. Mocket, TMV-3 and Sevahatik varieties were of average height (33.6–36.7 cm). The lowest height (30.5 cm) was recorded in the Chinese variety (Table 4).

The study results of the yield structural elements in the piedmont zone have testified, that the mentioned varieties differ from each other in these indicators; as a result different yield amounts are recorded. Thus, the data of Table 4 show, that Mocket and Chinese varieties stand out for the number and weight of plants pods (Table 4). In Mocket variety these indexes have made 98.2 n, and 72.6 g, while in Chinese variety - 91.6 n and 71.9 g, respectively. It should be mentioned, that pods containing 2 grains are prevailing in the Mocket and Chinese varieties.

Table 4. Biological indicators and yield structural elements of groundnut varieties

Varieties	Plans height, cm	Number of stems, n	Per 1 plant				Weight of 1,000 seeds, g
			number of pods, n	weight of pods, g	number of grains/seeds in a pod, n	g	
Lia (control)	46.3	9.3	87.3	70.8	262.0	133.6	515
Virginia	32.2	10.3	90.7	69.9	179.8	106.0	520
Mocket	32.6	12.1	98.2	72.6	206.2	112.3	545
TMV - 3	32.3	11.0	89.0	70.6	179.2	99.3	525
Sevahatik	36.7	10.2	86.5	69.1	169.3	89.7	508
Chinese	30.5	11.8	91.6	71.9	183.2	110.7	535

Besides, the mentioned two varieties exceed the other ones by the grain size. Lia variety exceeds Mocket, Chinese, TMV and Sevahatik varieties by the seeds number per a pod (262 n), though Lia variety concedes the mentioned varieties by the number of pods (87.3 n). This is accounted for the fact that Lia variety has small seeds and mostly develops pods with 2–3 and often 4 grains, which promotes the increase of grains weight in a pod. There is almost no difference between the Virginia and TMV-3 varieties

regarding the yield structural elements, as a result of which equal amounts of yield was developed (3.0 and 3.02 t ha^{-1}). It is also necessary to mention, that pods with 2 grains/seeds prevail in these varieties as well. Sevahatik variety lags behind the other varieties by the number of pods (86.5 n), number of grains per pod (169.3 n) and grains weight (89.7 g).

In the piedmont zone the highest yield capacity and best properties were recorded in the Mocket (3.33 t ha^{-1}) and Chinese (3.28 t ha^{-1}) varieties (Table 5).

Table 5. The yield of groundnut varieties per years

Varieties	Yield t ha^{-1}			Average yield, t ha^{-1}	Yield surplus, t ha^{-1}
	2020	2021	2022		
Lia	2.95	3.00	3.03	2.99	--
Virginia	3.00	3.02	2.99	3.00	--
Mocket	3.32	3.39	3.28	3.33	0.33
TMV3	3.02	2.98	3.00	3.02	0.02
Sevahatik	2.78	2.80	2.74	2.77	--
Chinese	3.25	3.32	3.27	3.28	0.28
Sx, %	5.86	1.29	1.31	0.54	
*$LSD_{05,\ t}$	0.56	0.13	0.13	0.16	

*LSD_{05} – least significant difference.

The study of the grain qualitative properties is significant for the evaluation of leguminous crops (groundnut) efficiency. The content of protein in this crop grain is mostly related to the symbiotic nitrogen fixation efficiency. It is also known, that protein content in grain is related to a number of other factors, such as genotype of the variety, soil and climatic conditions, plants supply with nutrients, particularly with nitrogen, etc. (Babayan, 1980, Onianu, 1981).

Considering the primary significance of protein for the grain quality evaluation, the content of crude protein in the grain of the studied groundnut varieties has also been identified (Table 6). The crude protein in the grain was determined based on the determination of nitrogen by the Kjeldahl's method, then the nitrogen content was multiplied by 5.70.

Table 6. Qualitative indicators of the groundnut varieties

Varieties	Dry matters, %	N, %	Crude protein, %	Total sugar, %	Fat, %
Lia	94.41	4.48	25.54	14.11	44.79
Virginia	94.38	4.40	25.08	15.47	44.88
Mocket	95.21	4.60	26.22	16.63	47.62
TMV-3	94.51	4.47	25.48	15.29	46.67
Sevahatik	93.80	4.39	25.02	15.11	45.43
Chinese	94.89	4.61	26.28	16.55	47.97

The data of the Table indicate that Virginia, TMV-3 and Sevahatik varieties stand behind the Lia variety in crude protein amount. Hence, the crude protein amount in Lia variety has made 25.54%, whereas in Sevahatik, Virginia and TMV-3 varieties - 25.02, 25.08 and 25.48%, respectively. The discussed varieties have exceeded Lia variety (14.11%) by the total sugar content, while in other varieties this index fluctuated within 15.11–16.63%. Upon the results of multiple research works, it has been disclosed that 1–2% fat is accumulated in the grain of leguminous crops (cicer, lentil), anyhow the soybean and groundnut come forth as an exception in which 10–25% and 50% fat is accumulated, respectively.

The studies have indicated that in the grains of Virginia variety fat amount almost equal to that of Lia variety (44.88%) or by 0.09% more fats ate accumulated. All the other varieties were distinguished by high fat content: 45.43 to 47.97%. In the control variant this index makes 44.79%.

CONCLUSION

1. The climatic conditions of piedmont sub-zone at the Armenian semi-desert soil belts are quite favorable for the cultivation of groundnut varieties. The average 3-year yield amount for the studied groundnut varieties has fluctuated from 2.77 (Sevahatik) to 3.33 t ha^{-1} (Mocket), besides, as compared to Lia variety, significant yield difference was observed only in the Mocket and Chinese varieties (LSD_{05} -0.16 tons).

2. Among the experimented varieties Mocket and Chinese varieties stand out for their early-ripening characteristics. The latter can avoid early fall frostbites in the climatic conditions of piedmont zones, thus, ensuring high yield.

3. The studied varieties slightly differed from each other by their crude protein and fat content, whereas the content of total sugars in the tested varieties exceeded that of Lia variety by 1–2.44%.

4. Groundnut cultivation is a great problem in irrigated conditions, which is related to the struggling measures taken against the weed vegetation, since their above-ground mass and root system have an allelopathic (antibiosis) impact on the crops.

ACKNOWLEDGEMENTS. The work was supported by the Science Committee of RA, in the frames of the research project No. 21T-4B046.

REFERENCES

Agroclimatic resources of Armenia edited by R.S. Mkrtchyan, D.H. Melkonyan & V.H. Badalyan, 2011. Yerevan, 41–49 (in Armenian).

Arinushkina, E.B. 1970. *Guideline to chemical analysis of soils*. M. Publishing house of Moscow State University, 487 pp. (in Russian).

Arrendell, S., Wynne, J.C., Elkan, G.H. & Schneeweis, T.J. 1988. Selection for nitrogen-fixing ability in early hybrid generations of peanuts. (USA), *Peanut Science* **15**(2), 90–93.

Babayan, G.B. 1980. *Balance of nitrogen, phosphorus and potassium in the agriculture of the Armenian SSR*. Yerevan, pp. 13–180 (in Russian).

Basu, T.K. 2011. Effect of Cobalt, Rhizobium and Phosphobacterium Inoculations on Growth, Yield, Quality and Nutrient Uptake of Summer Groundnut (Arachis hypogaea). *American Journal of Experimental Agriculture* **1**(1), 21–26.

Colvin, D.L., Brecke, B.J. &Whitty E.B. 1988. Tillage variables for peanut production. *Peanut Science* **15**(2), 94–97.

Dospekhov, B.A. 1985. *Methodology of Field Practice*. Agropromizdat, Moscow, pp. 207–248 (in Russian).

Galstyan, M. & Matevosyan, L. 2015. *Evaluation of groundnut cultivars by yieldindices and economic efficiency.* Bulletin of National University of Armenia, №4, 5–9 (in Armenian).

Grichar, J.W., Dotray, P.A. & Etheredge, L.M. 2015. Weed Control and Peanut (Arachis hypogaea L.) Cultivar Response to Encapsulated Acetochlor. *American Peanut Research and Education Society,* **42**(2), *Peanut Science,* 100–108.

Hammons, R.O. 1981. Research and increased costs in getting high peanut yields in the United States. *Proc. Int. Workshopgroundnuts*, Patancheree, 13–17 Oct. 1980, AnghraPradesh, pp. 40–43.

Harutyunyan, S.S. & Sargsyan, K.Sh. 2018. *Ecological security*, pp. 266–281 (in Armenian).

Jana, P.K., Barik, A. & Chatak, S. 1990. The influence of mineral fertilizers on the groundnut yield and yield structure of the peanut crop. *Indian J. Agr. Sc*. **60**(1), 49–51.

Kalenska, S., Novytska, N., Kalenskii, V., Garbar, L., Stolyarchuk, T., Doctor, N., Kormosh, S. & Martunov, A. 2022. The efficiency of combined application of mineral fertilizers, inoculants in soybean growing technology, and functioning of nitrogen-fixing symbiosis under increasing nitrogen rates. *Agronomy Research* **20**(4), 730–750.

Kishlyan, N.V., Bemova, V.D., Matveeva, T.V. & Gavrilova, V.A. 2020. Biological peculiarities and cultivation of groundnut (a review). *Proceedings on applied botany, genetics and breeding* **181**(1), 119–127 (in Russian).

Matevosyan, L.G. 2014. Comparative efficiency of groundnut cultivars under the conditions of the Ararat valley. *Agriscience* **3–4**, Yerevan, 122–125 (in Armenian).

Matevosyan, L.G., Barbaryan, A.A. & Avetisyan, S.G. 2020. The Comparative Efficiency in the Cultivation of New Groundnut Varieties in the Piedmont Zones of Armenia. *Agriscience and Technology* **3**(71), 56–59 (in Armenian).

Morla, F.D., Giayetto, O., Fernandez, E.M., Cerioni, G.A. & Cerliani, C. 2018. Plant density and peanut crop yield (Arachisypogaea) in the peanut growing region of Córdoba (Argentina). *American Peanut, Research and Education Society* **45**(2), Peanut Science, 82–86.

Nazaryuk, V.M., Kalimuullina, F.R. & Klenova, M.I. 2016. Aftereffect of biological nitrogen fixed by different pea genotypes. *Agrochemistry* **5**, 3–10 (in Russian).

Nigam, Sh.N., Giri, D.I. & Reddy, A.G.S. 2004. Groundnut Seed Production Guideline. *Int. Research Institute of Plant Production for Semi-Arid Tropics*, India, 32 pp. (in Russian).

Onianu, O.G. & Margvelashvili, G.N. 1981. Balance of nitrogen, phosphorus and potassium and the use of fertilizers in agriculture of the SSR Countries for 1976–1979 years. *Regulation of soil fertility, cycle and balance of nutrients in agriculture of the USSR: Thesis Report. Pushchino*, pp. 112–114 (in Russian).

Orlova, A.N. & Litvak, Sh.I. 1983. *From nitrogen to yield*. Moscow, Publication, pp. 24–29 (in Russian).

Patil, R.B., Bharud, R.W. & Pokharkar, S.M. 1988. Comparative assessment of the damage degree to peanut seeds during manual and machine plowing (India). *Seed Research* **16**(1), 112–113.

Peterburgsky, A.V. 1968. *Workspon on agronomocal chemistry*. Kolos, Moscow, pp. 99–112 (in Russian).

Roy, R.C., Stonehouse, D.P., Francois, B. & Brown, D.M. 1988. The influence of water deficit during the vegetation period on the yield and quality of groundnut pods in the south of the province Ontario (Canada). *Peanut Science* **15**(2), 85–89.

Soil science edited by J.S. Kaurichev. 1982. Kolos, Moscow, pp. 25–30 (in Russian).

Stalker, 2017. Utilizing Wild Species for Peanut Improvement. *Crop Science* **57**(3), 110–1120.

Taille De La 1997. Le nouream plan proteins Vegetables. *Oleoscope* **40**, 7–8.

Tanchyk, S., Litvinov, D., Butenko, A., Litvinova, O., Pavlov, O., Babenko, A., Shpyrka, N., Onychko, V., Masyk, I. & Onychko, T. 2021. *Fixed nitrogen in agriculture and its role in agrocenoses. Agronomy Research* **19**(2), 601–611.

Yagodin, B.A. 1987.*Workshop on agricultural chemistry*. Agropromizdat, Moscow, 512 pp. (in Russian).

http://agroservice.am/hy/product/504

https://brand.am/products/?l=e&barcode=5852886000118

Agronomy Research **22**(1), 190–206, 2024
https://doi.org/10.15159/AR.24.015

Balance and coefficients of usage of nitrogen, phosphorus and potassium from the soil and fertilizers by tomatoes and peppers in the conditions of Ararat Plain of Armenia

L.G. Matevosyan, S.S. Harutyunyan*, M.H. Galstyan, R.H. Osipova, A.T. Mkrtchyan, K.Sh. Sargsyan and R.R. Sadoyan

Scientific Centre of Agriculture, Iss- Le- Mulino 1, AM 1101, Ejmiatsin, Armavir region, Armenia
*Correspondence: ss_harutyunyan@mail.ru

Received: October 25th, 2023; Accepted: January 12th, 2024; Published: March 28th, 2024

Abstract. The aim of the research is to reveal the biological removal, balance and coefficient rates of nitrogen, phosphorus and potassium use from soil, organo-mineral fertilizers and microbiological concentrates by tomato and sweet pepper in the conditions of Ararat Plain of Armenia. Field experiments were carried out in 2017–2019, on typical irrigated meadow brown soils in triplicate. It has been established that at tomato yields of 50–75 t ha^{-1}, the biological removal of nitrogen ranges from 110 (without fertilizers) to 178 kg ha^{-1} ($N_{150}P_{80}$), P_2O_5: 61–89, K_2O_5: 166–289 kg ha^{-1}, and at pepper yields of 23–32 t ha^{-1}, respectively - 55–76, 38–49 and 77–106 kg ha^{-1}. Tomato utilization rates from the soil (unfertilized version) are: N: 118, P_2O_5: 37, K_2O: 8%, and the negative balances are respectively: 107, 67 and 109 kg ha^{-1}, similar data for pepper were recorded at: N: 59, P_2O_5: 23, K_2O: 4% and 52, 44, 20 kg ha^{-1}. From fertilizers, tomato absorbs 27–45% nitrogen, 11–48% P_2O_5 and 48–72% K_2O with negative balances (N: 15–55, P_2O_5: 14–76, K_2O: 34–79 kg ha^{-1}), in poultry litter the balance P_2O_5 = + 94.2 kg ha^{-1}. For pepper, however, these data were respectively amounted to: N: 6–14, P_2O_5: 10–15, K_2O: 9–20%, and the balances were positive. Microbiological concentrates (Azoto + phosphate Barvar) showed poor effectiveness as compared to organo-mineral fertilizers. It was also found that the lower the amount of a mobile element in the soil, or in the fertilizer dose, the higher its utilization rate and vice versa.

Key words: tomato, pepper, soil, organo - mineral fertilizers, balance, coefficients of usage, nitrogen, phosphorus, potassium.

INTRODUCTION

Vegetable crops (tomato, pepper, cucumber, zucchini, cabbage, potatoes, herbs, etc.) occupy an important place in the human diet, providing the body with carbohydrates, vitamins and minerals. These plants are particularly sensitive to soil conditions and mineral nutrition, at the same time they intensively absorb and accumulate harmful substances in fruits (nitrates, nitrosamines, residual amounts of pesticides and heavy metals (HM), etc. Therefore, alternative farming and biotechnology should be primarily applied in these phytocenoses. Currently, many countries prohibit

the application of ammonium nitrate to vegetable crops to avoid the nitrate accumulation in their commercial products. From this point of view, tomato and pepper in the conditions of Ararat Plain (the main region of Armenia for the cultivation of these crops) provide high yields, absorbing a significant amount of nutrients from soil and fertilizers.

The coefficients of use of nutrients by plants from the soil (CUS) and fertilizers (CUF) vary widely and depend on the plant type and variety, soil and climatic conditions, the capacity and agrochemical properties of the root layer of the soil, moisture availability and the level of agricultural technology, fertilizer systems, and many other factors affecting the growth and development of plants. In thirty- year experiments at the Dolgoprudny agrochemical station, winter wheat, rye, potatoes, oats in crop rotation used 26% nitrogen, 27% P_2O_5 and 57% K_2O from manure, and 51, 32 and 67%, from mineral fertilizers, respectively (Bugaev & Osipova, 1966). Approximately the same CUF data were obtained on light loamy soils of Belarus, and the utilization coefficients from the soil were: nitrogen: 13.4; P_2O_5: 7.6–9.3; K_2O: 15.3–20.8% (Bragin, 1970). Eight-year studies showed that the CUS and CUF of nitrogen, phosphorus and potassium in peas were respectively: 7 and 15, 15 and 30, 10 and 20, in winter rye: 15 and 50, 10 and 20, 10 and 30, in spring wheat: 10 and 55, 7 and 18, 7 and 60, oats: 10 and 60, 10 and 25, 10 and 60, corn: 20 and 50, 15 and 15, 15 and 40% (Sharyapov, 1976). When $N_{90}P_{60}K_{90}$ was applied locally together with 2 t ha^{-1} straw, the N utilization rate of barley was higher by 6–18% compared to the scattered application method (Shmyreva et al., 2004).

The results of 11.5 thousand field experiments showed that the coefficients of the nutrient elements use from mineral and organic fertilizers are very low, with row crops and technical crops more than by grains (Makarov & Nikitina, 1976). It was also found that the application of organic fertilizers increased plant yield by 34.1%, and mineral fertilizers by 14.1%, and the losses of NO_2-, NO_3-, and NH_4^+ from various organic fertilizers were significantly reduced than from nitrogen fertilizers. Application of manure at 40, 60 and 80 t ha^{-1} + $N_{56}P_{48}K_{60}$, increased soil humus content by 0.18; 0.24; and 0.21%, P_2O_5-41, 61 and 61, K_2O-36, 46 and 54 mg kg^{-1}, respectively (Kristaponyte, 2005; Cesoniene & Rutkoviene, 2009). Application of organic fertilizers such as litter and non-litter manure, bird droppings, composts, siderate, straw increased the yield of agricultural crops from 21 to 69%, while complete mineral fertilizers from 29 to 97% (Merzlaya, 2017). Vermicomost at doses of 3, 5 and 7 t ha^{-1} increased the potato yield of Aramis variety and the soil humus content (Butenko et al., 2020). Nitrogen utilization by plants per year of application is 42% with large fluctuations from 12 to 70%. Afterwards, nitrogen fertilizers show very low effectiveness (Korenkov, 1976).

Research with ^{15}N has shown that the coefficients of use of nitrogen fertilizers by plants in the year of application are 35–54%, and in the second and third years they drop sharply (Burtseva, 1969; Zamyatina & Varyushkina, 1973). The isotope method also revealed that fertilizers significantly increase the absorption of nutrients from the soil itself. Depending on soil conditions and plant species, this shift varies for nitrogen from 6 to 119%, for phosphorus: 39–87 and for potassium: 50–100%. This is explained by the fact that, under the influence of fertilizer, a more powerful root system is formed, penetrating a large volume of soil, thereby increasing the absorption of nutrients from the soil (Dontsov & Kravchenko, 1985). Compared to field experiments, in lysimetric and vegetation experiments, the results for CUS and CUF are somewhat overestimated, which is due to the coverage of the entire volume of soil by the plant root system, because of which plants absorb nutrients from soil and fertilizers almost equally (Lavreva, 1971).

The degree of absorption of nutrients by wheat and barley plants in rainfed conditions strongly depends on soil moisture. In wet years, plants used 51–52% nitrogen, 24–29% P_2O_5 and 5.7% K_2O from the soil, and in dry years 24.3; 12.2 and 2.2% respectively. Similar data from fertilizers are 2–3 times less (Khachatryan & Abazyan, 1986). In studies on CUS and CUF by fruit crops very low levels of nutrient elements assimilation was registered. CUS constitute: N: 2–9, P_2O_5: 4.6–5.2; K_2O: 1.0–3.6%, and from fertilizers: 0.8–8.0% (Grigel et al., 1986).

Research data on establishing the balance and degree of use of nutrients from the soil and fertilizers by tomato and pepper are almost absent in the literature. However, some studies have investigated the changes in lycopene and ß-carotene content during fruit ripening of some tomato varieties (Radzevičius et al., 2009), as well as their quality and yield when the roots of these plants are colonized with arbuscular mycorrhizal (AM) fungi of the Funelliformis mosseae strain at the same time, the yield increased by 50%, and the content of sugars, amino acids, and ß-amylase also increased compared to the option without fungal colonization (Palumbo et al., 2020). In field and vegatation experiments, the effectiveness of organo-mineral fertilizers on the yield and quality of tomato, as well as the biological removal of macronutrients by these plants was established (Harutyunyan, 2009; Harutyunyan et al., 2020).

Purpose of the research and problems

Tomatoes and peppers cultivated in field and greenhouse conditions are used almost all year round by people of different countries, and modern technologies are aimed not only at increasing yields, but also at improving the quality of the fruits of these crops. The aim of our research is to find ways to stabilize mineral nutrition of these crops and preserve soil fertility. In accordance with the stated goal, the research objectives include: 1. to reveal qualitative indices of tomato and pepper fruits at moderate doses of organo-mineral fertilizers, 2. to calculate the coefficients of use of nitrogen, phosphorus and potassium from the soil and fertilizers by these crops in field experiments, 3. to determine the NPK balance on the background of equivalent doses of different fertilizers and microbiological concentrates. The presented research is conducted in Armenia for the first time, and its scientific novelty is directly related to the disclosure of the degree of absorption of nutrients from soil and fertilizers, which are important arguments for preventing soil dehumification in farms.

Materials and methods

Field experiments were carried out on typically irrigated meadow brown soils in 2017–2019 on tomato 'Lia' and sweet pepper 'Almond 55' varieties of Armenian selection in Voskehat educational and experimental farm of National Agrarian University of Armenia (NAUA), located almost in the center of Ararat Plain (Etchmiadzin region, 40°08′and 44°19′ at an altitude of 850 m above sea level). The experiments were carried out in triple repetition (70 tomato and 80 pepper plants in each repetition), the distance between their rows was 80 cm. The schemes of experiments are given in Tables 2–8, where the principles of the only difference and comparison between the options are preserved.

Ammonium nitrate (N: 33%), simple superphosphate (P_2O_5: 18%), potassium salt (K_2O: 40%), and organic fertilizers - semi-rotted cattle manure (N: 0.48; P_2O_5: 0.23; K_2O: 0.55%), granulated poultry manure (N: 3.45; P_2O_5: 3.64; K_2O: 2.87% - according to certificate), organomix (a mixture of biohumus, peat and compost from organic waste:

N: 2.0; P_2O_5: 0.52; K_2O: 1.20% - according to the certificate), manufactured by ´ORWACO CJSC: an Armenian-Norwegian joint company were used as mineral fertilizers. Microbiological concentrates (Azoto and Phosphate Barvar) are produced in Iran in the form of a husk-like powder in packages of 100–120 g and are used in the form of aqueous solutions (water volume per one package is 1,000 liters). According to the certificate, Azoto Barvar contains nitrogen-fixing bacteria, Phosphate Barvar bacteria decomposing phosphorus-containing organic-mineral compounds of the soil that are hard for plants to access, converting P_2O_5 into mobile and water-soluble forms. All fertilizers were applied to the soil in spring (around April 20–25) as the main fertilizer before planting - as a strip at a depth of 20–25 cm with embedding. Agrotechnical measures (watering, hilling, weeding, control of weeds, pests and diseases) were carried out according to all options and repetitions simultaneously.

Soil samples of field participants were taken from the upper layer (0–40 cm depth) where tomato and pepper root systems (rhizosphere layer) are distributed. Laboratory soil analyzes were carried out according to generally accepted methods: mechanical composition - by the classical pipette method and assessed according to the gradation of N.A. Kachinsky (Alexandrova & Naidionova, 1976; Soil science edited by I.S. Kaurichev, 1982) with a P^H potentiometer, humus by Tyurin, hygroscopic moisture by gravimetric method, CO^2 by calcimeter, dry residue of aqueous extract by calcination method, total nitrogen by Kjeldahl, easily hydrolyzed nitrogen by Tyurin & Kononova, mobile phosphorus and potassium by Machigin with the further use of FEC and a flame photometer (Yagodin, 1987). The yield and vegetative mass of plants were measured by the gravimetric method (fresh and air-dried form). In air-dried plant samples, the content of total nitrogen was determined by the Kjeldahl method, phosphorus and potassium by wet ashing according to Ginzburg, with further determination of phosphorus by FEC, and potassium by a flame photometer. The sugar content in tomato and pepper fruits was determined by the Bertrand method, vitamin C by I. Murri (Yagodin, 1987), nitrates by nitrate tester ´SOEKS´ (NUC-0.19-2), and dry substances by drying and weight method. Statistical processing of yield data was carried out by analysis of variance (Dospekhov, 1985).

The coefficients of NPK use by tomato and pepper were calculated on the basis of the biological removal of these elements from the soil in control variants and by the difference method from fertilizers (Yagodin, 1987) using the following formulas:

$$Cs = \frac{100 \cdot Bc}{Cs} \quad (1)$$

where Cs – coefficients of nutrient utilization by plants from the soil, %; Bc – biological nutrient removal in the control variant, kg ha^{-1}; Cs – content of mobile nutrients in the soil rhizosphere, kg ha^{-1},

$$Dc = \frac{Bf - Bc \cdot 100}{D} \quad (2)$$

where Dc – difference coefficient, %; Bf – biological removal of the element in the fertilized version, kg ha^{-1}; Bc – biological removal of the element in the control variant, kg ha^{-1}; D is the dose of fertilizer in the fertilized version, kg ha^{-1} of active substance.

Balance coefficients for the use of nutrients from fertilizers are determined by the formula:

$$Bc = \frac{Bf \cdot 100}{D} \quad (3)$$

where Bc – balance coefficient, %; Bf – biological removal of the element in the fertilized version, kg ha^{-1}; D is the dose of fertilizer in the fertilized version, kg ha^{-1} of active substance.

RESULTS AND DISCUSSION

The Ararat Plain (805–950 m altitude) is the most active agricultural region of Armenia. The sum of active temperatures (above 10 °C) per year reaches 4,000–4,300 °C (average temperature +10.6 °C), in winter the absolute minimum temperature reaches (-30) - (-35 °C), the amount of precipitation -200–260 mm, humidity coefficient according to Shashko is 0.20–0.25 (Agroclimatic resources of Armenian edited by R.S. Mkrtchyan et al., 2011). Two sites were selected for laying field experiments not far from each other in order to avoid soil fatigue (Table 1). After the 2017 experience, field No. 1 was left as black fallow in 2018. The volumetric weight of the soil in field No. 1 was 1.2 kg dm^3, and in field No. 2: 1.4 kg dm^3.

Table 1. Physico-mechanical and agrochemical characteristics of experimental soils Plots

Experimental plots, Experimental years and rhizosphere layer	Mechanical composition (sum of particles < 0.01 mm) of phys. Clay %	Hygroscopic moisture, %	$CaCo_3$ by CO_2, %	Dry residue of aqueous extract, %	pH(H_2O)	Humus, %	Total nitrogen, %	Mobile forms, mg per 100 g of soil		
								N	P_2O_5	K_2O
Field No. 1, 2017–2019, 0–40 cm	25.4	3.62	1.51	0.025	7.54	1.30	0.068	1.40	3.40	34
Field No. 2, 2018, 0–40 cm	32.4	4.34	4.60	0.064	7.46	1.84	0.120	2.15	3.08	46

Table 1 shows that by mechanical composition, the soil of experimental plot No. 1 is light loamy (25.4%), and No. 2 is medium loamy (32.4%). The soils of both plots are slightly alkaline (pH-7.54 and 7.46), slightly carbonate (1.51 and 4.60%), humus is 1.30 and 1.84%, respectively, the soils are not saline with easily soluble salts (dry residue of water extract does not exceed 0.064%), the availability of mobile forms of nitrogen according to the Tyurin and Kononova gradations in both plots is very low, P_2O_5 and K_2O according to the Machinin gradation are optimal.

The research has shown that the yield of tomato and pepper in experimental plot No. 2 was higher (due to relatively high fertility and active crop rotation there) than in the first one (where in recent years, including 2018 it was fallow). The average tomato yield for three years (Table 2) in the variant without fertilizers was 51.8 t ha^{-1} (2.71 t ha^{-1} in

terms of air-dry weight), and in the fertilized variants it ranged from 62.6 (3.08) - Azoto Phosphate Barvar up to 75.3 / 3.98 t ha^{-1} (NP_{150P80}). It should be noted that the tomato yield in 2017 variants of organomix (58.9/2.02 t ha^{-1}) and Azoto-Phosphate Barvar (59.9/2.00 t ha^{-1}, and also in 2018 69.8/5.07 t ha^{-1}) compared to control were unreliable (LSD_{05}: in 2017 9.94 t, 2018 - 7.28 t). Similar phenomenon in the observed variants was observed in 2017 in pepper experiment (Table 3, LSD_{05}: 6.07 t).

Table 2. The influence of organo-mineral fertilizers and microbiological concentrates on the yield, the content of nutrients in tomato fruits and their removal by fruits

Experiment options	Harvest t ha^{-1}, fresh air. dry				Average for 3 years on air-dry weight, content, % removal, kg ha^{-1}		
	2017	2018	2019	average	N	P_2O_5	K_2O
1. No fertilizer (control)	51.1	64.7	39.5	51.8	2.70	1.48	3.66
	2.01	4.48	1.64	2.71	73.2	40.1	99.2
2. Mineral fertilizers	66.5	90.7	66.3	74.5	2.63	1.43	3.78
($N_{150}P_{80}K_{150}$ kg ha^{-1})	3.18	6.28	2.36	3.94	103.6	56.3	148.9
3. Manure 30 t ha^{-1}	63.0	92.2	66.4	73.9	3.04	1.49	4.63
	2.09	6.38	2.96	3.81	115.8	56.8	176.4
4. Poultry manure 5 t ha^{-1}	61.2	88.7	65.8	71.9	2.89	1.44	3.90
	2.15	6.14	2.52	3.60	104.0	51.8	140.4
5. Organomix	58.9	90.0	61.0	70.0	3.04	1.49	4.15
(ORWACO) 9 t ha^{-1}	2.02	6.17	3.04	3.74	113.7	55.7	155.2
6. Azoto+PhosphateBarvar	59.9	69.8	58.2	62.6	3.57	1.49	4.45
(100 + 100 g ha^{-1} in 1,000 L water)	2.00	5.07	2.17	3.08	110.0	45.9	137.1
7. Mineral fertilizers	71.6	89.7	64.5	75.3	3.08	1.54	4.74
$N_{150}P_{80}$ kg ha^{-1}	2.94	6.20	2.79	3.98	122.6	61.3	188.7
Sx$^-$, %	5.2	2.8	3.9	4.0	-	-	-
*LSD_{05}, t for fresh weight	9.94	7.28	7.24	8.39	-	-	-

**LSD* – Lowest Significant Difference.

Pepper yield was almost 2 or more times lower than that of tomato, and the content of nutrients in the components of the fruit and their removal by these plants was comparatively less (Table 3). The table shows that the average yield pepper for three years in the control variant was 23.1 t ha^{-1} (1.61 t ha^{-1} in terms of air-dry weight), and in fertilized variants this figure varied from 28.7/1.82 t ha^{-1} (Azoto +Phosphate Barvar) up to 32.0/2.17 t ha^{-1} (poultry manure). Pepper fruits were divided into two components: fruit pulp and seedpod with petioles in order to establish the nutrient content of these components separetrly, as well as to account for the excretion by these organs.

Table 3 shows that the fresh fruit pulp of pepper variety 'Almond 55' made up 75–80% of the weight of the fruit, and in terms of air-dry weight: 64–72%, i.e. testes with petiole in fresh fruits account for 20–25%. Table 3 also shows that in the fruit pulp of pepper the nutritional elements within the studied options were: N: 1.55–1.96; P_2O_5: 1.27–1.35 and K_2O: 2.11–3.29%, and in the seedpod with a petiole, respectively: 1.84–2.30; 1.29–1.37; 2.96–3.88%.

Table 3. The influence of organo-mineral fertilized and microbiological concentrates on the yield, the content of nutrients in pepper fruits and their removal by fruits

Experiment options	Harvest componens	Harvest, t ha^{-1}, fresh air. dry				3 – year average by air-dry weight, content, % removal, kg ha^{-1}		
		2017	2018	2019	Average	N	P_2O_5	K_2O
1. No fertilizer (control)	Fruits	14.7	41.2	13.5	23.1		-	-
		1.01	2.82	0.99	1.61			
	Fruit pulp	10.8	30.5	10.6	17.3	1.66	1.32	2.17
		0.63	1.47	0.68	1.03	17.1	13.6	22.4
	Seed with a petiole	3.9	10.7	2.9	5.8	2.06	1.37	3.82
		0.38	1.05	0.31	0.58	11.9	7.9	22.2
2. Mineral fertilizers ($N_{150}P_{80}K_{150}$ kg ha^{-1})	Fruits	21.6	54.5	19.1	31.7	-	-	-
		1.45	3.01	1.31	1.92			
	Fruit pulp	15.8	40.3	14.8	23.6	1.55	1.31	3.29
		0.88	2.39	0.87	1.38	21.4	18.1	45.4
	Seed with a petiole	5.8	14.2	4.3	8.1	1.84	1.35	3.88
		0.57	0.62	0.44	0.54	9.9	7.3	21.0
3. Manure 30 t ha^{-1}	Fruits	22.1	54.5	18.4	31.7	-	-	-
		1.41	3.64	1.28	2.11			
	Fruit pulp	16.7	42.0	13.0	23.9	1.74	1.35	2.37
		0.90	2.44	0.85	1.40	24.4	18.9	33.2
	Seed with a petiole	5.4	12.5	5.4	7.8	1.94	1.30	3.42
		0.51	1.20	0.43	0.71	13.8	9.2	24.3
4. Poultry manure 5 t ha^{-1}	Fruits	23.4	54.8	17.7	32.0	-	-	-
		1.56	3.64	1.30	2.17			
	Fruit pulp	17.5	41.6	12.5	23.9	1.66	1.27	2.11
		0.98	2.37	0.84	1.40	23.2	17.8	29.5
	Seed with a petiole	5.9	13.2	5.2	8.1	2.13	1.34	2.96
		0.58	1.27	0.46	0.77	16.4	10.3	22.8
5. Organo-mix (ORWACO) 9 t ha^{-1}	Fruits	19.0	53.3	17.6	30.0	-	-	-
		1.02	3.72	1.26	2.00			
	Fruit pulp	14.8	42.0	13.6	23.5	1.96	1.35	2.24
		0.73	2.51	0.84	1.36	26.7	18.4	30.5
	Seed with a petiole	4.2	11.3	4.0	6.5	1.97	1.29	3.16
		0.29	1.21	0.42	0.64	12.6	8.3	20.2
6. Azoto+phosphate Barvar (100 + 100 g ha^{-1} in 1,000 L water)	Fruits	20.8	49.2	16.1	28.7	-	-	-
		1.14	3.27	1.04	1.82			
	Fruit pulp	17.2	40.8	12.5	23.5	1.67	1.30	2.89
		0.71	2.27	0.69	1.23	20.5	16.0	35.6
	Seed with a petiole	3.6	8.4	3.6	5.2	2.00	1.30	3.22
		0.43	1.00	0.35	0.59	11.8	7.7	19.0
7. Mineral fertilizers $N_{150}P_{80}$ kg ha^{-1}	Fruits	22.7	54.8	18.1	31.9	-	-	-
		1.40	3.79	1.05	2.08			
	Fruit pulp	18.2	44.2	11.4	24.6	1.83	1.29	2.57
		1.11	2.45	0.71	1.42	26.0	18.3	36.5
	Seed with a petiole	4.5	10.6	6.7	7.3	2.30	1.35	3.88
		0.29	1.34	0.34	0.66	15.2	8.9	25.6
Sx^-,%	-	9.5	1.7	3.2	3.7	-	-	-
LSD_{05}, t for fresh weight	-	6.07	2.68	1.70	3.36	-	-	-

Thus, the removal of nitrogen from the fruit pulp of pepper in the unfertilized version was: 17.1; P_2O_5: 13.6 and K_2O: 22.4 kg ha^{-1}, and seedpod with petioles: 11.9; 7.9 and 22.2 kg ha^{-1}, respectively. In fertilized variants, these indicators were in the range: nitrogen: 20.5–26.7 and 9.9–16.4; P_2O_5: 16.0–18.9 and 7.3–10.3; K_2O: 29.5–45.4 and 19.0–25.6 kg ha^{-1}, respectively. From the above data, it is evident that organo-mineral fertilizers significantly increased the pulp of the fruit, reducing the removal of nutrients through the seedpod with petioles.

The dry matter content in tomato fruits varied from 4.75 to 5.11%, total sugars: 4.0–5.2%, and vitamin C: 22.7–29.8 mg %, and in some fertilized varieties these indicators were lower than the control option, which can be explained by the increase in yield in these options (Table 4). As for the content of nitrates in fruits, it should be noted that in all variants these compounds were 28 (control) to 35 mg kg^{-1} ($N_{150}P_{80}K_{150}$ and organomix) higher than the maximum permissible concentration MPC for open ground (150 mg kg^{-1}), which may be due to varietal characteristics and a particularly active effect on the plant of soil No. 2, which has always been in intensive exploitation with the use of organo-mineral fertilizers.

Table 4. Effect of organo-mineral fertilizers and microbiological concentrates on the content of nitrates and quality indicators of tomato and pepper fruits

Crop	Experiment options	Nitrates, mg kg^{-1}				3 – year average		
		2017	2018	2019	average	dry matter, %	total sugars, %	vitamin C, mg %
Tomato	1. Without fertilizer (control)	185	191	159	178	5.00	4.0	25.3
	2. Mineral fertilizers $N_{150}P_{80}K_{150}$ kg ha^{-1}	173	203	180	185	5.09	4.4	25.7
	3. Manure 30 t ha^{-1}	178	197	171	182	4.90	4.8	29.8
	4. Poultry manure 5 t ha^{-1}	174	195	178	182	4.75	5.2	26.6
	5. Organomix (ORWACO) 9 t ha^{-1}	179	196	179	185	5.09	4.1	22.9
	6. Azoto+phosphate Barvar (100 + 100 g ha^{-1} in 1,000 L water)	173	202	174	183	4.78	4.3	26.4
	7. Mineral fertilizers ($N_{150}P_{80}$ kg ha^{-1})	173	190	177	180	5.11	3.6	22.7
Pepper	1. Without fertilizer (control)	52	56	48	52	6.98	5.9	163
	2. Mineral fertilizers with $N_{150}P_{80}K_{150}$ kg ha^{-1}	59	76	68	68	7.87	5.4	138
	3. Manure 30 t ha^{-1}	54	81	64	66	6.64	5.4	150
	4. Poultry manure 5 t ha^{-1}	59	73	62	65	6.80	5.8	146
	5. Organomix (ORWACO) 9 t ha^{-1}	57	60	66	61	6.74	5.3	150
	6. Azoto+phosphate Barvar (100 + 100 g ha^{-1} in 1,000 L water)	58	72	58	62	6.18	6.8	146
	7. Mineral fertilizers ($N_{150}P_{80}$ kg ha^{-1})	58	67	51	59	6.43	5.6	158

The data in Table 4 also show that in comparison with tomatoes, pepper fruits contained more dry matter, sugars, and especially vitamin C, which is 5–6 times higher than the content in tomato. At the same time, it is observed that in the unfertilized version these substances were much higher than in the target variants (except for dry substances in option $N_{150}P_{80}K_{150}$ and total sugars in the option of microbiological concentrates). As

for nitrates, in pepper fruits these compounds were 3–3.5 times lower than the MPC for open ground (200 mg kg^{-1}).

Table 5. Effect of organo-mineral fertilizers and microbiological concentrates on the above-ground and root mass of tomato and pepper, t ha^{-1} (fresh/air-dry weight)

Crop	Experiment options	Above ground mass				Root mass			
		2017	2018	2019	average	2017	2018	2019	average
Tomato	1. Wihout fertilizer (control)	15.77	29.31	12.36	19.15	1.75	2.96	1.89	2.20
		2.52	5.16	2.20	3.29	0.39	0.65	0.54	0.53
	2. Mineral fertilizers	18.21	38.31	23.88	26.80	2.34	4.54	3.18	3.35
	($N_{150}P_{80}K_{150}$ kg ha^{-1})	3.06	6.92	4.24	4.74	0.71	1.10	0.90	0.90
	3. Manure 30 t ha^{-1}	18.13	35.94	25.44	26.50	2.42	3.84	3.39	3.22
		3.26	6.80	4.53	4.86	0.76	0.93	0.96	0.88
	4. Poultry manure 5 t ha^{-1}	17.64	35.92	23.07	25.54	2.10	3.10	3.10	2.77
		2.99	6.84	4.10	4.64	0.62	0.74	0.88	0.75
	5. Organomix (ORWACO)	17.78	32.54	22.37	24.23	1.98	3.32	2.90	2.73
	9 t ha^{-1}	3.03	6.04	3.98	4.35	0.60	0.72	0.83	0.72
	6. Azoto+phosphate Barvar	17.07	29.67	13.36	20.03	1.90	2.92	2.27	2.36
	(100 + 100 g ha^{-1} in	3.03	5.61	2.38	3.67	0.54	0.65	0.65	0.61
	1,000 L in water)								
	7. Mineral fertilizers	17.74	36.68	24.11	26.18	2.22	4.51	3.20	3.31
	($N_{150}P_{80}$ kg ha^{-1})	3.09	7.16	4.29	4.85	0.68	1.07	0.91	0.89
Pepper	1. Wihout fertilizer	7.94	6.59	6.70	7.08	0.77	1.25	0.73	0.92
	(control)	2.30	1.43	1.59	1.77	0.35	0.34	0.24	0.31
	2. Mineral fertilizers	8.31	8.98	8.24	8.51	0.85	2.22	1.04	1.37
	($N_{150}P_{80}K_{150}$ kg ha^{-1})	2.41	2.04	1.95	2.13	0.41	0.56	0.35	0.44
	3. Manure 30 t ha^{-1}	7.49	9.35	8.11	8.32	0.77	1.76	1.09	1.21
		2.19	2.18	1.78	2.05	0.35	0.48	0.36	0.40
	4. Poultry manure 5 t ha^{-1}	8.95	8.52	7.49	8.32	0.85	1.75	0.95	1.18
		2.63	1.86	1.78	2.09	0.38	0.46	0.32	0.39
	5. Organomix (ORWACO)	6.71	9.21	7.50	7.81	0.66	1.98	1.00	1.21
	9 t ha^{-1}	1.90	2.06	1.78	1.91	0.31	0.51	0.33	0.38
	6. Azoto+phosphate Barvar	10.11	7.84	6.87	8.27	1.01	1.58	0.79	1.13
	(100 + 100 g ha^{-1} in	2.97	1.65	1.63	2.08	0.46	0.41	0.26	0.38
	1,000 L in water)								
	7. Mineral fertilizers	10.48	9.05	7.89	9.14	0.73	2.11	1.07	1.30
	($N_{150}P_{80}$ kg ha^{-1})	3.04	2.03	1.87	2.31	0.34	0.55	0.36	0.42

Biological removal of nitrogen and ash elements from the soil and fertilizers by the commercial yield and vegetative mass of cultivated crops is considered to be the main basis for establishing the degree of nutrient assimilation. Table 5 shows data on the above-ground and root mass of the studied crops for the studied year. The vegetative mass of tomato varied over the years according to the yield pattern, i.e. the highest aboveground and root mass was formed in the 2nd field plot (2018), when, as in pepper, there was no big difference between years. On average for 3 years the wet above-ground mass of tomato in the control variant was 19.15 t ha^{-1} (3.29 t ha^{-1} air-dry weight), while the root mass was 2.20 and 0.53 t ha^{-1}. In fertilized versions the above-ground mass varied from 20.03/3.67 t ha^{-1} (Azoto+phosphate Barvar) to 26.80/4.74 t ha^{-1} ($N_{150}P_{80}K_{150}$), and the root mass in the same variants: 2.36/0.61 and 3.35/0.90 t ha^{-1}. As for pepper, its

above-ground wet weight for 3 years in the control variant was 7.08 t ha^{-1} (1.77 t ha^{-1} air-dry weight), root weight: 0.92 and 0.31 t ha^{-1}. In fertilized variants, these data ranged from 7.81/1.91–9.14/2.31 t ha^{-1} and 1.13/0.38–1.37/0.44 t ha^{-1}, respectively. According to Table 5, the wet root mass of a tomato averages 10–11% of the total vegetative mass, while for pepper it is 11.5–14%, and in terms of air-dry weight, these data increase relatively.

In average samples (mixed sample from all variants) of the above-ground mass of tomato, the total nitrogen was: 0.99; P_2O_5: 0.56 and K_2O: 1.74%, in roots: 0.86; 0.54 and 1.76% by air-dry weight. In similar organs of pepper, these data were respectively: 1.28; 0.78; 1.53 and 1.14; 0.86; 1.68% by air-dry weight. Based on the above data and average air-dry data for three years of vegetative mass (Table 5), the removal of nutrients by the above-ground and root mass of tomato and pepper was determined (Table 6). This table shows that the removal of nitrogen by the above-ground mass of tomato varied from 32.6 (control) to 48.1 kg ha^{-1} (manure 30 t ha^{-1}), P_2O_5: 18.4–27.2 and K_2O: 57.2–84.6 kg ha^{-1} in the same variants, and the root mass, respectively, was 4.6–7.7; 2.9–4.9 and 9.3–15.8 kg ha^{-1} in control and $N_{150}P_{80}K_{150}$ options. Nitrogen removal by the above-ground pepper mass varied from 22.7 (control) to 29.6 kg ha^{-1} ($N_{150}P_{80}$), P_2O_5: 13.8–18.0; K_2O: 27.1–35.3 kg ha^{-1} in the same variants, and root mass, respectively: 3.5–5.0; 2.7–3.8 and 5.2–7.4 kg ha^{-1} in the control and $N_{150}P_{80}K_{150}$ options.

Table 6. Removal of main nutrients by the vegetative mass of tomato and pepper, kg ha^{-1} per air-dry weight (according to average data for 2017–2019)

Crop	Experiment options	Above ground mass			Root mass		
		N	P_2O_5	K_2O	N	P_2O_5	K_2O
Tomato	1. Without fertilizer (control)	32.6	18.4	57.2	4.6	2.9	9.3
	2. Mineral fertilizers ($N_{150}P_{80}K_{150}$ kg ha^{-1})	46.9	26.5	82.5	7.7	4.9	15.8
	3. Manure 30 t ha^{-1}	48.1	27.2	84.6	7.6	4.8	15.5
	4. Poultry manure 5 t ha^{-1}	45.9	26.0	80.7	6.5	4.1	13.2
	5. Organomix (ORWACO) 9 t ha^{-1}	43.1	24.4	75.7	6.2	3.9	12.7
	6. Azoto+phosphate Barvar (100 + 100 g ha^{-1} in 1,000 L water)	36.3	20.6	63.9	5.2	3.3	10.7
	7. Mineral fertilizers ($N_{150}P_{80}$ kg ha^{-1})	48.0	27.2	84.4	7.7	4.8	15.7
Pepper	1. Without fertilizer (control)	22.7	13.8	27.1	3.5	2.7	5.2
	2. Mineral fertilizers ($N_{150}P_{80}K_{150}$ kg ha^{-1})	27.3	16.6	32.6	5.0	3.8	7.4
	3. Manure 30 t ha^{-1}	26.2	16.0	31.4	4.6	3.4	6.7
	4. Poultry manure 5 t ha^{-1}	26.8	16.3	32.0	4.4	3.4	6.6
	5. Organomix (ORWACO) 9 t ha^{-1}	24.4	14.9	29.2	4.3	3.3	6.4
	6. Azoto+phosphate Barvar (100 + 100 g ha^{-1} in 1,000 L water)	26.6	16.2	31.8	4.3	3.3	6.4
	7. Mineral fertilizers ($N_{150}P_{80}$ kg ha^{-1})	29.6	18.0	35.3	4.8	3.6	7.1

On the basis of nutrient elements removal by tomato and pepper fruits (Tables 2 and 3) and the vegetative mass of these plants (Table 6), the annual biological removal of nitrogen, phosphorus and potassium was determined, the data of which are the basis for accounting the coefficients of their use from soil and fertilizers (Table 7). This table shows that the main part of the annual biological removal of nutrients from tomatoes

was produced by the fruits, which on average was: nitrogen: 68, P_2O_5: 65 and K_2O: 63%. 28–30% of NPK was: removed by the above-ground mass of tomato, and only 3–4% by the root system. At 50–75 tha^{-1} of tomato yield, the applied doses of fertilizers remain in deficit, if we also take into account that about 30–50% of the elements of the fertilizers applied to the soil are absorbed by the plants. In pepper, the biological removal of NPK at a yield of 23–32 t ha^{-1} does not exceed the dose of applied fertilizers. As for microbiological concentrates, they showed poor effectiveness on both crops, due to the low efficiency of bacterial strains.

In addition to biological removal, to calculate the coefficients of use of nutrients from the soil (in non-fertilized variants), it is necessary to have general data of the mobile forms of NPK in the rhizosphere layer of the studied plants. The active rhizosphere of tomato and pepper in the irrigated conditions of Ararat Plain lies in a layer of 0–40 cm, and individual roots deepen to 60–80 cm depth. Based on the data of the 40 cm soil layer and the volumetric weights of the experimental plots (field No. 1–1.2 and field No. 2–1.4 kg dm^{-3}), the total soil mass was determined, which for the fields was 4,800 and 5,600 t ha^{-1}, respectively. The mass of medium loamy soil with an arable horizon of 20 cm per hectare is on average 3 million kg and each mg of nutrient element per 100 g of soil is equivalent to 30 kg ha^{-1} (Yagodin, 1987). Thus, according to Table 1, the content of mobile nitrogen in the rhizosphere of field No. 1 is: 67.2; P_2O_5: 163.2 and K_2O: 1632.0 kg ha^{-1}, and in field No. 2, respectively: 120.4; 172.5 and 2576.0 kg ha^{-1}. Total nitrogen on average for the two fields is: 93.8; P_2O_5: 167.9 and K_2O: 2104 kg ha^{-1}, on the basis of which the degree of use of NPK by tomato and pepper from the soil in unfertilized variants, in the Azoto+phosphate Barvar variant, as well as K_2O in the $N_{150}P_{80}$ variant were calculated.

Table 7 shows that the coefficients of use of nutrients from the soil by tomato on average per year are: nitrogen: 117.7; P_2O_5: 36.6 and K_2O: 7.9%, and for pepper, respectively: 58.8; 22.6 and 3.7%.

High degree of nitrogen absorption by tomato (117.7%) and pepper (58.8%) is due to its low content in soils (1.40 and 2.15 mg per 100 g of soil). Regarding CUF, nitrogen uptake in tomato ranges from 26.7 (poultry manure) to 45.3% ($N_{150}P_{80}$). P_2O_5: 11.3– 9.9 in the same variants and K_2O: 47.8 (poultry manure) - 72% (organomix). The same dynamics on the use of nutrients from fertilizers is repeated in pepper, at a significantly low level of biological removal. The coefficients of use of nutrients from soil and organic-mineral fertilizers show that the less a nutrient element is in the substrate, the higher the coefficient of its use by the plant and vice versa. For example, a high content of P_2O_5 in poultry manure (182.0 kg at a dose of 5 t ha^{-1}) reduces the degree of absorption of this element (11.3% in tomato and 5.4% in pepper).

Balance coefficients give an idea not only about the degree of absorption of nutrients from fertilizers and soil by plants, but also about the possible change in soil availability when applying this fertilizer. Naturally, balance coefficients are always higher than difference coefficients, and on poor soils they are always lower than on rich soils. If the balance coefficient is 100%, then the balance is zero and the supply of soil with elements does not change; if the coefficient is less than 100%, the balance is positive and the soil will be enriched with this element. If the coefficient is more than 100%, the balance is negative, and the soil will be depleted of this element (Yagodin, 1987). From these considerations it follows that in tomato, in addition to nitrogen and phosphorus in the dose of poultry manure (90.7 and 45%) and nitrogen in

the organomix (90.6%) in fertilized variants, the balance coefficients of nutrients are mainly negative, while in pepper, they are positive.

Table 7. Biological removal and utilization rates of nitrogen, phosphorus and potassium from soil and fertilizers by tomato and pepper

Crop	Experiment options	Biological output, kg ha^{-1}			CUS and CUF, %			Balance coefficients, %		
		N	P_2O_5	K_2O	N	P_2O_5	K_2O	N	P_2O_5	K_2O
Tomato	1. Without fertilizer (control)	110.4	61.4	165.7	117.7	36.6	7.9	-	-	-
	2. Mineral fertilizers ($N_{150}P_{80}K_{150}$ kg ha^{-1})	158.2	87.7	247.2	31.9	32.9	54.3	105.5	109.6	164.8
	3. Manure 30 t ha^{-1}	171.5	88.8	276.5	42.4	39.7	67.2	119.1	128.7	167.6
	4. Poultry manure 5 t ha^{-1}	156.4	81.9	234.3	26.7	11.3	47.8	90.7	45.0	163.3
	5. Organomix (ORWACO) 9 t ha^{-1}	163.0	84.0	243.5	29.2	48.3	72.0	90.6	179.5	225.5
	6. Azoto+phosphate Barvar (100 + 100 g ha^{-1} in 1,000 L water)	151.5	69.8	211.7	161.5	41.6	10.1	-	-	-
	7. Mineral fertilizers ($N_{150}P_{80}$ kg ha^{-1})	178.3	93.3	288.8	45.3	39.9	13.7	118.9	116.6	-
Pepper	1. Without fertilizer (control)	55.2	38.0	76.9	58.8	22.6	3.7	-	-	-
	2. Mineral fertilizers ($N_{150}P_{80}K_{150}$ kg ha^{-1})	63.6	45.8	106.4	5.6	9.8	19.7	42.4	57.2	70.9
	3. Manure 30 t ha^{-1}	69.0	47.5	95.6	9.6	13.8	11.3	47.9	68.8	57.9
	4. Poultry manure 5 t ha^{-1}	70.8	47.8	90.9	9.0	5.4	9.8	41.0	26.3	63.3
	5. Organomix (ORWACO) 9 t ha^{-1}	68.0	44.9	86.3	7.1	14.7	8.7	37.8	95.9	79.9
	6. Azoto+phosphate Barvar (100 + 100 g ha^{-1} in 1,000 L water)	63.2	43.2	92.7	67.4	25.7	4.4	-	-	-
	7. Mineral fertilizers ($N_{150}P_{80}$ kg ha^{-1})	75.6	48.8	104.5	13.6	13.5	5.0	50.4	61.0	-

The balances of basic nutrients and humus in world agriculture are highly variable and clearly depend on human activity. In the middle of the 20th century, the assessment of the economic balance in agriculture became most widespread, and included in its structure the removal of NPK by main and by-products, all losses and gains of nutrients, including symbiotic and non-symbiotic nitrogen fixation (Yurkin, 1974, 1975). The balance deficit in agriculture of the USSR in 1940 was for nitrogen: 73.8, phosphorus: 68.3 and potassium: 76.1%, meanwhile, on soils with an average level of actual fertility, the balance of nutrients should be positive, for nitrogen by 10–20, phosphorus - 80–100 and potassium 10% (Pryanishnikov, 1945). The negative balance of basic nutrients (N: 37, P_2O_5: 5 and K_2O: 31 kg ha^{-1}) in grain crops of the USSR continued until 1976 (Peterburgsky, 1979).

The maximum amount of mineral fertilizers in Russia and Ukraine was used in the second half of the 1980s - about 13 million tons of NPK, which was only 60% of the need, and since 1990 their use decreased by 3 times, organic fertilizers and lime by 2.5 times, because of which the NPK balance for 1991–1995 amounted to (-58), for 1998–1999 (-65) kg ha^{-1}, and the yield of grain crops in 1999–2000 was 1.56 t ha^{-1}, while

in France it was 7.26; in England- 7.17; Germany- 6.37; USA- 5.85 t ha^{-1} (Lebed et, al., 1997; Miloshchenko, 1999; Mineev, 2000; Mineev & Bichkova, 2003; Shafran, 2004).

In arable soils of Belarus for 1993–2001 the K_2O balance was +33 kg ha^{-1}, and in Western Siberia of Russia for 1988–2017 at NPK 75, 100, 125% was also positive (Bogdevich et al., 2004; Yakimenko, 2019), but in Russia in general the NPK balance from 1992 to 2018 was negative. The nitrogen deficit in agriculture in 2018 was 26 kg ha^{-1} (Kudeyarov, 2018, 2021; Shafran, 2020). Potassium plays a huge role in the mineral nutrition of plants. The gross content of potassium in the arable soil layer is 5–50 times more than nitrogen and 8–40 times more than phosphorus. However, the removal of potassium by agricultural crops on average exceeds the amount of nitrogen and phosphorus. In plants, potassium is in ionic form and is not included in the organic compounds of cells. Potassium increases winter hardiness and plant resistance to fungal and bacterial diseases (Agrochemistry edited by Yagodin, 1982). In a stationary field experiment on the light chestnut soil of the Saratov Trans-Volga region, the decisive role of the essential forms of potassium in the potassium nutrition of plants and in replenishing the negative balance of this element was established (Kononchuk & Nikitina, 2002). The balance of the main nutrients in the conditions of Armenia was formed according to the same dynamics as in Russia. According to long-term studies, after 1975, the gross and economic balances of nitrogen and phosphorus changed in a positive direction, and after the collapse of the USSR, all three elements in all lands became negative (Babayan, 1978, 1980, 1985; Harutyunyan et al., 2023).

It should also be noted that numerous political, economic, social, military, environmental, cultural and educational problems have been revealed in the post-Soviet countries, which have a strong negative impact on agriculture and the environment (Raukas, 2010; Harutyunyan & Sargsyan, 2018).

In our research, the balance of nutrients was deduced in order to establish all items of inputs and expenditures in tomato and pepper phytocenoses (Table 8). The expenditure items include: biological removal of elements, losses of nutrients by erosion (mainly irrigation), which for row crops in Ararat Plain is: N: 5.56; P_2O_5: 8.42 and K_2O: 12.86 kg ha^{-1} and by leaching: N: 6.80; P_2O_5: 1.25 and K_2O: 14.06 kg ha^{-1} (Babayan, 1980), gaseous nitrogen losses from applied doses of organic-mineral fertilizers are assumed to be on average 20% (Korenkov, 1976). In the inputs used: NPK intake with fertilizers, with irrigation water, with precipitation (N: 3.60; P_2O_5: no, K_2O: 7.0 kg ha^{-1}) and nitrogen from non-symbiotic nitrogen fixation. In the zone of brown chestnut and brown soils, as well as carbonate humus of Armenia, the supply of nitrogen by free-living nitrogen fixers is assumed to be 5.2 kg ha^{-1} per year (Babayan, 1980).

For irrigation of tomato and pepper phytocenoses, artesian water from Ararat Plain from a depth of 100–120 m is used. During the growing season, these plantations are watered 17 times with an irrigation rate of 600 m^3 ha^{-1} (irrigation rate during the vegetation 10,200 m^3 ha^{-1}). Laboratory analyzes of some artesian water sources showed that the total nitrogen content is: 0.65; P_2O_5: 0.37 and K_2O: 7.50 mg L^{-1}. Based on these data and irrigation rates, the amount of NPK per hectare of tomato and pepper was established, which was: N:6.63; P_2O_5: 3.77 and K_2O:76.5 kg ha^{-1}. However, under irrigation conditions it is extremely difficult to neutralize the influence of weeds on cultivated annual crops. Throughout the growing season, there is a fierce competition plants and weeds, and only active ecological, agrotechnical and biological methods of struggle against them ensure the expected yield. In a flax crop rotation which included

potatoes, barley, winter wheat, winter rye, annual and perennial weeds consumed a significant amount of NPK, which negatively affected crop productivity (Conova & Samoilov, 2015).

Table 8. Balance of main nutrients in tomato and pepper plantations between cultivated

Crop	Experiment options	Total losses include: biological removal, erosion, leaching, gaseous losses of nitrogen from fertilizers, kg ha^{-1}			Total revenue include: fertilizers, irrigation water, precipitation, non-symbiotic nitrogen fixation, kg ha^{-1}			Balance, + - kg ha^{-1}, balance intensity, %		
		N	P_2O_5	K_2O	N	P_2O_5	K_2O	N	P_2O_5	K_2O
Tomato	1. Without fertilizer (control)	122.8	71.1	192.6	15.4	3.8	83.5	-107.4 12.5	-67.3 5.3	-109.1 43.4
	2. Mineral fertilizers ($N_{150}P_{80}K_{150}$ kg ha^{-1})	200.6	97.4	274.1	165.4	83.8	233.5	-35.2 82.5	-13.6 86.0	-40.6 85.2
	3. Manure 30 t ha^{-1}	212.9	98.5	303.4	159.4	72.8	248.5	-53.5 74.9	-25.7 73.9	-54.9 81.9
	4. Poultry manure 5 t ha^{-1}	202.8	91.6	261.2	187.9	185.8	227.0	-14.9 92.7	+94.2 202.8	-34.2 86.9
	5. Organomix (ORWACO) 9tha^{-1}	211.4	93.7	270.4	195.4	50.6	191.5	-16.0 92.4	-43.1 54.0	-78.9 70.8
	6. Azoto+phosphate Barvar (100 + 100 g ha^{-1} in 1,000 L water)	163.9	79.5	238.6	15.4	3.8	83.5	-148.5 9.4	-75.7 4.8	-155.1 35.0
	7. Mineral fertilizers ($N_{150}P_{80}$ kg ha^{-1})	220.7	103.0	315.7	165.4	83.8	83.5	-55.3 74.9	-19.2 81.4	-232.2 26.4
Pepper	1. Without fertilizer (control)	67.6	47.7	103.8	15.4	3.8	83.5	-52.2 22.8	-43.9 8.0	-20.3 80.4
	2. Mineral fertilizers ($N_{150}P_{80}K_{150}$ kg ha^{-1})	106.0	55.5	133.3	165.4	83.8	233.5	+59.4 156.0	+28.3 151.0	+100.0 175.2
	3. Manure 30 t ha^{-1}	110.4	57.2	122.5	159.4	72.8	248.5	+49.0 144.4	+15.6 127.3	+126.0 202.9
	4. Poultry manure 5 t ha^{-1}	117.2	57.5	117.8	187.9	185.8	227.0	+70.7 160.3	+128.3 323.1	+109.2 192.7
	5. Organomix (ORWACO) 9 t ha^{-1}	116.4	54.0	113.2	195.4	50.6	191.5	+79.0 167.9	-4.0 92.7	+78.3 169.2
	6. Azoto+phosphate Barvar (100 + 100 g ha^{-1} in 1,000 L water)	75.6	52.9	119.6	15.4	3.8	83.5	-59.7 20.5	-48.7 7.2	-35.3 70.3
	7. Mineral fertilizers ($N_{150}P_{80}$ kg ha^{-1})	118.0	58.5	131.4	165.4	83.8	83.5	+47.4 140.2	+25.3 143.2	-47.9 63.5

Both balance coefficients and balances of nutrients, as well as their intensity, directly reflect the level of deficiency or surplus of nutrients in agrocenoses, revealing the dynamism of soil fertility. Table 8 shows that in the tomato phytocenosis, except for P_2O_5 introduced by poultry manure, the nutrients in all fertilized options are negative, and in the pepper plantation they are positive: nitrogen: 52.2–148.5; P_2O_5: 43.9–75.7 and K_2O: 20.3– 55.1 kg ha^{-1}. Nitrogen balance intensity in tomato ranges from 75–93, P_2O_5: 54–86.7 and K_2O: 71–87%. In the $N_{150}P_{80}$ variant, the negative K_2O balance and the

intensity of the balance in tomato was: 232.2 kg ha^{-1} and 26.4%, and in pepper: 47.9 kg ha^{-1} and 63.5%.

The data in Table 8 show that in order to ensure a high tomato yield in Ararat Plain, it is necessary to increase the doses of nitrogen and potassium by 50, and P_2O_5 by 20%. It is necessary to maintain the applied doses of complete mineral and organic fertilizers to stabilize the yield at the level of 35 t ha^{-1} in pepper plantations.

CONCLUSION

1. In all phytocenoses of Ararat Plain of Armenia, the first limiting factor among macroelements is nitrogen, because the soils of this zone are poor in humus and nitrogen, and P_2O_5 and K_2O in certain field areas are moderately and optimally provided.

2. In tomato and pepper plantations, the effectiveness of equivalent doses of mineral fertilizers ($N_{150}P_{80}K_{150}$ kg ha^{-1}), semi-freshened manure (30 t ha^{-1}), granulated poultry manure (5 t ha^{-1}), and organomix (9 t ha^{-1}) are estimated at almost the same level, and bacterial concentrations (Azoto+phosphate Barvar) turned out to be weaker.

3. The biological removal of basic nutrients at tomato yield of 70–75 t ha^{-1} exceeds the doses of applied fertilizers, and in pepper 30–32 t ha^{-1} these doses remain in excess.

4. Under intensive irrigation conditions, tomato at 51 t ha^{-1} yield absorbs 118% nitrogen, 37% P_2O_5 and 8.0% K_2O from the soil, while pepper at 23 t ha^{-1} yield, respectively: 59, 23 and 4%. The low utilization coefficient of K_2O by plants is due to its relatively high content in the soil.

5. The coefficient of nitrogen use by tomato from mineral fertilizers varies from 32 to 45%, P_2O_5: 33–40 and K_2O: 54%, and from manure, poultry manure and organomix, respectively: 27–42, 11–48 and 48–72%. Similar data in pepper are significantly low. The balance coefficients of nutrients in tomato mostly exceed 100%, while in pepper it reaches a maximum of 70%.

6. Nitrogen losses by irrigation erosion and leaching from irrigated meadow brown soils of Ararat Plain are: 12.4 P_2O_5: 9.7; K_2O: 26.9 kg ha^{-1} per year. The input from atmospheric precipitation, irrigation waters and non-symbiotic nitrogen fixation are: N: 15.4; P_2O_5: 3.8; K_2O: 83.5 kg ha^{-1}.

7. In tomato phytocenosis, except for phosphorus introduced by poultry manure, the balance of nutrients in all fertilized options is negative, and in pepper plantation it is positive. The intensity of the nitrogen balance in tomato at full organic-mineral fertilization varies in the ranges from 75–93, P_2O_5: 54–88 and K_2O: 71–87%, and in pepper all three elements exceeded 100%.

PRACTICAL SUGGESTION: To provide high yield of tomatoes (70–75 h kg^{-1}) and to ensure positive balance of main nutrients in the Ararat Plain the farmers are recommended to fertilize the soil with mineral fertilizers in doses $N_{200}P_{120}K_{200}$ k ha^{-1}, 40 t ha^{-1} of semi-rotten manure or 6 t ha^{-1} of granulated poultry manure.

REFERENCES

Agrochemistry. Ed. B.A.Yagodin. 1982. Kolos, Moscow, 574 pp. (in Russian).

Agroclimatic resources of Armenian. Ed. R.S. Mkrtchyan, D.H. Melkonyan & V.H. Badalyan. 2011. Yerevan, pp. 41–49 (in Armenian).

Alexandrova, L.N. & Naidionova, O.A. 1976. *Laboratory-practical trainings on soil science.* 3-rd edition, Kolos, Leningrad, 280 pp. (in Russian).
Babayan, G.B. 1978. Balance of nitrogen phosphorus and potassium in the agriculture of the Armenian SSR. *Agrochemistry* **10**, 68–74 (in Russian).
Babayan, G.B. 1980. B*alance of nitrogen, phosphorus and potassium in the agriculture of the Armenian SSR*. Yerevan, pp. 13–180 (in Russian).
Babayan, G.B. 1985. Balance of nutrient elements in the agriculture of the Armenian SSR. *Biological journal of Armenia* **38**(5), 415–422 (in Russian).
Bogdevich, I.M., Lapa, V.V., Ochkovskaya, L.V., Vasilyuk, G.V., Kalenik, G.I. & Konashenko, Yu.I. 2004. Balance and chages in the content of exchangeable potassium in Arable soils of Belorus. *Agrochemistry* **1**, 46–50 (in Russian).
Bragin, A.M. 1970. Balance and coefficients of usage of main nutrient elements of the soil and fertilizers. *Conclusion of scientific proceedings of Belorussian agricultural academy*. Minsk, **62**, 24–43 (in Russian).
Bugaev, V.P. & Osipova, Z.M.1966. Innfluence of mineral fertilizers and manure on agrochemical properties of soils and removal of nutrient elements by harvest in a perennial experiment. *Agrchemistry* **4**, 59–70 (in Russian).
Burtseva, S.V. 1969. Usag of nitrogen fertilizers with the application of ^{15}N in field conditions. *Bull. of All union SRI*. Moscow, **6**, 48–53 (in Russian).
Butenko, M.S., Ulyanova, O.A., Khalipsky, A.N. & Khizhnyak, S.V.2020. Influence of increasing doses of vermicompost on agrochemical properties of soil, yield and quality of potato tubers. *Agrochemistry* **7**, 47–56 (in Russian).
Cesoniene, L. & Rutkoviene, V. 2009. Lysimetric research of nutrient losses from organic fertlizers. *Agronomy Research* **7**(special issue 1), 224–232.
Conova, A.M. & Samoilov, L.N. 2015. Removal of nutrients cultural and weeds in the crop rotation. *Agrochemistry* **5**, 46–53 (in Russian).
Dontsov, M.B. & Kravchenko, C.H. 1985. Coefficients of usage of nutrient elements from fertilizers by crops. *Bull. of agricultural science* **4**, Moscow, pp. 55–61 (in Russian).
Dospekhov, B.A. 1985. *Methodology of Field Practice*. Agropromizdat, Moscow, pp. 207–248 (in Russian).
Grigel, G.I., Bandegru, D.I., Berezovski, V.N. & Postukhova, A.A. 1986. Removal nutrient elements by fruit crops. *Efficiency of application of fertilizers in intensive horticulture*, Kishinev, pp. 47–57 (in Russian).
Harutyunyan, S.S. 2009. Biological removal of nitrogen, phosphorus and potassium by tomatoes in different background of fertilizing. *Biological journal of Armenia* **61**(4), 43–50 (in Russian).
Harutyunyan, S.S. & Sargsyan, K.Sh. 2018. *Ecological security*, 476 pp. (in Armenian).
Harutyunyan, S.S., Sargsyan, K.Sh. & Mikayelyan H.A., 2020. The efficiency of application of organic-mineral fertilizers and microbiological concentrates in vegetation experiments of tomato and pepper. *Biological journal of Armenia* **72**(1–2), 82–88 (in Russian).
Harutyunyan, S.S., Ghukasyan, A.G. & Ghazaryan, G.R. 2023. Economic balance of nitrogen, phosphorus and potassium in the plantations of winter wheat and barley in the conditions of Ararat valley. *Annali D'Italia*, Florence, **29**, 3–12 (in Russian).
Khachatryan, A.S. & Abazyan, S.P. 1986. Application of nutrient elements by winter wheat and spring barley depending on provision of humidity. *Bull. of agricultural sciences of Armenia* **10**, 76–82 (in Armenian).
Kononchuk, V.V. & Nikitina, L.V. 2002. Effect of systematic application of fertilizers on the balance of potassium and several indices of potassium regime of liht chestnut soils during irrigation. *Agrochemistry* **6**, 53–58 (in Russian).
Korenkov, D.A. 1976. *Agrochemistry of nitrogen fertilizers*, Moscow, Nauka, 3–222 (in Russian).
Kristaponyte, I. 2005. Effect of fertilization systems on the balance of plant nutrients and soil agrochemical properties. *Agronomy Research* **3**(1), 45–54.

Kudeyarov, V.N. 2018. The balance of nitrogen, phosphorus and potassium in agriculture of Russia. *Agrochemistry* **10**, 3–11 (in Russian).
Kudeyarov, V.N. 2021. Nitrous oxide emission factor from Russian Arable soils at the fertilizers application. *Agrochemistry* **11**, 3–15 (in Russian).
Lavreva, U.A.1971. Mobilization of nitrogen of the soil under the influence of nitrogen fertilizers. *Bull. of All union SRI*. Moscow, **9**, 25–30 (in Russian).
Lebed, E.M., Kramaryev, S.M. & Podgornaya, L.G.1999. Balance of nutrient elements in crop rotation and application of fertilizers. *Agriculture* **6**, 25 (in Russian).
Makarov, N.B. & Nikitina, M.M. 1976. Coefficients of application of nutrient elements of fertilizers by the first crop. *Bull. of All union SRI*. Moscow **29**, 7–11 (in Russian).
Merzlaya, G.E. 2017. Biological factors in fertilizer systems. *Agrochemistry* **10**, 24–36 (in Russian).
Miloshchenko, N.Z. 1999. Fertility of soils as a central question of agriculture. *Agriculture* **5**, 15–16 (in Russian).
Mineev, V.G. 2000. Ecological functions of agrochemistry in modern agriculture. *Agrochemistry* **5**, 5–13 (in Russian).
Mineev, V.G. & Bichkova, L.A.2003. Situation and presspectives of application of mineral fertilizers in world and domestic agriculture. *Agrochemistry* **8**, 5–12 (in Russian).
Palumbo, G., Carfagna, S., Stolru, V., Torino, V., Romano, P.M., Letizie, F. & Di Martino, C. 2020. Environmental substainability fruit quality and production in mycorrhizal tomato plants without P fertilizing. *Agronomy Research* **18**(4), 2535–2549.
Peterburgsky, A.V. 1979. *Cycle and balance of nutrients in agriculture*. Science, Moscow, pp. 30–47 (in Russian).
Pryanishnikov, D.N. 1945. *Nitrogen in the life of plants and in Agriculture in the USSR*. Moscow, Publ. of Acad. of science of the USSR, 134–171 (in Russian).
Radzevičius, A., Karkleliene, R., Viskelis, P., Bobinas, C., Bobinaite, R. & Sakalauskiene, S. 2009. Tomato (Licopersicon esculentum Mill) fruit quality and physiological paramaters at different ripening stages of Lithuanian cultivars. *Agronomy Research* **7**(Special Issue II), 712–718.
Raukas, A.2010. Sustainable development and environmental risks in Estonia. *Agronomy Research* **8**(Special Issue II), 351–356.
Shafran, S.A. 2004. Dinamics of fertilization and soil fertility in Russia. *Agrochemistry* **1**, 9–17 (in Russian).
Shafran, S.A. 2020. Nitrogen balance in Agriculture of Russia and its regulation in modern conditions. *Agrochemistry* **7**, 47–56 (in Russian).
Sharyapov, M.M. 1976. Removal of nitrogen, phosphorus and potassium by harvest, coefficients of their usage and balance of nutrient elements in crop rotation on dark grey forest soils. *Proceedings of Tatar SRI of agriculture*, part **6**, 45–50 (in Russian).
Shmyreva, N.Ya., Khuzin, I.A., Feshchenko, N.S. & Bystrov, A.V. 2004. The use of fertilizer nitrogen by barley plants grown on soddy-podzolic soils of northern and southern slopes. *Agrochemistry* **10**, 27–32 (in Russian).
Soil science edited by I.S. Kauricheva. 1982. Kolos, Moscow, pp 34–35 (in Russian).
Yagodin, B.A. 1987. *Workshop on agricultural chemistry*. Agropromizdat, Moscow, 512 pp. (in Russian).
Yakimenko, V.N. 2019. Balance of potassium, yield and potash status of the soil in long-term field experiements in forest-steppe of Western Siberia. *Agrochemistry* **10**, 16–24 (in Russian).
Yurkin, S.N. 1974. Methodical issues of balance development in agriculture. *Bulletin of VIUA*, **20**, 12–37 (in Russian).
Yurkin, S.N. 1975. *Balance of nitrogen, phosphorus and potassium in the condition of intensify cation of the agriculture*. Moscow, 3–95 (in Russian).
Zamyatina, V.B. & Varyushkina, N.M. 1973. Transition and balance of nitrogen in fertilizers. In comp. *'Application of stable isotope ^{15}N in investigation of agriculture'*. Kolos, Moscow, 178–188 (in Russian).

Agronomy Research **22**(1), 207–216, 2024
https://doi.org/10.15159/AR.24.008

Integration of low-cost technologies for real-time monitoring of pigs in pre-fattening stage

A.P. Montoya[1,*], F.A. Obando[2], J.A. Osorio[3] and V. Gonzalez[3]

[1]Institución Universitaria Digital de Antioquia, Carrera 55#42-90, postal code 050015 Medellín, Colombia
[2]Universidad de Antioquia, Facultad de Ingeniería, Calle 67 #53-108, postal code 050010 Medellín, Colombia
[3]Universidad Nacional de Colombia, sede Medellín, Facultad de Ciencias Agrarias, Carrera 65 #59A-110, postal code 050034 Medellín, Colombia
[*]Correspondence: apmontoy@gmail.com

Received: February 1st, 2023; Accepted: December 27th, 2023; Published: January 29th, 2024

Abstract. Measurement of environmental, behavioural, and physiological variables is essential for decision making in intensive animal production systems. Data collection and analysis, in real time, employing low-cost tools are fundamental to increase competitiveness and animal wellness. In this context, the goal of this research was to develop a low-cost measurement system for monitoring bioclimatic and behavioural parameters in the production of pigs in the pre-fattening stage. Internet of things technologies was employed in order to increase control over the production and as a tool for decision-making in real time. Sensor Networks were developed using low-cost sensors open-source platforms and code. The system was validated in a pig farm located in Antioquia-Colombia with two groups of 10 pigs in the pre-fattening stage. Parallel tests with three sequential repetitions were carried out. The system was validated through continuous environmental data collection and periodic physiological measurements. The developed system includes temperature, relative humidity, global radiation, wind speed, pressure, and lighting sensors. A high microclimatic variability was found inside the facilities, presenting thermal discomfort conditions in some hours of the day, which impacted the development and behaviour of the animals. The adaptation of low-cost technologies for real-time monitoring of pigs is viable and facilitate decision-making in real time improving the productive efficiency, supplying important information at a productive and scientific level.

Key words: bioclimatic, comfort, ethology, pig farming, sensors, precision livestock farming.

INTRODUCTION

The 4.0 technology emerged in Germany in 2011 as a result of the fourth industrial revolution. This technology is based on the automation of processes and the incorporation of the Internet of Things to objects and systems in order to connect devices, collect information through the Internet and create interconnected intelligent devices in the digital world. This technology has spread around the world and it has made possible to improve the productive efficiency of different industries. The application of this

technology to the livestock sector is known as Precision Livestock Farming (PLF), an idea that was presented in the 90s in the United States of America (Morrone et al., 2022). The PLF focuses on the incorporation of different technologies in intensive systems to have real-time monitoring and more precise control over the physiological and environmental parameters in livestock production, in order to provide an early solution to possible problems that may arise in the production system (Buller et al., 2020).

It is estimated that by the year 2050 the world population will increase to more than 9 billion people, an aspect that requires intensifying food production in the world, in order to meet the needs of the population. The use of this type of technology is associated, among other things, with an increase in productive efficiency, therefore, the implementation of these technologies in PLF it is crucial (Benjamin & Yik, 2019b; Zhang et al., 2021).

Additionally, to facilitate the analysis of productive parameters in real time, PLF also provides tools for the monitoring and evaluation of environmental variables and animal welfare (Morrone et al., 2022). In this context, pig production is impacted by environmental factors determining the heat exchange of the animal with its surroundings. Because these animals are homeothermic, to regulate their temperature under unfavourable conditions, pigs employ energy that could be used in physiological processes associated with weight gain.

Bioclimatic management is very important at PLF. Many bioclimatic indices have been developed to represent the effect of different variables on the comfort of production facilities and animals. The THI is one of the most widespread, due to its easy calculation and the variables involved. This index represents the combined effect of air temperature and humidity on animal comfort in livestock production facilities. It is an empirical calculation that depends on the air temperature, relative humidity, genetics and physiology of the animal, among others. For this reason, different authors propose indices to monitor animal heat stress in intensive production facilities. In this work, the equation proposed by Cao, et al. (2021) will be used, this being one of the most up-to-date equations, obtained for conditions like those of our experiment.

$$THI = 0.8T + \left(\frac{RH(T - 14.4)}{100}\right) + 46.4 \quad (1)$$

In general, Colombian swine production is carried out in open or semi-open facilities without controlled climatic conditions, where climate regulation is carried out through natural ventilation through the windows of the facilities. In these spaces, it is possible that stress conditions associated with high temperatures are generated affecting the welfare and production of the animals (Machado et al., 2016). There are predetermined temperature and relative humidity conditions that can increase the production efficiency enhancing the genetic conditions of animals (Kuhl et al., 2023; Sales et al., 2008).The integration of technologies for the measurement of environmental variables in real time in this type of facilities plays a very important role in preventing the appearance of stressful situations and in decision-making (Buller et al., 2020).

Within the pork production sector these technological tools have been implemented for the measurement of productive parameters (Terrasson et al., 2017). The estimation of live weight, behaviour, movement patterns and posture are some of the measurements that can be performed (Benjamin & Yik, 2019a). Sensors, software and artificial vision have been employed in the measurement of biophysical, behavioural and physiological

parameters in intensive animal production systems (Berckmans, 2017; Aceto et al., 2019; Morrone et al., 2022). Image analysis and detection of body dimensions can estimate the weight of pigs in real time (Li et al., 2014). Infrared devices have been employed in the measurement of physiological and pathological processes in animals (Lu et al., 2018). Low-cost sensors have been used in the monitoring of the environmental space variability in different pig production facilities (Osorio et al., 2021). Additionally, mathematical models that predict productive parameters in pig production systems have been developed (Montoro et al., 2020).

In general, small and medium-sized Colombian pork producers do not have facilities with monitoring and control systems, the piggeries are usually natural ventilated and some climatic variables are measured manually. It is required adapted and low-cost systems that allow them to make informed decisions on climatic and productive management. This study seeks to implement a low-cost sensor network for real-time monitoring of bioclimatic, physiological and behavioural conditions of pre-fattening pigs, in order to support business decision-making in real time, through the incorporation of technology 4.0.

MATERIALS AND METHODS

Sensor network

The cost of the monitoring equipment employed in LPF can difficult its implementation in medium and small pig production farms (Sumiahadi et al., n.d.). Therefore, a low-cost open-source IoT tool for monitoring livestock production was developed. The sensor network was composed by two modules: internal environmental monitoring (Figs 1, B; C and D) and external monitoring (Fig. 1, A). For the measurement of internal environment, an ESP32 microprocessor was employed, this module was equipped to measure air temperature, relative humidity, pressure, light intensity and wind velocity. For the external module an ESP8266 microprocessor was used, this module was equipped to measure air temperature, relative humidity, atmospheric pressure, global radiation, wind speed and direction. The characteristics of the installed sensors are detailed in Table 1. All the sensors were installed outside the cases (Fig. 1, C).

Table 1. Low-cost sensor characteristics

Variable	Reference	Range	Resolution
Temperature	SHT31(Sensirion)	-40 to 90 °C	0.015 °C
Relative Humidity	SHT31(Sensirion)	0–100%	0.01%
Pressure	BMP280(Bosh)	300–1,100 hPa	0.16 hPa
Light	MAX44009(Maxim)	0.045–188,000 Lux	Variable

Internal modules were located in the middle of each pen at 1.5 m over the slat floor (Fig. 1, B). Outside module was installed over a ceiling at 3.5 m over de floor as can be detailed in Fig. 1, A).

The ESPNow communication protocol were employed to communicated the internal and external modules, sending the information wireless to the Raspberry Pi module, using the MQTT protocol through the open-source message broker Eclipse Mosquitto.

The measurements of all devices were stored in a micro-SD memory. All data and video can be online access employing Bluetooth protocol as can be seen in Fig. 1, D.

Swine tests

The customized network was tested in the monitoring a production of pigs in pre-fattening stage. Environmental and physiological conditions of the pigs were measured allowing the study of the thermal comfort inside the facility employing the THI index (Cao et al., 2021).

The tests were carried out at the Universidad Nacional San Pablo agrarian station, located in the department of Antioquia-Colombia (6°07'56"N 75°27'17"W 2.154 m.o.s.l). The place has an average temperature of 16.2 °C, mean RH of 82% and rainfall average of 2,645 mm. Two groups of pigs in pre-fattening stage were used, each group was composed of 10 pigs, as can be seen in Fig. 2.

Figure 1. A) External module and experimental piggery (red circle); B) Internal module location. C) Internal module detail; D) Internal module interior.

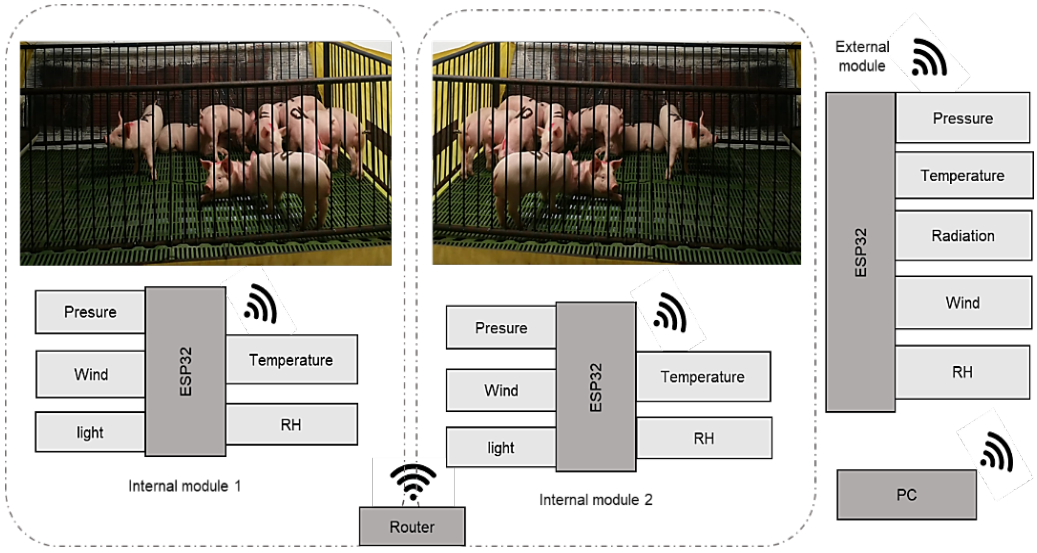

Figure 2. Test assembly description.

All piglets in the same band (within a range of three days of birth) were weighed at weaning, with 26 days of birth. Ten males and ten females weighing between 8–10 kg of live weight at weaning were selected for the trials. The sex and weight at the beginning of the experiment were homogeneous, separating males from females on each pen. Three repetitions were made, with a total of 60 animals. Each test started seven days after weaning, with duration of 42 days, with separation between test of 30 days.

The piggery where the trials were carried out contained two pens elevated 0.5 m above the ground. Two identical 2×2 m pens, with a 1m distance between them were used. The facilities did not have controlled climatic conditions. The entry and exit of air were controlled manually by opening the window shades, which remained closed along the night (5:00PM to 7:00AM).

At weaning the piglets were taken to the pre-fattening module. Ten animals were placed in each of the of the elevated pens with the aim of isolate them from the cold floor. Each pen had steel bars on the sides and was open at the top. The floor was of plastic slats for aeration and waste management. In addition, each pen had four drinkers and two linear feeders with 16 stalls each.

The facilities have double curtains in the ventilation to isolate the animals from the cold when was needed. Additionally, IR heating lamps were also used to adapt the piglets when they were transferred to the pre-fattening module.

The animals had a diet with commercial concentrate during all trials, with water and food ad libitum.

All the tests and production conditions of the animals were approved by the Ethics and Bioethics committee of the National University of Colombia-Medellín. The trials were carried out respecting the principles of animal welfare, guaranteeing the health, comfort and nutrition of the animals and following the guidelines of the ARRIVE (https://arriveguidelines. org) with the supervision of a zootechnician.

Automatic measurements of environmental variables were saved along the experiments. Manual air temperature and relative humidity were also taken at the high of the animals in the middle of the piggery, as usually is made in this production system. A Fluke 971 sensor with a resolution of 0.1 °C for temperature and 0.1% for relative humidity was used. Additionally, animal temperature was also taken employing a thermographic camera (Flir i3). Variable measurements allowed the analysis of the relationship between the environmental variables and the comparison between the THI computed using automatic and manual data.

RESULTS AND DISCUSSION

A large amount of data associated to the manual and automatic monitoring of bioclimatic variables was obtained. 239,660 data for each variable per test was saved, with a sample time of 10 s. The temperature is one of the most important variables to be consider in animal production systems. Temperature data shows high temporal and space variability between test and along them. When temporal variation of temperature along tests were analysed, it was found differences between the means and variances of the manual and automated data, also differences in the dynamic behaviour of the variable. Comparison of the temporal variability of the temperature in the same test and different pens (males and female) also showed different means and variances, but with similar

dynamic behaviour. Fig. 3 shows the comparison of the temperature behaviour along the first test in the male pen.

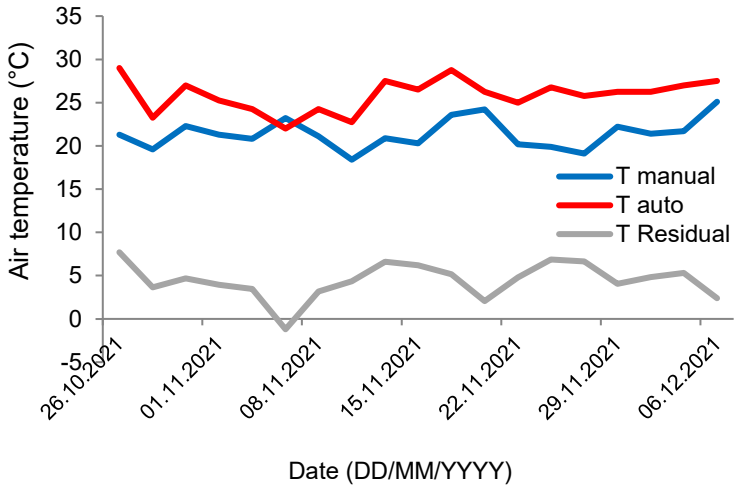

Figure 3. Comparison of the air temperature measurement employing manual and automatic sensor.

As can be seen in Fig. 3 manual and automatic temperatures are different, being the automatic temperature higher than the manual one, with means of 25.9 °C and 21.4 °C respectively, as can be seen in Table 2. The difference can be associated to the location of the sensor, due to the automatic sensor is near to the animals than the manual one, the radiation of the pigs' body heat increases the measurement, considering that both measurement systems (manual and automatic) were exposed to the air of the pig pen and were calibrated together with the same stimuli. In addition, the dynamic behaviour of the manual and automatic variables differs, as in November the 5th, when the manual temperature increases and the automatic one, decreases. Residuals (T automatic-T manual difference) are not constant, with a summatory different to zero. The standard deviation of the temperatures is higher than the accuracy and resolution of the sensor and the Person correlation between the two variables are 0.13, showing that no biased error is made in the measurement and the relation between the variable is no linear or other variables must be considered in the model.

Table 2. Descriptive statistics for the first experiment

Variable	T animal (°C)	T manual (°C)	T auto (°C)	T Residual (°C)	RH manual (%)	RH auto (%)	RH Residual (%)	THI manual	THI auto	THI Residual
Mean	37.1	21.4	25.9	4.5	77.4	81.3	4.0	68.8	76.3	7.5
Median	36.9	21.3	26.3	4.7	79.7	81.1	3.5	68.6	76.7	7.6
Variance*	1.6	2.9	3.4	4.0	175.3	122.5	142.9	4.2	5.5	7.2
SD	1.3	1.7	1.9	2.0	13.2	11.1	12.0	2.0	2.3	2.7
Max	39.3	25.1	29.0	7.7	95.2	100	25.1	73.3	80.2	13.3
Min	34.2	18.4	22.0	-1.2	38.6	60.8	-13.8	64.6	71.2	0.1

*Variance units are elevated to the square.

Relative humidity has an inverse relation with air temperature. An heterogenous behaviour of this variable was found between tests, piggeries and sensors. Even though there was nonspecific trend in the temporal analysis of the variable. Sometimes, manual humidity was higher or lower than the automatic one as can be seen in Fig. 4. In general, the mean of the automatic humidity was higher than the manual one, as is showed Table 2. This behaviour can be explained by the location of the sensor, where the sensor nearest to the animals is more exposed to the water vapor of waste evaporation and animal respiration.

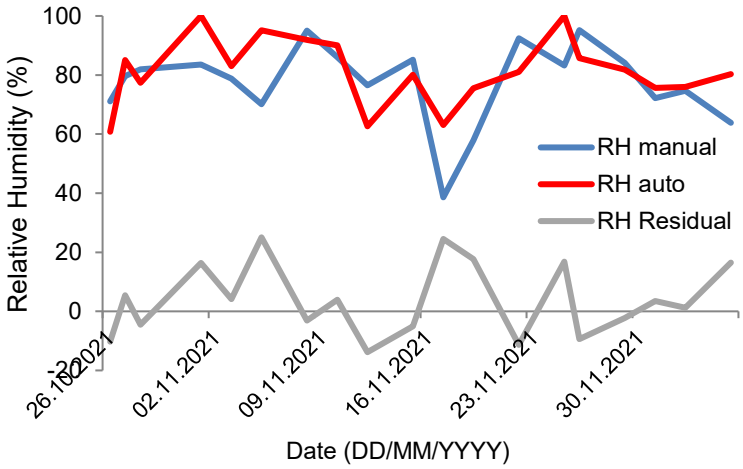

Figure 4. Comparison of the relative humidity measurement employing manual and automatic sensor.

The residual of the relative humidity variable has the same behaviour than in the temperature one. The standard deviation of the manual humidity was higher than the automatic one showing higher variability. But as the same in as temperature the standard deviations are higher than the sensor accuracy and resolution. Person correlation between the manual an automatic humidity was 0.28, showing a poor linear relation between them. Based in this result, it can be said that the measurement error is not biased and the relation between the variable is no linear or multivariable.

THI was computed employing Cao's equation. THI manual was calculated using manual taken temperature and humidity, while THI automatic was computed using the automatic values. As can be seen in Fig. 5 the automatic THI has higher values than the manual one with different dynamic behaviour and means of 76.3 and 68.8 respectively. The standard deviation of the THI auto, and variation range are higher than the manual one, showing more variability than the THI manual.

The threshold employed to define different rages of heat stress levels are: suitable for $THI < 74$, mild for $74 \leq THI < 78$, moderate for $78 \leq THI < 82$ and severe for $THI \geq 82$ (Cao et al., 2021). These values are depicted in Fig. 5 as horizontal lines. As can be seen in Fig. 5, all the values of THI manual are below of the suitable line, with a maximum value of 73.3, while for the THI automatic, the heat stress level goes from suitable to moderate, with a big portion of the values in mild level. Therefore, big

differences can be found when automatic or manual data are used, that can lead to a poor decision for environmental management inside the facilities.

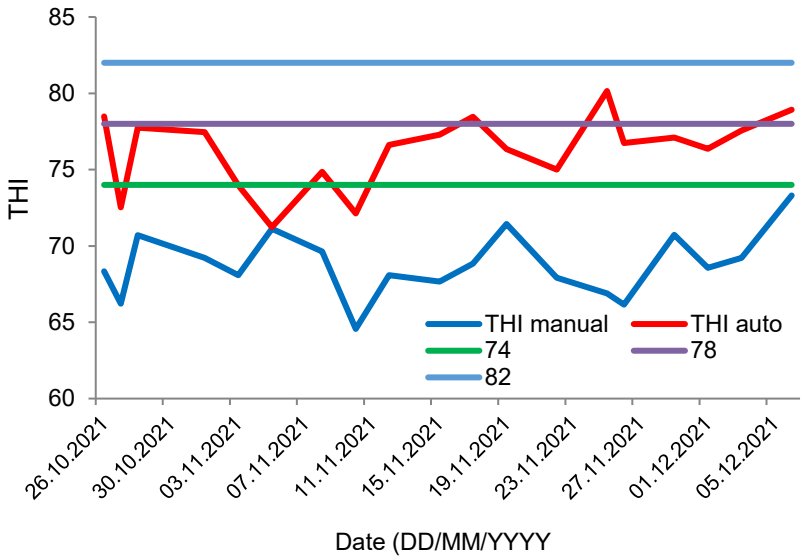

Figure 5. Comparison of the computed temperature and humidity index employing manual and automatic measurements.

Li et al. (2022) studied a combination of techniques for identifying an animal through video, recognizing their behaviour and analysing other variables such as outside temperature and humidity. They report that these kinds of information are the basis to generated an advance analysis of animal behaviour and wellness, being the accurate measurement of environmental variables a key for his study. In this case, the results of temperature and relative humidity in the Figs 3–4, shows that the manual data underestimate the automatic one, causing a significant difference in the computing of THI (Fig. 5). A similar behaviour was found by Neethirajan (2020) and Osorio et al. (2021b), were the authors highlight that the automatic sensors network can overestimate or underestimate the manual data.

Another important result is that the measurements of body temperature obtained using a thermographic camera were suitable, and could be an alternative to explore automated body temperature monitoring technology and have been developed in other researches employing visible and thermographic cameras (Taylor et al., 2022; Xie et al., 2023) using. If the THI data are analysed taking into account the statistics values of the animals' superficial temperature, presented in Table 2, it can be concluded that the animals were indeed subjected to thermal stress, since their average surface temperature was found to be 37.1 °C with a maximum of 39.3 °C, considering that superficial temperature measured with thermographic camera has a linear relation with rectal temperature and is usually bellow it (Zhang et al., 2019). Finally, could be consider that making climate management decisions with the manual data could cause productivity and welfare problems for the animals.

CONCLUSIONS

The development of low-cost sensor networks for monitoring environmental and physiological variables in pig production can contribute to real-time decision-making that impacts production and animal welfare. Production facilities with manual climate management are associated with high temporal and spatial variability of air temperature and relative humidity, which in many conditions can be found outside the comfort zone of the animals. In general, Colombian medium and small pig production facilities employs a single manual measurement of temperature and humidity in the middle of the piggery to calculate the temperature and humidity index, this practice can lead to an underestimation of the index that negatively affects the management of the animals and system production. The adaptation of low-cost technologies for real-time monitoring of pigs is viable and facilitate decision-making in real time improving the productive efficiency, supplying important information at a productive and scientific level.

REFERENCES

Aceto, G., Persico, V. & Pescapé, A. 2019. A Survey on Information and Communication Technologies for Industry 4.0: State-of-the-Art, Taxonomies, Perspectives, and Challenges. *IEEE Communications Surveys and Tutorials* **21**(4), 3467–3501. Institute of Electrical and Electronics Engineers Inc. https://doi.org/10.1109/COMST.2019.2938259

Benjamin, M. & Yik, S. 2019a. Precision Livestock Farming in Swine Welfare: A Review for Swine Practitioners. *Animals* **9**(133), 1–21. https://doi.org/10.3390/ani9040133

Benjamin, M. & Yik, S. 2019b. Precision livestock farming in swine welfare: A review for swine practitioners. *Animals* **9**(4). https://doi.org/10.3390/ani9040133

Berckmans, D. 2017. General introduction to precision livestock farming. *Animal Frontiers* **7**(1), 6–11. https://doi.org/10.2527/af.2017.0102

Buller, H., Blokhuis, H., Lokhorst, K., Silberberg, M. & Veissier, I. 2020. Animal welfare management in a digital world. *Animals* **10**(10), 1–12). MDPI AG. https://doi.org/10.3390/ani10101779

Cao, M., Zong, C., Zhuang, Y., Teng, G., Zhou, S. & Yang, T. 2021. Modeling of heat stress in sows part 2: Comparison of various thermal comfort indices. *Animals* **11**(6). https://doi.org/10.3390/ani11061498

Kuhl, R., Dias, C.H.F.Z., Alberton, G.C., Granzotto, F., Vicentin, J.H. & Santos, A.L. dos. 2023. Thermal comfort and photoperiod on the productive performance of sows and piglets. *Ciência Rural* **53**(5). https://doi.org/10.1590/0103-8478cr20210894

Li, J., Green-Miller, A., Hu, X., Lucic, A., Mohan, M.M.R., Dilger, R., Condotta, I., Aldridge, B., Hart, J.M. & Ahuja, N. 2022. Barriers to computer vision applications in pig production facilities. *Computers and Electronics in Agriculture*, **200**(September 2022), 107227. https://doi.org/10.1016/j.compag.2022.107227

Li, Z., Luo, C., Teng, G. & Liu, T. 2014. Estimation of Pig Weight by Machine Vision: A Review. In: *Li, D., Chen, Y. (eds) Computer and Computing Technologies in Agriculture VII. CCTA 2013.* IFIP Advances in Information and Communication Technology **420**, 42–49. Springer, Berlin, Heidelberg. https://doi.org/10.1007/978-3-642-54341-8_5

Lu, M., He, J., Chen, C., Okinda, C., Shen, M., Liu, L., Yao, W., Norton, T. & Berckmans, D. 2018. An automatic ear base temperature extraction method for top view piglet thermal image. *Computers and Electronics in Agriculture* **155**(September), 339–347. https://doi.org/10.1016/j.compag.2018.10.030

Machado, S.T., Nääs, I. de A., Neto, M.M., Vendrametto, O. & dos Reis, J.G.M. 2016. Effect of transportation distance on weight losses in pigs from dehydration. *Engenharia Agricola* **36**(6), 1229–1238. https://doi.org/10.1590/1809-4430-Eng.Agric.v36n6p1229-1238/2016

Montoro, J.C., Manzanilla, E.G., Solà-Oriol, D., Muns, R., Gasa, J., Clear, O. & Díaz, J.A.C. 2020. Predicting productive performance in grow-finisher pigs using birth and weaning body weight. *Animals* **10**(6), 1–14. https://doi.org/10.3390/ani10061017

Morrone, S., Dimauro, C., Gambella, F. & Cappai, M.G. 2022. Industry 4.0 and Precision Livestock Farming (PLF): An up to Date Overview across Animal Productions. *Sensors* **22**(12). MDPI. https://doi.org/10.3390/s22124319

Neethirajan, S. 2020. The role of sensors, big data and machine learning in modern animal farming. *Sensing and Bio-Sensing Research* **29**(1), 1–8. https://doi.org/10.1016/j.sbsr.2020.100367

Osorio, J.A.O., Castrillón, N., Gonzalez, V., Soto, Y.P.Q., Montoya, A.P. & Castrillon, E.G. 2021a. Assessment of spatial variability of environmental conditions in different swine production typologies in tropical conditions. *Journal of Animal Behaviour and Biometeorology* **9**(3), 1–8. https://doi.org/10.31893/jabb.21031

Osorio, J.A., Gonzalez, V.C., Ferraz, G.A.S., Ferraz, P.F.P. & Damasceno, F.A. 2021b. Thermal comfort assessment in a typological non-isolated maternity pig sheds with different types of farrowing systems. *Agronomy Research* **19**(S2), 1087–1098, 2021. https://doi.org/10.15159/ar.21.089

Sales, G.T., Fialho, E.T., Yanagi, T., Freitas, R.T.F.D., Teixeira, V.H., Gates, R.S. & Day, G.B. 2008. Thermal environment influence on swine reproductive performance. In: *Livestock Environment VIII - Proceedings of the 8th International Symposium*, 767–772. https://doi.org/10.13031/2013.25582

Sumiahadi, A., Direk, M. & Acar, R. (n.d.). *Economic Assesment of Precision Agriculture. A Short Review, Pasture and Forage Crops View project The Social Structure and the Levels of Perception of the Problems of the Students in the Campus Dormitory Konya-Turkey View project*. https://www.researchgate.net/publication/337744890

Taylor, C., Guy, J. & Bacardit, J. 2022. Prediction of growth in grower-finisher pigs using recurrent neural networks. *Biosystems Engineering* **220**(1), 114–134. https://doi.org/10.1016/j.biosystemseng.2022.05.016.

Terrasson, G., Llaria, A., Villeneuve, E. & Pilnière, V. 2017. Precision Livestock Farming: A Multidisciplinary Paradigm. In: S*MART 2017 The Sixth International Conference on Smart Cities, Systems, Devices and Technologies*, 55–59. https://www.researchgate.net/publication/331373949

Xie, Q., Wu, M., Bao, J., Zheng, P., Liu, W., Liu, X. & Yu, H. 2023. A deep learning-based detection method for pig temperature using infrared thermography. *Computers and electronics in agriculture* **213** (2023).

Zhang, M., Wang, X., Feng, H., Huang, Q., Xiao, X. & Zhang, X. 2021. Wearable Internet of Things enabled precision livestock farming in smart farms: A review of technical solutions for precise perception, biocompatibility, and sustainability monitoring. *Journal of Cleaner Production* **312**(February), 127712. https://doi.org/10.1016/j.jclepro.2021.127712

Zhang, Z., Zhang, H. & Liu, T. 2019. Study on body temperature detection of pig based on infrared technology: A review. *Artificial Intelligence in Agriculture* **1**(2019), 14–26.

Agronomy Research **22**(1), 217–226, 2024
https://doi.org/10.15159/AR.24.042

Theoretical study of the movement of the wide span machine in quasi-static turning mode

J. Olt[1,*], V. Bulgakov[2], V. Adamchuk[3], V. Kuvachov[4] and O. Liivapuu[1]

[1]Estonian University of Life Sciences, Institute of Forestry and Engineering, 56 Kreutzwaldi Str., EE 51006 Tartu, Estonia
[2]National University of Life and Environmental Sciences of Ukraine, 15 Heroyiv Oborony Str., UA 03041 Kyiv, Ukraine
[3]Institute of Mechanics and Automation of Agricultural Production of the National Academy of Agrarian Sciences of Ukraine, 11 Vokzalna Str., Glevakha stl, Fastiv Dist., UA 08631 Kyiv Region, Ukraine
[4]Dmytro Motornyi Tavria State Agrotechnological University, 18B Khmelnytsky Ave., UA 72310 Melitopol, Zaporozhye Region, Ukraine
[*]Correspondence: jyri.olt@emu.ee

Received: March 14th, 2024; Accepted: May 14th, 2024; Published: May 16th, 2024

Abstract. Wide span machines represent sophisticated energy and technological tools for controlled traffic farming. The curvilinear movement (turning) of these machines are often decisive in the design of new or evaluation of existing models of equipment. The application of classical theory of turning in researching wide span machines faces certain challenges due to limitations imposed when describing the force or kinematic interaction of their movers with the supporting surface along a constant technological track. Additionally, non-traditional control schemes further complicate the use of the classical turning theory. The present research aims to study the curvilinear motion of wide span vehicles in a quasi-static turning mode, allowing for the modelling of their turns with combined or non-traditional movers under various control schemes. As a result of the conducted research, it was established that a promising non-traditional turning scheme for a wide span machine is one where one rear wheel is driving, and the other is braking, with controllable front wheels. In this case, the turning radius of the machine is 1.5 times smaller compared to traditional turning schemes. It was experimentally proven that the practical implementation of this new non-traditional turning scheme for the wide span machine is limited by the magnitude of the load on its front wheels relative to the rear ones.

Key words: controlled traffic farming, curvilinear motion, turning, wide span machine.

INTRODUCTION

Contemporary agricultural development trends, amidst heightened competition, necessitate the reduction of production costs per unit (McHugh et al., 2009; Tullberg, 2009; Bindi et al., 2013; Antille et al., 2015; Chamen, 2015; Antille et al., 2019). A pivotal focus of ongoing global research involves formulating a comprehensive set of technological measures to implement resource-efficient technologies and technical

instruments, thereby diminishing the demand for material, technical, and energy resources. A prospective initiative in this context involves the implementation of wide span (gantry) systems in agriculture (Bochtis et al., 2010; Pedersen, 2011; Onal, 2012; Pedersen et al., 2016). The distinctive feature of these systems is the allocation of a portion of the overall field area for an engineering zone, encompassing a transportation system for the mobility of all mechanization equipment, communication infrastructure for energy and water supply, telecommunication channels, and an orientation system. The area of the engineering zone is primarily contingent upon the specifications of the transportation system, which, in a reciprocal manner, are dictated by the characteristics of technological and transport machinery. In controlled traffic farming systems, a promising innovation is a gantry machine modeled after the Dowler tractor. Within the operational cycle of any wide span machine, there exists a curvilinear motion (turning). The characteristics of this movement often play a decisive role in the design of new equipment or the assessment of existing models. Consequently, numerous scientists engage in the study of this specific type of motion (Rohde & Yule, 2003; Gasso et al., 2013; Gasso et al., 2014; Bulgakov et al., 2017; Bulgakov et al., 2019). Numerous scientific papers have been dedicated to the investigation of the turning of conventional machine-tractor aggregates (Gurudatta et al., 2018; Bulgakov et al., 2022), as the parameters of this type of motion largely determine its operational efficiency. Presently, two primary directions have emerged in the theory of turning, each employing distinct approaches to describing the motion. These directions encompass the theory of turning for wheeled and tracked machines. However, among contemporary tractor aggregates, machines featuring a combined or non-traditional type of mover are increasingly gaining prevalence (Ruiz-Garcia & Sanchez-Guerrero, 2022).

Attempts to apply existing models to describe the motion of such tractors (Hac et al., 2009; Adamchuk et al., 2016; Li et al., 2016; Bulgakov et al., 2018; Bulgakov et al., 2020) have generally been unsuccessful, primarily due to the constraints imposed when describing the force and kinematic interaction of their movers with the supporting surface. For instance, using the theory of turning for tracked vehicles (Ding & Tang, 2020) is deemed impractical for crawler tractors (such as those from Komatsu) or articulated-steering tractors (such as those from Case) due to inherent limitations in kinematics (non-turning supports of the mover).

To study the motion of conventional machine-tractor aggregates during turns, models based on the theory of lateral slip are most commonly employed (Nadykto et al., 2015). These models have found broad application in describing vehicles equipped with inter-axle differentials that operate virtually without wheel slip. Conversely, the classical theory of rotation for wheeled vehicles, based on the utilization of elastic side slip, precludes slipping relative to the ground. Simultaneously, non-traditional control schemes are increasingly being implemented in the models of experimental wide span machines. For example, additional braking during turns, accompanied by inevitable wheel slip (Bulgakov et al., 2019). In light of the aforementioned considerations, it is suggested to employ a methodology for simulating the curvilinear motion of wide span vehicles, conceptualized as a controlled entity whose curvilinear movement is governed by the constraints imposed on it, facilitated through the machine's design and its control system.

The aim of this study is to investigate the curvilinear motion of a wide span machine during a quasi-static turning mode, thereby enabling the simulation of its turning with a combined or non-traditional mover under various control schemes.

MATERIALS AND METHODS

An experimental research subject consisted of a prototype of a wide span machine (Fig. 1). The depicted wide span machine incorporates a power truss (1) functioning as a rigid frame connected to both the left (2) and right (3) platforms. Brackets (4) with wheels (5) are attached to platforms (2) and (3). The rotation of the wheels (5) is carried out using two gear motors (6) installed inside the platforms (2) and (3) and synchronous mechanisms (7) that drive the front and rear wheels (5) on each side of the machine. In the upper part of the left platform (2) there is a control cabinet (8) with chassis control devices. Supporting pillars (9) with power jacks for lifting the machine's sides from any direction are installed between the front and rear wheels (5) on the lower surface of platforms (2 and 3). Additional components of the machine's hydraulic system, including a hydraulic fluid reservoir (10), an electric motor (11) for driving the hydraulic pump (12), and a hydraulic distributor (13), are positioned on the crossbars of the frame (1). Additionally, a hydraulic suspended mechanism (14) is situated in the central part of the wide span machine.

The main technical specifications of the prototype (Fig. 1): operation mass 1,158 kg, wheel gauge 3.5 m, wheelbase 2.3 m, pneumatic tire size 9.5R32.

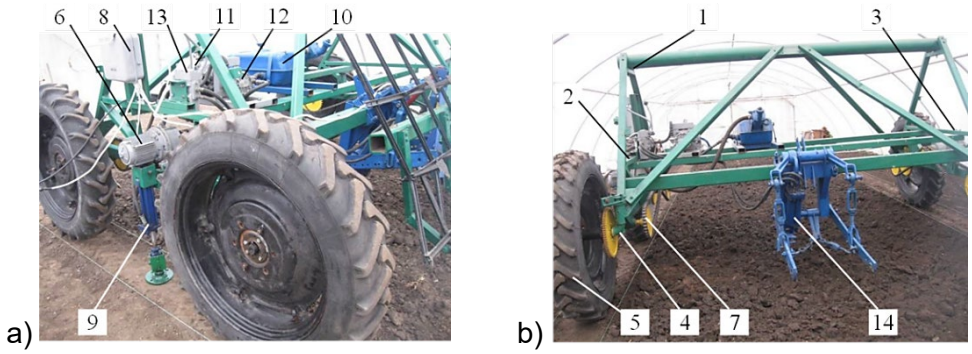

Figure 1. Overall view of the experimental wide span machine design: a) side view; b) front view: 1 – frame-truss; 2, 3 – left and right platforms; 4 – brackets; 5 – wheels; 6 – motor-reducers; 7 – wheel drive mechanism; 8 – control cabinet; 9 – support pillars with power jacks; 10 – hydraulic reservoir; 11 – electric motor; 12 – hydraulic pump; 13 – hydraulic distributor; 14 – suspended mechanism.

In the course of experimental investigations, the turning diameter of the machine was measured using a tape measure along the trajectory demarcated by inkjet markers affixed at the centre of its frame. The precision of the turning diameter measurement was within the range of ±1%.

The design of any agricultural gantry system permits two configurations: one with a wheeled mover and the other with a tracked mover. The wheeled mover configuration of the wide span machine continues to be the most promising. An evaluative analysis of

the turning capability of the wide track vehicle equipped with a wheeled mover system facilitated the identification of the most rational area of application for each of its potential configurations (Fig. 2).

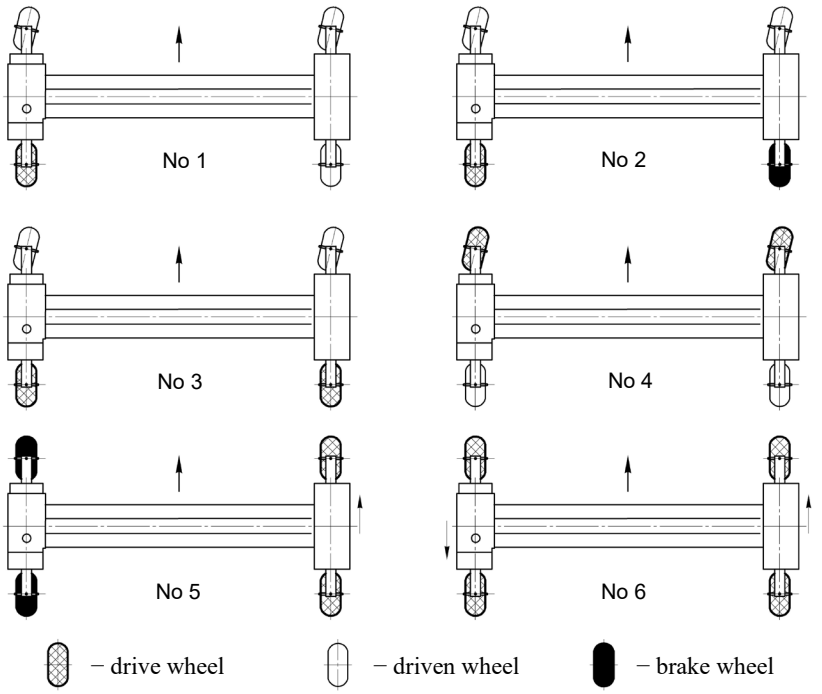

Figure 2. Schemes for controlling the turning of a wide span machine using one of its structural bases.

Initial investigations into the turning capacity of the wide-span machine indicate that Scheme No 1 is virtually unaffected by the vertical load on its drive wheels. Scheme No 2 exhibits the smallest turning radius among the configurations of the wide span machine. Nevertheless, when equipped with a front-mounted agricultural tool, resulting in an additional vertical load on the front of the machine, it forfeits its ability to move due to binding loss on the drive wheel. Schemes No 3 and No 4 are distinguished by their larger turning radius, yet they represent the most conventional and straightforward options for practical implementation. A wide span vehicle employing a skid steering turning, as demonstrated in Schemes No 5 and No 6, exhibits enhanced manoeuvrability. However, the utilization of a wheel propulsion device on a solid surface during turning results in increased slippage, leading to heightened wear on the vehicle wheels' tires.

In the course of the investigation, two non-traditional control schemes for the rotation of the wide span machine were examined: Scheme No 1 and No 2 (Fig. 2).

Theoretically, the analysed scheme of curvilinear motion of a physical wide span machine can be described in the mode of quasi-static turn (Fig. 3). This pertains to motion characterized by a variable radius, wherein inertial forces can be neglected and an equilibrium system of forces is present at each moment of time.

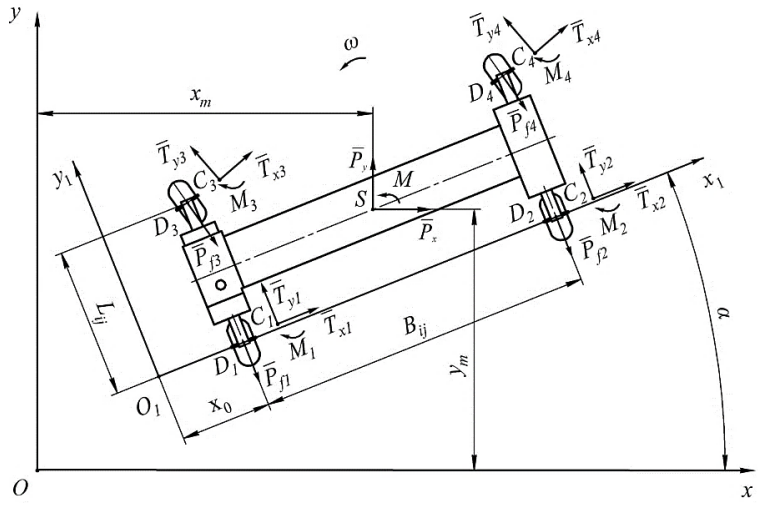

Figure 3. Scheme of quasi-static turning of a wide span machine with front swivel wheels.

The mathematical model of quasi-static turn of a wide span machine (Fig. 3) with n axes (i = 1...n) and m supports on each axis (j = 1...m) consists of 3 equations of motion:

$$\left.\begin{aligned}\sum_{i=1}^{n}\sum_{j=1}^{m} F_{xij} = 0,\\ \sum_{i=1}^{n}\sum_{j=1}^{m} F_{yij} = 0,\\ \sum_{i=1}^{n}\sum_{j=1}^{m} M_{O_{ij}} = 0,\end{aligned}\right\} \qquad (1)$$

where $\sum_{i=1}^{n}\sum_{j=1}^{m} F_{xij}$ – the sum of the projections of all forces on the x axis; $\sum_{i=1}^{n}\sum_{j=1}^{m} F_{yij}$ – the sum of the projections of all forces on the y axis; $\sum_{i=1}^{n}\sum_{j=1}^{m} M_{O_{ij}}$ – the sum of the moments of all forces about point O of each ij support of the wide span machine.

We write the equations of motion (1) of the wide span machine in the form:

$$\left.\begin{aligned}0 = \sum_{i=1}^{n}\sum_{j=1}^{m}\left(T_{xij}\cdot\cos\gamma_{ij} - T_{yij}\cdot\sin\gamma_{ij} + P_{fij}\cdot\sin\gamma_{ij}\right) + P_x,\\ 0 = \sum_{i=1}^{n}\sum_{j=1}^{m}\left(T_{xij}\cdot\sin\gamma_{ij} + T_{yij}\cdot\cos\gamma_{ij} + P_{fij}\cdot\cos\gamma_{ij}\right) + P_y,\\ 0 = \sum_{i=1}^{n}\sum_{j=1}^{m}\left[-M_{ij} + T_{yij}\cdot\sqrt{x_{cij}^2 + y_{cij}^2} - P_{fij}\cdot\left(\sqrt{x_{cij}^2 + y_{cij}^2} - x_{ij}\right)\right] + M,\end{aligned}\right\} \qquad (2)$$

where x_m, y_m, α – coordinates of the center of mass and the turning angle of the vehicle body in a fixed Cartesian system; P_{fij} – tractive resistance of ij supporting wheel; P_x, P_y, M – external forces and torque reduced to the center of mass of the machine; T_{xij}, T_{yij}, M_{ij} – force factors in contact of ij support wheel with the permanent tramline track; yij – turning angles of the ij support relative to the frame of wide span machine.

In non-stationary curvilinear motion, the steering wheels participate in two rotational movements about to parallel axes (Fig. 4). The first movement is the turning of the wheel together with the machine frame about the center of turning (point *O*), the second is a turning relative to the frame (point D_{ij}).

In this case, the constraint equations have the form:

$$(x_{cij} - x_{kij}) \cdot \sin(\alpha + \gamma_{ij}) - (y_{cij} - y_{kij}) \cdot \cos(\alpha + \gamma_{ij}) = 0, \quad (3)$$

$$(x_{cij} - x_{kij}) \cdot \sin(\alpha + \gamma_{ij}) - (y_{cij} - y_{kij}) \cdot \cos(\alpha + \gamma_{ij}) = 0, \quad (4)$$

where x_{kij}, y_{kij} – coordinates of point K_{ij} of ij support of wide span machine; x_{cij}, y_{cij} – coordinates of instantaneous center of zero velocity C_{ij} of support ij; α, γ_{ij}, $\dot{\alpha}$, $\dot{\gamma}_{ij}$ – turning angles and their time derivatives of the frame and ij support relative to the frame of wide span machine.

After transforming the coordinates and solving the equilibrium equations for the unknown coordinates of the instantaneous velocity center x_{ij}, y_{ij} of the wide span machine, we obtain:

$$x_{ij} = \frac{[\dot{x}_m \cdot \sin(\alpha + \gamma_{ij}) + V_{Tij} - \dot{y}_m \cdot \cos(\alpha + \gamma_{ij}) - \dot{\alpha} \cdot (B_{ij} \cdot \cos\gamma_{ij} + L_{ij} \cdot \sin\gamma_{ij})]}{\dot{\alpha} + \dot{\gamma}_{ij}} \quad (5)$$

$$y_{ij} = \frac{[\dot{x}_m \cdot \cos(\alpha + \gamma_{ij}) + \dot{y}_m \cdot \sin(\alpha + \gamma_{ij}) + \dot{\alpha} \cdot (B_{ij} \cdot \sin\gamma_{ij} - L_{ij} \cdot \sin\gamma_{ij})]}{\dot{\alpha} + \dot{\gamma}_{ij}}, \quad (6)$$

where B_{ij}, L_{ij} – transverse and longitudinal base of ij support of the wide span machine.

Mathematical models (5) and (6) represent equations of nonholonomic kinematic constraints for controlled curvilinear motion, reflecting the design parameters of the wide span machine and its control system.

The transformation of the coordinates of the instantaneous center of zero velocity (x_{cij}, y_{cij}) for any of its design of chassis is carried out by shift and turning. Equations of geometric constraints (Fig. 4), reflecting the construction arrangement and parameters of the wide span machine (base, track, number of supports and their relative positions) take the form:

$$\left.\begin{aligned} y_0 + y_1 &= 0, \\ y_1 &= y_2, \\ x_{c3} \cdot \sin\gamma_3 &= y_{c3} \cdot \cos\gamma_3, \\ x_{c4} \cdot \sin\gamma_4 &= y_{c4} \cdot \cos\gamma_4, \end{aligned}\right\} \quad (7)$$

where x_{c3}, x_{c4}, y_{c3}, y_{c4} – coordinates of the instantaneous center of zero velocity of support wheels 3 and 4 of the system of the wide span machine; y_{c3}, y_{c4} – turning angles of the support wheels 3 and 4 about the vertical axes in the system of the wide span machine.

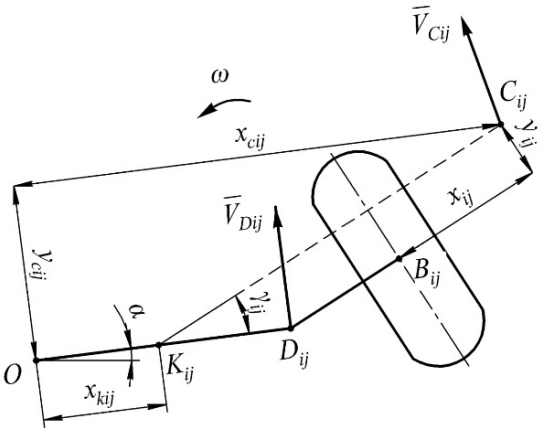

Figure 4. Kinematics of the steered wheel of a wide span machine.

The equations of kinematic constraints (4), depending on the implemented turning pattern of the wide span machine, reflecting the mode of motion of each support (driven, driving, brake) of the wide span machine, have the form:

$$\left.\begin{array}{r} T_{y1} = 0, \\ x_0 + x_1 = 0, \\ T_{y3} = 0, \\ T_{y4} = 0. \end{array}\right\} \quad (8)$$

First order differential equations for constructing the turning trajectory of a wide span machine have the form:

$$\left.\begin{array}{r} dx_m = ds \cdot \cos\alpha, \\ dy_m = ds \cdot \sin\alpha, \\ d\alpha = \dfrac{ds}{\rho_m}, \end{array}\right\} \quad (9)$$

where $ds = V_m \cdot dt$ – differential of the trajectory arc of the center of mass of the wide span machine; V_m – theoretical velocity of the center of mass; ρ_m – radius of curvature of the trajectory of the center of mass.

To construct the trajectory of the center of mass of the wide span machine using the radius of curvature ρ_m, as a function of the time parameter τ, we will apply the theory of a curvilinear integral. Under zero initial conditions, this integral will take the following form:

$$x_m = \int_0^T V_m \cdot \cos\left(\int_0^t \frac{V_m}{\rho_m} d\tau\right) dt, \quad (10)$$

$$y_m = \int_0^T V_m \cdot \sin\left(\int_0^t \frac{V_m}{\rho_m} d\tau\right) dt, \quad (11)$$

where t, T – current time and process time, respectively.

The radius of curvature ρ_m of the trajectory of the center of mass of the wide span machine in this case is equal to

$$\rho_m = x_0 + x_m, \quad (12)$$

where x_0 – the initial coordinate of the trajectory curve of the center of mass of the wide span machine.

The information above indicates that constructing the trajectory of the center of mass of the wide span machine involves determining the values of x_0 and x_m in the moving coordinate system. The values of x_0 and x_m are easily calculated when solving the problem of initial motion, expressed in the form of equilibrium conditions for the wide span machine at different moments in time.

Therefore, theoretical modelling of the motion of the wide span machine in quasi-static turning mode allowed establishing a connection between the coordinates of the instantaneous centre of velocities of an arbitrarily located support of the mover and the centre of turning of the wide span machine. It enables the formulation of the missing constraint equations. Combining various geometric constraints (reflecting the structural scheme and parameters of the machine) with kinematic ones (reflecting the control system) allows describing all types of constraints imposed on the wide span machine during its curvilinear motion.

RESULTS AND DISCUSSION

The adequacy of theoretical models for the curvilinear motion of the wide span machine in quasi-static turning mode was assessed based on a kinematic parameter – the diameter of turning under different loads applied to its running gear.

The simulation of the load mode for the wide span machine was carried out by installing additional ballast located at its front part. The degree of loading on the front wheels of the wide span machine relative to the rear wheels varied in the range of G_f/G_r = 0.5–2.5. In the experiment, using traces of jet markers attached to the center of the wide span machine, the diameter of turning was measured.

The results of comparing the theoretical and experimental dependencies of the turning diameter of the wide span machine for control schemes No 1 and No 2 (Fig. 2) with the degree of loading on the front wheels of the wide span machine relative to the rear wheels are presented in Fig. 5 and Fig. 6, respectively.

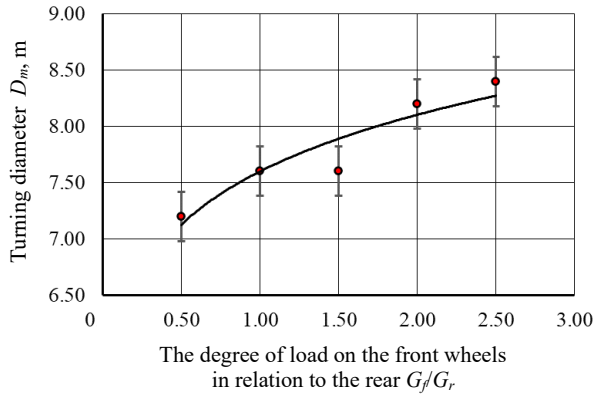

Figure 5. Comparison of theoretical and experimental dependences of the turning diameter of a bridge vehicle according to its control scheme No 1 (Fig. 2) on the degree of load on the front wheels in relation to the rear wheels.

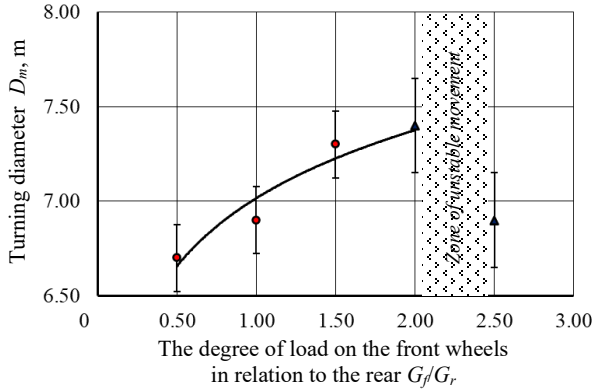

Figure 6. Comparison of theoretical and experimental dependences of the turning diameter of a bridge vehicle according to its control scheme No 2 (Fig. 2) on the degree of load on the front wheels in relation to the rear wheels.

The analysis of comparing the theoretical and experimental dependencies (Figs 5, 6) of the turning diameter of the wide span machine under different control schemes No 1 and No 2 (Fig. 2) with the degree of loading on its front wheels in relation to the rear ones showed that the maximum relative deviation of experimental points from the calculated curves across the entire load range G_f/G_r = 0.5–2.5 for both schemes did not exceed 11%.

It was experimentally established and theoretically confirmed that braking the rear inner wheel (scheme No 2, Fig. 2) leads to a 1.5-fold reduction in the turning radius. However, with an overload G_f/G_r of more than 2 times, the wide span machine loses its ability to move. During the experiments, this manifested as increased slipping, deviation from the stationary turning trajectory, and was characterized by a large spread in measurement results.

CONCLUSIONS

1. As a result of the conducted research, it has been established that a promising non-traditional turning scheme for the wide span machine is one where one rear wheel serves as the driving wheel, while the other functions as the braking wheel, with controllable front wheels. In this case, the turning radius of the wide span machine is 1.5 times smaller compared to traditional turning schemes.

2. When modelling the movement of the wide span machine in quasi-static turning mode, it is sufficient to have 3 equations of motion, 4 equations of geometric constraints, 3 equations of kinematic constraints, and 3 equations for constructing the turning trajectory. The adequacy of theoretical studies has been confirmed by experiments, where the deviation from theoretical dependencies does not exceed 11%.

3. It has been experimentally proven that the practical implementation of the mentioned new non-traditional turning scheme for the wide span machine is limited by the magnitude of the load on its front wheels in relation to the rear ones. With a load on the front wheels of the wide span machine more than 2 times that of the rear wheels, it loses the ability to move, resulting in increased slipping, and deviation from the stationary turning trajectory, and is characterized by a significant spread in measurement results.

REFERENCES

Adamchuk, V., Bulgakov, V., Nadykto, V., Ihnatiev, Y. &, Olt J. 2016. Theoretical research into the power and energy performance of agricultural tractors. *Agronomy Research* **14**(5), 1511–1518. ISSN 1406-894X

Antille, D.L., Chamen, W.C.T. & Tullberg, J.N. 2015. The potential of controlled traffic farming to mitigate greenhouse gas emissions and enhance carbon sequestration in arable land: a critical review. In Transactions of the *ASABE* **58**(3), 707–731.

Antille, D.L., Peets, S., Galambošová, J., Botta, G.F., Rataj, V., Macak, M., Tullberg, J.N., Chamen, W.C.T., White, D.R., Misiewicz, P.A., Hargreaves, P.R., Bienvenido, J.F. & Godwin, R.J. 2019. Review: Soil compaction and controlled traffic farming in arable and grass cropping systems. *Agronomy Research* **17**(3), 653–683. doi: 10.15159/AR.19.133

Bindi, I., Blackwell, P., Riethmuller, G., Davies, S., Whitlock, A. & Neale, T. 2013. Controlled traffic farming technical manual. *Technical manual bulletin* **4607**. Department of Agriculture and food, NACC, Western Australia, 80 pp. ISBN: 978-0-9923323-03

Bochtis, D.D., Sørensen, C.G. & Busatob, P. 2010. Tramline establishment in controlled traffic farming based on operational machinery cost. *Biosystems Engineering* **107**(3), 221–231.

Bulgakov, V., Adamchuk, V., Kuvachov, V., Arak, M. & Olt, J. 2017. Study into movement of wide span tractors (vehicles) used in controlled traffic farming. In: *Proceedings of the 28th DAAAM International Symposium*. Vienna, Austria, pp. 0199–0208. doi: 10.2507/28th.daaam.proceedings.027

Bulgakov, V., Kuvachov, V. & Olt, J. 2019. Theoretical Study on Power Performance of Agricultural Gantry Systems. In: *Proceedings of the 30th DAAAM International Symposium*. Vienna, Austria, pp. 0167–0175. doi: 10.2507/30th.daaam.proceedings.022

Bulgakov, V., Melnik, V., Kuvachov, V. & Olt, J. 2018. Theoretical Study on Linkage Unit of Wide Span Tractor. – In: *Proceedings of the 29th DAAAM International Symposium*. Vienna, Austria, 0180–0189. 10.2507/29th.daaam.proceedings.026

Bulgakov, V., Olt, J., Kuvachov, V. & Smolinskyi, S. 2020. A theoretical and experimental study of the traction properties of agricultural gantry systems. *Agraarteadus* **31**(1), 10–16. doi: 10.15159/jas.20.08

Bulgakov, V., Olt, J., Pascuzzi, S., Adamchuk, V., Gadzalo, J., Kuvachov, V., Kaletnik, H., Kaminskiy, V. & Lillerand, T. 2022. Theoretical Research of Gantry Tractor Turning. In: *Proceedings of the 33rd DAAAM International Symposium*. Vienna, Austria, pp. 0380–0389. doi: 10.2507/33rd.daaam.proceedings.054

Chamen, T. 2015. Controlled traffic farming – from worldwide research to adoption in Europe and its future prospects. *Acta Technologica Agriculturae Nitra* **18**(3), 64–73. doi: 10.1515/ata-2015-0014

Ding, Z., Li, Y. & Tang, Z. 2020. Theoretical Model for Prediction of Turning Resistance of Tracked Vehicle on Soft Terrain. *Mathematical Problems in Engineering*. Article ID4247904, 1–9. doi: 10.1155/2020/4247904

Gasso, V., Sørensen, C.A.G. & Oudshoorn, F.W. 2013. Controlled traffic farming: A review of the environmental impacts. *European Journal of Agronomy* **48**, 66–73.

Gasso, V., Sørensen, C. &, Pedersen H. 2014. An environmental life cycle assessment of controlled traffic farming. *Cleaner Production* **73**, 175–182.

Gurudatta, M. Anche, Velmurugan, M.A., Arun Kumar, S., Shankar C. Subramanian. 2018. Model Based Compensator Design for Pitch Plane Stability of a Farm Tractor with Implement. *IFAC-PapersOnLine* **51**(1), 208–213. doi: 10.1016/j.ifacol.2018.05.043

Hac, A., Fulk, D. & Chen H. 2009. Stability and Control Considerations of Vehicle-Trailer Combination. *SAE Int. J. Passeng. Cars – Mech. Syst*. **1**(1), 925–937. doi: 10.4271/2008-01-1228

Li, Z., Mitsuoka, M., Inoue, E., Okayasu, T., Hirai, Y. &, Zhu Z. 2016. Parameter sensitivity for tractor lateral stability against Phase I overturn on random road surfaces. *Biosystems Engineering* **150**(1), 10–23. doi: 10.1016/j.biosystemseng.2016.07.004

McHugh, A.D., Tullberg, J.N. & Freebairn, D.M. 2009. Controlled traffic farming restores soil structure. *Soil Tillage Research* **104**(1), 164–172, doi: 10.1016/j.still.2008.10.010

Nadykto, V., Arak, M. & Olt, J. 2015. Theoretical research into the frictional slipping of wheel-type undercarriage taking into account the limitation of their impact on the soil. *Agronomy Research* **13**(1), 148–157.

Onal, I. 2012. Controlled Traffic farming and Wide Span Tractors. *Journal of Agricultural Machinery Science* **8**(4), 353–364.

Rohde, K. & Yule, D. 2003. Soil compaction and Controlled Traffic Farming research in Central Queensland. *Proceedings ISTRO* **16**, 1020–1027.

Ruiz-Garcia, L. & Sanchez-Guerrero, P. 2022. A Decision Support Tool for Buying Farm Tractors, Based on Predictive Analytics. *Agriculture* **12**(3), 331. doi: 10.3390/agriculture12030331

Pedersen, H.H. 2011. Harvest Capacity Model for a Wide Span Onion Bunker Harvester. *Automation and System Technology in Plant Production, CIGR section V & NJF section VII conference*, pp. 27–36.

Pedersen, H.H., Oudshoorn, F.W., McPhee, J.E. & Chamne, W.C.T. 2016. Wide span - Re-mechanising vegetable production. *Acta horticulturae*, **1130**, 551–557. doi: 10.17660/ActaHortic.2016.1130.83

Tullberg, J.N. 2009. Avoiding soil compaction in CA: controlled traffic systems for mechanized conservation agriculture and their effect on greenhouse gas balances In: *Proceedings 4th World Congress on Conservation Agriculture*, February 2009, New Delhi, 85–190.

Agronomy Research **22**(1), 227–237, 2024
https://doi.org/10.15159/AR.23.108

Phytoremediation potential of oat (*Avena sativa* L.) in soils contaminated with cadmium

B. Piršelová[1,*] Ľ. Galuščáková[1], L. Lengyelová[1], V. Kubová[1], R. Matúšová[2], K. Bojnanská[3] and M. Havrlentová[3,4]

[1]Department of Botany and Genetics, Faculty of Natural Sciences and Informatics, Constantine the Philosopher University in Nitra, Nábrežie mLádeže 91, SK949 74 Nitra, Slovak Republic
[2]Institute of Plant Genetics and Biotechnology, Plant Science and Biodiversity Centre, Slovak Academy of Sciences, Akademická 2, P.O. Box 39A, SK950 07 Nitra, Slovak Republic
[3]National Agricultural and Food Centre, Research Institute of Plant Production in Piešťany, SK921 68 Piešťany, Slovak Republic
[4]Department of Biotechnologies, Faculty of Natural Sciences, University of Ss. Cyril and Methodius in Trnava, 917 01 Trnava, Slovak Republic
[*]Correspondence: bpirselova@ukf.sk

Received: October 1st, 2023; Accepted: November 28th, 2023; Published: December 15st, 2023

Abstract. Human activities can cause enormous damage to agricultural soils through the accumulation of toxic metals in the soil. The identification of plants capable of accumulating relatively large amounts of these compounds in plant tissues with the aim of reducing or limiting soil toxicity is of great interest. Two independent pot experiments were conducted to evaluate the phytoremediation potential of different varieties of oat (*Avena sativa* L.) grown in soil contaminated with cadmium (Cd, 50 mg kg^{-1} soil). Eight varieties were cultivated for 21 days in Cd- contaminated soil. Five varieties of oat were exposed to Cd at the third leaf stage, followed one week later by exposure to oat powdery mildew (*Blumeria graminis* f. sp. *avenae*) for 35 days. In general, the tested varieties accumulated more Cd in the roots than in the shoots and showed a high tolerance to Cd. Metal accumulation in shoots was lower after 21 days of cultivation (8.30–17.27 mg Cd kg^{-1}) than after 42 days (13.72–35.20 mg Cd kg^{-1}) and was the highest in tissues of plants infected with *B. graminis* (48.17–96.20 mg kg^{-1}). In conclusion, our results indicate a good phytostabilization and remediation potential of oat (varieties Racoon and Vaclav) for soil contaminated with cadmium.

Key words: *Avena sativa* L., cadmium tolerance, phytostabilization, remediation.

INTRODUCTION

Soil contamination by heavy metals is a serious environmental problem due to industrialization, urbanization, and intensive agricultural practices. Soil detoxification is quite complicated and technologically difficult. Current remediation methods include

physicochemical and biological remediation with the aim of reducing the bioavailability of heavy metals and thus their toxic effects. Physicochemical remediation involves redox, adsorption, and complexation reactions, but it is expensive and it is not possible to completely eliminate toxic compounds (Luo & Zhang, 2021). A promising approach is so-called phytoremediation. Phytoremediation involves the use of plants that accumulate larger amounts of toxic compounds in their tissues. Plants suitable for soil phytoremediation should grow rapidly, produce substantial biomass, have accumulation of toxic elements in their tissues without causing damage, and the overall management should be done in a simple manner (Raskin et al., 1997; Kasiuliene et al., 2016). Plants that are able to accumulate large amounts of risk compounds are hyperaccumulators. However, hyperaccumulators are often not suitable for phytoremediation due to their slow growth and low biomass production. Therefore, the identification of alternative plants that are tolerant to toxic compounds and can produce a considerable amount of biomass with relatively good accumulation potential is of interest.

Cadmium (Cd) is a non-essential element for plants and is considered one of the most toxic heavy metals due to its high mobility and ability to induce toxicity even at low concentrations in organisms (Benavides et al., 2005). Agricultural soils in many parts of the world are contaminated with cadmium as a result of the long-term use of phosphate fertilizers, various wastes in the form of composts and sludge from wastewater treatment plants (Niño-Savala et al., 2019; Tytła, 2019).

Limit for Cd in soil of Slovak Republic is 1.0 mg kg^{-1} of dry matter (Decree No. 59/2013). Cadmium content above 3 mg kg^{-1} soil is generally thought to indicate contaminated soils (Alloway, 1995). The toxic effects of cadmium on plant growth and metabolism are well documented: Cd inhibits cell division, impairs photosynthesis, nutrient assimilation, and the activity of various enzymes (Benavides et al., 2005, Lux et al., 2011; Alle et al., 2019; Pivková et al., 2022). Previous studies indicate large differences in metal accumulation among plant species and varieties (Murtic et al., 2019). Hyperaccumulators of cadmium are plant species that accumulate more than 100 mg Cd kg^{-1} dry weight in shoots (Baker & Walker, 1990). However, several studies with tolerant plants in remediation programs were unsuccessful because the specific interactions between genotype and environment were not considered.

Oat (*Avena sativa* L.), which belongs to the *Poaceae* family, is a multi-purpose cereal grown in many parts of the world. Oat is an exceptional crop in terms of its use in crop production, as it is not only an important forage crop, but also a food with high dietary and nutritional value (Ibrahim et al., 2022). Although several studies indicated a good accumulation potential of oat for Cd from soils contaminated with heavy metals (Azizian et al., 2011; Boros-Lajszner et al., 2020), data on the remediation potential of oat for Cd are scarce. Interesting in this respect is black oat (*Avena strigosa* Schreb.). Uraguchi and co-workers (2006) grew black oat seedlings for 4 weeks in hydroponic culture and then treated them with Cd for four days. *A. strigosa* showed high tolerance to Cd at a dose of 5 mg L^{-1}. Long-term Cd treatment of black oat (seedlings were grown on vermiculite for 2 weeks and then transferred to a hydroponic solution containing 1.1 mg L^{-1} Cd for 4 weeks) resulted in the accumulation of 74 mg Cd kg^{-1} dry weight (DW) in leaves, 140 mg kg^{-1} DW in stems, and 958 mg kg^{-1} DW in roots, placing black oat among the Cd-hyperaccumulating species (Uraguchi et al., 2009).

The aim of this study was to evaluate the remediation potential of oat varieties for soils contaminated with cadmium, of uninfected oats and of oats infected with the fungal pathogen *Blumeria graminis* f. sp. *avenae* in the case of short- and long-term exposure of oat seedlings to cadmium.

MATERIAL AND METHODS

Ten varieties of oat (*Avena sativa* L., Pushinskij, Vok, Valentin, Vaclav, V2 6/19, Prokop, Racoon, Aragon, Bay Yan 2, and Ivory) were used for the present study. Varieties Valentin, Vaclav and Prokop are Slovak registered varieties commonly available in the European Union (EU). The unregistered variety V2 6/19 is a variety bred in Slovakia, but it is not commonly available in the EU. Other varieties - Russian Pushkinskij, Chinese Bay Yan 2, German Aragon, German Ivory, Czech Vok and British Racoon are not commonly available in the EU. The seeds were obtained from the Gene Bank of the Slovak Republic. The genotypes used in the experiment were selected according the content of beta-glucans (cell wall polysaccharide of selected Poales with putative protecting function in the cell) (unpublished data). Another way for genotypes selection was the availability and possibility of cultivation of these materials.

Pot experiment 1

Seeds of eight oat varieties (Pushinskij, Vok, Valentin, Vaclav, V2 6/19, Prokop, Racoon, and Aragon) were sown in pots (15 seeds/pot, pot diameter 15 cm) containing a white peat potting substrate (Klasmann KTS 2, Klasmann-Deilmann GmbH, Germany, pH KCl 6.7, gravimetric soil water content max. 70%, EC in µS 400, total cadmium content 1.2 mg kg^{-1}, nitrogen content 1.65 g kg^{-1}, carbon content (C organic) 81.59 g kg^{-1}, phosphorus content 0.38 g kg^{-1}, potassium content 0.43 g kg^{-1}). The plants were grown in the FitotronII plant growth chamber under working conditions: temperature 24 °C, humidity 60%, with a 12/12 hour photoperiod and a light intensity of 20, 000 lux.

The plants were treated with tap water (control) or with a Cd solution irrigated at a dose of 50 mg Cd per kg substrate in three biological replicates. Cd was used in the form of $CdCl_2.2H_2O$. Plants were watered regularly throughout the experiment to maintain the maximum sorption capacity of the soil.

After three weeks, the seedlings were removed from the substrate and carefully cleaned from the substrate. The fresh weight (FW) of the roots and shoots of each plant was determined. The samples were then dried at 60 °C for two days to determine the dry weight (DW). The shoot tolerance index was calculated: TI (%) = (average biomass content of Cd treated plants/average biomass content of control plants) x 100.

Pot experiment 2

Seeds of five oat varieties (Aragon, Bay Yan 2, Ivory, Vaclav, and Racoon) were sown in plastic pots (diameter 25 cm) filled with 1,250 g Klasmann TS 2 substrate and grown in the FitotronII plant growth chamber under working conditions: temperature 15–24 °C, humidity 62–82%, with a 16/8 hour photoperiod and a light intensity of 20,000 lux, at 10 plants per pot.

After 22 days of cultivation in the given conditions (at the third leaf stage), 50 mg Cd per kg soil was added to the soil. After a seven-day Cd treatment, some seedlings were exposed to Cd for another 35 days (total of 42 days of Cd treatment) and some were also inoculated with the fungal pathogen *Blumeria graminis* f. sp. *avenae* for 35 days (variant Cd + *Bg*). The seedlings were inoculated with spores of *B. graminis* at a dose of 1,000–2,500 spores per cm^2 in a settling tower. The spores were dispersed in turbulent air in a settling tower, the density of inoculation was determined on Petri dishes with agar medium placed on the inoculated pots. Control plants were grown under conditions without Cd and infection. The experiment was performed with three biological replicates. After 64 days of growth, the roots were separated from the shoots and the dry matter was determined by drying the biomass at 60 °C for 48 hours.

Detection of cadmium in plant tissue and soil

Plant material and soil sample (0.5 g each) were digested in a mixture of 5 mL water, 5 mL HNO_3 (Merck, Darmstadt, Germany), and 1.5 mL H_2O_2 (30%, Slavus, Bratislava, Slovakia) using the Mars Xpress microwave oven (CEM Corporation, Matthews, NC, USA). Cadmium was detected by inductively coupled plasma optical emission spectroscopy (ICP-OES 725, Varian 725 ES ICP, Melbourne, Australia) according to Kováčik et al. (2019).

Evaluation of the efficiency of plant uptake

Based on the Cd content in the tissues, the bioaccumulation factor (BAF) was calculated to measure the relative Cd concentration in the plant organ compared to the cadmium content in the soil and the translocation factor (TF), which indicates the ability of the plant to transport Cd from the below-ground parts to the above-ground parts (Usman et al., 2019): BAF = cadmium content in plant organ/cadmium content in soil; TF = cadmium content in shoots/cadmium content in roots.

Statistical analyses

The obtained results were statistically analysed using the XLSTAT software. The basic statistical characteristics (arithmetic mean, standard deviation) were determined. The differences between the experimental variants were analysed using the t-test or the Kruskal-Wallis test followed by a Dunn's post hoc test ($p < 0.05$).

RESULTS

To evaluate the phytoremediation potential of different varieties of oat (*A. sativa* L.) grown in soil contaminated with cadmium (Cd), we conducted two independent experiments. The results are presented grouped by experiment. The tested oats showed a high tolerance to 50 mg kg^{-1} Cd in the soil.

As a result of the tested dose of Cd, in the case of the varieties Pushinskij, Vok, Valentin, Racoon and Aragon, there was even a significant elongation of shoots by 6.9%, 5.6%, 6.8%, 4.7% and 9.0% respectively. An increase in the fresh biomass of the shoots (by 25.9%, 16.7% and 20%) was observed in Pushinskij, Vok and Aragon varieties. An increase in dry matter content (by 11.1%) was also observed in the Aragon variety (Table 1).

Table 1. Effect of cadmium on shoot growth parameters of oat varieties

Variety	Variant of experiment	Length (cm)	Fresh weight (g)	Dry weight (g)
Pushinskij	Control	29.46 ± 5.10	0.27 ± 0.07	0.030 ± 0.010
	Cd	31.48 ± 5.03*	0.34 ± 0.06*	0.037 ± 0.009
Vok	Control	30.11 ± 4.76	0.36 ± 0.05	0.041 ± 0.006
	Cd	31.79 ± 4.68*	0.42 ± 0.05*	0.043 ± 0.005
Valentin	Control	29.28 ± 4.14	0.39 ± 0.06	0.039 ± 0.006
	Cd	31.26 ± 3.95*	0.41 ± 0.06	0.042 ± 0.004
Vaclav	Control	31.83 ± 3.95	0.37 ± 0.06	0.041 ± 0.006
	Cd	30.16 ± 4.24	0.39 ± 0.07	0.040 ± 0.009
V2 6/19	Control	29.33 ± 3.23	0.31 ± 0.08	0.032 ± 0.008
	Cd	29.36 ± 4.17	0.35 ± 0.06	0.035 ± 0.004
Prokop	Control	30.29 ± 4.35	0.37 ± 0.05	0.038 ± 0.006
	Cd	30.98 ± 5.00	0.35 ± 0.05	0.035 ± 0.004
Racoon	Control	31.13 ± 4.48	0.39 ± 0.06	0.040 ± 0.006
	Cd	32.59 ± 4.64*	0.41 ± 0.06	0.039 ± 0.005
Aragon	Control	30.49 ± 4.26	0.35 ± 0.05	0.036 ± 0.005
	Cd	33.22 ± 5.09*	0.42 ± 0.06*	0.040 ± 0.006*

Data are presented as *means* ± *SD* of three biological replicates. * the significance level of the differences compared to the control at $p < 0.05$ (*t*-test).

The tolerance indexes ranged from 93.50 to 125.43% (for the fresh weight of the shoots) and 94.53–122.96 (for the dry matter content of the shoots). The highest tolerance was found in the Pushinskij variety (TI_{DW} = 122.96%) and the lowest in the Prokop variety (TI_{DW} = 94.53 for the DW) (Fig. 1).

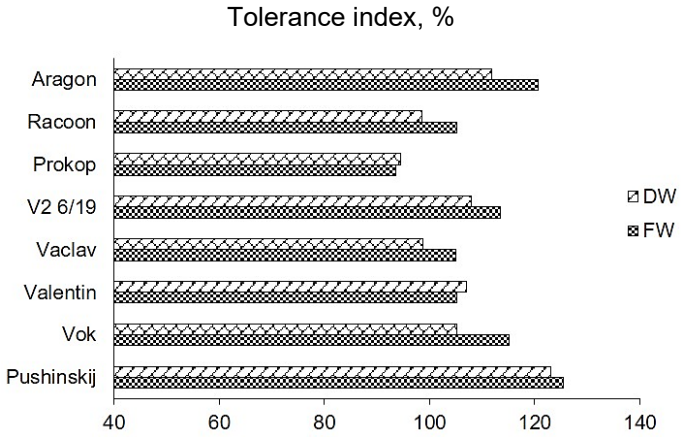

Figure 1. The tolerance index determined based on the fresh weight (FW) and the dry weight (DW) of the shoots.

The varieties differed in the amount of Cd accumulated in the tissues. Seedlings grown for 21 days in the presence of Cd accumulated from 8.3 mg Cd kg^{-1} in the variety Valentin to 17.27 and 14.67 mg Cd kg^{-1} shoot DW in the V2 6/19 and Pushinskij. The accumulation of cadmium in roots was higher in all samples and ranged from

28.4 mg Cd kg^{-1} DW in the variety Vok to 50.45, 49.35, and 48.05 mg Cd kg^{-1} DW in the V2 6/19, Aragon, and Pushinskij, respectively (Fig. 2).

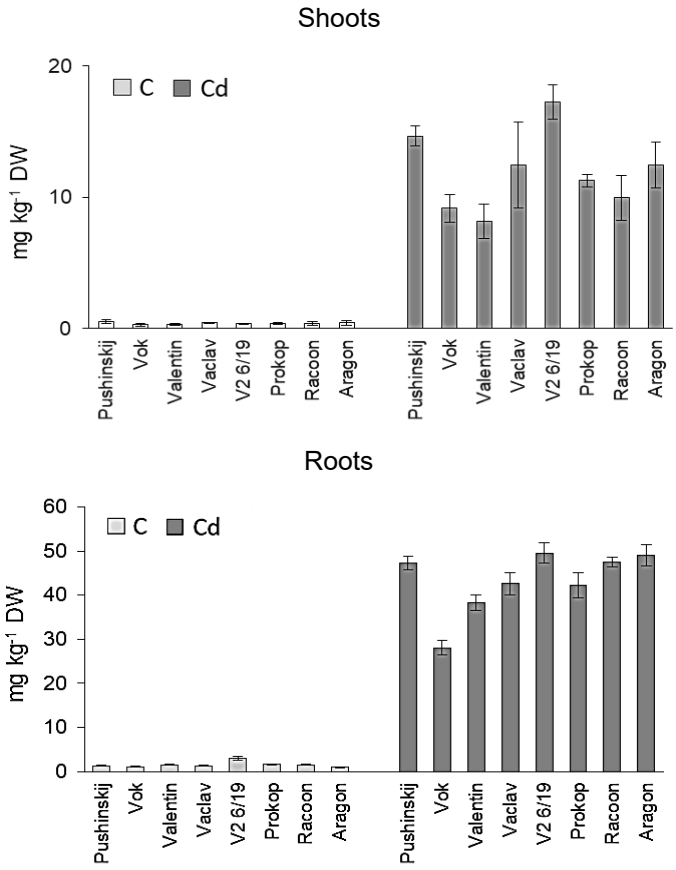

Figure 2. Cadmium content in shoots and roots of the tested oat varieties exposed to cadmium (Cd 50 mg kg^{-1} soil) for 21 days. Data are presented as *means* ± *SD* of three biological replicates. Control plants (C), cadmium-treated plants (Cd).

To evaluate the remediation potential of oat, the bioaccumulation factor (BAF) and translocation factor (TF) were determined. The BAF expresses the efficiency of metal accumulation in the plant tissue in relation to the amount in the soil and the TF expresses the ability of the plants to translocate the metal into the shoots. The BAF values reflect the amount of Cd in the tissues. BAF values for roots were higher (0.57–1.00) than for shoots (0.18–0.29). The highest values of BAF for roots were achieved by the varieties V2 6/19 (1.00), Aragon (0.99), Pushinskij and Racoon (0.96), the lowest by the varieties Vok (0.57) and Valentin (0.77). The highest values of BAF for shoots were achieved by the varieties Pushinskij (0.29), Vaclav and Aragon (0.25), the lowest by the varieties Vok (0.18) and Valentin (0.19).

Relatively low TF values (0.21–0.35) also indicate low metal transport from roots to shoots (Table 2). The most efficient Cd transport to the shoot was shown by the varieties V2 6/19 (0.35), Vok (0.32) and Pushinskij (0.30).

Table 2. Bioaccumulation factor (BAF) and translocation factor (TF) for the tested oat varieties (Experiment 1)

Variety	BAF for roots	BAF for shoots	TF shoots/roots
Pushinskij	0.96 ± 0.01 ^{ab}	0.29 ± 0.02 ^{a}	0.30 ± 0.02 ^{abc}
Vok	0.57 ± 0.03 ^{d}	0.18 ± 0.02 ^{b}	0.32 ± 0.06 ^{ab}
Valentin	0.77 ± 0.03 ^{cd}	0.19 ± 0.02 ^{b}	0.22 ± 0.05 ^{cd}
Vaclav	0.85 ± 0.05 ^{bcd}	0.25 ± 0.07 ^{ab}	0.29 ± 0.06 ^{acd}
V2 6/19	1.00 ± 0.04 ^{a}	0.22 ± 0.09 ^{ab}	0.35 ± 0.01 ^{a}
Prokop	0.86 ± 0.06 ^{bcd}	0.22 ± 0.01 ^{ab}	0.26 ± 0.01 ^{bcd}
Racoon	0.96 ± 0.02 ^{abc}	0.21 ± 0.06 ^{b}	0.21 ± 0.03 ^{d}
Aragon	0.99 ± 0.05 ^{ab}	0.25 ± 0.03 ^{ab}	0.25 ± 0.04 ^{bcd}

Data are given as *means* ± *SD* of three biological replicates. Differences between varieties were determined using the Kruskal-Wallis test followed by the Dunn's post-hoc test for multiple comparisons. Different letters indicate a significant difference ($p < 0.05$) between varieties for each parameter tested.

In experiment 2, as in experiment 1, higher Cd accumulation was observed in the roots compared to the shoots (Fig. 3), with the roots of infected plants accumulating slightly more Cd (151.00–307.33 mg kg^{-1} DW) than those of uninfected plants (63.52–308.85 mg kg^{-1} DW). Ivory and Racoon varieties accumulated the most Cd (Fig. 3).

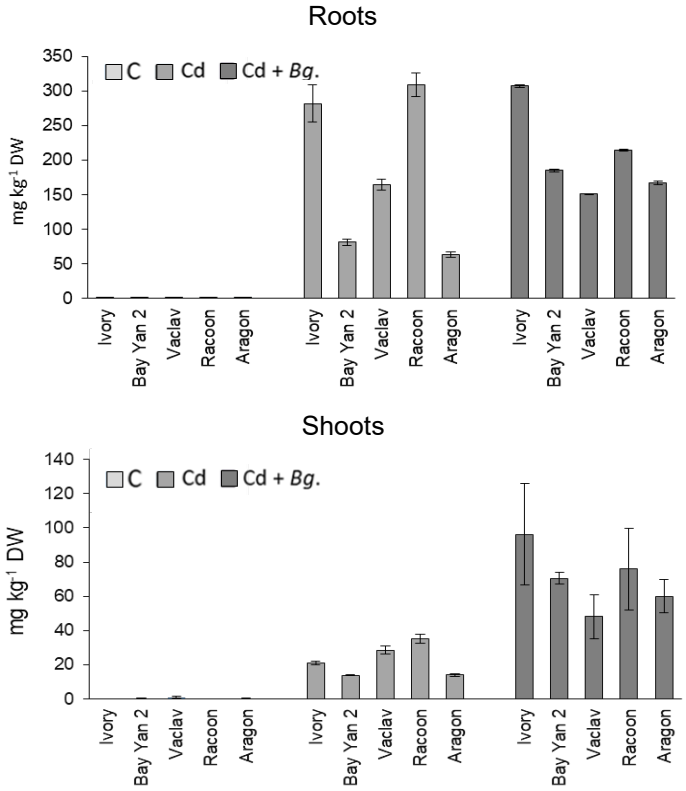

Figure 3. Cadmium (Cd) content in shoots and roots of the tested oat varieties grown in pots for 22 days and then exposed to Cd for 42 days or to Cd for 42 days plus *Blumeria graminis* (*Bg*) for 35 days. Data are presented as *means* ± *SD* of three biological replicates. Control plants (C), cadmium-treated plants (Cd), cadmium plus *Blumeria graminis* (Cd + *Bg*).

The Cd accumulation in the shoots also differed significantly depending on the type of exposure. 1.69–5.14 times more Cd was accumulated in the shoots of infected plants than in plants exposed to Cd only. Cadmium accumulated most in shoots of the Cd-exposed variety Racoon (35.20 mg kg^{-1} DW) and in infected shoots with the fungus *B. graminis* in the variety Ivory (96.20 mg kg^{-1} DW) (Fig. 3). In the experiment 2, the growth parameters were not evaluated, the infected variants showed signs of chlorosis and infection (white growth mycelium).

The accumulated Cd amounts in the tissues also reflect the BAF and TF values (Table 3). BAF for roots reached values of 1.27–6.18 for the Cd variant and 3.02–6.15 for the Cd + *Bg* variant. BAF values for shoots were lower, 0.27–0.70 for the Cd variant and 0.96–1.92 for the Cd + *Bg* variant. Thus, translocation of Cd from roots to shoots was higher for the Cd + *Bg* variant (TF = 0.31–0.38) than for the Cd variant (TF = 0.08–0.22) (Table 3).

Table 3. Bioaccumulation factor (BAF) and translocation factor (TF) for the tested oat varieties (Experiment 2)

Variety	BAF for roots	BAF for shoots	TF shoot/root
	Cd		
Ivory	5.63 ± 0.54^{ab}	0.42 ± 0.02^{cde}	0.08 ± 0.01^{d}
Bay Yan 2	1.63 ± 0.10^{de}	0.27 ± 0.01^{e}	0.17 ± 0.01^{cd}
Vaclav	3.28 ± 0.16^{bcde}	0.57 ± 0.05^{bcde}	0.17 ± 0.02^{bcd}
Racoon	6.18 ± 0.33^{a}	0.70 ± 0.05^{bcde}	0.11 ± 0.01^{d}
Aragon	1.27 ± 0.09^{e}	0.28 ± 0.02^{de}	0.22 ± 0.06^{abcd}
	Cd + *Bg*		
Ivory	6.15 ± 0.04^{a}	1.92 ± 0.59^{a}	0.31 ± 0.09^{abc}
Bay Yan 2	3.70 ± 0.04^{abcd}	1.41 ± 0.07^{ab}	0.38 ± 0.02^{a}
Vaclav	3.02 ± 0.02^{cde}	0.96 ± 0.26^{abcd}	0.32 ± 0.08^{abc}
Racoon	4.29 ± 0.03^{abc}	1.52 ± 0.48^{ab}	0.35 ± 0.11^{ab}
Aragon	3.35 ± 0.05^{bcde}	1.20 ± 0.19^{abc}	0.36 ± 0.05^{a}

Data are presented as *means* ± *SD* of three biological replicates. Differences between varieties/variants were determined using the Kruskal-Wallis test followed by the Dunn's post-hoc test for multiple comparisons. Different letters indicate a significant difference ($p < 0.05$) between the varieties/variants for each parameter tested. Cadmium-treated plants (Cd), cadmium plus *Blumeria graminis* (Cd + *Bg*).

DISCUSSION

The aim of this study was to evaluate and compare the remediation potential of selected oat varieties within different experimental approaches to abiotic and biotic stress.

The eight tested oat varieties showed high tolerance after 21 days of growth in contaminated soil (Tables 1, 2). The plants exposed to the metal for 42 days (experiment 2) also showed no visible symptoms of toxicity. Data evaluating the tolerance of oat to Cd ions are relatively sparse and controversial. High tolerance to Cd up to 20 mg kg^{-1} soil is indicated, for example, by Ciecko et al. (2004), Uraguchi et al. (2009), Tůma et al. (2014), and Marchel et al. (2018). On the other hand, growth inhibition, a decrease in photosynthetic pigment content and lower yield were already at doses of 10 mg kg^{-1} soil (Rolka, 2015; Boros-Lajszner et al., 2020). Astolfi et al. (2004) recorded a 32% and 33% decrease in fresh shoot biomass content and dry matter content of oat shoots exposed to a Cd dose of 0.154 mg kg^{-1} soil for 21 days. A significant reduction in fresh shoot biomass

was also observed after 10 days of growth in soils with a Cd dose of 6.25 mg kg^{-1} soil (da Rosa Corrêa et al., 2006).

The amount of accumulated Cd in plant tissues was dependent on both genotype and experimental conditions, with plants preferentially accumulating Cd in roots, in agreement with other studies (Uraguchi et al., 2009; Tůma et al., 2014; Kasiuliene et al., 2016; Boros-Lajszner et al., 2020). Metal accumulation in the tissues was lower after 21 days of cultivation (experiment1) than after 42 days (experiment 2) and was higher in the tissues of infected plants (Figs 1, 2). Thus, the highest remediation potential was achieved by infected plants, while the Cd content in the shoots of some varieties (Ivory & Racoon) approached that of the hyperaccumulating species (96.20 and 75.83 mg kg^{-1} DW). These varieties also reached relatively high BAF values (0.42 and 0.70) after 42 days of cultivation in Cd-contaminated soil.

The higher accumulation of Cd in the shoots of infected plants is probably the result of the failure of defense mechanisms that help to prevent the transport of Cd to higher parts of the plant. Oats accumulated relatively high levels of Cd in the roots, 28.40–50.45 mg kg^{-1} DW after 21 days of cultivation, 63.52–308.85 mg kg^{-1} DW after 42 days of Cd exposure, and 151.00–307.33 mg kg^{-1} DW in the case of infected plants (Figs 1, 2).

The higher BAF values also correspond to the given data (Tables 3, 4). Comparable levels of Cd were also found in the tissues of oat (variety Moozart) at a dose of 53.61 mg kg^{-1} soil (Azizian et al., 2011). Tůma et al. (2014), on the other hand, measured 11.37 mg kg^{-1} Cd in younger leaves, 55.97 mg kg^{-1} Cd in older leaves, and 235.33 mg kg^{-1} Cd in roots at a dose of 20 mg Cd on 1 kg soil. The present results suggest genotypic variability in Cd accumulation. It is also interesting to note that Cd translocation from roots to shoots was comparable in infected plants (TF = 0.31–0.36) and in plants cultivated in Cd-contaminated soil for 21 days (0.21–0.34), but was generally slightly lower in plants exposed to Cd for 42 days (TF = 0.08–0.22). Relatively low values of TF (0.072) at a dose of 16 mg kg^{-1} soil were also found by Boros-Lajszner et al. (2020) for oat shoots. Our study shows that the remediation potential of oat is significantly determined by genotype, time of Cd exposure, and other environmental factors. The preferential and significant accumulation of Cd in the roots indicates a high phytostabilization potential of this plant species. The choice of varieties for remediation or phytostabilization of contaminated soils requires a complex approach and optimization of the methodology applied, taking into account the possible effects of different environmental factors.

CONCLUSION

The presented study showed that the tested oat varieties had a high tolerance to cadmium and accumulated Cd preferentially in the roots. Metal accumulation in tissues was lower after 21 days of cultivation than after 42 days and was higher in tissues of plants infected with *B. graminis.* Thus, the remediation potential of oat was the highest in infected plants which were simultaneously exposed to the metal for 42 days (BAF for shoots = 0.96–1.92). In non-infected plants, the BAF after 42 days of Cd exposure reached the highest values in the varieties Vaclav and Racoon (BAF = 0.57 and 0.70, respectively). The high tolerance of the tested oat genotypes to Cd and at the same time, the high accumulation potential of the roots both indicate the possibility of using these

oat varieties for phytostabilization of Cd-contaminated soils. A more detailed investigation of the mechanisms of Cd tolerance of oat may help to increase the accumulation and remediation potential of oat.

ACKNOWLEDGEMENTS. This work was supported by the Slovak Research and Development Agency under Contract No. APVV-18-0154 and by the Ministry of Education, Science, Research and Sport of the Slovak Republic: grant VEGA 1/0073/20. We thank Ing. Peter Hozlár, PhD. for providing the seeds used within this work.

REFERENCES

Alle, V., Osvalde, A., Vikmane, M. & Kondratovics, U. 2019. The effect of cadmium and lead pollution on growth and physiological parameters of field beans (*Vicia faba*). *Agronomy Research* **17**(S2), 1261–1272.

Alloway, B.J. 1995. *Heavy Metals in Soils*. Blackie Academic and Professional, Chapman and Hall, London, 368 pp.

Astolfi, S., Zuchi S. & Passera, C. 2004. Effects of cadmium on the metabolic activity of *Avena sativa* plants grown in soil or hydroponic culture. *Biologia Plantarum* **48**, 413−418.

Azizian, A., Amin, S., Noshadi, M., Maftoun, M. & Emam, Y. 2011. Phytoremediation potential of corn and oat for increased levels of soil cadmium under different irrigation intervals. *Iran Agricultural Research* **30**, 47−59. doi: 10.22099/IAR.2012.493

Baker, A.J.M. & Walker, P.L. 1990. *Ecophysiology of metal uptake by tolerant plants*. In Shaw A.J. (ed.): Heavy Metal Tolerance in Plants: Evolutionary Aspects, Boca Raton, FL: CRC Press, 155–177.

Benavides, M.P., Gallego, S.M. & Tomaro, M.L. 2005. Cadmium toxicity in plants. *Brazilian Journal of Plant Physiology* **17**, 21−34. doi: 10.1590/S1677-04202005000100003

Boros-Lajszner, E., Wyszkowska, J. & Kucharski, J. 2020. Application of white mustard and oats in the phytostabilisation of soil contaminated with cadmium with the addition of cellulose and urea. *Journal of Soils and Sediments* **20**, 931–942. doi: 10.1007/s11368-019-02473-6

Ciecko, Z., Kalembasa, S., Wyszkowski, M. & Rolka, E. 2004. The effect of elevated cadmium content in soil on the uptake of nitrogen by plants. *Plant Soil Environment* **50**, 283–294. doi: 10.17221/4034-PSE

Da Rosa Corrêa, A., Rörig, L., Verdinelli, M., Cotelle, S., Férard, J. & Radetski, C. 2006. Cadmium phytotoxicity: Quantitative sensitivity relationships between classical endpoints and antioxidative enzyme biomarkers. *Science of the Total Environment* **357**, 120−127. doi: 10.1016/j.scitotenv.2005.05.002

Decree of the Ministry of Agriculture and Rural Development of the Slovak Republic No. 59/2013 (Decree No. 59/2013). Available online: https://www.slov-lex.sk/pravne-predpisy/SK/ZZ/2013/59/20130401. Accessed 18.11. 2023.

Ibrahim, M., Aav, A. & Jõudu, I. 2022. The potential and limitations for applications of oat proteins in the food industry. *Agronomy Research* **20**(1), 161–173. doi: 10.15159/AR.22.008

Kasiuliene, A., Paulauskas, V. & Kumpiene, J. 2016. Influence of nitrogen fertilizer on Cd and Zn accumulation in rapeseed (*Brassica napus* L.) biomass. *Agronomy Research* **14**(2), 418–427.

Kováčik, A., Tvrdá, E., Miškeje, M., Árvay, J., Tomka, M., Zbynovska, K., Andreji, J., Hleba, L., Kováčiková, E., Fik, M., Čupka, P., Nahácky, J. & Massányi, P. 2019. Trace metals in the freshwater fish *Cyprinus carpio*: Effect to serum biochemistry and oxidative status markers. *Biological Trace Element Research* **188**, 494–507. doi: 10.1007/s12011-018-1415-x

Luo, J.S. & Zhang, Z. 2021. Mechanisms of cadmium phytoremediation and detoxification in plants. *The Crop Journal* **9**, 521−529. doi: 10.1016/j.cj.2021.02.001

Lux, A., Martinka, M., Vaculík, M. & Philip, J.W. 2011. Root responses to cadmium in the rhizosphere: A review. *Journal of Experimental Botany* **62**, 21–37. doi: 10.1093/jxb/erq281

Marchel, M., Kaniuczak, J., Hajduk, E. & Właśniewski, S. 2018. Response of oat (*Avena sativa*) to the addition cadmium to soil inoculation with the genus *Trichoderma fungi*. *Journal of Elementology* **23**, 471–482. doi: 10.5601/jelem.2017.22.1.1391

Murtic, S., Jurkovic, J., Basic, E. & Hekic, E. 2019. Assessment of wild plants for phytoremediation of heavy metals in soils surrounding the thermal power station. *Agronomy Research* **17**(1), 234–244. doi:10.15159/AR.19.005

Niño-Savala, A.G., Zhuang, Z., Ma, X., Fangmeier, A., Li, H., Tang, A. & Liu, X. 2019. Cadmium pollution from phosphate fertilizers in arable soils and crops: an overview. *Frontiers of Agricultural Science and Engineering* **6**, 419–430. doi: 10.15302/J-FASE-2019273

Pivková, I., Kukla, J., Hniličková, H., Hnilička, F., Krupová, D. & Kuklová, M. 2022. Content of cadmium and nickel in soils and assimilatory organs of park woody species exposed to polluted air. *Life* **12**, 2033. doi:10.3390/life12122033

Raskin, I., Smith, R.D. & Salt, D.E. 1997. Phytoremediation of metals: Using plants to remove pollutants from the environment. *Current Opinion* in *Biotechnology* **8**, 221–226. https://doi.org/10.1016/S0958-1669(97)80106-1

Rolka, E. 2015. Effect of soil contamination with cadmium and application of neutralizing substances on the yield of oat (*Avena sativa* L.) and on the uptake of cadmium by this crop. *Journal of Elementology* **20**, 975–986. doi: 10.5601/jelem.2014.19.4.810

Tůma, J., Skalický, M., Tůmová, L. & Flidr, J. 2014. Influence of cadmium dose and form on the yield of oat (*Avena sativa* L.) and the metal distribution in the plant. *Journal of Elementology* **19**, 795–810. doi: 10.5601/jelem.2014.19.3.448

Tytła, M. 2019. Assessment of heavy metal pollution and potential ecological risk in sewage sludge from municipal wastewater treatment plant located in the most industrialized region in Poland-Case study. *International Journal of Environmental Research and Public Health* **16**, 2430. doi: 10.3390/ijerph16132430

Uraguchi, S., Kiyono, M., Sakamoto, T., Watanabe, I. & Kuno, K. 2009. Contributions of apoplasmic cadmium accumulation, antioxidative enzymes and induction of phytochelatins in cadmium tolerance of the cadmium-accumulating cultivar of black oat (*Avena strigosa* Schreb.). *Planta* **230**, 267–276. doi: 10.1007/s00425-009-0939-x

Uraguchi, S., Watanabe, I., Yoshitomi, A., Kiyono, M. & Kuno, K. 2006. Characteristics of cadmium accumulation and tolerance in novel Cd-accumulating crops, *Avena strigosa* and *Crotalaria juncea*. *Journal of Experimental Botany* **57**, 2955–2965. doi:10.1093/jxb/erl056

Usman, K., Al-Ghouti, M.A. & Abu-Dieyeh, M.H. 2019. The assessment of cadmium, chromium, copper, and nickel tolerance and bioaccumulation by shrub plant *Tetraena qataranse*. *Scientific Reports* **9**, 5658. doi: 10.1038/s41598-019-42029-9

Agronomy Research **22**(1), 238–252, 2024
https://doi.org/10.15159/AR.24.036

Influence of the farm location and seasonal fluctuations on the composition and properties of the milk

Xh. Ramadani[1], A. Kryeziu[2*], M. Kamberi[2] and M. Zogaj[3]

[1]University of Prishtina, Faculty of Agriculture and Veterinary, Department of Food Technology with Biotechnology, 10000 Prishtinë, Republic of Kosovo
[2]University of Prishtina, Faculty of Agriculture and Veterinary, Department of Biotechnology in Animal Science, 10000 Prishtinë, Republic of Kosovo
[3]University of Prishtina 'Hasan Prishtina', Faculty of Agriculture and Veterinary, Department of Plant Production, 34 Str. Tahir Zajmi, 10000 Prishtinë, Republic of Kosovo
[*]Correspondence: alltane.kryeziu@uni-pr.edu

Received: February 24 th, 2024; Accepted: April 30th, 2024; Published: May 7th, 2024

Abstract. The aim of this research was to investigate the variations in the chemical composition as well as the physical and microbiological properties of raw milk depending on the farm location and the season. Seven dairy farms located in seven different geographic regions of Kosovo were included in the experiment. Milk composition (total solids – TS, milk fat – MF, solids non-fat – SNF, protein – P, lactose – L, active acidity – AA (pH), density – D, colony formatting unit – CFU, and somatic cells count – SCC) were analysed during a one-year period from December 2021 to November 2022. In a total of 252 analysed milk samples, the research showed an average good composition in accordance with the Kosovo regulation for milk quality: TS (13.71%), MF (5.12%), SNF (8.60%), P (3.25%), L (3.87%), AA (6.83), D (1.028 g cm^{-3}), but higher number of CFU (194,048 mL^{-1}), and SCC (418,429 mL^{-1}). Farm location showed significant differences ($P < 0.01$) in TS, MF, SNF, P, D, CFU and SCC, whereas L content and AA value were statistically non-significant. The lower value of TS, MF, and CFU were detected in summer, AA, and P in spring, SNF and L in autumn, D value was similar in all seasons, whereas only SCC was present in winter season. The differences in all analysed parameters with respect to the season were statistically non-significant.

Key words: milk composition and properties, farm location, season.

INTRODUCTION

Modern dairy farming in Kosovo is relatively new and still developing. Kosovo is a small and landlocked country in Southeastern Europe and strategically is positioned in the centre of the Balkan Peninsula. The territory of Kosovo is positioned between the Latitude: 42° 39' 50.18" N, Longitude: 21° 05' 46.00" E, and covers a surface area of 10,887 km^{-2} with an average altitude of 800 m above sea level. It is inhabited by 1.873 million inhabitants. Additionally, Kosovo is administratively subdivided into seven geographic regions (districts), such as (Prishtinë-Pr, Mitrovicë-M, Pejë-Pe, Prizren-Pz, Ferizaj-Fe, Gjilan-Gji, and Gjakovë-Gja) (Fig. 1). According to the Green report (2022),

the cattle stock in Kosovo in 2021 was 260,528 heads. Dairy cows continue to have over 50% (132,076 heads) share in the total cattle stock. The total milk production in 2021 was 278,746 tons, which is about 2% higher than in 2020 because the number of dairy cows was higher. According to Bytyqi et al. (2009), daily milk yield differs from 12.34 to 18.92 kg per day depending on the cow breed. Milk consumption per capita was 171 kg per year, which means that a person consumes 0.47 kg per day including milk and its products.

Milk represents a high-quality and valuable food for humans. According to Kabil et al. (2015), it can provide a wide range of readily available nutrients to maintain health and normal growth of organism. The composition and properties of milk are different and depend on many factors. These factors include species (Roy et al., 2020); breed (Kebede, 2018 and Sanjayaranj et al., 2022); stage of lactation (Mishra et al., 2022). However, the composition of milk is also largely affected by other factors i.e. season (Sahu et al., 2018; Gajbhiye et al., 2019; Li et al., 2019; Shibru et al., 2019; Czyzak-Runowska et al., 2020; Kheowsri et al., 2023; and Yap et al., 2024); as well as months of the year (Singh et al., 2018 and Araújo et al., 2023). Kabil et al. (2015) described seasonality of milk as the change in composition, quality, and suitability for processing into a dairy-based product throughout the year. According to Habteghiorghis (2019), seasonal changes in milk are result of regional climatic conditions. Additionally, milk composition can differ by the geographic location of the farms (Khatun et al., 2018; Asefa & Teshome, 2019 Mitani et al., 2021 and Yap et al., 2024) etc. Milk composition also differs among countries, because different countries use different breeds and feeding regimens, and have different calving patterns and breeding practices. In addition, altitude also plays important role (Alrhmoun, et al., 2023; and Ramadani et al., 2023). On the other hand, Timlin et al., 2021; Magan, 2021; and O'Callaghan et al., 2016 emphasize that milk production and composition can be directly influenced by the feeding systems. Among factors affecting milk composition and properties, a great importance has the frequency of milking - morning, evening milking (Singh et al., 2018), as well as weather conditions - rainfall and temperature ´- (Hayes et al., 2023). In addition, one of the most important factors to be mentioned is health of the animal (Kul et al., 2019; Özlem & Kul, 2020 and Ali et al., 2022), which cause economic losses in dairy farms (Azooz et al., 2020). The influence of these factors on the

Figure 1. The map of Kosovo.
Source: https://www.mapsofindia.com/world-map/kosovo/districts-and-capital-list-map.html

composition and properties of milk is well known and studied worldwide but is not sufficient under the conditions of Kosovo. Therefore, the aim of this research was to examine the influence of farm location and seasonal variations as factors affecting milk composition and characteristics under the conditions in Kosovo in the years 2021 and 2022, with a particular emphasis in the seven administrative regions mentioned above.

MATERIAL AND METHODS

Research design and milk sampling

According to the aim of this research, seven dairy farms located in seven above - mentioned regions of Kosovo were included. With the aim to preserve the confidence of the results, the farms are lettered A through G. Herd size in the farms were from 32–188 milking cows (Table 1). Dairy farms were composed with different dairy breeds, mostly predominantly by Holstein Friesian breed (specialized dairy) and Simmental breed (dual-purpose: milk and meat production). The dairy cows in this research were kept indoors throughout the research period, in tie-up keeping, and in some cases with loose keeping. The animals did not use grazing in warm weather but were mainly fed with pre-prepared dry feed. In all season's animals were fed hay and haylage, with the addition of concentrated feed. Cows were milked twice a day at 06:00 h and 18:00 h daily, and raw milk was collected in farm cooling tanks.

Table 1. The research design of milk sampling

Region/farm	Number of cows (multi-breed herds)	Simmental breed (dual-purpose)	HF breed (specialized dairy)	Sample per Region/farm for one year Sample replication	Total samples per Region/farm
Pr/A	36	17	19	12	3	36
M/B	188	152	36	12	3	36
Pe/C	29	13	16	12	3	36
Pz/D	107	-	107	12	3	36
Fe/E	32	20	12	12	3	36
Gji/F	46	27	19	12	3	36
Gja/G	62	7	62	12	3	36
	500	236	271			
Total samples per research						252

Sample preparations of fresh raw milk for analysis.

After the complete milking, raw bulk milk in the farm cooling tanks was thoroughly mixed. The milk sampling was carried out once per month during the period from December 2021 to November 2022. Seasonal variations included spring (March, April, and May), summer (June, July, and August) autumn (September, October, and November) and winter (December, January, and February). A total of 252 milk samples with about 250 mL were collected in a plastic flask according to ISO 707:2008 (IDF 50:2008), (2008). Samples were conserved with 0.03% sodium azide, and with a portable hand-held mini refrigerator transported immediately at a temperature of 4–8 °C to the laboratory of the Food Technology with Biotechnology in the Faculty of Agriculture and Veterinary - University of Prishtina, for physical-chemical and microbiological analyses. For analysis, milk samples in a bottle were heated to around 40 °C in a water bath. The samples were then stirred and poured to allow the melted milk fat to emulsify. The sample was then cooled to approx. 20 °C.

Milk analyses

The analyses of raw milk samples were carried out on the following methods and instruments: MF, SNF, P, L and D were analysed with the 'Lactostar' - Funke Gerber 3510-070702, Germany, based on a combined thermo-optical procedure. TS content was calculated using MF and SNF values. AA value was measured by using pH meter GLP 21 'Crison' (ISO 11869:2012). CFU is analysed by the method of counting colonies of microorganisms in nutrient bases (agar-agar) and following the standard procedures recommended by ISO 4833–2:2013, whereas SCC was measured with the somatic cell counter MT05. The principle of method is based on adding to the milk a substance which causes a change in viscosity of the milk proportional to the quantity of somatic cells. Through measuring the viscosity of the milk sample, it is possible to measure the number of somatic cells. All analyses of raw milk were carried out in triplicate.

Statistical analyses

The obtained results were statistically analysed using the JMP-IN 7.0 statistical package (SASS unit) to find the influence of the farm location and the season in the chemical composition as well as the physical and microbiological properties of raw milk. The results of the analyses are presented in tabular form and were expressed as mean ± standard error of mean (SEM). To find whether significant differences exist, one way Anova was used, and if significance was observed, the Tukey's post hock test was used to find where and to what extent these differences are. The borderline of significance was set at the alfa level of 0.01.

RESULTS AND DISCUSSION

The influence of the farm location on the composition and properties of milk

The results regarding the influence of the farm location on the composition and properties of milk are presented in the Table 2 and 3.

Table 2. Milk composition depending on region/farm location (Mean ± SEM) (n = 252)

Region/farm location	TS (%)	MF (%)	SNF (%)	P (%)	L (%)
Pr/A	14.82 ± 0.51^{ab}	6.23 ± 0.56^{ab}	8.59 ± 0.15^{bcd}	3.57 ± 0.16^{ab}	3.50 ± 0.15
M/B	13.26 ± 0.52^{c}	4.58 ± 0.55^{bc}	8.68 ± 0.15^{bc}	3.01 ± 0.08^{c}	4.16 ± 0.12
Pe/C	13.60 ± 0.13^{bc}	4.35 ± 0.09^{c}	9.25 ± 0.05^{a}	3.69 ± 0.05^{a}	4.00 ± 0.08
Pz/D	13.32 ± 0.34^{c}	5.13 ± 0.42^{bc}	8.20 ± 0.16^{cd}	2.99 ± 0.10^{c}	3.72 ± 0.10
Fe/E	15.11 ± 0.23^{a}	7.31 ± 0.72^{a}	8.10 ± 0.21^{d}	3.13 ± 0.16^{c}	3.75 ± 0.12
Gji/F	13.20 ± 0.44^{c}	4.27 ± 0.33^{c}	8.74 ± 0.09^{ab}	3.21 ± 0.07^{bc}	3.99 ± 0.07
Gja/G	12.66 ± 0.14^{c}	3.99 ± 0.07^{c}	8.67 ± 0.07^{bc}	3.12 ± 0.06^{c}	4.00 ± 0.07
P	<.0001	<.0001	<.0001	<.0001	ns

TS – Total solids (%), MF – Milk fat (%); SNF – Solids non-fat (%); P – Proteins (%); L– Lactose (%); ns – non-significant. ^{a,b,c}Means with different superscript in the same column differ significantly ($P < 0.01$).

Based on the results presented in the Table 2, it is observed that content of the total solids has shown values within the limits prescribed in Administrative instruction MA 20/2006. The average value of this parameter was 13.71% (from 12.66 ± 0.14% to 15.11 ± 0.23%). This value is relatively high and good for milk processing, especially for cheese production. Among the analysed farms, TS showed variations that were

statistically significant ($P < 0.01$). Possible reason of differences observed between regions could be due to differences in farming practices or breed structure of the farms. Mean value of TS in this research is almost similar with results reported by Khatun et al. (2018), which observed significant differences in TS (13.62%; 13.15% and 14.12%) between farms in three different regions (South-Central, North-Western, and Western regions) of Bangladesh. A slightly lower value of TS reached Kouřimská et al. (2014) in their investigation with the aim to compare organic and conventional farming systems. They found higher contents of TS (12.73%) in conventional farming, compare to 12.69% in organic farming, emphasizing that differences could have been affected by the feeding composition which differs between organic and conventional farming systems. A slightly lower content of TS (12.72–13.3%) was reported by Yap et al. (2024) during evaluation of the quality of raw milk produced from nine different locations across Ireland over 12 months.

Milk fat content has shown values of $3.99 \pm 0.07\%$ (farm G) to $7.31 \pm 0.72\%$ (farm E). Differences in MF between farms could be described to feeding composition and regimes. The mean value of MF (5.12%) can be considered as a high valuable content. A valuable milk product with a high MF content (milk cream, buttermilk), etc. can be obtained from this milk. Among the farms analysed in this research, MF showed variations that were significantly different ($P < 0.01$). The results of this research are higher compared with the results reported by Kunda et al. (2015). They found out significantly different ($P > 0.05$) MF content averaging 3.90% (3.85% and 5.10%) in 83 farms around the two largest cities in Burkina Faso. Lower content of MF compared to ours reported Kouřimská et al. (2014) in analysed raw milk samples coming from organic and conventional farming systems. They stated higher contents of MF (4.03%) in organic farming, compared to 3.99% in conventional farming. Gaworski et al. (2018) in eight Estonian dairy farms with automatic milking system, milking parlour, and pipeline milking system, obtained these results for milk fat content (Mean ± SD): respectively $3.99 \pm 0.08\%$, $3.91 \pm 0.21\%$ and $4.26 \pm 0.33\%$. In addition, lower content of MF compared to ours was reported by Kvapilík et al. (2017), who obtained the MF 3.84% (from 3.23% to 4.46%) of the 522 monthly bulk milk samples from 11 experimental farms. Also, Nyokabi et al. (2021) reported lower content of milk fat (3.61%) compared to our results and stated no differences in the quality of raw milk between locations.

The solids non-fat content resulted in an average value of 8.60% (from $8.10 \pm 0.21\%$ to $8.74 \pm 0.09\%$) and is therefore within the limits provided for in Administrative Instruction MA 20/2006. Among the farms analysed, SNF showed variations that were statistically significant at the $P < 0.01$ level. In two farms (D, E), the milk analysed showed lower values than those provided in the above-mentioned regulation, according to which milk with an SNF content of less than 8.50% is considered adulterated by the addition of water. However, this doubt does not exist because the authors of the research strictly carried out the activities from milking to sampling, therefore low values can be attributed to other possible factors. Results obtained in this research seems to be lower, compared to those reported by Nyokabi et al. (2021) in the amount of 9.18%, which stated no differences in the quality of raw milk between locations. The higher content of SNF (9.30%) in milk of 83 farms is also reported by Kunda et al. (2015).

The overall mean of protein content (3.25%) in this research was within Kosovo standards for milk quality. The lowest value of this parameter was on the farm D (2.99 ± 0.10%) and farm B (3.01 ± 0.08%), which could be ascribed to feeding management. The highest value of protein content was detected on the farm C (3.69 ± 0.05%). Generally, milk with such protein content, could be a good resource for milk products, especially for cheese production. Among the farms analysed, P content showed variations that were statistically significant at the $P < 0.01$ level. Nyokabi et al. (2021) reported a slightly higher content of milk P (3.46%) compared to our results. Petrovska et al. (2017) in individual milk samples from the Latvian cow breeds, collected across different Latvian regions, obtained results for P content in amount of 3.45%, 3.50% and 3.43% respectively. Kvapilík et al. (2017) found that P content of bulk milk samples from 11 experimental farms was 3.39% (from 3.04 to 3.75%). In addition, Kunda et al. (2015), found out P content in milk of 83 farms in amount of 3.70%.

The lactose content in this research was not at the desired level. The lower content is registered on the farm A (3.50 ± 0.15%) whereas the higher on the farm B (4.16 ± 0.12%). The mean value of this parameter was 3.87%, which is significantly lower than the normal value provided by the regulation. The low lactose content of milk is an important indicator of milk quality, which could be due to the high SCC as well as low energy intake and malnutrition. Therefore, better hygiene and feeding management should be carried out on the farms to improve lactose content as well as milk quality in general. The lactose content in this research is lower to those reported by Rahman et al. (2014) in cows of two different regions of Bangladesh (both 5.29%), with non-significant differences. Ruska et al. (2017) analysed cow milk in farms located in different Latvia region with different holding system and obtained L content in amount of 4.65% and 4.71% with significant differences ($P < 0.05$). Kouřimská et al. (2014) in their research reached results for L content (4.84%) in conventional farming, compared to 4.80% in organic farming with significant differences. Yap et al. (2024) in 9 farms observed L content of 4.58 – 4.81% during evaluation of the quality of raw milk produced from nine different locations across Ireland over 12 months.

Table 3. Some physical properties, bacteriological quality and SCC of milk depending on region/farm location (mean ± SEM) ($n = 252$)

Region/farm location	AA (pH)	D (g cm^{-3})	CFU mL^{-1}	SCC mL^{-1}
Pr/A	6.83 ± 0.08	1.026 ± 0.00^{bc}	138,750 ± 37,387^{bc}	541,667 ± 63,614^{a}
M/B	6.76 ± 0.11	1.029 ± 0.00^{ab}	116,667 ± 24,721^{c}	300,000 ± 42,580^{c}
Pe/C	6.74 ± 0.07	1.031 ± 0.00^{a}	259,167 ± 45,167^{b}	483,333 ± 41,439^{ab}
Pz/D	6.98 ± 0.07	1.027 ± 0.00^{bc}	138,333 ± 26,136^{bc}	575,000 ± 58,225^{a}
Fe/E	6.88 ± 0.06	1.024 ± 0.00^{c}	136,250 ± 29,549^{bc}	575,000 ± 53,831^{a}
Gji/F	6.81 ± 0.12	1.029 ± 0.00^{ab}	115,000 ± 19,365^{c}	370,833 ± 34,520^{bc}
Gja/G	6.81 ± 0.09	1.030 ± 0.00^{a}	454,167 ± 50,923^{a}	83,167 ± 1,854^{d}
P	ns	<.0001	<.0001	<.0001

AA – Active acidity (pH); D – Density (g cm^{-3}); CFU – Colony Formatting Unit (CFU mL^{-1}); SCC – Somatic Cell Count (SCC mL^{-1}); ns – non-significant. ^{a,b,c}Means with different superscript in the same column differ significantly ($P < 0.01$).

The mean value of active acidity (pH = 6.83) was a slightly higher than frames of the Kosovo standards for milk quality for this parameter. A higher pH value indicates a

mastitis infection in the cow. As in the case of lactose, the hygiene management of the farm and dairy cows should be necessary and continuous, with the aim of ensuring healthy and high-quality milk. Among the farms analysed, AA showed statistically non-significant differences at the $P < 0.01$ level. A lower value compared to ours reported Asefa & Teshome (2019). They stated a significant difference between each study site with the lower pH of 6.02 and 6.17 in Debrezeit and Sebeta milk shade whereas in milk from Wolmera and Selale cloth to normal pH range.

Milk density on all farms was within the limits for normal and unadulterated milk. The overall mean value was 1.028 g cm^{-3} (1.024 to 1.031 g cm^{-3}), with variations that were statistically significant at the $P < 0.01$ level. The differences between lower and higher density values could be due to changes in total solids content. Asefa & Teshome (2019) reported almost similar results of density (1.029, 1.030, 1.029 and 1.031 g cm^{-3}) of milk samples from different locations, but with no significant ($P > 0.05$) difference. In addition, Nyokabi et al. (2021) reported a slightly higher value of milk density (1.031 g cm^{-3}) compared to our results and stated significant differences between locations.

The average value of CFU (194,048 mL^{-1}) was significantly above the threshold provided by the Kosovo regulation (< 80,000 mL^{-1}), and the analysed milk was categorized in the second quality class (< 300,000 CFU mL^{-1}). This may be attributed to poor hygiene practices that may have been implemented in these farms. It is recommended that in the future more work should be done to diligently implement hygienic measures on farms, with the aim of improving the microbiological quality of milk. However, this would affect the maintenance of the animals' health condition, but also the improvement of the milk payment, which is based, among other things, on the values of this parameter. In comparation to our results for this parameter, Kvapilík et al. (2017) found higher contents (250,000 mL^{-1}) in the bulk milk samples from 11 experimental farms during the period from 2012 to 2015. Contrary to this, Kouřimská et al. (2014) in conventional and in organic farming concluded contents of CFU (48,000 mL^{-1} and 45,000 mL^{-1} respectively), which are much lower compared to ours. Ivanov et al. (2017) found in milk samples from three regions of western Turkey that the maximum permissible values of 100,000 CFU mL^{-1} were exceeded and there were no statistically significant ($P < 0.05$) differences.

The average number of SCC (418,429 SCC mL^{-1}) although a little high, was almost within the limits for normal milk derived from healthy animals, and according to the Kosovo regulation it is categorized in the second quality class. Only farm B, F and G showed good results of SCC. However, the results recommend implementing the best hygienic practices to improve the quality of milk and healthy status of milking animals. These measures are necessary to prevent the occurrence of breast diseases that could, among other things, cause economic damage. Among the farms analysed, SCC showed variations that were statistically significant at the $P < 0.01$ level. Kouřimská et al. (2014) reported lower contents of SCC in conventional (230,000 mL^{-1}) and organic farming (218,000 mL^{-1}) compared to ours. Lower contents of SCC also reported Leso et al. (2019). He studied 30 commercial dairy farms located in the Po Valley, Italy over a period of one year. SCC was between 259,000 mL^{-1} and 354,000 mL^{-1}. Ducková et al. (2019) reported higher mean value of SCC (50,767 mL^{-1}) in milk samples from farm dairies compared to ours. Ivanov et al. (2017) found very high SCC levels in milk samples from three regions of western Turkey. These values are well above the maximum permitted by European legislation of 400,000 mL^{-1} in cow's milk.

The influence of the seasonal fluctuations on the composition and properties of milk

Based on the results presented in Table 4 and 5, it can be noted that all analysed indicators showed slight fluctuations within seasons with statistically non-significant differences.

Total solids content showed an average value of 13.71%, which meets the quality standards for milk in Kosovo. The lowest value was in the summer season (13.55 ± 0.32%) while the highest was in the spring season (13.97 ± 0.38%). The differences between the seasons were statistically non-significant. This can be justified by the fact that on all farms the animals were kept in an indoor system and were mainly fed with the almost similar pre-prepared dry feed, while the feed from free pasture has not been applied. Baset et al. (2016) reported that season (dry and wet) did not affect TS. This finding is consistent with the results obtained in our research. However, many other authors emphasize the influence of the season on changes in the value of TS in milk. Thus, Kabil et al. (2015) reported seasonal influence in mean values of TS, which in winter was 12.40%, and in summer 11.10% respectively. Both winter and summer values of TS were lower, compared to results in our research. Lower TS values in the summer season were also reported by Cowley et al. (2015). He dealt with the fact that days in summer are getting longer, and the temperature is rising, which results in heat stress to cows, decreases dry matter intake (DMI) in cattle, and that also declines milk production. Sahu et al. (2018) found that the overall mean for TS content of milk was 12.61%. He also showed non-significant influence of seasons on TS content of milk of Kosali cows, being highest in rainy season (12.81%) followed by winter (12.67%) and lowest in summer season (12.36%). According to Shibru et al. (2019), TS content was higher in dry season from October to May (13.38%) and lower in wet season from June to September (12.96%) with non-significant differences. Parmar et al. (2020) showed significantly higher value of TS in autumn (14.72%), compared to spring (13.95%) and summer (13.68%). Nateghi et al. (2014) suggested that summer milk has significantly higher TS content (13.31%) than winter milk (12.02%).

Table 4. Milk quality depending on season (Mean ± SEM) (n = 252)

Season	TS (%)	MF (%)	SNF (%)	P (%)	L (%)
Spring	13.97 ± 0.38	5.29 ± 0.43	8.57 ± 0.14	3.16 ± 0.10	4.02 ± 0.05
Summer	13.55 ± 0.32	4.88 ± 0.33	8.63 ± 0.13	3.24 ± 0.13	3.94 ± 0.11
Autumn	13.58 ± 0.31	4.97 ± 0.36	8.55 ± 0.11	3.27 ± 0.07	3.74 ± 0.10
Winter	13.73 ± 0.29	5.35 ± 0.52	8.67 ± 0.13	3.32 ± 0.08	3.80 ± 0.08
P	ns	ns	ns	ns	ns

TS – Total solids (%); MF – Milk fat (%); SNF – Solids non-fat (%); P – Proteins (%); L – Lactose (%); ns – non-significant.

Milk fat is considered one of the quality parameters that varies depending on various factors, including the influence of the season. MF content in the samples collected in the summer (4.88 ± 0.33%) was non-significantly lower compared with samples of winter season (5.35 ± 0.52%), with the average value of 5.12%. The slightly lower MF during summer season could be attributed to differences in nutrient intake or specific effects of climate such as environmental temperature. Statement regarding non-significantly differences of MF in our research is consistent with the statements of

Madruga et al. (2016), who reported that the MF content did not vary according to the seasons. On the other hand, Kabil (2015) reported a significant seasonal influence in cows MF with lower mean values in summer (3.10%) compared to winter (3.60%). Pacheco-Pappenheim et al. (2021) reported that MF levels were significantly higher ($P < 0.05$) between months, where the maximum content was observed in March (4.60%) and the minimum in June (4.08%). Also, according to Gajbhiye et al. (2019) MF content was significantly different between seasons ($P < 0.01$). The highest MF content being produced in the Rainy-winter season (4.34% and 4.26%) and lowest in Spring-Summer season (4.14% and 3.88%). Habteghiorghis (2019) in his research showed significant variation of MF ($P < 0.05$) between different seasons. The highest average of MF content (6.15%) was recorded in autumn, while the lowest (4.73%) was in spring. Czyzak-Runowska et al. (2020) reported significantly higher MF content ($P \leq 0.01$) in autumn-winter (3.79%) while lower content in spring-summer season (3.19%). Parmar et al. (2020) reported significantly higher content of MF in autumn (5.13%) and spring (5.00%) than in summer (4.71%). Bertocchi et al. (2014) reported significantly higher amount of MF in winter (4.01%) and autumn (3.91%) than in spring (3.85%) and summer (3.75%). Looper (2014) also reported the highest MF content during the autumn and winter, and lowest during the spring and summer season, reasoning mainly due to changes in both the types of feed availability and climatic conditions.

Solids non-fat content showed an average value of 8.60%. The lowest value was in the autumn season ($8.55 \pm 0.11\%$) while the highest was in the winter season ($8.67 \pm 0.13\%$), with statistically non-significant differences between seasons. However, a slightly lower SNF value in autumn could be due to feed composition or other factors (e.g. environmental conditions, temperature, etc.). SNF content in all seasons was under limits, prescribed in Administrative instructions of Kosovo for good and unadulterated milk. These findings are almost consistent with those emphasized by Singh et al. (2018), who reported average value of SNF 8.72% with the range from 7.97% in summer to 9.42% in winter season. Wangdi et al. (2016) recorded overall mean milk composition in milk produced in Bhutan and find out that SNF content was lower in spring and summer (8.35%), than in winter (8.40%) and autumn (8.61%). Mishra et al. (2022) found that SNF content varied by season and was highest in winter (9.46%), followed by summer (9.31%) and rainy season (8.92%). Kheowsri et al. (2023) reported that the SNF was significantly ($P < 0.01$) lower in the rainy (8.51%), in comparison to cold (8.54%) and hot season (8.55%).

Protein content of milk is highly important due to influence on its nutritional value and processing properties, since milk protein content may increase milk product yield such as cheese. The mean value of milk protein in this research was 3.25%. The lowest protein content in this research was detected in the spring season ($3.16 \pm 0.10\%$). It could be as a results of feed availability and climatic conditions. The highest content was registered in the winter season ($3.32\% \pm 0.08$) However, non-significant differences were detected between seasons. Similar conclusions emphasised in their research Baset et al. (2016); Wangdi et al. (2016); Lin et al. (2017). Contrary to this, Kabil, (2015) reported higher values of P in winter (3.50%) compared to summer (3.10%) respectively. Sahu et al. (2018) reported significantly differences of *P* levels between the seasons ($P < 0.01$), in which case the higher levels were registered in winter season (3.13%) followed by summer (2.98%) and lowest in the rainy season (2.82%). However, the

noted that the mean differences between summer and rainy season were nonsignificant. Chanda et al. (2021) reported average value of P (3.45%) in winter and 3.36% in summer with significantly differences ($P < 0.05$). In addition, Bertocchi et al. (2014) reported higher content of P during winter (3.44%) and autumn (3.48%) compared to spring (3.39%) and in summer (3.32%). Similar to this, Looper (2014) reported that the highest *P* content was recorded during the autumn and winter, and lowest during the spring and summer season resulting mainly due to changes in both the types of feed availability and climatic conditions.

The average lactose content in this study was 3.87%, which can be considered low for normal milk. In addition, lower values were found in all seasons. This could be related to several genetic factors and the health of the mammary gland. For this reason, maintaining general hygiene and udder health should be a necessary activity on all farms. Differences between the autumn season (3.74 ± 0.10%) and spring season (4.02 ± 0.05%) were statistically non-significant. Almost all authors cited below reported a higher amount of L in their research. Some of them (Parmar et al., 2020) obtained higher L amount in the autumn (4.68%) compared to spring (4.59%) and summer (4.62%). Sahu et al. (2018) reported that L level was significantly higher ($P < 0.01$) during the winter (4.69%) and lower in the summer (4.49%) and rainy season (4.22%). On the other hand, Baset et al. (2016) reported that season (dry and wet) did not affect L content. Nateghi et al. (2014) noted non-significant difference regarding L content between summer (4.61%) and winter milks (4.58%) respectively.

Table 5. Some physical properties, bacteriological quality and SCC of milk depending on season (Mean ± SEM) ($n = 252$)

Season	AA (pH)	D (g cm^{-3})	CFU mL^{-1}	SCC mL^{-1}
Spring	7.05 ± 0.26	1.028 ± 0.00	222,857 ± 43,612	447,857 ± 50,996
Summer	7.17 ± 0.29	1.028 ± 0.00	174,762 ± 23,408	445,000 ± 50,509
Autumn	7.54 ± 0.22	1.028 ± 0.00	189,524 ± 36,097	433,714 ± 51,168
Winter	7.47 ± 0.25	1.029 ± 0.00	189,048 ± 39,430	347,143 ± 41,000
P	ns	ns	ns	ns

AA – Active acidity (pH); D – Density (g cm^{-3}); CFU – Colony Formatting Unit (CFU mL^{-1}); SCC – Somatic Cell Count (SCC mL^{-1}); ns – non-significant.

The active acidity (pH) value of fresh whole cow milk normally varies within a quite narrow range of 6.5 and 6.8. In this study, this parameter could be considered slightly high because there is a high probability that it indicates udder inflammation. The lowest value of AA was in the spring (7.05 ± 0.26) while the highest was in the autumn (7.54 ± 0.22), with an average value of 7.31 and non-significant differences between seasons. This is consistent with the results obtained from Lin et al. (2017), who emphasized that season did not significantly affect AA value. Contrary to this, the statistically significant differences of pH between the seasons reported Özlem & Kul. (2020) with highest value in winter (6.76) and lowest value in spring (6.33). In addition, Habteghiorghis (2019) noted a significant variation ($P < 0.05$) in AA value between the samples from different seasons. Thus, the highest AA value recorded in winter (6.72) and lowest in summer (6.67).

The milk density in this research showed the mean value of 1.028 g cm^{-3}, which meets the requirements of the regulation for normal and undiluted milk. The lowest value

was in the spring, summer, and autumn (1.028 g cm^{-3}) while the highest was in the winter season (1.029 g cm^{-3}). The differences between the seasons were statistically non-significant. Similar results to ours reported Wangdi et al. (2016) with the D value of 1.028 g cm^{-3} in all seasons and non-significant differences. Moreover, Nateghi et al. (2014) noted that D value of summer and winter milks were 1.032 g cm^{-3} and 1.030 g cm^{-3} respectively, being statistically similar (non-significant). Contrary to this, Parmar et al. (2020) obtained the highest D value in the summer (1.0314 g cm^{-3}) while the lowest in the spring (1.0304 g cm^{-3}) with significant differences in all the seasons.

Analysed milk in our research showed the mean value of 194,048 CFU mL^{-1}. This value significantly exceeds the limit for extra class described in the regulation (80,000 CFU mL^{-1}). This can be attributed to lack of hygienic conditions during milking and handling of the milk. The lowest value was in the summer season (174,762 ± 23,408) while the highest was in the spring season (222,857 ± 43,612). The differences between the seasons were statistically non-significant. Hajmohammadi et al. (2021) noted that the samples collected in summer had higher ($P < 0.05$) CFU mL^{-1} than in winter, highlighting that these results indicate that most of the traditional milk production in the studied region occurs under unsatisfactory hygienic conditions. Like this, Bertocchi et al. (2014) found an increase in CFU during the summer months and emphasized that this is closely related to the greater bacterial growth and higher contamination of the udder compared to the other seasons. Contrary to this, Nateghi et al. (2014) gained a significantly higher microbial load of winter milk (78,262.54 CFU mL^{-1}) than that of summer milk (72,345.12 CFU mL^{-1}) suggesting that summer milk was produced under more favourable hygienic conditions.

The somatic cell counts in this research gave a mean value of 418,429 SCC mL^{-1}. The lowest value was in the winter season (347,143 ± 41,000) while the highest in the spring season (447,857 ± 50,996) and summer season (445,000 ± 50,509). These levels are relatively high, especially in the spring and summer season, which can lead to health problems of the mammary gland. Between seasons statistically non-significant differences were detected for this parameter. Contrary to this, Kheowsri et al. (2023) reported a significantly highest SCC in the rainy season (321.21 ± 3.93 x 1,000 cell mL^{-1}), and the lowest in cold season (297.29 ± 94.34 x 1,000 cell mL^{-1}). In addition, Heck et al. (2009) determined a minimum of SCC value in the winter and a maximum value in the summer season. Similar findings were offered by Bertocchi et al. (2014) and Hajmohammadi et al. (2021) reporting that the SCC was higher in the summer months.

CONCLUSIONS

Based on the results obtained in this research, it can be concluded that the geographical location of farms in Kosovo during 2021 and 2022, with the focus on the seven administrative regions significantly influenced majority of tested milk parameters, such as: TS, MF, SNF, P, D, CFU, and SCC. However, this factor did not significantly influence L content and AA value.

On the other hand, season did not have a significant influence on the measured parameters. Nevertheless, lower levels of TS, MF, and CFU in summer; AA and P in spring; SNF and L in autumn, and SCC in the winter season were observed.

Based on these findings, it is recommended for farmers to continue working in better hygienic practices on their farms to further improve milk quality and the health of

milking animals. Additionally, further research, especially regarding the influence of feeding and overall farm management practices, is suggested to better identify factors that influenced the variations in milk quality between farms and seasons observed in this research.

REFERENCES

Administrative Instruction MA–No. 20/2006. Quality Standards and Grade of Fresh Milk. *Provisional Institution of Self Government. Government of Kosovo. Ministry of Agriculture Forestry and Rural Development.* https://www.mbpzhr-ks.net/en/administrative-instructions/?dy=2006. Accessed 20. 10. 2023.

Ali, H.R., Ali, S.F., Abd-Algawad, R.H., Sdeek, F.A., Arafa, M., Kamel, E. & Shahein, M.A. 2022. Impact of udder infections on biochemical composition of milk in context of pesticides exposure. *Veterinary world* **15**(3), 797–808. https://doi.org/10.14202/vetworld.2022.797-808

Alrhmoun, M., Zanon, T., Katzenberger, K., Holighaus, L. & Gauly, M. 2023. Exploring the heights: Impact of altitude on dairy milk composition. *JDS communications* **5**(2), 139–143. https://doi.org/10.3168/jdsc.2023-0448

Araújo, V.M. de, Barbosa, S.B.P., Rangel, A.H. do N., Borba, L.H.F., Oliveira, J.P.F. de, & Batista, Â.M.V. 2023. Quality of raw bulk-tank milk produced in northeast Brazil. *Bioscience Journal* **39**, e39064. doi: https://doi.org/10.14393/BJ-v39n0a2023-59825.

Asefa, Z. & Teshome, G. 2019. Physical properties and chemical compositions of raw cow milk in milk shades around addis ababa, Ethiopia. *Journal of Natural Sciences Research* **9**(19), 33-37. DOI: 10.7176/JNSR/9-19-04

Azooz, M.F., El-Wakeel, S.A. & Yousef, H.M. 2020. Financial and economic analyses of the impact of cattle mastitis on the profitability of Egyptian dairy farms. *Veterinary world* **13**(9), 1750–1759. https:// doi.org/ 10.14202/ vetworld. 2020.1750-1759

Baset, M., Huque, K., Sarker, N., Hossain, M. & Islam, M. 2016. Influence of season, genotype and lactation on milk yield and composition of local and crossbred dairy cows reared under different feed base region. *Bangladesh Journal of Livestock Research* **19**(1–2), 50–65. https://doi.org/10.3329/bjlr.v19i1–2.26427

Bertocchi, L., Vitali, A., Lacetera, N., Nardone, A., Varisco, G. & Bernabucci, U. 2014. Seasonal variations in the composition of Holstein cow's milk and temperature–humidity index relationship. *Animal* **8**(4), 667–674 © The Animal Consortium. doi: 10.1017/S1751731114000032

Bytyqi, H., Rrustemi, M., Mehmeti, H., Kryeziu, A., Gjinovci, V. & Gjonbalaj, M. 2009. Milk production in commercial cattle dairy farms in Kosovo. *Stočarstvo* **63**(4) 275–285.

Chanda, T., Khan, M.K.I., Chanda, G.C. & Debnath, G.K. 2021. A Study on Farming Conditions and Production Performance of Available Genotypes under Commercial Dairying of Chittagong Bangladesh. *Asian Journal of Dairy and Food Research* **40**(2), 142–146. doi: 10.18805/ajdfr.DR-205

Cowley, F.C., Barber, D.G., Houlihan, A.V. & Poppi, D.P. 2015. Immediate and residual influences of heat stress and restricted intake on milk protein and casein composition and energy metabolism. *Journal of dairy science* **98**(4), 23562368, ISSN 0022–0302. https://doi.org/10.3168/jds.2014–8442

Czyzak-Runowska, G., Wójtowski, J., Bielinska-Nowak, S., Wojtczak, J. & Markiewicz-Keszycka, M. 2020. Seasonal variation in the quality parameters of milk from an extensive, small family farm. *Acta Sci. Pol. Zootechnica* **19**(3), 63–70. doi: 10.21005/asp.2020.19.3.08

Ducková, V., Čanigová, M., Zajác, P., Remeňová, Z., Kročko, M. & Nagyová, L. 2019. Influences of Somatic Cell Counts occurred in milk on quality of Slovak traditional cheese–Parenica. *Potravinarstvo Slovak Journal of Food Sciences* **13**(1), 675–680. https://doi.org/10.5219/1099

Gajbhiye, P.U., Ahlawat, A.R., Sharma, H.A. & Parikh, S.S. 2019. Effect of Stage, Season and Parity of Lactation on Milk Composition in Gir Cattle. *International Journal of Current Microbiology and Applied Sciences* **8**(03), 2419–2425. ISSN: 2319-7706. doi: https://doi.org/10.20546/ijcmas.2019.803.285

Gaworski, M., Leola, A., Kiiman, H., Sada, O., Kic, P. & Priekulis, J. 2018. Assessment of dairy cow herd indices associated with different milking systems. *Agronomy Research* **16**(1), 83–93. https://doi.org/10.15159/AR.17.075

Green report 2022. Source: KAS – Agricultural Households Survey ('17,'18,'19,'20,'21); *KAS, Foreign Trade Statistics; calculations by DEAAS – MAFRD*. Chrome extension: //efaidnbmnnnibpcajpcglclefindmkaj, /https://www.mbpzhr–ks.net/repository/ docs/Kosovo__Green_Report_ 2022. pdf.

Habteghiorghis, A.T. 2019. *The impact of seasonal variations of New Zealand raw milk on the heat stability of skim milk.* Abstract of a thesis submitted in partial fulfilment of the requirements for the Degree of Master of Food Science. https://hdl.handle.net/10182/11143. Accessed 16. 03. 2023.

Hajmohammadi, M., Valizadeh, R., Ebdalabadi, M.N., Naserian, A. & Oliveira, C.A.F. 2021. Seasonal variations in some quality parameters of milk produced in Khorasan Razavi Province, Iran. *Food Science and Technology (Campinas)* **41**(2), 718–722. doi:10.1590/fst.35120.

Hayes, E., Wallace, D., O'Donnell, C., Greene, D., Hennessy, D., O'Shea, N., Tobin, J.T. & Fenelon, M.A. 2023. Trend analysis and prediction of seasonal changes in milk composition from a pasture-based dairy research herd. *J. Dairy Sci*. **106**, 2326–2337. https://doi.org/10.3168/jds.2021-21483

ISO 4833–2:2013, 2013. Microbiology of the food chain – Horizontal method for the enumeration of microorganisms – Part 2: Colony count at 30 degrees C by the surface plating technique – Technical Corrigendum 1 (ISO 4833–2:2013/Cor1:2014).

ISO 707:2008 (IDF 50:2008), 2008. Milk and milk products – Guidance on sampling.

ISO/TS 11869:2012 (IDF/RM 150:2012). Fermented milks – Determination of titratable acidity Potentiometric method. https:// www. iso.org/ standard/ 56875.html.

Ivanov, G.Y., Bilgucu, E., Balabanova, T.B., Ivanova, I.V. & Uzatici, A. 2017. Influence of animal breed, season and milk production scale on somatic cell count and composition of cow milk. *Bulg. J. Agric. Sci*. **23**(6), 1047–1052.

JMP-in 7.0 (1989–2004). The statistical Discovery SoftwareTM. SAS Institute.

Kabil, O., Ali, M., Ibrahim, E. & El Barbary, H. 2015. Influence of seasonal variation on chemical composition of Cow's milk. *Benha Veterinary Medical Journal* **28**(1), 150–154. doi: 10.21608/bvmj.2015.32728

Kebede, E. 2018. Effect of Cattle Breed on Milk Composition in the same Management Conditions. *Ethiop. J. Agric. Sci*. **28**(2), 53–63.

Khatun, M.A., Roy, B.K., Hossain, A., Rahman, A., Munshi, M.K., Islam, M., Hossain, M.A., Islam Bhuiya, M.A., Rahman, M.M. & Huque, R. 2018. Biochemical and Microbial Quality Attributes of Cow's Milk in Respect to Regional Discrimination in Bangladesh. *Archives of Current Research International* **12**(4), 1–12. https://doi.org/10.9734/ACRI/2018/39451

Kheowsri, S., Rojanasthien, S., Semmarath, W., James Stott, C., Sungkatavat, P., Phetkarl, T., Rueangareerat, P., Suprasert, A., Atthi, R., Chaimongkol, C., Lavilla, C., Singhanetr, S., Yiengvisavakul, V., Pisetpaisan, A., Choongkittaworn, N., Sansamur, C. & Lewchalermvong, K. 2023. Factors affecting milk composition in dairy farms located in Northern, Thailand: *Veterinary Integrative Sciences* **21**(1), 157–173. https:// doi.org/ 10.12982/ VIS.2023.013

Kouřimská, L., Legarová, V., Panovská, Z. & Pánek, J. 2014. Quality of cows' milk from organic and conventional farming. *Czech Journal of Food Sciences* **32**(4), 398–405. doi: 10.17221/510/2012–CJFS

Kul, E., Şahİn, A., Atasever, S., Uğurlutepe, E. & Soydaner, M. 2019. Effects of somatic cell count on milk yield and milk composition in Holstein cows. *Vet. arhiv* **89**, 143–154. doi: 10.24099/vet.arhiv.0168

Kunda, B., Pandey, G.S. & Muma, J.B. 2015. Compositional and sanitary quality of raw milk produced by small holder dairy farmers in Lusaka Province of Zambia. *Livestock Research for Rural Development* **27***(*10). http://www.lrrd.org/lrrd27/10/pand27201.html

Kvapilík, J., Jedelská, R., Hanuš, O., Urban, P., Říha, J., Kopunecz, P., Seydlová, R., Roubal, P., Zlatníček, J. & Klimeš, M. 2017. Somatic cell count in milk from individual dairy cows and selected indicators. *Acta Universitatis Agriculturae et Silviculturae Mendelianae Brunensis* **65**(3), 879–892.

Leso, L., Pellegrini, P. & Barbari, M. 2019. Effect of two housing systems on performance & longevity of dairy cows in Northern Italy. *Agronomy Research* **17**(2), 574–581. https://doi.org/10.15159/AR.19.107

Li, S., Ye, A. & Singh, H. 2019. Seasonal variations in composition, properties, and heat-induced changes in bovine milk in a seasonal calving system. *J. Dairy Sci* **102**, 7747–7759. https://doi.org/10.3168/jds.2019-16685

Lin, Y., O'Mahony, J.A., Kelly, A.L. & Guinee, T.P. 2017. Seasonal variation in the composition and processing characteristics of herd milk with varying proportions of milk from spring – calving and autumn – calving cows. *Journal of Dairy Research* **84**(4), 444–452. doi:10.1017/S0022029917000516

Looper, M. 2014. Factors Affecting Milk Composition of Lactating Cows. *Agriculture and Natural Resources, Department of Agric. Res. and Extension, University of Arkansas System*. http://www.uaex.edu/publications/pdf/fsa–4014. url={https://api.semanticscholar.org/CorpusID:46639752}.

Madruga, R.C., Rangel, A.H.N., Urbano, S.A., Novaes, L.P., Borba, L.H.F., Sales, D.C., Silva, J.B.A. & Lima, E.R. 2016. Evaluation of the quality of tank milk for herds of Guzerat and F1 Guzolando cross. *Livestock Research for Rural Development* **28**(8). Retrieved January 30, 2024, from http://www.lrrd.org/lrrd28/8/madr28140.html.

Magan, J.B., O′ Callaghan, T.F., Kelly, A.L. & McCarthy, N.A. 2021. Compositional and functional properties of milk and dairy products derived from cows fed pasture or concentrate-based diets. *Comprehensive Reviews in Food Science and Food Safety* **20**(3), 2769–2800. doi: 10.1111/1541-4337.12751

Mishra, G., Goswami, S.C., Jhirwal, A.K. & Paliwal, S. 2022. Effect of Breed, Season and Stage of Lactation on Different Milk Parameters at Organized Farm. *Asian Journal of Dairy and Food Research*. doi: 10.18805/ajdfr.DR-1937

Mitani, T., Kobayashi, K., Ueda, K. & Kondo, S. 2021. Regional differences in the fatty acid composition, and vitamin and carotenoid concentrations in farm bulk milk in Hokkaido, Japan. *Animal science journal* **92**(1), e13570.

Nateghi, L., Yousefi, M., Zamani, E., Gholamian, M. & Mohammadzadeh, M. 2014. The influence of different seasons on the milk quality. *European Journal of Experimental Biology* **4**(1), 550–552. url={https:// api.semanticscholar. org/ CorpusID:28881907.

Nyokabi, S.N., De Boer, I.J.M., Luning, P.A., Korir, L., Lindahl, J., Bett, B. & Oosting, S.J. 2021. Milk quality along dairy farming systems and associated value chains in Kenya: An analysis of composition, contamination and adulteration. *Food Control* **119**(107482). https: //doi. org/10.1016/j. foodcont. 2020.107482

O'Callaghan, T.F., Hennessy, D., McAuliffe, S., Kilcawley, K.N., O'Donovan, M., Dillon, P., Ross, R.P. & Stanton, C. 2016. Effect of pasture versus indoor feeding systems on raw milk composition and quality over an entire lactation. *Journal of dairy science* **99**(12), 9424–9440. https://doi.org/10.3168/jds.2016-10985

Özlem, O. & Kul, E. 2020. Effects of some environmental factors on somatic cell count and milk chemical composition in cow bulk tank milk. *Akademik Ziraat Dergisi* **9**(1), 163–170 ISSN: 2147-6403 e-ISSN: 2618-5881. doi: http://dx.doi.org/10.29278/azd.725884

Pacheco-Pappenheim, S., Yener, S., Heck, J.M.L., Dijkstra, J. & Van Valenberg, H.J.F. 2021. Seasonal variation in fatty acid and triacylglycerol composition of bovine milk fat. *Journal of dairy science* **104**(8), 8479–8492. https://doi.org/10.3168/jds.2020-19856

Parmar, P., Lopez-Villalobos, N., Tobin, J.T., Murphy, E., McDonagh, A., Crowley, SH.V., Kelly, A.L. & Shalloo, L. 2020. The Influence of Compositional Changes Due to Seasonal Variation on Milk Density and the Determination of Season–Based Density Conversion Factors for Use in the Dairy Industry. *Foods* **9**(8), 1004. doi:10.3390/foods9081004 www.mdpi.com/journal/foods.

Petrovska, S., Jonkus, D., Zagorska, J. & Ciprovica, I. 2017. The influence of k-casein genotype on the coagulation properties of milk collected from the local Latvian cow breeds. *Agronomy Research* **15**(S2), 1411–1419.

Rahman, M.M., Mahmud, M.A.A., Baset, M.A., Mahfuz, S.U., Mehraj, H. & Jamal Uddin, A.F.M. 2014. Milk Nutritional Composition in Relation to Cow Genotype and Location of Bangladesh. *International Journal of Business, Social and Scientific Research* **01**(03), 155–160. Retrieve from http://www.ijbssr.com/currentissueview/14013027/

Ramadani, Xh., Kryeziu, A., Kamberi, M. & Zogaj, M. 2023. Influence of altitude and lactation period on composition and physical properties of milk in crossbred Sharri sheep. *Agronomy Research* **21**(3), 1278–1292. https://doi.org/10.15159/AR.23.044

Roy, D., Ye, A., Moughan, P.J. & Singh, H. 2020. Composition, Structure, and Digestive Dynamics of Milk From Different Species–A Review. *Front. Nutr.* **7**:577759. doi: 10.3389/fnut.2020.577759

Ruska, D., Jonkus, D. & Cielava, L. 2017. Monitoring of ammonium pollution from dairy cows farm according of urea content in milk. *Agronomy Research* **15**(2), 553–564.

Sahu, J., Bhonsle, D., Mishra, Sh., Khune, N.V. & Chaturvedani, A.K. 2018. Factors affecting the milk composition of Kosali cow. *Int. J. Curr. Microbiol. App. Sci.* **7**(8), 3795–3801. doi: https://doi.org/10.20546/ijcmas.2018.708.387

Sanjayaranj, I., Lopez-Villalobos, N., Blair, H.T., Janssen, P.W.M., Holroyd, S.E. & MacGibbon, A.K.H. 2022. Effect of Breed on the Fatty Acid Composition of Milk from Dairy Cows Milked Once and Twice a Day in Different Stages of Lactation. *Dairy* **3**, 608–621. https://doi.org/10.3390/dairy3030043.

Shibru, D., Tamir, B., Kasa, F. & Goshu, G. 2019. Effect of season, parity, exotic gene level and lactation stage in milk yield and composition of Holstein friesian crosses in central highlands of Ethiopia. *European Journal of Experimental Biology* **9**(4), 15.**ISS** http://www.imedpub.com/. ISSN 2248-92152248.

Singh, R.P., Herbert, S., Singh, B. & Verma, D.K. 2018. Quantification of immediate and subsequent responses in milk production, its components and body weight of Gangatiri cows at SHUATS dairy farm. *IOSR Journal of Agriculture and Veterinary Science (IOSR-JAVS)* e-ISSN: 2319-2380, p-ISSN: 2319-2372. Volume **11**, Issue 1 Ver. III PP 31–34 www.iosrjournals.org. doi: 10.9790/2380-1101033134

Timlin, M., Tobin, J.T., Brodkorb, A., Murphy, E.G., Dillon, P., Hennessy, D., O'Donovan, M., Pierce, K.M. & O'Callaghan, T.F. 2021. The Impact of Seasonality in Pasture-Based Production Systems on Milk Composition and Functionality. *Foods***10**, 607. https://doi.org/ 10.3390/foods10030607

Wangdi, J., Zangmo, T., Karma, K., Mindu, M. & Bhujel, P. 2016. Compositional quality of cow's milk and its seasonal variations in Bhutan. *Livestock Research for Rural Development* **28**(1).

Yap, M., O'Sullivan, O., O'Toole, P.W., Sheehan, J.J., Fenelon, M.A. & Cotter, P.D. 2024. Seasonal and geographical impact on the Irish raw milk microbiota correlates with chemical composition and climatic variables. *Msystems*, e01290-23. doi:10.1128/msystems.01290-23

Agronomy Research **22**(1), 253–273, 2024
https://doi.org/10.15159/AR.24.025

Semi-natural grassland abandonment in relation to agricultural land management under Common Agricultural Policy in boreonemoral Europe

S. Rūsiņa[1*], P. Lakovskis[2] and L. Ieviņa[2]

[1]University of Latvia, Faculty of Geography and Earth Sciences, Jelgavas iela 1, LV-1004 Riga, Latvia
[2]Institute of Agricultural Resources and Economics, Struktoru iela 14, LV-1039 Riga, Latvia
[*]Correspondence: solvita.rusina@lu.lv

Received: February 11th, 2024; Accepted: April 11th, 2024; Published: April 26th, 2024

Abstract. The Common Agricultural Policy (CAP) has had a major impact on agricultural land use changes in Europe. While grassland abandonment in mountain areas is well-documented, there is a gap in research regarding lowland regions. We investigated how changes in CAP regulations between two periods (2007–2013 and 2014–2020) influenced the pattern of semi-natural grassland (SNG) abandonment in boreonemoral Europe. We used 25 km^2 grid cells as the basic research unit. The relationship between agricultural land management variables and SNG abandonment was analyzed by regression methodology and non-linear relationships were detected. We observed a decrease in the overall rate of SNG abandonment during the second CAP period (2014–2020), suggesting that recent CAP modifications have had some positive impact on grassland conservation. However, the impact of CAP on SNG abandonment varied between the two regions differing in land capability for agriculture and between productive and unproductive SNG types. The study highlights the importance of understanding the complex processes that influence abandonment in strongly non-linear ways. It underscores the importance of tailored conservation strategies and the role of the CAP in shaping SNG management practices.

Key words: agri-environment, CAP support, grassland loss, Habitats Directive, intensification, land capability for agriculture.

Used abbreviations. AES agri-environmental scheme, LCA land capability for agriculture, PG permanent grassland, SNG semi-natural grassland.

INRODUCTION

Semi-natural permanent grasslands (SNG) are among the most valuable ecosystems for biodiversity conservation in agricultural landscapes in the European Union, with most of them being habitats listed in Annex I of Directive 92/43/EEC (Bengtsson et al., 2019; Herzon et al., 2022; Prangel et al., 2023). However, starting from the mid-20th century, considerable areas of SNG have been abandoned or converted into arable land or improved grassland (Pe'er et al., 2014). Particularly high risks of agricultural

intensification have been shown for the Baltic States in boreonemoral Europe (European Commission, 2019). At the same time, the risk of agricultural land abandonment is also rated as one of the highest in the Baltics (Terres et al., 2015).

While a bulk of literature examines grassland abandonment in mountain areas (due to the dominance of this agricultural land management type) (MacDonald et al., 2000; Gellrich et al., 2007; Hinojosa et al., 2016; Argenti, et al., 2020; Dax et al., 2021), there are surprisingly few studies exploring the driving factors of grassland abandonment in lowland regions (Biro et al., 2013). This could be related to the fact that grassland loss in lowland areas is more linked to their conversion to croplands and to a much lesser extent to abandonment (Wittig et al., 2010; Ridding et al., 2015). In addition, the majority of agricultural land abandonment studies do not distinguish between arable land and grassland, assuming the same driving factors for both land management types (Pazúr et al., 2014; Terres et al., 2015; Filho et al., 2016; Ustaoglu & Collier, 2018).

However, in boreonemoral Europe, mixed land-use agricultural landscapes at a farm level were common until the mid-20th c. The common practice was to have grasslands only on soils that were the least suitable for agricultural use. Thus, abandonment affected grasslands more than arable land in the mid-20th c. (Penēze et al. 2009; Aune et al., 2018; Rūsiņa et al., 2021). From the mid-20th century, the largest abandonment has been induced by the Common Agricultural Policy (CAP) in Western European countries and by the fall of the communist regime in Central and Eastern European countries (Biro et al., 2013; Pazúr et al., 2014; Lasanta et al., 2017). In latter, the overall rate of agricultural land abandonment declined after EU accession but it still continued in the more marginal areas where also the share of grasslands was historically higher (Nikodemus et al., 2005; Vanwambeke et al., 2012; Jepsen et al., 2015). CAP rules are therefore one of the main socio-economic factors behind the abandonment of agricultural land.

Socio-economic drivers of the decline in the area of SNG in boreal Europe (including the boreonemoral ecotone) are summarized by Herzon et al. (2022) in a conceptual model of a socio-ecological extinction vortex. The authors identify four highly interlinked and mutually reinforcing socio-economic processes: (1) receding importance for agricultural production, (2) diminishing attention in policy, research, and development; (3) disappearance of the topic in vocational education in the fields of agricultural sciences; and (4) decaying experience of the public.

We were particularly interested in the manifestation of the second process on the pattern of abandonment of SNG. In post-socialist countries, diminished attention to SNG in policy, research, and development that detached SNG from other agricultural land uses was strong until accession to the European Union (Sutcliffe et al., 2015; Herzon et al., 2021). After accession to the EU, agri-environment schemes became available and started to function as the main tool to conserve SNG biodiversity (King, 2010). Thus, attention to SNG in policy has been increasing in the past decades. There is evidence for both positive and negative changes in permanent grassland conservation due to CAP regulations. For example, in Germany, a special legal grassland status reduced grassland conversions to other land-use types and lowered the share of permanent grassland converted to cropland (Haensel et al., 2023). On the other hand, Bulgaria experienced a dramatic loss of permanent grasslands between 2006 and 2010 caused by the intensification of agriculture fostered by CAP (Dobrev et al., 2014). In Slovenia, only

3% of high nature value grasslands were reached by the agri-environmental support, which did not reverse the abandonment (Kaligarič et al., 2019). The contrasting outcomes of CAP illustrate the complexity of policy effects which can be evident even within a single policy measure. For instance, attempts to encourage more active farming through restrictions on the eligibility of certain maintenance practices (e.g. grazing instead of cutting) may result in abandonment of permanent grasslands due to higher expenses for some farmers (Viira et al., 2020). Again, most studies on SNG in relation to CAP have focused on managed grasslands or the loss of SNG due to intensification, but the emphasis on abandonment is almost lacking.

Our study addressed this knowledge gap by focusing on the relationships between SNG abandonment and agricultural land management under CAP in Latvia. We aimed to investigate how alterations in CAP regulations for grassland management between two periods (2007–2013 and 2014–2020) influenced the landscape-scale pattern of SNG abandonment. We hypothesized that the increased focus on grassland conservation in the CAP from 2007–2013 to 2014–2020 would result in a reduction of SNG abandonment, reflected in the altered response of abandonment rates to the landscape-scale pattern of agricultural land management.

Latvia is a suitable example to demonstrate relationships between agricultural land management and abandonment of SNG in boreonemoral Europe since it lies in the central part of the boreonemoral ecotone in Europe (Breckle, 2002) and the share of the area of SNG and other grassland types is comparable with neighbouring countries (Herzon et al. 2021). Joining the EU in 2004 accelerated the intensification of agriculture (Jepsen et al., 2015). During 2010–2016, the number of small (< 30 ha) farms declined by 15.5%, while the number of large (> 200 ha) farms increased by +12.7%. Similarly, the area of meadows and pastures declined from 651,100 ha in 2010 to 631,900 ha in 2020, while the proportion of arable land increased (Agriculture in Latvia, 2017; Agriculture in Latvia, 2020, Auzins et al., 2023). The amount of fertilizer and plant protection products per hectare increased by 10 to 40%, and in some regions, it increased by over 40% between 2012/13 and 2015/16 (European Commission, 2019).

MATERIALS AND METHODS

Study area

Latvia is a lowland country located on the eastern coast of the Baltic Sea in the boreonemoral ecotone of the Northern needle-leaved and Central European broad-leaved forest biome. The mean annual temperature is 6.2 °C, and the precipitation is 650 mm. The vegetation period lasts for 180–200 days. Forests cover ca. 50%, mires cover ca. 6% and agricultural land covers ca. 38%, while semi-natural grasslands occupy less than 1% of the country (Nikodemus et al., 2018). According to the national-level agricultural land classification (Boruks, 2004), the country is divided into five regions according to land capability for agriculture (LCA) (Fig. 1). These regions highly correspond to the intensity of agriculture characterized by the number of households and area of intensive (cereal fields) and extensive (grasslands) agricultural land (Table 1) at the beginning of our study period. Thus, we selected two areas to compare - the region LCA-High included Region 1 (high land capability for agriculture) and Region 2 (land capability for agriculture above intermediate), while the region LCA-Low corresponded to the borders of the

Region 4 (low land capability for agriculture). Regions 1 and 2 are considered to have lower risk of abandonment of utilized agricultural land (UAA) than Region 4 (Perpiña Castillo et al., 2021).

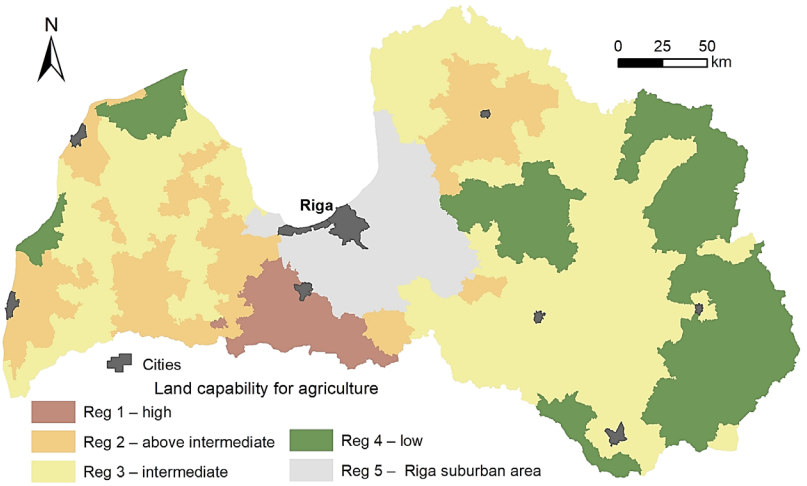

Figure 1. Regions by LCA (Boruks, 2004).

Table 1. Characteristics of five LCA regions as of 2014 (Integrated Administration and Control System data for 2014 from the Rural Support Service)

Region	Number of house-holds per 1,000 ha SAP*	SAP*, ha per 1,000 ha land	Cereal fields, ha per 1,000 ha SAP	Permanent grassl., ha per 1,000 ha SAP	Land capability for agriculture
Reg 1	20	625	637	20	High: fertile loam and clay soils; plain terrain
Reg 2	30	316	457	150	Above intermediate: sandy loam and loam soils; plain and undulating terrain
Reg 3	45	242	323	300	Intermediate: sandy loam and loam soils; undulating and hilly terrain
Reg 4	68	207	205	549	Low: sandy to clay soils; hilly terrain
Reg 5	42	166	302	258	Riga suburban area (intermediate-low): sandy and sandy loam soils; plain to undulating terrain; agricultural constraints mainly socioeconomic, related to active urbanization processes

* SAP – Single Area Payment.

Our data covered the implementation periods of the Rural Development Programme 2007–2013 and 2014–2020. During the first period, SNG conservation management was addressed by the action-oriented agri-environment scheme 'Maintenance of Biodiversity in Grasslands,' aimed at fostering biodiversity-friendly management of SNG across the country. The amount of financial support was 123 EUR

per hectare. Eligible areas included all SNG. The management requirements were common for all eligible habitat types and included mowing with or without hay removal once per season from 1 August until 15 September or grazing (0.4–0.9 animal units), and any improvement of grassland was forbidden. Permanent grasslands that were not eligible for the agri-environment scheme could receive a single area payment (direct area-based payments) with the condition that grasslands were cut at least once per season with or without hay removal. No other restrictions were in place.

The same AES continued for SNG in CAP 2014–2020 but with some changes. Concerning management prescriptions, two important changes were introduced. Firstly, the late mowing date (1 August) was cancelled due to farmers' complaints that it significantly reduced the chances of harvesting hay due to bad weather. Secondly, mulching or mowing without hay removal was forbidden, and grass cuttings were required to be removed from the field by 15 September. It should be noted that the same requirement was also imposed on permanent grasslands for single area payments. In addition, the payment calculation for AES changed. Starting in 2015, differentiation of the payment into three classes based on grassland productivity was introduced (83–155 EUR for productive grasslands and 206 EUR for unproductive grasslands). Finally, 'greening' measures were introduced.

To summarize, the important CAP modifications in relation to potential changes in trajectories of SNG abandonment between the two periods in Latvia were (1) introduction of a ban to convert environmentally sensitive permanent grasslands into arable land (in Latvia they included all SNG types across the country); (2) maintenance of the ratio of permanent grassland to agricultural land with a 5% margin of flexibility at national level without precise spatial mapping; (3) substantial increase in the financial support for unproductive SNG and partial decrease for productive grasslands; (4) more flexibility in choosing the mowing date but the option for grass mulching was cancelled.

Data on SNG distribution and productivity

We divided the country into 2,778 grid cells of 25 km^2 and used these cells as the basic landscape-scale unit of research. We analyzed seven SNG habitat types occurring in Latvia. They were split into two groups of productivity according to the habitat-specific national data on productivity (Rūsiņa, 2017). Productive SNG (dry hay more than 1 t ha^{-1} yr^{-1}) included Habitats Directive habitat types (European Commission, 2013; Auniņš, 2013) 6270* (asterix denotes priority habitats), 6450, and 6510, while unproductive SNG (dry hay less than 1 t ha^{-1} yr^{-1}) included 6120*, 6210*, 6230* (see Rūsiņa et al., 2023 for details). We collected data on SNG area and distribution from georeferenced EU grassland habitat maps maintained by the Nature Conservation Agency at the national level. For our first study period, we utilized all polygons mapped between 2001 and 2012, while for the second study period, we used data from 2013 to 2021. It's important to note that we included all polygons in our analysis, regardless of their management status (whether they were managed or abandoned) at the time of mapping.

Data on agricultural land management

Data on agricultural land management were obtained from different sources (Table 2). There are different approaches to define abandonment ranging from detailed use of vegetation parameters, like functional traits (Targetti et al., 2018) to simple… To analyze the state of grassland management, we defined the following management

status: (1) abandoned - SNG polygons not included in the agricultural parcel register of the Rural Support Centre and did not receive any payments from CAP instruments; (2) grasslands managed in AES – permanent grassland (PG) polygons (incl. SNG) that received subsidies under the action-oriented agri-environment scheme 'Maintenance of Biodiversity in Grasslands'. All polygons registered in the agricultural parcel register of the Rural Support Centre as arable land were omitted from the analysis.

Table 2. Description of data categories collected per grid cell, their type, and data sources

Data category	Data type	Data source
Area of abandoned semi-natural grasslands (SNG) (response variable)	Continuous; area (ha) per grid cell	SNG parcels not registered in Integrated Administration and Control System of Rural Support Service.
Area of SNG, total	Continuous; total area (ha) of SNG per grid cell	Nature Conservation Agency. Each polygon mapped only once and no update of the fate of the polygon during the two study periods.
Area of permanent grasslands (PG) managed under AES	Continuous; area (ha) per grid cell.	Integrated Administration and Control System of Rural Support Service.
Area of managed PG	Continuous; area (ha) per grid cell	Integrated Administration and Control System of Rural Support Service.
Agricultural land under organic farming	Continuous; area (ha) per grid cell	Integrated Administration and Control System of Rural Support Service.
Arable land area	Continuous; area (ha) per grid cell	Integrated Administration and Control System of Rural Support Service.
Land capability for agriculture (Land quality)	Categorical, 3-point scale (low, medium and high quality). Weighted average per grid cell calculated from all parcels of agricultural land per grid cell	Digitized land quality maps 1: 10,000 from 1960s to 1980s; https://geolatvija.lv/geo/p/317.

To examine the relationships between SNG abandonment and a landscape-scale agricultural land management patterns, we selected a set of explanatory variables that align with our study's objectives, as informed by previous research (Table 2). Previous studies have shown that land capability for agriculture and the total area of arable land tend to have a positive correlation with agricultural land management intensity (Latruffe & Piet, 2014; Vinogradovs, 2018) and grassland loss (Hatna & Bakker, 2011; Biro et al., 2013), while exhibiting a negative association with the preservation of high nature value agricultural lands (Stoate et al., 2009; Reif & Hanzelka, 2016). Additionally, research indicates that the proportion of permanent grasslands under agricultural management and the extent of agricultural land under organic farming have the potential to positively impact agricultural biodiversity (Hole et al., 2005).

Statistical analysis

Our analysis was conducted at the landscape scale, utilizing a study unit consisting of 5 km × 5 km (2,500 ha) grid cells, with a total of 2,778 cells (Krampis, 2012). To ensure the robustness of our findings, all variables underwent testing for spatial autocorrelation using Moran's I statistic (Anselin, 2002). The response variable, which represents the area of abandoned SNG, followed a Tweedie distribution due to its positive continuous nature and a high proportion of zero values. To prepare for modeling, we conducted a test for multicollinearity among the explanatory variables using a Spearman's correlation matrix. Multicollinearity occurs when explanatory variables are highly correlated, violating the assumption of independence. In such cases, it's advisable to retain only one variable from a group of highly correlated ones (Millington et al., 2007). We applied a correlation limit of $R > |0.8|$, but no explanatory variables displayed high correlations with each other, so all were retained in the models.

Upon visually inspecting the relationships between the response variable and each explanatory variable using scatter plots with a LOESS curve, we observed non-linear relationships. Consequently, we opted for generalized additive modeling (GAM) as our modeling approach (Wood, 2017). GAM is an extension of generalized linear models that offers greater flexibility by accommodating non-linear relationships between predictors and the response variable. Rather than assuming a linear relationship, GAM allows for the fitting of smooth, non-linear functions to individual predictors. This approach enables the visualization and understanding of each predictor's effect, and the amount of smoothing for each predictor is typically determined automatically by the model, helping to prevent overfitting.

Eight models were created for this study. Four of these models aimed to uncover relationships between the abandonment of productive SNG and the type of agricultural land management, focusing on two CAP periods (2014 and 2021) and two regions characterized by differing land capability for agriculture (LCA-High and LCA-Low). The remaining four models were developed for the same CAP periods and regions but focused on unproductive SNG. To capture non-linear relationships and make them more interpretable, smooth splines were employed with a constraint of 3 degrees of freedom. Model fit was assessed using the 'gam.check' function, and degrees of freedom were adjusted for variables exhibiting non-randomly distributed residuals, followed by model re-fitting. The stepwise regression technique, guided by Akaike's information criterion (AIC), was used to select the best-fitting model. In order to investigate whether the models adhered to their assumptions, residual analysis was conducted, and diagnostic plots were examined. All calculations and analyses were performed using the R 4.3.1 software package 'mgcv' (Wood, 2017).

RESULTS

Descriptive statistics

In 2014, abandoned SNG covered 20,336 ha, accounting for 39.7% of the total SNG area, and in 2021, they amounted to 17,761 ha, representing 27.9% of the total SNG area. The distribution of abandoned SNG was uneven (see Fig. 2).

The structure of agricultural land management in the two examined regions, LCA-High and LCA-Low, exhibited significant variation, particularly in the ratio of

arable land to permanent grasslands (see Fig. 3). Over the two CAP periods, both regions underwent changes in their agricultural land composition. In the LCA-High region, arable land increased by 9%, while in the LCA-Low region, it saw a more significant increase of 18%. In contrast, permanent grasslands expanded by 6% in the LCA-High region but decreased by 2% in the LCA-Low region. These alterations in land use predominantly occurred within sown grasslands (temporary grasslands), which experienced reductions in both regions.

In 2014, the LCA-High region had 2,114 ha of abandoned productive SNG and 1,870 ha of abandoned unproductive SNG. In 2021, the abandoned area was 865 ha and 1,051 ha, respectively. In the LCA-Low region, there were 3,164 ha of abandoned productive SNG and 2,965 ha of abandoned unproductive SNG in 2014. However, by 2021, these numbers changed to 396 ha and 1,203 ha, respectively.

The Moran's I test for spatial autocorrelation revealed significant positive spatial autocorrelation for all variables, except for the abandoned area of unproductive SNG in the LCA-Low region in 2014. This suggests that neighboring cells tend to exhibit similar land management patterns. Consequently, we incorporated spatial autocovariates into all of our Generalized Additive Models (GAMs). The relationships between our response variable, which is the abandoned area of SNG, and the explanatory variables varied across the two observation years, between the regions LCA-High and LCA-Low, and between the two SNG types (productive and unproductive), respectively.

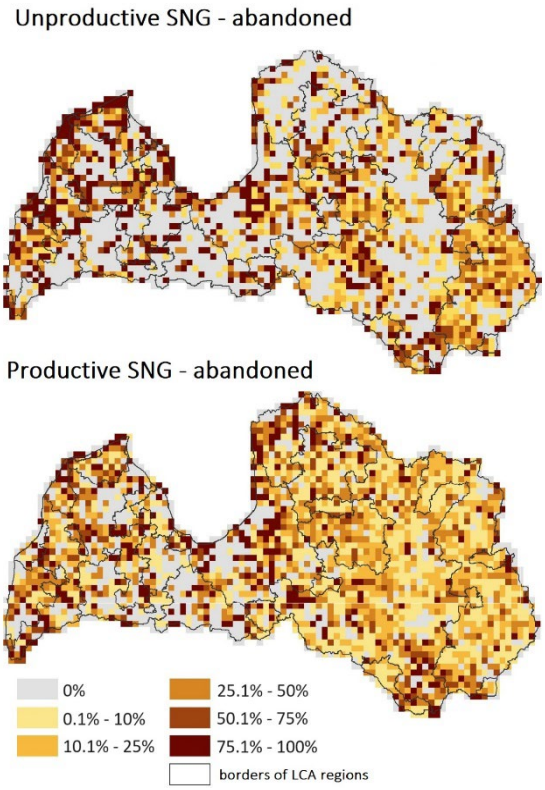

Figure 2. Share of abandoned SNG in Latvia in 2021 as a percentage of the total area of SNG per grid cell.

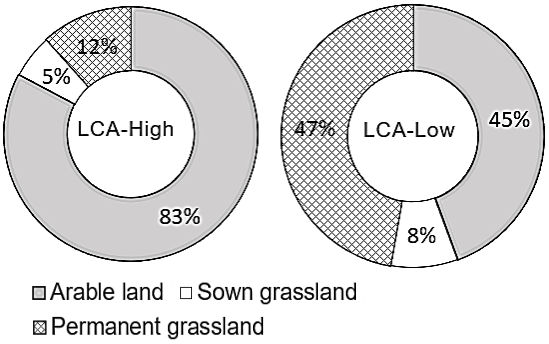

Figure 3. The share of agricultural land management types in 2021 in two studied regions.

Agricultural land management related to abandonment of productive SNG

The Generalized Additive Models (GAMs) applied to both LCA regions and both study periods revealed significant non-linear relationships between the abandonment of productive SNG, the total area of SNG, and the area of permanent grasslands (PG) supported by the agri-environmental scheme for grassland biodiversity (AES) (Fig. 4., Table 3).

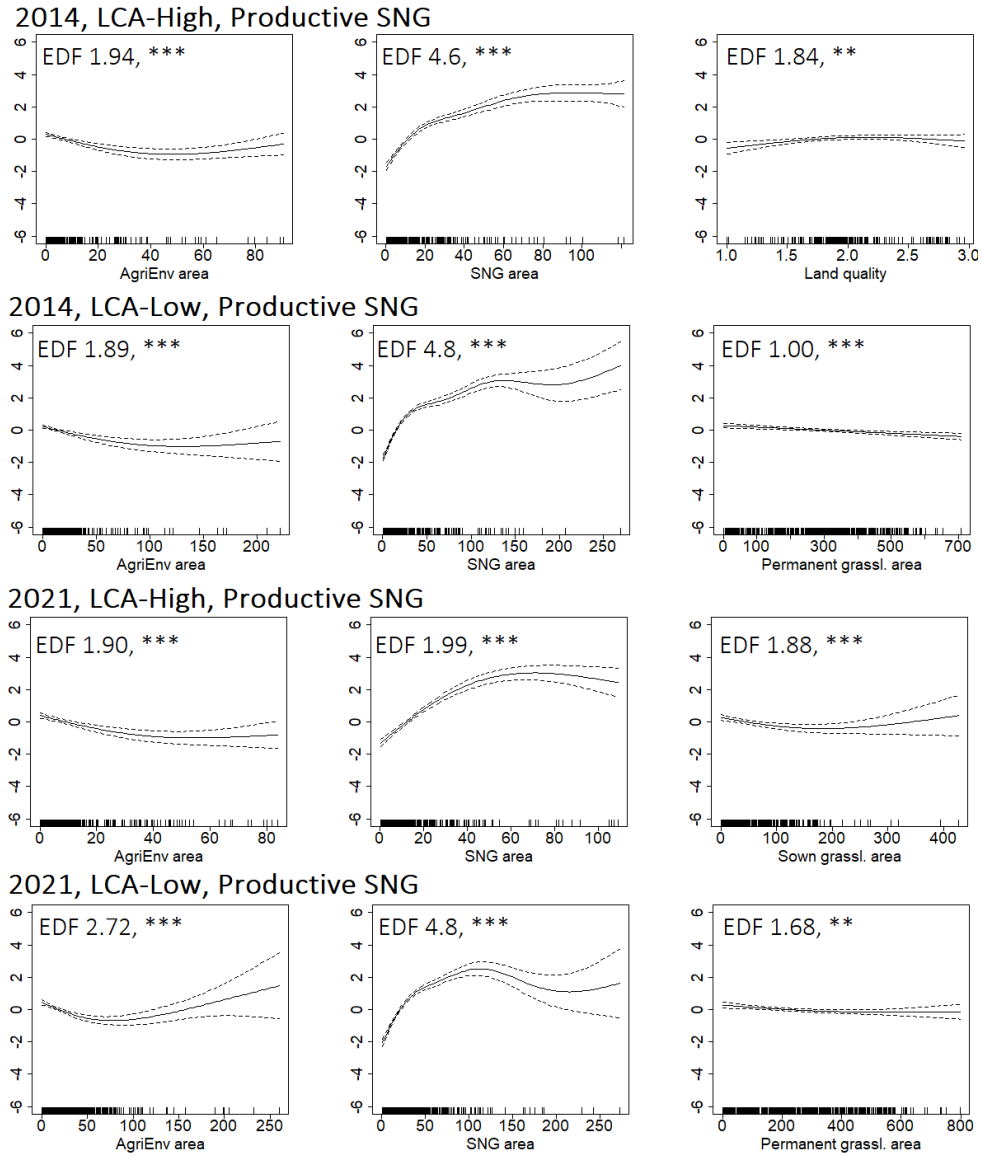

Figure 4. Predictors on *x*–axis against estimated values of response variable (splines) on y–axis for productive SNG. Higher values on the y–axis indicate larger abandoned area. Estimates are represented by a solid line. Dashed lines are 95% confidence limits. Only significant relationships are shown for each model. Significance levels for approximate significance of smooth terms: *** – $p < 0.001$, ** – $p < 0.01$, * – $p < 0.05$, (*) – $p < 0.1$.

Grid cells with a smaller total area of PG managed by AES per grid cell tended to experience higher abandonment rates. However, when grid cells had exceptionally large areas of PG managed by AES (100 ha or more), abandonment rates increased. The significance of land quality, represented by LCA, was associated with abandonment only in the LCA-High region in 2014. It was not significant in the LCA-Low region. In the LCA-High region, a larger area of sown grassland (temporary grasslands) was associated with higher SNG abandonment rates in 2021. In the LCA-Low region, the area of managed permanent grasslands was significantly associated with lower abandonment rates in both study periods.

Table 3. GAM model results for productive SGN

	2014, LCA-High				2021, LCA-High			
	Esti-mate	Std. Error	*t value*	*p*	Esti-mate	Std. Error	*t value*	*p*
(Intercept)	1.28	0.05	26.92	***	0.66	0.06	11.55	***
	edf	*Ref.df*	*F*	*p*	*edf*	*Ref.df*	*F*	*p*
s(PG managed by AES)	1.95	2.00	18.82	***	1.90	1.99	16.22	***
s(Permanent grassl. area)	1.89	1.98	4.19	*	*ns*			
s(Sown grassl. area)	*ns*				1.88	1.99	8.30	***
s(SNG area)	4.60	4.92	97.53	***	1.99	2.00	127.65	***
s(Land quality)	1.85	1.97	5.60	**	*ns*			
s(autocovariate)	*ns*				1.00	1.00	12.41	***
R-sq.(adj)	0.67				0.50			
Deviance explained	67.40%				48.80%			
REML	592.47				604.63			
Scale estimate	0.83				1.32			
Number of observations	257				355			
	2014, LCA-Low				2021, LCA-Low			
	Esti-mate	Std. Error	*t value*	*p*	Esti-mate	Std. Error	*t value*	*p*
(Intercept)	1.26	0.03	36.03	***	1.07	0.04	28.85	***
	edf	*Ref.df*	*F*	*p*	*edf*	*Ref.df*	*F*	*p*
s(PG managed by AES)	1.89	1.99	16.43	***	2.73	2.94	15.80	***
s(Permanent grassl. area)	1.00	1.00	18.12	***	1.68	1.89	6.56	**
s(SNG area)	4.89	4.99	145.2	***	4.83	4.98	91.86	***
R-sq.(adj)	0.73				0.55			
Deviance explained	71.40%				53.40%			
REML	960.15				1209.8			
Scale estimate	0.76				1.01			
Number of observations	434				569			

*** – $p < 0.001$, ** – $p < 0.01$, * – $p < 0.05$, (*) – $p < 0.1$, *ns* – not significant.

These findings underscore the complex interplay of factors influencing the abandonment of productive SNG, with variations between regions and study periods. The total area of PG managed by AES, land capability for agriculture, the area of sown grasslands, and the presence of managed permanent grasslands all contribute to shaping abandonment patterns.

Agricultural land management related to abandonment of unproductive SNG

Abandonment of unproductive SNG was significantly related to the total area of SNG and area of PG managed by AES (Fig. 5., Table 4). Area of sown grasslands was a significant factor in GAM for the region LCA-High in 2014, while in 2021 it was replaced by the area of organic farming. In addition, abandonment of unproductive SNG in region LCA-Low was significantly associated with the arable land area in 2014 and with managed permanent grassland area in 2021.

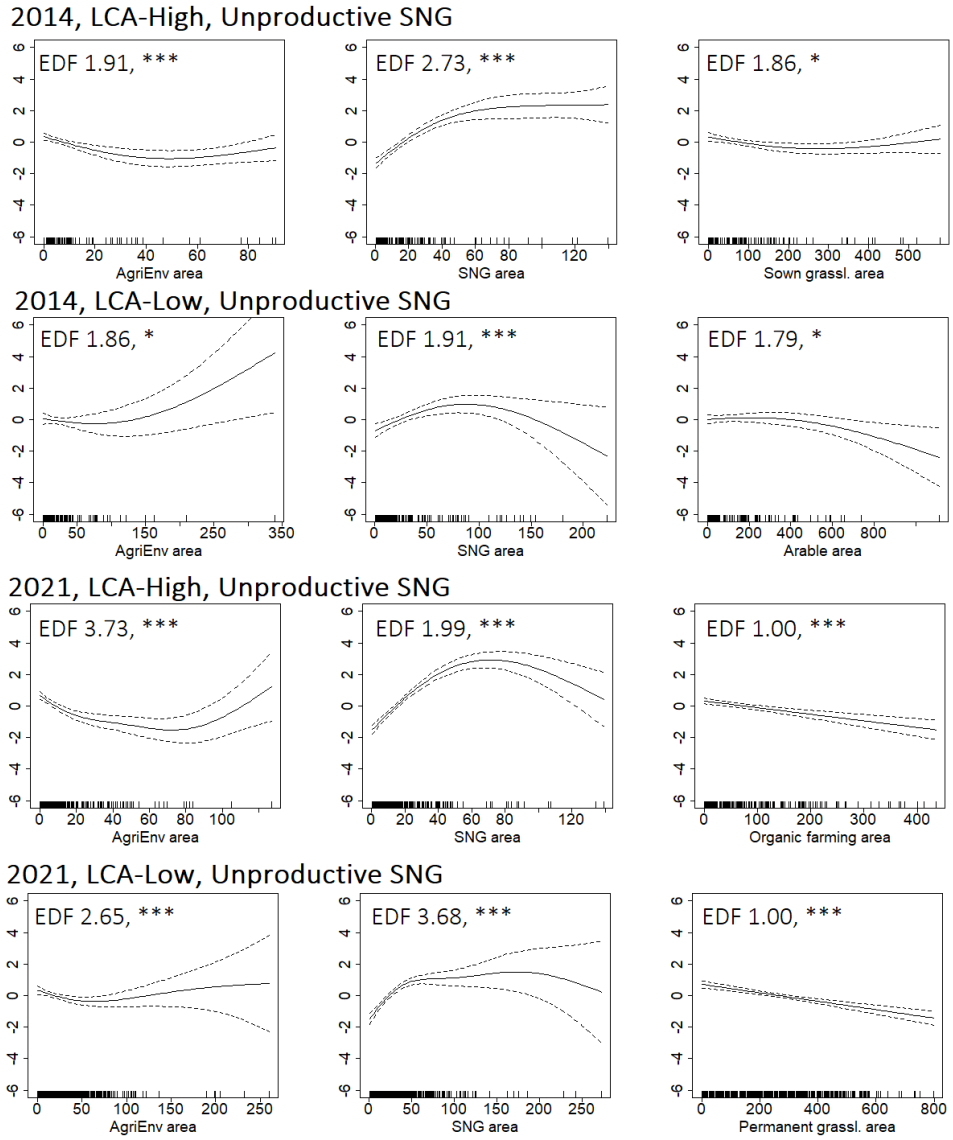

Figure 5. Predictors on x–axis against estimated values of response variable (splines) on y–axis for unproductive SNG. Higher values on the y–axis indicate larger abandoned area. Estimates are represented by a solid line. Dashed lines are 95% confidence limits. Only significant relationships are shown for each model. Significance levels for approximate significance of smooth terms: *** – $p < 0.001$, ** – $p < 0.01$, * – $p < 0.05$, (*) – $p < 0.1$.

Table 4. GAM model results for unproductive SGN

	2014, LCA-High				2021, LCA-High			
	Esti-mate	Std. Error	*t value*	*p*	Esti-mate	Std. Error	*t value*	*p*
(Intercept)	1.13	0.08	14.35	***	0.71	0.07	9.81	***
	edf	*Ref.df*	*F*	*p*	*edf*	*Ref.df*	*F*	*p*
s(PG managed by AES)	1.91	1.99	9.51	***	3.73	4.35	11.30	***
s(Sown grassl. area)	1.86	1.98	5.14	*	*ns*			
s(Organic farming area)	*ns*				1.00	1.00	26.32	***
s(SNG area)	2.73	2.94	33.82	***	1.99	2.00	85.81	***
s(autocovariate)	1.46	1.71	4.23	*	1.51	1.76	8.21	**
R-sq.(adj)	0.58				0.68			
REML	242.35				433.99			
Deviance explained	71.30%				48.50%			
Scale estimate	0.73				1.43			
Number of observations	110				242			
	2014, LCA-Low				2021, LCA-Low			
	Esti-mate	Std. Error	*t value*	*p*	Esti-mate	Std. Error	*t value*	*p*
(Intercept)	0.91	0.10	9.11	***	0.58	0.05	10.65	***
	edf	*Ref.df*	*F*	*p*	*edf*	*Ref.df*	*F*	*p*
s(Arable area)	1.79	1.96	2.87	*	*ns*			
s(PG managed by AES)	1.86	1.97	2.82	*	2.65	3.18	3.15	*
s(PG area)	*ns*				1.00	1.00	46.68	***
s(SNG area)	1.91	1.99	7.92	***	3.68	3.92	24.42	***
s(autocovariate)	*ns*				1.28	1.48	25.18	***
R-sq.(adj)	0.19				0.23			
REML	262.35				717.86			
Deviance explained	18.20%				26.90%			
Scale estimate	1.35				1.49			
Number of observations	134				448			

*** – $p < 0.001$, ** – $p < 0.01$, * – $p < 0.05$, (*) – $p < 0.1$, *ns* – not significant.

DISCUSSION

Our findings partly support our hypothesis that the increased focus on grassland conservation in the CAP from 2007–2013 to 2014–2020 would result in a reduction of SNG abandonment. Overall rate of abandonment decreased during the second CAP period. However, SNG abandonment varied between two CAP periods, showing both positive and negative changes depending on SNG productivity and LCA region.

Relationships between SNG abandonment and agricultural land management

In boreonemoral Europe, semi-natural grassland abandonment ranks as the second most influential factor contributing to the loss of these ecosystems (Penēze et al. 2009; Aune et al., 2018; Rūsiņa et al., 2021). Our study reveals the presence of non-linear relationships between abandonment rates and agricultural land management pattern. Among the seven variables investigated, only two consistently demonstrated significance across all models. Regardless of SNG productivity, CAP period, or LCA region, the lowest proportion of abandoned SNG was most strongly and consistently

associated with the higher total area of SNG and the higher area of permanent grassland supported by agri-environment schemes (AES). This finding underscores the influence of historical land use and grassland distribution legacies, aligning with similar observations in other European Union countries. There is a positive link between the success of long-term maintenance of SNG and their total area at the landscape and property levels both in Western European (Guerci et al., 2013; Walden & Lindborg, 2018) and in post-socialist countries. For instance, in Hungary, factors such as grassland patch area and proximity to other grasslands emerged as significant contributors to grassland loss due to abandonment (Biró et al., 2013). Overall, in mosaic-type landscapes agricultural land abandonment is less probable in areas with larger total area of agricultural land (Levers et al., 2016).

In landscapes where the overall area of PG managed under AES was relatively small (less than 100 ha), an increase in latter was effective in slowing down the rate of SNG abandonment. This suggests that CAP subsidies play a crucial role in mitigating the abandonment of SNG in landscapes characterized by small and fragmented grassland areas. However, when the total area of PG supported by AES surpassed this threshold, the rate of SNG abandonment began to increase once more. This phenomenon may be attributed to the fact that eligible areas for AES included not only SNG but also permanent grasslands important for bird species. Research indicates that grassland birds do not necessarily favor botanically rich semi-natural grasslands (Żmihorski et al., 2016). Notably, there was a significantly higher rate of abandonment in the unproductive SNG group when compared to productive SNG in response to an increase in the total area of PG managed under AES. This discrepancy may be attributed to the same underlying factor, albeit with a more pronounced effect. In general, unproductive SNG types hold less importance for grassland birds, often comprising small, fragmented areas that do not provide sufficient open space to meet the needs of these avian species. For instance, many wader species are closely associated with floodplains (Auniņš et al., 2001; Żmihorski et al., 2018; Opermanis et al., 2008), primarily falling within the category of productive SNG (unless subjected to agricultural improvements) under the EU habitat type 6450 *Northern boreal alluvial meadows*. Another crucial grassland bird species, the corncrake *Crex crex*, predominantly relies on post-agricultural permanent grasslands and fallow-lands that do not align with any specific SNG types or EU-designated habitat types (Bellebaum & Koffijberg, 2018; Keišs, 2005; Koffijberg et al., 2016).

These observations suggest that the driving factors behind abandonment differ between these two grassland groups. This divergence is further evidenced by the second most important variable in GAMs - the total area of SNG in the landscape. Notably, the trajectories and steepness of response curves exhibited significant variation between the two SNG productivity groups. The GAMs response curve for productive SNG consistently indicated an increase in SNG abandonment with the enlargement of the total SNG area in the landscape, up to a certain threshold (approximately 50 ha per grid cell), beyond which it plateaued, suggesting a slight positive impact of the total SNG area on their management. Conversely, the GAMs for unproductive SNG displayed a much stronger positive effect of larger SNG areas on the management outcomes of unproductive SNG, resulting in a reversal of the abandonment trajectory.

These findings imply that productive and unproductive SNG tend to be spatially distinct in a landscape, each exhibiting distinct management prospects. Our results align with studies in Central and Western Europe, suggesting considerable differences in threats and pressures among SNG habitat types. For instance, more productive mesic and some wet grassland types in Central Europe are more threatened by intensification (e.g., fertilization and sward improvement through reseeding or plowing), while the majority of unproductive wet and dry grasslands are susceptible to abandonment (Ridding et al., 2015; Janssen et al., 2016; Dengler & Tischew, 2018). Our results confirm this for the boreonemoral region.

In addressing SNG that are threatened by opposing processes (abandonment or conversion to cropland), a one-size-fits-all approach in AES design may not be effective. Instead, result-oriented AES schemes targeting specific problems should be favored over simplistic action-oriented AES (Sabatier et al., 2012). However, AES programs alone may not suffice to reverse the abandonment of SNG. A more integrated approach to nature conservation within the CAP and holistic development strategies are essential to prevent further abandonment (Šumrada et al., 2021).

The differences between two CAP periods

The differences in the response of SNG abandonment to landscape-scale agricultural land management pattern between the two CAP periods indicate both positive and negative changes, depending on the SNG productivity group and LCA region.

The response of productive SNG abandonment remained relatively stable between two CAP periods in both LCA regions. The main distinction was in the response curve to the SNG area in the second period. There, abandonment slowed down with an increased total SNG area, particularly in the LCA-Low region. A similar positive trend was observed for unproductive SNG. This suggests that the CAP 2014–2020 period was favorable for resuming the management of previously abandoned SNG, at least in certain areas. Most probably, unproductive SNG benefited from a substantial increase in the amount of aid from EUR 123 to EUR 206 in the second period, and farmers were more interested in resuming management of these economically non-viable grasslands. In addition, small-scale farmers have limited access to land for agricultural production, and SNG represent their only available option for expanding their production. In Latvia, livestock farming has predominantly been concentrated in regions with low and intermediate LCA, whereas crop farming prevails in regions with high LCA (Nikodemus et al., 2018). The number of cattle and sheep has been consistently increasing in Latvia in the last 20 years (Nipers et al., 2017). These findings align with some other studies examining grassland dynamics during the CAP 2014–2020 period. CAP changes introduced in 2014 led to reduced grassland conversion in Germany (Haensel et al., 2023) and Poland (Wrzaszcz, 2017). Gocht et al. (2017) also projected an increase in the cover of permanent grassland at the European level due to CAP 'greening' measures. On the other hand, SNG could not benefit from dairy farming because it favours intensive land management, minimizing grassland and maximizing the production of crop and maize for fooder (Stypinski, 2011). However, we couldn't find any studies specifically addressing the impact of CAP 2014–2020 on SNG abandonment rates.

The potential negative impact of CAP 2014–2020 on management of productive SNG (increased abandonment) in the LCA-High region could be linked to an increase in the area of sown (temporary) grasslands. Total area of the latter was a significant variable

in the GAM for the LCA-High region for productive SNG in 2021 but not in 2014. This suggests that grassland management became more intensive in the LCA-High region during CAP 2014–2020, and it was significantly related to a higher abandonment rate of productive SNG in landscapes with large areas of sown grasslands. On contrary, the area of organic farming was significantly related to a lower abandonment rate of unproductive SNG in the LCA-High region. It is documented that the area of organic farming increased substantially from 2013 to 2020 (Ušča et al., 2023).

Overall, the pattern of unproductive SNG abandonment exhibited less stability across CAP periods. In addition, GAMs for unproductive SNG in the LCA-Low region for both years explained only half as much variation as the other models. This implies that the driving factors behind unproductive SNG management and abandonment are more complex and likely related to socioeconomic factors not considered in this study. One possible explanation is the extreme marginality of these habitats for agriculture for nearly a century. They are most susceptible to abandonment when the profitability of these systems decreases. For instance, low profitability was a key factor driving the recurrent abandonment of recently restored SNG in Sweden. During the 20th century, forest cover in Latvia increased from 23% to more than 50%, primarily at the expense of SNG (Penēze et al., 2009; Rusina & Kiehl, 2010; Rūsiņa et al., 2021). Consequently, the abundance of these habitats was very low in all regions, averaging less than 3 hectares per 25 km² grid cell. This aligns with the socioecological habitat extinction vortex concept proposed by Herzon et al. (2022), where a considerable decline in the area under appropriate management eventually leads to diminishing importance for production and reduced attention from policy, research, and development efforts.

CONCLUSIONS

The study reveals significant differences between the abandonment rates of productive and unproductive semi-natural grasslands and intensity of agriculture suggesting that both grassland groups are spatially distinct and face different management challenges and threats.

The response of SNG abandonment to agricultural land management under two CAP periods varied depending on the productivity of the SNG and the land capability for agriculture. These variations suggest that the changes in CAP in relation to grassland conservation have had mixed impacts on SNG abandonment, reducing conversion in some cases but potentially increasing abandonment rates in others.

We conclude that context-specific, regionalized CAP instruments are needed to mitigate grassland abandonment outcomes. As with many similar studies, our study does not imply cause-and-effect relationships between abandonment of SNG and agricultural land management patterns; instead, it suggests that landscape-scale patterns of agricultural land management and land capability for agriculture are still important in shaping grassland biodiversity. It is now vital to investigate the direct effects of implementing CAP instruments on biodiversity at the landscape scale so that the cost-effectiveness of schemes can be evaluated.

Considering our findings, we suggest that result-based agri-environment schemes should be prioritized in landscapes with a high share of extensive agricultural land management. There is an urgent need for detailed research on socioecological drivers of the maintenance and conservation management of SNG, as our study showed their

extreme vulnerability to extinction because of their rarity and the lack of positive agricultural land use driving forces in helping to maintain them under appropriate management.

ACKNOWLEDGEMENTS. Authors are grateful to Gundega Vācere for her help with data collection, handling and spatial visualisation. The study was supported by the LIFE Integrated project 'Optimising the Governance and Management of the Natura 2000 Protected Areas Network in Latvia', LIFE19 IPE/LV/000010.

REFERENCES

Agriculture in Latvia, 2017. *Collection of Statistics*. In: Central Statistical Bureau of Latvia. https://www.csb.gov.lv/sites/default/files/publication/2017-05/Nr%2026%20Latvijas%20lauksaimnieciba%202016%20%2816_00%29%20LV%20EN.pdf (accessed 15 December 2021).

Agriculture in Latvia, 2020. *Collection of Statistics*. In: *Central Statistical Bureau of Latvia*. https://www.csb.gov.lv/sites/default/files/publication/2020-06/Nr_16_Latvijas_Lauksaimnieciba_2020_%2820_00%29_LV_EN.pdf (accessed 15 December 2021).

Anselin, L. 2002. Under the hood: Issues in the specification and interpretation of spatial regression models. *Agricultural Economics* **27**(3), 247–267. https://doi.org/https://doi.org/10.1016/S0169-5150(02)00077-4

Argenti, G., Del Serra, F., Stagliano, N. & Battaglini, I. 2020. Assessment of management effect on grasslands characteristics in an area of the Apennines (North Italy). *Agronomy Research* **18**(4), 2291–2302. https://doi.org/10.15159/ar.20.173

Aune, S., Bryn, A. & Hovstad, K.A. 2018. Loss of semi-natural grassland in a boreal landscape: impacts of agricultural intensification and abandonment. *Journal of Land Use Science* **13**(4), 375–390. https://doi.org/10.1080/1747423X.2018.1539779

Auninš, A., Petersen, B.S., Priednieks, J. & Prins, E. 2001. Relationships between birds and habitats in Latvian farmland. *Acta Ornithologica* **36**(1), 55–64. https://doi.org/10.3161/068.036.0114

Auniņš, A. 2013. *European Union protected habitats in Latvia*. Interpretation manual. Riga: Latvian Fund for Nature, Ministry of Environmental Protection and Regional Development. https://www.daba.gov.lv/upload/File/Publikacijas/ROKASGR_biotopi_EN.pdf (accessed 15 December 2023).

Auzins, A., Leimane, I., Krievina, A., Morozova, I., Miglavs, A. & Lakovskis, P. 2023. Evaluation of Environmental and Economic Performance of Crop Production in Relation to Crop Rotation, Catch Crops, and Tillage. *Agriculture* **13**(8), 1539. https://doi.org/10.3390/agriculture13081539

AREI 2016. Report. Lauku attīstības programma 2007–2013, Ex-post novērtējums [Ex-post evaluation ot the Rural Development Programme 2007–2013 of Latvia]. Agroresursu un ekonomikas institūts, Rīga. https://www.arei.lv/sites/arei/files/files/lapas/LAP%202007-2013%20ex-post%20nov%C4%93rt%C4%93jums.pdf (accessed 15 December 2023).

AREI 2019. Report. Līguma Nr. 2015/86 'Lauku attīstības programmas (LAP) 2014–2020 Nepārtrauktās novērtēšanas sistēmas uzturēšana' ietvaros. LAP 2014 – 2020 novērtēšana paplašinātajam Ikgadējam īstenošanas ziņojumam 2019. [Contract No 2015/86 'Maintenance of the Continuous Evaluation System of the Rural Development Programme (RDP) 2014–2020'. Evaluation of the RDP 2014–2020 for the extended Annual Implementation Report 2019] Agroresursu un ekonomikas institūts, Rīga. https://www.arei.lv/sites/arei/files/files/lapas/AIR2019_LAPnovert%20_zinojums_2019.%20%281%29.pdf (accessed 15 December 2023).

Bellebaum, J. & Koffijberg, K. 2018. Present agri-environment measures in Europe are not sufficient for the conservation of a highly sensitive bird species, the Corncrake Crex crex. *Agriculture, Ecosystems & Environment* **257**, 30–37. https://doi.org/10.1016/j.agee.2018.01.018

Bengtsson, J., Bullock, J.M., Egoh, B., Everson, C., Everson, T., O'Connor, T., O'Farrell, P.J., Smith, H.G. & Lindborg, R. 2019. Grasslands—more important for ecosystem services than you might think. *Ecosphere* **10**(2), e02582. https://doi.org/10.1002/ecs2.2582

Biro, M., Czucz, B., Horvath, F., Revesz, A., Csatari, B. & Molnar, Z. 2013. Drivers of grassland loss in Hungary during the post-socialist transformation (1987–1999). *Landscape Ecology* **28**, 789–803. doi: 10.1007/s10980-012-9818-0

Boruks, A. 2004. Dabas apstākļi un to ietekme uz agrovidi Latvijā [*Environmental conditions and their influence on agri-environment in Latvia*]. Latvijas Republikas Valsts zemes dienests, Rīga. 166 pp. (in Latvian).

Breckle, S.W. 2002. *Walter's Vegetation of the Earth*. The Ecological Systems of the Geo-Biosphere, 4th ed. Springer Berlin, Heidelberg, 527 pp.

Dax, T., Schroll, K., Machold, I., Derszniak-Noirjean, M., Schuh, B. & Gaupp-Berghausen, M. 2021. Land abandonment in mountain areas of the EU: An inevitable side effect of farming modernization and neglected threat to sustainable land use. *Land* **10**(6). https://doi.org/10.3390/land10060591

Dengler, J. & Tischew, S. 2018. Grasslands of western and northern Europe – between intensification and abandonment. In: Squires, V.R., Dengler, J., Feng, H. & Hua, L. (Eds.). *Grasslands of the World: Diversity, Management and Conservation.* Boca Raton: CRC Press, pp 27–63.

Dobrev, V., Popgeorgiev, G. & Plachiyski, D. 2014. Effects of the common agricultural policy on the coverage of grassland habitats in besaparski ridove special protection area (Natura 2000), southern bulgaria. *Acta Zoologica Bulgarica* **66**(January), 147–155.

European Commission 2013. *Interpretation manual of European Union habitats*. EUR 28, European Commission, DG Environment, Nature ENV B.3. In: European Commission, official website. https://ec.europa.eu/environment/nature/legislation/habitatsdirective/docs/Int_Manual_EU28.pdf (accessed 15 September 2021)

European Commission 2019. *Evaluation of the impact of the CAP on habitats, landscapes, biodiversity*. Final Report. Alliance Environment. European Commission, Directorate-General for Agriculture and Rural Development. AGRI-2018-0492 https://ec.europa.eu/info/sites/info/files/food-farming-fisheries/key_policies/documents/ext-eval-biodiversity-final-report_2020_en.pdf (accessed 15 September 2021)

Filho, W.L., Mandel, M., Al-Amin, A.Q., José, Feher, A. & Jabbour, C.C. 2016. An assessment of the causes and consequences of agricultural land abandonment in Europe. *International Journal of Sustainable Development & World Ecology* **24**(6), 554–560. https://doi.org/10.1080/13504509.2016.1240113

Gellrich, M., Baur, P., Koch, B. & Zimmermann, N.E. 2007. Agricultural land abandonment and natural forest re-growth in the Swiss mountains: A spatially explicit economic analysis. *Agriculture, Ecosystems & Environment* **118**(1–4), 93–108. https://doi.org/10.1016/j.agee.2006.05.001

Gocht, A., Ciaian, P., Bielza, M., Terres, J.M., Roder, N., Himics, M. & Salputra, G. 2017. EU-wide Economic and Environmental impacts of CAP greening with high spatial and farm-type detail. *Journal of Agricultural Economics* **68**(3), 651–681. https://doi.org/10.1111/1477-9552.12217

Guerci, M., Knudsen, M.T., Zucali, M., Sconbach, P. & Kristensen, T. 2013. Parameters affecting the environmental impact of a range of dairy farming systems in Denmark, Germany and Italy. *Journal of Cleaner Production* **54**, 133–141. https://doi.org/10.1016/j.jclepro.2013.04.035

Haensel, M., Scheinpflug, L., Riebl, R., Lohse, E.J., Röder, N. & Koellner, T. 2023. Policy instruments and their success in preserving temperate grassland: Evidence from 16 years of implementation. *Land Use Policy* **132**, 106766. https://doi.org/10.1016/j.landusepol.2023.106766

Hatna, E. & Bakker, M.M. 2011. Abandonment and expansion of arable land in Europe. *Ecosystems* **14**, 720–731. doi: 10.1007/s10021-011-9441-y

Herzon, I., Raatikainen, K., Rūsiņa, S., When, S., Helm, A. & Eriksson, O. 2022. Semi-natural habitats in the European boreal region: caught in the socio-ecological extinction vortex. *Ambio* **51**, 1753–1763. https://doi.org/10.1007/s13280-022-01705-3

Herzon, I., Raatikainen, K.J., When, S., Rūsiņa, S., Helm, A., Cousins, S.A.O., Rašomavičius, V. 2021. Semi-natural habitats in boreal Europe: a rise of a social-ecological research agenda. *Ecology and Society* **26**(2), 13. https://doi.org/10.5751/ES-12313-260213

Hinojosa, L., Napoléone, C., Moulery, M. & Lambin, E.F. 2016. The 'mountain effect' in the abandonment of grasslands: Insights from the French Southern Alps. *Agriculture, Ecosystems & Environment* **221**, 115–124. https://doi.org/10.1016/j.agee.2016.01.032

Hole, D.G., Perkins, A.J., Wilson, J.D., Alexander, I.H., Grice, P.V. & Evans, A.D. 2005. Does organic farming benefit biodiversity? *Biological Conservation* **122**, 113–130. https://doi.org/10.1016/j.biocon.2004.07.018

Janssen, J.A.M., Rodwell, J.S., García Criado, M., Gubbay, S., Haynes, T., Nieto, A., Sanders, N., Landucci, F., Loidi, J., Ssymank, A., Tahvanainen, T., Valderrabano, M., Acosta, A., Aronsson, M., Arts, G., Attorre, F., Bergmeier, E., Bijlsma, R.-J., Bioret, F., Biţă-Nicolae, C., Biurrun, I., Calix, M., Capelo, J., Čarni, A., Chytrý, M., Dengler, J., Dimopoulos, P., Essl, F., Gardfjell, H., Gigante, D., Giusso del Galdo, G., Hájek, M., Jansen, F., Jansen, J., Kapfer, J., Mickolajczak, A., Molina, J.A., Molnár, Z., Paternoster, D., Piernik, A., Poulin, B., Renaux, B., Schaminée, J.H.J., Šumberová, K., Toivonen, H., Tonteri, T., Tsiripidis, I., Tzonev, R. & Valachovič, M. 2016. European Red List of Habitats: Part 2. Terrestrial and Freshwater Habitats. In: Publications Office of the European Union, Luxembourg https://op.europa.eu/en/publication-detail/-/publication/22542b64-c501-11e7-9b01-01aa75ed71a1/language-en (accessed 15 September 2021)

Jepsen, M.R., Kuemmerle, T., Müller, D., Erb, K., Verburg, P.H., Haberl, H., Vesterager, J.P., Andrić, M., Antrop, M., Austrheim, G., Björn, I., Bondeau, A., Bürgi, M., Bryson, J., Caspar, G., Cassar, L.F., Conrad, E., Chromý, P., Daugirdas, V., Van Eetvelde, V., Elena-Rosselló, R., Gimmi, U., Izakovicova, Z., Jančák, V., Jansson, U., Kladnik, D., Kozak, J., Konkoly-Gyuró, E., Krausmann, F., Mander, Ü., McDonagh, J., Pärn, J., Niedertscheider, M., Nikodemus, O., Ostapowicz, K., Pérez-Soba, M., Pinto-Correia, T., Ribokas, G., Rounsevell, M., Schistou, D., Schmit, C., Terkenli, T.S., Tretvik, A.M., Trzepacz, P., Vadineanu, A., Walz, A., Zhllima, E. & Reenberg, A. 2015. Transitions in European land-management regimes between 1800 and 2010. *Land Use Policy* **49**, 53–64. https://doi.org/10.1016/j.landusepol.2015.07.003

Kaligarič, M, Čuš, J., Skornik, S. & Ivajnsic, D. 2019. The failure of agri-environment measures to promote and conserve grassland biodiversity in Slovenia. *Land Use Policy* **80**, 127–134. https://doi.org/10.1016/j.landusepol.2018.10.013

Keišs, O. 2005. Impact of changes in agricultural land use on the Corncrake Crex crex population in Latvia. *Biology* **691**, 93–109.

King, M. 2010. *An investigation into policies affecting Europe's semi-natural grasslands*. A report by The Grasslands Trust commissioned by the European Forum on Nature Conservation and Pastoralism & co-funded by the European Commission (DG Environment). In: *European Forum on Nature Conservation and Pastoralism* http://www.efncp.org/download/European-grasslands-report-phase1.pdf (accessed 15 September 2021)

Koffijberg, K., Hallman, C., Keišs, O. & Schäffer, N. 2016. Recent population status and trends of Corncrakes Crex crex in Europe. *Vogelwelt* **136**, 75–87.

Krampis, I. 2012. Sugu izplatības kartēšana Latvijā, metodes un rezultāti [Mapping the distribution of species in Latvia. Methods and Results]. *Ģeomātika* **8**(1), 43–48 (in Latvian).

Lasanta, T., Arnáez, J., Pascual, N., Ruiz-Flaño, P., Errea, M.P. & Lana-Renault, N. 2017. Space-time process and drivers of land abandonment in Europe. *Catena* **149**, 810–823. https://doi.org/10.1016/j.catena.2016.02.024

Latruffe, L. & Piet, L. 2014. Does land fragmentation affect farm performance? A case study from Brittany, France. *Agricultural Systems* **129**, 68–80. https://doi.org/10.1016/j.agsy.2014.05.005

Levers, C., Butsic, V., Verburg, P.H., Muller, D. & Kuemmerle, T. 2016. Drivers of changes in agricultural intensity in Europe. *Land Use Policy* **58**, 380–393. https://doi.org/10.1016/j.landusepol.2016.08.013

MacDonald, D., Crabtree, J.R., Wiesinger, G., Dax, T., Stamou, N., Fleury, P., Gutierrez Lazpita, J. & Gibon, A. 2000. Agricultural abandonment in mountain areas of Europe: Environmental consequences and policy response. *Journal of Environmental Management* **59**(1), 47–69. https://doi.org/10.1006/jema.1999.0335

Millington, J.D.A., Perry, G.L.W. & Romero-Calcerrada, R. 2007. Regression Techniques for Examining Land Use/Cover Change: A Case Study of a Mediterranean Landscape. *Ecosystems* **10**(4), 562–578. doi: 10.1007/s10021-007-9020-4

Nikodemus, O., Bell, S., Grīne, I. & Liepiņš, I. 2005. The impact of economic, social and political factors on the landscape structure of the Vidzeme Uplands in Latvia. *Landscape and Urban Planning* **70**, 57–67. https://doi.org/10.1016/j.landurbplan.2003.10.005

Nikodemus, O., Kļaviņš, M., Krišjāne, Z., Zelčs, V. (Eds.) 2018. *Latvija. Zeme, daba, tauta, valsts.* [Latvia. Land, Nature, Nation, State]. Rīga: Latvijas Universitātes Akadēmiskais apgāds.

Nipers, A., Pilvere, I., Zeverte-Rivza, S. & Krievina, A. 2017. Use of econometric model for developing an outlook for livestock sector in Latvia. *Proceedings of 16th International Scientific Conference 'Engineering for Rural Development'*, pp. 874–883. https://pdfs.semanticscholar.org/b83c/4a1f1ad6ae339dc8bb30ef4335a8cdbe7f6f.pdf

Opermanis, O., Račinskis, E. & Auniņš, A. 2008. EU Birds Directive Annex I vs national bird protection interests: legislative impact on bird conservation in Latvia. In Opermanis, O. & Whitelaw, G. (eds.), *Economic, social and cultural aspects in biodiversity conservation.* Press of the University of Latvia, pp. 94–102.

Pazúr, R., Lieskovský, J., Feranec, J. & Oťaheľ, J. 2014. Spatial determinants of abandonment of large-scale arable lands and managed grasslands in Slovakia during the periods of post-socialist transition and European Union accession. *Applied Geography* **54**, 118–128. https://doi.org/10.1016/j.apgeog.2014.07.014

Pe'er, G., Dicks, L.V., Visconti, P., Arlettaz, R., Báldi, A., Benton, T.G., Collins, S., Dieterich, M., Gregory, R.D., Hartig, F., Henle, K., Hobson, P.R., Kleijn, D., Neumann, R.K., Robijns, T., Schmidt, J., Shwartz, A., Sutherland, W.J., Turbé, A. & Scott, A.V. 2014. EU agricultural reform fails on biodiversity. *Science* **344**(6188), 1090–1092. https://doi.org/DOI: 10.1126/science.1253425

Penēze, Z., Nikodemus, O. & Krūze, I. 2009. Izmaiņas Latvijas lauku ainavā 20. un 21. gadsimtā [Changes in Latvian Rural Landscape during the 20th–21st century]. *Acta Universitatis Latviensis, Earth and Environment Sciences* **724**, 168–183.

Perpiña Castillo, C., Jacobs-Crisioni, C., Diogo, V. & Lavalle, C. 2021. Modelling agricultural land abandonment in a fine spatial resolution multi-level land-use model: An application for the EU. *Environmental Modelling & Software* **136**, 104946. https://doi.org/10.1016/J.ENVSOFT.2020.104946

Prangel, E., Kasari-Toussaint, L., Neuenkamp, L., Noreika, N., Karise, R., Marja, R., Ingerpuu, N., Kupper, T., Keerberg, L., Oja, E., Meriste, M., Tiitsaar, A., Ivask, M. & Helm, A. 2023. Afforestation and abandonment of semi-natural grasslands lead to biodiversity loss and a decline in ecosystem services and functions. *Journal of Applied Ecology* **60**, 825–836. https://doi.org/https://doi.org/10.1111/1365-2664.14375

Reif, J. & Hanzelka, J. 2016. Grassland winners and arable land losers: The effects of post-totalitarian land use changes on long-term population trends of farmland birds. *Agriculture, Ecosystems & Environment* **232**, 208–217. https://doi.org/10.1016/j.agee.2016.08.007

Ridding, L.E., Redhead, J.W. & Pywell, R.F. 2015. Fate of semi-natural grassland in England between 1960 and 2013: A test of national conservation policy. *Global Ecology and Conservation* **4**, 516–525. https://doi.org/10.1016/j.gecco.2015.10.004

Rusina, S. & Kiehl, K. 2010. Long-term changes in species diversity in abandoned calcareous grasslands in Latvia. *Tuexenia* **30**, 467–486.

Rūsiņa, S. 2017. *Protected Habitat Management Guidelines for Latvia.* Volume 3. Semi-natural grasslands. Sigulda: Nature Conservation Agency. https://nat-programme.daba.gov.lv/public/eng/documents_and_publications/

Rūsiņa, S., Prižavoite, D., Nikodemus, O., Brūmelis, G., Gustiņa, L. & Kasparinskis, R. 2021. Land-use legacies affect Norway spruce Picea abies colonisation on abandoned marginal agricultural land in Eastern Baltics. *New Forests* **52**, 559–583. https://doi.org/10.1007/s11056-020-09809-y

Rūsiņa, S., Vācere, G., Lakovskis, P. & Ieviņa, L. 2023. Changes in semi-natural grassland distribution in relation to CAP 2014–2020 area-based payments in Latvia. *Research for Rural Development* **38,** 16–22. Latvia University of Life Sciences and Technologies, Jelgava. DOI: 10.22616/rrd.29.2023.002

Sabatier, R., Doyen, L. & Tichit, M. 2012. Action versus result-oriented schemes in a Grassland agroecosystem: A dynamic modelling approach. *PLOS ONE* **7**(4). https://doi.org/10.1371/journal.pone.0033257

Stoate, C., Báldi, A., Beja, P., Boatman, N.D., Herzon, I., van Doorn, A., de Snoo, G.R., Rakosy, L. & Ramwell, C. 2009. Ecological impacts of early 21st century agricultural change in Europe – A review. *Journal of Environmental Management* **91**(1), 22–46. https://doi.org/10.1016/j.jenvman.2009.07.005

Stypinski, P. 2011. The Effect of Grassland-based Forages on Milk Quality and Quantity. *Agronomy Research* **9**(2), 479–488.

Sutcliffe, L.M.E., Batary, P., Kormann, U., Baldi, A., Dicks, L.V., Herzon, I., Kleijn, D., Tryjanowski, P., Apostolova, I., Arlettaz, R., Aunins, A., Aviron, S., Baležentiene, L., Fischer, C., Halada, L., Hartel, T., Helm, A., Hristov, I., Jelanska, S.D., Kaligarič, M., Kamp, J., Klimek, S., Koorberg, P., Kostiukova, J., Kovacs-Hostyanszki, A., Kuemmerle, T., Leuschner, C., Lindborg, R., Loos, J., Maccherini, S., Marja, R., Mathe, O., Paulini, I., Proenca, V., Rey-Benayas, J., Sans, F.X., Seifert, C., Stalenga, J., Timaeus, J., Torok, P., van Swaay, C., Viik, E. &Tscharntke, T.2015. Harnessing the biodiversity value of central and eastern European farmland. *Diversity and Distributions* **21**, 722–730. https://doi.org/10.1111/ddi.12288

Šumrada, T., Vreš, B., Čelik, T., Šilc, U., Rac, I., Udovč, A. & Erjavec, E. 2021. Are result-based schemes a superior approach to the conservation of High Nature Value grasslands? Evidence from Slovenia. *Land Use Policy* **111**(September). https://doi.org/10.1016/j.landusepol.2021.105749

Targetti, S., Messeri, A., Argenti, G & Stagliano, N. 2018. A comparative analysis of functional traits in semi-natural grasslands under different grazing intensities. *Agronomy Research* **16**(5), 2179–2196. https://doi.org/10.15159/AR.18.209

Terres, J.M., Scacchiafichi, L.N., Wania, A., Ambar, M., Anguiano, E., Buckwell, A., Coppola, A., Gocht, A., Källström, H.N., Pointereau, P., Strijker, D., Visek, L., Vranken, L. & Zobena, A. 2015. Farmland abandonment in Europe: Identification of drivers and indicators, and development of a composite indicator of risk. *Land Use Policy* **49**, 20–34. https://doi.org/10.1016/j.landusepol.2015.06.009

Ustaoglu, E. & Collier, M.J. 2018. Farmland Abandonment in Europe: An Overview of Drivers, Consequences and Assessment of the Sustainability Implications. *Environmental Reviews* **26**(4), 1–21. https://doi.org/10.1139/er-2018-0001

Ušča, M., Ieviņa, L., Lakovskis, P. 2023. Spatial disparity and environmental issues of organic agriculture. *Agronomy Research* **21**(3), 1374–1387. https://doi.org/10.15159/AR.23.077

Vanwambeke, S.O., Meyfroid, P., Nikodemus, O. 2012. 20 years of rural landscape changes in Vidzeme, Latvia. *Landscape and Urban Planning* **105**(3), 241–249. https://doi.org/10.1016/j.landurbplan.2011.12.009

Viira, A.H., Ariva, J., Kall, K., Oper, L., Jürgenson, E., Maasikamäe, S. & Põldaru, R. 2020. Restricting the eligible maintenance practices of permanent grassland – A realistic way towards more active farming? *Agronomy Research* **18**(Special Issue 2), 1556–1572. https://doi.org/10.15159/AR.20.018

Vinogradovs, I., Nikodemus, O., Elferts, D. & Brūmelis, G. 2018. Assessment of site-specific drivers of farmland abandonment in mosaic-type landscapes: A case study in Vidzeme, Latvia. *Agriculture, Ecosystems & Environment* **253**, 113–121. https://doi.org/10.1016/j.agee.2017.10.016

Walden, E. & Lindborg, R. 2018. Facing the future for grasslands restoration – What about the farmers? *Journal of Environmental Management* **227**, 305–312. https://doi.org/10.1016/j.jenvman.2018.08.090

Wittig, R., Becker, U. & Nawrath, S. 2010. Grassland loss in the vicinity of a highly prospering metropolitan area from 1867/68 to 2000—The example of the Taunus (Hesse, Germany) and its Vorland. *Landscape and Urban Planning* **95**(4) 175–180. https://doi.org/10.1016/j.landurbplan.2010.01.001

Wood, S. 2017. *Generalized Additive Models. An Introduction with R* (2nd ed.). Boca Raton, Chapman and Hall/CRC, 496 pp.

Wrzaszcz, W. 2017. The CAP greening effects – the Polish experience. *Proceedings of the 8th International Scientific Conference Rural Development 2017*. Aleksandras Stulginskis University. https://doi.org/10.15544/RD.2017.212

Żmihorski, M., Kotowska, D., Berg, Å. & Pärt, T. 2016. Evaluating conservation tools in Polish grasslands: The occurrence of birds in relation to agri-environment schemes and Natura 2000 areas. *Biological Conservation* **194**, 150–157. https://doi.org/10.1016/j.biocon.2015.12.007

Żmihorski, M., Krupiński, D., Kotowska, D., Knape, J., Pärt, T., Obłoza, P. & Berg, Å. 2018. Habitat characteristics associated with occupancy of declining waders in Polish wet grasslands. *Agriculture, Ecosystems and Environment* **251**(June 2017), 236–243. https://doi.org/10.1016/j.agee.2017.09.033

Agronomy Research **22**(1), 274–283, 2024
https://doi.org/10.15159/AR.24.010

Control of subacute ruminal acidosis in high-yielding dairy cow herd by measuring the rumen wall thickness

I. Sematovica*, A. Malniece and I. Duritis

Latvia University of Life Sciences and Technologies, Faculty of Veterinary Medicine, Clinical Institute, 8 Kristapa Helmana Str., LV-3004 Jelgava, Latvia
*Correspondence: ilga.sematovica@lbtu.lv

Received: October 1st, 2023; Accepted: January 21st, 2024; Published: February 13th, 2024

Abstract. The study aimed to investigate whether the rumen wall thickness (RWT) follows with the data from the collar sensor system and how deeply it depends on feeding management used in the high-yielding dairy cow farm, as well as what benefit it could bring to diagnose subacute rumen acidosis (SARA) in cows. The data obtained from the collar sensors about chewing activity were analysed in relation to milk recording results, the rumen wall thickness (RWT) and the context of the composition of feed easily digestible carbohydrate changes during the intensive lactation phase. The dynamic of RWT was evaluated concerning milk amount and quality, its relation to fertility, and the size of the cows, which were taken into account. The results showed that the sensor system provides information about cow behaviour but does not provide direct information about the SARA problem in the herd. The RWT was related to the changes in feed easily digestible carbohydrate content and chewing activity. In conclusion, the sensor system allows monitoring of feed ingestion, but overall data about productivity and milk composition are necessary to make conclusions and induce ideas about corrections. Additional RWT measures are necessary to monitor rumen health and SARA presence timely, so monitoring the RWT may lead to a longer productive life for the cow.

Key words: TMR, sensor systems, RWT, SARA.

INTRODUCTION

Subacute ruminal acidosis (SARA) is an actual subclinical problem with obvious consequences in high-producing dairy cattle if fed with a ration too high level of easily digestible carbohydrates (EDC). Due to its subacute nature and lack of clearly expressed clinical signs, this metabolic disease is difficult to monitor. However, information and parameters have been identified that indicate the presence and intensity of SARA in the herd or cow group less or more (Humer et al., 2017). Specialists of highly productive dairy farms manage the situation according to the financial and technological possibilities available to the farm.

Direct and indirect criteria and methods can be used to diagnose SARA. As a direct parameter is the dropping of pH in the rumen content below 5.6 for more than three hours (Kleen et al., 2003; Gozho et al., 2005). A pH value could be established by obtaining the ruminal content sample using an oro-gastral probe via rumen-centesis or using a

cannula previously operated surgically (Metwally et al., 2015; Lozier & Niehaus 2016). Monitoring of the milk fat and milk protein content and ratio, chewing score, monitoring of body condition score (BCS), appearance and consistency of faeces, urine pH and some blood biochemical parameters, and filling of rumen could be used as indirect criteria (Aditya et al., 2017; Antanaitis et al., 2019; Yang et al., 2020). All invasive methods disturb animals and are not in line with welfare standards if they are used just for prophylactic or just monitoring measures. A frequency of incidence of laminitis, rumenitis, and displacement of abomasum also could be indirect criteria proving SARA in the herd (Stone, 2004; Gasteiner et al., 2012). A questionnaire to monitor dairy herd health and investigate the causes of the SARA was elaborated based on evaluating feed composition and quality, farm management, animals and production (Liepa & Šematoviča, 2017). However, these methods are subjective and need to be monitored through regular visits provided by an educated and experienced specialist. The intra-ruminal boluses are elaborated to measure the reticulo-ruminal pH and temperature permanently, but a restricted time of battery capacity limits their wide use of them in practice.

The aim of the study was to determine whether the level of sensor systems (*Allflex Livestock Intelligence*^{TM}, *Heatime® Pro+*) and feeding management used in the high-yielding dairy farm allows them sufficient control of the presence and dynamics of SARA. To achieve the goal, the data obtained from sensors used in the farm were analysed in the context of cow milk monitoring results, the RWT, feed changes, and the cow size measured as the height at the sacrum dorsal point from the ground.

MATERIALS AND METHODS

The research took place in 2022 on a free-stall housing system farm of 660 dairy cows with an average milk yield of 12,300.00 kg per cow per year. The work was carried out using the data of 44 cows (16 primiparous and 28 older cows) in their intensive lactating period in May and June of 2022. Milk monitoring information (productivity, milk fat (MF), milk protein (MP), MF and MP ratio, somatic cell count (SCC) and artificial insemination (AI) times per pregnancy were taken from the Agricultural Database of Latvia ten days after changes in feeding recipes. The cows' size was taken into account.

Cow nutrition during the study period consisted of free accessible total mixed ration (TMR) delivered to cows 2 times per day and pushed closer to cows every 3 h. The recipe and preparation of the feed were not affected by the study. The study was conducted under the real production conditions of the farm. The feed's easily digestible carbohydrate (EDC) amount in the TMR was determined according to the recipes used during the study period (Table 2 and Table 3). Feed recipes before May included Beet pulp, which provided easily digestible fibre. A dry matter intake (DMI) during May reached 27–28 kg a day per cow because of the use of Beet pulp, but the first lactation cow reached 24–25 DMI kg per day, respectively.

During May, the Beet pulp ran out, and there was a sharp drop in edibility, even down to 23–24 kg of DMI, at the same time, the 1c grass ran out, and 2c grass was started. The quality of the two kinds of grass was different (Table 1). Grass 2c has less protein and was drier.

In May and June, cow chewing activity as time spent chewing feed (min per day) was obtained using sensors on neckties (*Allflex Livestock Intelligence system*). Data about everyday chewing activity were retrieved from *Allflex Livestock Intelligence software/system* corresponding to the study period.

Cow height in cm was established using a height measurement stick by related professionals on the farm. The RWT in cm was measured in the region of the middle third of the left abdomen (just under the paralumbar fossa) by the same veterinarian using ultrasound equipment MyLab30VetGold with a 7.7 MHz linear probe and according to the methodology previously described by (Roozbahani et al., 2013; Neubauer et al., 2017). The RWT measurements were recorded two times with 30-day intervals - 1st time was on May 2, and the 2nd time was on the 1st of June.

Table 1. Grass silage quality in the investigation period

	1c grass	2c grass
Moisture %	64.8	59.7
Dry matter %	35.2	40.3
Crude protein %	13.1	10.4
Adjusted protein %	13.1	10.4
Soluble protein %	9.1	6.2
Ammonia %	0.99	0.96
Rumen degradable protein %	11.1	8.3

Table 2. Feed recipe for the 1st lactation cow at the time of the study

	May		June	
Ingredients	Fresh kg	DM kg	Fresh kg	DM kg
Corn silage	21.32	6.80	23.51	7.50
Grass silage	11.36	4.00	15.24	5.70
Grass hay	0.60	0.51	1.10	0.93
Beet pulp	6.80	1.70	…	…
Glucose syrup	0.80	0.30	1.00	0.38
Rapu	7.10	6.18	0.70	0.61
Soybean meal 44%	1.20	1.08	4.90	4.41
Megalac	0.15	0.15	0.15	0.15
Mix Wheat50-Brley50	4.10	3.60	…	…
Soft wheat fine ground	…	…	5.20	4.50
High prod. concentrate	…	…	…	…
Sodium bicarbonate	0.20	0.19	0.15	0.14
Calcium carbonate	0.05	0.05	0.09	0.09
Calcium Phosphate	…	…	…	…
Sodium chloride	0.08	0.08	0.11	0.11
Premix Llet	0.10	0.10	0.10	0.10
Q-Boost	…	…	0.13	0.13
Totals	53.86	24.73 (45.9%)	52.38	24.73 (47.2%)

All procedures performed in the present study were in accordance with ethical standards. The Council for Ethical Treatment of Animals, Food and the Veterinary Service Republic of Latvia was approved for this study (No. 1.1-13E/20/891).

Mean ± standard deviation (SD) was used to express the data obtained and they were analysed using SPSS 18.0 software (*SPSS* Incorporated, Chicago, IL, USA). Graphical pictures were created using *MS Excel* software. The *Student's test* was

used to detect a statistically significant difference between related and non-related groups. A P value < 0.05 was considered statistically significant.

Table 3. Feed recipe for the 2nd and more lactation cows at the time of the study

	May		June	
Ingradients	Fresh kg	DM kg	Fresh kg	DM kg
Corn silage	26.65	8.50	26.65	8.50
Grass silage	10.80	3.80	15.24	5.70
Grass hay	0.50	0.42	0.90	0.76
Beet pulp	6.80	1.70	…	…
Glucose syrup	1.00	0.38	1.10	0.42
Rapu	…	…	0.60	0.52
Soybean meal 44%	4.60	4.14	5.20	4.68
Megalac	0.30	0.30	0.30	0.30
Mix Wheat50-Brley50	…	…	…	…
Soft wheat fine ground	6.50	5.63	6.50	5.63
High prod. concentrate	9.11	8.07	7.40	6.50
Sodium bicarbonate	0.14	0.14	0.14	0.14
Calcium carbonate	0.07	0.07	0.07	0.07
Calcium Phosphate	0.03	0.03	0.03	0.03
Sodium chloride	0.12	0.12	0.12	0.12
Premix Llet	0.10	0.10	0.10	0.05
Q-Boost	0.14	0.14	0.14	0.10
Totals	66.85	33.53 (50.2%)	64.49	33.51 (52%)

RESULTS AND DISCUSSION

When drawing up the feed composition for dairy cows on the farm, the mode and quality of the available feedstock must be considered. To fully satisfy the needs of yielding cows, some ingredients were bought and included in calculating a specific TMR. During the period of the study, the feed ingredients composition ratio was as follows (Fig. 1). The amount of EDC in TMR was higher in May than in June. Subsequently, the total productivity diminished from May to June (44.8 ± 8.83 vs 36.46 ± 7.06 kg day^{-1} per cow, $P > 0.05$). Milk composition average indices (MF, MP, SCC and MF:MP ratio see Table 5) were not changed statistically significantly, $P > 0.05$).

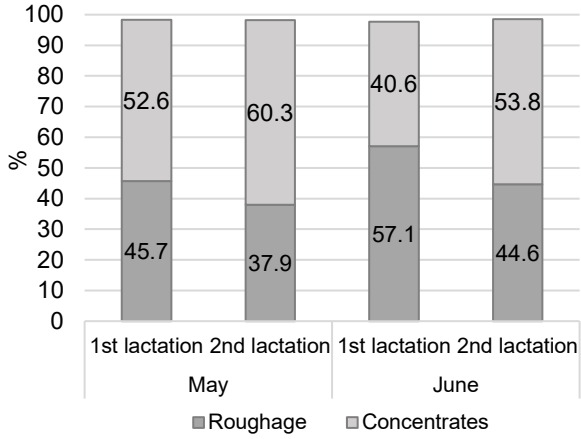

Figure 1. The proportion of EDC and roughage in the feed of the 1st and older cows in May and June.

In June, grass 2c (Table 1), which was included in TMR, was too dry and possibly prepared in too long fractions, and farm personnel noticed that the animals started sorting the feed. In June, a lower amount of EDC was included in the feed with almost the same amount of sodium bicarbonate, but most of the cows had increased RWT, which the noticed feed sorting can explain. In most cows (51.9%), the number of chewing movements decreased, and at the same time, the thickness of the rumen wall increased in 70.8% of cows. Most likely, this is due to the influence of the type of TMR preparation from the feed composition described earlier. In some cows (48.1%), the situation was the opposite, and 29.2% out of them were primiparous cows (Fig. 2). There may be hierarchy issues within the cow group and feed sorting due to the preparation and composition of the TMR. Individual qualities could be considered regarding feed metabolism in cow forestomach (Sematovica et al., 2017).

The mean results of the chewing activity during the study period in primiparous and older cows are represented in Table 4. They were kept in one group together and it was essential to rule out the superiority of older cows over young ones. So, it seemed that older cows ate more EDC as judged bys the significant increase in RWT ($P < 0.05$). It has been approved that older cows are more resistant to high-grain feeding than young cows (Neubauer et al., 2018).

Table 4. The dynamic of **c**hewing activity and RWT in the 1st lactation and older cows in the study period

Month	Lactation		Chewing activity min day^{-1}	Rumen wall thickness cm	Milk productivity day^{-1}
May	1st lactation	Min.	519	0.12	26.5
		Max	621	0.48	54.4
		Mean ± SD	583.4 ± 33.76	0.28 ± 0.146	41.0 ± 8.50
	More lactations	Min.	544	0.15	35.0
		Max	620	0.60	63.7
		Mean ± SD	570 ± 26.57	0.39 ± 0.134*	47.5 ± 8.24
June	1st lactation	Min.	541	0.10	30.5
		Max	638	0.65	50.0
		Mean ± SD	590.4 ± 27.19	0.42 ± 0.198	39.1 ± 6.49
	More lactations	Min.	508	0.21	21.9
		Max	643	0.94	50.0
		Mean ± SD	564.7 ± 37.46	0.64 ± 0.214*	34.3 ± 6.94

*($P < 0.05$).

No significant differences were observed between the mean chewing activity obtained in May and June ($P > 0.05$). However, the thickness of the RWT was increased statistically significantly (0.34 ± 0.161 vs 0.56 ± 0.224 cm, $P < 0.05$). Moreover, the following RWT data for individual cows (Fig. 2) brightly showed individual chewing behaviour for particular cows in that period. A negative statistical correlation was found between chewing activity and RWT dynamic ($r = 0.45$; $P < 0.01$). Interestingly, the thickness of the rumen wall changed statistically significantly in older cows (Table 5).

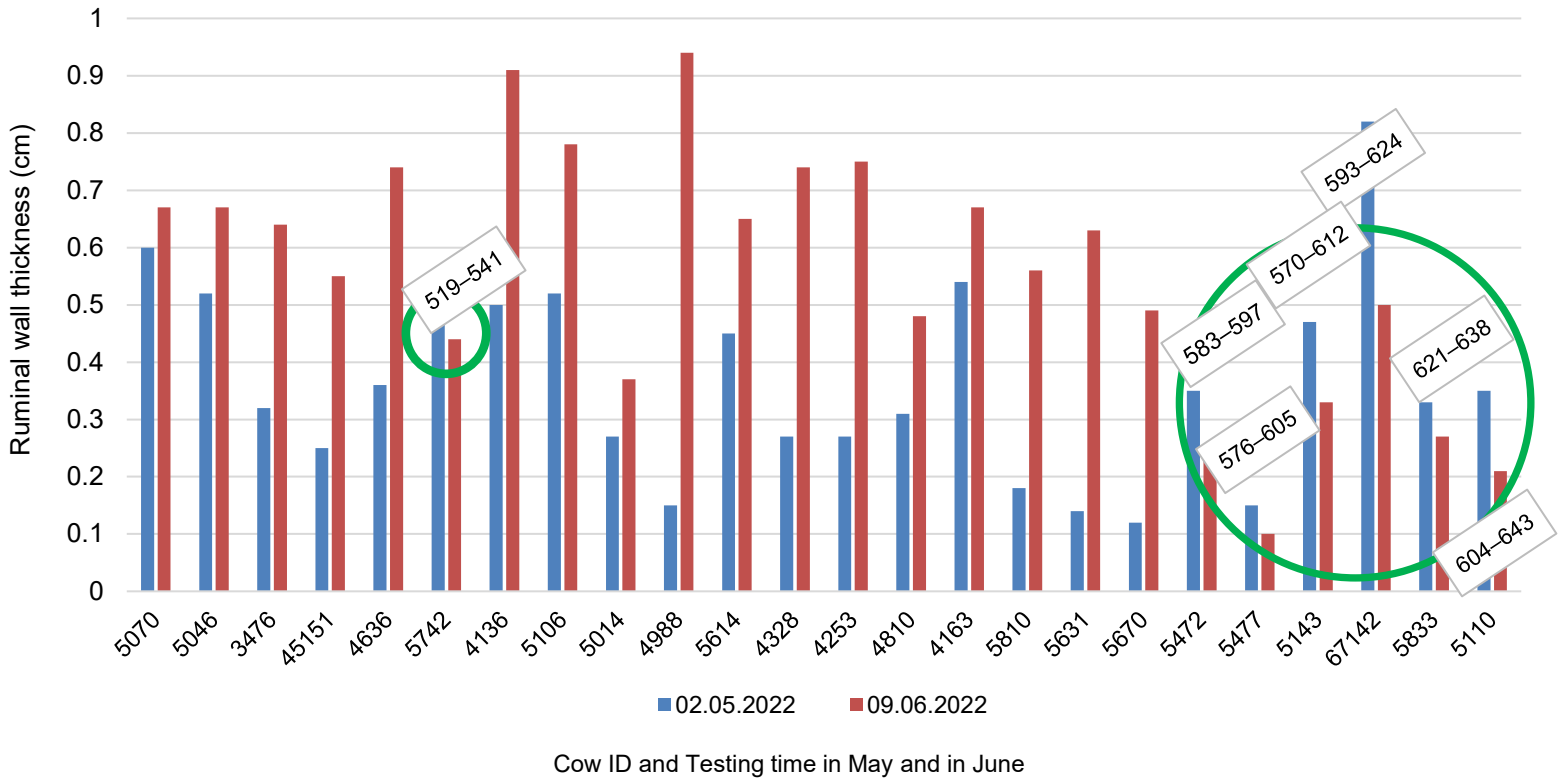

Figure 2. Dynamics of the rumen wall thickness (circle expresses some particular cow chewing activity increasing and simultaneous rumen wall thickness decreasing (indices in boxes)).

In cows whose chewing activity increased was higher productivity (38.2 ± 7.15 vs 35.8 ± 6.66 kg day^{-1}), their MF, MP, SCC AI times per pregnancy and size did not differ significantly ($P > 0.05$). Cows whose RWT increased became less productive (35.3 ± 6.94 vs 40.0 ± 8.14 kg day^{-1}) and other parameters like MF, MP, SCC, AI times per pregnancy and cow size were also not statistically different at the time of investigation ($P > 0.05$). It can be concluded that decreased chewing activity and increased RWT have a tendency to diminish cow productivity. These cows may become less productive despite higher EDC intake because in SARA there is a high concentration of lipopolysaccharides and inflammatory components in the rumen, which increase the expression and synthesis of pro- inflammatory cytokines in the rumen epithelium, thus causing ruminitis and opening the way for inflammation to the entire body (Zhao et al., 2018; Jiang et al., 2021).

Table 5. Parameter dynamic at time of investigation

Parameter/Time	May	June
Productivity kg day^{-1}	44.8 ± 8.83	36.5 ± 7.06**
MF %	3.5 ± 0.81	3.8 ± 0.77
MP%	3.4 ± 0.36	3.5 ± 0.32
SCC thousand mL^{-1}	395 ± 1,752.1	151 ± 412.1
Urea mmol L^{-1}	30.3 ± 7.84	32.8 ± 6.13
MF: MP ratio	1.0 ± 0.21	1.0 ± 0.17
AI per pregnancy	2.0 ± 1.67	2.2 ± 1.67
RWT mm	0.34 ± 0.161	0.56 ± 0.224**
Chewing activity time min day^{-1}	572.1 ± 28.83	574.1 ± 47.52

**($P < 0.05$).

It is well-known that reduced chewing activity could be one of the signals of SARA (Cao et al., 2021). The duration of chewing and rumination are closely related to dry matter intake. TMR particle size influences chewing activity and is closely related to the neutralisation of rumen composition by saliva. So, it is a direct criterion for rumen pH value. If TMR particles are too short, insufficient saliva rises to neutralise pH in the rumen. In our study despite the EDC proportion diminished, rumination/chewing activity proportionally did not reduce because of feed sorting which was noticed by farm personnel. During the study, the difference between minimal and maximum chewing value in 1st lactation cows was 100 ± 5 min day^{-1}, but in the older cow group, this value increased from 76 to 135 min day^{-1} in May and June, respectively.

Moreover, a big difference was noticed between minimal and maximal milk productivity levels in the older cow group (21.9 vs 56.2 kg day^{-1}), and it is obvious that different feeding requirements had to be considered.

At the time of the study, in 51.9%, the number of chewing movements decreased, and the thickness of the rumen wall increased in 70.8%, but in 48.1% of cows' the situation was the opposite, and 29.2% of them was primiparous cows. Thus, we cannot claim primiparous cows were more sensitive to changes in TMR and feed composition than older cows in our study. So, totally it could be explained by differences regarding the composition of TMR and grass quality, which particularly could affect the overall ruminal fermentation and metabolism in this field study. In addition, not possible to exclude feed sorting during June.

A weak but statistically significant correlation was found between RWT and MF content in milk ($r = 0.35$, $P < 0.05$).

A negative statistically significant correlation was found between cow size and MF% (r =−0.47; P = 0.01). It could be explained if a hierarchy existed and larger animals sorted feed. So, these animals could receive more easily digestible feed than smaller, physically weaker cows.

A negative statistically significant correlation was found between MF and MP ratio and artificial insemination times carried out (r = −0.33, P < 0.05). It could be because SARA cows eat digestive carbohydrates more easily, so they have a lower MF and MP ratio, and the SARA negative influence on reproduction is well known (Kh et al., 2014; Vallejo-Timarán et al., 2020).

Productivity has a mild negative correlation with RWT (r = −0.54, P < 0.001). So, in cows with thinner, healthier rumen walls, productivity is higher, and subsequently, these cows had to provide more time for chewing (r = 0.32, P < 0.05).

RWT has a statistically significant mild, negative correlation with chewing activity, showing that cows with lower chewing activity develop thicker ruminal wall, which can be connected with rumen mucosa proliferation caused by low pH levels in rumen during SARA (Mirmazhari-Anwar et al., 2013; Neubauer et al., 2018). The measurement of the rumen wall has attracted interest in recent years and more detailed measurements of the rumen wall have been carried out (Fiore et al., 2020).

CONCLUSIONS

The sensor system provides information about cow behaviour but does not provide direct information about the SARA problem in the herd. It can be seen that there is an individual response to feed change that requires further investigation to understand whether it is a feature of individual cows or a feed sorting option that cows use. Thickening of the rumen walls is a sign related to the effect of the ingested feed on the cow's organism and productivity. The long-term effects of long-term rumen wall thickening on the cow's productivity, health and longevity should be investigated. Monitoring the thickness of the rumen wall may lead to a longer productive life for the cow.

ACKNOWLEDGEMENTS. The study was supported by the project 'Low price bolus for monitoring rumen parameters and early detection of subacute rumen acidosis (SARA) in cows' which is funded by the European Agricultural Fund for Rural Development Program, 2014–2020

REFERENCES

Aditya, S., Humer, E., Pourazad, P., Khiaosa-ard, R., Huber, J.C. & Zebeli, Q. 2017. Intramammary infusion of Escherichia coli lipopolysaccharide negatively affects feed intake, chewing, and clinical variables, but some effects are stronger in cows experiencing subacute rumen acidosis. *Journal of Dairy Science* **100**(2), 1363–1377. doi.org/10.3168/jds.2016-11796

Antanaitis, R., Juozaitienė, V., Malašauskienė, D. & Televičius, M. 2019. Can rumination time and some blood biochemical parameters be used as biomarkers for the diagnosis of subclinical acidosis and subclinical ketosis? *Veterinary and animal science* **8**, 100077. doi.org/10.1016/j.vas.2019.100077

Cao, Y., Wang, D., Wang, L., Wei, X., Li, X., Cai, C., Lei, X. & Yao, J. 2021. Physically effective neutral detergent fiber improves chewing activity, rumen fermentation, plasma metabolites, and milk production in lactating dairy cows fed a high-concentrate diet. *Journal of Dairy Science* **104**(5), 5631–5642. doi.org/10.3168/jds.2020-19012

Fiore, E., Faillace, V., Morgante, M., Armato, L. & Gianesella, M. 2020. A retrospective study on transabdominal ultrasound measurements of the rumen wall thickness to evaluate chronic rumen acidosis in beef cattle. *BMC Veterinary Research* **16**(1). https://doi.org/10.1186/s12917-020-02561-7

Gasteiner, J., Guggenberger, T., Häusler, J. & Steinwidder, A. 2012. Continuous and Long-Term Measurement of Reticuloruminal pH in Grazing Dairy Cows by an Indwelling and Wireless Data Transmitting Unit. *Veterinary Medicine International* **2012**, 1–7. https://doi.org/10.1155/2012/236956

Gozho, G.N., Plaizier, J.C., Krause, D.O., Kennedy, A.D. & Wittenberg, K.M. 2005. Subacute Ruminal Acidosis Induces Ruminal Lipopolysaccharide Endotoxin Release and Triggers an Inflammatory Response. *Journal of Dairy Science* **88**(4), 1399–1403. doi.org/10.3168/jds.s0022-0302(05)72807-1

Humer, E., Aschenbach, J. R., Neubauer, V., Kröger, I., Khiaosa-ard, R., Baumgartner, W. & Zebeli, Q. 2017. Signals for identifying cows at risk of subacute ruminal acidosis in dairy veterinary practice. *Journal of Animal Physiology and Animal Nutrition* **102**, 380–392. doi: 10.1111/jpn.12850

Jiang, Y., Dai, P., Dai, Q., Ma, J., Wang, Z., Hu, R., Zou, H., Peng, Q., Wang, L. & Xue, B. (2021). Effects of the higher concentrate ratio on the production performance, ruminal fermentation, and morphological structure in male cattle-yaks. *Veterinary Medicine and Science* **8**(2), 771–780. https://doi.org/10.1002/vms3.678

Kh, H., Assadi-Alamouti, A., Mohammadi-Sangcheshmeh, A., Farzaneh, N. & Barmaki, S. 2014 Induction of Sub-Acute Ruminal Acidosis Affects Reproductive Performance in Holstein Heifers. Conference: *6th Iranian Congress on Animal Science*, Tabriz, 27-28 August 2014, accessed 30.07.2023 https://www.researchgate.net/publication/269872380_Induction_of_Sub-Acute_Ruminal_Acidosis_Affects_Reproductive_Performance_in_Holstein_Heifers

Kleen, J.L., Hooijer, G.A., Rehage, J. & Noordhuizen, J.P.T.M. 2003. Subacute Ruminal Acidosis (SARA): a Review. *Journal of Veterinary Medicine Series A*, **50**(8), 406–414. doi.org/10.1046/j.1439-0442.2003.00569.x

Liepa, L. & Šematoviča, I. 2017. The role of questionnaires in health control of the dairy herd affected by the subacute rumen acidosis. In: *Līdzsvarota lauksaimniecība*: zinātniski praktiskās konferences raksti, Jelgava, Latvija, 23.02.2017 / Latvijas Lauksaimniecības universitāte. Lauksaimniecības fakultāte. Latvijas Agronomu biedrība. Latvijas Lauksaimniecības un meža zinātņu akadēmija. Jelgava, 2017, pp. 130–134. Available at: http://llufb.llu.lv/conference/lidzsvar_lauksaim/2017/Latvia-lidzsvarota-lauksaimnieciba2017-130-134.pdf (in Latvian).

Lozier, J.W. & Niehaus, A.J. 2016. Surgery of the Forestomach. *Veterinary Clinics of North America: Food Animal Practice* **32**(3), 617–628. doi.org/10.1016/j.cvfa.2016.05.005

Metwally, A., Deml, M., Fahn, C. & Windisch, W. 2015. Effects of a Specific Blend of Essential Oil on Rumen Degradability, Total Tract Digestibility and Fermentation Characteristics in Rumen Fistulated Cows. *Global Veterinaria* **15**(5), 441–451., ISSN 1992-6197

Mirmazhari-Anwar, V., Sharifi, K., Mirshahi, A., Mohri, M., Grünberg, W. 2013. Transabdominal ultrasonography of the ruminal mucosa as a tool to diagnose subacute ruminal acidosis in adult dairy bulls: a pilot study. *Veterinary Quarterly* **33**(3), 139–147. doi: 10.1080/01652176.2013.854942

Neubauer, V., Humer, E., Kröger, I., Meißl, A., Reisinger, N. & Zebeli, Q. 2018. Technical note: Changes in rumen mucosa thickness measured by transabdominal ultrasound as a noninvasive method to diagnose subacute rumen acidosis in dairy cows. *Journal of Dairy Science* **101**(3), 2650–2654. https://doi.org/10.3168/jds.2017-13682

Neubauer, V., Humer, E., Kröger, I., Meißl, A., Reisinger, N. & Zebeli, Q. 2017. Technical note: Changes in rumen mucosa thickness measured by transabdominal ultrasound as a noninvasive method to diagnose subacute rumen acidosis in dairy cows. *Journal of Dairy Science* **101**(3). doi: 10.3168/jds.2017-13682

Roozbahani, M.A., Badiei, A., Nadalian, M.G., Veshkini, A., Buczinski, S. & Mashayekhi, M. 2013. Ultrasonographic Thicknesses of Ruminal and Abdominal Wall in High Yielding Holstein Dairy Cows. *Life Science Journal* **10**, 93–96. Available at https://www.lifesciencesite.com/lsj/life1005s/016_16676life1005s_93_96.pdf

Sematovica, I., Eihvalde, I. & Kairisa, D. 2017. Reticulo-ruminal pH and temperature relationship between dairy cow productivity and milk composition. *Agronomy Research* **15**(2), 576–584. URL: http://agronomy.emu.ee/wp-content/uploads/2017/05/Vol15nr2_Sematovica.pdf

Stone, W.C. 2004. Nutritional Approaches to Minimize Subacute Ruminal Acidosis and Laminitis in Dairy Cattle. *Journal of Dairy Science* **87**, E13–E26. doi.org/10.3168/jds.s0022-0302(04)70057-0

Vallejo-Timarán, D., Reyes-Vélez, J., VanLeeuwen, J., Maldonado-Estrada, J. & Astaiza-Martíneze, J. 2020. Incidence and effects of subacute ruminal acidosis and subclinical ketosis with respect to postpartum anestrus in grazing dairy cows. *Heliyon* **6**(4), e03712. doi: 10.1016/j.heliyon.2020.e03712

Yang, W., Xu, C., Lv, X., Zhang, B., Xia, C., Zhang, H., Wang, S., Zhao, Y., Ma, X., Gao, F., Wang, P. & Liu, G. 2020. Diagnosing bovine subacute rumen acidosis, involves determining calcium content in urine, pH in urine, acidic washing fiber content in feces, performing statistical analysis and diagnosing cows with subacute rumen acidosis. Patent Number: CN110702638-A. Patent Assignee: UNIV HEILONGJIANG BAYI AGRIC(UYON-C). Derwent Primary Accession Number2020-09725G, Indexed: 2020-02-26.

Zhao, C., Liu, G., Li, X., Guan, Y., Wang, Y., Yuan, X., Sun, G., Wang, Z. & Li, X. 2018. Inflammatory mechanism of Rumenitis in dairy cows with subacute ruminal acidosis. *BMC Veterinary Research* **14**(1). https://doi.org/10.1186/s12917-018-1463-7

Agronomy Research **22**(1), 284–300, 2024
https://doi.org/10.15159/AR.24.028

System dynamics modeling for precision beekeeping: Queen rearing optimization for advanced apiary management

A. Smilga-Spalvina[1,2,*], K. Spalvins[1] and I. Veidenbergs[1]

[1]Riga Technical University, Institute of Energy Systems and Environment, Āzenes street 12/1, LV-1048 Riga, Latvia
[2]Smilga Spalvina Llc., Planupes street 11A, LV-2141 Incukalns, Sigulda district, Latvia
[*]Correspondence: smilga.agnese@gmail.com

Received: February 1st, 2024; Accepted: April 17th, 2024; Published: April 30th, 2024

Abstract. The authors propose system dynamics modelling as a new direction in Precision Beekeeping. By modeling the production process in beekeeping, it is possible to forecast the potential production capacity before the season, using the resources available to the beekeeper. The model included in this article reflects one specialisation of beekeeping - queen bee rearing, from the process of queen bee breeding up to the sale of queen bees throughout the entire season. The model helps beekeepers make decisions about the workforce needed to maintain the desired production volume, expected income and costs and resource allocation.

Key words: apiary management, *Apis mellifera*, bee breeding, honey bee, precision beekeeping, system dynamic modeling, queen rearing.

INTRODUCTION

Precision beekeeping, or the incorporation of information technologies into beekeeping, is a recent innovation in the industry that has seen development over the last decade. Various monitoring systems are being developed, such as smart hive scales equipped with sensors that monitor, and process data on hive temperature, humidity, weight changes, sound variations, etc. (Zacepins et al., 2015; Zacepins et al., 2017; Hadjur et al., 2022; Zacepins et al., 2022; Danieli et al., 2023), as well as new tools to assess and precisely determine potential apiary locations and calculate bee colony amounts (Komasilova et al., 2020). Beekeepers can remotely access real-time data through applications. By incorporating machine learning and integrating AI into additional data processing and analysis, beekeepers will be able to receive specific notifications about particular bee colonies within applications, rather than dealing with large volumes of data (Zacepins et al., 2017; Hadjur et al., 2022). The implementation of remote apiary monitoring helps efficiently plan the beekeeper's time and prepare purposefully for apiary inspections.

Another tool that can help address questions related to effective resource planning is system dynamics modeling. This modeling is based on systemic thinking, or the exploration of cause-and-effect relationships between various variables and

understanding how each variable influences others and how everything is interconnected (Forrester, 1994). Models can simulate real-life processes. It is necessary to map out all variables, assign values to them (based on empirical data or theory), and describe relationships with formulas. Models drawn in specialized computer programs simulate behaviour, showing how one variable changes depending on another and how the system as a whole operates. At the core of modeling are problem formulation, dynamic hypothesis creation, model formulation and simulation, model testing, policy creation, and testing (Senge & Forrester, 1980; Forrester, 1994; Barlas, 1996). In beekeeping, various mathematical models have been developed, and system dynamics modeling has been applied. To inform important policy decisions, research has explored how the impact of beekeeping affects wild honey bee populations (Gill, 1996). Models have been used to test changes in the *Varroa* mite population and bee colony development (DeGrandi-Hoffman & Curry, 2004; Becher et al., 2014), as well as how bee colony development varies based on the availability of pollen and nectar sources, food reserves in the hive (Khoury et al., 2013; Russell et al., 2013; Myerscough et al., 2017; Hempel, 2022), and artificial feeding of bee colonies (Paiva et al., 2016). The influence of abiotic and biotic factors on bee colony health has been assessed, and productivity indicators have been forecasted (Gilioli et al., 2018). Profitability from migratory beekeeping has been modeled, taking into account the flowering crops at the apiary site (Pilati et al., 2018). It has been examined whether larger apiaries with a greater number of bee colonies have a higher prevalence of pathogens (Bartlett et al., 2019).

The aim of this article is to present a system dynamics model that can forecast production capacity in a subsector of beekeeping related to the breeding of queen bees. The model reflects the process of queen bee breeding for commercial purposes, aiding in decision-making regarding necessary human and bee colony resources to effectively meet planned production capacities. For the first time in beekeeping, a system dynamics model is described that comprehensively encompasses commercial beekeeping, incorporating human resources and reflecting queen bee rearing, which is essential in the reproductive material propagation subsector of beekeeping. The creation of such models, based on practical data that simulate the production process and capacity, enabling decisions for effective resource utilization, is presented as one of the subdirections of precision beekeeping.

MATERIALS AND METHODS

Definition of problem

The purpose of rearing queen bees is to propagate reproductive material that can be introduced into other colonies by acquiring either virgin queens or mated-laying queens. In Latvia, the queen bee rearing season is short, spanning 16 weeks from May 1st to August 31st. Honeybee colonies start actively collecting the first pollen from willows as early as the end of March (Klavins, 2024). This marks the beginning of active development for bee colonies. The queen bee rearing system requires strong bee colonies to ensure the queenless colonies for queen bee rearing and mating nuclei. The outcome of rearing new virgin and laying queen bees depends on both weather conditions (Büchler et al., 2013) and the efficiency of the rearing system. The establishment and maintenance of a queen rearing and mating system are time-consuming and complex. Therefore, system dynamics modeling will be employed to reflect the system, aiming to

understand the necessary resources for production, the production process, and limiting factors and to define indicators characterizing efficiency.

The model addresses the research question: What is the optimal size of the production system (production capacity) that a beekeeper with limited time resources (40 hours per week) can sustain as functional and profitable for the entire 16 weeks while maximizing the efficiency of resource utilization?

Background information

To understand the model, we must first delve into the biology and behaviour of bees. A bee colony is a superorganism comprising female organisms, the queen bee and worker bees, as well as male organisms known as drones. The queen bee, living for an average of 3–4 years, is the sole individual capable of laying fertilized eggs (Cobey, 2007). Worker bees maintain the colony: they feed and groom the queen, feed the larvae hatched from eggs, construct wax cells, collect water, pollen, and nectar, maintain cleanliness in the hive, defend it, and in summer, they also care for and feed the drones. Drones constitute 5% of the colony's population in summer, and their sole purpose is to take flight to mate with new queens, thus passing on their genes to other colonies (Oxley & Oldroyd, 2010).

It is possible to propagate bee colonies by isolating a portion of the bee population with honey and brood combs. When worker bees detect a queenless state, they decide to feed the youngest worker bee larvae with royal jelly, aiming to raise them into new queens. This behaviour is utilized in queen rearing. Strong colonies without queens are created, and beekeepers introduce grafted 12–24 hour-old larvae, derived from known bee breeding material, into artificial cells. Worker bees then start feeding and raising these larvae into queens (Büchler et al., 2013). A queenless colony can optimally rear 40 queen bees in one batch, and a total of around 160 queens in 3–4 weeks (Author's experience). After that, a new queenless colony must be formed for rearing queens. The queen bee develops in 16 days: 3 days in the egg stage, 6 days in the larval stage (a crucial period that can take place only within the bee colony), and 7 days as a pupa, during which development occurs in a sealed queen cell (this phase may take place within the bee colony or a special incubator) (Page & Peng, 2001).

The queen bee is introduced to a queenless bee unit (nucleus) a day before or after her birth, where worker bees feed and care for her (Büchler et al., 2013). The queen bee reaches sexual maturity within 5–6 days after birth (Page & Peng, 2001; Cobey et al., 2013). After maturation, on warm days (with an outdoor temperature of at least + 20 °C), the queen bee takes 1–3 mating flights, mating with an average of 10 drones and storing the sperm in a special organ - the spermatheca - for her entire lifespan (Page & Peng, 2001; Cobey et al., 2013). Upon returning to the nucleus, the queen bee starts laying eggs within an average of 5 days (Page & Peng, 2001). If the queen bee successfully mates, she lays fertilized eggs, which develop into worker bees. If not, she lays unfertilized eggs, which develop into drones. Therefore, it is necessary to check the brood comb 9 days after the start of laying, as the capping is visually different for workers and drones (Page & Peng, 2001; Büchler et al., 2013). The optimal time from the queen bee's birth to the examination of a mated, laying queen is 3 weeks. Both mated queen bees and virgin, unmated queens can be sold to other beekeepers, who introduce them into their colonies and renew the reproductive material.

To implement the breeding process, apiaries and main bee colonies are necessary. The recommended maximum number of bee colonies in one apiary is 30 (Büchler et al., 2013), linked to the availability of nectar sources. However, in Latvia, if both bee colonies and mating nuclei are placed in the same apiary, the maximum number of colonies in one apiary is 20, and for nuclei - 100 (author's recommendation based on experience). In the first half of the season (May, June), bee colonies actively develop, exhibiting a greater swarming tendency, and during this period, it is possible to create a maximum of 5 new nuclei from one parent colony. Regular inspections of bee colonies and nuclei are essential to establish and maintain bee colonies, as well as to assess the acceptance of new queens and the success of mating outcomes.

If queen bee rearing is the main source of income, then within 16 weeks, one must generate income to cover the annual costs of maintaining bee colonies, nuclei, etc. Therefore, the model includes the assumption that the annual costs for one bee colony are 100 EUR (winter feeding with sugar syrup, treatments, wear and tear on equipment, purchase of beeswax, transportation costs), and for a nucleus, the costs are 20 EUR (stimulative feeding during the absence of nectar flow, equipment wear and tear, transportation costs). To maintain the system, a person is also required, acting as the limiting factor - a time resource (40 hours per week) and as a cost component - labour wages. The model incorporates the average gross hourly wage for a beekeeper in Latvia in June 2023, which is 6.10 EUR/hour (SRS, 2023), assuming work specifically for 4 months for the purpose of queen rearing. Of course, there are other expenses related to marketing, customer service, and to some extent, processing of beekeeping products and preparation of equipment for the next season, which require additional human resources. Revenues are also influenced by demand and weather conditions affecting production volume. The primary goal of the model is to reflect the production process and the operational principles of the model, predicting production capacity in relation to limited human resources. The detailed income and expenditure section, along with factors influencing supply and demand, are additional model components that will remain beyond the scope of this article.

The dynamic hypothesis

Stocks, flows, and influencing factors. The model defines key resources as ‘stocks’ that accumulate and are utilized in the production process. Stocks also feature incoming and outgoing flows that regulate their value. Meanwhile, various additional factors or parameters influence these flows. The main resources in the queen rearing model are:

- Stock ‘Mating nuclei’: This stock has one incoming flow, ‘Formation of nuclei’, influenced by the resource ‘Bee colonies’. One strong bee colony can create 5 mating nuclei, and this formation is possible gradually only in May and June. Another influencing factor is the ‘Number of apiaries’, as the maximum capacity in one apiary location is 20 bee colonies and 100 mating nuclei.
- Stock ‘Production overtime’: This stock has an incoming flow ‘Time consumed for production’, influenced by the time spent on queen grafting, inspections of bee colonies and mating nuclei, and the packaging of queens for sale. The outgoing flow ‘Time has passed’ is constant and corresponds to the planned 40 hours per week.
- Stock ‘Virgin queens’: The incoming flow ‘Queen rearing’ depends on the defined number of rearing colonies, as each rearing colony can rear 40 virgin queens. If

overtime hours occur, the incoming flow ‘Queen rearing’ stops due to time constraints and resumes if overtime hours do not occur. The outgoing flows ‘Addition of virgin queens to mating nuclei’ depend on the number of mating nuclei created at the given moment, as one unit can accommodate 1 virgin queen. The outgoing flow ‘Sale of virgin queens’ depends on the surplus of virgins after adding them to mating nuclei.

- Stock ‘Queens in mating nuclei’ has two outgoing flows. After adding a queen to the nucleus, some queens may not be accepted or may disappear during the nuptial flight and not return. On average, the proportions of non-acceptance and disappearance are 30%. Meanwhile, 70% successfully mate, and within 3 weeks of being added to the nuclei, they become mated, laying, tested queens ready for sale (Smilga-Spalvina et al., 2024).
- Stock ‘Naturally mated, laying, tested queens’ accumulates all tested mated queens for sale. The stock has one outgoing flow ‘Sale of naturally mated queens’.
- The system includes additional stocks, ‘Virgin queens sold’, ‘Naturally mated queens sold’, and ‘Money in the bank’, which characterize production profitability. It should be noted that the model assumes that all queen bees are sold and does not investigate how changes in demand affect the circulation of queen bees in the system.

Causal loop diagrams. After defining stocks, flows, and influencing factors, causal relationships and their mutual impact on feedback loops are identified. Causal loop diagrams help visually represent these relationships (Fig. 1). If the variables within a loop act in opposite directions (if one variable increases, the other decreases), the influence is indicated by an arrow and a ‘minus’ sign. If there is an odd number of ‘minus’ signs within the loop, the loop is called balancing or negative. If the variables within a loop act in the same direction or ‘drive each other forward’ (if one variable increases, the other also increases), the influence is indicated by an arrow and a ‘plus’ sign. Conversely, if there are only ‘plus’ signs or an even number of ‘minus’ signs within the loop, the loop is called reinforcing or positive.

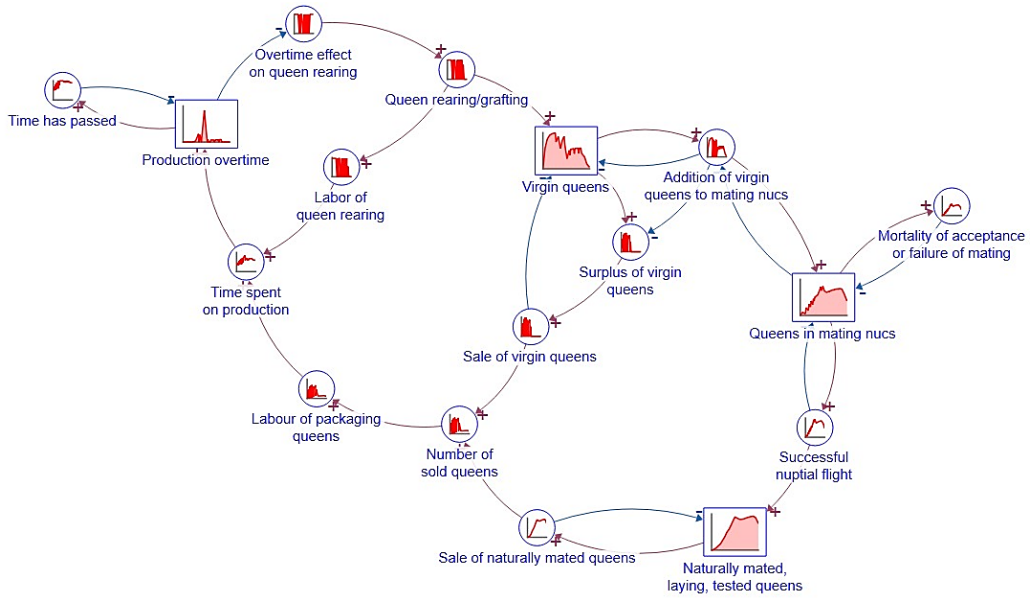

Figure 1. Causal loop diagram for the dynamic hypothesis of queen rearing process.

In the queen bee rearing model, the following causal loops are at play:

- Addition of virgin queens to mating nuclei: This action is governed by two balancing loops with the following relationships: the more virgin queens are added into mating nuclei, the fewer virgin queens remain in the stock, and vice versa. Another relationship is that the more virgin queens are added into mating nuclei, the more occupied the nuclei will be. The more occupied the nuclei, the fewer virgin queens can be added to them.
- Acceptance of virgin queens in nuclei and mating: Two balancing loops are also present here. The first: the more queens perish due to unsuccessful acceptance in the nuclei or during mating flights, the fewer queens will remain in the nuclei. The second: the more queens successfully mate, the fewer queens will remain in the nuclei.
- Sale of virgins and mated, laying queens: For mated queens, a balancing loop determines that the more queen bees are sold, the fewer queen bees will remain in the stock. In contrast, for virgin queens, a reinforcing loop dictates that the more queens are added to nuclei, the smaller the surplus of queens. The smaller the surplus, the fewer virgin queens need to be sold. Fewer queens sold result in a larger queen surplus.
- Regulation of production overtime: If the queen rearing system results in an increase in the time consumed by production, exceeding 40 hours per week, creating overtime, the system is regulated by the parameter 'overtime effect on queen rearing'. If overtime increases, the overtime effect coefficient decreases (from 1 to 0), and queen rearing is halted. Conversely, if overtime does not occur and does not exceed 40 hours per week, the overtime effect value increases from 0 to 1, restarting the queen rearing process. The creation of overtime is heavily influenced by packaging both types of queens. Meanwhile, the task related to the rearing of new queen bees in the system is the only one that can regulate the overall queen bee flow in the system.

The model itself is constructed using the *Stella Architect* software. The table of all parameters and equations in model is available in Annex 1 and Annex 2.

Within the framework of dynamic hypotheses, such a model, incorporating the previously described main stocks, flows, and causal loops will respond if any of the limiting factors of system capacity are exceeded, for instance, if the 40-hour workweek is exceeded. The model will precisely indicate the production capacity. Model validation is still required to ensure the model's reliable behaviour. The behaviour and forecasting results of the model will be described in the analysis section.

Validation

Model structure test: The model has been compared with a real system (based on empirical data and theoretical information about bee biology and behaviour). The stocks, flows, parameters and values included in the model correspond to real-life situations and theories. The level of detail is sufficient to analyse the mutual impact of each variable and its effect on the workload and time consumption. All structural elements included in the model, along with their values, are summarized in Annex 1 and Annex 2.

Model behaviour test: The model's variable quantities have been tested with extreme values, and the model's behaviour is consistent with real-life scenarios, avoiding any inexplicable behaviour. For instance, if there are no apiary locations, it is impossible to create mating nuclei. Only as many queen bees can be added to the nuclei as the number of mating nuclei that have been established or how many of them are queenless

at a given time. Since the model aims to forecast production capacity, it includes the time resource (time spent inspecting bee colonies and nuclei, queen rearing, queen packaging). Accumulation of overtime pauses queen rearing for a while. If the production capacity is optimal, the model exhibits S-shaped behaviour, as it is restricted by the system's capacity, i.e., the number of established mating nuclei. If overtime occurs in the system, the model generates a decline after an increase.

The policies that will be used to change behaviour:

• Policy – constants, parameters, numbers. Parameters such as 'count of mating nuclei' and the parameter 'planned virgin queens per week,' affecting the flow of 'queen rearing,' will be altered.

• Policy – the size of buffers and other stabilizing reserves relative to their flows. The stabilizing reserve is 'Production overtime'; if the stock becomes > 0, the parameter 'overtime effect on queen rearing' immediately influences the flow of 'queen rearing.'

• Policy – system rules. The system constraint is the parameter 'Expected time for production' – in the given model, it is set to 40 hours, and if exceeded, overtime hours accumulate, immediately regulating or temporarily halting the flow of 'queen rearing.

RESULTS AND DISCUSSION

In the Results section, 4 different production capacities will be examined to demonstrate the varying behaviour of the system dynamics model, which helps make decisions regarding production capacity planning.

Capacity: 200 queen bees per week and 200 mating nuclei (Fig. 2)

If a beekeeper has access to 2 apiaries, it is possible to gradually create 200 mating nuclei during the season, where new queen bees will be introduced. The plan is to rear 200 queen bees per week, meaning 200 new virgin queens will be born every week. The newly emerged queens will be added to the nuclei, from which, after 3 weeks, mated, laying and tested queen bees will be available. The surplus of virgin queens and mated, laying, tested queens are sold. Fig. 2, a illustrates the model's behaviour, where resources are utilized efficiently: all gradually created 200 mating nuclei are continuously filled with new queens throughout the entire season, and queen rearing occurs without interruptions, providing 200 virgin queens a week. Initially, in the first 4 weeks (May), there are significant surpluses of virgin queens, but during this period, there is the highest demand in the market for virgin queens, as mated queen bees appear in the market only at the end of May. Queen bee rearing is halted by the 13th week because, by the end of July, the colonies lose their swarming tendency, the season's peak nectar flows have ended, and the colonies refuse to rear queens intensively. The production capacity of 200 queens per week does not exceed 40 working hours per week (Fig. 2, b). Maximum time spent on production in this case is 27.1 hours/week. Queen rearing consumes 2.4 hours, queen bee packaging 8 hours, hive inspections 6.7 hours, and mating nuclei inspections reach 10 hours per week. Under ideal conditions with such capacity, it is possible to produce 1.42 thousand virgin queen bees and 471 laying queens (Fig. 2, c). The model predicts that all queen bees are sold (8 EUR/virgin queen, 22 EUR/laying queen), regardless of demand changes that may affect the circulation of queen bees in the system. Accordingly, with the selected production capacity, it is possible to cover the costs of maintaining bee colonies (100 EUR/colony) and mating nuclei maintenance costs

(20 EUR/nuclei) for the year, as well as provide seasonal salaries, resulting in forecasted surplus funds of 11.2 thousand EUR to cover additional expenses and investments (Fig. 2, d).

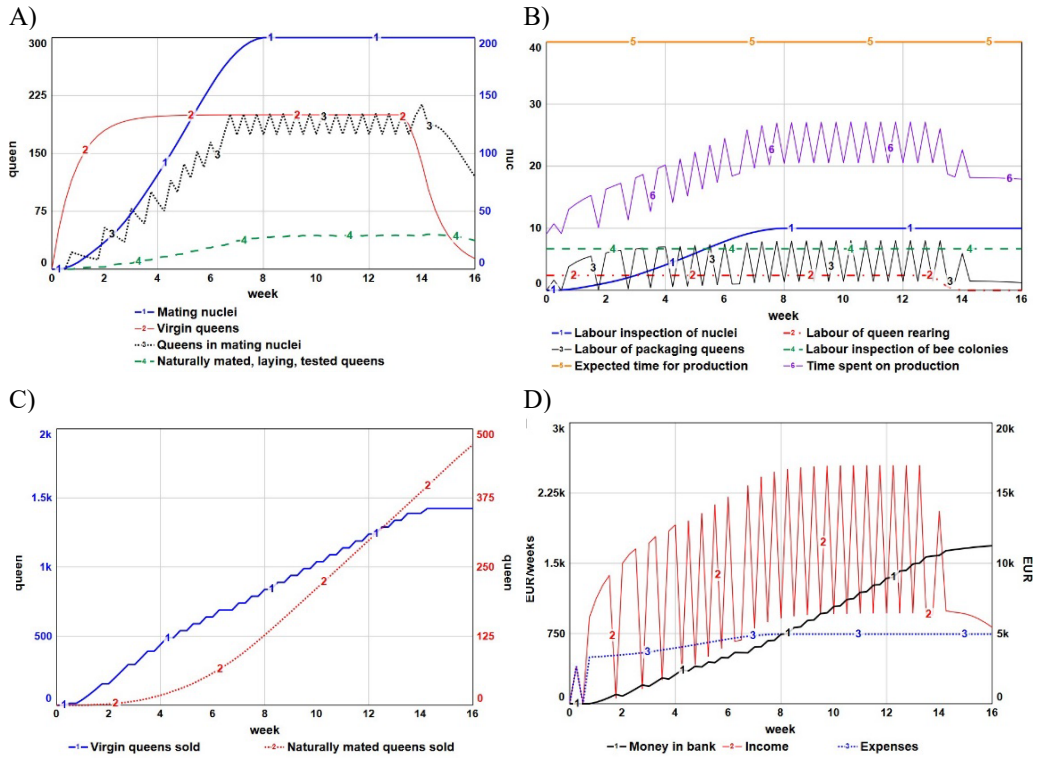

Figure 2. Simulation of the model behaviour by software *Stella Architect.* Production capacity (A), time resource consumption (B), the number of sold queen bees (C) and profit (D): rearing 200 queen bees per week, creating and maintaining 200 mating nuclei over a 16-week period with a 40-hour workweek.

Capacity: 300 queen bees per week and 300 mating nuclei (Fig. 3)

If beekeepers have access to additional apiaries and can increase queen rearing capacity, the system quickly reaches and exceeds 40 hours of production per week, hindering operations and temporarily or permanently interrupting queen rearing (Fig. 3, a, b). For example, by creating and maintaining 300 mating nuclei and rearing 300 queen bees per week, a beekeeper in the second half of the season, after 8 weeks, may encounter overtime hours, reaching 40.5 hours/week (Fig. 3, a, b). In this case, compared to the previous situation, work hours have increased in all positions: queen rearing consumes 3.6 hours, queen bee packaging 11.9 hours, hive inspection 10 hours, and nuclei inspection 15 hours. As the overtime hours are minimal, the system can be maintained functional until the end of the season by periodically suspending new queen rearing. With such capacity, it is possible to produce 1.9 thousand virgin queens and 713 laying queens during the season. Similar to the previous case, with a production capacity of 300 queen bees per week and 300 mating nuclei, it is possible to cover expenses

(994 EUR/week) and ultimately obtain surplus funds amounting to 17 thousand EUR. Of course, it should be noted that in this case, the system balances on the predicted production time limit of 40 working hours per week. As adjustments in the beekeeping process can be influenced by other external factors, it would be risky for a real farm to choose this option. With additional work appearing on the farm, the volume of overtime will definitely increase, and it may no longer be possible to effectively maintain the established queen rearing and mating system with only a few interruptions in queen rearing.

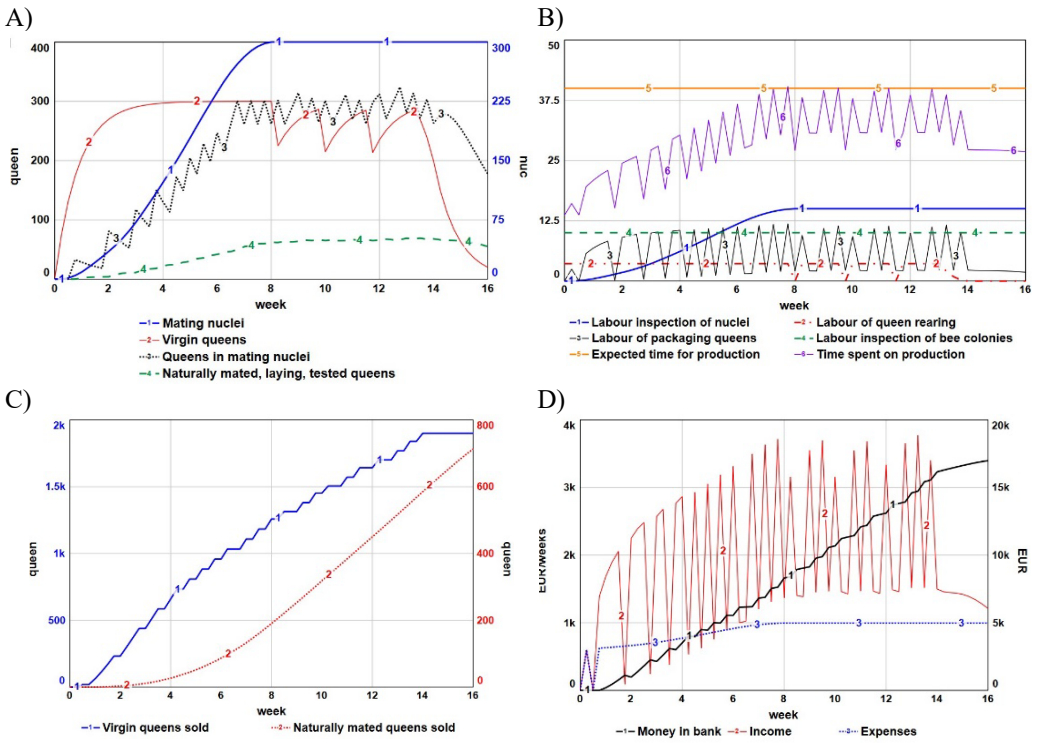

Figure 3. Simulation of the model behaviour by software *Stella Architect.* Production capacity (A), time resource consumption (B), the number of sold queen bees (C) and profit (D): rearing 300 queen bees per week, creating and maintaining 300 mating nuclei over a 16-week period with a 40-hour workweek.

Capacity: 400 queen bees per week and 400 mating nuclei (Fig. 4)

Increasing production capacity to 400 queen bees per week and 400 mating nuclei, the model shows that problems will arise in maintaining the system as early as the 4th week. In the fourth week, for the first time, 40.4 working hours are reached, and the rearing of new queen bees is interrupted (Fig. 4, b). With a larger production system, mating nuclei are formed from more bee colonies. It consumes more time for inspections than in previous cases with lower production capacity, i.e., 13.4 hours for 60 bee colonies. Queen rearing takes 4.8 hours per week, and queen packaging takes 14 hours per week. In total, for these three positions, it amounts to 32.2 hours per week. However, by establishing only a fraction of the intended mating nuclei, overtime hours rapidly

accumulate. It takes 20 working hours to inspect all 400 nuclei. In total, the necessary working hours to maintain the system would be 52.2 hours per week. However, in such a system with the corresponding amount of overtime, it is not possible to either resume queen rearing or fill all the created mating nuclei (Fig. 4, a). In case of overload, the number of produced queens also decreases (Fig. 4, c): by the 8th week, 1.34 thousand virgin queens are produced, after which there are no more virgin queens, but the number of produced laying queen bees is 886. Although production in this situation is inefficient, it is still possible to cover expenses and generate surplus funds of 12.9 thousand EUR (Fig. 4, d), which is significantly less than maintaining the system with 300 nuclei and 300 queen bees per week. In this capacity, the main consequence is the unnecessary maintenance of mating nuclei, which cannot be provided with new queen bees, resulting in the waste of bee resources.

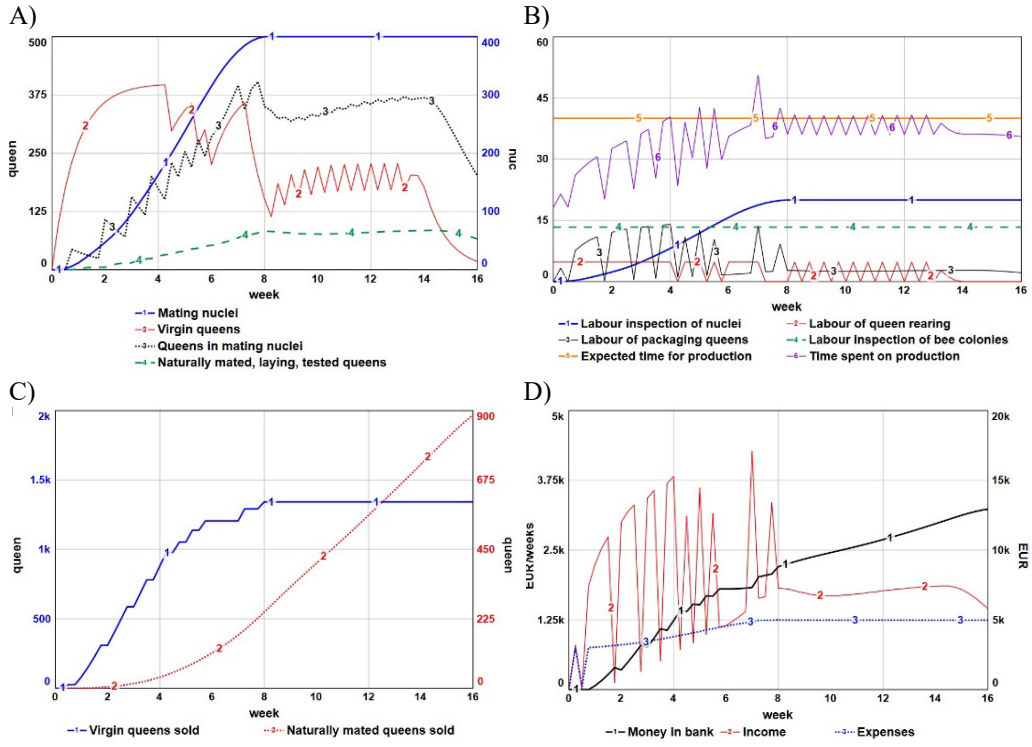

Figure 4. Simulation of the model behaviour by software *Stella Architect*. Production capacity (A), time resource consumption (B), the number of sold queen bees (C) and profit (D): rearing 400 queen bees per week, creating and maintaining 400 mating nuclei over a 16-week period with a 40-hour workweek.

Capacity: 500 queen bees per week and 500 mating nuclei (Fig. 5)

Increasing production capacity to 500 queen bees per week and 500 mating nuclei inevitably results in the first signs of inability to sustain such a volume, appearing as early as the 2nd week, while around the 6th to 7th week, the system completely and irreversibly collapses (Fig. 5, a, b). It requires 16.7 hours for maintaining bee colonies, 6 hours for queen rearing, 15.7 hours for queen packaging, and 25 hours per week for

maintaining all planned mating nuclei. At least 63.4 working hours per week are required to maintain such a system. The collapse of the system also reflects on the low number of produced queens for the chosen capacity (Fig. 5, c) and financial resources, running out by the 15th week (Fig. 5, d).

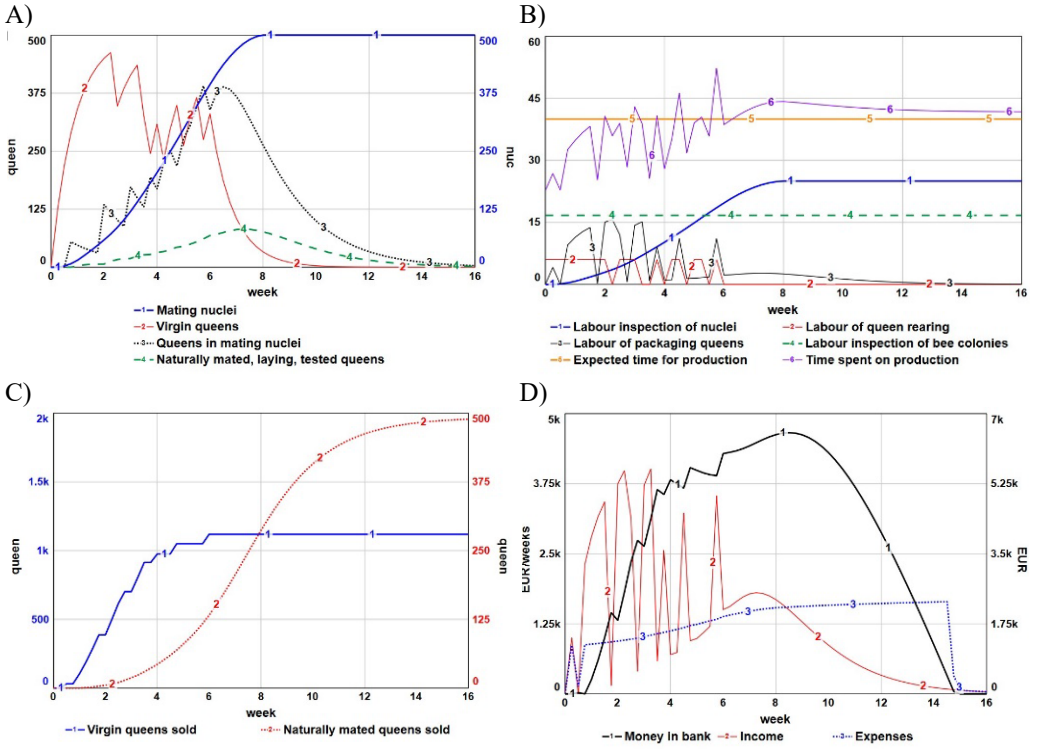

Figure 5. Simulation of the model behaviour by software *Stella Architect.* Production capacity (A), time resource consumption (B), the number of sold queen bees (C) and profit (D): rearing 500 queen bees per week, creating and maintaining 500 mating nuclei over a 16-week period with a 40-hour workweek.

The four scenarios described above illustrate what happens when an excessively large production capacity is chosen at the beginning of the beekeeping season, where the first signs appear when there is a shortage of time resources and what are the consequences of such decisions. Of course, in real life, after realizing that it is not possible to maintain the chosen production system, an alternative option can be selected: either hiring additional staff or reducing the production system's capacity to keep it functional until the end of the season, but making changes during the season also requires additional time. The model demonstrates that depending on the chosen production capacity (reared queens per week and maintained mating nuclei), the first signs or the first overtime hours may develop after 2, 4, or even 8 weeks after starting production, which may not be initially apparent. Therefore, modeling allows to plan for an appropriate production capacity before the season starts with a reserve of working hours necessary for unforeseen circumstances or to make timely decisions about hiring additional labour.

However, it should be noted that the specific model simulates the flow of queen bees without taking into account the prolonged adverse effects of weather conditions. If the weather conditions are consistently unfavourable (wind, rain, temperature below +20 °C), queen bees will be unable to go on nuptial flights, significantly delaying the circulation of queen bees in the nuclei and creating an excessive supply of virgin queens. Additionally, after the age of 14 days, the mating quality of the queen bee decreases; the queen bee may accumulate less sperm, resulting in a shorter lifespan (Cobey, 2013). Although the model already includes the assumption that 30% of queen bees will not be accepted or will be lost during mating flights (Smilga-Spalvina et al., 2024), in prolonged unfavourable weather conditions and periods of interrupted nectar yield, this percentage may be significantly higher.

CONCLUSIONS

System dynamics modeling is one of the precise tools in beekeeping that allows modeling the production process in software applications. Modeling helps to understand the production process in detail and make decisions about possible production capacities with the resources available to the beekeeper. It helps to identify weaknesses in the production process, for example, the time-consuming stages such as queen rearing, packaging of queens, inspection of bee colonies, and inspection of nuclei. To reduce time consumption in packaging of queens, packaging types can be changed, such as using wooden or plastic boxes for queen bees with accompanying worker bees, or employing padded envelopes or cardboard boxes for shipping. If too much time is spent on inspecting mating nuclei, where the acceptance, laying, and checking of brood take place, it may be necessary to reconsider the design of the nuclei or change the method of introducing queens to the nuclei (using queen cells or introducing a marked virgin queens).

The queen bee rearing model in the article demonstrates that with limited labour resources of 40 hours per week, it is possible to efficiently maintain 200 mating nuclei and rear 200 queen bees per week consistently without interruptions, utilizing the maximum capacity of the system. Of course, in this scenario, there remains a 32% reserve of time, which can be utilized by slightly increasing capacity or kept unused for unforeseen circumstances that may arise due to weather conditions, errors in planning and beekeeping practices, or variable demand. On the other hand, if the capacity is chosen to be too large, resources are inefficiently utilized, and it becomes impossible to temporarily halt the rearing of new queen bees and restore the system to its previous state. In such a case, quick solutions would be to reduce production capacity (the number of reared queen bees and mating nuclei) or to hire additional labour, which could be challenging during the season. To avoid overload, it is recommended to conduct planning before the season, including a buffer of working hours to address unforeseen circumstances, for example, prolonged unfavourable weather conditions and rapid changes of demand that will delay the circulation of queens.

REFERENCES

Barlas, Y. 1996. Formal aspects of model validity and validation in system dynamics. *System Dynamics Review: The Journal of the System Dynamics Society* **12**(3), 183–210.

Bartlett, L.J., Rozins, C., Brosi, B.J., Delaplane, K.S., de Roode, J.C., White, A., ... & Boots, M. 2019. Industrial bees: The impact of apicultural intensification on local disease prevalence. *Journal of Applied Ecology* **56**(9), 2195–2205. doi: 10.1111/1365-2664.13461

Becher, M.A., Grimm, V., Thorbek, P., Horn, J., Kennedy, P.J. & Osborne, J.L. 2014. BEEHAVE: a systems model of honeybee colony dynamics and foraging to explore multifactorial causes of colony failure. *Journal of applied ecology* **51**(2), 470–482.

Büchler, R., Andonov, S., Bienefeld, K., Costa, C., Hatjina, F., Kezic, N., Kryger, P., Spivak, M., Uzunov, A. & Wilde, J. 2013) 'Standard methods for rearing and selection of Apis mellifera queens,' *J. Apic. Res.* **52**(1). doi: 10.3896/IBRA.1.52.1.07

Cobey, S.W. 2007. Comparison studies of instrumentally inseminated and naturally mated honey bee queens and factors affecting their performance. *Apidologie* **38**(4), 390–410.

Cobey, S.W., Tarpy, D.R. & Woyke, J. 2013. 'Standard methods for instrumental insemination of Apis mellifera queens,' *J. Apic. Res*. **52**(4). doi: 10.3896/IBRA.1.52.4.09

Danieli, P.P., Addeo, N.F., Lazzari, F. Manganello, F. & Bovera, F. 2023. 'Precision Beekeeping Systems: State of the Art, Pros and Cons, and Their Application as Tools for Advancing the Beekeeping Sector.' *Animals*, vol., **14**(1), 70. doi: 10.3390/ani14010070

DeGrandi-Hoffman, G. & Curry, R. 2004. A mathematical model of Varroa mite (Varroa destructor Anderson and Trueman) and honeybee (*Apis mellifera* L.) population dynamics. *International Journal of Acarology* **30**(3), 259–274. doi: 10.1080/01647950408684393

Forrester, J.W. 1994. System dynamics, systems thinking, and soft OR. *System dynamics review*, **10**(2–3), 245–256. doi: 10.1002/sdr.4260100211

Gilioli, G., Simonetto, A., Hatjina, F. & Sperandio, G. 2018. Multi-dimensional modelling tools supporting decision-making for the beekeeping sector. *IFAC-PapersOnLine* **51**(5), 144–149. 10.1016/j.ifacol.2018.06.225

Gill, R.A. 1996. The Benefits to the Beekeeping Industry and Society from Secure Access to Public Lands and Their Melliferous Resources: Report to the Honeybee Research and Development Council of Australia. *Resource Systems Management Consulting.*

Hadjur, H., Ammar, D. & Lefèvre, L. 2022. Toward an intelligent and efficient beehive: A survey of precision beekeeping systems and services. *Computers and Electronics Agriculture* **192**. doi: 10.1016/j.compag.2021.106604

Hempel, M. 2022. BeeWare! A honeybee colony model - Exploring the mechanisms of early spring colony collapse. *The 2022 System Dynamics Conference.* Available at https://proceedings.systemdynamics.org/2022/supp/S1100.pdf. Accessed 30.01.2024

The 2022 System Dynamics Conference - Frankfurt Germany. Available: https://proceedings.systemdynamics.org/2022/supp/S1100.pdf [Accessed 30.01.2024.]

Khoury, D.S., Barron, A.B. & Myerscough, M.R. 2013. Modelling food and population dynamics in honey bee colonies. *PloS one* **8**(5), e59084. doi: 10.1371/journal.pone.0059084

Klavins, A. 2024. Latvian nature. Encyclopedia of species (Encyclopedia of species. Published by Gandrs Llc. Available at https://www.latvijasdaba.lv. Accessed 20.01.2024. (in Latvian).

Komasilova, O., Komasilovs, V., Kviesis, A., Bumanis, N., Mellmann, H. & Zacepins, A. 2020. Model for the bee apiary location evaluation. *Agronomy Research* **18**(S2), 1350–1358. doi: 10.15159/AR.20.090

Myerscough, M.R., Khoury, D.S., Ronzani, S. & Barron, A.B. 2017. Why do hives die? Using mathematics to solve the problem of honey bee colony collapse. In *The Role and Importance of Mathematics in Innovation: Proceedings of the Forum 'Math-for-Industry'* 35–50, Springer Singapore. doi: 10.1007/978-981-10-0962-4_4

Oxley, P.R. &. Oldroyd, B.P. 2010. The Genetic Architecture of Honeybee Breeding. *Adv Insect Physiol* **39**, 83–118. doi: 10.1016/S0065-2806(10)39003-5

Page, Jr, R.E. & Peng, C.Y.S. 2001. Aging and development in social insects with emphasis on the honey bee, Apis mellifera L. *Experimental gerontology* **36**(4–6), 695–711. doi: 10.1016/S0531-5565(00)00236-9

Paiva, J.P.L.M., Paiva, H.M., Esposito, E. & Morais, M.M. 2016. On the effects of artificial feeding on bee colony dynamics: a mathematical model. *PloS one* **11**(11), e0167054. doi: 10.1371/journal.pone.0167054

Pilati, L., Daris, R., Prestamburgo, M. & Sgroi, F. 2018. Modeling sequential production: The migratory beekeeper case. *Calitatea-Acces la Succes* **19**(162), 146–154.

Russell, S., Barron, A.B. & Harris, D. 2013. Dynamic modelling of honey bee (*Apis mellifera*) colony growth and failure. *Ecological Modelling* **265**, 158–169. doi: 10.1016/j.ecolmodel.2013.06.005

Senge, P.M. & Forrester, J.W. 1980. Tests for building confidence in system dynamics models. *System dynamics, TIMS studies in management sciences* **14**, 209–228.

Smilga-Spalvina, A., Spalvins, K. & Veidenbergs, I. 2024. Field study: Factors influencing virgin queen bee acceptance rate in Apis mellifera colonies. *Czech J. Anim. Sci.* **69**(4). doi: https://doi.org/10.17221/22/2024-CJAS

SRS (State Revenue Service of Latvia). 2023. Information about jobs in 2023 according to the profession classification. Available at https://www.vid.gov.lv/lv/informacija-par-darba-vietam-2023gada-atbilstosi-profesiju-klasifikatoram. Accessed 30.01.2024 (in Latvian).

Zacepins, A., Brusbardis, V., Meitalovs, J. & Stalidzans, E. 2015. Challenges in the development of Precision Beekeeping. *Biosyst. Eng.* **130**, 60–71. doi: 10.1016/j.biosystemseng.2014.12.001

Zacepins, A., Kviesis, A., Pecka, A. & Osadcuks, V. 2017. Development of Internet of Things concept for Precision Beekeeping. In Popescu, D., Sendrescu, D., Roman, M., Popescu, E., Barbulescu, L. (eds): *2017 18th International Carpathian Control Conference (ICCC),* IEEE, Sinaia, Romania, pp. 23–27, doi: 10.1109/CarpathianCC.2017.7970365

Zacepins, A., Ozols, N., Kviesis, A., Gailis, J., Komasilovs, V., Komasilova, O. & Zagorska, V. 2022. Evaluation of the honey bee colonies weight gain during the intensive foraging period. *Agronomy Research* **20**(2), 457–468. doi: 10.15159/AR.22.017

ANNEXES

Annex 1. Parameters and equations that represent functional relationships in a system dynamic model

Parameters	Equation	Units
Mating_nuclei (t)	Mating_nuclei (t - dt) + (Formation_of_nuclei) * dt; INIT Mating_nuclei = 0	nuclei
Money_in_bank (t)	Money_in_bank (t - dt) + (Income - Expenses) * dt; INIT Money_in_bank = 0	EUR
Naturally_mated_queens_sold (t)	Naturally_mated_queens_sold (t - dt) + (Sale_of_naturally_mated_queens) * dt; INIT Naturally_mated_queens_sold = 0	queen
Naturally_mated_laying_tested_queens (t)	Naturally_mated_laying_tested_queens (t - dt) + (Successful_nuptial_flight - Sale_of_naturally_mated_queens) * dt; INIT Naturally_mated_laying_tested_queens = 0	queen
Production_overtime (t)	Production_overtime (t - dt) + (Time_spent_on_production - Time_has_passed) * dt; INIT Production_overtime = 0	hour
Queens_in_mating_nuclei (t)	Queens_in_mating_nuclei (t - dt) + (Addition_of_virgin_queens_to_mating_nuclei - Successful_nuptial_flight - Mortality_of_acceptance_or_failure_of_mating) * dt; INIT Queens_in_mating_nuclei = 0	queen
Virgin_queens (t)	Virgin_queens (t - dt) + (Queen_rearing/grafting - Sale_of_virgin_queens - Addition_of_virgin_queens_to_mating_nuclei) * dt; INIT Virgin_queens = 0	queen
Virgin_queens_sold (t)	Virgin_queens_sold (t - dt) + (Sale_of_virgin_queens) * dt; INIT Virgin_queens_sold = 0	queen
Addition_of_virgin_queens_to_mating_nuclei	(IF Queens_in_mating_nuclei < Mating_nuclei THEN Virgin_queens ELSE 0)	queen/ week
Expenses	Expenses_for_wages_a_week + Expenses_bee_colonies_a_week + Expenses_for_nuclei_a_week	EUR/ week
Formation_of_nuclei	IF Bee_colonies * Formation_of_nuclei_factor/ Number_of_apiaries > Density_of_nuclei_in_one_apiary THEN Density_of_nuclei_in_one_apiary * Number_of_apiaries ELSE Bee_colonies * Formation_of_nuclei_factor	nuc/ week
Income	Income_from_the_sale_of_virgin_queens + Income_from_the_sale_of_naturally_mated_queens	EUR/ week
Mortality_of_acceptance_or_failure_of_mating	Queens_in_mating_nuclei * Mortality_rate	queen/ week
Queen_rearing/grafting	Total_grafting_places_for_rearing * Virgin_production_factor_(grafting_every_5_days) * Overtime_effect_on_queen_rearing	queen/ week
Sale_of_naturally_mated_queens	Naturally_mated_laying_tested_queens	queen/ week
Sale_of_virgin_queens	Surplus_of_virgin_queens	queen/ week
Successful_nuptial_flight	Queens_in_mating_nuclei * Ratio_of_mating_success * Time_for_laying_and_tested_queen	queen/ week
Time_has_passed	Expected_time_for_production	hour/ week
Time_spent_on_production	Labour_inspection_of_nuclei + Labour_inspection_of_bee_colonies + Labour_of_queen_rearing + Labour_of_packaging_queens	hour/ week
Bee_colonies	Density_of_bee_colonies_in_one_apiary * Number_of_apiaries	bee colony
Count_of_mating_nuclei	400 (user defined)	nuclei
Density_of_bee_colonies_in_one_apiary	20	bee colony/ apiary
Density_of_nuclei_in_one_apiary	100	nuc/ apiary

Expected_time_for_ production	40 (user defined)	hour
Expenses_bee_colonies_a_week	Bee_colonies * Expenses_for_one_bee_colony_a_week	EUR/ week
Expenses_for_nuclei_a_ week	Mating_nuclei * Expenses_for_one_nuc_a_week	EUR/ week
Expenses_for_one_bee_ colony_a_week	100/16	EUR/ bee colony/ week
Expenses_for_one_nuc_a_ week	20/16	EUR/ nuc/ week
Expenses_for_wages_a_ week	Labor_a_week * Gross_labor_wage_rate	EUR/ week
Formation_of_nuclei_ factor	GRAPH(TIME) Points: (0.00, 0.000), (1.00, 0.400), (2.00, 0.500), (3.00, 0.800), (4.00, 0.900), (5.00, 1.000), (6.00, 0.900), (7.00, 0.500), (8.00, 0.000), (9.00, 0.000), (10.00, 0.000), (11.00, 0.000), (12.00, 0.000), (13.00, 0.000), (14.00, 0.000), (15.00, 0.000), (16.00, 0.000)	percent
Gross_labor_wage_rate	6.10	EUR/ hour
Income_from_the_sale_of_naturally_mated_queens	Price_of_naturally_mated_queen * Sale_of_naturally_mated_queens	EUR
Income_from_the_sale_of_virgin_queens	Price_of_virgin_queen * Sale_of_virgin_queens	EUR/ week
Labour_inspection_of_ bee_colonies	Bee_colonies * Labour_inspection_of_one_bee_colony	hour/ week
Labour_inspection_of_ nuclei	Labour_inspection_of_one_nuc * Mating_nuclei	hour/ week
Labour_inspection_of_one _bee_colony	0.167	hour/ bee colony/ week
Labour_inspection_of_one_ nuclei	0.05	hour/ nuc/ week
Labor_a_week	Expected_time_for_production + Production_overtime	hour/ week
Labor_of_queen_rearing	Queen_rearing/grafting *Labor_of_queen_rearing_one_unit	hour/ week
Labor_of_queen_rearing_ one_unit	GRAPH(TIME) Points: (0.00, 0.012), (1.00, 0.012), (2.00, 0.012), (3.00, 0.012), (4.00, 0.012), (5.00, 0.012), (6.00, 0.012), (7.00, 0.012), (8.00, 0.012), (9.00, 0.012), (10.00, 0.012), (11.00, 0.012), (12.00, 0.012), (13.00, 0.012), (14.00, 0.000), (15.00, 0.000), (16.00, 0.000)	hour/ queen/ week
Labour_of_packaging_ one_queen	0.033	hour/ queen/ week
Labour_of_packaging_ queens	Number_of_sold_queens * Labour_of_packaging_one_queen	hour/ week
Mortality_rate	0.3	percent
Number_of_apiaries	Count_of_mating_nuclei/100	apiary
Number_of_grafting_places _in_one_rearing_colony	40	place
Number_of_rearing_ colonies	Planned_queens_per_week/40	bee colony
Number_of_sold_queens	Sale_of_virgin_queens + Sale_of_naturally_mated_queens	queen
Overtime_effect_on_ queen_rearing	IF Production_overtime >0 THEN 0 ELSE 1	percent
Planned_queens_per_week	400 (user defined)	queen
Price_of_naturally_mated_ queen	22	EUR/ queen
Price_of_virgin_queen	8	EUR/ queen
Ratio_of_mating_success	0.7	percent
Surplus_of_virgin_queens	IF Virgin_queens > Addition_of_virgin_queens_to_mating_nuclei THEN Virgin_queens - Addition_of_virgin_queens_to_mating_nuclei ELSE 0	queen
Time_for_laying_and_ tested_queen	0.33	week

Annex1 (continued)

Total_grafting_places_for_rearing	Number_of_rearing_colonies * Number_of_grafting_places_in_one_rearing_colony	place
Virgin_production_factor	GRAPH(TIME) Points: (0.00, 1.000), (1.00, 1.000), (2.00, 1.000), (3.00, 1.000), (4.00, 1.000), (5.00, 1.000), (6.00, 1.000), (7.00, 1.000), (8.00, 1.000), (9.00, 1.000), (10.00, 1.000), (11.00, 1.000), (12.00, 1.000), (13.00, 1.000), (14.00, 0.000), (15.00, 0.000), (16.00, 0.000)	percent

Annex 2. Run Specs for model in software *Stella Arhitect*

Run Specs	Value	Run Specs	Value
Start Time	0	Pause Interval	0
Stop Time	16	Integration Method	Euler
DT	1/4	Keep all variable results	True
Fractional DT	True	Run By	Run
Save Interval	0.25	Calculate loop dominance information	True
Sim Duration	1.5	Exhaustive Search Threshold	1000
Time Units	week		

Agronomy Research **22**(1), 301–312, 2024
https://doi.org/10.15159/AR.24.001

Influence of feeding area on development, productivity and nutritional value of chicory

O. Tkach[1], H. Pantsyreva[2,*], O. Ovcharuk[3], V. Ovcharuk[1], T. Padalko[1], L. Tkach[1] and O. Amorcite[1]

[1]Higher Educational Institution 'Podillia State University', Department of postgraduate studies, Shevchenko, 12, UA 32316 Kamianets-Podilskyi, Ukraine
[2]Vinnytsia National Agrarian University, Faculty of Agronomy and Forestry, Sonyachna street, 3, UA21008 Vinnytsia, Ukraine
[3]National University of Life and Environmental Sciences of Ukraine, agrobiological Faculty, Heroiv Oborony, 15, UA03041 Kyiv, Ukraine
[*]Correspondence: apantsyreva@ukr.net

Received: March 19th, 2023; Accepted: August 16th, 2023; Published: December 15th, 2024

Abstract. One of the main agrotechnical measures, which largely depends on the yield and quality of root chicory, is the correct placement of plants on the area. With different methods of sowing, placement schemes make it possible to ensure favorable conditions for plant growth and development and the maximum use of mechanization during the period of care for crops and harvesting. It was determined that the structure of the feeding area of the root chicory plant affects photosynthetic productivity. Therefore, the highest indicators of the net productivity of photosynthesis were distinguished by the placement of plants on the feeding area according to the scheme 45×22.5 cm and 22.5×45 cm, which had a positive effect on the yield of root crops and their content of inulin polysaccharide. The article presents the results of experimental studies that solve the scientific and practical problem of studying the elements of root chicory growing technology due to the optimization of the area of plant nutrition and the uniformity of their placement on productivity and quality indicators. It has been experimentally proven that with an increased rate of photosynthetic potential at a feeding area of 60×60 cm (with a plant density of 30,000 ha, the Umansky-97 variety was 9.2 $10^3 \times m^{-2}$ ha^{-1} per day, Umansky-99 - 9.3 $10^3 \times m^{-2}$ ha^{-1} per day with a decrease in the feeding area (45×45, 35×35, 45×22.5 cm), this indicator slightly increased, on average by variety, it was 10.1 to 10.8 $10^3 \times m^{-2}$ ha^{-1} per day. The highest indicator of inulin content in chicory root crops is the feeding area of 35×35 cm and was in the variety Umansky-97 - 18.5%, Umansky-99 - 18.7%, and the feeding area of 45×22.5 cm - 18.2% and 18.4%, respectively. Similarly, it was recorded that the feeding area of chicory plants significantly affects the yield of root crops. Thus, it was established that from a plant density of 60 to 120 $10^3 \times$ ha^{-1}, the productivity was on average 30 t ha^{-1} with an average weight of the root crop from 500 to 250 g, with an inulin content of 17.3 to 19.0%. According to the structure of the root crop, the productive part occupies on average from 82.7% to 91.6% of the total mass with inulin content from 17.3 to 19.0%.

Key words: root chicory, feeding area, variety, photosynthetic productivity, quality indicators.

INTRODUCTION

The soil and climatic conditions of the Right Bank Forest-Steppe of Ukraine differ significantly among themselves, which makes it necessary to sow root chicory at different times, because they are an important element of cultivation technology. Well-chosen sowing dates make it possible to obtain friendly seedlings, ensure the optimal onset of plant growth and development phases, uniform ripening of the crop and its suitability for long-term storage, while maintaining high quality indicators. A delay in sowing leads to a decrease in seed germination and a subsequent decrease in the yield. Also, the conducted studies established that the delay in sowing leads to the thinning of crops, unfriendly chicory seedlings due to the increase in soil temperature and loss of moisture at the depth of seed wrapping (Petrychenko et al., 2018; Tokarchuk et al., 2020; Honcharuk, et al., 2022).

The majority of scientists believe that the optimal conditions are when the seeds are placed at the depth of hard, dense soil with available moisture, while the top layer is loose, with good aeration. For this, it is important to correctly choose the calendar dates for sowing, taking into account the nature of the weather and climate conditions of the region, especially the spring period, the type of soil and the biological characteristics of the variety (Baranovsky & Potapenko, 2017; Ferrare et al., 2018; Hnatiuk et al., 2018; Reimer et al., 2020; Ebrahimi, et al., 2022).

Due to the warming observed in recent years, sowing too early in waterlogged, immature soil can usually lead to seed rot, disease damage and significant crop thinning. Scientists claim that the optimal time for sowing root chicory comes when the soil temperature at a depth of 2–3 cm 99 reaches 12–15 ℃, and the soil is physically fertile. They also noted that the timing of sowing is related to the quality of soil preparation. High-quality soil cultivation is achieved with optimal humidity. When determining the timing of sowing, it is necessary to take into account not only the general soil and climatic conditions of the zone, but also the microclimate and topography of the field, the nature of the weather in spring, varietal characteristics and the method of preparing seeds for sowing. It is also important to note that in order to create the most favorable conditions for the appearance of friendly uniform chicory seedlings, their further development and the formation of a high yield, as well as the high-quality use of mechanization tools, the sowing of seeds should be carried out in the optimal agrotechnical terms, the optimal sowing rate and the depth of seed wrapping should be established (Barcaccia et al., 2016; Pouille et al., 2020; Mazur et al., 2021).

In the conditions of the Right Bank Forest-Steppe of Ukraine, one of the main conditions for increasing the yield and quality of marketable root chicory products is the use of purposeful elements of cultivation technology, one of them is the area of plant nutrition taking into account the varietal characteristics of the culture and natural and climatic resources. Taking into account the main elements of the root chicory growing technology, the presented research results are characterized by relevance. They consist in the scientific, theoretical and practical improvement of the study of the area of nutrition, which is based on the analysis of the laws of the formation of productivity, indicators of the quality of root crops and growing conditions.

MATERIALS AND METHODS

In the conditions of the Right Bank Forest-Steppe of Ukraine in recent years, not fully favorable weather and climatic conditions for the potential productivity of root chicory plants have been formed. The research region is characterized by a sufficient amount of effective air and soil temperatures, with an insufficient amount of precipitation per year, and their uneven distribution by growing season.

The soil cover at the experimental sites of the Khmelnytskyi DSGDS of the ICSHP of the National Academy of Sciences of Ukraine, where field experiments were conducted in 2017–2020, is represented mainly by podzolized chernozem of coarse silt-medium loam composition. The thickness of the humus horizon reaches 100–120 cm, while the humus content (according to Tyurin) is 2.2–2.8%. The soil is moderately supplied with nutrients - total nitrogen (according to Kjeldahl) - 0.157–0.169%, mobile forms of phosphorus and potassium (according to Chirikov) 16.5 and 11.5 mg per 100 g of soil, respectively.

Weather conditions during the research period were different. The average daily air temperature during the growing season was higher than the long-term average by 2.7 °C, and the amount of precipitation exceeded the long-term average by only 33.8 mm, or 6.8%. A significant deficit of precipitation, and thus of productive moisture in the soil, was noted in the critical periods of root chicory growth and development (July - 73.0%, August - 16.5% to the average multi-year value).

Agricultural technology in experimental studies is generally accepted for the cultivation zone.

Root chicory seeds were sown according to the scheme: - square 35×35 cm, 45×45 cm, 60×60 cm; rectangles 45×22.5 cm, 45×(27 + 18) cm, 45×(40 + 27) cm; rhombic - 22.5×45 cm. Varieties: Umansky-97; Umansky-99. Scheme of the experiment: two-factorial in three repetitions.

RESULTS AND DISCUSSION

The possibility of increasing the productivity of root chicory crops by optimizing the density of planting plants and the uniformity of their placement on the feeding area has not yet been fully studied. In addition, there is insufficient scientific information about the reaction of modern chicory varieties to changes in the feeding area, both in terms of the length of the rows and the width of the rows. In this regard, a study was conducted to study the geometric structure of the plant feeding area and the optical properties of chicory crops as the main factors and their influence on photosynthetic productivity (Tkach, 2020; Ivanyshyn, 2021; Bondarenko et al., 2022).

Various studies confirm that in most cases, depending on the variety of chicory and the place of its cultivation, the carbohydrate complex of chicory (inulides + sugars) can have quite high indicators, which are close to the indicators of sugar beets, which are rich in dry matter content. Even the analysis of the chemical composition of chicory seeds and seeds does not give a complete idea of its composition. 42% is ash, water, nitrogenous compounds, fats and carbohydrates, and 58% should be fiber and soluble carbohydrates. The fat content in chicory seeds is quite high - 17.78%, which should warn farmers about the conditions and terms of storage of chicory seeds, because it is known that seeds with a high fat content lose their germination faster than seeds with a low fat content.

When growing chicory as an industrial plant, the chemical composition of the root and leaves (as valuable waste) is of primary importance (Mazur et al., 2019). Therefore, it is necessary to study in detail the chemical and technical characteristics of root chicory and analyze, if possible, changes in its composition, depending on the requirements of the industry. Chicory processing is currently focused on the production of coffee drinks, powdered medicinal and prophylactic products, the production of inulin and medical supplements. In the production of coffee drinks, the industry makes demands for an increased content of inulin, as the main nutritional and taste substrate, an increased content of intibin glucoside, which gives a specific coffee taste and aroma, and a reduced protein content. The sugar industry studies such matters as the percentage of inulin and other soluble carbohydrates that easily turn into sugars, as well as a small amount of intibin, which can give the juice a bitter taste, as well as a reduced protein content, since it is proteins that contribute to the formation of thick molasses, and this makes it harder for the sugar to be released. The alcohol industry, like the sugar industry, is interested in a high content of soluble carbohydrates, as the main raw material for alcohol, in a high content of soluble proteins, which is a nutrient medium for the development of yeast cultures during sugar fermentation, as well as a high content of phosphorus and potassium salts, necessary for successful yeast reproduction (Dragan et al., 2004; Das et al., 2016; Mazur et al., 2020; Tkach, 2020; Pantsyreva, 2021; Puyu et al., 2021).

All other conditions being equal, variants with the same feeding area, but with a different geometric shape, were included in the experimental schemes, which were conventionally classified according to the following characteristics: rectangular with the placement of one, two and three plants from the center of symmetry of the feeding area: rhombic with the placement of one plant in the center opposite spaces free of plants in adjacent rows and a square with the placement of plants in dense crops on adjacent rows (Sabzevari et al., 2010; Zayova et al., 2016).

In this regard, a study was conducted to study the geometric structure of the plant feeding area and the optical properties of chicory crops as the main factors and their influence on photosynthetic productivity (Lyashuk et al., 2018; Didur et al., 2019; Bhunia et al., 2021).

The variants with the placement of plants on the area (rectangular 45×22.5 cm and rhombic 22.5×45 cm) were distinguished by the highest indicators of the net productivity of photosynthesis, which had a positive effect on the yield of chicory root crops and their content of inulin polysaccharide, which had a uniform placement of plants with an interval 20×25 cm along the row, and wrapping the seeds to a depth of 1–1.5 cm. Also, the options with the placement of plants according to the rectangular 45×22.5 cm and rhombic 22.5×45 cm schemes differed in terms of the net productivity of photosynthesis (Table 1).

The study of the influence of the rational placement of plants (with the shape of the feeding area close to a square) on the productivity of root chicory deserved special attention. Observations were made with the set of geometric structures of crops, which were created in the form of a square shape of the feeding area for one plant - 35×35 cm, 45×45 cm, 60×60 cm and rectangular - 45×22.5 cm, it was established that crops with a square shape of the feeding area 35×35 cm and a plant density of 80,600 ha^{-1} ensured a greater collection of root crops, which is 1.4 t ha^{-1} higher compared to the variant (45×22.5 cm with a plant density of 100,000 ha).

Table 1. The influence of plant density, the size and shape of the feeding area on the photosynthetic potential (FP, $10^3\times$ m^{-2} days ha^{-1}) and the net productivity of photosynthesis (NPF, g m^{-2} leaf per day) (average for 2017–2020)

Indicator	The shape of the feeding area, cm^2 (Factor A)							
	60×60		45×45(c)*		35×35		45×22.5	
Plant density, $10^3\times$ ha^{-1}	30		50		80		100	
Feeding area, cm^2	3,600		2,025		1,225		1,012.5	
Seed variety (Factor B)	Umansky-97	Umansky-99	Umansky-97	Umansky-99	Umansky-97	Umansky-99	Umansky-97	Umansky-99
Accounting days	NPF, g m^{-2} leaf per day							
10.07	3.5	3.7	3.7	3.9	3.9	4.2	3.5	3.6
26.07	7.8	8.1	7.3	7.5	7.1	7.3	5.8	6.0
28.08	6.7	7.0	5.7	5.9	6.0	6.2	3.7	3.9
30.09	5.3	5.5	3.8	3.9	3.3	3.4	2.9	3.1
Accounting days	FP, $10^3\times$ m^{-2} days ha^{-1}							
10.07	0.6	0.7	1.0	1.1	1.3	1.5	1.2	1.4
26.07	2.7	2.9	3.1	3.3	3.5	3.7	3.2	3.5
28.08	5.8	6.0	6.8	7.1	7.6	7.7	7.4	7.5
30.09	9.2	9.3	9.8	10.1	10.6	10.8	10.2	10.4

Note: (c)* – control.

Thus, with an increase in the indicators of the net productivity of photosynthesis, it was noted in chicory plants 26.07 with a feeding area of 60×60 (plant density 30 $10^3\times$ ha^{-1}) in the Umansky-97 variety - 7.8 g m^{-2} leaf per day, Umansky-99 - 8.1 g m^{-2} leaf per day, in the future, the NPF indicator decreased.

However, the photosynthetic potential (FP) increased with the growth and development of plants, which was affected by the feeding area. Thus, with a feeding area of 60×60 (with a plant density of 30 $10^3\times$ ha^{-1}), the FP indicator for the period of 30.09 was 9.2 in the Umansky-97 variety, and 9.3 $10^3\times$ m^{-2} ha^{-1} in the Umansky-99 variety. With a decrease in the feeding area (45×45, 35×35, 45×22.5 cm) with a plant density of 50, 80 and 100 $10^3\times$ ha^{-1}, the FP indicator increases and on average by varieties was 10.1 to 10.8 $10^3\times$ m^{-2} ha^{-1} per day.

The analysis of the complex effect of the investigated factors showed that crops with a square shape of the feeding area (35×35 cm) and a plant density of 80 $10^3\times$ ha^{-1} ensured the collection of inulin by 6.1 t ha^{-1}, which is 0.9 t ha^{-1} more, compared to the area nutrition (45×22.5 cm with a plant density of 100 $10^3\times$ ha^{-1}) (Table 2).

In terms of yield of root crops, on average, during the years of research, the feeding area of 35×35 cm variety Umansky-97 was - 31.1 t ha^{-1}, Umansky-99 - 32.4 t ha^{-1}. With reduced yield indicators, the feeding area of 60×60 cm stands out, the Umansky-97 variety - 24.0 t ha^{-1}, Umansky-99 - 24.1 t ha^{-1}. An intermediate place is occupied by the feeding area of 45×45 cm (c) - 30.1 to 30.3 t ha^{-1} and 35×35 cm - 31.1 to 32.4 t ha^{-1}, respectively.

Table 2. Productivity of root chicory varieties depending on the shape of the plant nutrition area (average for 2017–2020)

Indicator	The shape of the feeding area, cm (Factor A)							
	square						rectangular	
	60×60		45×45(c)*		35×35		45×22.5	
	Seed variety (Factor B)							
	Umansky-97	Umansky-99	Umansky-97	Umansky-99	Umansky-97	Umansky-99	Umansky-97	Umansky-99
Yield of root crops, t ha^{-1}	24.0	24.1	30.1	30.3	31.1	32.4	27.5	28.7
Inulin content, %	16.7	16.8	17.7	17.9	18.5	18.7	18.2	18.4
Collection of inulin, t ha^{-1}	3.3	3.4	5.3	5.4	5.9	6.1	5.1	5.2

Note: (c)* – control.

The content of inulin in root crops also depended on the feeding area. With the highest indicator, the feeding area of 35×35 cm stands out and was 18.5% in the Umansky variety-97, 18.7% in the Umansky-99 variety, 18.2% and 18.4% in the 45×22.5 cm feeding area, in accordance. The intermediate place is occupied by the feeding area of 45×45 cm (c) with indicators of 17.7% and 17.9%, corresponding to the variety. With reduced indicators, the feeding area of 60×60 cm stands out and was 16.7% of the Umansky-97 variety - 16.8% of the Umansky-99 variety - 16.8%.

Also, experimental studies have established that for the formation of high productivity of root chicory crops, the uniformity of the distribution of plants on the area is of great importance and affects the development and average mass of the root crop (Table 3).

Table 3. The relationship between the density of root chicory plants Umansky-99 by qualitative characteristics (average for 2017–2020)

Indicator	Plant density, 10^3× ha^{-1}			
	60	80	100	120
The average mass of the root crop, g	500	375	300	250
Daily weight gain of the root crop, g	4.16	3.12	2.5	2.08
Inulin content, %	17.3	18.1	18.7	19.0
Collection of inulin, t ha^{-1}	5.19	5.43	5.64	5.7
Amount of dissolved ash, %	0.362	0.271	0.217	0.181
The ratio of the total mass of the root crop, % to the mass:				
head	12.3	9.5	7.1	5.1
productive part	82.7	84.2	87.2	91.6
actually the root	5.0	6.3	5.7	3.3

However, the larger the feeding area, the more significant the decrease in yield was observed. From the plant density of 60 and 120 10^3× ha^{-1}, the yield of root crops was 30.0 t ha^{-1}, the average weight of the root crop was 500 and 250 g, respectively; inulin content - 17.3 to 19.0%; inulin output - 5.19 and 5.7 t ha^{-1}. At the same time, root crops weighing more than 500 g made up almost 55% of the total mass of the crop in sparse sowing, and 13% in thickened sowing. At the same time, the experimental variety Umansky-99 was used.

It was established that an important indicator in the accumulation of quality indicators in chicory root crops is the productive part, which occupies an average of 82.7% (of the total mass) to 91.6%, regardless of plant density with a plant density of 60.000 ha^{-1} 12.3%, and the density of 120 $10^3\times$ ha^{-1} - 5.1%. A similar pattern is observed in the part of the root - the root itself, from 5.0 to 3.3%. From the total weight of the root crop, the head occupies a larger percentage in thinned sowing. This indicates that the content of inulin in root crops largely depends on the productive part of the root crop and on average at different densities was from 17.3% to 19.0%, with a harvest of 5.19 t ha^{-1} to 5.7 t ha^{-1}.

The analysis of the complex action of the studied factors showed that the average mass of root crops (Rk, g) depends on the density of plants (Sr, $10^3\times$ ha^{-1}) (Fig. 1). On average, over the years of research with an increased average mass of root crops, the density of plants was 60–80 $10^3\times$ plants per 1 ha, depending on the variety, was from 385 to 500 g. From a plant density of 120 $10^3\times$ ha^{-1}, the indicators of the average mass of root crops were from 235 g^{-1} to 250 g^{-1}, respectively varieties.

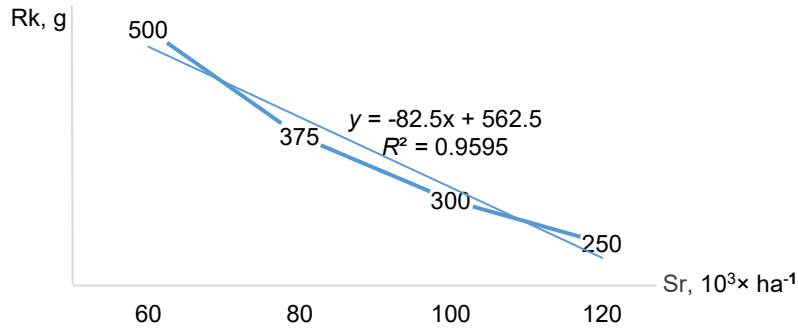

Figure 1. Dependence of the average root weight of root chicory (Rk, g) on plant density Sr, $10^3\times$ ha^{-1} (Average for 2017–2020).

The established analytical dependence between the density of chicory plants in the range of 60–120 10^3 ha^{-1}, and their qualitative indicators made it possible to realize the biological potential of plants in relation to the accumulation of root mass on the basis of a complex methodical approach. According to the assessment of the quality of chicory root crops, the content of inulin differed depending on the density of the plants (Fig. 2).

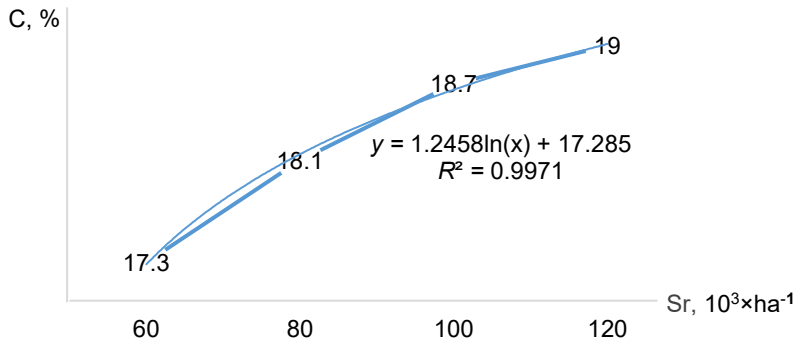

Figure 2. Dependence of the content of inulin in chicory roots (C, %) on the density of plants Sr, $10^3\times$ ha^{-1} (Average for 2017–2020).

The highest rate of inulin content was noted in root crops at a density of 120,000 plants ha^{-1} and averaged from 18.95 to 19.0%. The density of plants in general influenced and depended on the accumulation and collection of inulin from 1 ha (Fig. 3).

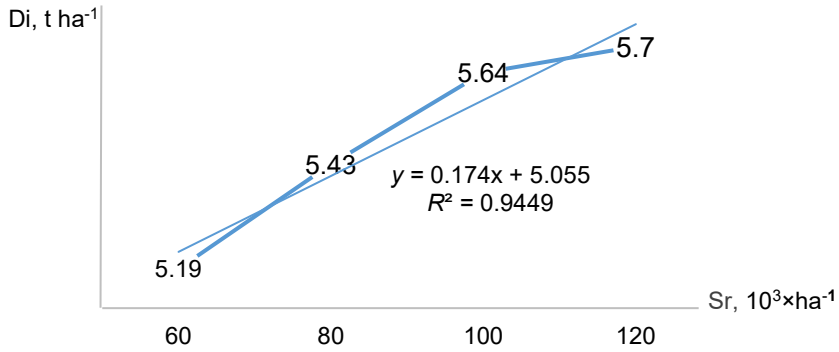

Figure 3. Dependence of inulin accumulation in root crops of root chicory (Di, t ha^{-1}) on plant density Sr, $10^3\times$ ha^{-1} (Average for 2017–2020).

Thus, the dependence of inulin collection in root crops with plant density from 60,000 ha^{-1} of plants to 120,000 ha^{-1} of plants from 5.12 t ha^{-1} to 5.75 t ha^{-1} was established, which confirms the dependence of this indicator on plant density.

According to the results of mathematical calculations, the dependence of the quality indicators of root chicory is shown in Table 4.

Table 4. Mathematical models of the dependence of quality characteristics of root chicory on the density of plants, Sr, $10^3\times$ ha^{-1} (average for 2017–2020)

Indicator	Regression equation	Multiple correlation coefficient, g	Coefficient of determination, R^2
Rk, g	y = -82.5x + 562.5	0.95	0.96
Dr, g	y = -0.686x + 4.68	0.98	0.96
C,%	y = 1.2458ln(x) + 17.285	0.96	0.99
D_i, t ha^{-1}	y = 0.174x + 5.055	0.97	0.94
D_a, %	y = -0.131ln(x) + 0.3618	0.98	0.99

Note Rk, g – mass of the root crop; D_r – daily increase in the mass of the root crop during the growing season, g; C – inulin content in root crops, %; D_i – collection of inulin polysaccharide from one hectare, t ha^{-1}; D_a – dissolved ash, %.

As the calculations show, between the quality indicators of root chicory and the density of plants - agrocenosis in the range of 60–120 $10^3\times$ha^{-1} with an almost constant yield of root crops of 30.0 t ha^{-1}, namely: the mass of the root crop; daily weight gain of the root crop during the growing season; there is an analytical dependence, which was determined by the equation of a linear function of the form:

$\bar{y} = a \times b^x$;

Between the content of inulin – C, %; output of dissolved ash – D_a, % – by the equation of a logarithmic curve of the form:

$\bar{y} = b \times log\, x - a$;

Indicators of the feeding area of the experimental plot of root chicory according to the distribution of the distance between root crops, the size, shape and aspect ratio of the feeding area, as well as the distribution of root crops in relation to size and weight and their significance in the formation of the crop according to the initial parameters before harvesting at a plant density of 90 10^3× ha^{-1}, root crops yield of 32 t ha^{-1} and vegetative mass of 19 t ha^{-1} of the Umansky-99 variety are shown in Table 5.

Table 5. Indicators of the feeding area and intervals between chicory roots of the Umansky-99 variety before harvesting (average for 2017–2020)

Indicator	Intervals between root crops, cm			
	0–15	15–30	30–45	45–60
Power area, $\frac{\text{см}^2}{\%}$	$\frac{337.5}{24.3}$	$\frac{1{,}012.5}{47.6}$	$\frac{1{,}687.5}{20.9}$	$\frac{2{,}362.5}{7.2}$
The shape of the feeding area, cm×cm	7.5×45	22.5×45	37.5×45	52.5×45
Aspect ratio of the feeding area, $K = \frac{L_p}{M}$	0.17	0.5	0.83	1.17

Note: L_p – distance between root crops in a row; M – row width 45 cm.

As a result of the research, it was established that the feeding area of root chicory plants, which was determined by the sowing structure under the existing cultivation technology with a row width of 45 cm at a plant density of almost 90 10^3×ha^{-1} (close to the optimum) varies within large limits (V = 64.5%), and the number of plants with placement at close intervals in a row (0–15 cm) and a feeding area of 337.5 cm reached 24.3%. This led to a decrease in the degree of illumination of the leaf apparatus (shading) of adjacent plants, as well as to a decrease in the net photosynthetic productivity (NPF). On the contrary, when placing plants at intervals of 40 cm with a feeding area of almost 2,000 cm, the net potential of photosynthesis increased. However, only 7.2% of plants were placed on such intervals. An increase in the feeding area, as a rule, is associated with a decrease in the density of plants, and therefore there was a decrease in the overall productivity of root chicory per unit area.

Thus, the optimal feeding area of root chicory plants, which is close to a square, should be formed by the structure of sowing, taking into account its biological features, both by choosing a rational width between rows, and by evenly placing plants in rows with intervals of not less than 25 and not more than 35 cm with the aspect ratio of the feeding area corresponding to the rectangle K = 0.8–1.2.

The size and shape of the feeding area have a significant influence on the size and mass of root crops and, therefore, on the formation of the mass of the harvest of the Umansky-99 variety (Table 6). If the number of root crops with a diameter of 10–20 mm corresponded to a percentage value of 9% of their total collection, then their significance in the formation of the mass of the crop was only 2.1%, while with 7% of root crops with a diameter of 80–100 mm, the significance of their mass was 16.7% of the harvest or 9.1 t ha^{-1}, i.e. eight times more than the mass of root crops of the 10–20 mm fraction.

Table 6. Distribution of quality indicators of the Umansky-99 variety depending on the diameter of the root crop (average for 2017–2020)

Indicator	Root diameter, mm				
	10–20	20–40	40–60	60–80	80–100
Number of root crops, %	19	41	26	11	3
Significance in the formation of crop mass, %	12.1	15.2	34.5	27.5	10.7
Root mass Mr, g^{-1}	77.9	164.4	274.2	384.3	575.7
The ratio of leaf weight to root weight, D_r / D_a	1.68	1.57	1.14	0.82	0.69

For high-quality cutting of the gorse, the root crops were smaller (d_k = 10–20 mm), and were placed in a row at a distance of up to 10 cm and lay below the level of the soil surface. Therefore, when stored in the kagata (burta), root crops with a gichka or with a high cut are damaged and poorly stored.

CONCLUSION

The structure of the feeding area of root chicory plants affects photosynthetic productivity. Placement of plants on the feeding area according to the 45×22.5 cm and 22.5×45 cm scheme was distinguished by the highest indicators of net productivity of photosynthesis, which had a positive effect on the yield of root crops and their content of inulin polysaccharide.

With an increased rate of photosynthetic potential, it was noted at a feeding area of 60×60 cm (with a plant density of 30 10^3× ha^{-1} of the Umansky 97 variety was - 9.2 10^3× $10^3 m^{-2}$ ha^{-1} per day, Umansky-99 - 9.3 10^3× m^{-2} ha^{-1} per day with with a decrease in the feeding area (45×45, 35×35, 45×22.5 cm^{-1}), this indicator slightly increased, on average by variety, it was 10.1 to 10.8 10^3× m^{-2} ha^{-1} per day. The highest indicator of inulin content in chicory root crops is the feeding area of 35×35 cm and was in the variety Umansky-97 - 18.5%, Umansky-99 - 18.7%, and the feeding area of 45×22.5 cm - 18.2% and 18.4%, respectively.

The feeding area of chicory plants significantly affects the yield of root crops. From a plant density of 60,000 to 120,000 ha^{-1}, the yield averaged 30 t ha^{-1} with an average root weight of 500 to 250 g, with an inulin content of 17.3 to 19.0%.

According to the structure of the root crop, the productive part occupies on average from 82.7% to 91.6% of the total mass with inulin content from 17.3 to 19.0%.

REFERENCES

Baranovsky, V. & Potapenko, M. 2017. Theoretical analysis of the technological feed of lifted root crops. INMATEH: *Agricultural Engineering* **51**(1), 29–38.

Barcaccia, G., Ghedina, A. & Lucchin, M. Current Advances in Genomics and Breeding of Leaf Chicory (Cichorium intybus L.). 2016. *Agriculture* **6**(50). doi: 10.3390/agriculture6040050

Bhunia, S., Bhowmik, A., Mallick, R. & Mukherjee, J. 2021. Agronomic efficiency of animalderived organic fertilizers and their effects on biology and fertility of soil: A review. *Agronomy* **11**(5), 823.

Bondarenko, V., Havrylianchik, R., Ovcharuk, O., Pantsyreva, H., Krusheknyckiy, V., Tkach, O. & Niemec, M. 2022. Features of the soybean photosynthetic productivity indicators formation depending on the foliar nutrition. *Ecology, Environment and Conservation*. Vol. **28**(August Suppl. Issue), pp. 20–26. doi: 10.53550/EEC.2022.v28i04s.004

Das, S., Vasudeva, N. & Sharma, S. 2016. Cichorium intybus: A concise report on its ethnomedicinal, botanical, and phytopharmacological aspects. *Drug Dev. Ther*. **7**(1), 1–12. doi:10.4103/2394-6555.180157

Didur, I., Prokopchuk, V. & Pantsyreva, H. 2019. Investigation of biomorphological and decorative characteristics of ornamental species of the genus Lupinus L. *Ukrainian Journal of Ecology* **9**(3), 287–290. doi: 10.15421/2019_743

Dragan, Z., Joze, O. & Stanislav, T. 2004. Plant characteristics for distinction of red chicory (Cichorium intybus L. var. silvestre Bisch.) cultivars grown in central Slovenia. *Acta Agric. Slov* (**83**):251–260.

Ebrahimi, M., Pouyan, M. & Mahdi Nezhad, M. 2020. Studying the possibility of replacing manure with other organic amendments in saffron (Crocus sativus L.) cultivation at different mother corm weights. *Saffron agronomy and technology* **8**(1), 37–57.

Ferrare, K., Bidel, L.P., Awwad, A., Poucheret, P., Cazals, G., Lazennec, F., Azay-Milhau, J., Tournier, M., Lajoix, A.D. & Tousch, D. 2018. Increase in insulin sensitivity by the association of chicoric acid and chlorogenic acid contained in a natural chicoric acid extract (NCRAE) of chicory (Cichorium intybus L.) for an antidiabetic effect. *J. Ethnopharmacol*. **215**, 241–248. doi: 10.1016/j.jep.2017.12.035.

Honcharuk, I., Matusyak, M., Pantsyreva, H., Kupchuk, I., Prokopchuk, V. & Telekalo, N. 2022. Peculiarities of reproduction of pinus nigra arn. in Ukraine. *Bulletin of the Transilvania University of Brasov, Series II: Forestry, Wood Industry, Agricultural Food Engineering* **15**(64), 33–42.

Hnatiuk, T.T., Zhitkevich, N.V., Petrychenko, V.F., Kalinichenko, A.V. & Patyka, V.P. 2019. Soybean Diseases Caused by Genus. *Pseudomonas Phytopathenes Bacteria*. *Mikrobiol. Z.* **81**(3), 68–83. doi: https://doi.org/10.15407/microbiolj81.03.068

Ivanyshyn, O., Khomina, V. & Pantsyreva, H. 2021. Influence of fertilization on the formation of grain productivity in different-maturing maize hybrids *Ukrainian Journal of Ecology* **11**(3), 262–269. doi: 10.15421/2021_170

Lyashuk, O., Sokil, M., Vovk, Y., Tson, A., Gupka, A. & Marunych, A. 2018. Torsional oscillations of an auger multifunctional conveyor's screw working body with consideration of the dynamics of a processed medium continuous flow. *Ukrainian Food Journal* **7**(3), 499–510. doi: https://doi.org/10.24263/2304-974X-2018-7-3-14

Mazur, V., Pantsyreva, H., Mazur, K., Myalkovsky, R. & Alekseev, O. 2020. Agroecological prospects of using corn hybrids for biogas production. *Agronomy Research* **18**(1), 177–182.

Mazur, V., Tkachuk, O., Pantsyreva, H., Kupchuk, I., Mordvaniuk, M. & Chynchyk, O. 2021. Ecological suitability peas (Pisum sativum) varieties to climate change in Ukraine. In: Agraarteadus: *Journal of Agricultural Science* **32**(2), 276–283. doi: 10.15159/jas.21.26

Mazur, V.A., Pantsyreva, H.V., Mazur, K.V. & Didur, I.M. 2019. Influence of the assimilation apparatus and productivity of white lupine plants. *Agronomy Research* **17**, 206–219.

Pantsyreva, H. 2021. Morphological and ecological-biological evaluation of the decorative species of the genus *Lupinus* L. *Ukrainian Journal of Ecology* **9**(3), 74–77. doi: 10.15421/2019_711

Petrychenko, V.F., Kobak, S.Ya., Chorna, V.M., Kolisnyk, S.I., Likhochvor, V.V. & Pyda, S.V. 2018. Formation of the Nitrogen-Fixing Potential and Productivity of Soybean Varieties Selected at the Institute of Feeds and Agriculture of Podillia of NAAS. *Mikrobiol. Z.* **80**(5), 63–75.

Pouille, C.L., Jegou, D., Dugardin, C., Cudennec, B., Ravallec, R., Hance P., Rambaud, C., Hilbert, J.L. & Lucau-Danila, A. 2020. Chicory root flour – A functional food with potential multiple health benefits evaluated in a mice model. *J. Funct. Foods*. **74**, 104174. doi: 10.1016/j.jff.2020.104174

Puyu, V., Bakhmat, M., Pantsyreva, H., Khmelianchyshyn, Y., Stepanchenko, V. & Bakhmat, O. 2021. Social-and-Ecological Aspects of Forage Production Reform in Ukraine in the Early 21st Century. *European Journal of Sustainable Development* **10**(1), 221–228. doi:10.14207/ejsd.2021.v10n1p221

Reimer, R.A., Soto-Vaca, A., Nicolucci, A.C., Mayengbam, S., Park, H., Madsen, K.L., Menon R. & Vaughan E.E. 2020. Effect of chicory inulin-type fructan–containing snack bars on the human gut microbiota in low dietary fiber consumers in a randomized crossover trial. *Am. J. Clin. Nutr*. **111**, 1286–1296. doi: 10.1093/ajcn/nqaa074

Sabzevari, S., Khazaei, H. & Kafi, M. 2010. The effect of humic acid on germination of four cultivars of fall wheat (Saions and Sabaln) and spring wheat. *Journal of Agricultural Research* **8**(3), 473–480.

Tkach, O. 2020. Yield of root crops of chicory depending on the density of plants. *Scientific journal.* Kherson **112**, pp. 150–156.

Tokarchuk, D.M., Pryshliak, N.V., Tokarchuk, O.A. & Mazur, K.V. 2020. Technical and economic aspects of biogas production at a small agricultural enterprise with modeling of the optimal distribution of energy resources for profits maximization. *Inmateh. Agricultural Engineering* **61**(2), 339–349.

Zayova, E., Nikolova, M., Dimitrova, L. & Petrova, M. 2016. Comparative study of in vitro, ex vitro and in vivo propagated Salvia Hispanica (Chia) plants: morphometric analysis and antioxidant activity. *Agro Life Scientific Journal* **5**(2), 166–174.